Aus
der Universitätsklinik für Urologie und Kinderurologie
der Medizinischen Fakultät
der Otto-von-Guericke-Universität Magdeburg
(Direktor: Prof. Dr. med. Martin Schostak)

„Irreversible Elektroporation in der Uroonkologie – die systematische Evaluation eines neuartigen, nonthermalen Gewebeablationsverfahrens am Nierentumormodell zur minimal-invasiven, perkutanen, kurativ-intendierten Therapie des lokal begrenzten Nierenzellkarzinoms und Prostatakarzinoms.“

H A B I L I T A T I O N S S C H R I F T

(kumulativ)

zur Erlangung des akademischen Grades
Dr. med. habil.
(doctor medicinae habilitatus)

an der Medizinischen Fakultät
der Otto-von-Guericke-Universität Magdeburg

vorgelegt von Dr. med. Johann Jakob Wendler
aus Berlin
wohnhaft Magdeburg
vom 13.05.2019

Widmung

Diese Arbeit widme ich aus Überzeugung
der Irreversiblen Elektroporation und ihrer Entwicklung
zum potenten, fokaltherapeutischen Tumorgewebeablationsverfahren.

Vorwort

Diese Habilitationsarbeit beruht im Sinne einer kumulativen Habilitationsschrift auf dem Inhalt der nachfolgend aufgelisteten Publikationen (1) - (17). Damit wird die nach der Habilitationsordnung gegebene Möglichkeit „zur Vorlage publizierter Forschungsergebnisse, die in ihrer Gesamtheit einer Habilitationsschrift gleichwertige wissenschaftliche Leistung darstellen“, genutzt. Die vollständige Publikationsliste des Habilitanden ist im separaten Abschnitt eingefügt.

(1) Liehr UB, **Wendler JJ**, Blaschke S, Porsch M, Janitzky A, Baumunk D, Pech M, Fischbach F, Schindele D, Grube C, Ricke J, Schostak M. **[Irreversible electroporation: the new generation of local ablation techniques for renal cell carcinoma].** Urologe A. 2012 Dec;51(12):1728-34.

(2) **Wendler JJ**, Pech M, Blaschke S, Porsch M, Janitzky A, Ulrich M, Dudeck O, Ricke J, Liehr UB. **Angiography in the isolated perfused kidney: radiological evaluation of vascular protection in tissue ablation by nonthermal irreversible electroporation.** Cardiovasc Intervent Radiol. 2012 Apr;35(2):383-90.

(3) **Wendler JJ**, Pech M, Porsch M, Janitzky A, Fischbach F, Buhtz P, Vogler K, Hühne S, Borucki K, Strang C, Mahnkopf D, Ricke J, Liehr UB. **Urinary tract effects after multifocal nonthermal irreversible electroporation of the kidney: acute and chronic monitoring by magnetic resonance imaging, intravenous urography and urinary cytology.** Cardiovasc Intervent Radiol. 2012 Aug;35(4):921-6.

(4) **Wendler JJ**, Porsch M, Hühne S, Baumunk D, Buhtz P, Fischbach F, Pech M, Mahnkopf D, Kropf S, Roessner A, Ricke J, Schostak M, Liehr UB. **Short- and mid-term effects of irreversible electroporation on normal renal tissue: an animal model.** Cardiovasc Intervent Radiol. 2013 Apr;36(2):512-20.

(5) Pech M, Janitzky A, **Wendler JJ**, Strang C, Blaschke S, Dudeck O, Ricke J, Liehr UB. **Irreversible electroporation of renal cell carcinoma: a first-in-man phase I clinical study.** Cardiovasc Intervent Radiol. 2011 Feb;34(1):132-8.

(6) **Wendler JJ**, Porsch M, Fischbach F, Pech M, Schostak M, Liehr UB. **Letter to the Editor Concerning "Irreversible Electroporation (IRE) Fails to Demonstrate Efficacy in a Prospective Multicenter Phase II Trial on Lung Malignancies: The ALICE Trial"** by Ricke et al. 2015 (doi:10.1007/s00270-014-1049-0). Cardiovasc Intervent Radiol. 2015 Aug;38(4):1064-5.

(7) **Wendler JJ**, Ganzer R, Hadaschik B, Blana A, Henkel T, Köhrmann KU, Machtens S, Roosen A, Salomon G, Sentker L, Witzsch U, Schlemmer HP, Baumunk D, Köllermann J, Schostak M, Liehr UB; Working Group for Focal and Microtherapy, Academy of the German Society of Urology. **[Irreversible electroporation. Current value for focal treatment of prostate cancer].** Urologe A. 2015 Jun;54(6):854-62.

(8) **Wendler JJ**, Ganzer R, Hadaschik B, Blana A, Henkel T, Köhrmann KU, Machtens S, Roosen A, Salomon G, Sentker L, Witzsch U, Schlemmer HP, Baumunk D, Köllermann J, Schostak M, Liehr UB. **Why we should not routinely apply irreversible electroporation as an alternative curative treatment modality for localized prostate cancer at this stage.** World J Urol. 2017 Jan;35(1):11-20.

(9) **Wendler JJ**, Klink F, Seifert S, Fischbach F, Jandrig B, Porsch M, Pech M, Baumunk D, Ricke J, Schostak M, Liehr UB. **Irreversible Electroporation of Prostate Cancer: Patient-Specific Pretreatment Simulation by Electric Field Measurement in a 3D Bioprinted Textured Prostate Cancer Model to Achieve Optimal Electroporation Parameters for Image-Guided Focal Ablation.** Cardiovasc Intervent Radiol. 2016 Nov;39(11):1668-1671.

(10) **Wendler JJ**, Fischbach K, Ricke J, Jürgens J, Fischbach F, Köllermann J, Porsch M, Baumunk D, Schostak M, Liehr UB, Pech M. **Irreversible Electroporation (IRE): Standardization of Terminology and Reporting Criteria for Analysis and Comparison.** Pol J Radiol. 2016 Feb 17;81:54-64.

(11) **Wendler JJ**, Porsch M, Nitschke S, Köllermann J, Siedentopf S, Pech M, Fischbach F, Ricke J, Schostak M, Liehr UB. **A prospective Phase 2a pilot study investigating focal percutaneous irreversible electroporation (IRE) ablation by NanoKnife in patients with localised renal cell carcinoma (RCC) with delayed interval tumour resection (IRENE trial).** Contemp Clin Trials. 2015 Jul;43:10-9.

(12) **Wendler JJ**, Ricke J, Pech M, Fischbach F, Jürgens J, Siedentopf S, Roessner A, Porsch M, Baumunk D, Schostak M, Köllermann J, Liehr UB. **First Delayed Resection Findings After Irreversible Electroporation (IRE) of Human Localised Renal Cell Carcinoma (RCC) in the IRENE Pilot Phase 2a Trial.** Cardiovasc Intervent Radiol. 2016 Feb;39(2):239-50.

(13) **Wendler JJ**, Friebe B, Baumunk D, Blana A, Franiel T, Ganzer R, Hadaschik B, Henkel T, Köhrmann KU, Köllermann J, Kuru T, Machtens S, Roosen A, Salomon G, Schlemmer HP, Sentker L, Witzsch U, Liehr UB, Ricke J, Schostak M. **[Focal therapy for small renal masses: Observation, ablation or surgery].** Urologe A. 2016 May;55(5):594-606.

(14) Zondervan PJ, Wagstaff PG, Desai MM, de Bruin DM, Fraga AF, Hadaschik BA, Köllermann J, Liehr UB, Pahernik SA, Schlemmer HP, **Wendler JJ**, Algaba F, de la Rosette JJ, Laguna Pes MP. **Follow-up after focal therapy in renal masses: an international multidisciplinary Delphi consensus project.** World J Urol. 2016 Dec;34(12):1657-1665. Epub 2016 Apr 22.

(15) **Wendler JJ**, Ricke J, Pech M, Fischbach F, Jürgens J, Porsch M, Janitzky A, Baumunk D, Siedentopf S, Köllermann J, Schostak M, Liehr UB. **Initial assessment of clinical feasibility, safety and efficacy of NanoKnife irreversible electroporation (IRE) in the focal treatment of localized renal cell carcinoma (RCC) with delayed interval tumor resection (IRENE trial).** 32nd Annual EAU Congress, London. Eur Urol Suppl 2017; 16(3);e102.

(16) **Wendler JJ**, Pech M, Köllermann J, Friebe B, Siedentopf S, Blaschke S, Schindele D, Porsch M, Baumunk D, Jürgens J, Fischbach F, Ricke J, Schostak M, Böhm M, Liehr UB. **Upper-Urinary-Tract Effects After Irreversible Electroporation (IRE) of Human Localised Renal-Cell Carcinoma (RCC) in the IRENE Pilot Phase 2a Ablate-and-Resect Study.** Cardiovasc Intervent Radiol. 2017 Sep 19.

(17) **Wendler JJ**, Pech M, Fischbach F, Jürgens J, Friebe B, Baumunk D, Porsch M, Blaschke S, Schindele D, Siedentopf S, Ricke J, Schostak M, Köllermann J, Liehr UB. **Initial Assessment of the Efficacy of Irreversible Electroporation in the Focal Treatment of Localized Renal Cell Carcinoma with Delayed-interval Kidney Tumor Resection (Irreversible Electroporation of Kidney Tumors before Partial Nephrectomy [IRENE] Trial-An Ablate-and-Resect Pilot Study).** Urology. 2018 Apr;114:224-232.

Inhaltsverzeichnis

8.7	**Wendler JJ**, Ganzer R, Hadaschik B, Blana A, Henkel T, Köhrmann KU, Machtens S, Roosen A, Salomon G, Sentker L, Witzsch U, Schlemmer HP, Baumunk D, Köllermann J, Schostak M, Liehr UB; Working Group for Focal and Microtherapy, Academy of the German Society of Urology. **[Irreversible electroporation. Current value for focal treatment of prostate cancer].** Urologe A. 2015 Jun;54(6):854-62.	157
8.8	**Wendler JJ**, Ganzer R, Hadaschik B, Blana A, Henkel T, Köhrmann KU, Machtens S, Roosen A, Salomon G, Sentker L, Witzsch U, Schlemmer HP, Baumunk D, Köllermann J, Schostak M, Liehr UB. **Why we should not routinely apply irreversible electroporation as an alternative curative treatment modality for localized prostate cancer at this stage.** World J Urol. 2017 Jan;35(1):11-20.	166
8.9	**Wendler JJ**, Klink F, Seifert S, Fischbach F, Jandrig B, Porsch M, Pech M, Baumunk D, Ricke J, Schostak M, Liehr UB. **Irreversible Electroporation of Prostate Cancer: Patient-Specific Pretreatment Simulation by Electric Field Measurement in a 3D Bioprinted Textured Prostate Cancer Model to Achieve Optimal Electroporation Parameters for Image-Guided Focal Ablation.** Cardiovasc Intervent Radiol. 2016 Nov;39(11):1668-1671.	178
8.10	**Wendler JJ**, Fischbach K, Ricke J, Jürgens J, Fischbach F, Köllermann J, Porsch M, Baumunk D, Schostak M, Liehr UB, Pech M. **Irreversible Electroporation (IRE): Standardization of Terminology and Reporting Criteria for Analysis and Comparison.** Pol J Radiol. 2016 Feb 17;81:54-64.	182
8.11	**Wendler JJ**, Porsch M, Nitschke S, Köllermann J, Siedentopf S, Pech M, Fischbach F, Ricke J, Schostak M, Liehr UB. **A prospective Phase 2a pilot study investigating focal percutaneous irreversible electroporation (IRE) ablation by NanoKnife in patients with localised renal cell carcinoma (RCC) with delayed interval tumour resection (IRENE trial).** Contemp Clin Trials. 2015 Jul;43:10-9.	194

Abkürzungsverzeichnis

A	Ampere
Abb.	Abbildung
AKFM	Arbeitkreis für Fokale und Mikrotherapie der DGU
AS	Active Surveillance
ASA	American Society of Anaesthesiologists
AUA	American Urological Assoziation
AWMF	Arbeitsgemeinschaft der Wissenschaftlichen Medizinischen Fachgesellschaften
BfArM	Bundesinstitut für Arzneimittel und Medizinprodukte
BT	Brachytherapie
CE	Communauté Européenne
CEUS	Contrast-enhanced Ultrasound
CT	Computertomographie
CTRP	Clinical Trials Reporting Program
DAfMT	Deutsche Akademie für Mikrotherapie
DGU	Deutsche Gesellschaft für Urologie
DIMDI	Deutsche Institut für Medizinische Dokumentation und Information
DRKS	Deutsche Register Klinischer Studien
EAU	European Assosiation of Urology
EEC	European Economic Community
EKG	Elektrokardiographie
ESWL	Extrakorporale Stoßwellenlithotripsie
FDA	Food and Drug Administration
GCP	Good Clinical Practice
GS	Gleason-Score
Gy	Gray
HDR-BT	High-Dose-Rate-Brachytherapy
HE	Hämatoxylin-Eosin
H-FIRE	Hochfrequente Irreversible Elektroporation
HIFU	Hochintensiver fokussierter Ultraschall
IMRT	Intensity-modulated Radiotherapy
INKA	Intelligente Katheter
IRE	Irreversible Elektroporation

IRENE	IRreversible Elektroporation von Nierentumoren vor Ektomie
KA	Kryoablation
KDIGO	Kidney Disease: Improving Global Outcomes
LDR-BT	Low-Dose-Rate-Brachytherapie
MPG	Medizinproduktegesetz
mpMRT	Multiparametrische Magnetresonanztomographie
MRT	Magnetresonanztomographie
MWA	Mikrowellenablation
NBKS	Nierenbeckenkelchsystem
NTIRE	Nonthermale Irreversible Elektroporation
NZK	Nierenzellkarzinom
OP	Operation
PCA	Prostatacarcinom
PSA	Prostata-spezifisches Antigen
RCC	Renal cell carcnioma
RFA	Radiofrequenzablation
RKI	Robert-Koch-Institut
SABR	Stereotaktische Ablative Radiotherapie
SRM	Small renal mass
STIMULATE	Solution Centre for Image Guided Local Therapies
Tab.	Tabelle
TNM	Tumor (Primärtumor), Nodus (Lmyphknoten), Metastasen (Fernmetastasen)
UICC	Union International Contre le Cancer
USA	United States of America
UTN	Universal trial number
V	Volt
WHO	World Health Organization

Abbildungsverzeichnis

Abb.12	Simulation der theoretischen Ablationszone anhand der Ablations-parametereinstellungen. Nummerierung der Elektrodenpositionen, welche sich zur Planung verschieben lassen. Der gelbe Ring entspricht der Tumorzone (lesion zone). Das blaue Areal entspricht dem peritumoralem Sicherheitssaum. Die graue Fläche entspricht der theoretischen Ablationszone. In tabellarischer Auflistung können die Ablationsparameter justiert werden.
Abb.13	CT-gestützte IRE-Elektroden-Platzierung unter Fluoroskopie und sterilen Kautelen. Beispiel für IRE mittels NanoKnife-System eines Nierentumors (IRENE-Studie, Wendler et al. 2015b) mit Patient in Bauchlage und Intubationsnarkose mit Muskelrelaxation und EKG-Synchronisierung.
Abb.14	Eingabe der CT-kontrollierten Elektrodenpositionen und –abstände zueinander.
Abb.15	Graphische Übersicht der Kurvenverläufe für Spannung und Stromstärke (NanoKnife™, AngioDynamics®). Pro Gruppe von zehn aufeinanderfolgenden IRE-Impulsen fällt die Spannung und Stromstärke leicht ab. Insgesamt nimmt die Stromstärke und Spannung vom Anfang bis zum Ende der Ablation zu. In der Vergrößerung der IRE-Pulse zeigt sich ein typischer Rechteckimpuls mit leichtem Stromanstieg innerhalb eines Rechteckimpulses.
Abb.16	Videofotografische Darstellung der bipolaren NanoKnife-IRE-Elektrode im Hühnerflüssigeiweiß mit Lichtblitzen (links). Schematische Darstellung der bipolaren NanoKnife-IRE-Elektrode mit Lokalisation der Lichtblitze (Mitte). Fotografische Darstellung der bipolaren NanoKnife-IRE-Elektrode im Hühnerflüssigeiweiß mit Schaumbildung (rechts).
Abb.17	Hohlraum um IRE-Nadelspitze, zur besseren Darstellung im Speise-gelatine-Modell.
Abb.18	Intraoperative IRE: sonografisch-gestützte IRE-Sonden-Einlage (links) und IRE-Puls-Applikation (rechts). Bipolare IRE-Elektrode des NanoKnife-Systems.
Abb.19	Typisches klarzelliges Nierenzellkarzinom (HE-Färbung) in 200-facher Vergrößerung ohne akute IRE-Veränderungen nach intraoperativer NanoKnife-System-Anwendung mit unmittelbar anschließender Nieren-tumorresektion (Nierenteilresektion) aus der Safety-Studie.
Abb.20	Anzahl der Publikation zur IRE in PubMed seit 2005 (Stand PubMed 26.04.2019).
Abb.21	Study Content Flow Chart zur IRENE-Studie.
Abb.22	Algorithmus verschiedener Therapieoptionen des T1a-Nierenzell-karzinoms (NZK) nach OP-/ Narkose-Risiko und Tumorlokalisation mit künftig möglichem Stellenwert der IRE/ HF-IRE als Behandlungsalternative.
Abb.23	Algorithmus verschiedener Therapieoptionen des lokal begrenzten Prostatakarzinoms (PCA) nach PCA-Risikoprofil und OP-/ Narkose-Risiko mit künftig möglichem Stellenwert der IRE / HF-IRE als Behandlungs-alternative.
Abb.24	Poster presentation of “Initial assessment of clinical feasibility, safety and efficacy of NanoKnife irreversible electroporation (IRE) in the focal treatment of localized renal cell carcinoma (RCC) with delayed interval tumor resection (IRENE trial). 32nd Annual EAU Congress, London. Eur Urol Suppl 2017; 16(3);e102.”

Tabellenverzeichnis

1. Einleitung

Minimalinvasive Gewebeablationsverfahren finden gegenüber den konventionellen Operationsmethoden eine immer größere, interdisziplinäre Anwendung in der Uroonkologie. Deren stetige Weiterentwicklung ermöglicht zunehmend einen entsprechend häufigeren oder größeren Organ- sowie Funktionserhalt mit einer damit verbundenen höheren Lebensqualität und geringeren, komorbiditätsbedingten Mortalität bei teils gleichwertigen onkologischen Ergebnissen. Entsprechend bedürfen jedoch neue Ablationsverfahren, neben der allgemeinen Anwendungszulassung zur Weichgewebeablation, vor allem einer fachspezifischen und indikationsbasierten Prüfung. Etabliert sind im Allgemeinen strahlentherapeutische Methoden, wie die perkutane Radiatio bzw. stereotaktische ablative Radiotherapie und die Brachytherapie, sowie thermoablative Techniken, wie die Radiofrequenzablation, der Hochintensive fokussierte Ultraschall und die Kryoablation. Andere Ablationsverfahren gelten bisher weitgehend als experimentell oder sind noch nicht etabliert. Die o.g. bisherigen Techniken wirken nicht selektiv, d.h. dass verfahrensbedingt keine Unterscheidung zwischen Tumorgewebe und gesundem Gewebe, sowie keine Trennung anatomischer Grenzstrukturen stattfindet. So ergibt sich für diese Verfahren ein spezifisches Anwendungsprofil unter Berücksichtigung der möglichst effektiven Zielgewebszerstörung und der möglichst geringen Nebenwirkungen auf das gesunde Umgebungsgewebe bzw. funktionelle Leitstrukturen. Bei den o.g. Techniken muss ein zentrifugaler Abfall des Wirkungsgradienten berücksichtigt werden, so dass per notwendigem, peritumoralem Sicherheitssaum von 5-10 mm stets ein Teil des angrenzenden gesunden Gewebes mitgeschädigt wird. Zusätzlich ist die Thermoablationswirkung durch den kühlenden Effekt bei hyperthermalen Techniken (heat-sink effect) und den wärmenden Effekt bei hypothermalen Techniken (cold-sink effect) bei einer starken Vaskularisation eingeschränkt.
Seit 2005 steht die Irreversible Elektroporation (IRE) als neuartiges, nonthermales Weichgewebeablationsverfahren im Fokus der klinischen Medizin, insbesondere der Onkologie. Nach ersten experimentellen Publikationen wurde eine nonthermoablative, gewebeselektive Wirkweise der IRE mit scharfbegrenzten Ablationsarealen ohne die bekannten Nachteile bisher bekannter Ablationsverfahren postuliert. Die Matrix sowie Grenz- und Leitstrukturen sollen erhalten bleiben. 2007 erhielt die Firma AngioDynamics Inc. (NY, U.S.A.) die Zulassung der zuständigen US-amerikanischen Behörde FDA für ihr Medizinprodukt „NanoKnife®“ zur Ablation von Weichgewebe. 2008 folgte dafür die EC-Kennzeichnung für Medizinprodukte mit kommerzieller Anwendungszulassung durch die Europäische Kommission. Bis dato beschränkten sich die Anwendungserfahrungen dabei lediglich auf in-vitro- und tierexperimentelle Untersuchungen, vorrangig am Lebergewebe.

Die Anwendung der IRE mittels NanoKnife-Systems zur Weichgewebeablation wurde entsprechend für verschiedene Organe und Tumorentitäten beworben.

Im o.g. Kontext bestand konsekutiv das Interesse zur Anwendung der IRE und des NanoKnife-Systems als minimalinvasive Ablationsmethode für lokal begrenzte urologische Tumoren. Dabei ergeben sich mögliche Indikationen zur organschonenden und organerhaltenden Ablation von lokal begrenzten Nieren-, Blasen-, Hoden- und Prostata-tumoren, respektive -karzinomen.

Zum Zeitpunkt des Beginns unserer Untersuchungen (2008/ 2009) standen keine ausreichenden Erkenntnisse zum klinischen Einsatz dieses Verfahrens zur Verfügung, was zur eigenen Evaluation des NanoKnife-Systems bzw. der IRE als Zielsetzung führte.

Die folgende Arbeit ist eine zusammenfassende Darstellung dieser systematischen, experimentellen und klinischen Evaluation der IRE und des NanoKnife-Systems als neues Gewebeablationsverfahren aus uroonkologischer Sicht.

2. Zielsetzung

Da zum Zeitpunkt der Gerätezulassung des NanoKnife-Systems keine klinischen, tumorentitätsspezifischen Wirksamkeitsnachweise zur Irreversiblen Elektroporation vorlagen, führte das zur eigenen Zielsetzung, die postulierten Funktionseigenschaften der Irreversiblen Elektroporation und die vom Hersteller angegebenen Eigenschaften des NanoKnife-Systems im Hinblick auf eine minimalinvasive, perkutane Anwendung zunächst bei Nierenkarzinomen und Prostatakarzinomen im Rahmen einer Wirksamkeitsnachweisstudie zu prüfen.

Als primäres Organmodell zur klinisch-experimentellen Evaluation wurde die Niere gegenüber der Prostata favorisiert, da hier insgesamt eine höhere klinische Expertise zur fokalen Therapie von Nierentumoren bestand, und die Niere ein leichter zu simulierendes und zu monitorierendes Organ darstellt. Die kumulative Habilitationsschrift stellt die Weiterführung der präklinisch-experimentellen Grundarbeiten in die klinische Anwendung dar. Daraus abgeleitete Erkenntnisse aus der Anwendung an der Niere bzw. der Behandlung des lokal begrenzten Nierenzellkarzinoms sollen auf das Prostatamodell zur Anwendung beim lokal begrenzten Prostatakarzinom übertragen und im Rahmen der laufenden internationalen wissenschaftlichen Untersuchungen diskutiert werden.

3. Grundlagen

3.1 Nierenzellkarzinom

3.1.1 Epidemiologie des Nierenzellkarzinoms

Das Nierenzellkarzinom (NZK) ist das dritthäufigste maligne Tumorleiden in der Urologie und mit rund 90% das häufigste Malignom der Niere, wobei die 5-Jahres-Prävalenz (n = 58.100) und Inzidenz (n = 14.960) in Deutschland stetig zunehmen (RKI 2016; Lindblad 2004). Die relative 5-Jahres-Überlebensrate beträgt für lokal begrenzte Nierenzellkarzinome in Abhängigkeit von weiteren Risikofaktoren 87-97% und für metastasierte Nierenzellkarzinome je nach Metastasenlokalisation und Patientenkondition <20% (mittlere Überlebenszeit 6-9 Monate) (MacLennan et al. 2012; Neves et al. 1988). Neben der mit zunehmendem Alter ansteigenden Krebserkrankungsrate kommt es auch zu einem Anstieg der Komorbidität bis Multimorbidität durch andere Organ- oder Systemerkrankungen, die sowohl direkten oder indirekten Einfluss auf die Therapie und den Verlauf der malignen Erkrankungen als auch die Nierenfunktion haben (Kirchberger et al. 2012). Insbesondere die chronische Niereninsuffizienz geht mit einer schlechteren Lebenserwartung und -qualität einher (KDIGO 2012). Aufgrund des technischen Fortschritts in der schnittbildgebenden Diagnostik erfolgt zunehmend die Erkennung des NZK gezielt oder als Zufallsbefund im Frühstadium mit dem Vorteil einer fokalen nierenerhaltenden Behandlung (Tsili et al. 2015).

3.1.2 Wachstumsverhalten des Nierenzellkarzinoms

Das NZK entsteht in der Nierenrinde (Cortex renalis) mit meist unilateraler und unifokaler Lokalisation. Das Wachstumsmuster wird histomorphologisch in kompakt, azinär, tubulopapillär oder zystisch bzw. als deren Mischform unterschieden. Eine zystische Degeneration ist bei 10-25 % aller NZK zu finden und häufiger mit dem papillären NZK und einem multifokalen, beidseitigen sowie oft metachronen Wachstum vergesellschaftet (Wein et al. 2016).

Der Begriff „kleiner Nierentumor“ ist zunächst eine bildmorphologische Beschreibung einer soliden Raumforderung des kortikalen Nierenparenchyms ohne Wertung der Entität, Dignität und genauen Lokalisation. Im angloamerikanischen Raum gilt dies als „small renal mass“ (SRM) mit einer Größe bis 3 cm Durchmesser (AUA 2017).

Im europäischen und deutschsprachigen Raum wurde dieser Begriff als „kleiner Nierentumor“ für solide Raumforderungen des Nierenparenchyms mit einer Größenausdehnung bis 4cm analog zur T-Kategorie der UICC-Klassifikation 2017 für das lokal begrenzte nichtmetastasierte NZK cT1a cN0 cM0 Stadium 1 übernommen (AWMF 2017; EAU 2019; Brierley et al. 2017; Wittekind et al. 2013). Der prognostische Grenzwert von 4 cm für T1a ist historisch bedingt und korreliert nicht mit neueren Daten, wobei die Wachstums- und die Metastasierungsrate bereits ab einer Tumorgröße von 3 cm exponentiell zunehmen.

Zahlreiche Studien zum Progress kleiner T1a-Nierentumoren (≤ 4 cm) zeigten eine relativ langsame Wachstumsrate mit pro Jahr und eine sehr geringe Metastasierungsrate in den ersten 5 Jahren, wobei diese Daten eine nicht unerhebliche Anzahl histologisch ungesicherter oder benigner Tumoren und verschiedene NZK-Subtypen enthalten (Frank et al. 2003, Wein et al. 2016). Chawla et al. errechneten aus einer Metaanalyse für die Subgruppe bioptisch gesicherter pT1a-NZK (n = 120) mit einer medianen Tumorgröße von 2,48 (1,7–4,0) cm eine mediane Wachstumsrate von 0,35 cm pro Jahr (0,42–1,6 cm pro Jahr) bei einem mittleren Nachbeobachtungszeitraum von 30 (25–39) Monaten, wobei die initiale Tumorgröße nicht mit der Wachstumsrate signifikant korrelierte (Chawla et al. 2006). Thompson et al. beschrieben eine Metastasierungsquote von 0,13 % bei NZK <3 cm (1/178), wobei das Metastasierungsrisiko um 24 %/cm zusätzlichem Wachstum stieg (Thompson et al. 2009). Somit ist die Tumorgröße einer der wichtigsten Prognosefaktoren für den Erkrankungsverlauf und eine Metastasierung.

Im Anfangsstadium wächst das lokalisierte NZK vorrangig verdrängend und teilweise infiltrierend, wobei sich häufig eine peritumorale Pseudokapsel als „chirurgische Kapsel“ durch Kompression von gesunden Zellen des Umgebungsgewebes, von randständigen Tumorzellen und von angrenzendem Bindegewebestroma (Matrix) (Wein et al. 2016) findet. Diese durchschnittlich nur 0,5mm dicke Pseudokapsel ist jedoch individuell ausbildet und existiert in variabler Ausprägung von einer kompletten oder inkompletten Pseudokapsel mit und ohne Tumorinfiltration bis hin zu einer komplett fehlenden Pseudokapsel (Kim et al. 2015; Xi et al. 2017). Gelegentlich sind mikroskopische Satellitentumore in unmittelbarer Umgebung zum makroskopischen Tumor zu finden (Raz et al. 2007).

Histologisch wird das NZK nach prognostisch relevanten Subtypen unterschieden, wobei zu den drei häufigsten Haupttypen das klarzellige NZK (80-90%), das papilläre bzw. chromophile NZK (10-15%) und das chromophobe NZK (4-5%) zählen (AWMF 2017; EAU 2019; Eble et al. 2004). Das NZK weist eine histologisch und genetisch große intratumorale und intertumorale Heterogenität auf, sowohl des Primärtumors als auch seiner Metastasen, welche ein differenziertes Wachstumsmuster und eine unterschiedliche medikamentös-tumortherapeutische Ansprechrate begründet (Beksac et al. 2017).

Bei fortschreitendem Wachstum infiltriert das NZK angrenzende Strukturen (Nierenbeckenkelchsystem, Nierenkapsel, Nebenniere, perirenales Fettgewebe, Gerota-Faszia) bzw. schreitet über diese hinaus (Terrone et al. 2004). Ebenso steigt das Risiko zur Ausbildung von Tumorthromben der Nierenvenen bis Vena cava und deren Wandinfiltration. Der lokale und systemische Progress des unbehandelten NZK hängt von mehreren Prognosefaktoren die wie Tumorgröße und -lokalisation sowie dem histologischen Subtyp ab. Das NZK metastasiert häufig lymphogen retroperitoneal in die regionalen hiliären, paracavalen und paraaortalen Lymphknoten und weit häufiger hämatogen, wie in die Lunge (50-60%), das Skelett (30-40%), die Leber (30-40%) und das Gehirn (5-11%) (Ritchie et al. 1983; Hellsten et al. 1990).

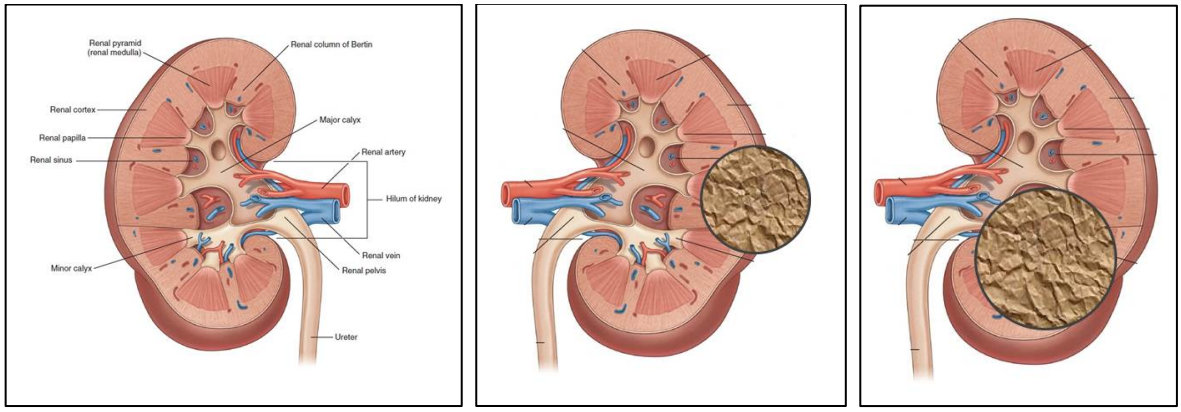

Abb.1: Links: Anatomie der Niere (Wein et al. 2016). Mittig: Beispiel kortikaler Nierentumor (Nierenzellkarzinom) im Mittelgeschoss. Rechts: Beispiel zentraler Nierentumor (Nierenzellkarzinom) im Unter- bis Mittelgeschoss mit direkter Lagebeziehung zum Nierenhilus (Nierengefäße und Nierenbecken).

Das lokal begrenzte bis lokal fortgeschrittene, nicht-metastasierte NZK wird anhand Tumorgröße und Tumorausdehnung per T-Kategorie der TNM-Klassifikation UICC 2017 eingestuft (EAU 2019; Brierley et al. 2017; Wittekind et al. 2013). Anatomische Klassifikationssysteme zur Nierentumorlokalisation wie der PADUA-Score („preoperative aspects and dimensions used for an anatomical classification“), der RENAL-Score („radius, exophytic/endophytic, nearness to collecting system or sinus, anterior/posterior and location relative to polar lines“) oder der C-Index stellen eine Entscheidungshilfe in der Therapiewahl dar (Joshi et al. 2017).

3.1.3 Therapieoptionen des lokal begrenzten Nierenzellkarzinoms

3.1.3.1 Active Surveillance des Nierenzellkarzinoms

Besteht die Indikation oder der Wunsch zum Aufschub einer invasiven Therapie des lokal begrenzten kleinen Nierenzellkarzinoms, stellt die aktive Überwachung zunächst eine Behandlungsoption dar. Das Konzept der aktiven Überwachung (Active Surveillance, AS) sieht im Fall kleiner, lokal begrenzter asymptomatischer Nierentumoren (SRM, cT1a, ≤4 cm) mit geringer Größenprogredienz und Metastasierungstendenz ein Kontrollieren mittels regelmäßiger Bildgebung nach initialer histologischer Sicherung per Biopsie vor. Erst bei einer Größenprogredienz oder auf Patientenwunsch soll die kurativ intendierte Behandlung eingeleitet werden. Es gibt weder objektive Kriterien zur Selektion adäquater Patienten noch eine einheitliche Definition zur AS (AWMF 2017). Ein Tumormarker zur Verlaufskontrolle des Nierentumors existiert nicht; das Konzept der Rebiopsie zur Verlaufskontrolle des Nierentumors unter AS ist nicht etabliert. Somit wird als AS lediglich die bildgebende Kontrolluntersuchung definiert, wobei bislang kein empfohlenes Schema zu Bildgebungsart und Intervall existiert. Zur AS von SRM und pT1a-NZK liegen neben retrospektiven Studien und Metaanalysen keine prospektiv randomisierten Studiendaten vor (AWMF 2017). Jewett et al. analysierten bei 101 bioptisch gesicherten pT1a-NZK eine Progressionsrate von 0,13 cm/Jahr und einer Metastasierungsrate von 1,1 % über eine mediane Nachbeobachtungszeit von 28 Monaten (Jewett et al. 2011). Lane et al. fanden bei 537 SRM-Patienten mit einem Alter ≥ 75 Jahren keinen signifikanten Überlebensunterschied zwischen AS und OP, wobei von 148 Todesfällen in einer medianen Nachbeobachtungszeit von 3,9 Jahren lediglich 4 % auf einen klinischen Progress eines NZK zurückzuführen waren (Lane et al. 2010). Insgesamt wird die AS nicht für Nierentumoren bei einer Größe >3cm, unscharfer Begrenzung, deutlicher Inhomogenität, NZK-suspektem Kontrastmittel-enhancement, biopsiehistologisch aggressivem NZK und nicht wesentlich eingeschränkter Lebenserwartung empfohlen (Wein et al. 2016). Für die „richtige Indikationsstellung oder Praktizierung“ der AS bedarf es demnach der Berücksichtigung bestimmter Fakten im interdisziplinären Setting aus Urologen, Radiologen und Pathologen. Mit den Möglichkeiten einer bildgestützten lokalen Ablation, neben der nierenerhaltenden Chirurgie, tritt die aktive Überwachung aufgrund ihrer Limitationen zunehmend in den Hintergrund, zumal sie das Risiko der Untertherapie im noch kursiven Stadium birgt.

3.1.3.2 Operative Therapieoptionen des Nierenzellkarzinoms

Die operative Nierentumorentfernung gilt als Therapie der Wahl bzw. Goldstandard beim lokal begrenzten, nicht metastasierten NZK. Das historische Konzept der radikalen Tumornephrektomie (en-bloc-Resektion) mit Entfernung der tumortragenden Niere, der ipsilateralen Nebenniere, Gerota-Faszie, anhaftenden Peritoneum, Nierengefäße und der ipsilateralen Lymphknoten vom Diaphragma bis zur Aortenbifurkation (Robson et al. 1969) ist aufgrund fehlender, onkologischer Vorteile als Standardtherapie weitgehend verlassen worden. Als operativer Standard kommt zum einen die Tumornephrektomie (Entfernung der tumortragenden Niere) in Frage, welche einerseits offen-chirurgisch von lumbal, transperitoneal oder thorakoabdominal und andererseits laparoskopisch bzw. retroperitoneoskopisch durchgeführt werden kann (Wein et al. 2016) Zum anderen können Nierentumore organerhaltend offen chirurgisch oder laparoskopisch bzw. retroperitoneoskopisch reseziert werden (Nierentumorresektion). Die Indikationsstellung bezüglich des Zugangswegs hängt stark von der Patientenkonstitution, der Tumorlage (Tumor-Scores) und der Operationserfahrung ab. Um eine chronische Niereninsuffizienz bzw. deren Verstärkung oder Verschlechterung bis hin zur Nierenersatztherapie (Dialyse) samt einhergehender Komorbidität und Mortalität zu vermeiden, sollte stets möglichst viel gesundes Nierenparechym erhalten werden (nephron sparing surgery) (EAU 2019; MacLennan et al. 2012; Kirchberger et al. 2012; KDIGO 2012). Daher sollte – wann immer möglich – eine nierenerhaltende und -schonende Nierentumorresektion durchgeführt werden (EAU 2019; AWMF 2017). Die postoperative Nierenfunktion bei der operativen Nierentumorentfernung ist abhängig vom Grad des Kollateralschadens des angrenzenden, peritumoralen, gesunden Nierengewebes. Dieser wird durch die Ischämiezeit der Niere (hypoxischer Parenchymschaden), der Resektionsgrundversorgung (Koagulation und Kompression des Parenchyms) und den Resektionsrand (Anteil des mitresezierten Parenchyms) definiert. Die Ischämiezeit sollte so kurz wie möglich sein, wobei bei einer zu erwartenden Ischämiezeit >25 min wird eine Kühlung (kalte Ischämie) empfohlen wird. Bei einer günstigen, insbesondere peripheren Tumorlage und einer zu erwartenden geringen Blutung kann auch ohne Nierengefäßausklemmung (Zeroischämie) nierenteilreseziert werden (Klatte et al. 2015). Systematische Untersuchungen zum Parenchymschaden in Abhängigkeit von der Resektionsgrundversorgung fehlen. Weiterhin sollte maximal viel gesundes Parenchym im Rahmen der chirurgischen Tumorentfernung belassen werden („nephron-sparing surgery“) (AWMF 2017; EAU 2019). Der Anteil der Parenchymschädigung wächst exponential mit dem Grad der Nierenteilresektion und der Tumorgröße. Anzustreben sei, wenn chirurgisch möglich, der maximale Nierenparenchymerhalt durch eine Nierentumorenukleation (Präparation direkt entlang des Tumorrands bzw. der Tumorkapsel)

gegenüber einer Enukleoresektion (Resektion mit minimalem Sicherheitssaum aus gesundem Parenchym) und einer Nierenteilresektion (keilförmige Resektion des Tumors im gesunden Nierenparenchym), (siehe Abbildung 2) (Marconi et al. 2016; Serni et al. 2015). Minervini et al. beschrieben in ihrer Metanalyse 2017 aus 33 Studien mit insgesamt 11.282 Patienten keine Unterlegenheit einer Enukleation („simple enucleation“) gegenüber der Nierenteilresektion bezüglich positiver Absetzungsränder und Lokalrezidiven (Minervini et al. 2017). Insgesamt ist dies individuell abhängig vom Tumorwachstumsverhalten, der Ausprägung einer peritumoralen Pseudokapsel und dem Vorhandensein von mikroskopischen Tumorausläufern bzw. Satellitentumoren (siehe 3.1.2).

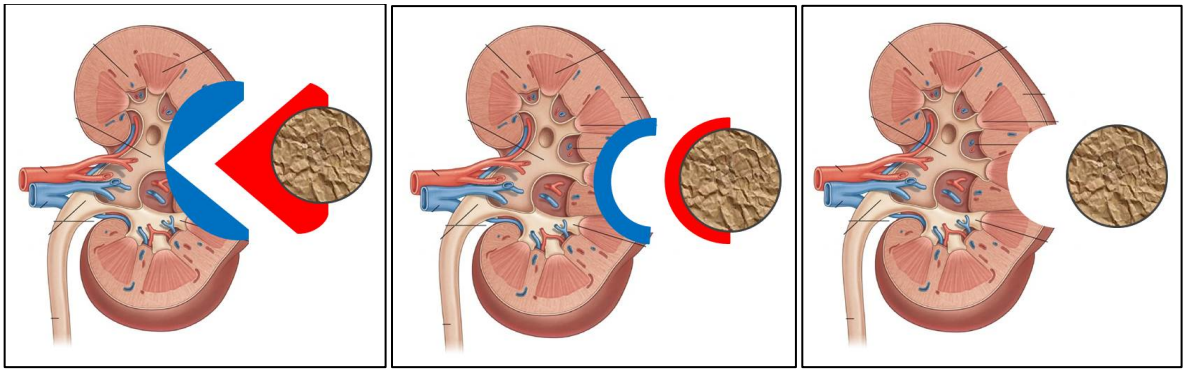

Abb.2: Operationstechniken der Nierentumorentfernung (rot = mitentferntes gesundes, peritumorales Nierenparenchym durch Resektion; blau = sekundär geschädigtes, gesundes Nierenparenchym durch blutungsstillende und adaptierende Resektionsrandversorgung). Links: Nierenteilresektion. Mittig: Enukleoresektion. Rechts: Enukleation („Ideal“) (Wendler et al. 2018c).

Die Operationsindikation muss unter Berücksichtigung der Patientenkonstitution und Tumorkonstellation gestellt werden. Bei ausgeprägter chronischer Niereninsuffizienz, anatomischen oder funktionellen Einzelnieren, multifokalem Tumorwachstum zeigt sich eine imperative Indikation zum Nierenparenchymerhalt Bei zentral gelegenen Nierentumoren besteht das Risiko eines frustranen Nierenerhalts mit notwendiger Tumornephrektomie.

Es sollte also für jeden Patienten die kritische Nutzen-Risiko-Abwägung einer kurativ intendierten Therapie mittels chirurgischer Tumorresektion oder interventioneller Ablation erfolgen. Bei dieser Betrachtung müssen auch der Grad und die Summe der Invasivität einzelner Maßnahmen diskutiert werden (Wendler et al. 2018c). Der Begriff „Minimalinvasivität“ für invasive Verfahren wird häufig nur auf den äußeren Zugang bzw. die äußere Wunde reduziert. Bezogen auf den Nierentumor, hat aber auch der innere Zugang zum Tumor und der Kollateralschaden am Nierenparenchym einen großen Einfluss auf das perioperative Komplikationsrisiko und die Lebensqualität des Patienten. Bei dieser Betrachtung kommt insbesondere dem Patientenalter und der -kondition eine prognostische Bedeutung zu, wobei der Höhepunkt der Neuerkrankungen im 7. Lebensjahrzehnt liegt. Somit handelt es sich bei der Mehrheit der Betroffenen um alte Patienten (junge alte

Menschen: 65–74 Jahre, mittlere alte Menschen: 75–84 Jahre, ältere alte Menschen: ≥85 Jahre; SIOG International Society of Geriatric Oncology-Definition (Wagener 2017; Surbone et al. 2007). Ein strukturiertes geriatrisches Assessment (Barthel-Index, Mini-Mental-State-Test, Tinetti-Test) und eine systematische Erfassung der Komorbiditäten (Charlson Comobidity Index, ASA-(American Society of Anaesthesiologists)-Score, Sarkopeniegrad, ECOG (Eastern Cooperative Oncology Group) -Status) ermöglichen eine individuelle Entscheidungsfindung und führen in etwa der Hälfte der Fälle zu einer Änderung des Therapiekonzepts (Puts at al. 2012; Wedding 2016; Charlson et al. 1987; Panella et al. 2008; Peyton et al. 2016) durch Berücksichtigung von Mobilität, Alltagskompetenz, Belastbarkeit und Lebenserwartung des Patienten. Mit dem Alter und der Morbidität des Patienten steigen sein Risiko für peri- und postoperative Komplikationen sowie das Risiko, an komorbiditätsbedingten Ursachen zu versterben. So beträgt die Komplikationsrate der Nierenteilresektion bei den unter 50-jährigen Patienten rund 30% und bei den über 80-jährigen Patienten rund 50%. Kommen relevante Komorbiditäten (Charson- Index: ≥2) hinzu, steigt die Komplikationsrate für die Nierenteilresektion und die Tumornephrektomie auf das 6-Fache gegenüber Patienten ohne relevante Nebenerkrankungen (Abouassaly et al. 2011). Bei den über 80-Jährigen kommt es in 35% der Fälle zu schweren, interventionsbedürftigen Komplikationen (Clavien-Dindo ≥III) und zu einer Mortalität von rund 3% (Berger et al. 2012). Lane et al. fanden bei 537 Patienten mit SRM mit einem durchschnittlichen Alter von 75 oder mehr Jahren keinen signifikanten Überlebensunterschied zwischen AS und den operativen Therapien Nierenteilresektion und Tumornephrektomie. Dabei verstarben 28% der Patienten (n=148) innerhalb einer medianen Nachbeobachtungszeit von rund 4 Jahren, wobei 24% auf andere Todesursachen als ein progressives, metastasiertes NZK, vorrangig kardiovaskuläre Erkrankungen, zurückzuführen waren (Lane et al. 2010). Auch Sun et al. konnten keinen Überlebensvorteil der chirurgischen Resektion kleiner NZK bezüglich der karzinomspezifischen Mortalität bei über 75-Jährigen oder bei Charlson Comorbidity Index von 2 oder mehr nachweisen (Sun et al. 2013; Sun et al. 2014).

Risikofaktoren, wie ein fortgeschrittenes Patientenalter oder eine sehr hohe kardiovaskuläre und pulmonale Komorbidität, können somit eine relative Kontraindikation zur Resektion bedeuten. In diesen Fällen können nichtoperative Ablationsverfahren (siehe 3.1.3.3) eine Therapiealternative darstellen (AWMF 2017; EAU 2019).

3.1.3.3 Ablationsverfahren beim Nierenzellkarzinom

Die allgemeine Operabilität des lokalisierten, kleinen NZK ergibt sich vorrangig noch aus der Komorbidität des Patienten, seinem Behandlungswunsch sowie aus dem perioperativen Narkoserisiko und der postoperativen Rekonvaleszenzprognose. Bei einer relativen oder absoluten Kontraindikation für eine operative Nierentumorentfernung in Allgemein-/Intubationsnarkose mit Muskelrelaxation stehen leitlinienbasiert die Radiofrequenzablation (RFA) und die Kryoablation (KA) als Tumorablationsverfahren zur Option. Vor einer geplanten ablativen Therapie ist eine histologische Diagnosesicherung einer bildgebend unklaren Nierenraumforderung cT1a eine Biopsie als zweifache koaxiale Zylinderbiopsie (18 Gauge) außerhalb der möglichen zentralen Tumornekrose notwendig (EAU 2019; AWMF 2017). Die europäisch-urologischen Leitlinie der EAU (European Association of Urology) und die deutsch-urologische Leitlinie der AWMF/ DGU (Arbeitsgemeinschaft der Wissenschaftlichen Medizinischen Fachgesellschaften / Deutsche Gesellschaft für Urologie) bieten die RFA und die KA als Behandlungsalternative zur operativen Tumorentfernung für Nierentumoren cT1a bzw. <3cm bei ausgewählten Patienten an (EAU 2019; AWMF 2017). Weiterhin diskutiert die aktuelle, deutsch-urologische Leitlinie die stereotaktisch-ablative Bestrahlung als künftige, potentielle Therapieoption (AWMF 2017; Siva et al. 2017). Andere Ablationsverfahren bzw. Therapiemethoden werden derzeit noch als experimentell bewertet (EAU 2019; AWMF 2017).

3.1.3.3.1 Etablierte, thermale Ablationsverfahren beim Nierenzellkarzinom

In den Leitlinien der deutschen, europäischen und US-amerikanischen Gesellschaften für Urologie und Radiologie werden die Radiofrequenzablation (RFA) und Kryoablation (KA) als alternative kurative Therapieoption kleiner Nierentumoren gewertet (AUA 2017; AWMF 2017; EAU 2019). Zwar existieren hierzu aufgrund ihrer längeren Anwendung die meisten Daten, jedoch liegen keine prospektiv randomisierten Studiendaten vor (Whitson et al. 2012; Wendler et al. 2018c; Wendler at al. 2016c; EAU 2019). Neben der Effektivität zur Tumorkontrolle spielt die Bewertung der Komplikationsraten und Lebensqualität eine entscheidende Rolle. Im direkten Vergleich von RFA und KA konnte keine Überlegenheit eines der beiden Verfahren bezogen aufs krankheitsspezifische, rezidivfreie und gesamte Überleben nachgewiesen werden (AUA 2017; AWMF 2017; Zhou et al. 2018; EAU 2019). Entscheidend für die Erfolgs- und Komplikationsrate ist die Lage und Größe des Nierentumors. Camacho et al. demonstrierten, dass eine RENAL-Score > 8 eine höhere Lokalrezidiv- und Komplikationsrate für RFA und KA vorhersagen kann (Camacho et al. 2015). Eine endgültige Bewertung der RFA oder KA als Therapiealternative kann bei der

aktuellen Datenlage nicht getroffen werden, so dass die Verfahren aktuell als Therapieoption bei nicht zentral gelegenen T1a-Nierentumoren für ältere Patienten mit höherer Morbidität und erhöhten operativen bzw. anästhesiologischen Risiken oder Kontraindikationen empfohlen werden (AUA 2017; AWMF 2017; EAU 2019). Aufgrund der weniger komplexen Durchführbarkeit der RFA findet die RFA gegenüber der KA eine größere Verbreitung und Anwendung. Berufspolitische Aspekte haben jedoch ebenso einen Einfluss auf die Anwendung, wobei die perkutane, bildgeführte RFA in den Händen der interventionellen Radiologie und die bisher vorrangig laparoskopische KA in den Händen der operierenden Urologen liegt.

3.1.3.3.1.1 Radiofrequenzablation des Nierenzellkarzinoms

Die Radiofrequenzablation (RFA) stellt ein hyperthermes Ablationsverfahren dar, bei dem es durch die Applikation von hochfrequentem Wechselstrom (375–480 kHz) über aktive Elektroden zum alternierenden Ionenstrom mit resultierender Reibungswärme (Joule-Effekt) über 100°C und Koagulationsnekrose im Zielgewebe kommt. Diese Friktionswärme wird radiär zur Elektrode durch das Gewebe fortgeleitet (Konduktionsprinzip). Insgesamt werden somit Temperaturen von 50–105 °C mit multipel variabler Wirkung erreicht. Im niedrigeren Temperaturbereich kommt es zur Proteindenaturierung, chromosomalen Alteration, Membranschädigung der Zellen und Zellorganellen sowie zur Schädigung des Gefäßsystems. Im höheren Temperaturbereich um ca. 100°C kommt es zur Verkochung, Vaporisation (Verdampfung) und Karbonisation (Verkohlung) des Gewebes (Duffey et al. 2010). Als Elektroden werden monopolare oder bipolare Elektroden, kompakte Einzel-, Cluster- oder vorrangig expandierbare Schirmelektroden unterschiedlicher Größen verwendet. Die Sondenart, Applikationszeit (ca. 10–12 min) und Temperaturhöhe beeinflusst dabei die Größe und Homogenität der Ablationszone (2–7 cm). Ein Sicherheitssaum von 5–10 mm wird empfohlen.

Die RFA ist bei zentral gelegenen NZK wegen der Nähe zum Nierenhilus und Nierenbeckenkelchsystems (NBKS) neben den möglichen Perforationsrisiken wegen des Hitzeabtransports durch Blut- und Harnfluss (konvektionsbedingter „heat sink effect“) nur eingeschränkt anwendbar. Zur Reduzierung des Heat-sink-Effekts durch arterielle Nierengefäße kann die vorherige transarterielle Embolisation des Ziel- und Grenzgewebes eingesetzt werden.

Zur Behandlung von Nierentumoren wurde die RFA erstmals 1997 eingesetzt (Zlotta et al. 1997). Bisherige Anwendungsversuche an der Niere schlossen offen-chirurgische, perkutane und laparoskopische Verfahren ein. Die perkutane RFA ist die am häufigsten angewendete energieablative Methode zur alternativen Behandlung des NZK, da sie technisch sehr

einfach und mit relativ geringem zeitlichen (10–20 min Ablationsdauer) und apparativen Aufwand durchgeführt werden kann. Aufgrund der sehr guten Platzierungsmöglichkeit der RFA-Applikatoren unter Fluoroskopie (CT oder MRT) und Effektivität wurde und wird die RFA vorrangig perkutan in Analgosedierung angewandt. Für die hypertherme, möglichst vollständige Gewebezerstörung sind etwa Temperaturen von ca. 80°C über 8–10 min notwendig. Die starke Inhomogenität und Vaskularisation von Nierentumoren führt durch den oben genannten Heat-sink-Effekt und durch entsprechende Impedanzsprünge häufig zur inkompletten Ablation (Skipping-Läsionen), (Rendon et al. 2002; Klingler et al. 2007). Die primäre Erfolgsrate der RFA bei SRM liegt zwischen 90–100 % in Abhängigkeit von der Tumorgröße und -lage, wobei die Rate technisch bedingt bei SRM < 3 cm und kortikalperipherer Lokalisation höher ist (Varkarakis et al. 2005; Clark et al. 2006; Breen et al. 2007; Ferakis et al. 2010; Zagoria et al. 2011). Diverse Studien beschrieben eine Lokalrezidivrate für pT1a-NZK zwischen 2 und 12 % in den ersten 5 Jahren nach RFA (Breen et al. 2007; Kunkle et al. 2008; Wah et al. 2014; Olweny et al. 2012; Psutka et al. 2013; Kroeger et al. 2014). Darüber hinaus ermöglicht die RFA eine Wiederholung, wobei deren Sekundärerfolgsrate auf nahezu 100% steigt (Tracy et al. 2010). Die Metastasierungsraten nach RFA sind vergleichbar mit Active-Surveillance-Daten (metastasenfreie und erkrankungsspezifische Überlebensraten von 95–99 %) (Jewett et al. 2011; Ferakis et al. 2010; Zagoria et al. 2011; Tracy et al. 2010; Georgiades at al. 2013). Komplikationen nach renaler RFA treten meist leichtgradig zwischen 0–19 % auf (AWMF 2017; Varkarakis et al. 2005; Ferakis et al. 2010; Zagoria et al. 2011; Wah et al. 2014; Gervais et al. 2005). Insbesondere von einer renalen RFA im Kontakt zum NBKS oder Harnleiter wird wegen der Perforations-, Fistel- und Strikturgefahr abgeraten (AWMF 2017; EAU 2019; Wah et al. 2014). Insgesamt zeigen sich bei der RFA vergleichbare Ergebnisse zur Nierenteilresektion unter Vorbehalt fehlender randomisierter Studien (AWMF 2017; EAU 2019; Olweny et al. 2012; Takaki et al. 2010; Hoffmann et al. 2010). Mit ausstehenden Langzeitdaten ist eine Indikationsausweitung und breitere Anwendung der RFA zur Therapie von T1a-NZK zu erwarten – nicht zuletzt bei imperativem Nierenfunktionserhalt bei Einzelnieren und Nephron-sparender Ablation (Hoffmann et al. 2010).

3.1.3.3.1.2 Kryoablation des Nierenzellkarzinoms

Die Kryoablation (KA) stellt das einzige hypotherme Ablationsverfahren dar. Über eine eingeführte Kältesonde kommt es durch 2–3 zyklische aktive Einfrier- (−60°C bis −70°C) und passive Auftauphasen (>10°C/min) mit konsekutiver Zelldehydrierung, mechanischer Zerreißung durch Eiskristallbildung und minderperfusionsbedingter Ischämie schließlich zur Koagulationsnekrose im Zielgewebe (Bischoff et al. 1999). Die Thermoregulation erfolgt über

gasdurchströmte Kryosonden mit thermoisoliertem Schaft und nichtisolierter Spitze per Joule-Thomson-Effekt (dichte- und druckabhängige Temperaturveränderung), wobei Argongas (−180 °C) zur Kühlung und Heliumgas zur Erwärmung genutzt wird (Berger et al. 2009). Je nach Tumorgröße werden 3–5 Kryonadeln und 2 Thermonadeln bildgeführt platziert. Ein Sicherheitssaum von 5–10 mm wird empfohlen. Die starke Inhomogenität und Vaskularisation von Nierentumoren führt durch den oben genannten Cold-sink-Effekt und durch entsprechende Impedanzsprünge häufig zur inkompletten Ablation (Skipping-Läsionen) (Camacho et al. 2015; Berger et al. 2009). Zur Reduzierung des Cold-sink-Effekts kann die vorherige, transarterielle Embolisation des Ziel- und Grenzgewebes eingesetzt werden (Duffey et al. 2010). Die KA bietet im Gegensatz zu hyperthermalen Ablationstechniken keinen ausreichend hämostyptischen Effekt mit entsprechend erhöhtem Blutungsrisiko (Berger et al. 2009).

Die KA ist bei zentral gelegenen NZK wegen der Nähe zum Nierenhilus und NBKS neben den möglichen Perforations- und Thrombembolierisiken wegen der Erwärmung durch den Blut- und Harnfluss (konvektionsbedingter „cold sink effect“) nur eingeschränkt anwendbar.

Die KA wurde als älteste thermale Ablationstechnik erstmal 1995 zur Behandlung von Nierentumoren eingesetzt (Uchida at al. 1995). Bisherige Anwendungsversuche der renalen KA schlossen offen-chirurgisch, perkutane, laparoskopische, transluminale und endoskopische Verfahren ein. Zwar erreicht die perkutane Anwendung bei günstiger Tumorlage akzeptable Ergebnisse, jedoch stellt die laparoskopische Anwendung in Allgemeinnarkose die gängigste und sicherste Technik aufgrund der endoskopischen und endosonographischen Kontrollmöglichkeit der KA-Applikation (Eisball) und größeren Blutungskontrolle dar (EAU 2019; Jiang et al. 2017). Statistisch signifikante Unterschiede in der Komplikationsrate zwischen der perkutanen und laparoskopischen KA konnten Jiang et al. nicht festgestellen (Jiang et al. 2017). Hierfür muss zuvor die Niere wie bei einer standardisierten laparoskopischen Nierenteilresektion vom anlagernden Fett operativ befreit werden. Nach der KA wird der Eisball für 5–10 min mechanisch komprimiert und für weitere 5–10 min unter einem reduzierten intraabdominellen Gasdruck kontrolliert. Die Hämostase kann durch Applikation von Hämostyptika oder Klebstoffen, sowie bei persistierenden Blutungen auch mittels Umstechung versorgt werden (Bischoff et al. 1999; Gill et al. 2003).

Die primäre Erfolgsrate der KA bei SRM liegt zwischen 90–100 % in Abhängigkeit von der Tumorgröße und -lage, wobei die Rate technisch bedingt bei SRM <3cm und kortikalperipherer Lokalisation höher ist (Atwell et al. 2008; Georgiades et al. 2008). Diverse Studien beschrieben in den ersten 5 Jahren nach KA eine Lokalrezidivrate für pT1a-NZK zwischen 3 und 17 % (Pirasteh et al. 2011; Atwell et al. 2013; Gill et al. 2005; Aron et al. 2010; Finley et al. 2008; Klatte et al. 2011; Strom et al. 2011). Die Metastasierungsraten nach KA entsprechen Active-Surveillance-Daten (metastasenfreie und erkrankungs-

spezifische Überlebensraten von 93–98 %) (EAU 2019; AWMF 2017; Gill et al. 2005, Haber et al. 2012; Jiang et al. 2017). Das perioperative Outcome der laparoskopischen KA ist vergleichbar zur laparoskopischen Nierenteilresketion (EAU 2019; Gill et al. 2003; Klatte et al. 2011; Haber et al. 2012; Desai et al. 2005; Jiang et al. 2017). Komplikationen nach renaler KA treten meist leichtgradig zwischen 2–19 % auf (AWMF 2017; Klatte et al. 2011; Haber et al. 2012; Jiang et al 2017). Von einer renalen KA im Kontakt zum NBKS oder Harnleiter wird wegen der Perforations-, Fistel- und Strikturgefahr abgeraten (EAU 2019; AWMF 2017; Gill et al. 2005; Jiang et al. 2017). Aufgrund des höhren apparativen und kostenintensiveren Aufwands wird diese Technik eher wenigen Zentren vorbehalten bleiben.

3.1.3.3.2 Alternative nonthermale Ablationsverfahren beim Nierenzellkarzinom

Thermale Ablationsverfahren, wie der Radiofrequenz- und Kryoablation, sind verfahrensbedingt limitiert einsetzbar. Einerseits wird die Hitzewirkung hyperthermaler Ablationsverfahren durch die kühlende Durchblutung (heat sink effect) (Lu et al. 2002), andererseits die Kältewirkung hypothermaler Techniken durch die erwärmende Durchblutung (cold sink effect) (Ladd et al. 1999) reduziert. Somit ist das Risiko einer imkompletten Ablation im Zielgewebe mit einer eigenen ausgeprägten Vaskularisation oder in Angrenzung zu größeren Gefäßen, wie zum Beispiel bei Nierentumoren, erhöht (Johnson et al. 2018; Farrag et al. 2017). Weiterhin ist aufgrund des zentrifugalen Temperaturabfalls und dem damit notwendigen, peritumoralen Sicherheitssaum keine scharfe Begrenzung auf das Tumorgewebe möglich. Damit ist die Aussparung und Schonung von angrenzenden, vulnerablen Strukturen erschwert bzw. nicht möglich. Bei Nierentumoren stellen das Nierenbeckenkelchsystem, der Harnleiter und die nierenversorgenden Blutgefäße für den Nierenfunktionserhalt essentielle Strukturen dar. Bei thermoablativen Techniken ergeben sich bei Involvierung dieser Leitstrukturen Komplikationen durch Nierenbecken- und Harnleiterfisteln mit Urinextravasation (Urinombildung), Harnleiter- und Nierenkelchhals-strikturen mit Harnstauung und konsekutiver Nierenparenchymschädigung, sowie Perfusionsstörungen mit Ischämie des Nierenparenchyms. Folglich ergeben sich Tumorgrößen- und Tumorlagelimitierungen für ablative Maßnahmen (Tacke 2007). Andere thermale Ablationsverfahren, wie der hochintensive fokussierte Ultraschall (HIFU) und die Mikrowellenablation (MWA), sind derzeit noch als experimentell zu bewerten, bieten aktuell keine Vorteile gegenüber der RFA oder KA und sind technisch derzeit aufwendiger (Klingler et al. 2008; Ritchie et al. 2011; Moreland et al. 2014; Carrafiello et al. 2013).

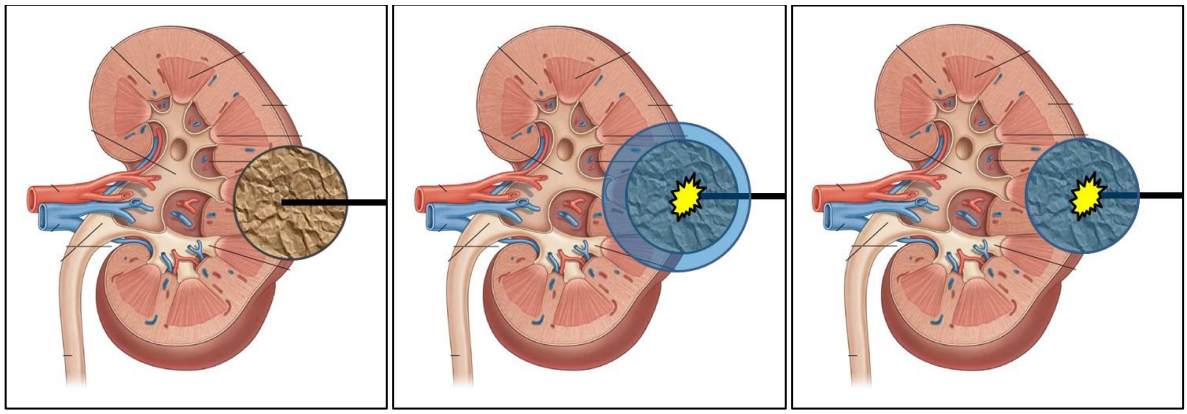

Abb.3: Links: Schema einer in den kortikalen Nierentumor eingeführter Ablationselektrode. Mittig: Schema einer Nierentumorablation mit Sicherheitssaum und Schädigung des peritumoralen gesunden Nierenparenchyms. Rechts: Schema einer Nierentumorablation ohne Sicherheitssaum und ohne Schädigung des peritumoralen gesunden Nierenparenchyms („Ideal“) (Wendler et al. 2018c).

Aufgrund der o.g. Limitationen thermoablativer Techniken sind nonthermale Tumortherapie-verfahren interessant, welche derzeit in Studien untersucht werden. Insbesondere beim multifokalen, asymmetrisch wachsenden oder zentralen Nierenzellkarzinom könnten nonthermoablative Verfahren einen Vorteil aufweisen.

3.1.3.3.2.1 Perkutane Strahlentherapie des Nierenzellkarzinoms

Die primäre, perkutane, konventionelle, fokale Strahlentherapie des lokal begrenzten NZK galt historisch als unwirksam und unbrauchbar. Grundlage dafür ist die relativ hohe „Strahlenunempfindlichkeit“ des NZK und die durch mangelnde technische Aussparungsmöglichkeit bedingte, hohe Nebenwirkungsrate der strahlensensiblen, perirenalen Risikoorgane (radiogene Enteritis und Harnleiterstriktur). Neuere radiotherapeutische Techniken ermöglichen als stereotaktische ablative Radiotherapie („sterotactic ablative body radiotherapy“, SABR) eine präzise, fokale, hypofraktionierte Bestrahlung („Radiochirurgie“) über eine oder wenige Fraktionen (24–42 Gy über 1–5 Fraktionen à 4–25 Gy Einzeldosen) (Siva et al. 2012; Zondervan et al. 2019). Dies ermöglicht eine Bandbreite an Techniken (robotergestützte Linearbeschleuniger, moderne Immobilisationsmaßnahmen, neue softwarebasierte Bestrahlungsgeometrie und -algorithmen, 3D/4D-CT-Simulation, Atmungstriggerung, Bestrahlungsmarker, Cone-Beam, intensitätsmodulierte Radiotherapie IMRT etc.).

Im Kontrast zur konventionellen Strahlentherapie, die über eine DNA-Schädigung zur Apoptose führt, wirkt die SABR auf verschiedene strukturelle und signaltransduktorische Bereiche der Zelle mit konsekutiv letaler, nonthermaler Zellschädigung. Campbell et al. fassten die Ergebnisse der SABR von lokal begrenzten Nierenzellkarzinomen von 138 Patienten respektive 166 T1a- bis T1b-Tumoren aus 14 Studien von 2003–2015 zusammen (Campbell et al. 2015). Für eine einheitliche Beurteilung ist hierbei die

Heterogenität der Behandlungsschemata, Tumordaten und Bewertungskriterien zur Lokalkontrolle limitierend. Siva et al. untersuchten 223 Patienten mit einer SABR (118 single-fraktioniert und 105 multi-farktioniert), wobei sich eine lokale Kontrolle von 97,8 % nach 4 Jahren bei einer geringen Toxizität (35,6% G1-2 und 1,3% G3-4) zeigte (Siva et al. 2018). Die Autorengruppe schließt auf eine mögliche künftige Therapieoption des lokalen NZK mittels primärer SABR (Siva et al. 2017; Siva et al. 2018; Correa et al. 2019).

3.1.3.3.2.2 Brachytherapie des Nierenzellkarzinoms

Bei der Brachytherapie (BT) werden im Zielgewebe sehr hohe Strahlendosen über temporär eingebrachte Strahlenquellen erreicht. Durch den typischen steilen Dosisabfall kann eine hohe unerwünschte Strahlenexposition des Umgebungsgewebes bzw. der benachbarten Risikoorgane vermieden werden. Beim bildgeführten Afterloading werden sekundär zu beladende, d. h. zunächst inaktive Applikatoren im Tumor (interstitielle Brachytherapie) unter CT- oder MR-Fluoroskopie platziert und dann sekundär durch das Nachladegerät mit der divergenten Strahlenquelle beladen. Ein exakter Bestrahlungsplan (Dosisverteilung) wird durch die räumlich individuelle Lage und Verweildauer der Applikatoren kalkuliert.
Die High-dose-rate-Brachytherapie (HDR-BT) zeichnet sich durch eine kontinuierliche Hochdosisleistung (HDR > 12 Gy/h) aus, wobei aktuell vorzugsweise 192-Iridium als βstrahlendes Isotop verwendet wird. Dies führt über die Wirkung auf verschiedene strukturelle und signaltransduktorische Bereiche der Zelle zu einer letalen, nonthermalen Zellschädigung. Nach Positionierung der Brachytherapiekatheter in Seldinger-Technik und in intravenöser Analgosedierung eingebrachte fixierte Schleusen (z. B. Angiographie-schleusen) wird eine kontrastmittelgestützte Planungs-CT oder -MRT (Atemanhaltetechnik, Schichtdicke ≤5 mm) zur Determinierung der exakten Lage in Beziehung zur Tumorausdehnung (Koordinaten x, y, z) akquiriert. Die Bestrahlungszeit von etwa 20–90 min ist von der Größe des zu therapierenden Tumorvolumens (GTV) abhängig, wobei idealerweise 100 % (D100) des Zielvolumens (GTV + Sicherheitssaum von wenigen Millimetern) von der avisierten Dosis erfasst werden sollten. Gegebenenfalls werden in einer zweiten Sitzung unterexponierte Tumoranteile erneut behandelt.
Mit dieser Technik können irregulär geformte Tumoren ohne Größenlimitation und unabhängig von der respiratorischen Bewegung behandelt werden. Klinische Daten zur Behandlung des lokal begrenzten NZK mittels perkutaner HDR-BT wurden bisher nicht publiziert. In einer prospektiven Phase-I- bis -II-Studie wird derzeit die Bestrahlung von NZK und die Toleranzdosis des nichttumorösen Nierenparenchyms untersucht (Klinik für Radiologie und Nuklearmedizin der Universität Magdeburg, Deutschland) (Bretschneider et al. 2012). Die noch unveröffentlichten Zwischenergebnisse (30 von 50 Patienten) zeigen

eine gute Steuerbarkeit und ein gutes Ansprechen von Nierenkarzinomen (nicht publizierte Daten EMMA-1- und EMMA-2-Studie Magdeburg – *under review*: Damm, Pech, Ricke et al. 2019).

3.1.3.3.2.3 Irreversible Elektroporation des Nierenzellkarzinoms

Die Irreversible Elektroporation (IRE) weist ein hohes Potential in der perkutanen, nonthermalen Ablation des lokal begrenzten Nierenzellkarzinoms auf. Gegenüber der Brachytherapie (Afterloading) und der Stereotaktisch-ablativen Radiatio (SABR) bietet die IRE als strahlenexpositionsfreies Gewebeablationsverfahren einen möglichen Vorteil. Aktuell gilt Anwendung der IRE als experimentell und sollte nur im Rahmen von Studien zur weiteren Evaluation durchgeführt werden. Die bisherige Entwicklung und der gegenwärtige Anwendungsstand der Technik beim NZK soll im Rahmen der eigenen Arbeiten erläutert und diskutiert werden (siehe 3.2 bis 6.)

3.2 Irreversible Elektroporation

3.2.1 Entwicklung der Irreversiblen Elektroporation zum Ablationsverfahren

Mit der Erfindung des elektrostatischen Generators machte Otto von Guericke aus Magdeburg den elektrischen Strom nutzbar und schaffte damit quasi die Basis für erste Untersuchungen von Strom auf lebendes Gewebe und den menschlichen Körper (Guericke 1672). Hautrötungen nach Applikation von Funken und Lichtbögen, sowie direkten Stromeinwirkungen wurde bis zum 18. Jahrhundert noch als Wärmeeffekt interpretiert, welche jedoch rückwirkend betrachtet auf dem Phänomen der Elektroporation basierten. 1802 beobachtete Ritter mit tetanischen Muskelkontraktionen nach Starkstromimpulsen indirekt das Elektroporationsprinzip als Modulation des elektrischen Spannungsgradienten und den elektrischen Zusammenbruch der vitalen Zellmembran (Hodkin 1951). Fuller entdeckte 1898 als erster die zytotoxische, nonthermale Wirkung von Hochspannungs-stromentladungen auf Bakterien in Wasserproben (Fuller 1898), woraus sich letztlich die „Elektroplasmolyse“ als Sterilisationsverfahren in der heutigen Lebensmittelindustrie entwickelte (Doevenspeck 1961; Schilling et al. 2008; Toepfl et al. 2006). Anfang des 20. Jahrhunderts wurden die Hämolyse durch kurze Starkstromimpulse und gewebeschädigende Effekte durch Lichtbögen und Blitze auf den menschlichen Körper beschrieben (Rockwell 1903; Jex-Bake 1913). 1925 fand Fricke heraus, dass sich die Zellmembran wie eine dielektrische Schicht verhält, welche im starken elektrischen Feld zusammenbricht (Fricke 1925). Elf Jahre später wurde der mögliche Nutzen von hochfrequenten elektrischen Feldern zur nonthermalen, minimalinvasiven Gewebeablation postuliert (McKinley 1936). Stämpfli konnte 1957 den reversiblen und irreversiblen elektrischen Zusammenbruch des membranösen Potentials, der wie ein Kondensator funktionierenden Doppellipidmembran, aufzeigen (Stämpfli 1957). 1967 gelang der Nachweis, dass ultrakurze, starke elektrische Impulse im Mikrosekundenbereich mit langen Intervallen im Sekundenbereich einen irreversiblen Semipermeabilitätverlust der Zellmembran durch einen zytotoxisch wirkenden Ionenstrom bewirken (Sale et Hamilton 1967). Die Idee der Gewebeablation durch eine elektrisch induzierte Zytolyse fand jedoch zunächst keine medizinisch-wissenschaftliche Anwendung. Stattdessen richtete sich in den 1970er bis 1990er Jahren der Fokus auf die reversible Zellmembranveränderung durch elektrische Impulse als „reversible Elektro-poration“. Zimmermann erreichte erstmals durch die „reversible Elektroporation“ eine Zellfusion („Elektrofusion“) (Zimmermann 1982). 1997 beschrieben Kinesota und Tsong die nicht-thermische, elektrische Erzeugung von wenigen Nanometer großen Membranporen (Kinosita et Tsong 1977). Dies führte zur noch heute angewandten Idee der intrazellulären Einschleusung von zytotoxischen Chemotherapeutika als Krebstherapie, als sog.

„Elektrochemotherapie“ (Mir et al. 1991). Der eigentliche Begriff der „Elektroporation“ nach einem erfolgreichen transmembranösen intrazellulärer Gentransfer wurde jedoch erst 1982 durch Neumann geprägt (Neumann et al. 1982), womit das Verfahren eine zentrale Rolle in der in der heutigen Mikrobiologie und Biotechnologie erlangte.

In den 1990er Jahren griffen Lee und Piñero den Gedanken zur medizinischen Nutzung der „irreversible Elektroporation“ (IRE) induzierten Apoptose als alternatives Tumorgewebe-ablationsverfahren wieder auf (Bhatt et al. 1990; Piñero et al. 1997). Yao et al. konnten 2004 die nonthermale Gewebeablationsfähigkeit der IRE erstmal physikalisch nachweisen (Yao et al. 2004). Im gleichen Jahr ließen Rubinsky und Davalos die nonthermale IRE als Weichgewebeablationsverfahren patentieren und beschrieben damit deren spezielle Eigenschaften (Davalos et Rubinsky 2004; Davalos et Rubinsky 2007; Davalos et al. 2005). Patentinhaber war das von der Forschungsgruppe gegründete Biotechnologie-Unternehmen Oncobionic Inc. ® (CA, U.S.A.).

Schließlich publizierten Miller et al. 2005 die erste IRE von Leberkarzinomzellen in-vitro (Miller et al. 2005). Edd et al. beschrieben 2006 das tumorselektive Potential der nonthermalen IRE von in-vivo-Leberparenchym mit Ausbildung einer scharf begrenzten Ablationszone (Nekrose) mit Erhalt der azellulären Gewebematrix und von darin gelegenen, größeren funktionellen Strukturen wie Blutgefäßen und Gallengängen (Edd et al. 2006). Es folgten experimentelle Versuche an verschiedenen Geweben.

Im Verlauf wurden die Rechte und der Vertrieb des IRE-Verfahrens, sowie der hierfür entwickelten Medizinprodukte durch die Firma AngioDynamics® zur weiteren Entwicklung und Vermarktung übernommen. 2007 erhielt die Firma AngioDynamics Inc. (NY, U.S.A.) die Zulassung der zuständigen US-amerikanischen Behörde FDA für ihr Medizinprodukt „NanoKnife®“ zur Ablation von Weichgewebe (510k). 2008 folgte dafür die CE-Kennzeichnung (CE 0050 und CE 0051) für Medizinprodukte (nach 93/42/EWG) mit kommerzieller Anwendungszulassung durch die Europäische Kommission. 2008/2009 wurden weltweit Applikationssysteme durch die Firma AngioDynamics® für experimentelle und klinische Studien einzelnen Zentren zur Verfügung gestellt.

Durch das Institut für Medizinische Dokumentation und Information (DIMDI) des Deutschen Bundesministeriums für Gesundheit (BMG) erfolgte 2015 die Bekanntgabe von OPS-Kodes (Operationen- und Prozedurenschlüssel) für die IRE mittels NanoKnife® auf Beantragung durch den Hersteller AngioDynamics Inc. für die IRE an Gallengängen, Knochen, Leber, Lunge, Magen, Nebennieren, Nieren, Ösophagus, Prostata, Pankreas und Rektum wurden eingeführt. Ausreichende Prüfdaten für eine Anwendungsempfehlung lagen bis dato nicht vor (Wendler et al. 2015a).

3.2.2 Eigenschaften der Irreversiblen Elektroporation

Die irreversible Elektroporation (IRE) ist ein neues minimal-invasives, nonthermal wirkendes Gewebeablationsverfahren. Durch die lokale Applikation von repetitiven (90-100 pro Elektrodenpaar) ultrakurzen, rektangulären Starkstromimpulsen mit 2000–3000 V und 30–50 A im Mikrosekundenbereich (Pulsdauer 70-100 µs in Pulsintervallen von 1-0,25 sec) über in das Zielgewebe eingebrachte nadelförmige Elektroden wird eine kritische, elektrisch induzierte Störung des dipolelektrischen Zellmembranpotenzials verursacht (Rubinsky 2010). Dies führt zu einem elektrischen Zusammenbruch der Zellmembran mit konsekutiv irreversibler Bildung von etwa 100 Nanomembranporen („irreversible Elektroporation“) pro Zelle mit einer Größe von 80-490 nm (Lee et al. 2012; Kinesota et al. 1992).
Die Poren verursachen eine permanente Erhöhung der Zellmembranpermeabilität und führen damit zum unkontrollierten Ioneneinstrom und Verlust von Makromolekülen. Die folgliche Störung der Zellhomöostase mündet in einer Apoptose durch Zytolyse im Zielgewebe innerhalb von 1–7 Tagen (Rubinsky 2010).

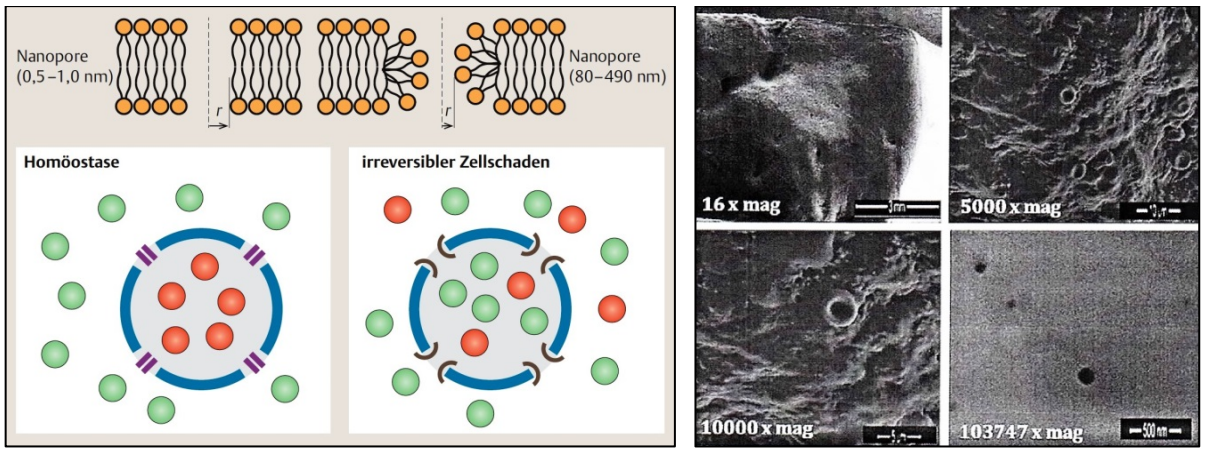

Abb.4: Links: Induktion und Entstehungsprinzip von irreversiblen Nanoporen in der Zellmembran durch die irreversible Elektroporation (Jürgens et al. 2016). Rechts: Erster kryoelektronen-mikroskopischer Nachweis von Nanoporen durch Irreversible Elektroporation (Hepatozyten-zellmembran), (Lee et al. 2012).

Damit wirkt die IRE nur auf vitale Zellen. Durch den nonthermoablativen Charakter bleibt die Matrix (Bindegewebsstroma) erhalten. Aufgrund der postulierten Alles-oder-Nichts-Reaktion ab einem „kritischen“ induzierten Transmembranpotenzial (ca. 1000V/cm) soll das Ablationsareal eine sehr kleine Transitionszone (<1mm) und damit scharfe Begrenzung zum Umgebungsgewebe aufweisen. Unterhalb des „kritischen“ Transmembranpotentials kommt es zu reversiblen Elektoporation oder zu keiner zytotoxischen Reaktion mit Zellerhalt. (Rubinsky 2010).

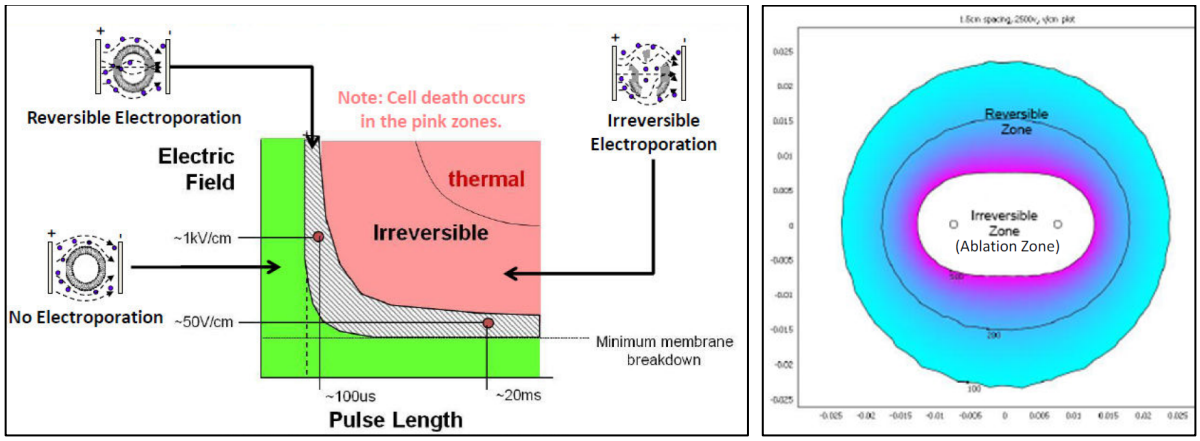

Abb.5: Links: Schematische Beziehung zwischen elektrischer Feldstärke und Pulslänge zur irreversiblen Elektroporation in Abgrenzung zur reversiblen Elektroporation und Thermoablation (Radiofrequenzablation). Rechts: Schematische Darstellung der ellipsoiden IRE-Ablationszone um zwei monopolare IRE-Elektroden sowie der konzentrischen umgebenden reversible Elektroporations-zone, (Manual 2011).

Aufgrund der postulierten nonthermalen Ablationswirkung der IRE sollen vaskularisations-bedingte Kühleffekte („heat-sink-effect“ wie bei der Radiofrequenzablation, RFA) keine Rolle spielen. Die Größe des gesamten Ablationsareals ist von der verwendeten Elektroden-anzahl und -konfiguration abhängig.

Für die IRE wird eine gewisse Gewebeselektivität postuliert, wobei unter Erhalt der extrazellulären Matrix größere Gewebestrukturen und anatomische Grenzstrukturen innerhalb des Zielvolumens oder im Randbereich geschont werden, denen ein matrixbasiertes Grundgerüst zugrunde liegt (Davalos et al. 2005; Rubinsky 2010). So wurde in den ersten experimentellen Untersuchungen demonstriert, dass Blutgefäße, intrahepatische Gallengänge trotz umgebender Parenchymablation erhalten bleiben (Rubinsky 2010). Aus diesen publizierten Eigenschaften wurde ein scheinbarer klinischer Vorteil der IRE gegenüber anderen Ablationsmethoden (insbesondere gegenüber Thermoablationstechniken) postuliert (Davalos et al. 2005; Rubinsky 2010). Unter-schiedliche elektrische Eigenschaften verschiedener Zielgewebe lassen jedoch eine unterschiedliche Wirkung vermuten (Golberg et al. 2015). Darüber hinaus gibt es bislang keine systematische Evaluation der spezifisch elektrischen Konduktivität in verschiedenen Tumorgeweben.

3.2.3 NanoKnife-Ablationssystem zur Irreversiblen Elektroporation

Das NanoKnife-System (HPV01) ist eine Medizinprodukt zur Applikation von Starkstromimpulsen über temporär in den Körper eingebrachte nadelförmige Elektroden (Risiko-Geräteklassifikation IIb nach FDA und nach EEC 93/42). Aktuell ist das NanoKnife-System der Firma Angiodynamics (AngioDynamics Inc., Queensbury, NY, USA) weltweit das einzige kommerziell erhältliche System zur klinischen Anwendung der irreversiblen

Elektroporation. Es besteht im Wesentlichen aus zwei Komponenten: dem NanoKnife-Generator („IRE-Generator“) und den NanoKnife-Elektroden („IRE-Elektroden“).
Der IRE-Generator ist als mobiles Rollwagengerät (56 cm + 68 cm x 15 cm, 66 kg) konzipiert, der sich aus einem Korpus mit integriertem Generator und Kondensator sowie aus einem Bedienpult (Tastatureinheit, Computer, 15“ LCD-Monitor) (Abb.6).

Abb.6: Links: IRE-Generator des NanoKnife-Systems der Firma AngioDynamics Inc.. Im vorderen, oberen Teil des Korpus befinden sich die 6 möglichen Steckplätze für die IRE-Elektroden des NanoKnife-Systems. Rechts oben: EKG-Synchronisationsgerät Accu-Sync 72. Rechts unten: Fußschalter zum Generatorstart (Kondensatorladung und Pulsapplikationsstart) des NanoKnife-Systems, (Manual 2011).

Für die IRE-Elektroden befinden sich 6 Steckplätze am IRE-Generatorkorpus. Die IRE-Pulsapplikation kann EKG-getriggert und in festen Intervallen 90 bpm oder 240 bpm erfolgen. Üblicherweise erfolgt die IRE-Pulsapplikation EKG-getriggert in der refraktären Phase des Myokards im Moment der vollständigen Depolarisation des Kammermyokards (Systole), um keine Herzrhythmusstörungen zu induzieren. Vor allem bei der IRE-Applikation in Herznähe ist die EKG-Synchronisation notwendig. Zur EKG-Triggerung wird ein digitales externes EKG-Synchronisationsgerät AccuSync® 72 (Medical Research Corporation®, Milford, CT U.S.A.) im 3-Kanal- oder 5-Kanal-Modus mit Echtzeitmonitoring konnektiert. Weiterhin kann ein IRE-Generator per Fußschalter zur Kondensatorladung und Einleitung der automatischen IRE-Pulsapplikation verwendet werden. Der Generator samt Fußschalter und EKG-Synchronisationsgerät befinden sich im unsterilen Arbeitsbereich. Die IRE-Elektroden sind als nadelförmige Einmalelektroden steril verpackt (Werksterilisation mit

Ethylenoxid) und werden nach Platzierung im Zielgewebe über ein fest fixiertes Kabel mit dem Generator verbunden.

Für die IRE mittels NanoKnife-System stehen bipolare und monopolare Elektroden zur Verfügung. Die Elektroden übertragen die Impulsenergie als Gleichstrom vom Generator des NanoKnife-Systems ins Zielgewebe.

Variablen	**Bipolare Elektrode**	**Monopolare Elektrode**
Elektrodenlänge	150 mm (300 mm)	150 mm (300 mm)
Elektrodendurchmesser	1,67mm	1,2 mm
Elektrodenform	zylindrisch	zylindrisch
Spitze distaler Pol	Pyramidenschliff	Pyramidenschliff
Elektrodenpole	2	1
Pollänge	7mm je Pol; Polabstand 7mm	regulier-/adaptierbar (5-40mm)
Steckplätze Generator	2	1
Zeitgleiche Anwendung	1	2-6 (davon 1 Aktivatorelektrode)
Maximale Spannung	3000 V	3000 V
Maximale Stromstärke	50 A	50 A
Ablationsareal	30 x 15 x 15 mm	variabel, abhängig von Elektrodenzahl und -anordnung
Ablationsvolumen	3,5 ccm	variabel, max. 60 ccm
Ablationsareal	rotationssymmetrisches gestrecktes Ellipsoid	variabel, ellipsoid-förmig

Tab.1: Technische Spezifikationen der bipolaren und monopolaren IRE-Elektroden des NanoKnife-Systems.

Die bipolare Elektrode wird singulär angewendet. Sie besteht an der Spitze aus voneinander elektrisch isolierten, freiliegenden Polen. Die Elektrodenspitze sollte so platziert werden, dass das Zentrum des Zielgewebes zwischen den beiden Polen liegt. Die bipolare Elektrode wurde weitestgehend für die klinische Anwendung aufgrund ihrer Limitationen vom Markt genommen. Gängiger für die individuelle Anwendung sind die monopolaren Elektroden (Abb.7). Die monopolaren Elektroden werden zeitgleich in Kombination von 2-6 verwendet.

Eine Elektrode fungiert systembedingt als Aktivator-Elektrode (blau) für die Prozedurerkennnung (Abb.7). Die Pollänge ist von 0mm bis 40mm in 5mm-Schritten regulierbar (Abb.8). Die Elektrodenspitzen sollten dabei möglichst parallel platziert werden und das Zielgewebe einschließen, da sonst eine unvollständige Ablation resultiert (Abb.7). Jede monopolare Elektrode bildet funktionell einen elektrischen Pol. Die monopolaren Elektroden werden je nach Programmierung nacheinander paarweise vom Generator elektrisch angesteuert. Der ideale Elektrodenabstand liegt zwischen 11mm und 23mm, um „Kurzschlüsse“ (high current) oder Aussparungen (skipping leasons) zu vermeiden (Wendler et al. 2016a).

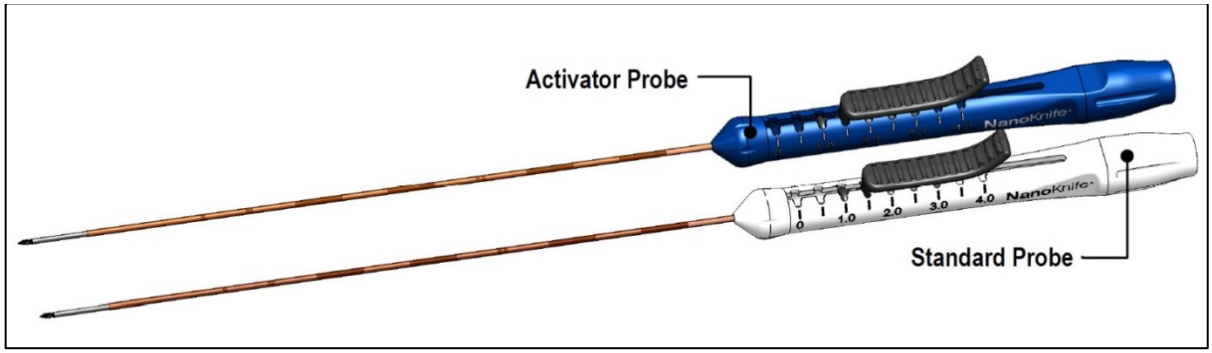

Abb.7: Monopolares Elektrodenpaar mit Aktivatorelektrode (blau) und Zusatzelektrode (weiß). Parallele Elektrodenausrichtung mit gleicher Länge der aktiven Elektrodenspitze, (Manual 2011)

Abb.8: Monopolare Elektrode mit Einstellmechanismus (Schieberegler) für die Länge der aktiven Elektrodenspitze.

Die Ablationsplanung erfolgt über die integrierte Gerätesoftware (Microsoft™ Windows®) des NanoKnife-Systems. Die anwendungsspezifischen Geräteinstellungen werden über eine Tastatur und ein Touchpad nach entsprechender Vorplanung vorgenommen. Die zu abladierende Raumforderung wird zunächst in ihrer Größenausdehnung in 3 Ebenen anhand einer 3D-Schnittbildgebung (CT, MRT) definiert. Mit Festlegung des peritumoralen Sicherheitssaums ergibt sich die Ablationszone in ihrer Größenausdehnung (gewünschtes Zielvolumen) in 3 Ebenen.

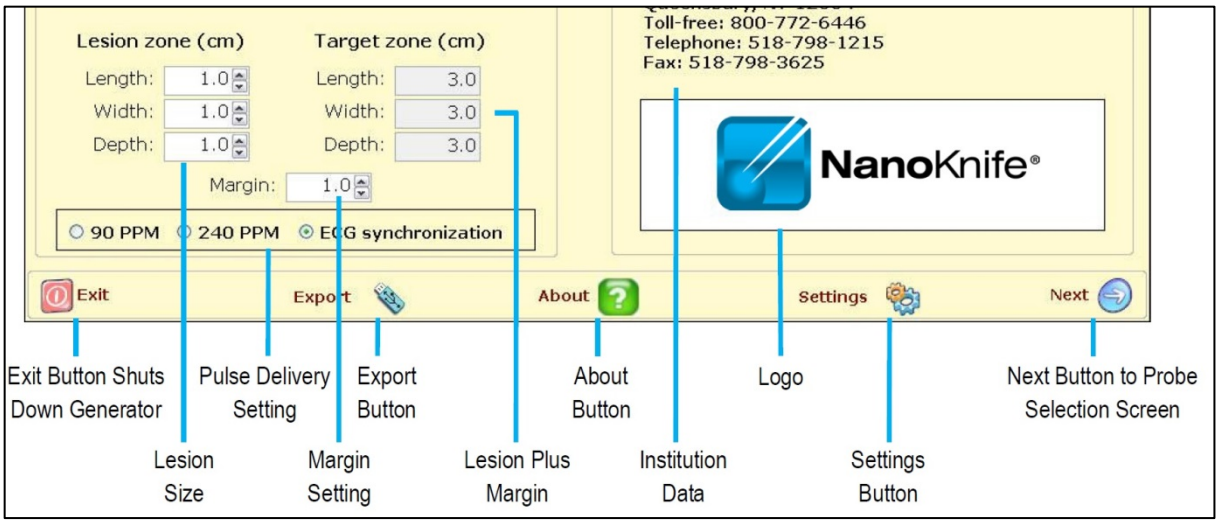

Abb.9: Zielparametereinstellung in der nanoKnife-Software mit Tumorausdehnung (Lesion zone), Sicherheitssaum (Margin) und Ablationszone (Target zone), (Manual 2011).

Anhand der Ablationszonenparameter erfolgt zunächst die Festlegung der zu verwendenden Elektrodenzahl im maximalen Querschnitt der Raumforderung (2D-Planung), (Abb.10). Durch eine individuelle Geometrie der Elektrodenanordnung im Zielgewebe sind verschiedene Ablationsfeldgrößen und -formen möglich (Abb.11).

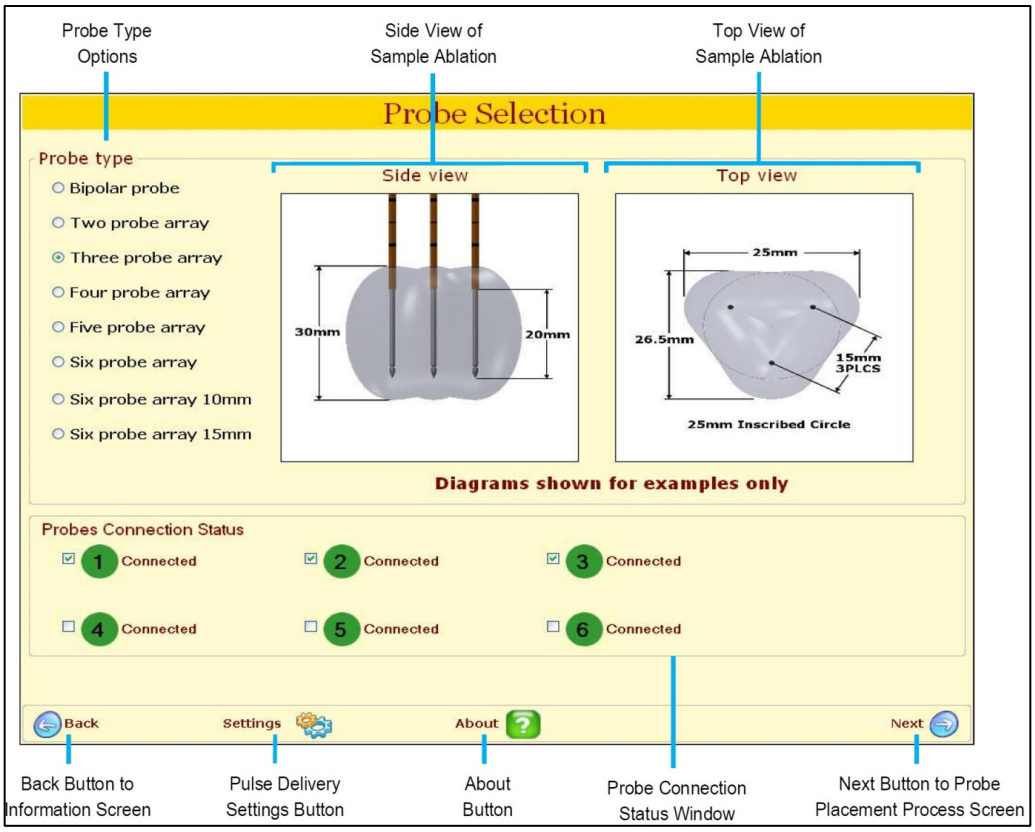

Abb.10: Festlegung der Elektrodenzahl mit jeweiliger, ungefährer Elektrodengeometrie bezogen auf den Querschnitt der Ablationszone (Manual 2011).

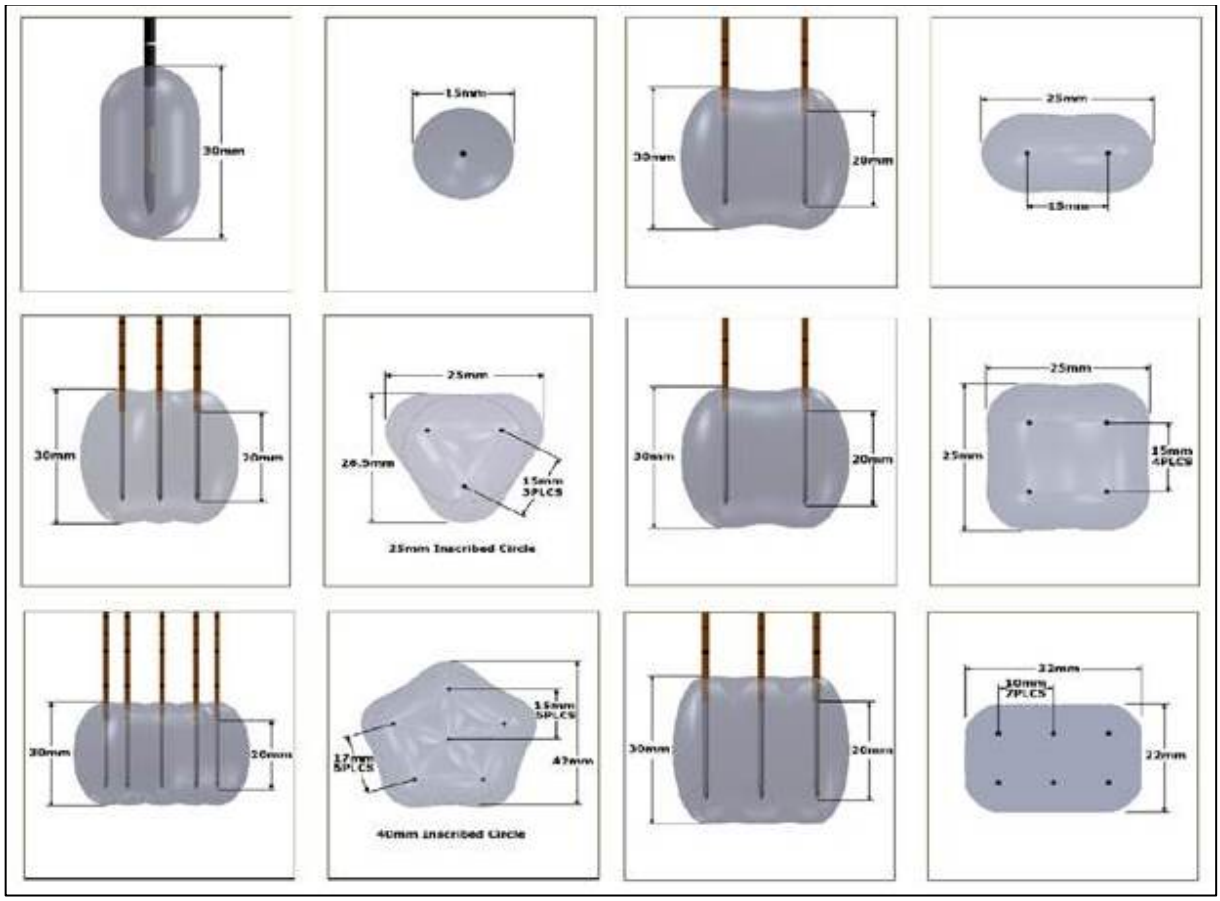

Abb.11: Transversale und longitudinale Darstellung der verschiedenen, symmetrischen Elektrodengeometrie je nach Elektrodenzahl pro Ablationszone für bipolare Elektrode und für monopolare Elektroden (Manual 2011).

Die hypothetische Ablationszone wird nun automatisch von der Gerätesoftware berechnet und im Querschnitt grafisch dargestellt (Abb.12). Anhand einer Simulation mit den Standardeinstellung kann überprüft werden, ob die Elektrodenanzahl und –geometrie ausreicht, um den Tumor und ggf. den Sicherheitssaum vollständig mit einer theoretischen Ablationszone abzudecken (Abb.12). Hierbei können einzelne Parameter, wie die Elektrodenpositionen und –abstände, sowie die Spannung zwischen dem jeweiligen Elektrodenpaar justiert werden, um die theoretische Ablationszone in ihrer Morphologie im Querschnitt an die Zielstruktur anzupassen.

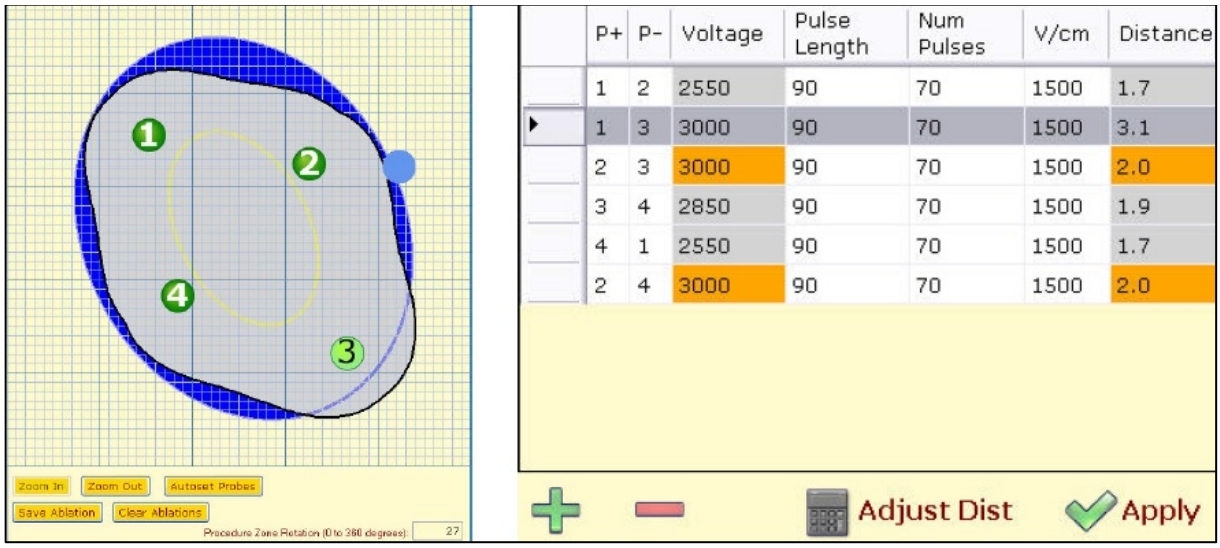

Abb.12: Simulation der theoretischen Ablationszone anhand der Ablationsparametereinstellungen. Nummerierung der Elektrodenpositionen, welche sich zur Planung verschieben lassen. Der gelbe Ring entspricht der Tumorzone (lesion zone). Das blaue Areal entspricht dem peritumoralem Sicherheitssaum. Die graue Fläche entspricht der theoretischen Ablationszone. In tabellarischer Auflistung können die Ablationsparameter justiert werden (Manual 2011).

Im Folgenden werden die Elektroden entsprechend der Planung der o.g. Simulation im Zielgewebe mit Hilfe bildgebender Verfahren positioniert. Die Platzierung erfolgt idealerweise CT-gestützt (Abb.13), da per Sonographie eine dreidimensionale Visualisierung nicht ausreichend möglich ist, und die ferromagnetischen Elektroden nicht MRT-kompatibel sind.

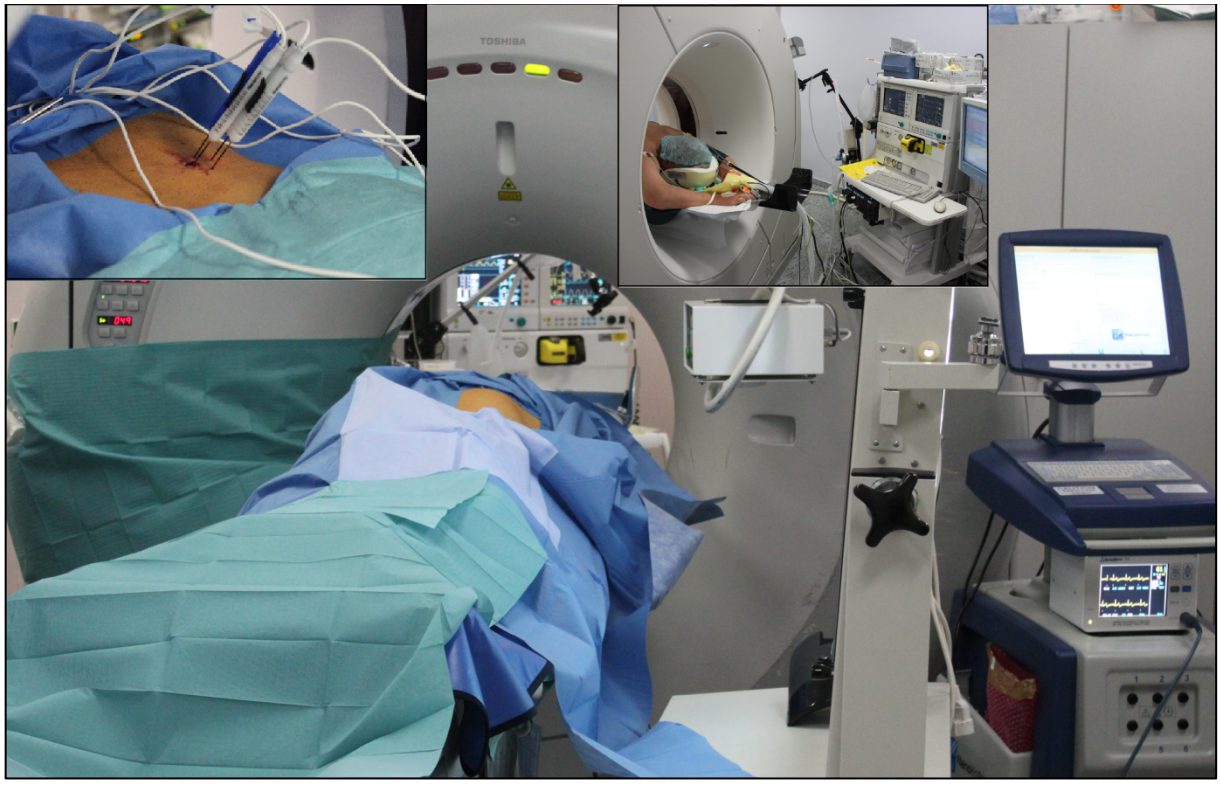

Abb.13: CT-gestützte IRE-Elektroden-Platzierung unter Fluoroskopie und sterilen Kautelen. Beispiel für IRE mittels NanoKnife-System eines Nierentumors (IRENE-Studie, Wendler et al. 2015b) mit Patient in Bauchlage und Intubationsnarkose mit Muskelrelaxation und EKG-Synchronisierung.

Nach Elektrodenplatzierung erfolgt eine Kontroll-CT zur Beurteilung der Elektrodenlage. Hierbei erfolgt die Messung der Elektrodenposition zueinander und zum Tumor. Die tatsächlichen Lageparameter werden anhand einer Skizze (Abb.14) nun erneut in das NanoKnife-Simulationsprogramm eingegeben. Nach entsprechender Simulation der Ablationszone kann eine Anpassung der Spannungsparameter pro Elektrodenpaar vorgenommen werden, um eine möglichst ideale Ablation zur erreichen. Sollte die Elektrodenposition unzureichend sein, wird der Vorgang einer erneuten Planungssimulation und Elektrodenplatzierung wiederholt.

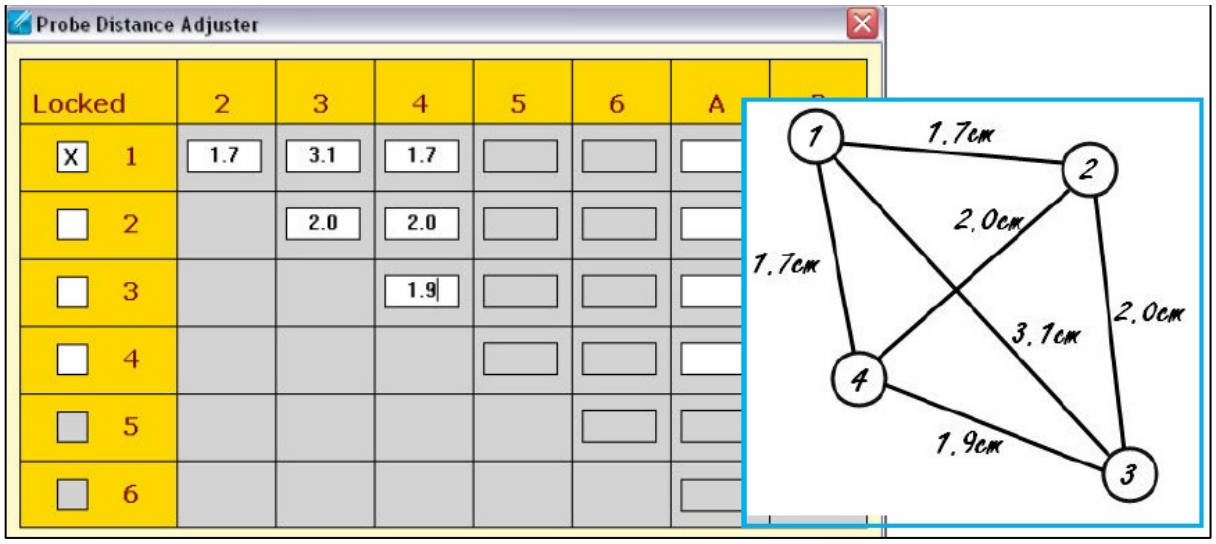

Abb.14: Eingabe der CT-kontrollierten Elektrodenpositionen und –abstände zueinander, (Manual 2011).

Im Falle einer guten Elektrodenplatzierung und IRE-Parameterfestlegung werden pro Elektrodenpaar 10 Testpulse appliziert, um zu testen, ob die Elektroden in einem IRE-tauglichen Abstand zueinander liegen und die elektrische Impedanz des Zielgewebes überwunden wird. Nach einem erfolgreichen Testdurchlauf erfolgt die eigentliche Ablation. Während der Pulsapplikation werden die erfolgreich oder nicht erfolgreich applizierten IRE-Pulse sowie der Status der abgeschlossenen Behandlung pro Elektrodenpaar als Balkenanzeige (in %) im Geräte-Display angezeigt. Nach Abschluss der Ablationsrunde erscheint eine Dokumentation der Pulsparameter für den gesamten Applikationszyklus. Dieser lässt sich pro Elektrodenpaar in verschiedenen Vergrößerungen für die Stromstärke (A) und Spannung (V) als graphischer Verlauf auswerten (Abb.15). Die Strom- und Spannungskurven sollten idealerweise eine geforderte IRE-typische Konfiguration aufweisen (Abb.15). Im Falle einer unzureichend wirkenden Ablation kann die Ablation mit gleichen oder geänderten Parameter wiederholt werden.

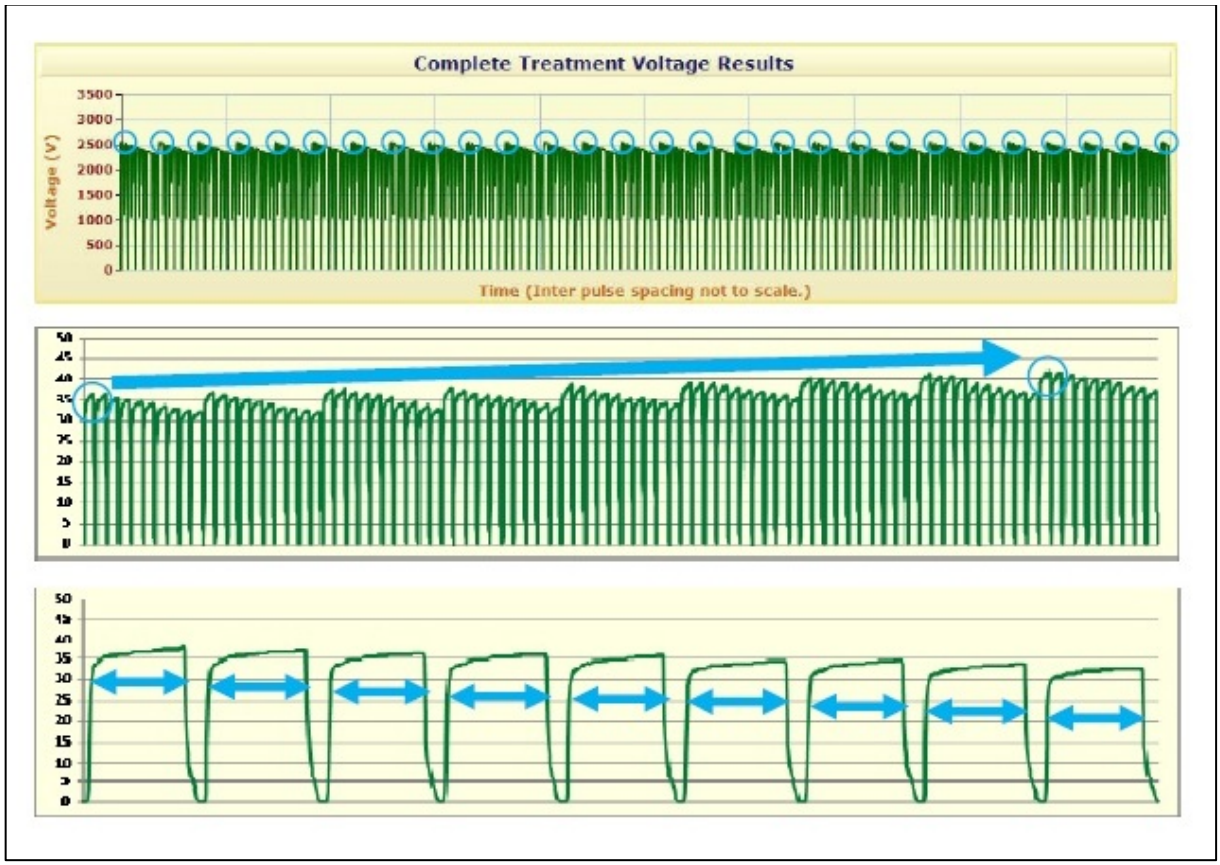

Abb.15: Graphische Übersicht der Kurvenverläufe für Spannung und Stromstärke (NanoKnife™, AngioDynamics®). Pro Gruppe von zehn aufeinanderfolgenden IRE-Impulsen fällt die Spannung und Stromstärke leicht ab. Insgesamt nimmt die Stromstärke und Spannung vom Anfang bis zum Ende der Ablation zu. In der Vergrößerung der IRE-Pulse zeigt sich ein typischer Rechteckimpuls mit leichtem Stromanstieg innerhalb eines Rechteckimpulses, (Manual 2011).

Nach erfolgreich wirkender Ablation kann die Behandlung beendet werden. Die Elektroden werden hierzu aus dem Zielgewebe und dem Patienten entfernt. Im Gegensatz zu thermischen Ablationsverfahren, wie der Radiofrequenzablation (RFA), erfolgt verfahrensbedingt bei der IRE keine Koagulation des Stichkanals.

Als absolute Kontraindikationen zur Anwendung des NanoKnife-Systems werden von der Firma Angiodynamics ein QT-Intervall >550ms im EKG, eine intrathorakale Applikation bei vorhandenem Herzschrittmacher oder Defibrillator, eine Applikation in der unmittelbarer Nähe von metallischen Implantaten, eine Anwendung im Augenbereich und bei bekannter Epilepsie genannt. Als relative Kontraindikationen gelten die Applikation bei elektrischen Implantaten, Schwangerschaft, Herzrhythmusstörungen ohne Möglichkeit einer EKG-Synchronisation und ein Zustand nach Myokardinfarkt. Der Hersteller empfiehlt hierbei eine konsiliarische Rücksprache mit der jeweilig zuständigen medizinischen Fachrichtung für eine Risiko-Nutzen-Analyse.

4. Darstellung und Diskussion der Arbeiten im Kontext

Für die Irreversible Elektroporation (IRE) wurde eine nonthermal elektroablative Eigenschaft mittels repetitiver, hochenergetischer, ultrakurzer Starkstrompulse (90-100 Pulse, 2000-3000 Volt, >1000V/cm, 30-50 Ampere, 70-100 µs Pulsdauer) postuliert und publiziert (Davalos et al. 2005). Zum Untersuchungsbeginn in dieser Klinik (2008/ 2009) waren keine systematischen Daten zur IRE mittels NanoKnife-System in verschiedenen Medien verfügbar. Die zulassungsrelevanten Untersuchungen basierten in-vivo-Anwendungen an der Leber, Prostata sowie großer Blutgefäße (Edd et al. 2006; Rubinsky 2010). Für die verschiedenen Organe bzw. Weichgewebe wurden unterschiedliche elektrische Leitfähigkeiten definiert (Rubinsky 2010). Die Definition und Kalkulation der nonthermalen Irreversiblen Elektroporation (NTIRE) beruhten hauptsächlich auf komplexen mathematischen Modellen (Rubinsky 2010). Da zum Zeitpunkt der Gerätezulassung des NanoKnife-Systems keine klinischen, tumorentitätsspezifischen Wirksamkeitsnachweise zur Irreversiblen Elektroporation vorlagen, führte das zur eigenen Zielsetzung, die postulierten Funktions-eigenschaften der Irreversiblen Elektroporation und die vom Hersteller angegebenen Eigenschaften des NanoKnife-Systems im Hinblick auf eine minimal-invasive, perkutane Anwendung zunächst bei Nierenkarzinomen und Prostatakarzinomen im Rahmen einer Wirksamkeitsnachweisstudie zu prüfen. Als primäres Organmodell zur klinisch-experimentellen Evaluation wurde die Niere gegenüber der Prostata favorisiert, da hier insgesamt eine höhere klinische Expertise zur fokalen Therapie von Nierentumoren bestand, und die Niere ein leichter zu simulierendes und zu monitorierendes Organ darstellt.

Entsprechend wurde zur systematischen Betrachtung eine eigene Untersuchungskaskade von einfachen physikalischen in-vitro-Modellen, über in-vivo-Tierversuchmodelle bis hin zur klinischen Wirksamkeitsnachweisstudie gewählt:

- physikalische Untersuchungen der IRE im experimentellen Eiweißmodell und Gelmodell
- physikalische Untersuchungen der IRE im ex-vivo-Nierenfrischpräparat
- radiologische Untersuchungen der IRE im ex-vivo-Nierenperfusionsmodell
- präklinische Studie zur IRE im in-vivo-Nierentierversuchsmodell
- klinische Studie zur IRE im in-vivo-Nierentumorhumanmodell (Sicherheit)
- klinische Studie zur IRE im in-vivo-Nierentumorhumanmodell (Wirksamkeit)

Dabei stellt die Fortsetzung der o.g. experimentellen Grundarbeiten mit der Durchführung der ersten Pilot-Wirksamkeitsnachweisstudie per Ablations-Resektions-Sequenz den entscheidenden Schritt als Überführung der IRE zur klinischen Anwendung beim Nierenzellkarzinom dar.

Im Verlauf unserer Untersuchungen wurden eigene Erfahrungen und Ergebnisse stets im Kontext zu anderen Publikationen diskutiert. Entsprechend wurden auch die zu berücksichtigenden Fragestellungen für eine weitere Anwendung der IRE in Stellungnahmen, Reviews und Empfehlungen zum Thema Nierenzellkarzinom- und Prostatakarzinom-Ablation publiziert. Die nachfolgenden Publikationen sollen abschnittsweise erläutert und in ihrem zeitlichen und aktuellen wissenschaftlichen Kontext diskutiert werden.

4.1 Physikalische Untersuchungen der IRE im experimentellen Eiweiß- und Gelmodell, sowie im ex-vivo-Nierenfrischpräparat

Vor einer eigenen klinischen Anwendung des NanoKnife-Systems zur IRE sollte demzufolge zunächst eine „Austestung“ in einfachen experimentellen Modellen erfolgen.

Liehr UB, **Wendler JJ**, Blaschke S, Porsch M, Janitzky A, Baumunk D, Pech M, Fischbach F, Schindele D, Grube C, Ricke J, Schostak M. **[Irreversible electroporation: the new generation of local ablation techniques for renal cell carcinoma].** Urologe A. 2012 Dec;51(12):1728-34.

Im Flüssighühnereiweißmodell (24°C, 200ml) erfolgte die Applikation von IRE-Impulsen mit der vom Hersteller empfohlenen Einstellung zur Ablation von Weichgeweben (bipolare Elektrode 15cm 5Ch, NanoKnife-System, 90 Impulse zu je 2700V und 22A für je 70µs, 375 kJ) bei einer berechneten IRE-Ablationszone von 30x15mm eines verlängerten Rotationsellipsoids. Dabei zeigten sich reproduzierbar knallartige Impulsgeräusche mit zeitgleicher Lichtblitzausbildung an den vier Polenden der bipolaren Elektrode sowie eine Schaumbildung um die Elektrode herum und einer filmartigen, bräunlichen Eiweiß-verfestigung an den nichtisolierten Elektrodenpolen (Abb. 16). Der Versuchsaufbau demonstrierte eine Knallreaktion, Lichtbogenbildung, Gasausbildung und Eiweiß-denaturierung. Dies ließ eine mögliche elektromechanische Umwandlung der IRE-Impulse in Lichtbögen (bis 20.000°C, eine (Wasser-)Elektrolyse mit Gasbildung, eine explosionsartige Druckausdehnung mit intensiver Schallemission und eine thermoablative Hitzentwicklung mit Eiweißdenaturierung vermuten.

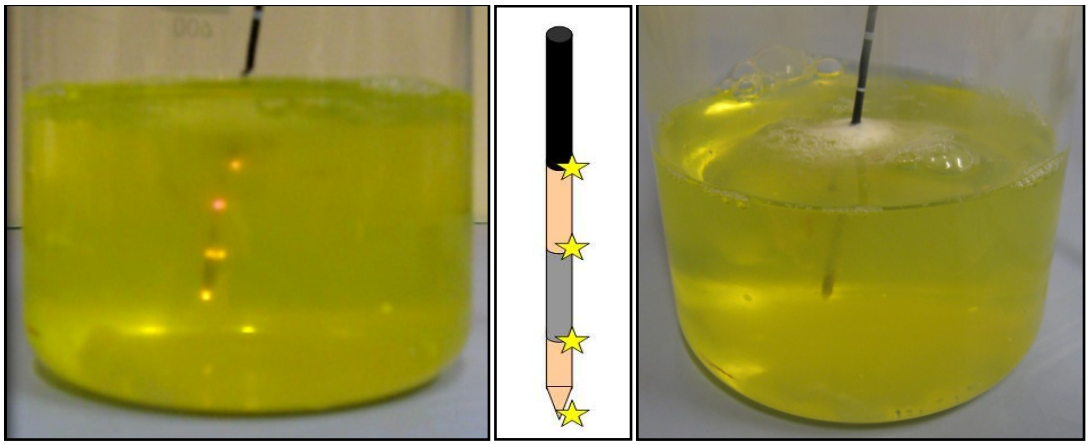

Abb.16: Videofotografische Darstellung der bipolaren NanoKnife-IRE-Elektrode im Hühner-flüssigeiweiß mit Lichtblitzen (links). Schematische Darstellung der bipolaren NanoKnife-IRE-Elektrode mit Lokalisation der Lichtblitze (Mitte). Fotografische Darstellung der bipolaren NanoKnife-IRE-Elektrode im Hühnerflüssigeiweiß mit Schaumbildung (rechts), (Liehr 2014).

Diese Phänomene waren bis dato nicht publiziert worden. Bei den o.g. Beobachtungen konnte somit für die IRE-Ablation per NanoKnife-System in flüssigkeitsreichen Weichgeweben (starke Vaskularisation, flüssigkeitsgefüllte anatomische Hohlsysteme, Drüsen, Zysten, zystische Tumoren etc.) ein möglicher Wirkverlust sowie mechanischer, chemischer und thermischer Kollateralschaden nicht ausgeschlossen werden. Die Beobachtungen wurden mit der Forschungsgruppe um Rubinsky et al. sowie der Fa. AngioDynamics Inc. 2009/ 2010 kommuniziert. Ein eigener Versuchsaufbau zum Nachweis der vermuteten Elektrolyse mit Wasserstoffgasbildung und Knallgasreaktion konnte leider nicht umgesetzt werden. Die Forschungsgruppe um Rubinsky et al. veröffentlichte seit 2015 verschiedene Phänomene zur Elektrolyse, während der IRE, wobei eine entsprechende Gasbildung und Knallgasreaktion in Abhängigkeit vom Medium und pH-Wert beschrieben werden konnte (Meir 2015; Meir et Rubinsky 2015). Weiterhin wurde diskutiert, dass diese Gasbildung zu einer Veränderung der Impedanz am Zielgewebe sowie der Ankopplung zwischen der IRE-Elektrode und dem Zielgewebe mit entsprechendem Wirkungsverlust führen (van Es et al. 2016). Anderseits ist zu diskutieren, ob das Phänomen einer Gasbildung und entsprechend hyperechogenen Darstellung im Ultraschall als sogenanntes Real-Time-Monitoring der IRE-Ablationszone zu nutzen ist (Schmidt et al. 2012).

Im Hydrogelmodell (Roth 240 Bloom Granulat-Gelatine für Laboruntersuchungen und handelsüblicher Speisegelatine) erfolgte in einem Acrylglasblock (80x50x70mm, Volumen 280ccm) die systematische Temperaturmessung (faseroptisches, digitales Thermometer TempSens72® von OpSens®) in definierten Abständen (5, 10, 15mm) zur NanoKnife-IRE-Elektrode während der Applikation der IRE-Impulse (bipolare Elektrode 15cm 5Ch, NanoKnife-System, 90 Impulse zu je 2700V und 22A für je 70µs, 375 kJ, 120sec.). Dabei konnte beobachtet werden, dass sich während der der IRE-Applikation ein zylindrischer Hohlraum um die NanoKnife-IRE-Elektrode bildete, wobei es zu nach Applikations-wiederholung zur Fehlermeldung „high-current“ bei gleichzeitiger Lichtbogenbildung an den Polenden kam. In der Temperaturmessung zeigten sich ein maximaler Temperaturanstieg von 11,5°C im Abstand von 5mm zur Elektrode und ein zentrifugaler Temperaturabfall, wobei im Abstand von 15mm bereits keine Temperaturveränderung mehr messbar war. Nach Auffüllen des entstandenen Hohlraums mit NaCl 0,9% stellte sich eine maximale Temperaturerhöhung auf 13,3°C im Abstand von 5mm zur Elektrode dar (Blaschke SB 2013; Liehr UB 2014).
Im gleichen Versuchsaufbau mit in-vitro-Nierenfrischpräparatmodell (schlachtfrische Nieren vom Hausschwein/ Deutschen Landschwein, Gut Glüsig GmbH Sachsen-Anhalt, Deutschland) zeigte sich ein maximaler Temperaturanstieg von 17,3°C im Abstand von 5mm

zur Elektrode und ein zentrifugaler Temperaturabfall, wobei im Abstand von 15mm bereits keine Temperaturveränderung mehr messbar war.
Mit den o.g. experimentellen Untersuchungen konnten wir zeigen, dass die geringen Temperaturanstiege um <15°C über 90-120 Sekunden bei der IRE nicht für eine hyperthermale Gewebeablation mit konstant >60°C über >10-40 Minuten erreicht werden. Somit zeigt sich zwar keine nonthermale IRE im wortwörtlichen Sinne, jedoch eine nonthermo-ablative IRE wie postuliert (Blaschke SB 2013; Liehr UB 2014).

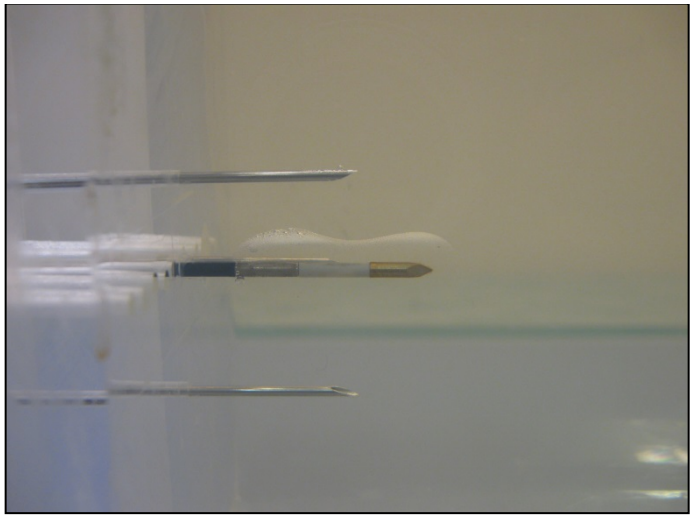

Abb.17: Hohlraum um IRE-Nadelspitze, zur besseren Darstellung im Speisegelatine-Modell.

Die Ergebnisse dieser experimentellen Untersuchungen wurden jedoch nicht detailliert PubMed-gelistet publiziert (Liehr et al. 2012; Blaschke SB 2013; Liehr UB 2014). In den Folgejahren wurde immer wieder der nonthermoablative Charakter der IRE per NanoKnife-System mit möglichen thermalen Kollateralschäden besonders in Nähe zur Hohlorganen oder Metallimplantaten in Frage gestellt (Faroja et al. 2013; Scheffer et al. 2016; Ruarus et al. 2018). Van den Bos et al. konnten 2016 in einem Hydrogelversuch (Poylacrylamidgel) ebenso eine Gasbildung mit einer Kavitationsbildung um die Elektrode herum und einen Temperaturanstieg durch IRE nachweisen (van den Bos et al. 2016c). Bei der Gasbildung und Kavitation postulierten sie eine Ursache aus einer Vaporisation und einer Hydrolyse von Wasser in molekularen Sauerstoff und Wasserstoff. Der Temperaturanstieg korrelierte mit der Spannungsstärke, Pulslänge, Elektrodenlänge, dem Winkel der Elektroden und dem Elektrodenabstand zu einander. Hierbei zeigte sich ein maximaler Temperaturanstieg um +40,4°C über 150 sec., weshalb die Autorengruppe eine Validierung dieser Parameter in Tierversuchs- und klinischen Studien empfehlen (van den Bos et al. 2016c).

4.2 Radiologische Untersuchungen im ex-vivo-Nierenperfusionsmodell

In den o.g. Untersuchungsmodellen konnte gezeigt werden, dass es zwar zu keiner thermoablativen Temperaturerhöhung durch die IRE im Gel- und Nierenfrischpräparatmodell kam. Jedoch zeigten sich im Eiweiß- und Gelmodell Begleitphänome mit explosionsartigen Knallgeräuschen, Gasbildung, Lichtbögen und Eiweißdenaturierung im unmittelbaren Kontakt zur IRE-Elektrode, die auf eine mögliche akute Gewebeschädigung hindeuten könnten. Neben den bekannten histopathologischen Nierenparenchymschäden durch thermoablative Techniken (Duffey et al. 2010), konnten Köhrmann et al. auch die akute , mechanische Zerstörung mikrovaskulärer Strukturen im Nierenparenchym durch die extrakorporale Stoßwellentherapie (ESWL, nonthermaler Ultraschall) mittels angiographischer Untersuchungen nachweisen (Köhrmann et al. 1994).

Wendler JJ, Pech M, Blaschke S, Porsch M, Janitzky A, Ulrich M, Dudeck O, Ricke J, Liehr UB. **Angiography in the isolated perfused kidney: radiological evaluation of vascular protection in tissue ablation by nonthermal irreversible electroporation.** Cardiovasc Intervent Radiol. 2012 Apr;35(2):383-90.

Mit unseren experimentellen Untersuchungen zur IRE im in-vitro-Nierenfrischpräparat-Perfusionsmodell konnten per dynamischer, digitaler Substranktionsangiographie (DSA, Iod-haltiges Kontrastmittel) und statischer, hochauflösender Angiographie (Mammographie-Technik, Barium-haltiges Kontrastmittel) akute elektromechanische Blutgefäßschäden mit Kontrastmittelextravasat oder Unterbrechung des Endstromgebietes des Nierenparenchyms ausgeschlossen werden (Wendler et al. 2012a). Damit unterscheidet sich die IRE grundlegend von thermoablativen oder mechanischen Ablationstechniken. Zusätzlich beobachteten wir in der DSA eine wellenartige, IRS-Impuls-synchrone, zentrifugale Kontrastmittelbewegung im Nierenparenchym ausgehend von den IRE-Elektrodenpolen, welche auf einem kapillären, wellenartigen Kontrastmittelabstrom durch die IRE-Impulsbedingten Schalldruckemissionen bei erhaltenem Kapillarbett hindeuten. Mit diesem Modell erfolgte die erstmalig und einzige, angiographisch-radiologische Beschreibung des morphologischen und funktionellen Erhalts des makro- und mikrovaskulären Nierenparenchymssystems nach IRE. Wir schlussfolgerten, dass kein sekundärer, ischämiebedingter Nierenparenchymfunktionsverlust aufgrund mechanischer Kollateralschäden am renovaskulären System im Rahmen der IRE entstehe. Bei einer scharf begrenzten Nierenparechymzellablation per nonthermoablativer IRE und bei einem gleichzeitigen Erhalt des renovaskulären Systems im und um das Ablationsareal postulierten wir, dass mit der IRE eine Nephron-sparendere Ablationsmethode im Vergleich zu thermaloablativen Techniken zur Verfügung stünde (Wendler et al. 2012a).

4.3 Präklinische Studie zur IRE im in-vivo-Nierentierversuchsmodell

Zum damaligen Zeitpunkt (2009) lagen keine publizierten präklinischen oder klinischen, histologischen oder bildgebenden Untersuchungsergebnisse zur IRE von in-vivo-Nierengewebe (Parenchym, Tumor, Nierenbeckenkelch- und Nierengefäßsystem) im Sinne einer Sicherheits- oder Wirksamkeitsnachweisstudie vor. Zur Narkoseführung, sowie für muskuläre und kardiovaskuläre bestanden bis dato nur limitierte Erkenntnisse (Rubinsky et al. 2007; Bertacchini et al. 2007; Rubinsky et al. 2008; Mali et al. 2008). Vor einem klinischen Einsatz der IRE als kurativ-intendierte Ablation von Nierenzellkarzinomen in einer Humanstudie galt es zunächst die postulierten, protrahierten Eigenschaften der IRE am in-vivo-Tier- und -Nierenmodell zu prüfen.

Dementsprechend konzipierten wir eine eigene Tierversuchsstudie (Tierversuchslabor Institute of Medical Technology and Research (IMTR) GmbH Rottmersleben sowie die Universitätskliniken für Urologie, Radiologie und Anästhesiologie Magdeburg) mit Prüfung durch die zuständige Ethikkommission des Landesamtes für Verbraucherschutz Sachsen-Anhalt und Genehmigung durch das Referat für Verbraucherschutz und Veterinärangelegenheiten Halle (Saale) des Landesverwaltungsamtes Sachsen-Anhalt (Aktenzeichen 42502-2-996 IMTR, GA-Nr.112). Hierbei erfolgte eine perkutane, multifokale, CT-gestützte IRE der Nieren von Hausschweinen in Allgemeinnarkose (Intubationsnarkose mit Muskelrelaxation) mit einer Nachbeobachtungszeit von 28 Tagen. Die IRE wurde mittels NanoKnife-System gemäß Herstellerangaben appliziert. Die Versuchstiere wurden gemäß Studienprotokoll klinisch, laborchemisch, Röntgen- und MRT-radiologisch, anästhesiologisch, histo- und zytopathologisch untersucht. Zum Beobachtungsendpunkt (28 Tage nach IRE) wurden die Nieren zur histologischen Analyse explantiert (Wendler et al. 2012b; Wendler et al. 2013).

Neben den Daten der u.g. Veröffentlichungen wurden weitere klinische und paraklinische Parameter im Sinne einer Safety-Analyse gemäß Studienprotokoll erfasst, jedoch nicht detailliert PubMed-gelistet publiziert. Alle Versuchstiere überlebten die Beobachtungsdauer. Nebenwirkungen außer eine temporäre, nicht interventionspflichtige, asymptomatische, postpunktionelle Makrohämaturie in einem Fall traten nicht auf. Elektrokardiographisch konnten während der IRE-Applikation in Allgemeinnarkose keine rhythmischen oder morphologischen Veränderungen festgestellt werden. Paraklinisch zeigte sich bei allen Versuchstieren eine temporäre, reaktive Leukozytose ohne klinische Infektzeichen.

Wendler JJ, Pech M, Porsch M, Janitzky A, Fischbach F, Buhtz P, Vogler K, Hühne S, Borucki K, Strang C, Mahnkopf D, Ricke J, Liehr UB. **Urinary tract effects after multifocal nonthermal irreversible electroporation of the kidney: acute and chronic monitoring by magnetic resonance imaging, intravenous urography and urinary cytology.** Cardiovasc Intervent Radiol. 2012 Aug;35(4):921-6.

Mit dieser präklinischen Untersuchung (Wendler et al. 2012b) erfolgte erstmals eine zytopathologische und radiographische Beschreibung der akuten und subakuten Auswirkungen der IRE auf das Nierenbeckenkelchsystem. Direkt nach IRE stellte sich ein leichtes Ödem ohne Gewebedefekt im Bereich der Ablationsareale dar. 7 Tage nach IRE konnten MRT-morphologisch ausgedehnte, scharfabgrenzbare Ablationsareale mit Angrenzung und Einbeziehung des Nierenkelchsystems nachgewiesen werden. 28 Tage nach IRE zeigten sich resektionshistopathologisch und MRT-morphologisch scharfabgrenzbare nekrotisch-narbige Defekte mit ausgeprägter Schrumpfung. Das Urothel des Nierenbeckenkelchsystem mit Angrenzung an die IRE-Ablationsareale wies Regenerationszeichen als reversiblen Epithelschaden auf. Urinzytologisch fanden sich passager abgestoßene Urothelzellen aus dem IRE-involvierten Nierenbeckenkelchsystem mit einer spezifischen Vakuolisierung und Zellmembranauflösung. Dieser Befund nach IRE wurde hiermit erstmals zytologisch nachgewiesen und deckt sich mit den postulierten Beschreibungen einer protrahiert wirkenden IRE mit degenerativen Zell- und Kernmembranveränderungen (Rubinsky et al. 2010). Mittels intravenöser Ausscheidungs- und MRT-Urographie wurde der morphologische und funktionelle Erhalt des Nierenbeckenkelchsystems nachgewiesen. Eine Perforation, Fistelung und Striktur des oberen harnableitenden Systems konnte ausgeschlossen werden, welche typische Risiken bzw. Nebenwirkungen von thermoablativen Techniken darstellen (Uhlig et al. 2019). Aus diesen Ergebnissen schlussfolgerten wir, dass mittels NanoKnife-IRE eine fokal begrenzte Nierenparenchymablation bei gleichzeitigem Erhalt der Organintegrität und des involvierten Nierenbeckenkelchsystems, sowie eine schnelle Urothelregeneration möglich sind. Daraus ergäben sich Anwendungsvorteile gegenüber den Leitlinien-basierten thermoablativen Techniken (RFA und Kryoablation), insbesondere im Hinblick auf zentral gelegene Nierentumoren.

Wendler JJ, Porsch M, Hühne S, Baumunk D, Buhtz P, Fischbach F, Pech M, Mahnkopf D, Kropf S, Roessner A, Ricke J, Schostak M, Liehr UB. **Short- and mid-term effects of irreversible electroporation on normal renal tissue: an animal model.** Cardiovasc Intervent Radiol. 2013 Apr;36(2):512-20.

Anhand dieser Publikation wurden erstmals detaillierte resektionshistopathologische und MRT-morphologische Befunde nach multifokaler IRE im in-vivo-Nierenparenchym beschrieben. Aufgrund einer postulierten spezifischen Wirkungsweise der IRE führten wir unmittelbar vor sowie 30min, 7 und 28 Tage nach IRE eine multiparametrische MRT der Nieren durch, bevor die Explantation am Tag 28 erfolgte. Die unterschiedlich großen Ablationszonen an Tag 7 wiesen einen inhomogenen, konzentrischen Aufbau auf. Wir postulierten einen zentrifugalen Wirkungsabfall mit Ausbildung einer zentralen Nekrose und kompletter Gewebeablation, einer peripheren Transitionszone mit möglich inkompletter Gewebeablation und eine perifokale Ödemzone. Die Limitation dieser Studie lag in der fehlenden, nicht geplanten Resektion am Tag 7 nach IRE zur histopathologischen Korrelation. Anhand verschiedener MRT-Sequenzen zu verschiedenen Zeitpunkten schlussfolgerten wir, dass die multiparametrische MRT als derzeit effizientere, bildgebende Methode zur Kontrolle der Ablationsbehandlung im Vergleich zur Sonographie und Computertomographie einzusetzen sei. MRT-Intensitätsmessungen des an die Ablationszonen angrenzenden Nierenparenchyms wiesen keine interventionsbedingten Veränderungen im Sinne von Kollateralschäden auf. Demzufolge sei eine Nierenparenchym-schonende, multifokal definierte Gewebeablation mittels perkutaner CT-gestützter IRE per NanoKnife-System möglich. Weiterhin postulierten wir jedoch, dass aufgrund prolongierter postinterventioneller Umbau- und Schrumpfungsprozesse der Ablationszone frühestens nach 4 Wochen eine histologische und MRT-morphologische Kontrolle des Ablationserfolgs sinnvoll sei. Eine unmittelbare MRT-Kontrolle nach IRE-Ablation ließ keine Rückschlüsse auf die Ausdehnung der Ablationszone und damit Effektivität der IRE zu. Histologisch beschrieben wir 28 Tage nach IRE-Ablation scharfbegrenzte Narben mit einer zentralen, dezellularisierten Nekrose und kompletten Verlust an Glomeruli und Tubuli, sowie einer peripheren Transitionszone (<1mm) aus teilweise erhaltenen, degenerierten Glomeruli und Tubuli. Die Ablationszonen wiesen eine lymphozytäre Infiltration und Calciumablagerungen mit Fremdkörperriesenzellen auf, sowie einen randständigen, perifokalen Siderophagen-saum. Das unmittelbar an die Ablationszone angrenzende Nierenmark wies erhaltene Sammelrohre mit epithelialer Regeneration analog zum angrenzenden Urothel des Nierenbeckenkelchsystems auf. Blutgefäße (Arteriolen) in der Ablationszone blieben erhalten und wiesen eine Intimafibrose sowie perivaskuläre Fibrose und Calciumspangenbildung mit

konsekutiver Wandverdickung auf. Insgesamt konnte die postulierte Eigenschaft der IRE mit einer Dezellularisation des Parenchyms und dem gleichzeitigem Erhalt der Bindegewebsmatrix mit einem entsprechenden Regenerationspotential des Gefäßendothels und Nierenbeckenkelchenepithels (Urothel) nachvollzogen werden. Wir schlussfolgerten, dass nach IRE spezifische, histopathologische Muster zu berücksichtigen sind, sowie der strukturelle Blutgefäßerhalt eine gewisse Schonung funktioneller, matrixbasierter Strukturen ermöglicht.

Vergleichbar mit unseren Ergebnissen waren die quasi zeitgleichen Tierversuchstudien von Tracy et al. (Tracy et al. 2011) und Deodhar et al. (Deodhar et al. 2011) zur IRE am in-vivo-Nierengewebe. Tracy et al. führten eine laparoskopisch-gestützte IRE an in-vivo-Schweinenieren mittels NanoKnife-System durch. Die resektionshistologische Befundung ohne bildgebende Untersuchen erfolgten von 18 Ablationen ≤7 Tage und 6 Ablationen 14 Tage nach IRE (Tracy et al. 2011). Deodhar et al. analysierten 23 Ablationen ≤36 Stunden und 6 Ablationen 21 Tage nach perkutaner CT-gestützter IRE mittels NanoKnife-System an in-vivo-Schweinenieren mittels Computertomographie und Resektionshistologie (Deodhar et al. 2011). Beide Gruppen demonstrierten die fokal begrenzte IRE-Ablation von Nierenparenchym unter Einbeziehung und Erhalt des Nierenbeckenkelchsystems bei Regeneration des Urothels. Eine differenzierte Betrachtung des Nierenparenchyms und der Ablationszonen nach dem tubulären, glomerulären und vaskulären Muster, sowie nach anderen Ablations- oder IRE-spezifischen Veränderungen erfolgte mit diesen Publikationen nicht. Zusammenfassend schlussfolgerten wir, dass neben einer notwendigen Wirksamkeitsnachweisstudie zur IRE im humanen in-vivo-Nierentumormodell auch weitere präklinische, tierexperimentelle Untersuchungen am in-vivo-Nierenmodell notwendig sind, um die Abhängigkeit der histopathologischen Wirkung von unterschiedlichen IRE-Parametern zu prüfen.

In den Folgejahren erschienen weiterführende Arbeiten zur Beurteilung der IRE-Wirkung in in-vivo-Nierengewebe aus analogen Tierversuchsstudien. Olweny et al. demonstrierten spezifische, histopathologische Unterschiede zwischen nonthermoablativer IRE und thermoablativer IRE (Olweny et al. 2013). Sommer et al. beschrieben die Abhängigkeit der Ablationsarealgrößen in Abhängigkeit verschieden geometrischer Elektrodenkonfigurationen (Sommer et al. 2013). Wimmer et al. untersuchten die Größendiskrepanz zwischen der IRE-Simulation sowie der CT-morphologischen Ausdehnung und der histopathologischen Größe der Ablationszone in Abhängigkeit verschiedener IRE-Parametereinstellungen. Dabei zeigte sich eine Größenüberschätzung der Simulation und des CT-Befundes gegenüber der zentralen Nekrosezone mit kompletter Gewebeablation bei bestehender inkompletter, peripherer Gewebeablation im Randsaum (Wimmer et al. 2014). Neal et al. korrelierten numerische IRE-Ablationsmodelle mit klinisch-histopathologischen Befunden in

Abhängigkeit verschiedener elektrischen Konduktivitäten (Neal et al. 2015). Dabei beschrieben sie eine sich während der IRE-Ablation verändernde Konduktivität des Zielgewebes, ein zentrale Nekrosezone und eine periphere Transitionszone mit heterogenem Muster von vitalen bis letalen Gewebestrukturen in Abhängigkeit der Parenchymzellart und der IRE-Ablationsparameter. Sie schlussfolgerten, dass eine asymmetrische, sigmoide, dynamisch Konduktivitätsfunktion am genauesten mit der tatsächlichen Ablationszone einhergehe, und dass die IRE möglicherweise bei gleichen Parametereinstellungen in inhomogenen und heterogenen Tumoren ein unterschiedliches Ablationsverhalten aufweise (Neal et al. 2015).

Srimathveeravalli et al. stellten nach intraluminaler IRE-Ablation des Harnleiters zwar ebenfalls eine erhaltenen Integrität der Harnleiter und eine Regeneration des Urothels fest, jedoch entstanden im Gegensatz zum muskelfreien, subepithelial zellarmen Nierenbeckenkelchsystem chronische Strikturen aufgrund eines narbigen Umbaus der Tunica muscularis ureteris (Srimathveeravalli et al. 2015; Srimathveeravalli et al. 2017).

Cornelis et al. verglichen die Ausdehnung der Ablationszonen nach IRE, RFA, Kryoablation (KA) und Mikrowellenablation (MWA). Dabei ergaben sich histologisch um die zentrale Nekrosezone größere Transitionszonen (Mischbild aus vitalen und avitalen Zellen) nach IRE und RFA als nach KA und MWA, während die CT-morphologische Darstellung der Ablationszonen als inadäquat bewertete Bildgebungsmethode dies nicht differenzieren konnte (Cornelis et al. 2017).

4.4 Klinische Studie zur IRE im in-vivo-Nierentumorhumanmodell (Safety-Studie, First-in-Man-Pilot-Studie Phase I)

Basierend auf unseren o.g. experimentellen Beobachtungen und der klinischen Zulassung des IRE-NanoKnife-Systems zur Weichgewebsablation wurde konsekutiv eine Sicherheits-analyse und Anwendungsstudie (Safety-Studie) zur IRE im in-vivo-Nierentumorhumanmodell konzipiert (Phase 1, Genehmigung durch zuständige Ethik-kommission Medizinische Fakultät Magdeburg 20.01.2009, Vorgangsnummer:12/09). Trotz klinischer Zulassung des IRE-NanoKnife-Systems waren zum Zeitpunkt der Planung und Durchführung dieser Pilotstudie keine wissenschaftlichen Daten oder Publikationen zur klinischen Anwendung am Menschen bekannt.

Pech M, Janitzky A, **Wendler JJ**, Strang C, Blaschke S, Dudeck O, Ricke J, Liehr UB. **Irreversible electroporation of renal cell carcinoma: a first-in-man phase I clinical study.** Cardiovasc Intervent Radiol. 2011 Feb;34(1):132-8.

In dieser Pilotstudie erfolgte die offen-chirurgische Anwendung der IRE mittels NanoKnife-System in Intubationsnarkose unter EKG-Triggerung nach Herstellervorgaben bei 6 Patienten mit einem lokalbegrenzten Nierenzelltumor (20-39mm) und einer Indikation zur offen-lumbalen Nierenteilresektion oder Tumornephrektomie nach Leitlinienempfehlung, um eine exakte Platzierung der IRE-Elektroden im Nierentumor sicherzustellen (Abb.18).

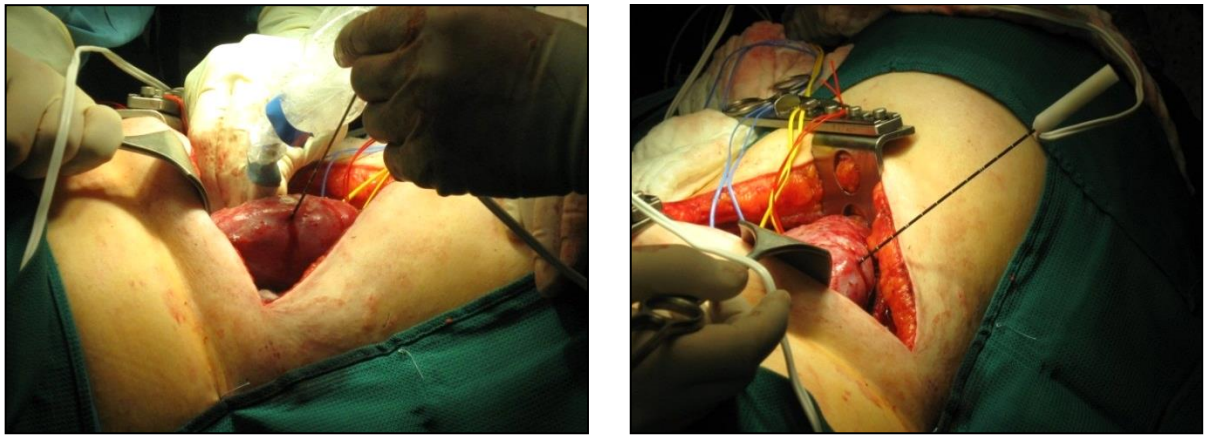

Abb.18: Intraoperative IRE: sonografisch-gestützte IRE-Sonden-Einlage (links) und IRE-Puls-Applikation (rechts). Bipolare IRE-Elektrode des NanoKnife-Systems.

Periinterventionelle Blutdruck- oder Laborveränderungen (Blutgasanalysen) wurden nicht beobachtet. Manifeste Herzrhythmusstörungen oder kardiale Ischämiezeichen konnten nicht festgestellt werden, wobei fünf Patienten unspezifische, nicht pathologische EKG-Veränderungen (verlängerte QTc-Zeit, inkompletter Rechtsschenkelblock. Pulmonale und

neuromuskuläre Komplikationen traten ebenfalls nicht auf (Pech et al. 2011). Wir schlussfolgerten, dass die renale IRE-Applikation mittels NanoKnife-System gemäß Herstellerempfehlungen eine sichere, nebenwirkungsfreie Technik darstellt. Darauf aufbauend müsse deren Tumorablationswirkung in einer Phase-2-Studie resektionshistologisch und MRT-bildgebend überprüft werden.

Analoge Sicherheitsstudien zur perkutan renalen, haptischen und pulmonalen IRE-Applikation mittels NanoKnife-System in Intubationsnarkose und EKG-Triggerung demonstrierten eine prinzipiell sichere, nebenwirkungsarme Anwendung unter Beobachtung von starken Muskelkontraktionen bei zu geringer Muskelrelaxation, IRE-assoziierten ventrikulären, selbstlimitierende Tachykardien (insbesondere in unmittelbarer Herznähe) und eine temporäre, systolische, nicht interventionspflichtige Blutdruckzunahme (Ball et al. 2010; Thomson et al. 2011).

Sicht- oder messbare, makroskopisch-intraoperative Veränderungen an der Niere zeigten sich nicht. Die histologischen Untersuchungen der Nierenteilresektate zeigten unmittelbar nach IRE keine akuten Gewebeschäden, welche auf die postulierte protrahierte Ablations-wirkung der IRE hindeuteten (Abb.19).

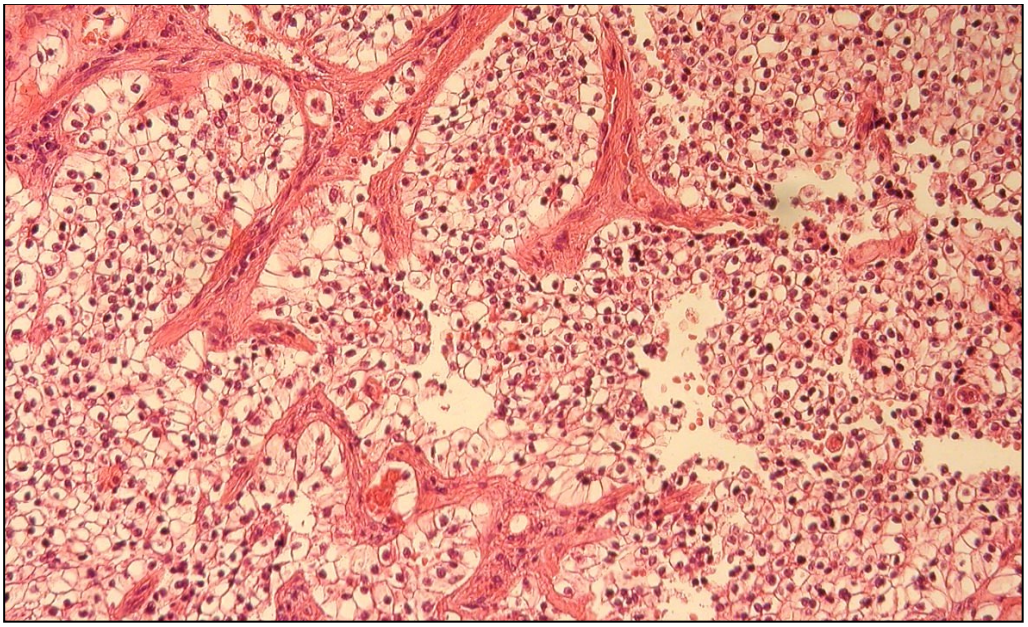

Abb.19: Typisches klarzelliges Nierenzellkarzinom (HE-Färbung) in 200-facher Vergrößerung ohne akute IRE-Veränderungen nach intraoperativer NanoKnife-System-Anwendung mit unmittelbar anschließender Nierentumorresektion (Nierenteilresektion) aus der Safety-Studie (Pech et al. 2011).

4.5 Stellungnahmen zur Anwendung der IRE bzw. des NanoKnife-Systems zur Behandlung von Lungentumoren und des lokalisierten Prostatakarzinoms basierend auf eigenen Untersuchungsergebnissen und verfügbarer Literatur

Aufgrund der postulierten Eigenschaften und klinischen allgemeinen Zulassung des NanoKnife-Systems zur IRE von Weichgewebe erfolgten international spezifische IRE-Anwendungen und Studien zu verschiedenen Organen. Vergleichend mit unseren eigenen Erfahrungen und im Hinblick auf die mögliche Übertragung dieser Ergebnisse auf eine Etablierung als tumorablatives, fokaltherapeutisches Verfahren in der Urologie erfolgte die Publikation kritischer Stellungnahmen.

Wendler JJ, Porsch M, Fischbach F, Pech M, Schostak M, Liehr UB. **Letter to the Editor Concerning "Irreversible Electroporation (IRE) Fails to Demonstrate Efficacy in a Prospective Multicenter Phase II Trial on Lung Malignancies: The ALICE Trial" by Ricke et al. 2015** (doi:10.1007/s00270-014-1049-0). Cardiovasc Intervent Radiol. 2015 Aug;38(4):1064-5.

Dupuy et al. beschrieben einen diffusen Alveolarschaden mit Fibrosierung und entzündlicher Infiltration bei gleichzeitig erhaltenen Bronchiolen und Blutgefäßen in gesunden in-vivo-Schweinelungen nach perkutaner IRE (Dupuy et al. 2011). Thomson et al. äußerten Schwierigkeiten, einen gewünschten Stromfluss gemäß IRE-Zielparameter in der Lunge zu erhalten und relativierten die Indikation zur möglich Anwendung in der Lunge (Thomson et al. 2011; Rubinsky et al. 2010). Usman et al. veröffentlichen die Behandlung von 2 Patienten mit größenregredienten Lungentumoren nach IRE (Usman et. al 2012).

Ricke et al. führten die erste klinische Pilotstudie zum Wirksamkeitsnachweis der IRE von Lungentumoren mit 23 Patienten durch (Ricke et al. 2015). Aufgrund einer nicht sicher reproduzierbaren IRE und einer konsekutiv unzureichenden Tumorkontrolle (61% Progression, 69% inkomplette Ablation, 30% komplette Remission, 13% Punktions-kanalmetastasen) schlussfolgerte die Studiengruppe, dass die IRE zur pulmonalen Anwendung nicht effektiv sei (Ricke et al. 2015).

Mit unserem „Letter to the Editor" stellten wir die generelle Zulassung der IRE bzw. des NanoKnife-Systems für die Ablation von Weichgewebe in Frage, da die IRE als nonthermoablatives Verfahren stark von der Textur und damit der elektrischen Leitfähigkeit (Konduktivität) des Zielgewebes abhängig ist. Bis dato gab es in der verfügbaren Fachliteratur nur vorläufige Ergebnisse zur IRE-Ablationseffektivität aus Phase-I-Safety-Studien zur Tumoren verschiedener Entitäten in Niere, Pankreas, Leber und Prostata ohne

Nachweis einer kurativen Malignomablation mittels IRE/ NanoKnife-System. Verfahrensspezifisch stellen hohe Impedanzsprünge in sehr inhomogenem Zielgewebe einen Wirkverlust der IRE dar. Zur Gewebeablation benötigen die IRE-Elektroden eine gute elektrische Ankopplung an das Zielgewebe. Mit dieser Stellungnahme postulierten wir, dass diese Bedingung aufgrund der schwammartigen Lungenstruktur nicht gegeben ist, weil Alveolarluft als starker, elektrischer Isolator wirkt. Weiterhin postulierten wir, dass größere inhomogene Hohlraumstrukturen mit einer Bindegewebsmatrix (größere Drüsengänge, Blutgefäße, Gallengänge, Harnröhre, Bronchien etc.) sowie Verkalkungen (Sklerose, Knochen, Lithiasis) zwar als funktionelle Strukturen im Rahmen der IRE geschont werden können, aber diese Strukturen ebenso eine IRE-Wirkung stören (conductivity sink effect). Daher seien die schlechten Ablationsergebnisse der IRE von Lungentumoren auch zu erwarten, weshalb wir für die IRE-Anwendung verfahrensspezifisch im Gegensatz zu thermoablativen Techniken eine Kontraindikation sehen.

Wendler JJ, Ganzer R, Hadaschik B, Blana A, Henkel T, Köhrmann KU, Machtens S, Roosen A, Salomon G, Sentker L, Witzsch U, Schlemmer HP, Baumunk D, Köllermann J, Schostak M, Liehr UB; Working Group for Focal and Microtherapy, Academy of the German Society of Urology. [**Irreversible electroporation. Current value for focal treatment of prostate cancer**]. Urologe A. 2015 Jun;54(6):854-62.

Ziel unserer eigenen Untersuchungsreihen war es, die Erkenntnisse aus der Anwendung an der Niere bzw. der Behandlung des lokal begrenzten Nierenzellkarzinoms auf das Prostatakarzinommodell zu übertragen und eine eigene Sicherheits- und Wirksamkeits-nachweisstudie zur IRE des lokalisierten Prostatakarzinoms durchzuführen. Aufgrund vorhandener etablierter, konkurrierender Verfahren wie die radikale Prostatektomie (offen, laparoskopisch, robotisch-assistiert), perkutane Strahlentherapie, Brachytherapie und HIFU war eine primäre Anwendung und Pilotstudiendurchführung zur IRE der Prostata ohne ausreichender Voruntersuchungen kritisch bewertet worden. Nach klinischer Zulassung der IRE für Weichgewebsablationen erfolgte außerhalb unseres Zentrums trotz fehlender Erkenntnisse eine kommerzielle Anwendung ohne Studien (Guenther et al. 2019).
Die Sicherheit und Wirkung der IRE mittels NanoKnife-System wurde in der Laienpresse als neue, schonende Therapiemethode gegen Prostatakrebs propagiert. Interessierte Patienten wurde gegen sehr hohe, private Kosten dieses Verfahren als Behandlungsalternative angeboten. Daraufhin publizierte der Arbeitskreis für fokale und Mikrotherapie der Akademie (AKFM) der Deutschen Gesellschaft für Urologie (DGU) e.V. eine kritische Stellungnahme und Übersichtarbeit zur IRE-Wendung an der Prostata. Wir schlussfolgerten im Konsens, dass die IRE bzw. das NanoKnife-System aufgrund der bisherigen Datenlage keine

Alternative zu etablierten Behandlungsmethoden des Prostatakarzinoms darstellt. Weiterhin ist eine nebenwirkungsfreie Anwendung im Bereich der Prostata nicht bewiesen. Eine kommerzielle Anwendung und Anwendung außerhalb von Studien könne nicht empfohlen werden. Die DGU reagierte daraufhin mit entsprechenden Stellungnahmen im Konsens, um gegen die fachlich ungerechtfertigte und ethisch nicht vertretbare Kommerzialisierung der IRE als neues Verfahren mit hohem Potential vorzugehen. Nach dieser deutschsprachigen und durchaus medizinpolitischen Publikation folgte das internationale englischsprachige Review.

Wendler JJ, Ganzer R, Hadaschik B, Blana A, Henkel T, Köhrmann KU, Machtens S, Roosen A, Salomon G, Sentker L, Witzsch U, Schlemmer HP, Baumunk D, Köllermann J, Schostak M, Liehr UB. **Why we should not routinely apply irreversible electroporation as an alternative curative treatment modality for localized prostate cancer at this stage.** World J Urol. 2017 Jan;35(1):11-20.

Mit diesem Review erfolgt die erste umfassende Zusammenfassung und Bewertung der aktuellen Datenlage nicht nur im Hinblick auf die Anwendung und Wirkung in der Prostata, sondern auch im Hinblick auf die möglichen Nebenwirkungen (Inkontinenz, Blasen-entleerungsstörungen, Strikturen, Darmläsionen) angrenzender Risikoorgane und –strukturen (periphere Nerven / Gefäß-Nervenbündel und Darm). Abschließend werteten wir gemäß dem Publikationstitel, dass die IRE derzeit nicht als alternative Therapiemethode des lokalisierten Prostatakarzinoms routinemäßig und nicht außerhalb von klinischen Studien angewendet werden sollte.

Die Europäischen Gesellschaft für Urologie (EAU) bewertete In ihrem aktuellen Positionspaper 2018 die klinisch verfügbaren Fokaltherapietechniken des lokalisierten Prostatakarzinoms (van der Poel et al. 2018). Dabei zitierte sie bestätigend die o.g. Publikation (Wendler et al. 2017a). Sie fasste zusammen, dass die IRE des Prostatakarzinoms zwar vielversprechend und weitgehend sicher sei, aber zum aktuellen Stand die IRE-Ablationszone weder exakt fokal und kalkulierbar zu applizieren, noch eindeutig zu monitorieren sei, wobei eine hohe Rate an Rezidiven bzw. Persistiven/ Residuen argumentativ angeführt wurde (van der Poel et al. 2018).

Neuere Studien zur IRE des lokal begrenzten Prostatakarzinoms sind jedoch sehr vielversprechend (Wiggermann et al. 2017; Ting et al. 2016; van den Bos et al. 2016a; van den Bos et al. 2016b; Gebauer et al. 2017; Baur et al. 2017; van den Bos et al. 2018; Scheltema et al. 2018; Guenther et al. 2019; Giganti et al. 2019).

Wendler JJ, Klink F, Seifert S, Fischbach F, Jandrig B, Porsch M, Pech M, Baumunk D, Ricke J, Schostak M, Liehr UB. **Irreversible Electroporation of Prostate Cancer: Patient-Specific Pretreatment Simulation by Electric Field Measurement in a 3D Bioprinted Textured Prostate Cancer Model to Achieve Optimal Electroporation Parameters for Image-Guided Focal Ablation.** Cardiovasc Intervent Radiol. 2016 Nov;39(11):1668-1671.

Ausgehend von den vorläufigen Untersuchungsergebnissen zur IRE der Prostata bzw. des Prostatakarzinoms (Wendler et al. 2017a) postulierten wir den Bedarf eines in-vivo-Prostatakarzinom-Prostatatmodells zur Simulation und Definition spezifischer und individualisierbarer IRE-Parameter zur fokalen, kurativen Therapie (Rubinsky et al. 2008; Neal et al. 2014; van den Bos et al. 2016a; van den Bos et al. 2016b). Hintergrund dieser Überlegung sind für eine fokale Therapie relevante, patientenindividuell variable Kenngrößen zum Prostatakarzinom, wie zum Beispiel Prostataform- und volumen, Tumorlage und –ausdehnung, Prostata- und Tumortextur, Gewebedichte, Zysten, Prostatolithiasis, Harnröhren- und Samenbläschen-konfiguration etc. (Ganzer et al. 2017; Ganzer et al. 2018).
Wir beschrieben einen möglichen experimentellen Versuchsaufbau aus einer in-vivo-3D-Prostatakarzinomtumor aus kultivierten PCA-Zelllinien mittels 3D-Bioprinttechnologie basierend auf patientenindividuellen MRT-Bildern einer multiparametrischen MRT der Prostata. Anhand dieses Modells wäre eine individualisierte IRE-Ablationssimulation zur Definition der individuellen „optimalen“ IRE-Anwendung (Elektrodenkonfiguration und IRE-Parameter) möglich.
Arena et al. schlugen bereits ein 3D-Tumormodell als in-vitro-Krebszellkultur in einem Kollagen-I-Hydrogel zur IRE-Parametertestung vor, was jedoch keine intratumorale Gewebsdichteunterschiede und keine Grenzstrukturen berücksichtigte (Arena et al. 2012). Sano et al. testeten in einem solchen Modell bereits die Ablationswirkung von high frequency IRE (H-FIRE) im Hinblick auf eine äquivalente IRE-Ablation ohne provozierende Muskelkontraktionen für eine Anwendung ohne Allgemeinnarkose und ohne Muskelrelaxation (Sano et al. 2018a; Sano et al. 2018b). Zhang et al. nutzen dieses Modell zur Klärung der Gwebekonduktivitäts-änderungen während und nach IRE (Zhang et al. 2019).

4.6 Standardisierung der Terminologie und Reportkriterien zur IRE für die Vergleichbarkeit von Studienergebnissen zur IRE und anderen Ablationsmethoden

Die IRE mittels NanoKnife-System als neuartige Methode stellt eine komplexe Ablationsbehandlung mit verfahrensspezifischen Parametereinstellungen dar (Manual 2011). Um die publizierten Ergebnisse solcher Studien vergleichen zu können, bedarf es einer einheitlichen Terminologie der IRE-spezifischen Geräteeinstellungen und Prozeduren.
Die Internationale Arbeitsgruppe für bildgeführte Tumorablationstechniken (International Working Group on Image-Guided Tumor Ablation) definierten 2003 und in einem Update 2014 definierten entsprechend international einheitliche Klassifikationskriterien für verschiedene Tumorablationsverfahren (Goldberg et al. 2003; Ahmed et al. 2014a; Ahmed et al. 2014b; Ahmed et al. 2014a; Ahmed et al. 2014c). Deren Hauptziel war die Kommunikation zu den Ablationstechniken zu präzisieren, um einen methodischen Vergleich und eine bessere Patientenbehandlung zu ermöglichen. Dabei wurde jedoch die IRE im Detail mit ihrer verfahrensspezifischen Wirkweise nicht ausreichend berücksichtigt (Ahmed et al. 2014a; Ahmed et al. 2014b). Da es meist an randomisierten Studien verschiedener Ablationsverfahren fehlt, sind Metaanalysen umso wichtiger. Diese benötigen vor allem eine vergleichbare, standardisierte Terminologie, Methodik und Reportkriterien.

Wendler JJ, Fischbach K, Ricke J, Jürgens J, Fischbach F, Köllermann J, Porsch M, Baumunk D, Schostak M, Liehr UB, Pech M. **Irreversible Electroporation (IRE): Standardization of Terminology and Reporting Criteria for Analysis and Comparison**. Pol J Radiol. 2016 Feb 17;81:54-64.

Die zahlreichen klinischen Publikationen zur IRE-Anwendung weisen eine sehr variable Terminologie auf. Weiterhin wurden und werden notwendige Kenndaten zur Beurteilung der IRE-Applikation und -Resultate nicht einheitlich bzw. oft nicht publiziert, was eine Interpretation und Metaanalyse deutlich erschwert. Als neuartiges Verfahren zeigte sich eine entsprechend exponentiell steigende Publikationszahl von Original- und Übersichtsarbeiten zur IRE (Abb.20).

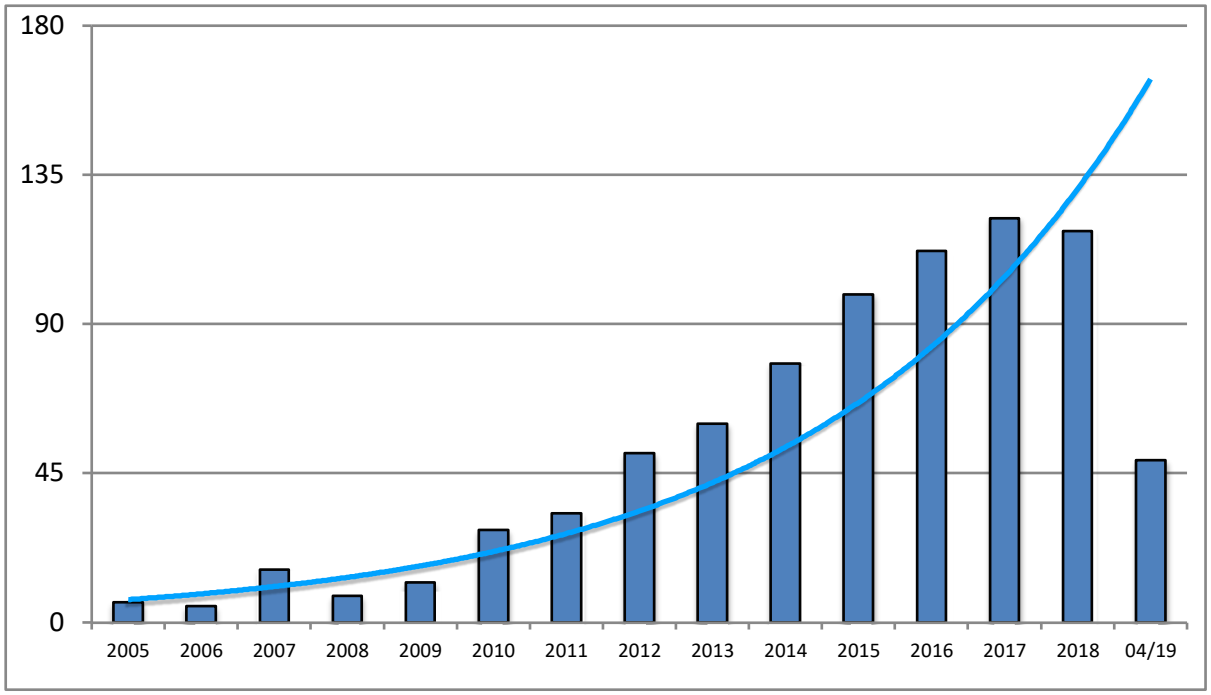

Abb.20: Anzahl der Publikation zur IRE in PubMed seit 2005 (Stand PubMed 26.04.2019).

Um diese Problematik und Anforderungen auf die IRE-Anwendung und -Publikationen zu übertragen, erfolgte unsererseits die erstmals notwendige Darstellung und Empfehlung einer einheitlichen Terminologie und Prozedurdarstellung der IRE mit Berücksichtigung internationaler Empfehlungen für bildgeführte Ablationsverfahren. In diesem Kontext ist dies die einzige Publikation zur IRE, welche frei verfügbar auch als Hilfestellung für andere Anwender des NanoKnife-Systems dienen soll. Darüber hinaus kalkulierten wir Empfehlungen zur IRE-Planung und IRE-Elektrodenkonfiguration für definierte Tumor- bzw. Zielvolumina.

4.7 Fokale Therapie des lokal begrenzten Nierentumors bzw. Nierenzellkarzinoms – Behandlung und Nachsorge

Diese Veröffentlichung verfasste der Arbeitskreis für fokale und Mikrotherapie der Akademie (AKFM) der Deutschen Gesellschaft für Urologie (DGU) e.V. auf Einladung durch das Journal „Der Urologe“ als Organ der Deutschen Gesellschaft für Urologie.
In dieser Übersichtsarbeit erfolgten u.a. die Darstellung des IRE-Verfahrens und deren derzeitiger Stellenwert in der fokalen Therapie des lokalbegrenzten, kleinen Nierentumors. Wir resümierten die ersten Ergebnisse resektionshistologischen Wirksamkeitsnachweise nach IRE von pT1a Nierenzellkarzinomen (Wendler et al. 2016b; Wendler et al. 2016c). Die IRE stellte damit ein neues, potentiell alternatives, nonthermales Ablationsverfahren von kleinen Nierentumoren mit möglichen Vorteilen gegenüber anderen thermoablativen Techniken (RFA, Kryoablation, Mikrowellenablation, HIFU) und strahlentherapeutischen Methoden (perkutaner Radiatio und Brachytherapie) dar. Weitere analoge Arbeiten zur Fokalen Therapie des lokalbegrenzten Nierentumors folgten (Wendler et al. 2018c; Wendler et al. 2018d).

Wendler JJ, Friebe B, Baumunk D, Blana A, Franiel T, Ganzer R, Hadaschik B, Henkel T, Köhrmann KU, Köllermann J, Kuru T, Machtens S, Roosen A, Salomon G, Schlemmer HP, Sentker L, Witzsch U, Liehr UB, Ricke J, Schostak M. [**Focal therapy for small renal masses: Observation, ablation or surgery**]. Urologe A. 2016 May;55(5):594-606.

Ein grundlegendes, methodisches Problem stellt die Nachbeobachtung und Befundbeurteilung nach fokaler Therapie von Nierentumoren dar. Die internationalen sowie deutschen Leitlinien zum Nierenzellkarzinom und die internationalen Empfehlungen zur Terminologie und zu den Reportkriterien nach bildgeführter Tumorablation (Goldberg et al. 2003; Ahmed et al. 2014a; Ahmed et al. 2014b; Ahmed et al. 2014a; Ahmed et al. 2014c; EAU 2019, AUA 2017, AWMF 2017) definierten keine detaillierten, konsensualen Bewertungsmaßstäbe zum Follow-up. Im Gegensatz zur chirurgischen Nierentumorentfernung verbleibt verfahrensspezifisch nach ablativen Methoden destruiertes Nierentumorgewebe im Zielgebiet. So weisen verschiedene Tumorablationsverfahren unterschiedlich Regressionsmuster des Tumors auf. Während thermoablative Verfahren eine unmittelbare Koagulationsnekrose verursachen, weisen zum Beispiel nonthermoablative Verfahren wie die Strahlentherapie eine prolongierte Tumor-involution auf. Die IRE am ehesten eher ein „Mischbild“ beider dar.
Aufgrund dieser Problematik einer fehlenden einheitlichen Empfehlung zur Nachsorge nach Ablation von Nierentumoren wurde 2015 im Rahmen des 8. Internationalen Symposiums für

Fokale Therapie und Bildgebung des Prostata- und Nierenzellkarzinoms eine interdisziplinäre Diskussion und mehrstufige Befragung der Mitglieder als Konsensverfahren angestrebt.

Zondervan PJ, Wagstaff PG, Desai MM, de Bruin DM, Fraga AF, Hadaschik BA, Köllermann J, Liehr UB, Pahernik SA, Schlemmer HP, **Wendler JJ**, Algaba F, de la Rosette JJ, Laguna Pes MP. **Follow-up after focal therapy in renal masses: an international multidisciplinary Delphi consensus project**. World J Urol. 2016 Dec;34(12):1657-1665. Epub 2016 Apr 22.

Mit dieser interdisziplinären Arbeit erfolgte durch die Expertengruppe zur Fokalen Therapie des Nierenzellkarzinoms eine detaillierte Definition von Rezidiv bzw. Persistiv, einer Risikostratifikation, der Follow-up-Intervalle, der risikoadaptierten Bildgebungstechniken zur Ablationskontrolle und zum Restaging, der Indikation von Kontrollbiopsien nach Ablation. Sie gilt als Handlungsempfehlung oder Grundlage für diese bisherigen „Graubereiche“, bis anhand einer eindeutigeren Datenlage eine Implementierung in die fachspezifischen Leitlinien erfolgt (Zondervan et al. 2016).
Die bildgebende Kontrolle sollte mittels feinschichtiger 3-Phasen-Kontrastmittel-CT oder multiparametrischer Kontrastmittel-MRT durch frühestens 3 Monate nach Ablation und mindestens für 5 Jahre, am besten 10 Jahre durchgeführt werden. Ein Residuum bzw. Persistiv des Tumors sei durch ein persistierendes, radiologisches Kontrastmittel-enhancement ab 3 Monate nach Ablation definiert. Ein Rezidiv sei durch ein neu- bzw. wiederaufgetretenes Kontrastmittelenhancement oder durch eine Größenprogredienz innerhalb oder am Rand der Ablationszone definiert. Nur im Fall eines o.g. radiologischen Verdachts eines Persistivs oder Rezidivs werden Kontrollbiopsien empfohlen.

4.8 Klinische Pilotstudie zum Wirksamkeitsnachweis der IRE im in-vivo-Nierentumorhumanmodell Phase II a

Trotz fehlender erkrankungsspezifischer Sicherheits- und vor allem Wirksamkeitsnachweise mittels prospektiver Studien erhielt die Firma AngioDynamics Inc. (NY, U.S.A.) 2007/ 2008 die Zulassung ihr Medizinprodukt „NanoKnife® System“ zur Ablation von Weichgewebe.

Für das NanoKnife-System wurde eine nonthermale, fokussierbare, perkutane leicht applizierbare, komplette IRE-Ablation von Nierentumoren/ Nierenzellkarzinomen <4cm postuliert (Pech et al. 2011; Liehr et al. 2012; Wendler et al. 2013). Verfahrensspezifisch soll die IRE-Ablationszone mit einer geringen Transitions-szone scharfbegrenzt sein, was einen geringen Kollateralschaden des angrenzenden gesunden Nierenparenchyms mit größtmöglichem Nephronerhalt bedeutet. Durch eine Schonung von angrenzendem Nierenbeckenkelchsystem und involvierten größeren Blutgefäßen sei ein funktioneller Nierenerhalt auch bei zentral gelegenen Nierentumoren mit Nierenhilus-naher IRE möglich. Diese Eigenschaften versprächen entsprechende Vorteile gegenüber etablierten, thermoablativen Techniken und der chirurgischen Resektion (Zondervan et al. 2019; Wah et al. 2014; Johnson et al. 2004; Patel et al. 2017; Pierorazio et al. 2016).

Aufbauend auf unsere eigenen experimentellen Untersuchungen, präklinischen Tierversuchsstudien und der Phase-1-Safety-Pilotstudie sollten nun die o.g. postulierten Eigenschaften des NanoKnife-Systems in einer klinischen Pilotstudie zum Wirksamkeitsnachweis der IRE von lokal begrenzten Nierenzellkarzinomen überprüft werden. Da es sich um eine Medizinproduktstudie zum Wirksamkeitsnachweis handelte, erfolgte die Beantragung zur Genehmigung beim Deutschen Institut für Medizinische Dokumentation und Information (DIMDI) sowie der Bundesinstitut für Arzneimittel und Medizinprodukte (BfArM) nach Erhalt eines positiven Votums der zuständigen Ethikkommission (Medizinische Fakultät Magdeburg). Der geforderte Prüfplan wurde gemäß SPIRIT Leitlinien (Schulz et al. 2013; Calvert et al. 2018) peer-reviewed, international publiziert und in internationalen und nationalen Studienregistern registriert.

Wendler JJ, Porsch M, Nitschke S, Köllermann J, Siedentopf S, Pech M, Fischbach F, Ricke J, Schostak M, Liehr UB. **A prospective Phase 2a pilot study investigating focal percutaneous irreversible electroporation (IRE) ablation by NanoKnife in patients with localised renal cell carcinoma (RCC) with delayed interval tumour resection (IRENE trial).** Contemp Clin Trials. 2015 Jul;43:10-9.

Diese Studienprotokollpublikation umfasst im Detail folgende GCP-konforme Aspekte: Einleitung und Grundlagen, Studientitel, Studien-registrierung, Studiengenehmigung, Studienmanagement, Studienrichtlinien, Studiendesign, Studienrationale, Studienziele (Primär- und Sekundärziele), Studienpopulation, Studienzugangs- und -teilnahme-bedingungen, Rekrutierungsbestimmungen, Ein- und Ausschlusskriterien, Studien-flussdiagramm (trial flow chart), Prüfplanalgorithmus, alle Untersuchungs- und Behandlungsmethoden, Nachsorgebestimmungen (follow-up), Definitionen und Management unerwünschter Wirkungen, Abbruchbestimmungen, Fallzahlkalkulation, Statistische Analyse, Monitoring, Auditing, Rechtliche und ethische Bestimmungen, Studienlimitationen, Diskussion der Studienrationale (Wendler et al. 2015b).
Ziel der Studie war die Evaluation der perkutanen, Irreversiblen Elektroporation (IRE) als primäres Ablationsverfahren von lokal begrenzten Nierenzellkarzinomen pT1a cN0 cM0 (≤4cm) mit anschließender sequentieller, operativer Tumorresektion nach 4 Wochen (short-follow-up). Dabei soll der Ablationserfolg der IRE bildgebend und histologisch überprüft werden (Proof of Principle).

Die Primärziele dieser Studie waren:

- Onkotherapeutische Effektivität, gemessen am Anteil vitaler Tumorreste im resektionshistopathologischen und bildgebenden Befund
- Klinische Durchführbarkeit der perkutanen Irreversiblen Elektroporation von lokalisierten Nierenzellkarzinomen mittels NanoKnife-System

Die Sekundärziele dieser Studie waren:

- Prozedurale Verträglichkeit der IRE und der nachfolgenden Turmorresektion
- Unerwünschte Wirkungen des prozeduralen Vorgehens zur Tumorentfernung, Safety

Unsere Pilot-Studie ist durch folgende Kenndaten gekennzeichnet:

- Studientitel
  - Lang: Prospektive, monozentrische, klinische Studie Phase-I/II zur Prüfung der klinischen Wirksamkeit perkutaner, irreversibler Elektroporation (IRE) bei Patienten mit lokal begrenzten Nierenzellkarzinomen – IRENE.
  - Kurz: IRreversible Elektroporation von Nierentumoren vor Ektomie – IRENE.
- Studiendesign:
  - Klinische Studie, Interventionsstudie, Phase 1-2 (2a), Pilot-Studie
  - Prüfung auf Durchführbarkeit und Wirksamkeit eines Medizinproduktes Klasse II b (MPG-Studie)
  - Prospektiv, monozentrisch
  - Einarmig, unkontrolliert, nicht-randomisiert, offen, nicht verblindet
- Studien-IDs:
  - Zentrum Urologische Univ.klinik Magdeburg Deutschland: DE-UKMD-URO-001
  - EUDAMED-Nummer (BfArM): CIV-12-04-006021
  - BfArM-Nr.: DE/EKST41/00020520
  - DIMDI: 00007531, 00020520, 00013378
  - Zuständige Ethikkommission (Med.Fakultät der Universität Magdeburg): 73/12
- Studienregistrierung:
  - Clinical-Trials-Gov: NCT01967407
  - Deutsches Register für Klinische Studien (DRKS): DRKS00004266
  - Clinical Trial Registry Platform (CTRP): DRKS00004266
  - WHO-Studienregister: DRKS00004266
  - Universal Trial Number (UTN): U1111-1140-0415
- Prüfprodukt:
  - NanoKnife-System von AngioDynamics (CE 0086) NanoKnife Electroporation Ablation System, AngioDynamics Inc., Latham, NY 12110, USA).
  - NanoKnife Generator (CE 0050) + NanoKnife Elektroden (CE 0051) – HVP 01
  - Medizinproduktklasse:
    - Class IIb device according to the Risk Classification for Medicinal Products of the FDA
    - Class II b according to the European regulation 93/42/EWG
  - NanoKnife-Procedure-Guide 2.2.0 German AngioDynamics Inc.
  - Planungssoftware: NanoKnife-ProcedureManage-2_2_0_23.msi windows
  - NanoKnife-Auslesesoftware: IRE Data conversion (xml) – AngioDynamics Inc.
  - EKG-Synchronisation: AccuSync® 72, AccuSync Medical Research Corp:, Milford,CT, USA)

Mit dieser Publikation des Studiendesigns ist es möglich die gesamte Methodik detailliert darzustellen. Dies ist aus kapazitären Gründen und der einschränkenden Publikationsvorgaben der jeweiligen Zieljournale für Folgepublikationen zu einzelnen Studienergebnissen nicht möglich. Ein zitierfähiger Verweis auf die Methode, sowie ein kritischer Abgleich zwischen Studienplanung, -durchführung und -ergebnispublikation ist somit jederzeit transparent möglich.

Zeitgleich zu unserem Studienprotokoll veröffentlichten Wagstaff et al. (Wagstaff et al. 2015) ein analoges Studienprotokoll zur IRE von lokalbegrenzten Nierentumoren mit Indikation zur Tumornephrektomie (Sicherheits- und Wirksamkeitsnachweisstudie). Bei 10 Patienten sollte die perkutane, CT-gestützte IRE des Nierentumors unmittelbar nach stanzbioptischer Sicherung, bildgebende Verlaufskontrollen mittels MRT- und Kontrastmittelultraschall (CEUS) sowie die Tumornephrektomie nach 4 Wochen durchgeführt werden (Wagstaff et al. 2015). Es wurden keine Daten zu dieser Studie publiziert. Nach Korrespondenz mit der Studiengruppe um de la Rosette at al. gelang diesem Studienzentrum aufgrund des zweizeitigen Interventionsschemas in Intubationsnarkose, der verzögerten definitiven, chirurgischen Therapie und des experimentellen Charakters der IRE keine Patientenrekrutierung für diese Studie.
Als Alternative dazu publizierte die gleiche Arbeitsgruppe ein Protokoll einer Phase-2-Studie zur perkutanen IRE von Nierentumoren (small renal masses) von 20 Patienten mit rein bildgeführter Kontrolle des IRE-Ablationserfolges per CEUS, CT und MRT (Buijs et al. 2017).
Zu weiteren klinischen Studien über IRE von Nierentumoren (Diehl et. al. 2016; Trimmer et al. 2015; de la Flor-Robledo et al. 2016; Canvasser et al. 2017) wurden keine separaten Studienprotokolle in gelisteten Fachjournalen publiziert.

Wendler JJ, Ricke J, Pech M, Fischbach F, Jürgens J, Siedentopf S, Roessner A, Porsch M, Baumunk D, Schostak M, Köllermann J, Liehr UB. **First Delayed Resection Findings After Irreversible Electroporation (IRE) of Human Localised Renal Cell Carcinoma (RCC) in the IRENE Pilot Phase 2a Trial.** Cardiovasc Intervent Radiol. 2016 Feb;39(2):239-50.

Mit dieser Publikation erfolgte die erste und detaillierte Veröffentlichung zu resektions-histologischen Analysen nach IRE von Nierenzellkarzinom der ersten 3 Patienten aus der o.g. IRENE-Studie. 4 Wochen nach IRE zeigten alle 3 Fälle eine hohen Grad an Tumorgewebsdestruktion bei jedoch einer jedoch überwiegend inhomogener Textur der Ablationszone. Die noch teilweise schemenhaft erkennbaren Tumorzellen wiesen unterschiedliche Regressionsgrade auf, für deren Zustandsbeschreibung eine adaptierte Regressionsgradklassifikation gewählt und empfohlen wurde. Mittels immunologischer Vitalitätsmarker wiesen 66% in den mikroskopischen Tumorresiduen lediglich avitale Tumorzellen auf. Die Tumoren und Ablationszonen wiesen eine deutliche Schrumpfung auf, wobei sich Ablationszone einen konzentrisch-zonalen Aufbau zeigte. Die innere Zone, bestehend aus einer ausgedehnten, homogen-amorphe Nekrose vom Koagulations-nekrosetyp, wurde umgeben von einer zweiten, schmaleren, konzentrischen, eher inhomogene Nekrosezone mit noch schemenhaft erkennbaren Tubuli und Glomeruli, sowie einer dritten, 1-5mm schmalen, konzentrischen Zone mit sekundären Ischämiezeichen bei teils okkludierten arteriellen Blutgefäßen mit Intimahyperplasie und a.e. reaktivem Granulationsgewebe. Das angrenzende Nierenparenchym wies keine Veränderungen auf. In die Ablation involvierte Nierenkelche zeigten urotheliale Regerationszeichen. Wir schlussfolgerten, dass eine komplette und Nieren-erhaltende Ablation von pT1a Nierenzellkarzinomen <3cm mittels perkutan CT-gestützter IRE per NanoKnife-System möglich ist. Die histologischen Befunde zeigen Momentaufnahmen einer protrahierten Tumordestruktion.

Cornelis et al. verglichen die Ablationszonen 24h nach IRE, RFA, Kryoablation (KA) und Mikrowellenablation (MWA) in Schweinenieren. Prinzipiell unterschieden diese Ablationstechniken histologisch nicht voneinander (Cornelis et al. 2017). Wie bei den thermoablativen Verfahren zeigte sich auch ein konzentrischer Aufbau der Ablationszone nach IRE. Dabei ergaben sich histologisch um die zentrale Nekrosezone größere und diffusere Transitionszonen (Mischbild aus vitalen und avitalen Zellen) nach IRE und RFA als nach KA und MWA, während die CT-morphologische Darstellung der Ablationszonen als inadäquat bewertete Bildgebungsmethode dies nicht differenzieren konnte (Cornelis et al. 2017).

Morgen et al. verglichen Nierengewebe von Schweinen 24h, 3,7, 14 und 28 Tage nach IRE, RFA und Nierenteilresektion (Morgan et al. 2016). Prinzipiell unterschieden IRE und RFA histologisch nicht voneinander (Morgan et al. 2016). Auch nach IRE zeigte sich auch ein konzentrischer Aufbau der Ablationszone. Aufgrund der Ausdehnung der Ablationszone samt Transitionszone sowie gleicher Nierenfunktionsparameter schlussfolgerten Morgen et al., dass die IRE keinen histologischen und funktionellen Vorteil gegenüber der RFA und Nierenteilresektion zeige (Morgan et al. 2016).

Wendler JJ, Ricke J, Pech M, Fischbach F, Jürgens J, Porsch M, Janitzky A, Baumunk D, Siedentopf S, Köllermann J, Schostak M, Liehr UB. **Initial assessment of clinical feasibility, safety and efficacy of NanoKnife irreversible electroporation (IRE) in the focal treatment of localized renal cell carcinoma (RCC) with delayed interval tumor resection (IRENE trial).** 32nd Annual EAU Congress, London. Eur Urol Suppl 2017; 16(3);e102.

Die vorläufigen Ergebnisse unserer Pilotstudie wurden zunächst in einer Übersichtsarbeit auf dem jährlichen Kongress der Europäischen Gesellschaft für Urologie (EAU) im März 2017 präsentiert (weltweit zweitgrößter und europäisch größter urologischer Kongress) (Wendler et al. 2017b). Hier erfolgte die zusammenfassende Darstellung der Patienten- und Tumordaten, IRE-Ablationsparameter, Interventionsdaten, MRT-Befunde, Nierenfunktionsparameter, Operationstechniken, makroskopisch-pathologischen Analysen, des histologischen Mappings, der mikroskopisch-histologischen Befunde, der Nebenwirkungen und des Ablationserfolges (Wendler et al. 2017b). Diese Befunde werden mittels nachfolgender Publikationen separat und detailliert dargestellt (Wendler et al. 2017b; Wendler et al. 2018a; Wendler at al. 2018b).

Die Pilot-Studie enthält folgende Kennzahlen:

- Studiendauer: 5,0 Jahre (01.09.2013 – 30.08.2018)
- Initiierung: 28.01.2013; Close-out-visit: 30.08.2018
- First patient in: 12.09.2013; Last patient out: 29.12.2015
- Avisierte Patientenzahl: 20 Patienten
- vorzeitige Beendigung der Studie nach 10 Rekrutierungen/ Patienten (3 drop-outs, siehe Abb.21)
- 7 auswertbare Patienten mit kompletter Prüfkaskade
- Datum des Prüfberichts / Abschlussberichts: 15.11.2018

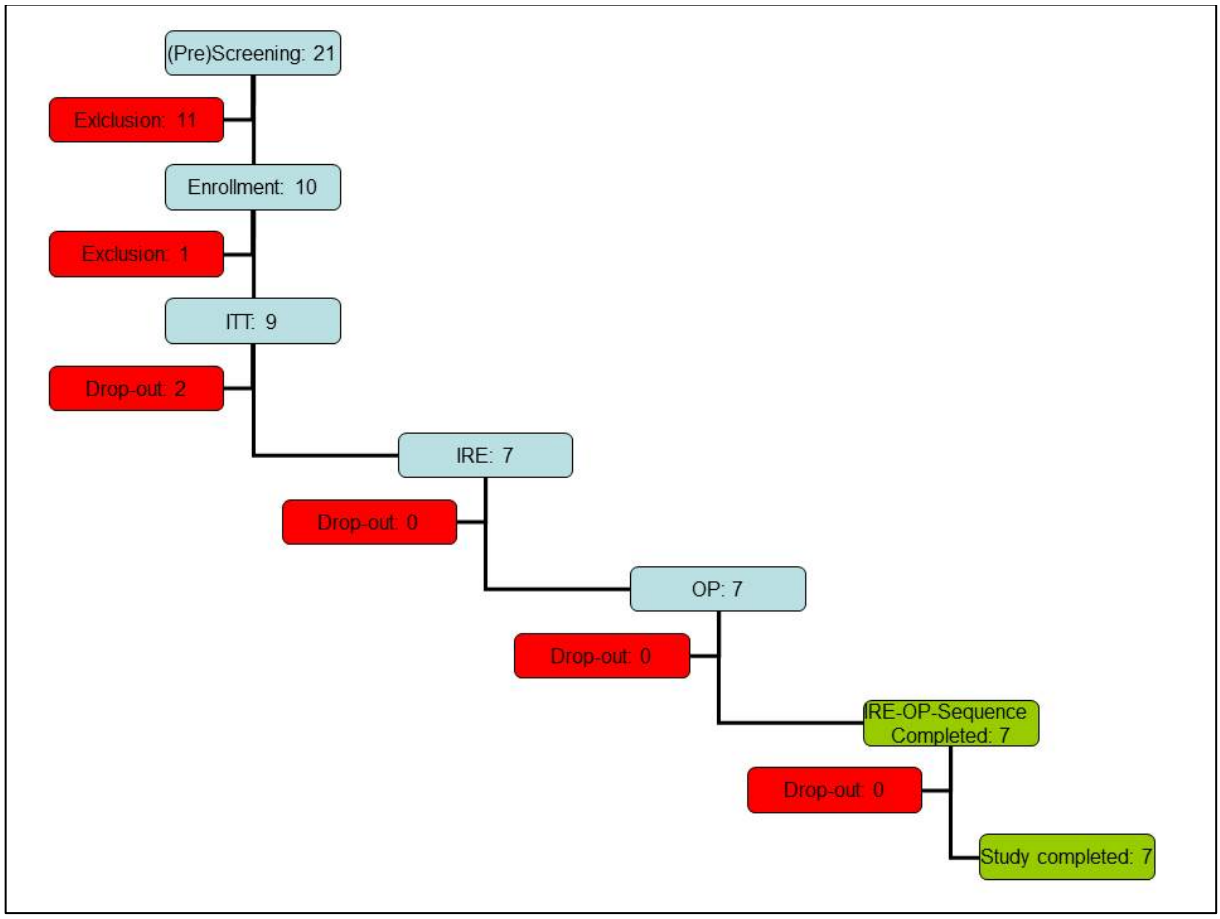

Abb.21: Study Content Flow Chart zur IRENE-Studie.

Sieben Patienten mit einem bioptisch-histologisch gesicherten Nierenzellkarzinom pT1a cN0 cM0 erhielten eine CT-gestützte, perkutane IRE des Nierentumors in Intubationsnarkose unter EKG-Triggerung. 28 Tage nach IRE erfolgte die komplette, offen-chirurgische Exploration und Resektion des Ablationsareals bzw. des Tumor oder die Tumornephrektomie nach urologischen Kautelen (siehe Abb.21). Die Resektate wurden detailliert histopathologisch befundet. Neben standardisierten, laborchemischen und klinischen Basisuntersuchungen wurden 1 Tag vor IRE sowie 2, 7 und 27 Tage nach IRE eine Kontrastmittel-MRT und Urinzytologie durchgeführt.

Die Ergebnisse der Pilot-Studie (IRENE) werden nachfolgend tabellarisch zusammengefasst. Einzelne Aspekte davon wurden davon separat publiziert und werden jeweils im Anschluss diskutiert (Wendler et al. 2017b; Wendler et al. 2018a; Wendler et al. 2018b).

Patient	**P1**	**P2**	**P3**	**P4**	**P5**	**P6**	**P7**
Age / Sex	44 / M	78 / M	74 / M	73 / M	74 / M	71 / F	61 / M
Tumour	**P1**	**P2**	**P3**	**P4**	**P5**	**P6**	**P7**
Targets	1	1	1	1	2	1	1
Location	UP, right, cortical, exophytic, ventrolateral	UP/MP, right, cortical, exophytic, dorsomedial	UP/MP, right, cortical, exophytic, dorsomedial, hilum (central)	UP, right, cortical, exophytic, lateral	LP/MP, right, cortical, exophytic, lateral, medio-central satellite	UP/MP, right, cortical, exophytic, ventrolateral	LP, left, cortical, exophytic, dorsomedial
PADUA	6	8	11	6	8	6	7
Size (cm)	1.7×1.7×1.6	1.5×1.5x1.4	1.6 ×1.5×1.5	2.2×2.1×1.9	3.9×3.8×3.1; 1.8×1.5×1.7	2.4×2.4×2.0	1.4×1.1×1.8
Volume (cm^3)	2.4	1.6	1.9	4.6	24.1+2.8=26.9	6.0	1.5
Shape	spherical,	spherical,	spherical,	spherical,	elliptic-spherical	spherical,	spherical,
Biopsy	papRCC,G2	eos-ccRCC, G1	ccRCC, G1	ccRCC, G1	ccRCC, G1	ccRCC, G2	papRCC, G2
Texture	solid	solid	solid	cystic-solid	solid	solid	solid
TNM	pT1a G2	pT1a G1	pT1a G1	pT1a G1	pT1a G1	pT1a G2	pT1a G2

Tab.2: Übersicht Patientendaten zur IRENE-Pilotstudie (Wendler et al. 2017b).

IRE	P1	P2	P3	P4	P5	P6	P7
Sessions; Ablations	1; 1	1; 1	1; 1	1; 1	1; 2	1; 1	1; 1
Rounds	4	2	3	4	2+2	2	2
No. of electrodes / pairs / configuration	4 / 6 / square	3 / 3 / triangular	4 / 6 / square	4 / 6 / square	3 / 3 / triangular; 6 / 10 / pentagonal with centre	3 / 3 / triangular	3 / 3 / triangular
Tip exposure	2.5 cm	1.5 cm	2.0 cm	2.0 cm	2.0 and 2.5 cm (pull-back)	2.5 cm	2.0 cm
Planned Treatm. zone (cm) / (cm^3)	2.4 × 2.9 × 3.5 / 12.7	2.5 × 2.5 × 2.5 / 8.2	3.5 × 4.0 × 3.0 / 22.0	3.0 × 3.0 × 2.9 / 13.7	2.7 × 2.7 × 2.7 / 10.3 and 4.4 × 4.4 × 4.5 / 45.6	3.0 × 3.3 × 3.0 / 15.6	2.4 × 2.9 × 2.8 / 10.2
Pulse length	90 µs	90 µs	90 µs	90 µs	70, 80, 90 µs	90 µs	70 and 90 µs
Pulses	1300	450	1320	840	570 + 880	450	510
Current min./ max.	30 / 49 A	30 / 42 A	30 / 49 A	25 / 49 A	22 / 50 A	28 / 50 A	20/ 35 A
Voltage min./max.	1800 / 2800 V	2200 / 2640 V	1960 / 3000 V	2160 / 3000 V	1800 / 2800 V	1850 / 2600 V	1820 / 2660 V
Intervention / Anaesthesia	131 / 193 min	126 / 162 min	163 / 208 min	123 / 194 min	203 / 317 min	53 / 91 min	104 / 181 min
Surgery	**P1**	**P2**	**P3**	**P4**	**P5**	**P6**	**P7**
Initial / pre-surgic. Crea	73 / 75 umol/l	69/ 66 umol/l	92 / 89 umol/l	96 / 101 umol/l	84 / 90 umol/l	101 / 102 umol/l	87 / 89 umol/l
Initial / pre-surgical GFR	107 / 106 ml/min	86 / 88 ml/min	70 / 73 ml/min	67 / 63 ml/min	78 / 72 ml/min	48 / 47 ml/min	82 / 80 ml/min
Resection type; access	Partial resection open lumbar	Partial resection open lumbar	Nephrectomy; open lumbar	Partial resection open-abdom.	Nephrectomy open lumbar	Partial resection open-abdom.	Partial resection open lumbar
OP/ Ischaem.	185 / 16 min	175 / 19 min	115 / 0 min	190 / 18 min	130 / 0 min	140 / 21 min	185 / 35 min
Pathology	**P1**	**P2**	**P3**	**P4**	**P5**	**P6**	**P7**
Ablation zone (cm) / (cm^3)	2.5 × 2.0 × 1.3 / 3.4	3.0 × 2.5 × 2.0 / 7.9	4.2 × 1.4 × 1.2 / 17.2	2.8 × 2.2 × 2.0 / 3.5	4.2 × 2.8 × 3.5 / 19.2	2.9 × 2.5 × 3.5 / 4.5	4.6 × 2.2 × 3.0 / 8.4
Tumour (cm) / (cm^3)	1.6 × 1.5 × 1.2 / 1.6	1.6 × 1.7 × 1.1 / 1.6	1.5 × 1.4 × 1.2 / 1.3	1.2 × 0.8 × 1.0 / 0.2	3.0 × 2.4 × 4.0 / 9.7	3.0 × 2.2 × 2.0 / 2.0	1.3 × 1.2 × 1.0 / 0.2
Coverage of tumour by ablation zone	complete	complete	complete	complete	incomplete	incomplete	complete
Residual tumour	0.28 cm^3; in-field	0.045 cm^3; in-field	1.185 cm^3; in-field	none	0.009 cm^3; out-field/margin	0.03 cm^3; out-field/margin	none
Regression	3°	4°	4°	4°	3°	3°	4°
Mib-1 index	0 %	0 %	0 %	0 %	1 %	1 %	0 %
viability	uncertain	non-viable	non-viable	non-viable	viable	viable	non-viable
TNM (IRE)	uncertain, ypT0-1a V0 L0 Pn0 R0-1	complete, ypT0 V0 L0 Pn0 R0	complete, ypT0 V0 L0 Pn0 R0	complete, ypT0 V0 L0 Pn0 R0	incomplete, ypT1a V0 L0 Pn0 R1	incomplete, ypT1a V0 L0 Pn0 R1	complete, ypT0 V0 L0 Pn0 R0
TNM (OP)	R0	R0	R0	R0	R0	R0	R0
Renal system	involved	involved	involved	involved	involved	involved	involved
Urothelium	regeneration	regeneration	regeneration	regeneration	regeneration	regeneration	regeneration
Urine cytology	temporary degeneration, vacuolisation	temporary degeneration, vacuolisation	temporary degeneration, vacuolisation	temporary degeneration, vacuolisation	temporary degeneration, vacuolisation	temporary degeneration, vacuolisation	temporary degeneration, vacuolisation

Tab.3: Übersicht Methodik und Ergebnisse zur IRENE-Pilotstudie (Wendler et al. 2017b).

Im Anschluss an die o.g. Erstbeschreibung initialer, histopathologischer Resektionsbefunde nach Irreversibler Elektroporation (IRE) an Nierentumoren (Wendler et al. 2016b) folgte die Veröffentlichung der Ergebnisse zur Auswirkung der IRE auf das Nierenbeckenkelchsystem bzw. das Urothel (Wendler et al. 2018b) analog zu unseren präklinischen Vorarbeiten am Tiermodell (Wendler et al. 2012b).

Wendler JJ, Pech M, Köllermann J, Friebe B, Siedentopf S, Blaschke S, Schindele D, Porsch M, Baumunk D, Jürgens J, Fischbach F, Ricke J, Schostak M, Böhm M, Liehr UB. **Upper-Urinary-Tract Effects After Irreversible Electroporation (IRE) of Human Localised Renal-Cell Carcinoma (RCC) in the IRENE Pilot Phase 2a Ablate-and-Resect Study.** Cardiovasc Intervent Radiol. 2017 Sep 19.

Dies stellt die erste Beschreibung von Effekten auf das Nierenbeckenkelchsystem mittels Magnetresonanztomographie (MRT), Urinzytologie und Resektionshistologie nach IRE von lokal begrenzten Nierenzellkarzinomen dar. Bei sieben von sieben Patienten war das Nierenbeckenkelchsystem im IRE-Ablationsareal involviert (bei 100% Nierenkelche und bei 29% Nierenbecken). Es zeigte sich bei allen Patienten eine postpunktionelle, leichtgradige, selbstlimitierende Makrohämaturie.

Die MRT 1-2, 7 und 27 Tage nach IRE demonstrierte in der Urographiephase bei allen Patienten ein erhaltenes Nierenbeckenkelchsystem ohne Urinextravasation (ohne Perforation) und normale Abflussverhältnisse des oberen Harntraktes ohne Stauung (ohne Striktur bzw. Obstruktion). Diese Beobachtung deckt sich mit den präklinischen Ergebnissen des Tierversuchs mittels MRT und Ausscheidungsurographie (Wendler et al. 2012b).

Mittels Urinzytologie konnte auch im Humanmodell erstmals die temporäre, spezifische Vakuolisierung des Zyto- und Karyoplasmas von abgeschilferten Urothelzellen 1-2 Tage nach renaler IRE nachgewiesen werden. Dieser Befund deckt sich mit den postulierten Beschreibungen einer protrahiert wirkenden IRE mit degenerativen Zell- und Kernmembranveränderungen (Rubinsky et al. 2010) und den eigenen präklinischen Erstbeschreibung aus dem Tierversuchsmodell (Wendler et. al 2012b). Bisher finden sich keine weiteren Zytologiebeschreibungen nach IRE in der verfügbaren Literatur. Diese o.g. Publikation stellen somit die ersten und einzigen Beschreibungen im klinischen Kontext dar, welche als scheinbar neues zytologisches, IRE-spezifisches Phänomen für die künftige Pathologiebefundung berücksichtigt werden sollte. Eine klinische Relevanz ließ sich bisher nicht ableiten.

Die Resektionshistologie 28 Tage nach IRE zeigte in allen Fällen ein an die Ablationszone bzw. Koagulationsnekrose und Narbe angrenzendes Nierenbeckenkelchsystem. Dessen Urothel wies Zeichen der Destruktion und Regeneration im Sinn eines reversiblen Epithelschadens auf. Diese Beobachtung konnte demzufolge im Humanmodell analog zum

Tierversuchsmodell reproduziert werden (Tracy et al. 2011; Deadhar et al. 2011; Wendler et al. 2012b). Grundlage für dieses Phänomen scheint die postulierte Schonung der nonzellulären Matrix der Submukosa und der Basalmembran zu sein (Phillips et al. 2010). Eine Perforation, Fistelung und Striktur des oberen harnableitenden Systems konnte ausgeschlossen werden, welche typische Risiken bzw. Nebenwirkungen von thermoablativen Techniken darstellen (Zondervan et al. 2019; Wah et al. 2014; Johnson et al. 2004; Patel et al. 2017; Pierorazio et al. 2016).

Im Gegensatz dazu beschrieben Srimathveeravalli et al. nach IRE des Harnleiters im Tierversuchsmodell zwar die ebenfalls keine Urinleckage, jedoch eine massive Granulation und Vernarbung der ureteralen Tunica muscularis mit konsekutiver Obstruktion und Harnstauung (Srimathveeravalli et al. 2015; Srimathveeravalli et al. 2017). Demzufolge scheint die IRE von Harnleitertumoren (Urothelkarzinome, Endometriose, Harnleiter-involvierende extraureterale Tumoren) keine Therapiealternative darzustellen. Vergleichsweise dazu berichteten Wendler et al. teilweise von einer luminalen Okklusion renaler Arteriolen aufgrund einer Hyperplasie der Tunica media (Wendler et al. 2016b). Diese Problematik stellt sich beim Nierenbeckenkelchsystem scheinbar nicht, da hier eine ausgeprägte Tunica muscularis fehlt.

Aus diesen Ergebnissen schlussfolgerten wir, dass mittels NanoKnife-IRE eine Nierentumorablation bei gleichzeitigem Erhalt der Organintegrität und des involvierten Nierenbeckenkelchsystems sowie einer schnellen Urothelregeneration möglich ist. Daraus ergäben sich Anwendungsvorteile gegenüber den Leitlinien-basierten thermoablativen Techniken (RFA und Kryoablation), insbesondere im Hinblick auf zentral gelegene Nierentumoren bzw. Nierenzellkarzinome.

Nach o.g. Beschreibung mit Hauptaugenmerk auf die Nebeneffekte und möglichen Kollateralschäden der renalen IRE auf das Nierenbeckenkelchsystem folgte nun die Publikation der detaillierten Tumorablationsergebnisse dieser Patienten (Übersicht siehe Tab. 2).

Wendler JJ, Pech M, Fischbach F, Jürgens J, Friebe B, Baumunk D, Porsch M, Blaschke S, Schindele D, Siedentopf S, Ricke J, Schostak M, Köllermann J, Liehr UB. **Initial Assessment of the Efficacy of Irreversible Electroporation in the Focal Treatment of Localized Renal Cell Carcinoma With Delayed-interval Kidney Tumor Resection (Irreversible Electroporation of Kidney Tumors Before Partial Nephrectomy [IRENE] Trial - An Ablate-and-Resect Pilot Study).** Urology. 2018 Apr;114:224-232.

Bisher existieren wenige klinische Publikationen zur Irreversiblen Elektroporation des kleinen Nierenzellkarzinoms, wobei in allen Zentren das NanoKnife-System zur Anwendung kam. Die meisten Studien basierten auf der bildgebenden und ggf. bioptischen Kontrolle der Ablationszone bzw. des abladierten Tumors.

Diehl et al. behandelten 7 kleine Nierentumoren (Mittel 24mm, Range 15-18mm) mittels perkutaner Irreversibler Elektroporation bei operativen Einzelnieren. Eine zunehmende Intensitätsminderung der Ablationszone in der Kontroll-MRT über durchschnittlich 6,4 Monate (Range 3-11 Monate) sollte eine Ansprechrate von 100% demonstrieren. Diese Studie war durch eine fehlende prä- und postinterventionelle histologische Sicherung des Nierentumor limitiert (Diehl et al. 2016).

Canvasser et al. berichteten von einer „suboptimalen onkologischen Effektivität“ nach perkutaner Irreversibler Elektroporation von 42 kleinen Nierentumoren (Mittel 20mm, Range 10-36mm), wobei die Kontroll-CTs und -MRTs ein Enhancementverlust und eine Involution des Tumors über 6 Monate nachweisweisen konnten. Davon zeigte sich jedoch in 3 Fällen eine inkomplette Ablation im Tumorrandbereich. Die Studie war ebenfalls durch eine fehlende systematische prä- und postinterventionelle histologische Sicherung des Tumors limitiert (20 Nierenzellkarzinome, 22 unklare Dignität, keine Re-Biopsie nach Ablation) (Canvasser et al. 2017).

Buijs et al. beschrieben die technisch erfolgreiche Durchführbarkeit einer perkutanen CT-gestützten IRE bei 9 von 10 Nierentumoren (8 NZK und 2 SRM, Mittel 22mm, Range 11-39mm) mit einer mittleren Narkosezeit von 3,7h (Range 3-5h), einer mitlleren Prozedurzeit von 2,1h (Range 1,7-2,5h), (Buijs et al. 2019). Relevante Nebenwirkungen (10% Clavien-Dindo 3) oder Serumkreatininveränderungen traten innerhalb von 12 Monaten nicht auf (Buijs et al. 2019).

Limitationen ergeben sich durch die nicht beschriebene bildgebende oder histologische Nachsorgeuntersuchung des Tumors bzw. Ablationsareals. Die beschriebene unmittelbare CT-Kontrolle zeigte in 90% einen technischen Ablationserfolg mit kompletter Abdeckung des Tumorareals per IRE-Ablationsareal ohne Kontrastmittelenhancement ist zu diskutieren.

Mit der vorliegenden klinischen Pilotstudie von Wendler at al. (Wendler at al. 2015b; Wendler et al. 2016b; Wendler et al. 2017b; Wendler et al. 2018a; Wendler et al. 2018b) erfolgte erstmals eine systematische resektionshistologische Untersuchung der mittels Irreversibler Elektroporation abladierten, histologisch gesicherten Nierenzellkarzinome pT1a. Diese Analyse repräsentiert einen „Schnappschuss“ 4 Wochen nach erfolgter Ablation mit verfahrensspezifischen Ergebnissen, wobei der Gewebeumbauprozess nach lokal gezielt induzierter Nekrose und Inflammation nach 4 Wochen noch nicht abgeschlossen zu sein scheint. Dabei zeigten die IRE-Areale eine zonale Gliederung der insgesamt scharf abgrenzbaren Ablationszone. Diese wiesen eine ausgedehnte zentrale Koagulationszekrose, umgeben von einem schmalen, reaktiven zweischichtigen Randsaum (Transitionszone) mit Gefäßveränderungen und Zeichen einer sekundären Ischämie. Die komplette Abdeckung des Tumors mit einem kalkulierten Ablationsfeld war mittels NanoKnife-System möglich, jedoch zeigten sich in 3 von 7 Fällen mikroskopisch residuelle Tumorzellnester. Eine konkrete Vorhersage des Ablationserfolgs mittels verfahrensspezifischer Surrogatparameter scheint vorerst nicht möglich. Relativierend dazu, sind solche mikroskopischen Residuen in einer reinen bildgebenden Kontrolle nicht sichtbar, weshalb entsprechende Studien mit CT- und MRT-Follow-Up klinisch sehr hohe Raten einer kompletten Ablation aufweisen. Mehrere Studien demonstrierten eine Lokalrezidivrate von pT1a Nierenzellkarzinom mit 2-12% nach Radiofrequenzablation und 3-17% nach Kryoablation in den ersten 5 Jahren Nachbeobachtungszeit (Wendler et al. 2016c).
Unter den aktuellen technischen Voraussetzungen der Irreversiblen Elektroporation mittels NanoKnife-System ist das Verfahren jedoch sehr komplex, sowie technisch, personell und zeitlich aufwendig. Insbesondere die möglichst exakte parallele Platzierung von mehreren IRE-Elektroden im Tumor unter Berücksichtigung einer dreidimensionalen Ablationszonenplanung und der Bewegung des Zielgewebes war sehr diffizil.
Relevante Komplikationen traten nicht auf. Makroskopisch und bildgebend deckten die IRE-Ablationszonen das Tumorzielvolumen komplett ab. Bezogen auf das Nebenwirkungsprofil dieser Studie scheint die Anwendung des NanoKnife-Systems zur perkutanen Nierentumorablation sicher. Die intendierte kurative Ablation von lokal begrenzten Nierenzellkarzinomen bis 3cm Größe mittels Irreversibler Elektroporation scheint möglich. Bemerkenswert sind auch die demonstrierten kompletten Ablationen der zentralen oder

hilusnah-gelegenen Nierentumore mit Nierenfunktionserhalt, dessen chirurgische Enukleation oder Thermoablation wahrscheinlich inkomplett oder mit einem kompletten Nierenverlust einhergegangen wäre. Dies deutet auf das hohe Potential der IRE als neues, therapeutisches Tool für zentralgelegene Nierentumoren mit relativer Kontraindikation für eine chirurgische Resektion oder Thermoablation hin.

Aus diesen Ergebnissen schlussfolgerten wir, dass mittels NanoKnife-IRE eine Nierentumorablation bei gleichzeitigem Erhalt der Organintegrität und des involvierten Nierenbeckenkelchsystems möglich ist. Daraus ergäben sich Anwendungsvorteile gegenüber den leitlinienbasierten, thermoablativen Techniken (RFA und Kryoablation), insbesondere im Hinblick auf zentral gelegene Nierentumoren bzw. Nierenzellkarzinome. Eine Option zur erneuten Ablation im Falle eines Persistivs oder Rezidivs ist potentiell gegeben.

5. Zusammenfassung

In den letzten zwei Jahrzehnten weist die Uroonkologie eine Entwicklung weg von der ultraradikalen Exzisionschirurgie hin zur fokalen Therapie mit größtmöglichem Organfunktionserhalt bei gleichwertiger onkologischer Sicherheit auf. Für ausgewählte Indikationen kommen zunehmend interventionelle Ablationsverfahren zum Einsatz.

Dieser Trend betrifft vor allem die Niere bei lokal begrenzten Nierentumoren. Der frühere Standard der radikalen Tumornephrektomie wurde zu Gunsten des Nierenfunktionserhalts per Nierenteilresektion bis hin zur Nierentumorenukleation zur Vermeidung einer höheren kardiovaskulären Morbidität und Mortalität, sowie der Dialysepflichtigkeit weitgehend verlassen. Bei Patienten mit erhöhten Operations- oder Narkoserisiken sowie ausdrücklichem Wunsch einer Behandlungsalternative stehen mittlerweile minimalinvasive Ablationstechniken wie die Kryotherapie und die Radiofrequenzablation (RFA) leitlinienetabliert zur Verfügung. Beim lokal begrenzten (low risk) Prostatakarzinom kommen, neben der radikalen Prostatektomie und der perkutanen Radiatio, fokale Ablationsverfahren wie der Hochintensive fokussierte Ultraschall (HIFU) und die Brachytherapie zur Anwendung. Beim lokal begrenzten, muskelinvasiven Harnblasenkarzinom ist in ausgewählten Fällen eine Harnblasenteilresektion als Alternative zur radikalen Zystektomie mit blasenersetzender Harnableitung möglich.

Für die verschiedenen Tumorentitäten werden inzwischen in der gesamten Uroonkologie zunehmend multimodale Konzepte aus chirurgischer Operation, ablativen Techniken und medikamentös-systemischer Therapie für lokal fortgeschrittene und oligometastasierte Tumorstadien mit nicht mehr nur palliativer Absicht, sondern auch kurativer Intention diskutiert. Dabei ergeben sich neue Bedürfnisse im Sinne einer „maßgeschneiderten“ individuellen Behandlung.

Die o.g. etablierten Thermoablations- und Bestrahlungstechniken wirken nicht gewebe- oder strukturselektiv und weisen spezielle, verfahrensbedingten Limitationen, Risiken und Nebenwirkungen auf.

Eine Alternative dazu verspricht die Irreversible Elektroporation (IRE, NTIRE), welche als neuartiges Weichgewebeablationsverfahren nonthermal, gewebeselektiv zelluläre Strukturen in einem wählbaren Zielbereich unter Erhalt der Matrix und damit Berücksichtigung von Organ- bzw. Leitstrukturen ohne die bekannten Nachteile bisher bekannter Techniken anzuwenden sei. Seit 2008 steht das Medizinprodukt NanoKnife-System® der Firma AngioDynamics Inc. (NY, U.S.A.) zur kommerziellen Anwendung der IRE als allgemeines Weichgewebeablationsverfahren zur Verfügung. Bis dato lagen keine ausreichenden, tumorentitätsspezifischen oder organspezifischen Wirksamkeitsnachweise vor, wobei die

Behandlungsparameter an ex-vivo-Modellen, insbesondere am Lebermodell entwickelt wurden. Eine Evidenz zur Anwendung der IRE wurde bis dato nicht erzielt.
Im o.g. Kontext bestanden konsekutiv Skepsis und Interesse zur Anwendung der IRE und des NanoKnife-Systems als minimal-invasive Ablationsmethode für lokal begrenzte urologische Tumoren. Dabei ergäben sich mögliche Indikationen zur organschonenden und organerhaltenden Ablation von lokal begrenzten Nieren-, Blasen-, Hoden- und Prostatatumoren, respektive -karzinomen.

Aufgrund dessen ergab sich für uns die Zielsetzung, die postulierten Funktionseigenschaften der Irreversiblen Elektroporation und die vom Hersteller angegebenen Eigenschaften des NanoKnife-Systems im Hinblick auf eine klinische Anwendung zur perkutane Tumorablation in der Uroonkologie zu prüfen. Als primäres Organmodell zur klinisch-experimentellen Evaluation wurde die Niere gegenüber der Prostata favorisiert, da hier insgesamt eine höhere klinische Expertise zur fokalen Therapie von Nierentumoren bestand, und die Niere ein leichter zu simulierendes und zu monitorierendes Organ darstellt. Dafür wurde eine entsprechende Untersuchungskaskade, welche einen größtmöglichen Erkenntnisgewinn unter Wahrung maximaler Sicherheitsaspekte in den Untersuchungsabschnitten zuließ:

- physikalische Untersuchungen der Irreversiblen Elektroporation im experimentellen Eiweißmodell und Gelmodell (Liehr et al. 2012; Blaschke 2013; Liehr 2014)
- physikalische Untersuchungen der Irreversiblen Elektroporation im tierischen ex-vivo-Nierenfrischpräparat (Liehr et al. 2012; Blaschke 2013; Liehr 2014)
- radiologische Untersuchungen der Irreversiblen Elektroporation im tierischen ex-vivo-Nierenperfusionsmodell (Wendler et al. 2012a)
- präklinische Studie zur Irreversiblen Elektroporation im tierischen in-vivo-Nierenversuchsmodell (Wendler et al. 2012b; Wendler et al. 2013)
- klinische Sicherheitsstudie zur Irreversiblen Elektroporation im humanen in-vivo-Nierentumormodell (Pech et al. 2011)
- klinische Wirksamkeitsstudie zur Irreversiblen Elektroporation im humanen in-vivo-Nierentumormodell (Wendler et al. 2015b; Wendler et al. 2016b; Wendler et al. 2017b; Wendler et al. 2018a; Wendler et al. 2018b)

Abgeleitete Erkenntnisse aus diesem Prozess und gegenwärtiger wissenschaftlicher Entwicklungen zur Irreversiblen Elektroporation und Fokalen Therapie sollten im Rahmen der laufenden internationalen wissenschaftlichen Untersuchungen diskutiert werden. Entsprechende Überlegungen sollten auf das Prostatamodell zur potentiellen Anwendung beim lokal begrenzten Prostatakarzinom übertragen werden:

- Stellenwert fokaler Therapiemethoden beim lokal begrenzten Nierenzellkarzinom (Wendler et al. 2016c; Wendler et al. 2018c; Wendler et al. 2018d)
- Nachsorgeempfehlungen nach fokaler Therapie des lokal begrenzten Nierenzellkarzinoms (Zondervan et al. 2016)
- Anwendungslimitationen der Irreversiblen Elektroporation bei verschiedenen Zielorganen und Entitäten (Wendler et al. 2015a; Wendler et al. 2015c)
- Gegenwärtiger Wissensstand, Anwendungsempfehlungen und Simulation zur Irreversiblen Elektropration des Prostatakarzinoms (Wendler et al. 2015a; Wendler et al. 2016d; Wendler et al. 2017a)
- Standardisierung der Terminologie und Reportkriterien zur Irreversiblen Elektroporation im Vergleich zu anderer Ablationstechniken (Wendler et al. 2016a)

Diese Habilitationsarbeit im Sinn einer kumulativen Habilitationsschrift ist eine zusammenfassende Darstellung ausgewählter Publikationen dieser systematischen, experimentellen und klinischen Evaluation zur Irreversiblen Elektroporation (IRE) bzw. des NanoKnife®-Systems als neues Gewebeablationsverfahren aus uroonkologischer Sicht.
Die physikalische Untersuchungskaskade an den Phantommodellen konnte zeigen, dass es in liquiden und gelatinösen Medien zur Ausbildung von Lichtbögen mit Gasbildung, sowie Kavitationsphänomen mit Denaturierungsprozessen in unmittelbarer Nähe zur IRE-NanoKnife-Elektrode kommt (Liehr et al. 2012; Blaschke 2013; Liehr 2014). Diese Phänome wurden bis dato in der Literatur nicht beschrieben und standen für Anwendungslimitationen und Kollateraleffekte in der klinischen Anwendung bisher nicht zur Diskussion. Im Gegensatz dazu konnten mittels Temperaturmessungen im in-vitro-Gel- und ex-vivo-Nieren-Modell die postulierten Eigenschaften einer nicht thermoablativen Temperaturentwicklung im IRE-Ablationsareal des NanoKnife-Systems bestätigt werden (Liehr et al. 2012; Blaschke 2013; Liehr 2014). Ebenso zeigte sich im angiographischen Versuchsaufbau keine unmittelbare Gewebezerstörung im tierischen ex-vivo-Nierenmodell durch die IRE, was auf eine gewebe- bzw. strukturselektive, verzögerte Ablationswirkung und den möglichen Erhalt von essentiellen vaskulären Strukturen hindeutete (Wendler et al. 2012a). Es folgte die Pilotstudie als Machbarkeits-, Sicherheits- und Wirksamkeitsnachweisstudie im Tierversuchmodell (Wendler et al. 2012b; Wendler et al. 2013). Hier konnten neben neuartigen MRT-radiologischen, zytologischen und histologischen Befunden die postulierten Eigenschaften der IRE bestätigt werden, wobei sich eine verzögerte, relativ scharfbegrenzte Koagulations-nekrose mit Erhalt von Blutgefäßen und des Nierenbeckenkelchsystems zeigte. Insgesamt war eine CT-gestützte, perkutane IRE der Niere in Vollnarkose mittels NanoKnife-System technisch durchführbar und procedural sicher, Komplikationen traten

nicht auf. Diese Erkenntnisse ermöglichten die nachfolgenden Studienanwendungen bei Patienten mit Nierentumoren. Es erfolgte zunächst eine Sicherheitsstudie als weltweit erste humane Pilot-studie zur IRE per NanoKnife-System als intraoperative IRE mit unmittelbarer Resektion des Nierentumors und IRE-Applikationsareals (Pech et al. 2011; Liehr 2012). Hier konnte keine akute Gewebezerstörung nachgewiesen werden, was auf den postulierten protrahierten Zelluntergang durch IRE hindeutete. Ebenso zeigten sich keine Komplikation oder Nebenwirkungen im Sinn einer sicheren Applikations- und Anwendungsmöglichkeit an der Niere bzw. im Retroperitoneum.
Daraufhin führten wir die erste Wirksamkeitsnachweisstudie zur IRE von lokal begrenzten Nierenzellkarzinomen mit resektionshistologischer Kontrolle durch (Wendler et al. 2015b; Wendler et al. 2017b). Zum einen konnten wir die Durchführbarkeit der perkutanen CT-gestützten IRE von pT1a Nierenzellkarzinomen und klinische Sicherheit ohne Auftreten von Komplikationen nachweisen. Dabei erwies sich jedoch die Prozedur der IRE- Elektroden-Platzierung und die Ablationsplanung per NanoKnife-System als sehr komplex und aufwendig umsetzbar. IRE-spezifische Komplikationen oder Nebenwirkungen traten nicht auf (Wendler et al. 2016b; Wendler et al. 2017b; Wendler et al. 2018a). Zum anderen konnten wir eine mögliche komplette Ablation des Nierentumors mittels IRE unter Funktionserhalt der Niere nachweisen. Dies gelang auch bei zentral gelegenen Nierentumoren mit Involvierung des Nierenhilus (Nierenbecken, Nieren-versorgende Blutgefäße) (Wendler et al. 2016b; Wendler et al. 2017b; Wendler et al. 2018a; Wendler et al. 2018b).

Zusammenfassend konnte unsere systematische Untersuchungskaskade, neben diversen Erstbeschreibungen zur IRE, sowohl die Durchführbarkeit und Sicherheit, als auch die Wirksamkeit der IRE zur fokalen, nierenfunktionserhaltenden, nonthermalen Ablation von Nierengewebe bzw. Nierenzellkarzinomen nachweisen. Damit stünde in der „Toolbox“ zur Behandlung des lokal begrenzten Nierenzellkarzinom bzw. von Nierentumoren ein neues „Werkzeug“ zur Verfügung. Durch die fehlenden Limitationen gegenüber Thermoablations-verfahren (RFA und Kryotherapie) deutet sich für die IRE als neues „Tool“ ein Behandlungsvorteil bzw. eine spezielle Indikation für zentral gelegene Nierentumoren an (Wendler et al. 2016b; Wendler et al. 2018a; Wendler et al. 2018b; Zondervan 2019).

Parallel zu unseren Erfahrungen im Rahmen der o.g. Untersuchungskaskade stand stets die Anwendung der IRE bzw. NanoKnife-Systems für andere Organe bzw. Tumorentitäten, (insbesondere des Prostatakarzinoms), die Kommerzialisierung des NanoKnife-Systems, die Vergleichbarkeit von Publikationen zur IRE und anderen Ablationsverfahren, sowie die Anwendung von und Nachsorge nach fokalen Therapiemethoden des Nierenzellkarzinoms im Fokus. Während die IRE ein vielversprechendes Verfahren für solide Tumoren in soliden

Weichgeweben parenchymatöser Organe verspricht, zeigen sich technisch- bzw. funktionsspezifische Limitationen der IRE, zum Beispiel in der Behandlung von Lungentumoren (Wendler et al. 2015c; Ricke et al. 2015).

Trotz zunehmender Publikationszahl zur IRE des lokal begrenzten Prostatakarzinoms zeigte die IRE hier noch keinen evidenten Wirksamkeitsnachweis und dürfte als experimentell anzusehendes Verfahren nicht als kommerzielle, routinemäßige Behandlungsalternative angeboten werden (Wendler et al. 2015a; Wendler et al. 2017a). Die eigenen Stellungnahmen dazu wurden in der Fachpresse und –literatur entsprechend aufgegriffen und übernommen (Ärzteblatt 2015; van der Poel et al. 2018). Da die IRE jedoch auch zur Behandlung des lokal begrenzten Prostatakarzinoms ein potentielles Verfahren darstellt, sollten indiviuelle und prostataspezifische IRE-Parameter experimentell getestet und definiert werden (Wendler et al 2016d). Die Publikationszahl zur IRE per NanoKnife-System stieg seit ihrer Verfügbarkeit exponentiell, bei gleichzeitig sehr heterogenen Publikationsinhalten, unterschiedlich genutzten Termini und teils intransparenten IRE-Parametern. Weiterhin unterscheidet sich die IRE technisch stark von thermoablativen Ablationsverfahren. Dies erschwert eine Auswertung der Publikationsergebnisse und macht einen direkten Vergleich teilweise unmöglich. Daher sollte eine Standardisierung der Terminologie und Reportkriterien zur IRE analog zu anderen Ablationsverfahren gefunden und eingehalten werden (Wendler et al. 2016a). Ebenso bedürfte es der Definition konkreter Nachsorgeempfehlungen nach fokaler Therapie von Nierentumoren bzw. Nierenzellkarzinomen, welche bisher in den Leitlinien nicht ausreichend definiert wurden (Zondervan et al. 2016).

Im Rahmen dieses Gesamtprojektes „Evaluation zur Anwendung der Irreversible Elektroporation per NanoKnife-System in der Uroonkologie“ zeigten sich zu diskutierende Limitationen dieser Arbeiten bzw. des NanoKnife-Systems. Bei den diskutierten Limitationen der o.g. Untersuchungen ist das Verfahren der IRE und die Anwendung des NanoKnife-Systems trotz klinischer Zulassung weiterhin als experimentell zu bewerten. Trotz klinischer Anwendungszulassung des NanoKnife-Systems ist aus Sicht der Studiengruppe die Anwendung für jede einzelne Indikation (Entität, Lokalisation, Organ, Dignität) neu zu prüfen und eine Anwendung außerhalb klinischer, registrierter und zu publizierender Studien nicht zu empfehlen. Unsere Pilotstudien wurden zu einer Zeit geplant, als die technischen Variablen des NanoKnife-Systems und der Irreversiblen Elektroporation noch nicht vollständig bekannt waren. Die Ergebnisse können nicht zur Empfehlung einer spezifischen Parameteränderung des NanoKnife-Systems oder der Irreversiblen Elektroporation verwendet werden. Die individuelle Tumorgewebetextur mit seinen sehr variablen, inhomogenen bioelektrischen Eigenschaften scheint eine große, jedoch aktuell nicht bestimmbare oder kalkulierbare Rolle zu spielen.

Anhand der vorliegenden Studienergebnisse ergeben sich, soweit beurteilbar, für die Irreversible Elektroporation keine besonderen verfahrensspezifischen Vorsichtsmaßnahmen oder Risiken. Das Risiko einer inkompletten Tumorentfernung gilt für alle ablativen und chirurgischen Verfahren. Eine abschließende Nutzen-Risiko-Bewertung für die perkutane Irreversible Elektroporation von Nierenkarzinomen <3cm mittels NanoKnife-Systems ist aufgrund der limitierten Daten dieser Pilotstudie nicht möglich.

Das NanoKnife-System weist jedoch derzeit noch verfahrens- und produktspezifische Limitationen für eine routinemäßige, breite Anwendung auf:

- Die softwarebasierte Ablationsplanung des NanoKnife-Systems ist nur in 2D in einem festen medianen Transversalschnitt zum Tumor bzw. zur IRE-Elektrodenachse darstellbar.
- Die möglichst streng parallele Platzierung der IRE-Elektroden ist kompliziert, insbesondere bei einem limitierten Punktionsfenster und tieferen Zielstrukturen, sowie bei beweglichen Zielorganen, wie die Niere.
- Die Ablationswirkung ist pro Impuls und während der Ablation nicht zeitgleich (real-time) zu beurteilen. Die Anzeige der verfahrensspezifischen Ablationsgraphen (elektrischen Impulse mit A, V und Kurvenform) erschien bisher erst zum Ende der Ablationsrunde.
- Die Ablationszone ist weder primär sicher planbar, noch im real-time-Verfahren oder unmittelbar postinterventionell bildgebend visualisierbar. Aufgrund nicht messbarer, dynamischer inter- und intraindividueller Impedanzunterschiede des Zielgewebes ist die Ablationszone somit nicht zwangsläufig gleich reproduzierbar. Die Ablations-zonenausdehnung zeigt sich bildgebend, verfahrensspezifisch (prolongierte Apoptose/ Nekrose / Irreversibel Elektroporation) erst im späteren klinischen Verlauf nach 7 bis 28 Tagen.
- Das NanoKnife-System ermöglicht die Irreversible Elektroporation nur in Vollnarkose/ Intubationsnarkose mit maximaler Muskelrelaxation, da nur so elektrisch induzierte, die Behandlung störende Muskelkontraktionen vermieden werden können. Der Einsatz als Behandlungsalternative zur chirurgischen Nierentumorresektion für Patienten mit einem hohen perioperativen Narkoserisiko ist somit bisher nicht möglich.

Abschließend betrachtet weist die Irreversible Elektroporation ein hohes Potential zur Tumorablation in der Uroonkologie, insbesondere von lokal begrnezten Nierenzell- und Prostatakarzinomen auf. Der nachfolgende Ausblick soll weitere Projekte unserer Arbeitsgruppen zu diesem Thema auflisten, sowie den aktuellen und künftig möglichen Stellenwert der IRE in der Uroonkologie nach entsprechend notwendiger, technischer Weiterentwicklung darstellen. Weitere experimentelle und klinische Studien mit spezifischen Indikationsstellungen sind notwendig, um eine Evidenz und Implementierung in die fachspezifischen Leitlinien zur erreichen.

6. Ausblick

Ausgehend von o.g. zusammengefassten Untersuchungsergebnissen und Limitation wären aus Sicht der Studiengruppe technische Weiterentwicklungen zur Irreversiblen Elektroporation bzw. des NanoKnife-Systems erforderlich:

- Die softwarebasierte Ablationsplanung des NanoKnife-Systems sollte eine dreidimensionale Ablationszonenplanung mit variablen Zugangsachsen in Ausrichtung zu den Körperachsen oder der spezifischen Tumorform ermöglichen, um eine indivuelle, exakte Ablationsplanung und damit konsekutiv effektive Ablation durchführen zu können.
- Die Platzierung der monopolaren IRE-Elektroden müsste leichter parallel und am besten navigationsgestützt ermöglicht werden, um die Prozedur der Elektrodenplatzierung zu vereinfachen und die Interventionszeit zu verkürzen.
- Der eigentliche IRE-Appliaktionsprozess sollte im Real-Time-Verfahren graphisch dargestellt werden, um bessere Rückschlüsse auf den Applikationserfolg zu erlauben. Die neueste Generation des NanoKnife-Systems soll dies laut Hersteller ermöglichen.
- Die Applikation bzw. die Wirkung der IRE-Impulse müsste so verändert werden, dass keine Muskelkontraktionen als Nebeneffekt entstehen. Damit wäre die Applikation der IRE ohne Vollnarkose durchzuführen. Die hochfrequente IRE (HF-IRE) soll dies möglich machen und wird derzeit experimentell durch diverse Arbeitsgruppen untersucht (Arena et al. 2011; Sano MB et al. 2018a; Zhao Y et al. 2018; Dong et al. 2018).

Diese Adaptionen der IRE- bzw. NanoKnife-Parameter würde eine routinemäßige Anwendung und einen breiteren Einsatz fachübergreifend ermöglichen.

Für das T1a-Nierenzellakarzinom könnte die IRE eine Behandlungsalternative zur thermalen Ablationsverfahren, insbesondere für zentrale oder hilusnahe Lokalisationen darstellen. Im Fall einer klinischen Zulassung für die HF-IRE in Lokalanästhesie stünde die IRE auch für Patienten mit einem hohen Narkoserisiko zur Option (siehe Abb.22).

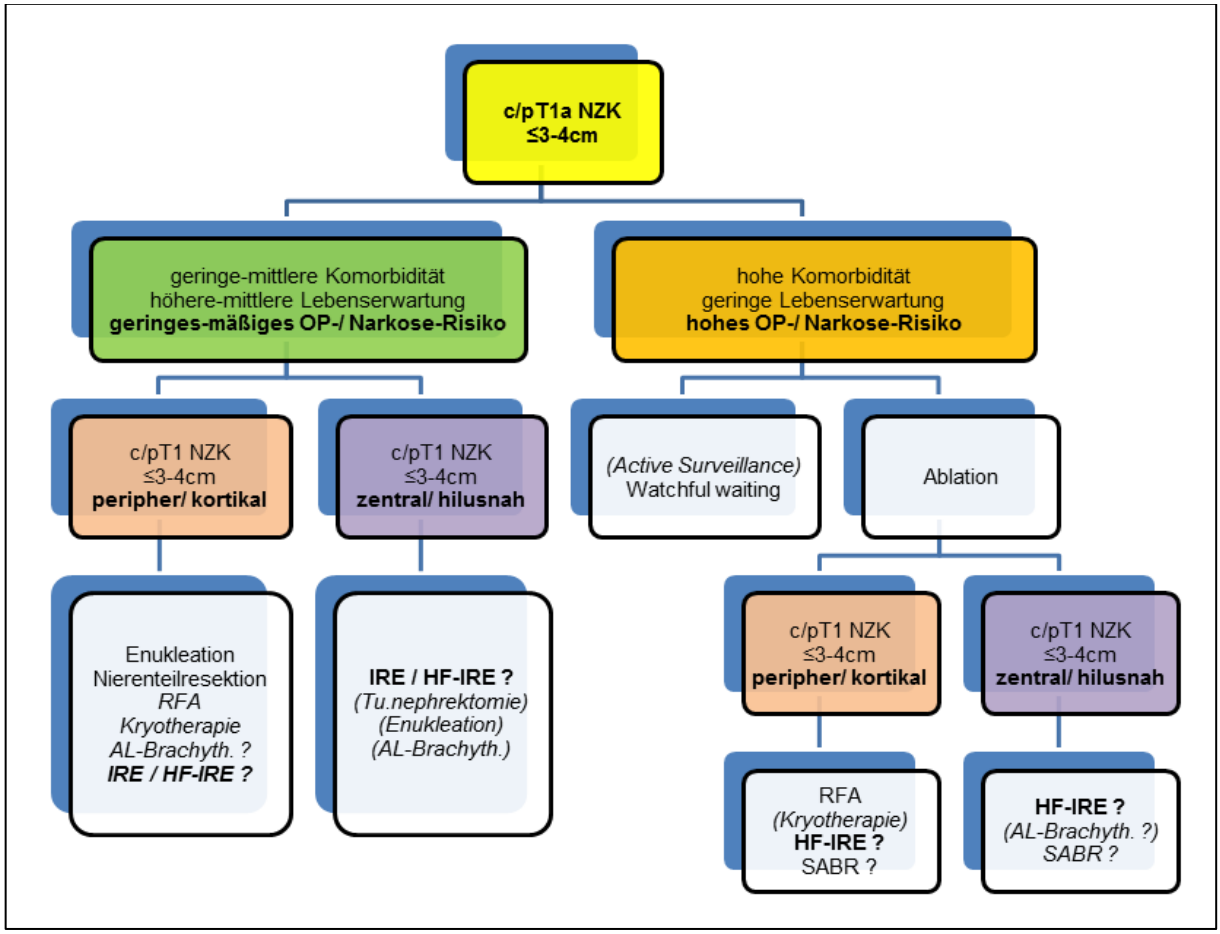

Abb.22: Algorithmus verschiedener Therapieoptionen des T1a-Nierenzellkarzinoms (NZK) nach OP-/ Narkose-Risiko und Tumorlokalisation mit künftig möglichem Stellenwert der IRE/ HF-IRE als Behandlungsalternative.

Für das lokal begrenzte Prostatakarzinom ist die Sicherheit und Wirksamkeit für jede einzelne Indikationsstellung an PCA-Risikoprofil und Tumorlage zu prüfen. Künftig könnte die IRE / HF-IRE für alle u.g. Risikosituationen als Therapieoption zur Verfügung stehen (siehe Abb.23). Zur zunehmende komplexe Entscheidungsfindung einer individualisierten Behandlung bei einer großen Bandbreite an Indikationen und Therapiemethoden beim lokal begrenzten Nierenzell- und Prostatakarzinom bedarf einer interdisziplinären Beratung in entsprechenden Spezialsprechstunden (Liehr et al. 2017; Ganzer et al. 2018; Edison et al. 2017). Hierfür werden orientierende und detaillierte, sich stets verändernde Algorithmen zur Visualisierung benötigt:

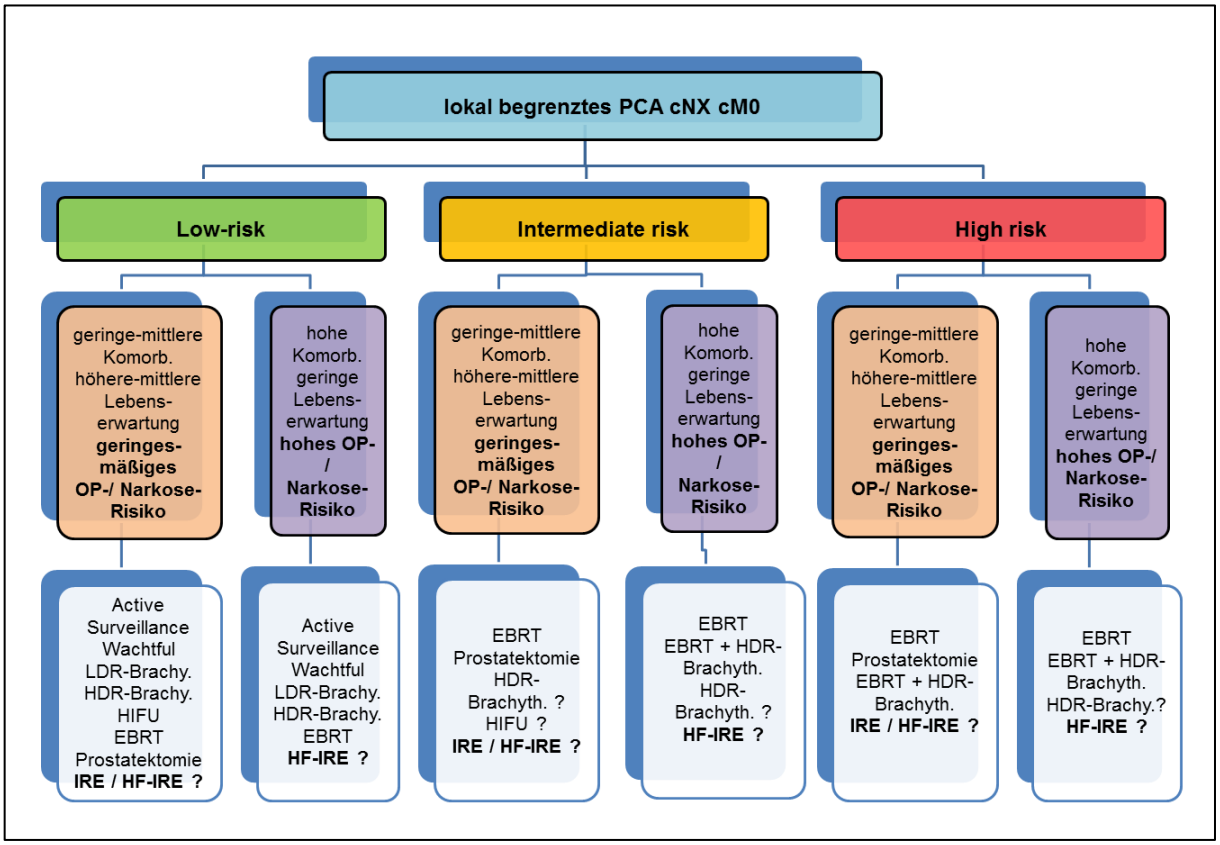

Abb.23: Algorithmus verschiedener Therapieoptionen des lokal begrenzten Prostatakarzinoms (PCA) nach PCA-Risikoprofil und OP-/ Narkose-Risiko mit künftig möglichem Stellenwert der IRE / HF-IRE als Behandlungsalternative.

Aktuelle Projekte zur Irreversiblen Elektroporation bzw. zum NanoKnife-System sind geplant:

- Analyse der MRT-Befunde in Korrelation zur Resektionshistologie aus der o.g. klinischen Phase-2-Studie zur Irreversiblen Elektroporation beim lokal begrenzten Nierenzellkarzinom (Wendler et al. 2015b; Wendler et a. 2017b).
- Safety- und Outcome-Publikation der o.g. klinischen Phase-1- und Phase-2-Studie zur Irreversiblen Elektroporation beim lokal begrenzten Nierenzellkarzinom (Wendler et al. 2015b).
- Experimentelle Untersuchung der Ablationsmuster verschiedener Elektroden- und Impedanzparameter der Irreversiblen Elektroporation am in-vitro-in-vivo-Modell (u.a. Zwiebelmodell).
- Analyse der periinterventionellen Immunreaktion im Rahmen der renalen Irreversiblen Elektroporation aus der o.g. experimentellen Tierversuchsstudie am Schweinemodell und der o.g. klinischen Phase-1- und Phase-2-Studie beim lokal begrenzten Nierenzellkarzinom (Pech et al. 2011; Wendler et al. 2012a; Wendler et al. 2013; Wendler et al. 2015b).
- Klinische Studie zur perkutanen Ablation des lokal begrenzten cT1a cN0 cM0 Nierenzellkarzinoms mittels (navigations-gestützter) Irreversiblen Elektroporation mit bildgestütztem Follow-up (Folgestudie zur IRENE-Studie Phase 2).
- Klinische Studie zur perkutan-perinealen mpMRT-TRUS-Fusions-gestützten Irreversiblen Elektroporation des lokal begrenzten, low-risk und intermediate-risk Prostatakarzinoms GS6-7a pT1c-cT2a cN0 cM0 PSA<10.
- Entwicklung einer automatisierten Vorrichtung zur perkutan-perinealen mpMRT-TRUS-Fusions-gestützten Irreversiblen Elektroporation des lokal begrenzten, low-risk und intermediate-risk Prostatakarzinoms (Zusammenarbeit mit INKA und STIMULATE Magdeburg).

7. Literaturverzeichnis

(1) Abouassaly R, Yang S, Finelli A, Kulkarni GS, Alibhai SM. What is the best treatment strategy for incidentally detected small renal masses? A decision analysis. BJU Int. 108(8 Pt 2):E223-31. (2011)

(2) Ahmed M, Solbiati L, Brace CL, Breen DJ, Callstrom MR, Charboneau JW, Chen MH, Choi BI, de Baère T, Dodd GD 3rd, Dupuy DE, Gervais DA, Gianfelice D, Gillams AR, Lee FT Jr, Leen E, Lencioni R, Littrup PJ, Livraghi T, Lu DS, McGahan JP, Meloni MF, Nikolic B, Pereira PL, Liang P, Rhim H, Rose SC, Salem R, Sofocleous CT, Solomon SB, Soulen MC, Tanaka M, Vogl TJ, Wood BJ, Goldberg SN; International Working Group on Image-guided Tumor Ablation; Interventional Oncology Sans Frontières Expert Panel; Technology Assessment Committee of the Society of Interventional Radiology,; Standard of Practice Committee of the Cardiovascular and Interventional Radiological Society of Europe. Image-guided tumor ablation: standardization of terminology and reporting criteria--a 10-year update. Radiology. 273(1):241-60. (2014a)

(3) Ahmed M, Solbiati L, Brace CL, Breen DJ, Callstrom MR, Charboneau JW, Chen MH, Choi BI, de Baère T, Dodd GD 3rd, Dupuy DE, Gervais DA, Gianfelice D, Gillams AR, Lee FT Jr, Leen E, Lencioni R, Littrup PJ, Livraghi T, Lu DS, McGahan JP, Meloni MF, Nikolic B, Pereira PL, Liang P, Rhim H, Rose SC, Salem R, Sofocleous CT, Solomon SB, Soulen MC, Tanaka M, Vogl TJ, Wood BJ, Goldberg SN; International Working Group on Image-Guided Tumor Ablation; Interventional Oncology Sans Frontières Expert Panel; Technology Assessment Committee of the Society of Interventional Radiology; Standard of Practice Committee of the Cardiovascular and Interventional Radiological Society of Europe. Image-guided tumor ablation: standardization of terminology and reporting criteria--a 10-year update. J Vasc Interv Radiol. 25(11):1691-705.e4. (2014b)

(4) Ahmed M; Technology Assessment Committee of the Society of Interventional Radiology. Image-guided tumor ablation: standardization of terminology and reporting criteria--a 10-year update: supplement to the consensus document. J Vasc Interv Radiol. 25(11):1706-8. (2014c)

(5) Arena CB, Sano MB, Rossmeisl JH Jr, Caldwell JL, Garcia PA, Rylander MN, Davalos RV. High-frequency irreversible electroporation (H-FIRE) for non-thermal ablation without muscle contraction. Biomed Eng Online 10:102. (2011)

(6) Arena CB, Szot CS, Garcia PA, Rylander MN, Davalos RV. A three-dimensional in vitro tumor platform for modeling therapeutic irreversible electroporation. Biophys J. 103(9):2033-42. (2012)

(7) Aron M, Kamoi K, Remer E, Berger A, Desai M, Gill I. Laparoscopic renal cryoablation: 8-year, single surgeon outcomes. J Urol. 183(3):889-95. (2010)

(8) Ärzteblatt. Nutzen der irreversiblen Elektroporation bei Prostatakrebs nicht belegt. http://www.aerzteblatt.de/nachrichten/61695. hil/aerzteblatt.de, 04.02.2015. (2015).

(9) Atwell TD, Farrell MA, Leibovich BC, Callstrom MR, Chow GK, Blute ML, Charboneau JW. Percutaneous renal cryoablation: experience treating 115 tumors. J Urol. 179(6):2136-40; discussion 2140-1. (2008)

(10) Atwell TD, Schmit GD, Boorjian SA, Mandrekar J, Kurup AN, Weisbrod AJ, Chow GK, Leibovich BC, Callstrom MR, Patterson DE, Lohse CM, Thompson RH. Percutaneous ablation of renal masses measuring 3.0 cm and smaller: comparative local control and complications after radiofrequency ablation and cryoablation. AJR Am J Roentgenol. 200(2):461-6. (2013).

(11) AUA - American Urological Association Education and Research Renal mass and localized renal cancer: AUA guideline. https://www.auanet.org/guidelines/renal-cancer-renal-mass-and-localized-renal-cancer-guideline; Zugegriffen: 24.04.2019. (2017)

(12) AWMF - Leitlinienprogramm Onkologie (Deutsche Krebsgesellschaft, Deutsche Krebshilfe, AWMF): Diagnostik, Therapie und Nachsorge des Nierenzellkarzinoms, Langversion 1.2, 2017, AWMF Registernummer: 043/017OL, http://leitlinienprogramm- onkologie.de/Nierenzellkarzinom.85.0.html. (2017)

(13) Ball C, Thomson KR, Kavnoudias H. Irreversible electroporation: a new challenge in "out of operating theater" anesthesia. Anesth Analg. 110(5):1305-9. (2010)

(14) Baur ADJ, Collettini F, Enders J, Maxeiner A, Schreiter V, Stephan C, Gebauer B, Hamm B, Fischer T. MRI-TRUS fusion for electrode positioning during irreversible electroporation for treatment of prostate cancer. Diagn Interv Radiol. 23(4):321-325. (2017)

(15) Beksac AT, Paulucci DJ, Blum KA, Yadav SS, Sfakianos JP, Badani KK. Heterogeneity in renal cell carcinoma. Urol Oncol. 35(8):507-515. (2017)

(16) Berger A, Kamoi K, Gill IS, Aron M. Cryoablation for renal tumors: current status. Curr Opin Urol. 19(2):138-42. (2009)

(17) Berger J, Fardoun T, Brassart E, Capon G, Bigot P, Bernhard JC, Rigaud J, Patard JJ, Descazeaud A. Detailed analysis of morbidity following nephrectomy for renal cell carcinoma in octogenarians. J Urol. 188(3):736-40. (2012)

(18) Bertacchini C, Margotti PM, Bergamini E, Lodi A, Ronchetti M, Cadossi R. Design of an irreversible electroporation system for clinical use. Technol Cancer Res Treat. 6(4):313-20. (2007)

(19) Bhatt DL, Gaylor DC, Lee RC. Rhabdomyolysis Due to Pulsed Electric Fields. Plastic and Reconstructive Surgery. 86(1):1-11. (1990)

(20) Bishoff JT, Chen RB, Lee BR, Chan DY, Huso D, Rodriguez R, Kavoussi LR, Marshall FF. Laparoscopic renal cryoablation: acute and long-term clinical, radiographic, and pathologic effects in an animal model and application in a clinical trial. J Endourol. 13(4):233-9. (1999)

(21) Blaschke, Simon. Experimentelle Betrachtungen zur Wirkung der Irreversiblen Elektroporation im Gelantinegelphantom und am Nierenfrischpräparat vom Schwein. Magdeburg, Univ., Med. Fak., Diss., 2013.

(22) Breen DJ, Rutherford EE, Stedman B, Roy-Choudhury SH, Cast JE, Hayes MC, Smart CJ. Management of renal tumors by image-guided radiofrequency ablation: experience in 105 tumors. Cardiovasc Intervent Radiol. 30(5):936-42. (2007)

(23) Bretschneider T, Peters N, Hass P, Ricke J. [Update on interstitial brachytherapy]. Radiologe. 52(1):70-3. (2012)

(24) Brierley, J.D., et al., TNM classification of malignant tumors. UICC International Union Against Cancer. 8th edn. Wiley-Blackwell, 2017.

(25) Buijs M, van Lienden KP, Wagstaff PG, Scheltema MJ, de Bruin DM, Zondervan PJ, van Delden OM, van Leeuwen TG, de la Rosette JJ, Laguna MP. Irreversible Electroporation for the Ablation of Renal Cell Carcinoma: A Prospective, Human, In Vivo Study Protocol (IDEAL Phase 2b). JMIR Res Protoc. 6(2):e21. (2017)

(26) Buijs M, Zondervan PJ, de Bruin DM, van Lienden KP, Bex A, van Delden OM. Feasibility and safety of irreversible electroporation (IRE) in patients with small renal masses: Results of a prospective study. Urol Oncol. 37(3):183.e1-183.e8. (2019)

(27) Calaway AC, Gondim DD, Flack CK, Jacob JM, Idrees MT, Boris RS. Anatomic comparison of traditional and enucleation partial nephrectomy specimens. Urol Oncol. 35(5):221-226. (2017)

(28) Calvert M, Kyte D, Mercieca-Bebber R, Slade A, Chan A-W, King MT. Guidelines for Inclusion of Patient-Reported Outcomes in Clinical Trial Protocols: The SPIRIT-PRO Extension. Jama 319(5):483–494. (2018)

(29) Camacho JC, Kokabi N, Xing M, Master VA, Pattaras JG, Mittal PK, Kim HS. R.E.N.A.L. (Radius, exophytic/endophytic, nearness to collecting system or sinus, anterior/posterior, and location relative to polar lines) nephrometry score predicts early tumor recurrence and complications after percutaneous ablative therapies for renal cell carcinoma: a 5-year experience. J Vasc Interv Radiol. 26(5):686-93. (2015)

(30) Campbell SP, Song DY, Pierorazio PM, Allaf ME, Gorin MA. Stereotactic Ablative Radiotherapy for the Treatment of Clinically Localized Renal Cell Carcinoma. J Oncol. 2015:547143. (2015)

(31) Wein A, Kavoussi L, Partin AW, Peters CA. Campbell-Walsh Urology. 11th ed. Elsevier, Philadelphia 2016.

(32) Canvasser NE, Sorokin I, Lay AH, Morgan MSC, Ozayar A, Trimmer C, Cadeddu JA. Irreversible electroporation of small renal masses: suboptimal oncologic efficacy in an early series. World J Urol. 35(10):1549-1555. (2017)

(33) Carrafiello G, Dionigi G, Ierardi AM, Petrillo M, Fontana F, Floridi C, Boni L, Rovera F, Rausei S, Mangano A, Spampatti S, Marconi A, Carcano G, Dionigi R. Efficacy, safety and effectiveness of image-guided percutaneous microwave ablation in cystic renal lesions Bosniak III or IV after 24 months follow up. Int J Surg. 11 Suppl 1:S30-5. (2013)

(34) Charlson ME, Pompei P, Ales KL, MacKenzie CR. A new method of classifying prognostic comorbidity in longitudinal studies: development and validation. J Chronic Dis. 40(5):373-83. (1987)

(35) Chawla SN, Crispen PL, Hanlon AL, Greenberg RE, Chen DY, Uzzo RG The natural history of observed enhancing renal masses: meta-analysis and review of the world literature. J Urol 175(2):425-431. (2006)

(36) Clark TW, Malkowicz B, Stavropoulos SW, Sanchez R, Soulen MC, Itkin M, Patel A, Mondschein JI, Wein AJ. Radiofrequency ablation of small renal cell carcinomas using multitined expandable electrodes: preliminary experience. J Vasc Interv Radiol. 17(3):513-9. (2006)

(37) Cornelis FH, Durack JC, Kimm SY, Wimmer T, Coleman JA, Solomon SB, Srimathveeravalli G. A Comparative Study of Ablation Boundary Sharpness After Percutaneous Radiofrequency, Cryo-, Microwave, and Irreversible Electroporation Ablation in Normal Swine Liver and Kidneys. Cardiovasc Intervent Radiol. 40(10):1600-1608. (2017)

(38) Correa RJM, Louie AV, Staehler M, Warner A, Gandhidasan S, Ponsky L, Ellis R, Kaplan I, Mahadevan A, Chu W, Swaminath A, Onishi H, Teh BS, Lo SS, Muacevic A, Siva S. Stereotactic Radiotherapy as a Treatment Option for Renal Tumors in the Solitary Kidney: A Multicenter Analysis from the IROCK. J Urol. 101097JU0000000000000111. (2019)

(39) Davalos RV, Mir IL, Rubinsky B. Tissue ablation with irreversible electroporation. Ann Biomed Eng. 33(2):223-31. (2005)

(40) Davalos RV, Rubinsky B, Mir LM. Theoretical analysis of the thermal effects during in vivo tissue electroporation. Bioelectrochemistry. 61(1-2):99-107. (2003)

(41) Davalos RV, Rubinsky B. Temperature considerations during irreversible electroporation. Int J Heat Mass Tran, 51:5617-5622 (2008)

(42) Davalos RV, Rubinsky B. Tissue ablation with irreversible electroporation. US 2007/0043345 A1, USPAP, USA (2004/ 2007)

(43) de la Flor-Robledo M, Solís-Muñoz P, Sanjuán-Álvarez M, Abadal-Villayandre JM, Asensio-Merino F. Percutaneous irreversible electroporation of a renal tumor: Anesthetic management. Rev Esp Anestesiol Reanim. 63(7):419-22. (2016)

(44) Deodhar A, Monette S, Single GW Jr, Hamilton WC Jr, Thornton R, Maybody M, Coleman JA, Solomon SB. Renal tissue ablation with irreversible electroporation: preliminary results in a porcine model. Urology. 77(3):754-60. (2011)

(45) Diehl SJ, Rathmann N, Kostrzewa M, Ritter M, Smakic A, Schoenberg SO, Kriegmair MC. Irreversible Electroporation for Surgical Renal Masses in Solitary Kidneys: Short-Term Interventional and Functional Outcome. J Vasc Interv Radiol. 27(9):1407-1413. (2016)

(46) Doevenspeck H. Influencing cells and cell walls by electrostatic impulses. Fleischwirtschaft 13:986-987. (1961)

(47) Dong S, Wang H, Zhao Y, Sun Y, Yao C. First Human Trial of High-Frequency Irreversible Electroporation Therapy for Prostate Cancer. Technol Cancer Res Treat. 17:1533033818789692. (2018)

(48) Duffey BG, Kyle Anderson J. Current and future technology for minimally invasive ablation of renal cell carcinoma. Indian J Urol. 26(3):410-7. (2010)

(49) Dupuy DE, Aswad B, Ng T. Irreversible electroporation in a Swine lung model. Cardiovasc Intervent Radiol. 34(2):391-5. (2011)

(50) EAU - European Association of Urology (EAU) - Guidelines on Renal Cell Carcinoma - limited update March 2019. https://uroweb.org/guideline/renal-cell-carcinoma/. Zugriffen: 24.04.2019. in EAU Guidelines. Edn. presented at the EAU Annual Congress Barcelona 2019.

(51) Eble JN, Sauter G, Epstein JI, Sesterhenn IA (eds). In: Pathology and genetics of tumours of the urinary system and male genital organs. World Health Organization Classification of Tumours. Lyons: IARC Press, 7. (2004)

(52) Edd JF, Horowitz L, Davalos RV, Mir LM, Rubinsky B. In vivo results of a new focal tissue ablation technique: irreversible electroporation. IEEE Trans Biomed Eng. 53(7):1409-15. (2006).

(53) Edison E, Tariq Shah T, Ahmed HU. Focal Ablation of Early-Stage Prostate Cancer: Candidate Selection, Treatment Guidance, and Assessment of Outcome. Urol Clin North Am. 44(4):575-585. (2017)

(54) Faroja M, Ahmed M, Appelbaum L, Ben-David E, Moussa M, Sosna J, Nissenbaum I, Goldberg SN. Irreversible electroporation ablation: is all the damage nonthermal? Radiology. 266(2):462-70. (2013)

(55) Farrag K, Sriprasad S. Non-Surgical Ablative Therapy for Management of Small Renal Masses-Current Status and Future Trends. Indian J Surg Oncol. 8(1):39-45. (2017)

(56) Ferakis N, Bouropoulos C, Granitsas T, Mylona S, Poulias I. Long-term results after computed-tomography-guided percutaneous radiofrequency ablation for small renal tumors. J Endourol. 24(12):1909-13. (2010)

(57) Finley DS, Beck S, Box G, Chu W, Deane L, Vajgrt DJ, McDougall EM, Clayman RV. Percutaneous and laparoscopic cryoablation of small renal masses. J Urol. 180(2):492-8; discussion 498. (2008)

(58) Frank I, Blute ML, Cheville JC, Lohse CM, Weaver AL, Zincke H. Solid renal tumors: an analysis of pathological features related to tumor size. J Urol. 170(6 Pt 1):2217-20. (2003)

(59) Fricke H. A mathematical treatment of the electric conductivity and capacity of disperse systems. II. The capacity of a suspension of conducting spheroids surrounded by a non-conducting membrane for a current of low frequency. Physical Review. 26. (1925)

(60) Fuller GW. Report on the investigations into the purification of the Ohio river water at Louisville Kentucky. D. Van Nostrand Company, New York; 1898.

(61) Ganzer R, Arthanareeswaran VKA, Ahmed HU, Cestari A, Rischmann P, Salomon G, Teber D, Liatsikos E, Stolzenburg JU, Barret E. Which technology to select for primary focal treatment of prostate cancer?-European Section of Urotechnology (ESUT) position statement. Prostate Cancer Prostatic Dis. 21(2):175-186. (2018)

(62) Ganzer R, Franiel T, Köllermann J, Kuru T, Baumunk D, Blana A, Hadaschik B, von Hardenberg J, Henkel T, Köhrmann KU, Liehr UB, Machtens S, Roosen A, Salomon G, Schlemmer HP, Sentker L, Wendler J, Witzsch U, Schostak M. [Focal therapy of prostate cancer]. Urologe A. 56(10):1335-1346. (2017)

(63) Gebauer B, Enders J, Baur ADJ, Hamm B, Collettini F. CT-Guided Irreversible Electroporation for Locally Recurrent Prostate Cancer following Radical Prostatectomy and Salvage Radiation Therapy. J Vasc Interv Radiol. 28(9):1280-1281. (2017)

(64) Georgiades C, Rodriguez R. Renal tumor ablation. Tech Vasc Interv Radiol. 16(4):230-8. (2013)

(65) Georgiades CS, Hong K, Bizzell C, Geschwind JF, Rodriguez R. Safety and efficacy of CT-guided percutaneous cryoablation for renal cell carcinoma. J Vasc Interv Radiol. 19(9):1302-10. (2008)

(66) Gervais DA, McGovern FJ, Arellano RS, McDougal WS, Mueller PR. Radiofrequency ablation of renal cell carcinoma: part 1, Indications, results, and role in patient management over a 6-year period and ablation of 100 tumors. AJR Am J Roentgenol. 185(1):64-71. (2005)

(67) Giganti F, Stabile A, Giona S, Marenco J, Orczyk C, Moore CM, Allen C, Kirkham A, Emberton M, Punwani S. Prostate cancer treated with irreversible electroporation: MRI-based volumetric analysis and oncological outcome. Magn Reson Imaging. 58:143-147. (2019)

(68) Gill IS, Matin SF, Desai MM, Kaouk JH, Steinberg A, Mascha E, Thornton J, Sherief MH, Strzempkowski B, Novick AC. Comparative analysis of laparoscopic versus open partial nephrectomy for renal tumors in 200 patients. J Urol. 170(1):64-8. (2003)

(69) Gill IS, Remer EM, Hasan WA, Strzempkowski B, Spaliviero M, Steinberg AP, Kaouk JH, Desai MM, Novick AC. Renal cryoablation: outcome at 3 years. J Urol. 173(6):1903-7. (2005)

(70) Golberg A, Bruinsma BG, Uygun BE, Yarmush ML. Tissue heterogeneity in structure and conductivity contribute to cell survival during irreversible electroporation ablation by "electric field sinks". Sci Rep. 5:8485. (2015)

(71) Goldberg SN, Charboneau JW, Dodd GD 3rd, Dupuy DE, Gervais DA, Gillams AR, Kane RA, Lee FT Jr, Livraghi T, McGahan JP, Rhim H, Silverman SG, Solbiati L, Vogl TJ, Wood BJ; International Working Group on Image-Guided Tumor Ablation. Image-guided tumor ablation: proposal for standardization of terms and reporting criteria. Radiology. 228(2):335-45. (2003)

(72) Guenther E, Klein N, Zapf S, Weil S, Schlosser C, Rubinsky B, Stehling MK. Prostate cancer treatment with Irreversible Electroporation (IRE): Safety, efficacy and clinical experience in 471 treatments. PLoS One. 14(4):e0215093. (2019)

(73) Guericke, Otto von: Experimenta nova (ut vocantur) Magdeburgica de vacuo spatio. 1672.

(74) Haber GP, Lee MC, Crouzet S, Kamoi K, Gill IS. Tumour in solitary kidney: laparoscopic partial nephrectomy vs laparoscopic cryoablation. BJU Int. 109(1):118-24. (2012)

(75) Häcker A, Chauhan S, Peters K, Hildenbrand R, Marlinghaus E, Alken P, Michel MS. Multiple high-intensity focused ultrasound probes for kidney-tissue ablation. J Endourol. 19(8):1036-40. (2005)

(76) Hellsten S, Johnsen J, Berge T, Linell F. Clinically unrecognized renal cell carcinoma. Diagnostic and pathological aspects. Eur Urol. 18 Suppl 2:2-3. (1990)

(77) Hodgkin AL. The ionic basis of electrical activity in nerve and muscle. Biological reviews of the Cambridge Philosophical Society 26: 339-409. (1951)

(78) Hoffmann RT, Jakobs TF, Kubisch CH, Trumm C, Weber C, Siebels M, Helmberger TK, Reiser MF. Renal cell carcinoma in patients with a solitary kidney after nephrectomy treated with radiofrequency ablation: mid term results. Eur J Radiol. 73(3):652-6. (2010)

(79) Huang WH, Chang CH, Huang CP, Wu HC, Hsieh I PF. The percentage of resected and ischemic volume determined by a geometric model is a significant predictor of renal functional change after partial nephrectomy. Int Braz J Urol. 43(1):80-86. (2017)

(80) Jewett MA, Mattar K, Basiuk J, Morash CG, Pautler SE, Siemens DR, Tanguay S, Rendon RA, Gleave ME, Drachenberg DE, Chow R, Chung H, Chin JL, Fleshner NE, Evans AJ, Gallie BL, Haider MA, Kachura JR, Kurban G, Fernandes K, Finelli A. Active surveillance of small renal masses: progression patterns of early stage kidney cancer. Eur Urol. 60(1):39-44. (2011)

(81) Jex-Blake A.J. Death by electric currents and by lightning. The Goulstonian lectures for 1913. British Medical Journal. 11: 425-552, 492-498, 548-552, 601-603. (1913)

(82) Jiang K, Tang K, Guo X, Liu H, Chen H, Chen Z, Xu H, Ye Z. Laparoscopic cryoablation vs. percutaneous cryoablation for treatment of small renal masses: a systematic review and meta-analysis. Oncotarget. 8(16):27635-27644. (2017)

(83) Johnson BA, Cadeddu JA. Current opinion in urology 2017: focal therapy of small renal lesions. Curr Opin Urol. 28(2):166-171. (2018)

(84) Johnson DB, Solomon SB, Su LM, Matsumoto ED, Kavoussi LR, Nakada SY, Moon TD, Shingleton WB, Cadeddu JA. Defining the complications of cryoablation and radio frequency ablation of small renal tumors: a multi-institutional review. J Urol. 172(3):874-7. (2004)

(85) Joshi SS, Uzzo RG. Renal Tumor Anatomic Complexity: Clinical Implications for Urologists. Urol Clin North Am. 44(2):179-187. (2017)

(86) Jürgens JHW, Liehr UB, Wendler JJ. Irreversible Elektroporation – ein neues Therapieverfahren auf dem Prüfstand. Interventionelle Radiologie Scan 04(01): 69-86. (2016)

(87) KDIGO 2012 Clinical Practice Guideline for the Evaluation and Management of Chronic Kidney Disease. Vol 3; Issue 1, January 2013. hhttps://kdigo.org/wp-content/uploads/2017/02/KDIGO_2012_CKD_GL.pdf, Zugegriffen: 24.04.2019. (2012)

(88) Kim M, Choi WS, Jeong CW, Ku JH, Kim HH, Moon KC, Kwak C. Differences in peritumoral pseudocapsule characteristics according to clinicopathological factors in clinical T1a renal tumors. Int J Clin Exp Pathol. 8(9):11323-31. (2015)

(89) Kinosita K, Hibino M, Itoh H, Shigemori M, Hirano K, Kirino Y, Hayakawa T. Events of membrane electroporation visualized on a time scale from microsecond to seconds. Guide to Electroporation and Electrofusion (1992) Chang, D. C., Chassy, B. M., Saunders, J. A., and Sowers, A. E., Eds., Academic Press (New York), pp.29-46. (1992)

(90) Kinosita KJ, Tsong TY. Formation and resealing of pores of controlled sizes in human erythrocyte membrane. Nature. 268: 438-441. (1977)

(91) Kirchberger I, Meisinger C, Heier M, Zimmermann AK, Thorand B, Autenrieth CS, Peters A, Ladwig KH, Döring A. Patterns of multimorbidity in the aged population. Results from the KORA-Age study. PLoS One. 7(1):e30556. (2012)

(92) Klatte T, Ficarra V, Gratzke C, Kaouk J, Kutikov A, Macchi V, Mottrie A, Porpiglia F, Porter J, Rogers CG, Russo P, Thompson RH, Uzzo RG, Wood CG, Gill IS. A Literature Review of Renal Surgical Anatomy and Surgical Strategies for Partial Nephrectomy. Eur Urol. 68(6):980-92. (2015)

(93) Klatte T, Mauermann J, Heinz-Peer G, Waldert M, Weibl P, Klingler HC, Remzi M. Perioperative, oncologic, and functional outcomes of laparoscopic renal cryoablation and open partial nephrectomy: a matched pair analysis. J Endourol. 25(6):991-7. (2011)

(94) Klingler HC, Marberger M, Mauermann J, Remzi M, Susani M. 'Skipping' is still a problem with radiofrequency ablation of small renal tumours. BJU Int. 99(5):998-1001. (2007)

(95) Klingler HC, Susani M, Seip R, Mauermann J, Sanghvi N, Marberger MJ. A novel approach to energy ablative therapy of small renal tumours: laparoscopic high-intensity focused ultrasound. Eur Urol. 53(4):810-6; discussion 817-8. (2008)

(96) Köhrmann KU, Back W, Bensemann J, Florian J, Weber A, Kahmann F, Rassweiler J, Alken P. The isolated perfused kidney of the pig: new model to evaluate shock wave-induced lesions. J Endourol. 8(2):105-10. (1994)

(97) Kroeger N, Choueiri TK, Lee JL, Bjarnason GA, Knox JJ, MacKenzie MJ, Wood L, Srinivas S, Vaishamayan UN, Rha SY, Pal SK, Yuasa T, Donskov F, Agarwal N, Tan MH, Bamias A, Kollmannsberger CK, North SA, Rini BI, Heng DY. Survival outcome and treatment response of patients with late relapse from renal cell carcinoma in the era of targeted therapy. Eur Urol. 65(6):1086-92. (2014)

(98) Kunkle DA, Uzzo RG. Cryoablation or radiofrequency ablation of the small renal mass: a meta-analysis. Cancer. 113(10):2671-80. (2008)

(99) Ladd AP, Rescorla FJ, Baust JG, Callahan M, Davis M, Grosfeld JL. Cryosurgical effects on growing vessels. Am Surg. 65(7):677-82. (1999)

(100) Lane BR, Abouassaly R, Gao T, Weight CJ, Hernandez AV, Larson BT, Kaouk JH, Gill IS, Campbell SC. Active treatment of localized renal tumors may not impact overall survival in patients aged 75 years or older. Cancer. 116(13):3119-26. (2010)

(101) Lee EW, Wong D, Prikhodko SV, Perez A, Tran C, Loh CT, Kee ST. Electron microscopic demonstration and evaluation of irreversible electroporation-induced nanopores on hepatocyte membranes. J Vasc Interv Radiol. 23(1):107-13. (2012)

(102) Liehr UB, Wendler JJ, Blaschke S, Porsch M, Janitzky A, Baumunk D, Pech M, Fischbach F, Schindele D, Grube C, Ricke J, Schostak M. [Irreversible electroporation: the new generation of local ablation techniques for renal cell carcinoma]. Urologe A. 51(12):1728-34. (2012)

(103) Liehr, Uwe-Bernd. Irreversible Elektroporation: präklinischen und klinische Evaluation eines neuen Verfahrens zur lokalen Ablation von lokalisierten Nierenzellkarzinomen. Magdeburg, Univ., Med. Fak., Habil.-Schr., 2014.

(104) Lindblad P. Epidemiology of renal cell carcinoma. Scand J Surg. 93(2):88-96. (2004)

(105) Lu DS, Raman SS, Vodopich DJ, Wang M, Sayre J, Lassman C. Effect of vessel size on creation of hepatic radiofrequency lesions in pigs: assessment of the "heat sink" effect. AJR Am J Roentgenol. 178(1):47-51. (2002)

(106) MacLennan S, Imamura M, Lapitan MC, Omar MI, Lam TB, Hilvano-Cabungcal AM, Royle P, Stewart F, MacLennan G, MacLennan SJ, Canfield SE, McClinton S, Griffiths TR, Ljungberg B, N'Dow J; UCAN Systematic Review Reference Group; EAU Renal Cancer Guideline Panel. Systematic review of oncological outcomes following surgical management of localised renal cancer. Eur Urol. 61(5):972-93. (2012)

(107) Mali B, Jarm T, Corovic S, Paulin-Kosir MS, Cemazar M, Sersa G, Miklavcic D. The effect of electroporation pulses on functioning of the heart. Med Biol Eng Comput. 46(8):745-57. (2008)

(108) Manual NanoKnife® System Procedure & Trouble Shouting Guide. Software version 2.2.0. AngioDynamics®, © AngioDynamics, Inc., 2011.

(109) Marconi L, Desai MM, Ficarra V, Porpiglia F, Van Poppel H. Renal Preservation and Partial Nephrectomy: Patient and Surgical Factors. Eur Urol Focus. 2(6):589-600. (2016)

(110) McKinley GM. Short electric wave radiation in biology. In: Duggar, B.M. (ed.) Biological effects of radiation. 1936; 1: 541-558. McGraw-Hill Book Co., New York. (1936)

(111) Meir A, Rubinsky B. Electrical impedance tomography of electrolysis. PLoS One. 10(6):e0126332. (2015)

(112) Meir A. A Study of Electrolytic Processes in Micro-Electroporation and Electroporation. A dissertation submitted in partial satisfaction of the requirements for the degree of Doctor in Philosophy In Biophysics in the Graduate Division of the University of California, Berkeley Committee in charge: Professor Boris Rubinsky, Chair, Professor Luke Lee, Professor Mohammad Mofrad, Professor Ralph Greif. Spring 2015.

(113) Miller L, Leor J, Rubinsky B. Cancer cells ablation with irreversible electroporation. Technology in Cancer Research and Treatment. 4: 699-706. (2005)

(114) Minervini A, Campi R, Sessa F, Derweesh I, Kaouk JH, Mari A, Rha KH, Sessa M, Volpe A, Carini M, Uzzo RG. Positive surgical margins and local recurrence after simple enucleation and standard partial nephrectomy for malignant renal tumors: systematic review of the literature and meta-analysis of prevalence. Minerva Urol Nefrol. 69(6):523-538. (2017)

(115) Mir LM, Orlowski S, Belehradek JJ, Paoletti C. Electrochemotherapy potentiation of antitumour effect of bleomycin by local electric pulses. European Journal of Cancer. 27: 68-72. (1991)

(116) Moreland AJ, Ziemlewicz TJ, Best SL, Hinshaw JL, Lubner MG, Alexander ML, Brace CL, Kitchin DR, Hedican SP, Nakada SY, Lee FT Jr, Abel EJ. High-powered microwave ablation of t1a renal cell carcinoma: safety and initial clinical evaluation. J Endourol 28(9):1046–1052. (2014)

(117) Morgan MS, Ozayar A, Lucas E, Friedlander JI, Shakir NA, Cadeddu JA. Comparative Effects of Irreversible Electroporation, Radiofrequency Ablation, and Partial Nephrectomy on Renal Function Preservation in a Porcine Solitary Kidney Model. Urology. 94:281-7. (2016)

(118) Neal RE 2nd, Garcia PA, Kavnoudias H, Rosenfeldt F, Mclean CA, Earl V, Bergman J, Davalos RV, Thomson KR. In vivo irreversible electroporation kidney ablation: experimentally correlated numerical models. IEEE Trans Biomed Eng. 62(2):561-9. (2015)

(119) Neal RE 2nd, Millar JL, Kavnoudias H, Royce P, Rosenfeldt F, Pham A, Smith R, Davalos RV, Thomson KR. In vivo characterization and numerical simulation of prostate properties for non-thermal irreversible electroporation ablation. Prostate. 74(5):458-68. (2014)

(120) Neumann E, Schaeffer-Ridder M, Wang Y, Hofschneider PH. Gene transfer into mouse lymphoma cells by electroporation in high electric fields. EMBO J. 1: 841-845. (1982)

(121) Neves RJ, Zincke H, Taylor WF. Metastatic renal cell cancer and radical nephrectomy: identification of prognostic factors and patient survival. J Urol. 139(6):1173-6. (1988)

(122) Olweny EO, Kapur P, Tan YK, Park SK, Adibi M, Cadeddu JA. Irreversible electroporation: evaluation of nonthermal and thermal ablative capabilities in the porcine kidney. Urology. 81(3):679-84. (2013)

(123) Olweny EO, Park SK, Tan YK, Best SL, Trimmer C, Cadeddu JA. Radiofrequency ablation versus partial nephrectomy in patients with solitary clinical T1a renal cell carcinoma: comparable oncologic outcomes at a minimum of 5 years of follow-up. Eur Urol. 61(6):1156-61. (2012)

(124) Panella L, Tinelli C, Buizza A, Lombardi R, Gandolfi R. Towards objective evaluation of balance in the elderly: validity and reliability of a measurement instrument applied to the Tinetti test. Int J Rehabil Res. 31(1):65-72. (2008)

(125) Patel HD, Pierorazio PM, Johnson MH, Sharma R, Iyoha E, Allaf ME, Bass EB, Sozio SM. Renal Functional Outcomes after Surgery, Ablation, and Active Surveillance of Localized Renal Tumors: A Systematic Review and Meta-Analysis. Clin J Am Soc Nephrol. 12(7):1057-1069. (2017)

(126) Pech M, Janitzky A, Wendler JJ, Strang C, Blaschke S, Dudeck O, Ricke J, Liehr UB. Irreversible electroporation of renal cell carcinoma: a first-in-man phase I clinical study. Cardiovasc Intervent Radiol. 34(1):132-8. (2011)

(127) Peyton CC, Heavner MG, Rague JT, Krane LS, Hemal AK. Does Sarcopenia Impact Complications and Overall Survival in Patients Undergoing Radical Nephrectomy for Stage III and IV Kidney Cancer? J Endourol. 30(2):229-36. (2016)

(128) Phillips M, Maor E, Rubinsky B. Nonthermal irreversible electroporation for tissue decellularization. J Biomech Eng. 132(9):091003. (2010)

(129) Pierorazio PM, Johnson MH, Patel HD, Sozio SM, Sharma R, Iyoha E, Bass EB, Allaf ME. Management of Renal Masses and Localized Renal Cancer: Systematic Review and Meta-Analysis. J Urol.196(4):989-99. (2016)

(130) Piñero J, Lopez-Baena M, Ortiz T, Cortes F. Apoptotic and necrotic cell death are both induced by electroporation in HL60 human promyeloid leukaemia cells. Apoptosis. 2: 330-336. (1997)

(131) Pirasteh A, Snyder L, Boncher N, Passalacqua M, Rosenblum D, Prologo JD. Cryoablation vs. radiofrequency ablation for small renal masses. Acad Radiol. 18(1):97-100. (2011)

(132) Psutka SP, Feldman AS, McDougal WS, McGovern FJ, Mueller P, Gervais DA. Long-term oncologic outcomes after radiofrequency ablation for T1 renal cell carcinoma. Eur Urol. 63(3):486-92. (2013)

(133) Puts MT, Hardt J, Monette J, Girre V, Springall E, Alibhai SM. Use of geriatric assessment for older adults in the oncology setting: a systematic review. J Natl Cancer Inst. 104(15):1133-63. (2012)

(134) Raz O, Mendlovic S, Leibovici D, Pantuck AJ, Sandbank J, Sella A, Lindner A, Zisman A. The prevalence of malignancy in satellite renal lesions and its surgical implication during nephron sparing surgery. J Urol. 178(5):1892-5; discussion 1895. (2007)

(135) Rendon RA, Kachura JR, Sweet JM, Gertner MR, Sherar MD, Robinette M, Tsihlias J, Trachtenberg J, Sampson H, Jewett MA. The uncertainty of radio frequency treatment of renal cell carcinoma: findings at immediate and delayed nephrectomy. J Urol. 167(4):1587-92. (2002)

(136) Ricke J, Jürgens JH, Deschamps F, Tselikas L, Uhde K, Kosiek O, De Baere T. Irreversible electroporation (IRE) fails to demonstrate efficacy in a prospective multicenter phase II trial on lung malignancies: the ALICE trial. Cardiovasc Intervent Radiol. 38(2):401-8. (2015)

(137) Ritchie RW, Leslie TA, Turner GD, Roberts IS, D'Urso L, Collura D, Demarchi A, Muto G, Sullivan ME. Laparoscopic high-intensity focused ultrasound for renal tumours: a proof of concept study. BJU Int. 107(8):1290-6. (2011)

(138) RKI (Robert Koch-Institut) 2016 - Bericht zum Krebsgeschehen in Deutschland 2016. Zentrum für Krebsregisterdaten im Robert Koch-Institut (Hrsg). Berlin, 2016.

(139) Robson CJ, Churchill BM, Anderson W. The results of radical nephrectomy for renal cell carcinoma. J Urol. 101(3):297-301. (1969)

(140) Rockwell AD. The Medical and surgical uses of electricity: including the X-ray, Finsen light, vibratory therapeutics, and high-frequency currents. E.B. Treat & Company, New York. (1903)

(141) Ruarus AH, Vroomen LGPH, Puijk RS, Scheffer HJ, Faes TJC, Meijerink MR. Conductivity Rise During Irreversible Electroporation: True Permeabilization or Heat? Cardiovasc Intervent Radiol. 41(8):1257-1266. (2018)

(142) Rubinsky B, Onik G, Mikus P. Irreversible electroporation: a new ablation modality - clinical implications. Technol Cancer Res Treat. 6(1):37-48. (2007)

(143) Rubinsky J, Onik G, Mikus P, Rubinsky B. Optimal parameters for the destruction of prostate cancer using irreversible electroporation. J Urol. 180(6):2668-74. (2008)

(144) Rubinsky, Boris (Ed.) Irreversible Electroporation. Series in Biomedical Engineering. 1. Auflage: eBook-ISBN: 978-3-642-05420-4; Springer-Verlag Berlin Heidelberg 2010.

(145) Sale AJH, Hamilton WA. Effects of high electric fields on microorganisms. Biochimica et Biophysica Acta. 148: 781-800. (1967)

(146) Sano MB, DeWitt MR, Teeter SD, Xing L. Optimization of a single insertion electrode array for the creation of clinically relevant ablations using high-frequency irreversible electroporation. Comput Biol Med95:107-117. (2018a)

(147) Sano MB, Fesmire CC, DeWitt MR, Xing L. Burst and continuous high frequency irreversible electroporation protocols evaluated in a 3D tumor model. Phys Med Biol. 63(13):135022. (2018b)

(148) Scheffer HJ, Vogel JA, van den Bos W, Neal RE 2nd, van Lienden KP, Besselink MG, van Gemert MJ, van der Geld CW, Meijerink MR, Klaessens JH, Verdaasdonk RM. The Influence of a Metal Stent on the Distribution of Thermal Energy during Irreversible Electroporation. PLoS One. 11(2):e0148457. (2016)

(149) Scheltema MJ, Chang JI, Böhm M, van den Bos W, Blazevski A, Gielchinsky I, Kalsbeek AMF, van Leeuwen PJ, Nguyen TV, de Reijke TM, Siriwardana AR, Thompson JE, de la Rosette JJ, Stricker PD. Pair-matched patient-reported quality of life and early oncological control following focal irreversible electroporation versus robot-assisted radical prostatectomy. 36(9):1383-1389. (2018)

(150) Schilling S, Schmid S, Jäger H, Ludwig M, Dietrich H, Toepfl S, Knorr D, Neidhart S, Schieber A, Carle R. Comparative study of pulsed electric field and thermal processing of apple juice with particular consideration of juice quality and enzyme deactivation. J Agric Food Chem. 56(12):4545-54. (2008)

(151) Schmidt CR, Shires P, Mootoo M. Real-time ultrasound imaging of irreversible electroporation in a porcine liver model adequately characterizes the zone of cellular necrosis. HPB (Oxford). 14(2):98-102. (2012)

(152) Schulz KF, Grimes DA. Get in the spirit with SPIRIT 2013: Protocol content guideline for clinical trials. Contraception 88:676-7. (2013)

(153) Serni S, Vittori G, Frizzi J, Mari A, Siena G, Lapini A, Carini M, Minervini A. Simple enucleation for the treatment of highly complex renal tumors: Perioperative, functional and oncological results. Eur J Surg Oncol. 41(7):934-40. (2015)

(154) Siva S, Louie AV, Warner A, Muacevic A, Gandhidasan S, Ponsky L, Ellis R, Kaplan I, Mahadevan A, Chu W, Swaminath A, Onishi H, Teh B, Correa RJ, Lo SS, Staehler M. Pooled analysis of stereotactic ablative radiotherapy for primary renal cell carcinoma: A report from the International Radiosurgery Oncology Consortium for Kidney (IROCK). Cancer. 124(5):934-942. (2018)

(155) Siva S, Pham D, Gill S, Corcoran NM, Foroudi F. A systematic review of stereotactic radiotherapy ablation for primary renal cell carcinoma. BJU Int. 110(11 Pt B):E737-43. (2012)

(156) Siva S, Pham D, Kron T, Bressel M, Lam J, Tan TH, Chesson B, Shaw M, Chander S, Gill S, Brook NR, Lawrentschuk N, Murphy DG, Foroudi F. Stereotactic ablative body radiotherapy for inoperable primary kidney cancer: a prospective clinical trial. BJU Int. 120(5):623-630. (2017)

(157) Sommer CM, Fritz S, Wachter MF, Vollherbst D, Stampfl U, Bellemann N, Gockner T, Mokry T, Gnutzmann D, Schmitz A, Knapp J, Longerich T, Kuhn-Neureuther C, Pereira PL, Kauczor HU, Werner J, Radeleff BA. Irreversible electroporation of the pig kidney with involvement of the renal pelvis: technical aspects, clinical outcome, and three-dimensional CT rendering for assessment of the treatment zone. J Vasc Interv Radiol. 24(12):1888-97. (2013)

(158) Srimathveeravalli G, Cornelis F, Wimmer T, Monette S, Kimm SY, Maybody M, Solomon SB, Coleman JA, Durack JC. Normal Porcine Ureter Retains Lumen Wall Integrity but Not Patency Following Catheter-Directed Irreversible Electroporation: Imaging and Histologic Assessment over 28 Days. J Vasc Interv Radiol. 28(6):913-919.e1. (2017)

(159) Srimathveeravalli G, Silk M, Wimmer T, Monette S, Kimm S, Maybody M, Solomon SB, Coleman J, Durack JC. Feasibility of catheter-directed intraluminal irreversible electroporation of porcine ureter and acute outcomes in response to increasing energy delivery. J Vasc Interv Radiol. 26(7):1059-66. (2015)

(160) Stämpfli R. Reversible electrical breakdown of the excitable membrane of a Ranvier node. Anais da Academia Brasileira de Ciencias. 30: 57-63. (1957)

(161) Strom KH, Derweesh I, Stroup SP, Malcolm JB, L'Esperance J, Wake RW, Gold R, Fabrizio M, Palazzi-Churas K, Gu X, Wong C. Second prize: Recurrence rates after percutaneous and laparoscopic renal cryoablation of small renal masses: does the approach make a difference? J Endourol. 25(3):371-5. (2011)

(162) Sun M, Becker A, Tian Z, Roghmann F, Abdollah F, Larouche A, Karakiewicz PI, Trinh QD. Management of localized kidney cancer: calculating cancer-specific mortality and competing risks of death for surgery and nonsurgical management. Eur Urol. 65(1):235-41. (2014)

(163) Sun M, Bianchi M, Trinh QD, Hansen J, Abdollah F, Hanna N, Tian Z, Shariat SF, Montorsi F, Perrotte P, Karakiewicz PI. Comparison of partial vs radical nephrectomy with regard to other-cause mortality in T1 renal cell carcinoma among patients aged ≥75 years with multiple comorbidities. BJU Int. 111(1):67-73. (2013)

(164) Surbone A, Kagawa-Singer M, Terret C, Baider L. The illness trajectory of elderly cancer patients across cultures: SIOG position paper. Ann Oncol. 18(4):633-8. (2007)

(165) Tacke J. [Interventional oncology in urology]. Radiologe. 47(12):1089-96. (2007)

(166) Takaki H, Yamakado K, Soga N, Arima K, Nakatsuka A, Kashima M, Uraki J, Yamada T, Takeda K, Sugimura Y. Midterm results of radiofrequency ablation versus nephrectomy for T1a renal cell carcinoma. Jpn J Radiol. 28(6):460-8. (2010)

(167) Terrone C, Cracco C, Guercio S, Bollito E, Poggio M, Scoffone C, Tarabuzzi R, Porpiglia F, Scarpa RM, Fontana D, Rocca Rossetti S. Prognostic value of the involvement of the urinary collecting system in renal cell carcinoma. Eur Urol. 46(4):472-6. (2004)

(168) Thompson RH, Hill JR, Babayev Y, Cronin A, Kaag M, Kundu S, Bernstein M, Coleman J, Dalbagni G, Touijer K, Russo P. Metastatic renal cell carcinoma risk according to tumor size. J Urol. 182(1):41-5. (2009)

(169) Thomson KR, Cheung W, Ellis SJ, Federman D, Kavnoudias H, Loader-Oliver D, Roberts S, Evans P, Ball C, Haydon A. Investigation of the safety of irreversible electroporation in humans. J Vasc Interv Radiol. 22(5):611-21. (2011)

(170) Ting F, Tran M, Böhm M, Siriwardana A, Van Leeuwen PJ, Haynes AM, Delprado W, Shnier R, Stricker PD. Focal irreversible electroporation for prostate cancer: functional outcomes and short-term oncological control. Prostate Cancer Prostatic Dis. 19(1):46-52. (2016)

(171) Toepfl S, Mathys A, Heinz V, Knorr D. Potential of High Hydrostatic Pressure and Pulsed Electric Fields for Energy Efficient and Environmentally Friendly Food Processing. Food Reviews International 22: 405-423. (2006)

(172) Tracy CR, Kabbani W, Cadeddu JA. Irreversible electroporation (IRE): a novel method for renal tissue ablation. BJU Int. 107(12):1982-7. (2011)

(173) Tracy CR, Raman JD, Donnally C, Trimmer CK, Cadeddu JA. Durable oncologic outcomes after radiofrequency ablation: experience from treating 243 small renal masses over 7.5 years. Cancer. 116(13):3135-42. (2010)

(174) Trimmer CK, Khosla A, Morgan M, Stephenson SL, Ozayar A, Cadeddu JA. Minimally Invasive Percutaneous Treatment of Small Renal Tumors with Irreversible Electroporation: A Single-Center Experience. J Vasc Interv Radiol. 26(10):1465-71. (2015)

(175) Tsili AC, Argyropoulou MI. Advances of multidetector computed tomography in the characterization and staging of renal cell carcinoma. World J Radiol. 7(6):110-27. (2015)

(176) Uchida M, Imaide Y, Sugimoto K, Uehara H, Watanabe H. Percutaneous cryosurgery for renal tumours. Br J Urol. 75(2):132-6; discussion 136-7. (1995)

(177) Uhlig J, Strauss A, Rücker G, Seif Amir Hosseini A, Lotz J, Trojan L, Kim HS, Uhlig A. Partial nephrectomy versus ablative techniques for small renal masses: asystematic review and network meta-analysis. Eur Radiol. 29(3):1293-1307. (2019)

(178) Usman M, Moore W, Talati R, Watkins K, Bilfinger TV. Irreversible electroporation of lung neoplasm: a case series. Med Sci Monit. 18(6):CS43-7. (2012)

(179) van den Bos W, de Bruin DM, Jurhill RR, Savci-Heijink CD, Muller BG, Varkarakis IM, Skolarikos A, Zondervan PJ, Laguna-Pes MP, Wijkstra H, de Reijke TM, de la Rosette JJ. The correlation between the electrode configuration and histopathology of irreversible electroporation ablations in prostate cancer patients. World J Urol. 34(5):657-64. (2016a)

(180) van den Bos W, de Bruin DM, Muller BG, Varkarakis IM, Karagiannis AA, Zondervan PJ, Laguna Pes MP, Veelo DP, Savci Heijink CD, Engelbrecht MR, Wijkstra H, de Reijke TM, de la Rosette JJ. The safety and efficacy of irreversible electroporation for the ablation of prostate cancer: a multicentre prospective human in vivo pilot study protocol. BMJ Open. 4(10):e006382. (2014)

(181) van den Bos W, Jurhill RR, de Bruin DM, Savci-Heijink CD, Postema AW, Wagstaff PG, Muller BG, Varkarakis IM, Skolarikos A, Zondervan PJ, Laguna Pes MP, de Reijke TM, de la Rosette JJ. Histopathological Outcomes after Irreversible Electroporation for Prostate Cancer: Results of an Ablate and Resect Study. J Urol. 196(2):552-9. (2016b)

(182) van den Bos W, Scheffer HJ, Vogel JA, Wagstaff PG, de Bruin DM, de Jong MC, van Gemert MJ, de la Rosette JJ, Meijerink MR, Klaessens JH, Verdaasdonk RM. Thermal Energy during Irreversible Electroporation and the Influence of Different Ablation Parameters. J Vasc Interv Radiol. 27(3):433-43. (2016c)

(183) van den Bos W, Scheltema MJ, Siriwardana AR, Kalsbeek AMF, Thompson JE, Ting F, Böhm M, Haynes AM, Shnier R, Delprado W, Stricker PD. Focal irreversible electroporation as primary treatment for localized prostate cancer. BJU Int. 121(5):716-724. (2018)

(184) van der Poel HG, van den Bergh RCN, Briers E, Cornford P, Govorov A, Henry AM, Lam TB, Mason MD, Rouvière O, De Santis M, Willemse PM, van Poppel H, Mottet N. Focal Therapy in Primary Localised Prostate Cancer: The European Association of Urology Position in 2018. Eur Urol. 74(1):84-91. (2018)

(185) van Es R, Vink J, Lajoinie G, Versluis M, Byrd I, Neven K, Doevendans P, Wittkampf F. 216-02: In vitro analysis of gas bubble formation and its effect on impedance during electroporation ablation. EP Europace, Volume 18, Issue suppl_1, 1 Pages i141. (2016)

(186) Varkarakis IM, Allaf ME, Inagaki T, Bhayani SB, Chan DY, Su LM, Jarrett TW, Kavoussi LR, Solomon SB. Percutaneous radio frequency ablation of renal masses: results at a 2-year mean followup. J Urol. 174(2):456-60; discussion 460. (2005)

(187) Wagener N. [Renal cell carcinoma in older and geriatric patients]. Urologe A. 56(8):1019-1024. (2017)

(188) Wagstaff PG, de Bruin DM, Zondervan PJ, Savci Heijink CD, Engelbrecht MR, van Delden OM, van Leeuwen TG, Wijkstra H, de la Rosette JJ, Laguna Pes MP. The efficacy and safety of irreversible electroporation for the ablation of renal masses: a prospective, human, in-vivo study protocol. BMC Cancer. 15:165. (2015)

(189) Wah TM, Irving HC, Gregory W, Cartledge J, Joyce AD, Selby PJ. Radiofrequency ablation (RFA) of renal cell carcinoma (RCC): experience in 200 tumours. BJU Int. 113(3):416-28. (2014)

(190) Wedding U. Geriatrisches Assessment in der Urologie. In: MichelMS, Thüroff JW, Janetschek Getal (Hrsg)Die Urologie. Springer, Heidelberg, SS2273–S2280. 2016.

(191) Wendler JJ, Damm R, Liehr UB, Brunner T, Pech M, Schostak M. [Small renal cell carcinoma-active surveillance and ablation]. Urologe A. 57(6):731-743. (2018c)

(192) Wendler JJ, Fischbach K, Ricke J, Jürgens J, Fischbach F, Köllermann J, Porsch M, Baumunk D, Schostak M, Liehr UB, Pech M. Irreversible Electroporation (IRE): Standardization of Terminology and Reporting Criteria for Analysis and Comparison. Pol J Radiol. 81:54-64. (2016a)

(193) Wendler JJ, Friebe B, Baumunk D, Blana A, Franiel T, Ganzer R, Hadaschik B, Henkel T, Köhrmann KU, Köllermann J, Kuru T, Machtens S, Roosen A, Salomon G, Schlemmer HP, Sentker L, Witzsch U, Liehr UB, Ricke J, Schostak M. [Focal therapy for small renal masses: Observation, ablation or surgery]. Urologe A. 55(5):594-606. (2016c)

(194) Wendler JJ, Ganzer R, Hadaschik B, Blana A, Henkel T, Köhrmann KU, Machtens S, Roosen A, Salomon G, Sentker L, Witzsch U, Schlemmer HP, Baumunk D, Köllermann J, Schostak M, Liehr UB; Working Group for Focal and Microtherapy, Academy of the German Society of Urology. [Irreversible electroporation. Current value for focal treatment of prostate cancer]. Urologe A. 54(6):854-62. (2015a)

(195) Wendler JJ, Ganzer R, Hadaschik B, Blana A, Henkel T, Köhrmann KU, Machtens S, Roosen A, Salomon G, Sentker L, Witzsch U, Schlemmer HP, Baumunk D, Köllermann J, Schostak M, Liehr UB. Why we should not routinely apply irreversible electroporation as an alternative curative treatment modality for localized prostate cancer at this stage. World J Urol. 35(1):11-20. (2017a)

(196) Wendler JJ, Klink F, Seifert S, Fischbach F, Jandrig B, Porsch M, Pech M, Baumunk D, Ricke J, Schostak M, Liehr UB. Irreversible Electroporation of Prostate Cancer: Patient-Specific Pretreatment Simulation by Electric Field Measurement in a 3D Bioprinted Textured Prostate Cancer Model to Achieve Optimal Electroporation Parameters for Image-Guided Focal Ablation. Cardiovasc Intervent Radiol. 39(11):1668-1671. (2016d)

(197) Wendler JJ, Liehr BU, Damm R, Powerski M, Brunner T, Schostak M, Pech M. Small renal carcinoma: the "when" and "how" of operation, active surveillance, and ablation. Pol J Radiol. 83:e561-e568. (2018d)

(198) Wendler JJ, Pech M, Blaschke S, Porsch M, Janitzky A, Ulrich M, Dudeck O, Ricke J, Liehr UB. Angiography in the isolated perfused kidney: radiological evaluation of vascular protection in tissue ablation by nonthermal irreversible electroporation. Cardiovasc Intervent Radiol. 35(2):383-90. (2012a)

(199) Wendler JJ, Pech M, Fischbach F, Jürgens J, Friebe B, Baumunk D, Porsch M, Blaschke S, Schindele D, Siedentopf S, Ricke J, Schostak M, Köllermann J, Liehr UB. Initial Assessment of the Efficacy of Irreversible Electroporation in the Focal Treatment of Localized Renal Cell Carcinoma with Delayed-interval Kidney Tumor Resection (Irreversible Electroporation of Kidney Tumors before Partial Nephrectomy [IRENE] Trial-An Ablate-and-Resect Pilot Study). Urology. 114:224-232. (2018b)

(200) Wendler JJ, Pech M, Köllermann J, Friebe B, Siedentopf S, Blaschke S, Schindele D, Porsch M, Baumunk D, Jürgens J, Fischbach F, Ricke J, Schostak M, Böhm M, Liehr UB. Upper-Urinary-Tract Effects After Irreversible Electroporation (IRE) of Human Localised Renal-Cell Carcinoma (RCC) in the IRENE Pilot Phase 2a Ablate-and-Resect Study. Cardiovasc Intervent Radiol. 41(3):466-476. (2018a)

(201) Wendler JJ, Pech M, Porsch M, Janitzky A, Fischbach F, Buhtz P, Vogler K, Hühne S, Borucki K, Strang C, Mahnkopf D, Ricke J, Liehr UB. Urinary tract effects after multifocal nonthermal irreversible electroporation of the kidney: acute and chronic monitoring by magnetic resonance imaging, intravenous urography and urinary cytology. Cardiovasc Intervent Radiol. 35(4):921-6. (2012b)

(202) Wendler JJ, Porsch M, Fischbach F, Pech M, Schostak M, Liehr UB. Letter to the Editor Concerning "Irreversible Electroporation (IRE) Fails to Demonstrate Efficacy in a Prospective Multicenter Phase II Trial on Lung Malignancies: The ALICE Trial" by Ricke et al. 2015 (doi:10.1007/s00270-014-1049-0). Cardiovasc Intervent Radiol. 38(4):1064-5. (2015c)

(203) Wendler JJ, Porsch M, Hühne S, Baumunk D, Buhtz P, Fischbach F, Pech M, Mahnkopf D, Kropf S, Roessner A, Ricke J, Schostak M, Liehr UB. Short- and mid-term effects of irreversible electroporation on normal renal tissue: an animal model. Cardiovasc Intervent Radiol. 36(2):512-20. (2013)

(204) Wendler JJ, Porsch M, Nitschke S, Köllermann J, Siedentopf S, Pech M, Fischbach F, Ricke J, Schostak M, Liehr UB. A prospective Phase 2a pilot study investigating focal percutaneous irreversible electroporation (IRE) ablation by NanoKnife in patients with localised renal cell carcinoma (RCC) with delayed interval tumour resection (IRENE trial). Contemp Clin Trials. 43:10-9. (2015b)

(205) Wendler JJ, Ricke J, Pech M, Fischbach F, Jürgens J, Porsch M, Janitzky A, Baumunk D, Siedentopf S, Köllermann J, Schostak M, Liehr UB. Initial assessment of clinical feasibility, safety and efficacy of NanoKnife irreversible electroporation (IRE) in the focal treatment of localized renal cell carcinoma (RCC) with delayed interval tumor resection (IRENE trial). 32nd Annual EAU Congress, London. Eur Urol Suppl 16(3);e102. (2017b)

(206) Wendler JJ, Ricke J, Pech M, Fischbach F, Jürgens J, Siedentopf S, Roessner A, Porsch M, Baumunk D, Schostak M, Köllermann J, Liehr UB. First Delayed Resection Findings After Irreversible Electroporation (IRE) of Human Localised Renal Cell Carcinoma (RCC) in the IRENE Pilot Phase 2a Trial. Cardiovasc Intervent Radiol. 39(2):239-50. (2016b)

(207) Whitson JM, Harris CR, Meng MV. Population-based comparative effectiveness of nephron-sparing surgery vs ablation for small renal masses. BJU Int. 110(10):1438-43; discussion 1443. (2012)

(208) Wiggermann P, Brünn K, Bäumler W. [Irreversible electroporation (IRE): A minimally invasive therapeutic option in prostate cancer]. Radiologe. 57(8):637-640. (2007)

(209) Wimmer T, Srimathveeravalli G, Gutta N, Ezell PC, Monette S, Maybody M, Erinjery JP, Durack JC, Coleman JA, Solomon SB. Planning irreversible electroporation in the porcine kidney: are numerical simulations reliable for predicting empiric ablation outcomes? Cardiovasc Intervent Radiol. 38(1):182-90. (2015)

(210) Wittekind B.J, C. Compton CC, Sobin LH (eds). A Commentary on Uniform Use. UICC International Union against cancer. 4th edition. Wiley-Blackwell. 106. 2013.

(211) Xi W, Wang J, Liu L, Xiong Y, Qu Y, Lin Z, Chen X, Wang Z, Xu J, Guo J. Evaluation of Tumor Pseudocapsule Status and Its Prognostic Significance in Renal Cell Carcinoma. J Urol. pii: S0022-5347(17)77849-4. (2017)

(212) Yao C, Sun C, Mi Y, Xiong L, Wang S. Experimental studies on Killing and inhibiting effects of steep pulsed electric field (SPEF) to target cancer cell and solid tumor. IEEE Trans. Plasma Science. 32: 1626-1633. (2004)

(213) Zagoria RJ, Pettus JA, Rogers M, Werle DM, Childs D, Leyendecker JR. Long-term outcomes after percutaneous radiofrequency ablation for renal cell carcinoma. Urology. 77(6):1393-7. (2011)

(214) Zhang B, Yang Y, Ding L, Moser MAJ, Zhang EM, Zhang W. Tumor Ablation Enhancement by Combining Radiofrequency Ablation and Irreversible Electroporation: An In Vitro 3D Tumor Study. Ann Biomed Eng. 47(3):694-705. (2019)

(215) Zhao Y, Bhonsle S, Dong S, Lv Y, Liu H, Safaai-Jazi A, Davalos RV, Yao C. Characterization of Conductivity Changes During High-Frequency Irreversible Electroporation for Treatment Planning. IEEE Trans Biomed Eng. 65(8):1810-1819. (2018)

(216) Zhou W, Arellano RS. Thermal Ablation of T1c Renal Cell Carcinoma: A Comparative Assessment of Technical Performance, Procedural Outcome, and Safety of Microwave Ablation, Radiofrequency Ablation, and Cryoablation. J Vasc Interv Radiol. 29(7):943-951. (2018)

(217) Zimmermann U. Electric field-mediated fusion and related electrical phenomena. Biochimica et Biophysica Acta. 694: 227-277. (1982)

(218) Zlotta AR, Wildschutz T, Raviv G, Peny MO, van Gansbeke D, Noel JC, Schulman CC. Radiofrequency interstitial tumor ablation (RITA) is a possible new modality for treatment of renal cancer: ex vivo and in vivo experience. J Endourol. 11(4):251-8. (1997)

(219) Zondervan PJ, Buijs M, De Bruin DM, van Delden OM, Van Lienden KP. Available ablation energies to treat cT1 renal cell cancer: emerging technologies. World J Urol. 37(3):445-455. (2019)

(220) Zondervan PJ, Wagstaff PG, Desai MM, de Bruin DM, Fraga AF, Hadaschik BA, Köllermann J, Liehr UB, Pahernik SA, Schlemmer HP, Wendler JJ, Algaba F, de la Rosette JJ, Laguna Pes MP. Follow-up after focal therapy in renal masses: an international multidisciplinary Delphi consensus project. World J Urol. 34(12):1657-1665. (2016)

8. Anhang – Verwendete Publikationen

8.1

Irreversible electroporation: the new generation of local ablation techniques for renal cell carcinoma.

Liehr UB, Wendler JJ, Blaschke S, Porsch M, Janitzky A, Baumunk D, Pech M, Fischbach F, Schindele D, Grube C, Ricke J, Schostak M.

Urologe A. 2012 Dec;51(12):1728-34. doi: 10.1007/s00120-012-3038-8. German.

BACKGROUND: Local ablation techniques are a major focus of current developments in oncology. The primary aim is to retain organs and preserve organ functions without compromising the oncological outcome.

METHOD: Irreversible electroporation (IRE) is a novel ablation technique that involves the application of high-voltage pulses to induce cell apoptosis without causing thermal damage to the target tissue or adjacent structures.

AIM: First published in 2005 IRE is currently undergoing preclinical and clinical trials in several areas of oncology and the initial results have been promising. The IRE technique could be a significant development in ablation treatment for renal cell carcinoma (RCC) but decisive proof of its effectiveness for local RCC has not yet been provided. This study presents the results of preclinical and initial clinical trials which are discussed and compared with those of other ablation techniques in order to demonstrate the current value of IRE.

Urologe 2012 · 51:1728–1734
DOI 10.1007/s00120-012-3038-8
Online publiziert: 10. November 2012

U.-B. Liehr[1] · J.J. Wendler[1] · S. Blaschke[1] · M. Porsch[1] · A. Janitzky[1] · D. Baumunk[1]
M. Pech[2] · F. Fischbach[2] · D. Schindele[1] · C. Grube[1] · J. Ricke[2] · M. Schostak[1]
[1] Klinik für Urologie und Kinderurologie, Universitätsklinikum Magdeburg A.ö.R., Magdeburg
[2] Klinik für Radiologie und Nuklearmedizin, Universitätsklinikum Magdeburg A.ö.R., Magdeburg

Irreversible Elektroporation

Die neue Generation lokaler Ablationsverfahren beim Nierenzellkarzinom

Hintergrund und Fragestellung

Aktuell gibt es in der onkologischen Chirurgie den Trend von der ultraradikalen Exzisionschirurgie zu fokalen Therapien. Idealerweise gelingt bei gleicher onkologischer Sicherheit der Funktionserhalt des betroffenen Organs. In der Urologie betrifft dieser Trend v. a. die Niere, eine Nierenteilresektion ist seit Jahren leitliniengerechte Behandlungsalternative zur Nephrektomie [1]. Bei ausgewählten Patienten (Morbidität, drohende Dialyse) kommen Kryotherapie und Radiofrequenzablation (RFA) nach histologischer Sicherung in Frage. Andere Ablationsverfahren gelten derzeit als experimentell [1]. Kein Verfahren selektiert Tumorgewebe oder respektiert Grenzstrukturen.

Die Wirkung thermaler Ablationstechniken ist aufgrund durchbluteter Gefäße (>3 mm; ca. 37°C) im Bereich des Zielgewebes limitiert. Die Hitzewirkung hyperthermaler Ablationsverfahren wird durch die kühlende Durchblutung („heat sink effect“ [2]), die Kältewirkung hypothermaler Techniken durch die erwärmende Durchblutung („cold sink effect“ [3]) reduziert. Da die Wirkung der bisherigen Ablationsmethoden im Tumorrandbereich zentrifugal nachlässt, ist eine scharfe Therapiebegrenzung auf den Tumor schwierig. Die irreversible Elektroporation (IRE) stellt als neue nichtthermale Ablationsmethode eine Alternative ohne die genannten Nachteile dar. 2005 wurde die IRE erstmals wissenschaftlich publiziert [17]. Seit 2008 hat die Technik eine europäische CE-Kennzeichnung und ist zur Anwendung im Rahmen von Medizinproduktstudien zugelassen.

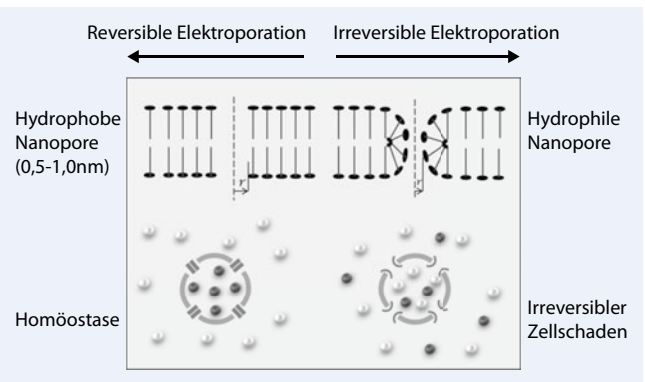

Abb. 1 ◀ Rechts schematische Darstellung der reversiblen und irreversiblen Elektroporation

Methodik

Im Folgenden wird die Technik, bisherige eigene Untersuchungen der IRE bei Nierenzellkarzinomen (NZK) und die aktuelle Wertigkeit des Verfahrens dargestellt.

Ergebnisse

- Technik: Die IRE ist ein minimal-invasives, nonthermales Gewebeablationsverfahren, welches eine permanente elektrische Permeabilisation der Zellmembran auf Molekularebene im Nanomillimeterbereich (NanoKnife) bewirkt (**Abb. 1**). Es werden pro Behandlung 90–100 hochenergetische, ultrakurze (Pulsdauer 20–200 µs), rektanguläre Starkstrompulse (Wechselstrom) mit bis zu 50 A und 3000 V durch nadelförmige Elektroden im Zielgewebe appliziert. Das elektrische Feld wirkt gewebeunspezifisch nur auf vitale Zellen ohne thermoablative Effekte und führt zum irreversiblen Zelltod im Applikationsbreich des elektrischen Feldes nach ca. 3 (1–7) Tagen. Die nachgewiesenen Mikroporen wiesen im Mittel einen Durchmesser von 340–360 nm auf [18].

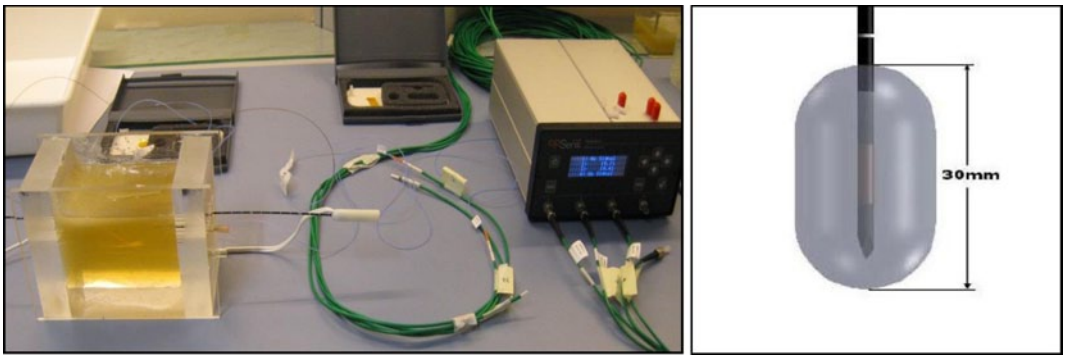

Abb. 2 ◀ Versuchsaufbau Temperaturmessung während IRE im Hydrogel-Acrylglasblock-Phantom (*links*), bipolare Ablationsgeometrie schematisch (*rechts*)

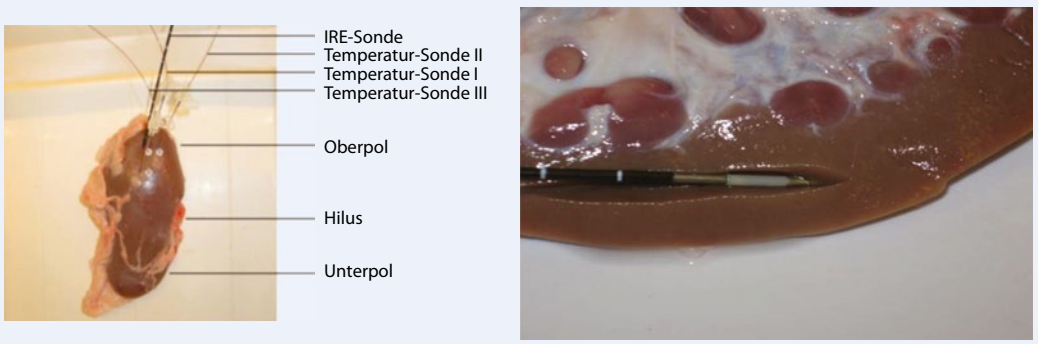

Abb. 3 ◀ Anordnung der Messsonden und Mikroporationselektrode (*links*), Markierung des Elektrodenkanals für die histologische Aufarbeitung (*rechts*)

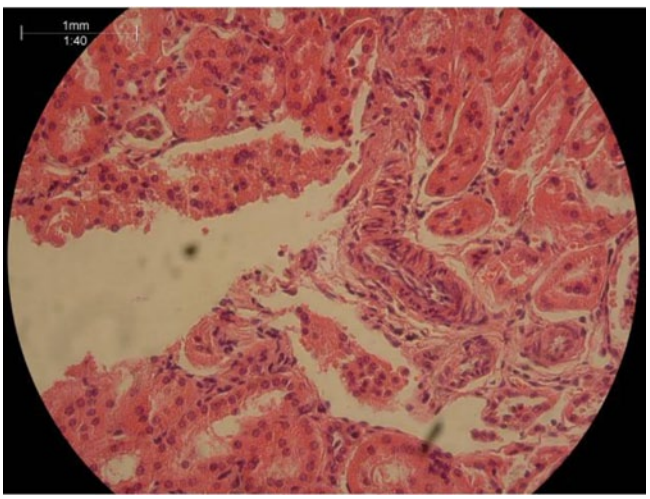

Abb. 4 ◀ Mikroskopisches Präparat, Vergrößerung 1:20: Kanalspitze markiert Lage der IRE-Elektrode zum Ablationszeitpunkt

- Studien: Bis September 2008 gab es weltweit keine Erkenntnisse zur Anwendung der IRE an der Niere. Eine systematische Überprüfung ihrer physikalischen Eigenschaften sowie der Anwendungsmöglichkeit an Nierengewebe und -tumoren wurde in unserer Klinik durchgeführt.

Physikalische Eigenschaften im Eiweißmodell

Zur Darstellung des Verhaltens der IRE-Elektrode in flüssigen bzw. viskösen, physiologischen Medien wurde die IRE versuchsweise in dekantiertem Hühnereieiweiß bei Raumtemperatur (24°C) durchgeführt. Hierzu wurde eine bipolare IRE-Elektrode (NanoKnife™, bipolar probe, 15 cm, 5 Charr., AngioDynamics® Inc. Queensbury, NY, USA) in einem Reagenzglas mit 200 ml flüssigem Hühnereiweiß fixiert und mittels des NanoKnife™-Electroporators (AngioDynamics® Inc. Queensbury, NY, USA) jeweils 90 IRE-Impulse (Gesamtenergie: 375 kJ) appliziert. An der Elektrode kam es pulssynchron zu Lichtblitzen, einhergehend mit einem lauten Knallgeräusch und wolkenartige Formationen im flüssigen Eiweiß mit zentrifugaler Ausbreitung (ca. 2 cm). Makroskopisch denaturiertes Eiweiß fand sich bis auf einen dünnen Film an der Elektrode nicht.

Physikalische Eigenschaften im Gelmodell

Die IRE ist für die Ablation von Weichteilgewebe zugelassen. In einem weichteilgewebeähnlichen Gel (Roth® 240 Bloom), welches in Konsistenz, Wärmeleitfähigkeit und Elektrolytzusammensetzung annähernd den physikalischen Eigenschaften der Niere entsprach, wurden Temperaturveränderungen durch IRE mit 2 Temperatursensoren (OTG1®, TempSens72® von OpSens®) gemessen (**Abb. 2**).

Es ergaben sich über die Dauer der IRE (90 s) bei einem Abstand von 5 mm und 10 mm zur IRE-Sonde Temperaturdifferenzen im Mittel von 13,3 und 2,0°C.

Physikalische Eigenschaften im Nierenfrischpräparat

Fünf schlachtfrische Schweinenieren wurden ex vivo zur Beobachtung der IRE-Effekte an organischem Material herangezogen, die Temperaturentwicklung während der Applikation in definierten Abständen zur IRE-Elektrode (5, 10 und 20 mm) gemessen, sowie der Einfluss der IRE auf die anatomischen Strukturen histologisch untersucht (**Abb. 3**). Die Platzierung der IRE-Nadel und Messsonden erfolgte sonographisch (Linear Array 7,5 MHz).

Es ergaben sich maximale Temperaturanstiege von im Mittel 14,5°C, 4,9°C und 0,4°C. Histologisch zeigten sich unauffällige Blutgefäße, Glomeruli und Nierentubuli ohne thermische Schäden (**Abb. 4**).

Physikalische Eigenschaften im Nierenperfusionsmodell

Einflüsse auf durchströmte Strukturen (arterielles, venöses System, harnleitendes System) sowie angiographische Veränderungen vor, während und nach IRE sollten am perfundierten In-vitro-Nierenfrischpräparat mittels digitaler Substraktionsangiographie (DSA; AXIOM Artis FA®, Siemens, Deutschland) und hochauflösender Mammographietechnik (Mammomat 3.000® Siemens, Deutschland; Bariumsulfatkontrastmittel) aufgezeigt werden.

Das Perfusionsmodell am Nierenfrischpräparat erwies sich als robuste und reproduzierbare Versuchsanordnung (**Abb. 5**). Die Organe zeigten eine komplette Perfusion mittels Indigoblaufarbstoffindikator und wiesen bei konstanten Druckverhältnissen und konstantem Perfusionszeitvolumen ein Verhältnis venöser Abfluss zu ureteralem Eluat von 9:1 auf. Während und nach der IRE zeigten sich keine Veränderungen in der Gefäßdarstellung, Extravasationen, Kontrastmittelakkumulationen oder -stasen (**Abb. 6,** [24]).

Zusammenfassung · Abstract

Urologe 2012 · 51:1728–1734 DOI 10.1007/s00120-012-3038-8

U.-B. Liehr · J.J. Wendler · S. Blaschke · M. Porsch · A. Janitzky · D. Baumunk · M. Pech F. Fischbach · D. Schindele · C. Grube · J. Ricke · M. Schostak

Irreversible Elektroporation. Die neue Generation lokaler Ablationsverfahren beim Nierenzellkarzinom

Zusammenfassung

Hintergrund. Lokale Ablationsverfahren stehen in der Onkologie im Fokus aktueller Entwicklungen. Vorrangiges Ziel ist es, ohne Kompromittieren der onkologischen Ergebnisse, Organe und Organfunktionen zu erhalten.

Methode. Die irreversible Elektroporation (IRE) ist ein neues Ablationsverfahren und beruht auf einer induzierten Zellapoptose nach Applikation von Starkstromimpulsen ohne thermische Schädigung des Zielgewebes und benachbarter Strukturen.

Ziel. 2005 erstmals publiziert, wird die IRE aktuell in einigen onkologischen Fachgebieten präklinischen und klinischen Untersuchungen unterzogen, die Ergebnisse sind bisher vielversprechend. Die IRE könnte eine deutliche Entwicklung in der Ablationstherapie beim Nierenzellkarzinom (NZK) bedeuten, der entscheidende Wirknachweis für das lokale NZK steht jedoch bisher aus. In dieser Arbeit werden eigene präklinische und erste klinische Untersuchungen und Ergebnisse dargestellt, diskutiert und mit anderen Ablationstechniken verglichen, um die aktuelle Wertigkeit der IRE aufzuzeigen.

Schlüsselwörter

Elektroporation, irreversible · Nierenzellkarzinom · Ablationsverfahren, lokale · Funktionserhalt · Zellapoptose, induzierte

Irreversible electroporation. The new generation of local ablation techniques for renal cell carcinoma

Abstract

Background. Local ablation techniques are a major focus of current developments in oncology. The primary aim is to retain organs and preserve organ functions without compromising the oncological outcome.

Method. Irreversible electroporation (IRE) is a novel ablation technique that involves the application of high-voltage pulses to induce cell apoptosis without causing thermal damage to the target tissue or adjacent structures.

Aim. First published in 2005 IRE is currently undergoing preclinical and clinical trials in several areas of oncology and the initial results have been promising. The IRE technique could be a significant development in ablation treatment for renal cell carcinoma (RCC) but decisive proof of its effectiveness for local RCC has not yet been provided. This study presents the results of preclinical and initial clinical trials which are discussed and compared with those of other ablation techniques in order to demonstrate the current value of IRE.

Keywords

Electroporation, irreversible · Renal cell carcinoma · Ablation, local · Function retention · Apoptosis, induced

Klinische Eigenschaften und Sicherheitsaspekte (In-vivo-Nierenmodell) im Tierversuch (Wirkungsnachweis und Safety-Studie)

Die Wirkungen der IRE ist nur in vivo nachweisbar. Die lokale Ablation von Nierenparenchym unter Erhaltung der Organintegrität waren das Primärziel, lokale, systemische, akute oder subakute Nebenwirkungen zu finden, das Sekundärziel der Studie. Drei Hausschweine wurden einer perkutanen IRE CT-gestützt an drei Geschossen der jeweils rechten Niere unter EKG-Triggerung und MRT-kompatibler Intubationsnarkose (ITN) unterzogen (Aktenzeichen 42502-2-996 IMTR). Periinterventionell, am Tag 7 und 28 nach IRE, erfolgte eine MRT-Untersuchung der Nieren und am Tag 28 die Tötung und Organexplantation der Versuchstiere.

Neben der histologischen Analyse der Explantate wurden die Versuchstiere ausscheidungsurographisch, klinisch, paraklinisch und laborchemisch bis zum Beobachtungsendpunkt untersucht. Abbruchkriterien gemäß Studienprotokoll

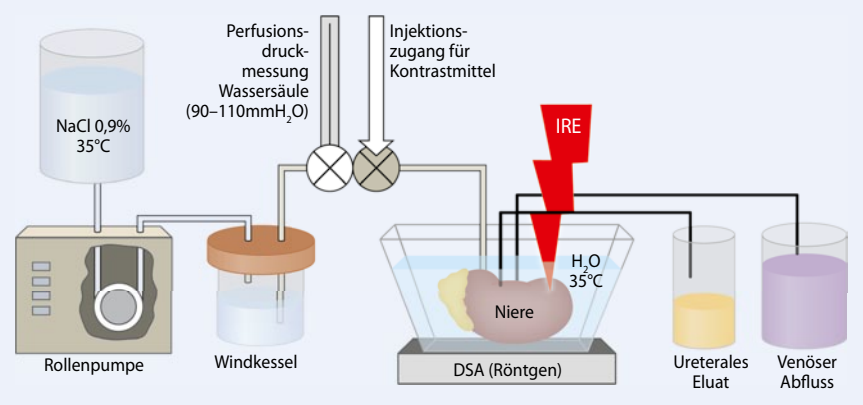

Abb. 5 ▲ Schematischer Versuchsaufbau des Nierenperfusionsmodells zur DSA unter IRE-Kautelen. (Adaptiert nach [24], mit freundl. Genehmigung)

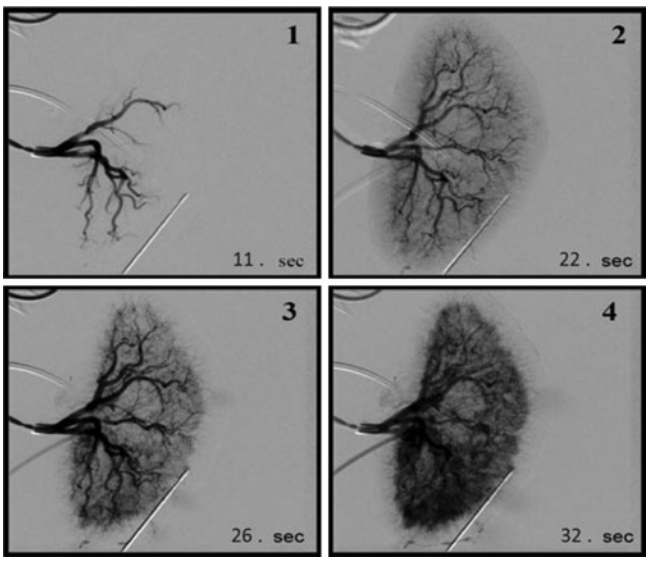

Abb. 6 ◀ DSA während IRE mittels bipolarer IRE-Elektrode am perfundierten Nierenfrischpräparat

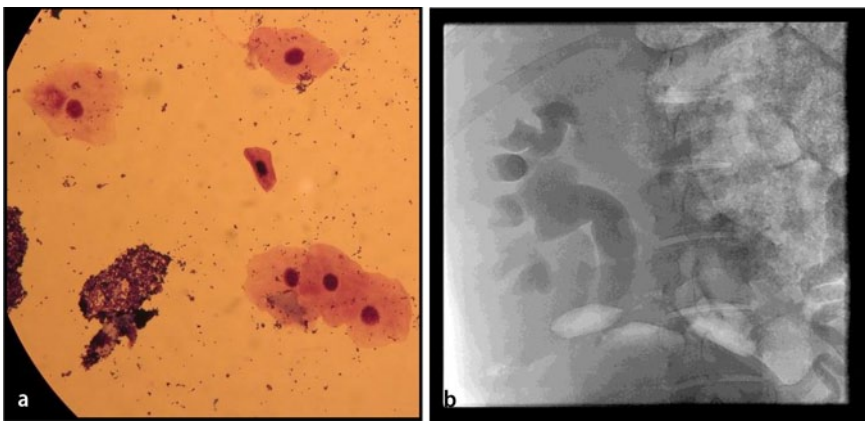

Abb. 7 ▲ **a** Urinzytologie, Spontanurin 3 Tage postoperativ in 400facher Vergrößerung und Durchlichtmikroskopie. **b** p.-a.-Aufnahme Niere 30 min p. i. (30 ml Ultravist®-370; Versuchstier 1) Tag 3 nach IRE

und Tierschutzgesetz ergaben sich nicht, ebenfalls keine Verhaltensänderungen, Schmerzanzeichen oder Infektzeichen. Die Punktionswunde, das Miktions- und Defäkationsverhalten sowie die Vitalparameter waren unauffällig. Urinzytologisch konnte eine temporäre, pathologisch degenerative Veränderung der Urothelzellen unmittelbar postoperativ beobachtet werden (**Abb. 7a**). Im Ausscheidungsurogramm zeigten sich unauffällige Befunde (**Abb. 7b**). Die intraoperativen Befunde im Rahmen der Organentnahme zeigten sich normal und ohne Auffälligkeiten.

Einen Anstieg der Kreatinkinase mit einem Maximum am 1. postoperativen Tag (im Mittel um 111,56 SI) und Abfall auf Ausgangsniveau, sowie einen Anstieg des Serumkreatinins bis zum 17. und 28. postoperativen Tag (im Mittel um 46 SI) zeigten alle Versuchstiere (**Abb. 8**). Serumeiweißelektrophoresen zeigten keine entzündlichen Reaktionen.

Verglichen mit der Computertomographie (CT) ergab die Magnetresonanztomographie (MRT) wegen der besseren Weichgewebedarstellung (T2-SPIR-w-MRT) detailliertere Lokalbefunde für das Monitoring der Ablationszone. In den Ablationszonen kam es zur vollständigen Ablation der Tubuli und Glomeruli, bei sehr scharfer Ablationsrandzone blieben angrenzende Strukturen (Bindegewebe, Harnableitungssystem) intakt. Mit IRE behandeltes Kelchsystem heilte ohne Vernarbung bei erhaltener Basalzellschicht. Die Obduktion zeigte keine makroskopischen und histologischen Veränderungen an den lebenswichtigen Organen [25].

Klinische Eigenschaften und Sicherheitsaspekte (In-vivo-Nierenmodell) im Humanmodell und erste klinische Anwendungs- und Sicherheitsstudie (Safety-Studie)

Prospektive, monozentrische, nicht-randomisierte klinische Phase-I-Studie

Das Primärziel war die Patientensicherheit während und nach IRE (akute, chronische unerwünschte Wirkungen, Sekundärziel die akute Ablationswirkung und die Praktikabilität des Verfahrens. Bei 6 Patienten mit lokal begrenztem, nicht metastasiertem Nierentumor wurde int-

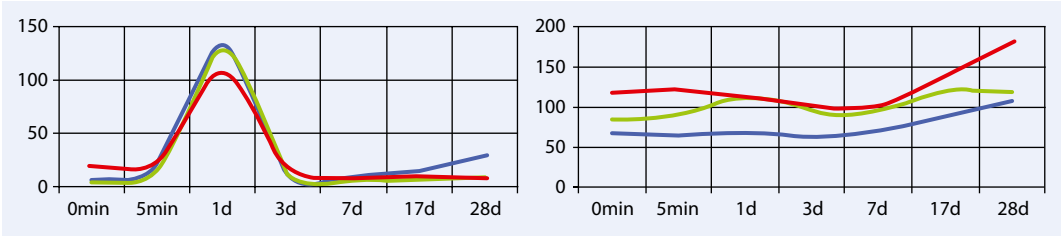

Abb. 8 ◀ Kreatinkinase (SI, *links*), Kreatinin (SI, *rechts*) im Verlauf, (*blau*, *grün*, *rot*: Schwein 1, 2, 3)

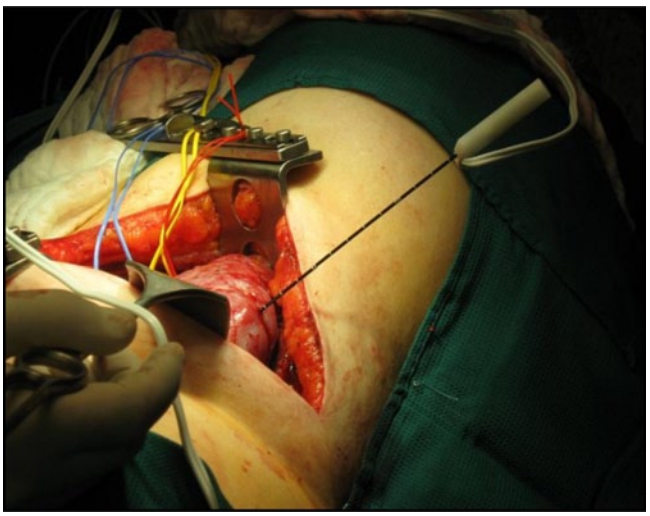

Abb. 9 ◀ Ultraschallgestützte Platzierung der IRE-Elektrode im Nierentumor

raoperativ eine sonographiegestützte IRE des Nierentumors durchgeführt und anschließend die Niere mit Tumor teilreseziert (◘ **Abb. 9**). Neben der histologischen Analyse der Teilresektate wurden die Patienten regelmäßig klinisch, paraklinisch, bildgebend (inklusive Staging), laborchemisch, immunologisch und elektrokardiographisch 12 Monate untersucht. Die IRE erfolgte mittels bipolarer IRE-Elektrode unter EKG-Synchronisierung mittels AccuSync® 72 (Medical Research Corporation®, Milford, CT, USA) und Vollnarkose (ITN) mit Relaxation.

Die Messung der Lebensqualität der Patienten erfolgte regelmäßig mittels EORTC-QLQ-C30-Fragebogen [26].

Kein Patient verstarb, entzog sich den Nachbeobachtungen oder musste ausgeschlossen werden. Es gab keinen Dropout. In den Verlaufskontrollen traten keine pathologischen Lagetypen, Lagetypveränderungen, Herzrhythmusstörungen oder hämodynamischen Veränderungen, keine relevanten hämatologischen oder biochemischen Veränderungen, keine Veränderungen der Herzfunktion oder der harnableitenden Systeme auf. Histologisch zeigten sich keine thermalen oder anderen adversen Effekte [20].

Klinische Eigenschaften und Wirknachweis (In-vivo-Nierentumormodell) im Humanmodell (Start: 10/2012)

Eine prospektive, monozentrische, klinische Phase-I/II-Studie zur Prüfung der klinischen Wirksamkeit perkutaner IRE bei Patienten mit lokal begrenzten NZK (EUDAMED-Nummer: CIV-12-04-006021) startet im Herbst 2012 an unserer Klinik.

Diskussion

Lokale Ablationstechniken beim NZK sind in der der EAU-Leitlinie 2010 für spezielle Indikationen verankert (Radiofrequenzablation, Kryotherapie), werden jedoch bisher limitationsbedingt wenig angewendet. Andere Verfahren kommen über präklinische Entwicklungsstadien nicht hinaus. Aufgrund ihrer vergleichsweise wenigen Nachteile eröffnet die IRE potentiell eine Therapieoptimierung.

Physikalische Eigenschaften (Eiweiß- und Gelmodell, Nierenfrischpräparat)

Durch IRE treten Lichtbogenbildung und pulssynchrone Druckwellen in flüssigen Medien auf, nicht jedoch in gelähnlicher Umgebung. Ein Wirkverlust (Energieumwandlung) sollte daher im Nierenparenchym gering sein, muss jedoch bei zystischen Strukturen der Niere (Hohlsystem, Tumore mit zystischen Anteilen) evaluiert werden. Die Temperaturmessungen im Eiweiß- und Gelmodell bestätigen die nonthermalen Eigenschaften der IRE.

Physikalische Eigenschaften im Nierenperfusionsmodell

Evaluationen der Wirkung von HIFU (thermales Ablationsverfahren) demonstrierten mittels hochauflösender Angiographie die akute Nierenparenchymschädigung im Nierenperfusionsmodell [21]. Ähnliche Zerstörungen an der Niere wurden bei anderen Ablationstechniken (RFA, Kryoablation, Mikrowellentherapie, Histotripsie, Laserablation, Chemoembolisation) festgestellt [5]. Präklinische Untersuchungen zur IRE zeigten echoreiche Ablationsareale in der Sonographie während der IRE, hypodense Areale in der CT nach IRE sowie hyperintense Areale in der MRT einen Tag nach IRE [23]. Ein weiteres Phänomen der IRE ist eine kurzzeitige Ischämie in In-vivo-Gewebe während der IRE („vascular lock") als Ausdruck elektrisch bedingter Vasokonstriktion oder druckschwankungsbedingter Verschlüsse der Arteriolen mit Thrombenbildung [19, 22]. Makro- und mikrovaskuläre Strukturen im Nierenparenchym und -tumorgewebe blieben hingegen erhalten [20]. Unsere Untersuchung ist die erste angiographische Untersuchung der akuten Nierengewebeveränderung durch IRE. Mit ihr gelang die Dar-

Tab. 1 NZK-Ablationsverfahren im Vergleich

Ablationstechnik	Wichtigste Nachteile	Applikation	Schonung sensibler Strukturen	EK
IRE (irreversible Elektroporation) [19, 20, 24, 25, 28]	Fehlender Wirknachweis NZK	Perkutan, offen-chirurgisch, laparoskopisch (Sono, CT)	Ja	V
RFA (Radiofrequenzablation) [1, 4, 5]	Nekrose („heat sink effect")	Perkutan, offen-chirurgisch laparoskopisch (Sono, CT, MRT)	Nein	IV
Kryoablation [1, 6, 7, 10]	Nekrose, Aufwand, Nachblutung („cold sink effect")	Laparoskopisch, perkutan, offenchirurgisch, transluminal, endoskopisch (Sono)	Nein	IV
Mikrowellenablation [8, 9]	Nekrose, Aufwand, Sondenkühlung	Perkutan, offen-chirurgisch	Nein	V
HIFU (hochintensiver fokussierter Ultraschall) [10]	Nekrose, Aufwand Technik	Perkutan-extrakorporal, laparoskopisch	Nein	IV
LITT (laserinduzierte interstitielle Thermotherapie) [11]	Nekrose, Aufwand	Perkutan (MRT)	Nein	V
Histotripsie [12]	Nekrose, Technik, Schallfenster	Perkutan-extrakorporal (Sono)	Nein	V
SIRT (Selektive interstitielle Radiotherapie) [13, 14]	Nekrose, Ischämie, Aufwand	Transarteriell (DSA)	Nein, stromgebietsabhängig, systemische NW	V
TACE, TAE (transarterielle Chemoembolisation) [15]	Nekrose, Ischämie, Wirkstofflimitationen	Transarteriell (DSA)	Nein, stromgebietsabhängig, systemische NW	V
PDT (photodynamische Therapie) mit Palladium-Bakteriochlorophyll (Tookad®) [16]	Nekrose, Eindringtiefe (mm), Lichtempfindlichkeit	Perkutan (offen-chirurgisch, laparoskopisch)	Nein	V

EK Evidenzklassen.

stellung der erhaltenen Perfusion und Integrität der Endstromgebiete in Ablationszonen von Nieren während und nach IRE [24].

Klinische Eigenschaften und Sicherheitsaspekte (In-vivo-Nierenmodell) im Tierversuch (Wirkungsnachweis und Safety-Studie)

Die IRE ist einfach und praktikabel. Mit EKG-Synchronisation ergaben sich perinterventionell und im Verlauf keine kardialen Nebenwirkungen. Die Punktion der IRE-Zielgebiete gelang sonographisch und computertomographisch ohne Nachblutungen. Aufgrund der bildgebenden Effekte der IRE-Ablationszonen in den Verlaufskontrollen scheint die MRT das geeignete Verfahren hierfür zu sein [27]. Die IRE von Nierentumoren ist mit Schonung angrenzender Strukturen möglich. Dies entspricht anderen Untersuchungsergebnissen [23]. Ob die IRE von zystischen Nierentumoren effektiv ist, muss in Studien geklärt werden.

Klinische Eigenschaften und Sicherheitsaspekte (in-vivo-Nierenmodell) im Humanmodell (Safety-Studie)

Bei Applikation von Starkstromimpulsen (Elektroporation) ist ein wichtiger Sicherheitsaspekt die Kardioprotektion. Zahlreiche Untersuchungen liegen hierzu vor [28]. Ball et al. [31] konnten im Rahmen der IRE-Anwendung (Leber, Niere, Lunge) bei 21 Patienten keinen Zusammenhang zwischen kardialen Komplikationen und der Distanz der IRE-Elektroden zum Herz feststellen, jedoch scheint eine EKG-Synchronisation essentiell [29]. Unsere EKG-Verlaufskontrollen zeigten keine therapieabhängigen Nebenwirkungen der IRE. Klinische und Paraklinische Verlaufsparameter waren unauffällig [20]. Eine Modifizierung der IRE-Pulse konnte Muskelkontraktionen eliminieren [30]. Eine IRE-Therapie ohne Muskelrelaxation in Lokalanästhesie wäre potentiell möglich.

IRE im Kontext anderer ablativer Verfahren beim NZK

Vorteile der IRE

Ein wichtiges IRE-Merkmal ist die fehlende thermale Gewebeschädigung. Die entstehende Stromwärme ist gering und im perfundierten Nierengewebe zu vernachlässigen [27]. Thermiebedingte Kollateralschäden sensibler Strukturen (NBKS, Gefäße, Drüsen etc.) sind nicht zu erwarten, da präzise Areale mit scharfem Rand im Wirkbereich des induzierten transmembranen Potentials abladiert werden. Eine gewisse Gewebeselektivität (Gefäße, Nerven, Bindegewebe, NBKS) scheint vorzuliegen. Die Elektroden sind bildgebend einfach perkutan zu platzieren und bergen kaum Risiken für Komplikationen. Der entscheidende Wirknachweis der IRE beim NZK steht jedoch aus. Hochwertige Studien müssen folgen.

Die **Tab. 1** stellt aktuell für das NZK zur Verfügung stehende Verfahren der IRE gegenüber.

Fazit für die Praxis

Die IRE besitzt aufgrund ihrer Eigenschaften das Potential, lokale Ablationstherapien des NZK zu revolutionieren.

Der technische Aufwand ist im Vergleich gering. Die bisherige Datenlage zur IRE ist vielversprechend, der entscheidende Wirksamkeitsnachweis steht jedoch aus. Ihr Vorteil im Vergleich zu anderen thermalen und nonthermalen Ablationsverfahren ist die Induktion einer Apoptose ohne thermische Zerstörung des Gewebes und angrenzender Strukturen. Aktuell nur in Narkose und Relaxation durchführbar, sind IRE-Ablationen in Lokalanästhesie in der Entwicklung, lokale Nierenzellkarzinome multimorbider Patienten könnten zukünftig ebenfalls therapiert werden.

Korrespondenzadresse

Dr. U.-B. Liehr
Klinik für Urologie und Kinderurologie,
Universitätsklinikum Magdeburg A.ö.R.,
Leipziger Straße 44,
39120 Magdeburg
liehr@med.ovgu.de

Interessenskonflikte. Der korrespondierende Autor gibt für sich und seine Koautoren an, dass kein Interessenkonflikt besteht.

Literatur

1. Ljundberg B, Cowan N, Hanbury DC et al (2010) Guidelines on renal cell carcinoma. European Association of Urology (eau) 2010, update version April 2010. Eur Urol 58(3):398–406
2. Lu DS, Raman SS, Vodopich DJ et al (2002) Effect of vessel size on creation of hepatic radiofrequency lesions in pigs: assessment of the „heat sink" effect. Am J Roentgenol 178(1):47–51
3. Ladd AP, Rescorla FJ, Baust JG et al (1999) Cryosurgical effects on growing vessels. Am Surg 65(7):677–682
4. Dib RE, Touma NJ, Kapoor A (2009) Review of the efficacy and safety of radiofrequency ablation for the treatment of small renal masses. Can Urol Assoc J 3(2):143–149
5. Duffey BG, Kyle Anderson J (2010) Current and future technology for minimally invasive ablation of renal cell carcinoma. Indian J Urol 26(3):410–417
6. Bischoff JT, Chen RB, Lee BR et al (1999) Laparoscopic renal cryoablation: acute and long-term clinical radiographic, and pathologic effects in an animal model and application in a clinical trial. J Endourol 13:233–239
7. Berger A, Kamoi K, Gill IS, Aron M (2009) Cryoablation for renal tumors: current status. Curr Opin Urol 19(2):138–142
8. Carrafiello G, Mangini M, Fontana F et al (2010) Single-antenna microwave ablation under contrast-enhanced ultrasound guidance for treatment of small renal cell carcinoma: preliminary experience. Cardiovasc Intervent Radiol 33(2):367–374
9. Brace CL (2009) Microwave ablation technology: what every user should know. Curr Probl Diagn Radiol 38(2):61–67
10. Klatte T, Marberger M (2009) High-intensity focused ultrasound for the treatment of renal masses: current status and future potential. Curr Opin Urol 19(2):188–191
11. Dick EA, Joarder R, De Jode MG et al (2002) Magnetic resonance imaging-guided laser thermal ablation of renal tumours. BJU Int 90(9):814–822
12. Kieran K, Hall TL, Parsons JE et al (2007) Refining histotripsy: defining the parameter space for the creation of nonthermal lesions with high intensity, pulsed focused ultrasound of the in vitro kidney. J Urol 178:672–676
13. Lang EK, Sullivan J (1988) Management of primary and metastatic renal cell carcinoma by transcatheter embolization with iodine 125. Cancer 62(2):274–282
14. MacKie S, Silva S de, Aslan P et al (2011) Super selective radio embolization of the porcine kidney with 90yttrium resin microspheres: a feasibility, safety and dose ranging study. J Urol 185(1):285–290
15. Tsuchiya K, Uchida T, Kobayashi M et al (2000) Tumor-targeted chemotherapy with SMANCS in lipiodol for renal cell carcinoma:longer survival with larger size tumors. Urology 55(4):495–500
16. Weersink RA, Forbes J, Bisland S et al (2005) Assessment of cutaneous photosensitivity of TOOKAD (WST09) in preclinical animal models and in patients. Photochem Photobiol 81(1):106–113
17. Davalos RV, Mir IL, Rubinsky B (2005) Tissue ablation with irreversible electroporation. Ann Biomed Eng 33(2):223–231
18. Lee EW, Wong D, Prikhodko SV et al (2012) Electron microscopic demonstration and evaluation of irreversible electroporation-induced nanopores on hepatocyte membranes. J Vasc Interv Radiol 23(1):107–113
19. Rubinsky B, Onik G, Mikus P (2007) Irreversible electroporation: a new ablation modality–clinical implications. Technol Cancer Res Treat 6(1):37–48
20. Pech M, Janitzky A, Wendler JJ et al (2012) Irreversible electroporation of renal cell carcinoma: a first-in-man phase i clinical study. Cardiovasc Intervent Radiol 35(4):921–926
21. Häcker A, Chauhan S, Peters K et al (2005) Multiple high-intensity focused ultrasound probes for kidney-tissue ablation. J Endourol 19(8):1036–1040
22. Sersa G, Jarm T, Kotnik T et al (2008) Vascular disrupting action of electroporation and electrochemotherapy with bleomycin in murine sarcoma. Br J Cancer 98(2):388–398
23. Lee EW, Loh CT, Kee ST (2007) Imaging guided percutaneous irreversible electroporation: ultrasound and immunohistological correlation. Technol Cancer Res Treat 6(4):287–294
24. Wendler JJ, Pech M, Blaschke S et al (2012) Angiography in the isolated perfused kidney: radiological evaluation of vascular protection in tissue ablation by nonthermal irreversible electroporation. Cardiovasc Intervent Radiol 35(2):383–390
25. Wendler JJ, Porsch M, Hühne S et al (2012) Short- and mid-term effects of irreversible electroporation on normal renal tissue: an animal model. Cardiovasc Intervent Radiol (Epub ahead of print)
26. Aaronson NK et al (1993) The European Organization for Research and Treatment of Cancer QLQ-C30: a quality-of-life instrument for use in international clinical trials in oncology. J Natl Cancer Inst 85(5):365–76
27. Wendler JJ, Pech M, Porsch M et al (2012) Urinary tract effects after multifocal nonthermal irreversible electroporation of the kidney: acute and chronic monitoring by magnetic resonance imaging, intravenous urography and urinary cytology. Cardiovasc Intervent Radiol 35(4):921–926
28. Vadim V, Fedorov VV, Nikolski VP, Efimov R (2008) Effect of electroporation on cardiac electrophysiology. In: Shulin Li (ed) Electroporation protocols – preclinical and clinical gene medicine, 1. edn. Humana Press, New York, pp 433–448
29. Mali B, Jarm T, Corovic S et al (2008) The effect of electroporation pulses on functioning of the heart. Med Biol Eng Comput 46(8):745–757
30. Arena C, Sano MB, Rossmeisl JH Jr et al (2011) High-frequency irreversible electroporation (H-FIRE) for non-thermal ablation without muscle Contraction. Bio Med Eng 10:102
31. Ball C, Thomson KR, Kavnoudias H (2010) Irreversible electroporation: a new challenge in „out of operating theater" anesthesia. Anesth Analg 110(5):1305–1309

8.2

Angiography in the isolated perfused kidney: radiological evaluation of vascular protection in tissue ablation by nonthermal irreversible electroporation.

Wendler JJ, Pech M, Blaschke S, Porsch M, Janitzky A, Ulrich M, Dudeck O, Ricke J, Liehr UB.

Cardiovasc Intervent Radiol. 2012 Apr;35(2):383-90

PURPOSE: The nonthermal irreversible electroporation (NTIRE) is a novel nonthermal tissue ablation technique by local application of high-voltage current within microseconds leading to a delayed apoptosis. The purpose of this experimental study was the first angiographic evaluation of the acute damage of renal vascular structure in NTIRE.

METHODS: Results of conventional dynamic digital substraction angiography (DSA) and visualization of the terminal vascular bed of renal parenchyma by high-resolution X-ray in mammography technique were evaluated before, during, and after NTIRE of three isolated perfused porcine ex vivo kidneys.

RESULTS: In the dedicated investigation, no acute vascular destruction of the renal parenchyma and no dysfunction of the kidney perfusion model were observed during or after NTIRE. Conspicuous were concentric wave-like fluctuations of the DSA contrast agent simultaneous to the NTIRE pulses resulting from NTIRE pulse shock wave.

CONCLUSION: The NTIRE offers an ablation method with no acute collateral vascular damage in angiographic evaluation.

Cardiovasc Intervent Radiol (2012) 35:383–390
DOI 10.1007/s00270-011-0187-x

LABORATORY INVESTIGATION

Angiography in the Isolated Perfused Kidney: Radiological Evaluation of Vascular Protection in Tissue Ablation by Nonthermal Irreversible Electroporation

Johann Jakob Wendler · Maciej Pech · Simon Blaschke · Markus Porsch · Andreas Janitzky · Matthias Ulrich · Oliver Dudeck · Jens Ricke · Uwe-Bernd Liehr

Received: 5 January 2011 / Accepted: 11 May 2011 / Published online: 2 June 2011

Abstract
Purpose The nonthermal irreversible electroporation (NTIRE) is a novel nonthermal tissue ablation technique by local application of high-voltage current within microseconds leading to a delayed apoptosis. The purpose of this experimental study was the first angiographic evaluation of the acute damage of renal vascular structure in NTIRE.
Methods Results of conventional dynamic digital substraction angiography (DSA) and visualization of the terminal vascular bed of renal parenchyma by high-resolution X-ray in mammography technique were evaluated before, during, and after NTIRE of three isolated perfused porcine ex vivo kidneys.
Results In the dedicated investigation, no acute vascular destruction of the renal parenchyma and no dysfunction of the kidney perfusion model were observed during or after NTIRE. Conspicuous were concentric wave-like fluctuations of the DSA contrast agent simultaneous to the NTIRE pulses resulting from NTIRE pulse shock wave.
Conclusion The NTIRE offers an ablation method with no acute collateral vascular damage in angiographic evaluation.

Johann Jakob Wendler and Maciej Pech are contributed equally to this study.

J. J. Wendler (✉) · S. Blaschke · M. Porsch · A. Janitzky · M. Ulrich · U.-B. Liehr
Department of Urology, University of Magdeburg, Leipziger Straße 44, 39120 Magdeburg, Germany
e-mail: johann.wendler@med.ovgu.de

M. Pech · O. Dudeck · J. Ricke
Department of Radiology and Nuclear Medicine, University of Magdeburg, Leipziger Straße 44, 39120 Magdeburg, Germany

Keywords Nonthermal irreversible electroporation · Angiography · Isolated perfused kidney · Tissue ablation · Vascular protection

Introduction

Nonthermal irreversible electroporation (NTIRE) is a novel nonthermal tissue ablation technique that applies high-voltage and high-current electrical pulses on the microsecond timescale with inserted needle-like electrodes to induce irreversible permeabilization of the cell membrane (nanopores) with consequent cell death by loss of homeostasis within approximately 4 (±3) days. Although the exact mechanism of electroporation, reversible as well as irreversible, is not completely understood, it is known that NTIRE alters in vivo cells on molecular level via induced high-electric field transmembrane voltage that causes an electrical breakdown of the dielectric lipid bilayer. NTIRE does not alter the extracellular matrix and does not cause protein denaturation or other side effects that are associated with thermal ablation modalities. Hence, anatomical borders and structures-like vessels and nerves as well as the integrity of an organ are safe [1]. Recent studies have shown a multidisciplinary potential in surgical oncology and ablation of benign lesions. It has been used in different preclinical models of tissue ablation of organs, such as kidney, prostate, liver, heart, pancreas, brain, lung, dermis, and vessels [2–12]. In contrast to current thermal ablative techniques, there is no reduction of effectiveness by vascularization ("cold- or heat-sink effect") [13] and no collateral damage to anatomical borders. Several investigations have demonstrated the persisting intactness of major vessels adjoining to or lying in the ablation zone as well as the necrosis and thrombosis of small vessels in

the ablation zone [1, 11]. So, the possible protection of the urine collecting system, such as the renal pelvis and ureter, as well as a nephron-sparing effect by sharply bounded ablation zone is postulated by using NTIRE in kidney [2, 6].

To date, there is no sufficient real-time imaging method that is able to correlate the ablation area during or immediately after NTIRE to the tumor extension [13–15]. Experimental studies have demonstrated the confirmation of a hyperechoic areal in real-time ultrasound respectively a hypodense areal in real-time computer tomography (CT) immediately after the NTIRE around the probe as well as a T2-hyperintense areal in MRT 1 day after NTIRE [11, 16]. These areals were correlated with the histopathological ablation zones in delayed exploration of in vivo target tissues and are explained as acute edema of the ablated area as a sign of local inflammatory tissue reaction on energy application [13, 16]. For follow-up after NTIRE, conventional imaging methods, such as CT or MRT, are reliable methods to investigate tumor ablation by showing necrosis, scar formation, tumor size reduction, and absence of enhancement [17]. Despite of all that, only postresection histological analysis in a closed interval of 2–4 weeks after NTIRE is able to prove complete tumor ablation.

With our investigations, we focused on NTIRE as a novel potential ablation modality for renal cell carcinoma (RCC). First results of clinical intraoperative trials have shown the possibility of safe application of NTIRE to the kidney using ECG-synchronization and general anesthesia with muscle relaxation [18, 19]. Pech et al. [18] performed an intraoperative ultrasound-guided NTIRE of localized RCC (tumor size 20–39 mm) in six patients scheduled for curative open lumbar resection (four partial and two total nephrectomies). For all patients a NanoKnife^{TM} system with bipolar single probe and 90 pulses up to 50 A and 3000 V by a NanoKnife^{TM} generator (AngioDynamics® Inc., NY, USA) was used. They observed no acute side effects during the peri- and postoperative (12 weeks) periods by measuring ECG, blood pressure, central hemodynamic values, standard blood values, acid-base values, and respiratory values. Thomson et al. [17] investigated ECG synchronized IRE in 38 humans with advanced malignancy of the liver ($n = 25$), kidney ($n = 7$), and lung ($n = 3$) and a total of 69 separate tumors (average 46 cm^3) that where unresponsive for alternative treatment. They observed a complete target tumor ablation verified by CT in 66% (46/69) without NTIRE-related adverse events.

The kidney offers a favorable target for tumor ablation because of its location for percutaneous access and its condition of severe vascularized parenchyma, which is easy to monitor by routine imaging procedures as well as blood and urine values. The therapy "gold standard" of small localized RCC (T1-2 TNM 2010 UICC) is the nephron-sparing surgery by partial tumor nephrectomy [20]. One basis of the nephron-sparing therapy to reduce the risk of renal failure is the maximum protection of the local vascular system and prevention of ischemia. For inoperable cases and patients with small, multilocular, or bilateral renal tumors as well as solitary kidney, the 2010 EAU guidelines recommended cryoablation and radiofrequency ablation (RFA) as therapeutic alternatives [20]. These thermal ablation techniques cause acute destruction of the vascular system and tissue, in both of the target tissue as well as the adjacent tissue in terms of collateral damage.

This experimental study was the first radiological evaluation of the acute vascular damage of renal parenchyma by NTIRE in relation to thermal ablation techniques.

Material and Methods

Selection and Preparation of the Kidneys

Three kidneys were obtained from three freshly slaughtered pigs (7 min) in warm ischemia. Only kidneys from pigs for slaughter of an accredited abattoire (estate Gut Glüsig GmbH, Germany) were taken after termination. The healthiness of the pigs (7 ± 1-month-old and weighed 120 ± 10 kg) was examined by veterinary. The preparations of the isolated kidneys were performed by two experienced urologists according to the technique of kidney transplantation.

The renal hilum was prepared immediately after organ explantation. The kidneys were directly intra-arterially perfused with 12.500 IE of heparin (0.5 ml of Heparin-Natrium-12.500-ratiopharm®, Ratiopharm, Germany) by a cannula to avoid vascular clotting (after 3 min).

The renal artery and renal vein were intubated with flexible tube sections of infusion elongation (Heidelberg Extension Tubing®, Braun, Germany) and fixed by ligature (Marlin® 1, Catgut, Germany). To avoid air embolization, these preparations were performed in a water bath of 4°C NaCl 0.9%. While unhinging the kidneys from adipose capsule, we researched pathological alterations to exclude any impact.

After 10 min, we intra-arterially perfused the kidneys with 500 ml of cold (4°C) NaCl 0.9% (Intrafix® Primeline Braun, Germany) with a pressure of 100 ± 5 cm H_2O by pressure infusion cuff (SafePress 1000 CC®, Dahlhausen, Germany), until nonbloody solution drain off the renal vein. The proximal ureter was intubated with a percutaneous nephrostomy balloon-catheter 10 Charr. (Uromed®, Germany) blocked with 2 ml in the renal pelvis.

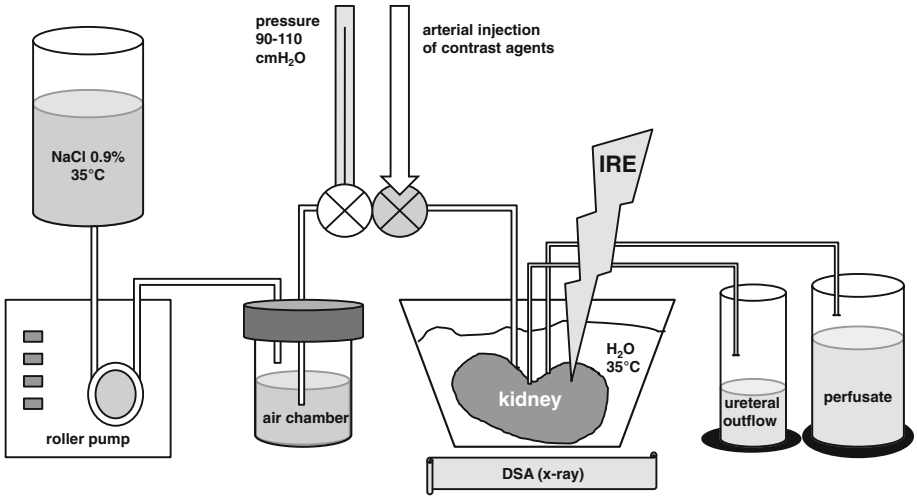

Fig. 1 Experimental setup for NTIRE and DSA in the isolated perfused kidney

Consequently, we stored the kidneys in NaCl 0.9% at 4°C until performing NTIRE.

Perfusion Model of the Isolated Kidney

To simulate a physiological temperature, the kidneys were completely lying in NaCl 0.9% (35°C) during NTIRE and digital substraction angiography (DSA) (50 min after isolation) and perfused continuously with NaCl 0.9% (35°C) through the renal arteries at 100 ml/min and a pressure between 100 ± 10 cm H_2O (measured by water column) using a commercial perfusion pump for percutaneous nephrolitholapaxy (Uropump®, Storz, Germany) and an air chamber. To exclude any extravasation and control complete perfusion of the organ, we applied indigo blue colorant (MonicoSpa, Spain). Venous and ureteral outflow were collected and measured separately (Fig. 1). A continuous, nearly physiological perfusion of the kidneys was feasible. We observed no relevant extravasation due to any leakage and the perfusion of the kidneys seemed to be complete by changing color while flushing with NaCl 0.9% and indigo blue colorant. Venous and ureteral outflow was constant at approximately 9:1 while constant pressure 100 ± 10 cm H_2O and constant perfusion 100 ± 10 ml/min.

Nonthermal Irreversible Electroporation

During the continuous perfusion of the isolated porcine kidneys, we performed NTIRE. Therefore, each of the three kidneys was punctured manually in the lower, middle, and upper part (total amount: nine ablation zones) per one NTIRE electrode (5 Charr. Resp. 1.6 mm). For all NTIRE applications, a NanoKnife™ Electroporator (AngioDyanmics® Inc.) with a bipolar single-needle electrode (NanoKnife™ bipolar probe 15 cm, AngioDyanmics® Inc.) was used. In each part, 90 pulses per minute were given with 2700 V approximately 22 A and 70 ms. As specified by the manufacturer, the calculated ablation zone is a prolate spheroid of 30 × 15 mm^2. The total energy averaged 375 kJ per ablation zone resp. approximately 1 mJ per kidney. Each kidney was examined by two independent and experienced urologists in consensus. Each NTIRE procedure was executed sufficiently, and no undelivered pulses were documented. During NTIRE, we observed no change of the perfusion performance.

Digital Substraction Angiography

To visualize the dynamic perfusion, we performed DSA (AXIOM Artis FA®, Siemens, Germany) of the perfused kidneys with three pictures per second. For each DSA series, 20 ml of iodine contrast agent (Imeron® 300, Bracco Imaging, Italy) was injected to the perfusion system. Each DSA series (Figs. 2, 3) was reviewed by two independent and experienced interventional radiologists and two independent and experienced urologists in consensus.

Marker and Digital Angiography in Mammography Technique (Static Angiography)

Marking the exact NTIRE probe position in the static angiography X-ray images in mammography technique (low-kV exposure technique, high resolution), we used self-made marker (5 Charr.) consisting of a 16 G venous in-dwelling catheter (BD Venflon™ Pro Safety, Becton Dickenson, USA). We used the tube fragment of approximately 30 mm and fixed a 10-mm piece of copper wire in the middle of the lumen. The ends of the tube were closed

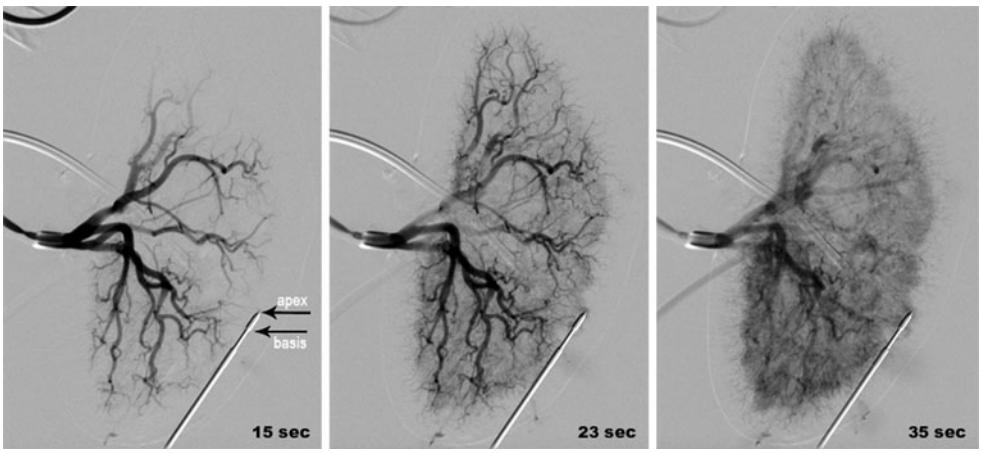

Fig. 2 Digital substraction angiography (DSA) while performing NTIRE with a single-needle bipolar probe to the lower part of the isolated perfused porcine kidney. The apex and the basis of the nonisolated lower pole of the NTIRE single-needle electrode are labeled

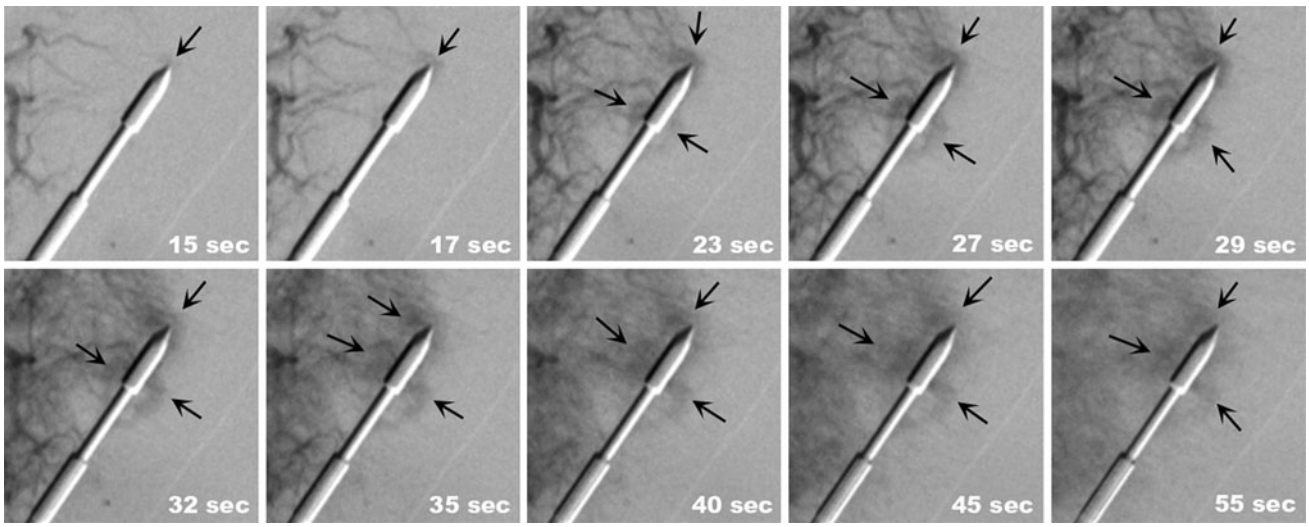

Fig. 3 Display detail of the surrounding area of the single-needle bipolar probe during digital substraction angiography (DSA) while performing NTIRE to the lower part of the isolated perfused porcine kidney. The *open black arrows* show the fluctuation of the X-ray contrast agent based on the apex and the basis of the nonisolated lower pole of the NTIRE single-needle electrode (see Fig. 2)

with the correspondent mandarin (10 mm). Each one marker was placed in Seldinger technique into one of the three puncture channels of each kidney after each NTIRE application by using a slim synthetic trocar of a 5 Charr. suprapubic catheter for children (EasyCyst®, Rüsch, Germany).

Directly afterwards each kidney was perfused with NaCl 0.9% (4°C) again until the iodine contrast agent for DSA was cleared out. Accordingly the kidneys were perfused with barium sulphate contrast agent (Barilux® HD, Sanochemia, Switzerland) into the renal artery until draining it off the renal vein. Then, the arterial, venous, and ureteral tubes were closed to keep the intravascular and nondiffusible contrast agent inside. Subsequently digital static angiography was performed by mammography technique with 50 cm, 24 kV (low-kV exposure technique, high resolution) and 80 mAs (Mammomat 3000®, Siemens, Germany). Each X-ray image (whole kidney and its 5-mm coronary transactions; Figs. 4, 5) was observed by two independent and experienced interventional radiologists and two independent and experienced urologists in consensus.

Results

Digital Substraction Angiography

Before NTIRE, we observed regular and physiological perfusion with flooding and complete draining off the vascular

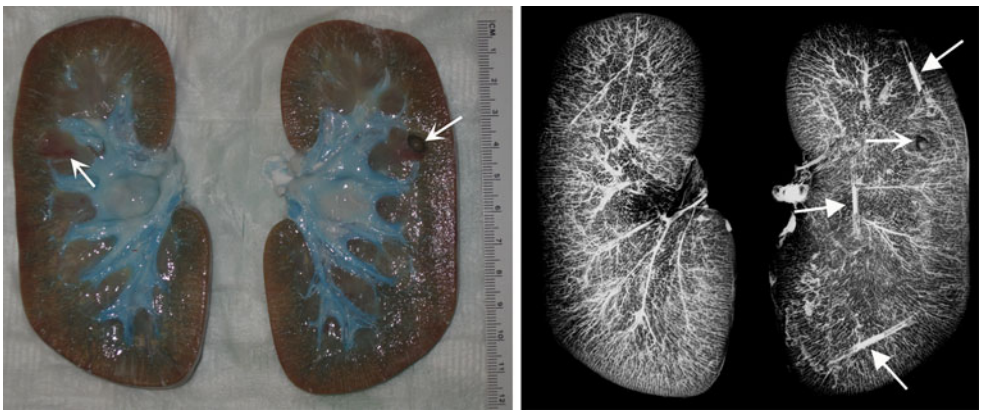

Fig. 4 Images of the half-split kidney (*left*) and correspondent digital static angiography per high-resolution X-ray imaging in low-kV exposure mammography technique (*right*). *Open arrows* show a small pre-existing cortical cyst. *Closed arrows* show the metal markers set to the NTIRE electrode channels (3 per kidney)

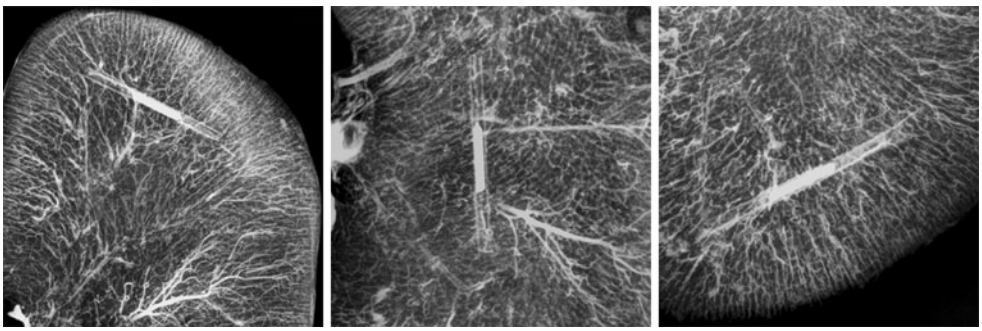

Fig. 5 Digital static angiography per high-resolution X-ray imaging in low-kV exposure mammography technique of the coronary kidney transactions display detailed the renal vascular system around the metal markers (*upper pole to the left*, *central zone in the middle*, *lower pole to the right*). Each metal marker shows one of the NTIRE puncturing channels

system of the renal parenchyma without any perfusion gaps. During (Figs. 2, 3) and after (Figs. 4, 5) NTIRE, we observed no relevant changes, such as extravasations, perfusion gaps, open areas, accumulations, or stases in the renal parenchyma. Conspicuous was a concentric wavelike fluctuation of the contrast agent, each based on the apex and basis of the nonisolated lower pole of the NTIRE single-needle bipolar probe, which appeared simultaneous to the NTIRE pulses (90/min), expanded around 1 cm and cleared away completely during perfusion (Fig. 3).

Overall it has to be noted that just major renal vessels, especially of the renal medulla, are detailed visible in DSA, whereas the vascular system of the renal cortex between the renal medulla and the renal capsule seems to be spared (Fig. 2). Because of that, in the following, these visible major vessels in DSA are defined as macrovascular system of the kidney.

Digital Angiography in Mammography Technique (Static Angiography)

The correlation of the NTIRE ablation zone to the angiography images was feasible by marking the NTIRE puncture channels per metal marker (Figs. 4, 5, closed arrows). The contrast agent stayed characteristically intraluminal of the complete organ. In correlation to the marked ablation zones, we observed no extravasation and no disruption of the terminal vascular bed of renal cortical parenchyma, such as gaps, open areas, or accumulations—neither around the seeds nor in the distant parenchyma (Figs. 4, 5). Additional to the DSA, also small vessels of the renal cortex are displayed straight to the renal capsule and can be well distinguished from each other (Fig. 5). In the following these small vessels, which are not detailed visible in DSA, are defined as microvascular system of the kidney.

Discussion

The principle of NTIRE is the local application of high-voltage current within microseconds with a delayed parenchyma ablation after 4 ± 1 days without destruction of the tissue scaffolding and the major vascular system [1, 21], preserving organ structure and the demonstrated

recovery of normal tissue with regenerative capacities [5]. Because of supposing no adverse effects, such as collateral damage of the surrounded tissue and vascular system as well as no fragmentary tumor destruction, NTIRE could be superior to current thermal ablation techniques, such as RFA and cryotherapy in kidney tumors [2, 6]. So far, there has been no radiological examination of the vascular system closed to the NTIRE ablation zone in the acute phase but only histological investigations [1, 21].

This experimental study is the first radiological approach to examine the renal vascular system in the acute phase of NTIRE. Conventional DSA before, during, and after NTIRE as well as digital static angiography per high resolution X-ray imaging in low-kV exposure mammography technique after NTIRE were used in isolated, perfused, porcine, ex vivo kidneys. This enables a qualitative radiological examination of the NTIRE ablation zone closed and surrounded terminal macro- and microvascular bed of renal parenchyma in the acute phase. Referred to its typical anatomy of the renal vascular system, the DSA shows the renal macrovascular system with vasa renales, segmentales, interlobares, and arcuatae of the renal medulla and columns (Fig. 2), whereas the angiography in mammography technique additionally shows the renal microvascular system with vasa corticales, rectae spuriae, and rectae verae of the renal cortex and pyramids (Figs. 4, 5).

By using this ex vivo model of the isolated porcine kidney, it is possible to simulate mechanically a current physiological perfusion of a human in vivo kidney to examine acute mechanical vascular reactions and tissue damage by NTIRE without interfering by kidney movement. Because of the restriction status, using NTIRE to humans just in clinical studies, it was not possible to observe percutaneous NTIRE to human unaffected in vivo kidneys by using DSA and static angiography in mammography technique.

We observed at first a remained vascular perfusion and integrity of the terminal vascular bed of renal parenchyma without any lesions in the ablation zone or the surrounded parenchyma by using contrast agent-based X-ray imaging during and after NTIRE. In contrast to that, previous reports on several energy-based kidney treatment methods in the isolated perfused kidney observed lesions of the terminal vascular bed of renal cortical parenchyma with petechial extravasations and open areas, such as in ESWL, respectively cavern-like thermolesions, such as in HIFU using angiography in mammography technique [22–24]. Similar characteristics were observed for other technologies for minimally invasive ablation of renal masses, such as cryoablation, RFA, and microwave [25].

Previous publications reported a remarkable phenomenon of blood perfusion disruption with consecutive ischemia during in vivo electroporation, referred to as the vascular lock and explained as electrical vasoconstriction reflex or collapse by decreased intravascular pressure of afferent arterioles [26]. Other experimental studies of histological analysis after NTIRE of in vivo porcine liver demonstrated intact major vascular structures and necrotic small vessels with organized intraluminal fibrin thrombi in the ablated area 24 hours after NTIRE [1, 11]. Histopathologic analyses of renal tumor resections immediately after NTIRE showed the preservation of the vasculature in the electroporated tissue and the urine collecting system [2, 6, 18].

Incidentally we discovered a conspicuous phenomenon of concentric wavelike fluctuation of the contrast agent simultaneous to the NTIRE pulses (90/min). Each was based on the apex and basis of the NTIRE single-needle bipolar probe with an extension of 1 cm and cleared away completely during perfusion. These contrast agent waves followed no macroscopic visible vascular pattern, if procurable to judge, what may be based on the limited resolution of the DSA. Given that the microvascular structure after NTIRE is maintained in high-resolution angiography imaging by mammography technique, we exclude any destructions, such as extravasation. In fact compared with barium X-ray contrast agent (mammography technique), iodine X-ray contrast agent (DSA) is diffusible, but the pulsatile contrast agent waves occur and clear away too fast and straightened for any physiological or electrical triggered diffusion into the extravascular space. Thus, we conclude that the phenomenon is based on a pulsatile propagation along the capillaries with a fast draining off, what is not detailed presentable in the DSA and may extends three-dimensional starting from the bipolar probe poles.

We hypothesize that the contrast agent waves result from the electrical pulse shock waves caused by the NTIRE strokes and based on the temporary increased intravascular concentration of the contrast agent. This observation is limited by the difficult demonstration of a rapid recurrent dynamic phenomenon in DSA sequence by means of freezed images. This first described radiological phenomenon in NTIRE could be a part for an approach to develop a perfusion-based and reliable modified real-time monitoring method of the NTIRE ablation zone with additional imaging of the tumor extension by its specific vascularization pattern.

This study is limited by the design of an ex vivo model and the small number of studied kidneys ($n = 3$) and ablation zones ($n = 9$). The DSA is a dynamic real-time imaging method but is limited by its low resolution and frame frequency. The static angiography per mammography technique is limited by its nonexisting real-time and dynamic imaging but features a high resolution. Moreover,

the study is limited to a conventional visualized qualitative evaluation of the renal vascular system without any quantitative analysis. No correlation to thermal ablation methods has been made by the same investigation method. Furthermore, no histological examination in view of vascular system was performed. The ex vivo model cannot reproduce the dynamic behavior of in vivo capillaries due to high-voltage current, the filtration or absorption of in vivo kidney, and the delayed histological or immunological behaviour to NTIRE. A histological analysis could be limited by artefacts of the nondiffusible barium sulphate contrast agent because of vessel obliteration.

In summary, this study is an additional module to demonstrate the preservation of the vascular system closed to the NTIRE ablation zone. This reveals the possible superiority of the NTIRE versus thermal ablation methods for nephron-sparing therapy to reduce the risk of renal failure. Further experimental and clinical in vivo studies are needed for complete understanding the NTIRE mechanism and developing it to a widely useable treatment modality especially of kidney tumors.

Conclusions

This experimental study is the first radiological approach to examine the acute dynamic vascular perfusion of the isolated perfused porcine kidney by conventional digital substraction angiography (DSA) during NTIRE and the morphology of the terminal vascular bed of the renal parenchyma by digital static angiography per high resolution X-ray imaging in low-kV exposure mammography technique after NTIRE. This study is an additional, radiological module to demonstrate the preservation of the macro- and microvascular system of the whole kidney after NTIRE. In contrast to thermal ablation methods, there seems to be no acute vascular damage by NTIRE. This reveals the possible superiority of the NTIRE versus thermal ablation methods for nephron-sparing therapy to reduce the risk of renal failure. Further experimental and in vivo studies are needed for complete understanding the NTIRE mechanism and using NTIRE for ablation of kidney tumors.

Conflict of interest The authors declare that they have no conflicts of interest. This study was performed independently of the manufacturer of the devices used.

References

1. Rubinsky B, Onik G, Mikus P (2007) Irreversible electroporation: a new ablation modality—clinical implications. Technol Cancer Res Treat 6(1):37–48
2. Tracy CR, Kabbani W, Cadeddu JA (2010) Irreversible electroporation (IRE): a novel method for renal tissue ablation. BJU Int. doi:10.1111/j.1464-410X.2010.09797.x
3. Onik G, Mikus P, Rubinsky B (2007) Irreversible electroporation: implications for prostate ablation. Technol Cancer Res Treat 6(4):295–300
4. Dupuy DE, Aswad B, Ng T (2011) Irreversible electroporation in a swine lung model. Cardiovasc Intervent Radiol 34:391–395
5. Sano MB, Neal RE 2nd, Garcia PA, Gerber D, Robertson J, Davalos RV (2010) Towards the creation of decellularized organ constructs using irreversible electroporation and active mechanical perfusion. Biomed Eng Online 9(1):83
6. Deodhar A, Monette S, Single GW Jr, Hamilton WC Jr, Thornton R, Maybody M, Coleman JA, Solomon SB (2011) Renal tissue ablation with irreversible electroporation: preliminary results in a porcine model. Urology 77:754–760
7. Garcia PA, Neal RE, Rossmeisl JH, Davalos RV (2010) Nonthermal irreversible electroporation for deep intracranial disorders. Conf Proc IEEE Eng Med Biol Soc 1:2743–2746
8. Charpentier KP, Wolf F, Noble L, Winn B, Resnick M, Dupuy DE (2010) Irreversible electroporation of the pancreas in swine: a pilot study. HPB (Oxford) 12(5):348–351
9. Maor E, Ivorra A, Mitchell JJ, Rubinsky B (2010) Vascular smooth muscle cells ablation with endovascular nonthermal irreversible electroporation. J Vasc Interv Radiol 21(11):1708–1715
10. Al-Sakere B, André F, Bernat C, Connault E, Opolon P, Davalos RV, Rubinsky B, Mir LM (2007) Tumor ablation with irreversible electroporation. PLoS One 2(11):e1135
11. Lee EW, Chen C, Prieto VE, Dry SM, Loh CT, Kee ST (2010) Advanced hepatic ablation technique for creating complete cell death: irreversible electroporation. Radiology 255(2):426–433
12. Hong J, Stewart MT, Cheek DS, Francischelli DE, Kirchhof N (2009) Cardiac ablation via electroporation. Conf Proc IEEE Eng Med Biol Soc 2009:3381–3384
13. Lee EW, Thai S, Kee ST (2010) Irreversible electroporation: a novel image-guided cancer therapy. Gut Liver 4(Suppl 1):S99–S104
14. Goldberg SN, Charboneau JW, Dodd GD 3rd, Dupuy DE, Gervais DA, Gillams AR, Kane RA, Lee FT Jr, Livraghi T, McGahan JP, Rhim H, Silverman SG, Solbiati L, Vogl TJ, Wood BJ, International Working Group on Image-Guided Tumor Ablation (2003) Image-guided tumor ablation: proposal for standardization of terms and reporting criteria. Radiology 228(2):335–345
15. Granot Y, Ivorra A, Maor E, Rubinsky B (2009) In vivo imaging of irreversible electroporation by means of electrical impedance tomography. Phys Med Biol 54(16):4927–4943
16. Lee EW, Loh CT, Kee ST (2007) Imaging guided percutaneous irreversible electroporation: ultrasound and immunohistological correlation. Technol Cancer Res Treat 6(4):287–294
17. Thomson KR, Cheung W, Ellis SJ, Park D, Kavnoudias H, Loader-Oliver D, Roberts S, Evans P, Ball C, Haydon A (2011) Investigation of the safety of irreversible electroporation in humans. J Vasc Interv Radiol 22(5):611–621
18. Pech M, Janitzky A, Wendler JJ, Strang C, Blaschke S, Dudeck O, Ricke J, Liehr UB (2011) Irreversible electroporation of renal cell carcinoma: a first-in-man phase I clinical study. Cardiovasc Intervent Radiol 34:132–138
19. Ball C, Thomson KR, Kavnoudias H (2010) Irreversible electroporation: a new challenge in "out of operating theater" anesthesia. Anesth Analg 110(5):1305–1309
20. Ljungberg B, Cowan N, Hanbury DC, Hora M, Kuczyk MA, Merseburger AS, Mulders PFA, Patard JJ, Sinescu IC (2010) Guidelines on Renal Cell Carcinoma. European Association of Urology (EAU). http://www.uroweb.org/. Accessed 25 May 2011

21. Maor E, Ivorra A, Leor J, Rubinsky B (2007) The effect of irreversible electroporation on blood vessels. Technol Cancer Res Treat 6(4):307–312
22. Häcker A, Chauhan S, Peters K, Hildenbrand R, Marlinghaus E, Alken P, Michel MS (2005) Multiple high-intensity focused ultrasound probes for kidney-tissue ablation. J Endourol 19(8):1036–1040
23. Köhrmann KU, Back W, Bensemann J, Florian J, Weber A, Kahmann F, Rassweiler J, Alken P (1994) The isolated perfused kidney of the pig: new model to evaluate shock wave-induced lesions. J Endourol 8(2):105–110
24. Peters K (2007) Experimetelle Untersuchungen zur nichtinvasiven Gewebeablation durch hochenergetischen fokussierten Ultraschall (HIFU). Dissertation, Tierärztliche Fakultät der LMU München. http://edoc.ub.uni-muenchen.de/6643/1/Peters_Kristina.pdf
25. Duffey BG, Kyle Anderson J (2010) Current and future technology for minimally invasive ablation of renal cell carcinoma. Indian J Urol 26(3):410–417
26. Sersa G, Jarm T, Kotnik T, Coer A, Podkrajsek M, Sentjurc M, Miklavcic D, Kadivec M, Kranjc S, Secerov A, Cemazar M (2008) Vascular disrupting action of electroporation and electrochemotherapy with bleomycin in murine sarcoma. Br J Cancer 98(2):388–398

8.3

Urinary tract effects after multifocal nonthermal irreversible electroporation of the kidney: acute and chronic monitoring by magnetic resonance imaging, intravenous urography and urinary cytology.

Wendler JJ, Pech M, Porsch M, Janitzky A, Fischbach F, Buhtz P, Vogler K, Hühne S, Borucki K, Strang C, Mahnkopf D, Ricke J, Liehr UB.

Cardiovasc Intervent Radiol. 2012 Aug;35(4):921-6.

PURPOSE: The nonthermal irreversible electroporation (NTIRE) is a novel potential ablation modality for renal masses. The aim of this study was the first evaluation of NTIRE's effects on the renal urine-collecting system using intravenous urography (IVU) and urinary cytology in addition to histology and magnetic resonance imaging (MRI).

METHODS: Eight percutaneous NTIRE ablations of the renal parenchyma, including the calyxes or pelvis, were performed in three male swine. MRI, IVU, histology, and urinary cytology follow-ups were performed within the first 28 days after treatment.

RESULTS: MRI and histological analysis demonstrated a localized necrosis 7 days and a localized scarification of the renal parenchyma with complete destruction 28 days after NTIRE. The urine-collecting system was preserved and showed urothelial regeneration. IVU and MRI showed an unaltered normal morphology of the renal calyxes, pelvis, and ureter. A new urinary cytology phenomenon featured a temporary degeneration by individual vacuolization of detached transitional epithelium cells within the first 3 days after NTIRE.

CONCLUSIONS: This first urographical, urine-cytological, and MRI evaluation after porcine kidney NTIRE shows multifocal parenchyma destruction while protecting the involved urine-collecting system with regenerated urothelial tissue. NTIRE could be used as a targeted ablation method of centrally located renal masses.

Cardiovasc Intervent Radiol (2012) 35:921–926
DOI 10.1007/s00270-011-0257-0

LABORATORY INVESTIGATION

Urinary Tract Effects After Multifocal Nonthermal Irreversible Electroporation of the Kidney: Acute and Chronic Monitoring by Magnetic Resonance Imaging, Intravenous Urography and Urinary Cytology

Johann Jakob Wendler · Maciej Pech · Markus Porsch · Andreas Janitzky · Frank Fischbach · Peter Buhtz · Klaus Vogler · Sarah Hühne · Katrin Borucki · Christof Strang · Dirk Mahnkopf · Jens Ricke · Uwe-Bernd Liehr

Received: 21 June 2011 / Accepted: 29 July 2011 / Published online: 26 August 2011

Abstract
Purpose The nonthermal irreversible electroporation (NTIRE) is a novel potential ablation modality for renal masses. The aim of this study was the first evaluation of NTIRE's effects on the renal urine-collecting system using intravenous urography (IVU) and urinary cytology in addition to histology and magnetic resonance imaging (MRI).
Methods Eight percutaneous NTIRE ablations of the renal parenchyma, including the calyxes or pelvis, were performed in three male swine. MRI, IVU, histology, and urinary cytology follow-ups were performed within the first 28 days after treatment.
Results MRI and histological analysis demonstrated a localized necrosis 7 days and a localized scarification of the renal parenchyma with complete destruction 28 days after NTIRE. The urine-collecting system was preserved and showed urothelial regeneration. IVU and MRI showed an unaltered normal morphology of the renal calyxes, pelvis, and ureter. A new urinary cytology phenomenon featured a temporary degeneration by individual vacuolization of detached transitional epithelium cells within the first 3 days after NTIRE.
Conclusions This first urographical, urine-cytological, and MRI evaluation after porcine kidney NTIRE shows multifocal parenchyma destruction while protecting the involved urine-collecting system with regenerated urothelial tissue. NTIRE could be used as a targeted ablation method of centrally located renal masses.

Keywords Non-thermal irreversible electroporation · Ablation · Kidney · Animal model · MRI · Urography · Urinary cytology

Electronic supplementary material The online version of this article (doi:10.1007/s00270-011-0257-0) contains supplementary material, which is available to authorized users.

J. J. Wendler (✉) · M. Porsch · A. Janitzky · S. Hühne · U.-B. Liehr
Department of Urology, University of Magdeburg, 39120 Magdeburg, Germany
e-mail: johann.wendler@med.ovgu.de

M. Pech · F. Fischbach · J. Ricke
Department of Radiology and Nuclear Medicine, University of Magdeburg, 39120 Magdeburg, Germany

P. Buhtz · K. Vogler
Institute of Pathology, University of Magdeburg, 39120 Magdeburg, Germany

K. Borucki
Institute of Clinical Chemistry, University of Magdeburg, 39120 Magdeburg, Germany

C. Strang
Department of Anaesthesiology, University of Magdeburg, 39120 Magdeburg, Germany

D. Mahnkopf
Institute of Medical Technology and Research, Rottmersleben, Germany

Introduction

Nonthermal irreversible electroporation (NTIRE) is a new nonthermal soft-tissue ablation technology that applies high current pulses with inserted needle-like electrodes that cause irreversible membrane permeabilization of in vivo cells by way of induced high electric-field transmembrane voltage leading into cell death by loss of homeostasis [1, 2]. We focused on NTIRE as a novel potential ablation modality for centrally located renal masses in our

investigations [3–5]. Whenever technically feasible, nephron-sparing surgery by kidney tumor resection is the "gold-standard" procedure in tumors ≤7 cm [6]. The partial resection of the kidney in cases of central kidney tumors is limited by their close location to the renal hilum, resulting in the risk of organ ischemia by major vessel destruction as well as urinary leakage (by insufficient organ reconstruction) that requires nephrectomy. Cryoablation (CRA) and radiofrequency ablation (RFA) are recommended as therapeutic alternatives in inoperable patients with cortical-located kidney tumors ≤3 cm [6–12]. NTIRE promises advantages compared with the current thermal tissue ablation techniques [5]. Wendler et al. [13] demonstrated angiographically the acute protection of the renal vascular system under renal NTIRE. Tracy et al. [14] and Deodhar et al. [18] demonstrated histologically the potential of NTIRE for complete cortical renal parenchyma ablation while sparing the urine-collecting system in a porcine kidney model. The first human kidney tumor studies, by Pech et al. [4] and Thomson et al. [3], demonstrated safe NTIRE application without general side effects. Intravenous urography (IVU) and urinary cytology are routine urological examinations of the upper urinary tract [15, 16]. Dynamic contrast-enhanced and diffusion-weighted magnetic resonance imaging (MRI) provides functional information of the kidney [17]. The aim of this study was to perform the first evaluation of NTIRE's effect on the renal urine-collecting system using urography and urinary cytology in addition to histological and MRI evidence of renal tissue ablation.

Materials and Methods

The study was approved by the Veterinary Ethic Commission of the State Office of Consumers and Health Protections and the Scientific Board. Three German domestic male pigs (weighing 28 to 33 kg and 3 months old) received professional care in compliance with the Principals of Good Laboratory Practice (GLP) and the German Animal Protection Act by the animal laboratory. In each pig, the right kidney was treated with two to three multifocal NTIRE ablations under general anaesthesia and muscle relaxation. After sterile preparation, applicator-needle electrodes (NanoKnife® Systems; AngioDynamics® Inc., USA) were percutaneously placed 10 to 20 mm into the right kidney in left-lateral position under computed tomography (CT) guidance (Toshiba Aquilion S16; Toshiba-MS) with the aim of multifocal ablation of the renal cortex and renal medulla, including renal calyxes and renal pelvis (Fig. 1a, b). We used a single 19G needle bipolar probe in six ablations and a triple pack of 16G needle monopolar probes in two ablations with a planned spacing of 10 mm each (see Table 1). The technical feasibility, differences in ablation efficacy, and histological results should be evaluated between these two probe techniques. Each NTIRE procedure (9 sets of 10 DC electrical pulses, pulse length 70 to 100 µs, input current 22 to 27 A, and input voltage 2300 to 2700 V) was performed under R-synchronization per continuous three-lead electrocardiogram (AccuSync72, MRC) until all pulse cycles were completed (no low or high currents were displayed) (Fig. 1c).

Sedation was accomplished using ketamine (6 to 8 mg), xylazin (4 to 7 mg), and propofol (3 to 4 mg/kg); general anaesthesia using isoflurane (1 to 2 vol%) and nitrous oxide (60 to 70%; 2 l/min); muscle relaxation using pancuronium bromide (1 to 2 mg); analgesia using meloxicam (0.4 ml/kg); and antibiosis using oxytetracycline (20 mg/kg). All animals were studied for a 28-day period and killed with an overdose (10 ml) of potassium chloride (25%) after nephrectomy. Blood and urine samples (midstream and bladder punction) were taken right before and 5 min as well as 1, 3, 7, 17, and 28 days after NTIRE.

Non-contrast-enhanced MRI, dynamic contrast-enhanced MRI, MR-diffusion-weighted imaging (MR-DWI), and T1-MR urogram scans of the kidneys (1.5 Tesla Achieva Philips, four-channel surface coil, and Gadovist; Bayer-Schering) were performed right before and 30 min as well as 7 and 28 days after NTIRE. The following MRI sequences were used: T1-survey-TFE, T2-SSH-TSE, T2-HR-SPIR-TSE, T2-HR-RT, DWI, T1-Dual-2D-GE, T1-Thrive1-4-3D-GE, and T1-Thrive5-3D-GE. Thrive2-4

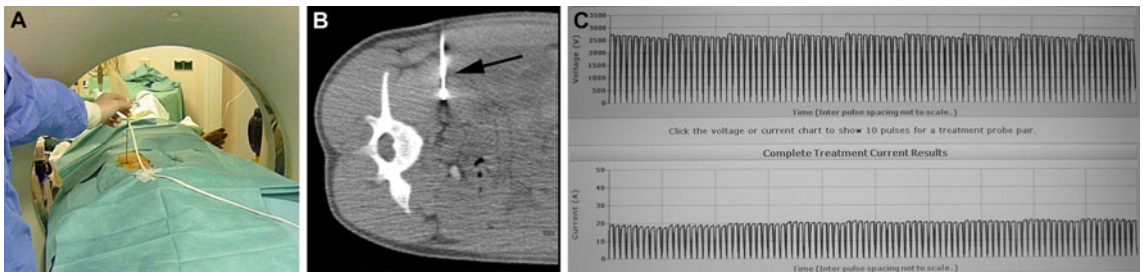

Fig. 1 CT-guided percutaneous NTIRE (**a** and **b**) of the right porcine kidney with the bipolar NTIRE probe (*arrow*). NTIRE application protocol of voltage and current amplitudes (**c**)

Table 1 Size and shape of eight kidney ablation zones immediately, 7 and 28 days after NTIRE per MRI radiological (T2HR-SPIR/SHH sequence) and histological findings

Pig no.	NTIRE, technique, electrodes	Renal position of ablation zone	Lesion size on MRI at day 7 (mm)	Lesion size on MRI at day 28 (mm)	Macroscopic lesion shape on surface at day 28 (mm)	Macroscopic lesion size on surface at day 28 (mm)	Microscopic lesion size at day 28 (mm)
1	1 Bipolar	UP, ventrolateral	26 × 13 × 13	13 × 10 × 5	Elongate	15 × 3	15 × 8 × 4
1	1 Bipolar	MP, ventrolateral	19 × 16 × 12	5 × 6 × 6	Circular	6 × 6	8 × 6 × 4
1	3 monopolar	LP, ventrolateral	15 × 17 × 10	4 × 10 × 4	Star-shaped	6 × 6 × 5	6 × 8 × 4
2	1 Bipolar	UP, dorsolateral	15 × 14 × 13	8 × 10 × 6	Circular	9 × 9	9 × 9 × 8
2	3 Monopolar	MP, dorsolateral	17 × 14 × 13	10 × 8 × 4	Circular	12 × 11	12 × 10 × 6
3	1 Bipolar	UP, ventrolateral	21 × 9 × 9	12 × 5 × 4	Elongate	20 × 4	20 × 6 × 5
3	1 Bipolar	MP, ventrolateral	10 × 13 × 12	7 × 7 × 7	Circular	5 × 4	5 × 9 × 7
3	1 Bipolar	LP, ventrolateral	9 × 11 × 9	6 × 6 × 4	Circular	6 × 4	8 × 8 × 7

Length × width × depth. Upper pole with upper principal calyxes (UP), lower pole with lower principal calyxes (LP), and middle part with medium principal calyxes and renal pelvis (MP)

images were obtained at 20, 40, and 70 s after administrating the contrast agent. T1-MR urogram (Thrive5) was performed between 9 and 19 min (average 14) after contrast agent administration. MRI scans were evaluated using Infinitt PACS software (INFINITT PACS, INFINITT Europe GmbH, Germany).

IVU by conventional X-ray imaging (Artis zee Floor-Mounted System; Siemens) was performed 3 days after NTIRE. Images were taken right before and every 5 min (during a 90-min period) after injection of 30 ml iodine contrast agent (Ultravist-370, 86 kV) (Fig. 2a).

Urinary cytology centrifugates were stained with May–Grünwald–Giemsa stain and then fixed with Canada balm for transmitted-light microscopy with and without oil immersion. Removed kidneys were fixed in 10% formalin. Sections of 5-mm intervals in the transverse plane were made, and the sections were embedded in paraffin. Representative 5-µm microtome sliced sections were stained with haematoxylin and eosin (HE), Elastica-van-Gieson, Berlin blue, Azan, and antihuman-cytoceratin-7-antibody for histological differentiation.

Results

All of the eight renal parenchyma ablations included the renal calyxes or pelvis (two to three ablations/right kidney) (Table 1). All animals survived the experiment with no severe complications. One animal presented a temporary macrohaematuria within the first 3 days after NTIRE. Serum creatinine values showed an increase from preoperative levels of 90 µmol/l (range 67–118) to post-NTIRE levels of 136 µmol/l (range 108–182) at day 28 after the procedure, but they remained within the standard value for German domestic pigs (≤191 µmol/l).

X-Ray IVU and MRI

IVU evaluation showed regular contrast media elimination and no extravasation or gap of the treated renal calyxes and pelvis. The first radiological detection of the X-ray contrast-agent excretion was noted 5 min after injection without disparity in side. The maximal contrast-agent excretion was between 30 and 80 min and showed a consecutive decrease along with increased bladder filling. There were no qualitative or morphological differences in the contralateral untreated kidneys with regard to physiological findings (Fig. 2a, b).

The highest contrast between NTIRE lesions and renal parenchyma was obtained by T2-SPIR-weighted MRI with the following findings: (1) Postinterventional localized hyperintense edema of the renal parenchyma with no substantial lesion immediately after NTIRE; (2) hypointense necrosis-like lesion ≤26-mm diameter with perifocal hyperintense edema 7 days after NTIRE; (3) nonintense scar-like lesion with cortical shrinkage ≤13-mm diameter 28 days after NTIRE (Fig. 3a–c, Table 1). The urographical late venous MRI phase (T1-Thrive5-3D-GE urogram scans) demonstrated normal morphological appearances and normal timing of contrast media excretion with no

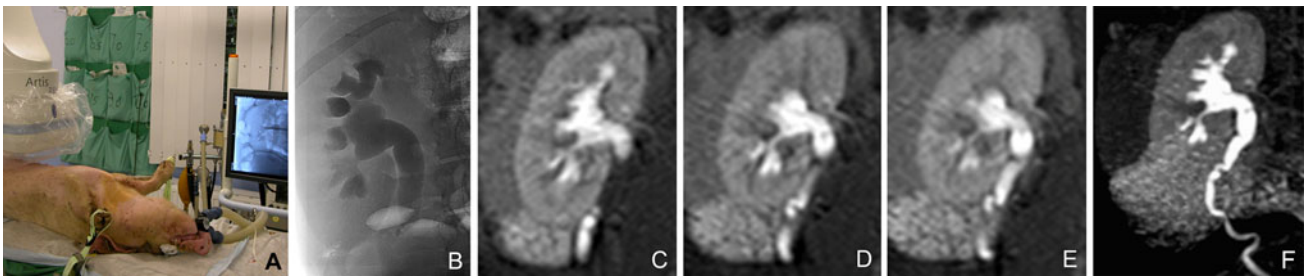

Fig. 2 X-ray IVU (60 minutes after injection) with the pig in supine position 3 days after NTIRE (**a** and **b**). Contrast-enhanced late venous MRI (Thrive5) with urographic phase of the right kidney 7 days after NTIRE (**c**, **d**, and **e**). 2D reconstruction of the superimposed coronary T1-MR urogram planes (**f**)

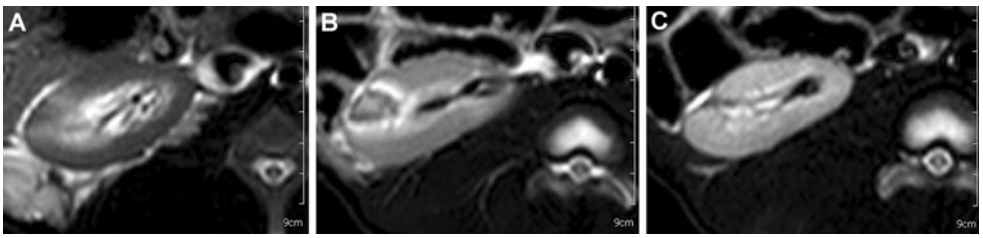

Fig. 3 Center part of the right kidney (pig no. 2) visualized with T2-SPIR MRI at 30 min (**a**), 7 days (**b**), and 28 days after NTIRE (**c**)

urine leakage or urinary obstruction. There were no qualitative or morphological differences in the contralateral untreated kidneys with regard to physiological findings of the renal calyxes and pelvis (Fig. 2c–f).

Histological Analysis and Urinary Cytology

A total of eight sharp circumscribed scars with concave retractions of the right renal surface were detected 28 days after NTIRE ablation (Table 1, Fig. 4b). The central area showed a fibrotic scar partly with fibrinoid necrosis of complete destructed tubules and glomeruli surrounded by granulomas of calcium containing foreign-body giant cells, siderin- and hematoidin-containing histiocytes, fibrotic atrophied glomeruli and tubules, follicular lymphocyte infiltrations, as well as arterioles and venules with circular calcium deposits and a thickened wall (Fig. 4c). All NTIRE ablation zones reached the renal calyxes or pelvis, which showed normal urothelium (Fig. 4d). No cicatrisation, shrinkage, or necrotic ulceration of the renal pelvis and calyxes were seen. There were no qualitative differences of histological results between the bipolar- and monopolar-probe techniques.

Urinary cytology had fundamentally changed by day 1 after NTIRE application. There were an increased number of isolated and partly aggregated transitional urothelium cells with massive degeneration: pale and partly cloudy cytoplasm with ongoing dissolution of the cell membrane as well as swollen cell nuclei with anisocaryosis, hypochromasia, and a dissoluted structure by differently sized pale vacuoles (Fig. 5a, b). From day 3 onward, normal urinary cytology of isolated transitional epithelium cells (regular relation between homogenous cytoplasm and cell nucleus) was seen (Fig. 5c).

Discussion

This preclinical study is the first examination of NTIRE's effect on the renal urine-collecting system using MRI, IVU, and urinary cytology in addition to histological evidence of renal tissue ablation. MRI of the ablation zones at day 28 correlated well with histological analysis at day 28 after NTIRE. Tracy's [14], Deadhar's [18] results, as well as ours, demonstrated histologically the potential of sparing the urine-collecting system by NTIRE of renal parenchyma in a normal porcine kidney. None of these previous studies observed the effect of the NTIRE on the urine-collecting system using urography and urinary cytology, which are routine urological examinations. Referring to a warranted tumor model for renal NTIRE, Thomson et al. [3] investigated seven patients with percutaneous NTIRE of renal masses verified by CT at 3-month follow-up. They observed complete tumor ablation in two renal cell carcinoma (RCC) patients, whereas five patients (one with bifocal RCC, one with singular RCC, one with a transitional cell carcinoma of the renal pelvis, and two with a kidney metastasis from colorectal carcinoma) did not respond to NTIRE treatment.

MRI and urography are favorable methods with which to monitor the success of renal NTIRE ablation as well as renal function and urine-collecting system morphology [15, 17]. This study demonstrated preservation and regeneration

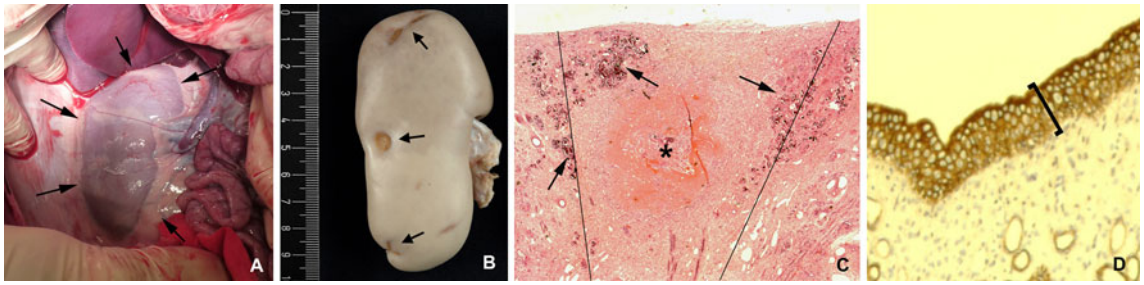

Fig. 4 Intraoperative transperitoneal view of the right kidney (**a**). Macroscopic view of the right kidney after fixing in formaldehyde and removing the connective tissue. *Arrows* show ablation zones as cortical scarred depressions (**b**). Histological analysis of the NTIRE ablation area shows a sharp delineated NTIRE ablation zone with central scar (*borderlines*) partly with a central fibrinoid necrosis (*asterisks*) and peripheral calcium deposits (*arrows*) stained with HE (**c**). The scar adjoining renal calyxes with normal urothelium (*bracket*) stained with cytoceratin-7 (**d**)

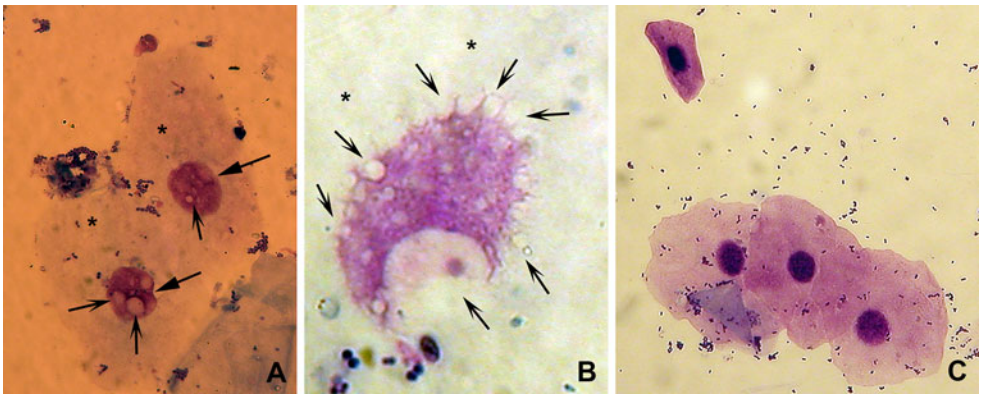

Fig. 5 Urinary cytology one day after NTIRE treatment (**a** and **b**) shows degenerated transitional urothelium cell nuclei (*closed arrows*) by vacuolization (*open arrows*) with pale cytoplasm and ongoing dissolution of the cell membrane (*asterisks*). Normal urinary cytology 3 days after NTIRE (**c**)

of the urine-collecting system after renal NTIRE. No urine extravasation or fistula, no urinary obstruction, no cicatrization or shrinkage, no necrotic ulceration, and no renal failure were observed. These observations are in direct contrast to the acute effects and early complications in the urine-collecting system seen using RFA and CRA [19]. Clinical RCC studies with sufficient outcome data after NTIRE are still warranted. In contrast, short and intermediate oncological outcome data after RFA and CRA of small renal masses (SRMs) have been extensively published, whereas the first long-term results are still awaited [8, 10, 11]. Kunkle and Uzzo [10] analysed CRA or RFA of 1375 localized SRMs (mean tumor size 26.4 mm) in 47 studies of 45 institutions: They reported local tumor progression in 5.2% of patients after CRA and in 12.9% of patients after RFA at mean 18.7-month follow-up, whereas 24.5% of patients had unknown or indeterminate primary pathology, and 33.5% had benign lesions. Rodriguez et al. [11] observed 81 percutaneous CRAs of biopsy-proven pT1-staged RCC (13 to 51 mm) with a complete ablation rate efficacy of 98%. Similarly, Zagoria et al. [12] performed percutaneous RFA of 125 biopsy-proven pT1-staged RCCs (6 to 88 mm) with a complete ablation rate efficacy of 93%.

The preserved and intact matrix, such as submucosa and the basement membrane of the urine-collecting system, as well as the regeneration capability of the urothelium may stimulate healing of the renal calyxes and pelvis after NTIRE. This study observation of urinary cytology after NTIRE represents a qualitative result of a new urinary cytological phenomenon. The current literature provides no similar observations of transitional cell alteration. We interpret this vacuolization of the detached transitional cells as an NTIRE-caused degeneration that seems to be specific in the sense of ongoing apoptosis and necrosis for cells after NTIRE. However, urinary cytology after NTIRE is unable to monitor the NTIRE ablation success, but it reflects NTIRE's individual effect on transitional cells of the urinary tract. Therefore, this new phenomenon must be taken into account when evaluating urinary cytology during the first 7 days after NTIRE. In summary, this study is an additional module by which to demonstrate preservation

and regeneration of the urine-collecting system and urothelium after NTIRE (Figs. 4, 5).

Limitations

This preclinical study of renal NTIRE ablation is limited by the missing swine kidney tumor model, the qualitative description of urinary cytology and urography only, and the small number of cases. Long-term complications, such as renal calyx obstruction, ureteropelvic junction obstruction, or ureter structures, were not assessed.

In general, percutaneous ablation of renal masses is limited by the tumor location because of the percutaneous lumbar access, close proximity to other organs, respiratory kidney motion compared with ribs having small intercostal access, and the difficult distinction between kidney tumor and renal parenchyma during the ablation procedure under non-contrast-enhanced imaging guidance. NTIRE ablation is limited by the requirement of general anaesthesia and muscle relaxation. In contrast, the NTIRE technique is limited by the need for combined multiple monopolar electrodes that are dependent on tumor size (ablation volume $\geq$3.5 cm^3), a maximum number of six probes (ablation volume $\leq$60 cm^3), precise electrode positioning (parallel distance range 5–15 mm), missing coagulation of the probe channel, and dependence on electrical impedance homogeneity of the target tissue [2].

Compared with current thermal ablative techniques, NTIRE plays a potential role in the ablation of centrally located kidney tumors by preserving the urine-collecting system and main vasculature without loss of targeted parenchyma ablation effectiveness [19].

Conclusion

This first urographical and urine-cytological evaluation after porcine kidney NTIRE shows multifocal parenchyma destruction with protection of the involved urine-collecting system. NTIRE could be used as a targeted method of ablating centrally located tumors. New histological phenomena should be taken into account by pathologists when evaluating histology and urinary cytology after NTIRE. Further human NTIRE studies of primary bioptic verified kidney tumors followed by tumor resection approximately 4 weeks after NTIRE are warranted to determine ablation efficacy of this novel technology in different kidney cancers.

Conflict of interests The authors declare that they have no conflict of interest. This study was performed independently of the manufacturer of the devices used.

References

1. Rubinsky B, Onik G, Mikus P (2007) Irreversible electroporation: a new ablation modality—clinical implications. Technol Cancer Res Treat 6(1):37–48
2. Rubinsky B (2009) Irreversible electroporation, 1st edn. Springer, Heidelberg
3. Thomson KR, Cheung W, Ellis SJ, Federman D, Kavnoudias H, Loader-Oliver D et al (2011) Investigation of the safety of irreversible electroporation in humans. J Vasc Interv Radiol 22(5):611–621
4. Pech M, Janitzky A, Wendler JJ, Strang C, Blaschke S, Dudeck O et al (2011) Irreversible electroporation of renal cell carcinoma: a first-in-man phase I clinical study. Cardiovasc Intervent Radiol 34(1):132–138
5. Duffey BG, Kyle Anderson J (2010) Current and future technology for minimally invasive ablation of renal cell carcinoma. Indian J Urol 26(3):410–417
6. Ljungberg B, Cowan N, Hanbury DC, Hora M, Kuczyk MA, Merseburger AS et al (2010) Guidelines on renal cell carcinoma. European Association of Urology. http://www.uroweb.org/. Accessed 25 May 2011
7. Tacke J (2007) Interventional oncology in urology [in German]. Radiologe 47(12):1089–
8. Breen DJ, Railton NJ (2010) Minimally invasive treatment of small renal tumors: trends in renal cancer diagnosis and management. Cardiovasc Intervent Radiol 33(5):896–908
9. Dib RE, Touma NJ, Kapoor A (2009) Review of the efficacy and safety of radiofrequency ablation for the treatment of small renal masses. Can Urol Assoc J 3(2):143–149
10. Kunkle DA, Uzzo RG (2008) Cryoablation or radiofrequency ablation of the small renal mass: a meta-analysis. Cancer 113(10):2671–2680
11. Rodriguez R, Cizman Z, Hong K, Koliatsos A, Georgiades C (2011) Prospective analysis of the safety and efficacy of percutaneous cryoablation for pT1NxMx biopsy-proven renal cell carcinoma. Cardiovasc Intervent Radiol 34(3):573–578
12. Zagoria RJ, Traver MA, Werle DM, Perini M, Hayasaka S, Clark PE (2007) Oncologic efficacy of CT-guided percutaneous radiofrequency ablation of renal cell carcinomas. AJR Am J Roentgenol 189(2):429–436
13. Wendler JJ, Pech M, Blaschke S, Porsch M, Janitzky A, Ulrich M, et al (2011) Angiography in the isolated perfused kidney: Radiological evaluation of vascular protection in tissue ablation by nonthermal irreversible electroporation. Cardiovasc Intervent Radiol (in press)
14. Tracy CR, Kabbani W, Cadeddu JA (2011) Irreversible electroporation (IRE): a novel method for renal tissue ablation. BJU Int 107(12):1982–1987
15. Strohmaier WL, Bartunek R (2008) Diagnostic imaging̃The end of intravenous urography [in German]? Urologe A 47(5):556, 558–562
16. Raisi O, Magnani C, Bigiani N, Cianciavicchia E, D'Amico R, Muscatello U et al (2011) The diagnostic reliability of urinary cytology: A retrospective study. Diagn Cytopathol (in press)
17. Notohamiprodjo M, Reiser MF, Sourbron SP (2010) Diffusion and perfusion of the kidney. Eur J Radiol 76(3):337–347
18. Deodhar A, Monette S, Single GW Jr, Hamilton WC Jr, Thornton R, Maybody M, Coleman JA et al (2010) Renal tissue ablation with irreversible electroporation: preliminary results in a porcine model. Urology 77(3):754–760
19. Igor Pinkhasov G, Raman JD (2010) Management and prevention of renal ablative therapy complications. World J Urol 28(5): 559–564

8.4

Short- and mid-term effects of irreversible electroporation on normal renal tissue: an animal model.

Wendler JJ, Porsch M, Hühne S, Baumunk D, Buhtz P, Fischbach F, Pech M, Mahnkopf D, Kropf S, Roessner A, Ricke J, Schostak M, Liehr UB.

Cardiovasc Intervent Radiol. 2013 Apr;36(2):512-20.

PURPOSE: Irreversible electroporation (IRE) is a novel nonthermal tissue ablation technique by high current application leading to apoptosis without affecting extracellular matrix. Previous results of renal IRE shall be supplemented by functional MRI and differentiated histological analysis of renal parenchyma in a chronic treatment setting.

METHODS: Three swine were treated with two to three multifocal percutaneous IRE of the right kidney. MRI was performed before, 30 min (immediate-term), 7 days (short-term), and 28 days (mid-term) after IRE. A statistical analysis of the lesion surrounded renal parenchyma intensities was made to analyze functional differences depending on renal part, side and posttreatment time. Histological follow-up of cortex and medulla was performed after 28 days.

RESULTS: A total of eight ablations were created. MRI showed no collateral damage of surrounded tissue. The highest visual contrast between lesions and normal parenchyma was obtained by T2-HR-SPIR-TSE-w sequence of DCE-MRI. Ablation zones showed inhomogeneous necroses with small perifocal edema in the short-term and sharp delimitable scars in the mid-term. MRI showed no significant differences between adjoined renal parenchyma around ablations and parenchyma of untreated kidney. Histological analysis demonstrated complete destruction of cortical glomeruli and tubules, while collecting ducts, renal calyxes, and pelvis of medulla were preserved. Adjoined kidney parenchyma around IRE lesions showed no qualitative differences to normal parenchyma of untreated kidney.

CONCLUSIONS: This porcine IRE study reveals a multifocal renal ablation, while protecting surrounded renal parenchyma and collecting system over a mid-term period. That offers prevention of renal function ablating centrally located or multifocal renal masses.

Cardiovasc Intervent Radiol (2013) 36:512–520
DOI 10.1007/s00270-012-0452-7

LABORATORY INVESTIGATION

Short- and Mid-term Effects of Irreversible Electroporation on Normal Renal Tissue: An Animal Model

J. J. Wendler · M. Porsch · S. Hühne · D. Baumunk · P. Buhtz · F. Fischbach · M. Pech · D. Mahnkopf · S. Kropf · A. Roessner · J. Ricke · M. Schostak · U.-B. Liehr

Received: 19 March 2012 / Accepted: 12 July 2012 / Published online: 15 August 2012

Abstract
Purpose Irreversible electroporation (IRE) is a novel nonthermal tissue ablation technique by high current application leading to apoptosis without affecting extracellular matrix. Previous results of renal IRE shall be supplemented by functional MRI and differentiated histological analysis of renal parenchyma in a chronic treatment setting.
Methods Three swine were treated with two to three multifocal percutaneous IRE of the right kidney. MRI was performed before, 30 min (immediate-term), 7 days (short-term), and 28 days (mid-term) after IRE. A statistical analysis of the lesion surrounded renal parenchyma intensities was made to analyze functional differences depending on renal part, side and posttreatment time. Histological follow-up of cortex and medulla was performed after 28 days.
Results A total of eight ablations were created. MRI showed no collateral damage of surrounded tissue. The highest visual contrast between lesions and normal parenchyma was obtained by T2-HR-SPIR-TSE-w sequence of DCE-MRI. Ablation zones showed inhomogeneous necroses with small perifocal edema in the short-term and sharp delimitable scars in the mid-term. MRI showed no significant differences between adjoined renal parenchyma around ablations and parenchyma of untreated kidney. Histological analysis demonstrated complete destruction of cortical glomeruli and tubules, while collecting ducts, renal calyxes, and pelvis of medulla were preserved. Adjoined kidney parenchyma around IRE lesions showed no qualitative differences to normal parenchyma of untreated kidney.
Conclusions This porcine IRE study reveals a multifocal renal ablation, while protecting surrounded renal parenchyma and collecting system over a mid-term period. That offers prevention of renal function ablating centrally located or multifocal renal masses.

Keywords Irreversible electroporation · Percutaneous ablation · Kidney · Animal model

J. J. Wendler (✉) · M. Porsch · S. Hühne · D. Baumunk · M. Schostak · U.-B. Liehr
Department of Urology, University of Magdeburg, Leipziger Straße 44, 39120 Magdeburg, Germany
e-mail: johann.wendler@med.ovgu.de

P. Buhtz · A. Roessner
Institute of Pathology, University of Magdeburg, Leipziger Straße 44, 39120 Magdeburg, Germany

F. Fischbach · M. Pech · J. Ricke
Department of Radiology, University of Magdeburg, Leipziger Straße 44, 39120 Magdeburg, Germany

D. Mahnkopf
Institute of Medical Technology and Research, Thomas-Müntzer-Platz 1, 39343 Rottmersleben, Germany

S. Kropf
Institute of Biometry, University of Magdeburg, Leipziger Straße 44, 39120 Magdeburg, Germany

Introduction

Irreversible electroporation (IRE) is a new, nonthermal tissue ablation technology [14, 15]. In our investigation, we focused on IRE as potential minimally invasive ablation modality for renal masses [3]. Increased rate of detected small renal cell carcinoma (RCC), also in elderly, probably functionally compromised population necessitates minimally invasive

procedures [1, 10, 13]. Whenever feasible, partial resection with a margin <5 mm is the "gold standard" for solitary RCC <7 cm [9, 16]. Central tumors require almost nephrectomy because of the closed location to the hilus with the risk of organ ischemia by major vessel destruction and the risk of urinary leakage by insufficient reconstruction. For inoperability, cryoablation and radiofrequency ablation are recommended as alternatives, except for tumors >3 cm, in the hilum, or near the collecting system [9]. IRE may have advantages compared with those thermal ablation techniques, which cause severe collateral damage of the normal adjacent tissue [3]. Wendler et al. [21] demonstrated the acute protection of the renal vessels during IRE. Previous animal studies of IRE revealed the protection of the involved urine collecting system [2, 19, 20]. First clinical results by Pech et al. [12] and Thomson et al. [17] demonstrated a safe renal IRE. To date, there is no sufficient IRE real-time imaging method [4, 5]. Renal dynamic contrast-enhanced (DCE-MRI) and diffusion-weighted magnetic resonance imaging (DWI-MRI) provide excellent morphological and functional information [11] and permit immediate depiction of the IRE zones [6–8, 22]. This study supplements previous investigations of renal IRE by the first MRI follow-up and a purposive histological differentiation of the renal parenchyma in a mid-term treatment setting to evaluate the minimally invasive potential of IRE.

Materials and Methods

Three domestic male pigs (28–33 kg, 3 months old) were obtained by animal laboratory and received veterinary medical care in compliance with the Good Laboratory Practice and German animal protection act. The study was approved by the ethic commission and scientific board (animal project no. 42502-2-996, IMTR-GA-no. 112). The animals were treated with two to three multifocal IRE ablations (NanoKnife™ System, AngioDynamics®) under general anesthesia with muscle relaxation and continuous 3-lead ECG-R-synchronization (AccuSync72, MRC®). 19G single bipolar (length 20 mm) and three parallel three-cornered placed 16G (distance 5–10 mm from each other, length 15 mm) were percutaneously placed 10–20 mm into the right kidney (Table 1) under CT guidance (Toshiba® Aquilion S16). Each IRE treatment with 22–27 A and 2,300–2,700 V consisted of 90 electrical pulses per 70 µs pulse duration using one bipolar probe and 3 × 90 electrical pulses (90 each probe pair) per 100 µs pulse duration using three monopolar probes. The intended ablation volume was 3.5 cm^3 of a rotationally symmetric prolate spheroid ($a = 15$ mm, $b = 7.5$ mm) for one bipolar electrode and 2.9–5.2 cm^3 of a triangular prism ($a = 15$–20 mm, $h = 30$ mm) for three monopolar electrodes with the above-mentioned setting due to the manufacturer's data. Probes were placed in the renal cortex and renal medulla with intended inclusion of the renal surface and the renal calyxes of the urine collecting system. The protocol intended multifocal IRE treatment of the renal parenchyma separated for each anatomical renal part (upper pole, middle part, lower pole) to avoid overlapping of the intended ablation volumes and to obtain nonablated parenchyma around and between these intended ablation zones. An exception was animal 2, which was without a third IRE treatment of the lower pole (interventionists decision), because of a nonintended, very caudal probe placement at the middle renal part (see "Study limitations") and a consecutive impossible separate, third IRE ablation of the lower renal part. All animals were studied for a 28 day period and euthanized with an overdose of potassium chloride after necropsy.

MR Imaging

Noncontrast-enhanced MRI (NCE-MRI), DCE-MRI, DWI-MRI, and T1-MR-urogram scans of the kidneys (1.5 tesla, 4 channel surface cardiology coil; gadobutrolum contrast agent, sequences: T1-survey-TFE, T2-SSH-TSE, T2-HR-SPIR-TSE, T2-HR-RT, DWI, T1-Dual-2D-GE, T1-Thrive1-4-3D-GE and T1-Thrive5-3D-GE) were made just before, and 30 min, 7 days, and 28 days after IRE. Thrive 2–4 images were obtained at 20 s, 40 s, 70 s, and Thrive5 between 9–19 min after administrating contrast agent. MRI was evaluated with INFINITT PACS®. Renal lesions were measured in each MRI sequence. Contrast ratios between lesions and renal parenchyma were calculated from the intensities of ROI (30 ± 2 mm^2) in each MRI sequences (240 overall) to evaluate the highest sequence contrast. Moreover, we hypothesized a collateral damage of the renal parenchyma. Different IRE effects in ablation area size, shape, and transition zone due to the protocol and the heterogenic parenchyma of the kidney should be taken into account. Therefore, the signal intensities (SI) of ROI of the renal cortical parenchyma of the upper pole, middle part, and lower pole in close vicinity to the ablation zones of the IRE-treated, right kidney, as well as the cortical parenchyma of the analogous renal part of the untreated, left kidney were measured for each animal, in each MRI sequence (SSH, T2SPIR, T2RT, DWI, Dual, Thrive 1–5) and at each point of time (before resp., 30 min, 7 days, and 28 days after IRE) (Table 2). The background noise was measured in each MRI sequence and subtracted from the SI of the parenchyma.

For statistical analysis, the mean of three measurements (SI and noise) with ROI (30 ± 2 mm^2) for each region by the same investigator was taken. The data were analyzed in a linear mixed model (SPSS, version 18.0, procedure "mixed") with the renal part, the time point, and laterality (corresponding to treated/untreated) as fixed factors and the animals as random factors. In addition to the three (fixed)

main factors, the interaction of time point and laterality were included in the model, because this interaction tests for different profiles in the time course of SI in the treated and untreated kidneys. A condensed description has been derived from separate mixed model analyses for treated and untreated kidneys with only renal part and time points as fixed factors (and again animal as random factor). Because the renal part showed no significance, we used the estimates of means and corresponding standard errors of means (SEM) of SI at the different time points, averaged over the levels of renal part (Table 3).

Pathological analysis

Immediately after nephrectomy, the kidneys were perfused and fixed with 10 % formalin. After removing perirenal connective tissue, the kidneys were photographed (Fig. 2), measured, and described. Each treated kidney was completely cut transversally in 3-mm-thick paraffin blocks; 3-µm-thick sections were stained with hematoxylin-eosin (HE), Elastica-van-Gieson, partly with Azan and occasionally, the PAS, Berlin-blue and Kossa reaction. The immunohistochemical reaction was positive with monoclonal antihuman-antibody cytokeratin-7 for staining the epithelium of the collecting ducts, distally convoluted tubuli and urothelium. The renal parenchyma, hilus, and urine collecting system was histologically examined at three sites each. To exclude systemic IRE effects, tissues specimens were taken from all organs at necropsy and processed in HE sections.

Results

MR imaging

ight renal IRE lesions were created. The highest visual contrast between the lesions and renal parenchyma was obtained by T2-SPIR-weighted MRI. The following MRI findings were seen (Fig. 1): immediately after IRE (0 days): a postinterventional localized renal parenchyma edema at the region of IRE ablation without any substantial lesions; 7 days after IRE: a hypointense necrosis-like lesion in the renal parenchyma at the region of IRE ablation with a perifocal hyperintense edema. The necrosis-like lesion contained a small central area that was isointense to the adjacent renal cortex on T2w and DWI while non-intense on the T1w; 28 days after IRE: a sharp delineated, nonintense, scar-like lesion with cortical shrinkage and without contrast enhancement and without perifocal edema, which was well delimitable from the spared renal parenchyma. The residual kidney parenchyma outside of the IRE lesions showed no pathological findings such as structural defects, urine leakage or urinary obstruction.

Lesion sizes were measured in three planes of the MRI sequences with the highest contrast and the largest extension of the lesions: T2-SSH for coronary axis and T2-HR-SPIR for transversal axis (Table 1). The perifocal hyperintense edema (T2w) 7 days after IRE measured 3–4 mm. All lesions included the renal surface and reached the urine collecting system in the MR images. The stated macroscopic lesion constitutes only a description of the size, which varies because of the different probe position and count with consecutive different shape on the renal surface.

In the mixed model analyses of SI (ROI of each MR sequences) of the renal parenchyma in close vicinity to the ablation zones were only significant effects of time point, but not of renal part, laterality and interaction of time point and laterality, indicating that there are special time courses due to physiological development and stress of operation in general, but no significant differences (mean ± SEM, Table 2; *P* values, Table 3; plots) in the time course of SI between treated and untreated kidneys. In this sense, we observed no collateral parenchyma damage of the treated kidney in close vicinity of the multifocal ablation zones compared with the untreated kidney.

Pathological analysis

Altogether, eight well-delineated ablation scars were macroscopically noted in the three right kidneys (Figs. 2, 3A; Table 1). The surface of the kidneys was retracted in the regions of the scar and showed yellowish-brown color centrally. The whole treated kidney was microscopically scanned for any lesions. All together, eight ablation zones could be noted. On the cut section, the wedge-like scars became narrower to the depth. One scar affected the cortex only and the other ones both the cortex and the medulla. Four lesions reached the renal calyx, i.e., pylon.

All kidney areas are representative analyzed to describe all different histological reactions after IRE. Histologically, the scar in the renal cortex lacks glomeruli and tubuli (Fig. 3E). The increased connective tissue contains ductal structures of different sizes, the epithelium of which is positive for cytokeratin-7. These ductal structures can be considered as collecting ducts with regenerative epithelium. In the cortex, the scars show a seam of atrophic tubuli and sclerotic or degenerating glomeruli, partly with periglomerular fibrosis, lying very close to each other (Fig. 3F). In some lesions, glomerular microcysts can be noted in this seam (Fig. 3G). In six scars, calcium plaques up to 300 µm lie in the scar tissue (mainly at the rim) either singly or as a conglomerate, each showing a foreign-body-giant cell granulomatous reaction (Figs. 3B, D, O). In the medulla, there are neither collecting ducts nor intermediary tubuli in the scar (left half), whereas the margin of the scar (right half) contains ducts of different width and configuration (Fig. 3I).

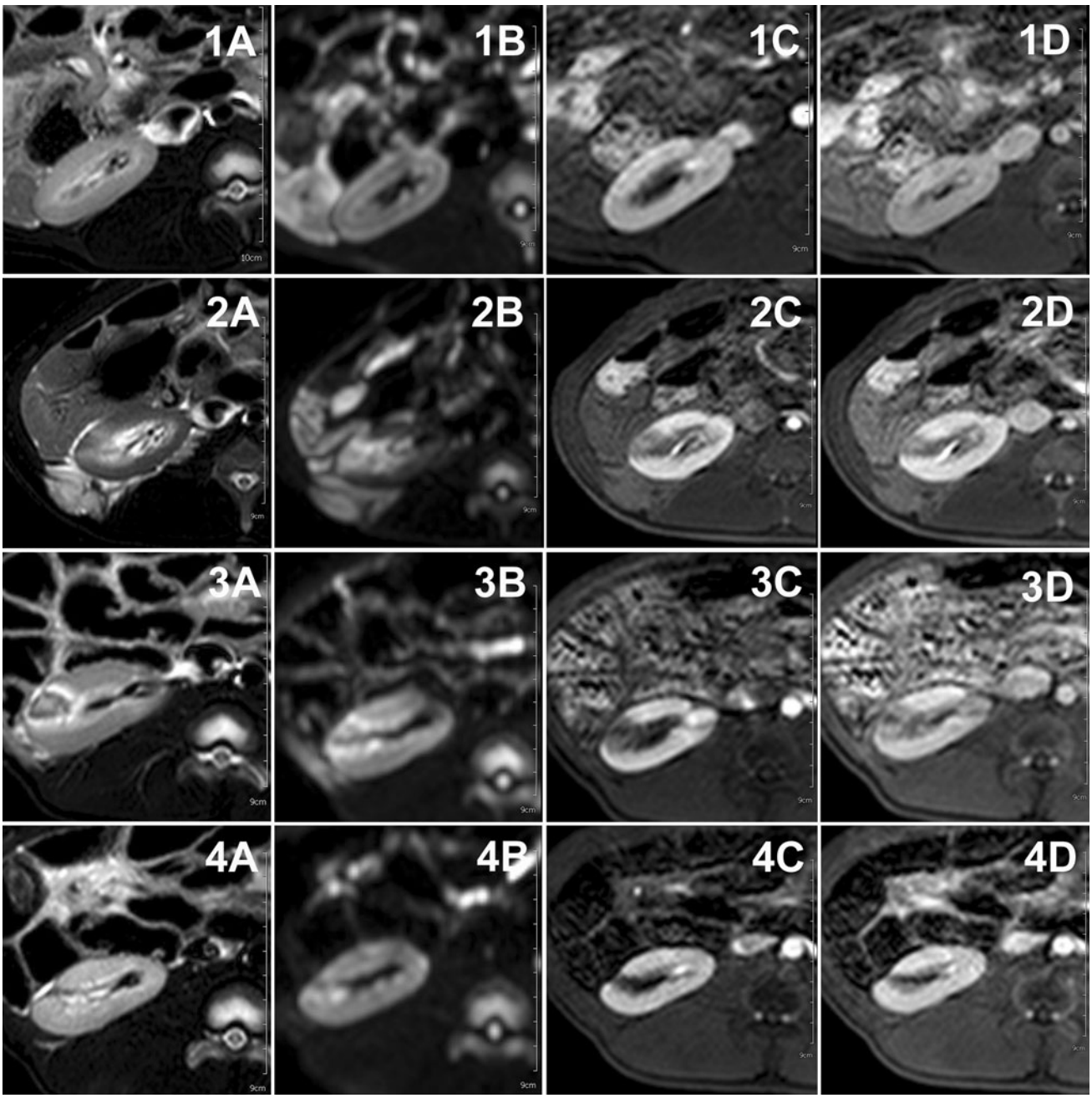

Fig. 1 MRI of center part of kidney (animal 2): before (*1*), 30 min after (*2*), 7 days after (*3*), and 28 days after (*4*) IRE. T2-HR-SPIR (*A*), DWI (*B*), T1-Thrive2 (*C*), and T1-Thrive4 (*D*)

Some of these contain hyaline casts, whereas others contain mucin positive for PAS, Alcian blue, and Mucicarmine. In the scars and predominantly at the rim of the scars, large nests of siderophages (blue) can be recognized in the cortex and medulla (Fig. 3D). Hematoidin pigment was found in only one lesion. All lesions contain lymphocytic infiltrates in the cortex and medulla (Fig. 3C), partly like follicles. The obviously regenerated urothelium over the scarred papillae and calyces is partly flattened (Fig. 3J). It shows mucinous metaplasia as does the normal urothelium of the swine. In only one site of ablation, the urothelium of a calyx lacks focally 1 mm (bracket; Fig. 3K), where a stronger interstitial nephritis can be seen in the adjacent renal parenchyma. In the cortical scars, the interlobular vessels are obliterated or show thickened intima and media (Fig. 3M). Such angiosclerosis also can be seen at the margin of the scars. In the renal parenchyma around and between the IRE lesions, the vessels are surrounded by circular fibrosis (Fig. 3N). Only one lesion

Table 1 Size and shape of eight kidney ablation zones immediately, 7 days, and 28 days after IRE in MRI radiological (T2HR-SPIR/SHH sequence) and histopathological findings (Length × width × depth)

Pig no.	IRE, technique, electrodes	Renal position of ablation zone (mm)	Lesion size on MRI at day 7 (mm)	Lesion size on MRI at day 28 (mm)	Macroscopic lesion shape on surface at day 28 (mm)	Macroscopic lesion size on surface at day 28 (mm)	Microscopic lesion size at day 28 (mm)
1	1 Bipolar	UP, ventrolateral	26 × 13 × 13	13 × 10 × 5	Elongate	15 × 3	15 × 8 × 4
	1 Bipolar	MP, ventrolateral	19 × 16 × 12	5 × 6 × 6	Circular	6 × 6	8 × 6 × 4
	3 Monopolar	LP, ventrolateral	15 × 17 × 10	4 × 10 × 4	Star-shaped	6 × 6 × 5	6 × 8 × 4
2	1 Bipolar	UP, dorsolateral	15 × 14 × 13	8 × 10 × 6	Circular	9 × 9	9 × 9 × 8
	3 Monopolar	MP, dorsolateral	17 × 14 × 13	10 × 8 × 4	Circular	12 × 11	12 × 10 × 6
3	1 Bipolar	UP, ventrolateral	21 × 9 × 9	12 × 5 × 4	Elongate	20 × 4	20 × 6 × 5
	1 Bipolar	MP, ventrolateral	10 × 13 × 12	7 × 7 × 7	Circular	5 × 4	5 × 9 × 7
	1 Bipolar	LP, ventrolateral	9 × 11 × 9	6 × 6 × 4	Circular	6 × 4	8 × 8 × 7

UP upper pole; *LP* lower pole; *MP* middle part with medium principal calyxes and renal pelvis

in the center of the scar (semicircle) shows a 3-mm-sized infarct (Fig. 3O). A foreign body giant cell granuloma points to a vanished vessel. At the margin of one lesion, the sections show an interlobar artery with an obviously thickened intima and media with surrounding calcium clamps up to 2 mm (Fig. 3P). Furthermore, large nests of siderophages in the surroundings of the artery can be interpreted as residues of bleeding. The findings of the renal parenchyma outside and adjacent to the scars are normal in the glomeruli, tubules, collecting tubes, extrarenal kidney vessels, and urinary system with an intact pelvic structure of muscularis and submucosa (Fig. 3H, L). A greater transition zone with intermediate histological reaction between the normal parenchyma and the decellularized parenchyma of the IRE scars cannot be found (<1 mm). In the surrounded medulla of six ablation sites, there is discrete tubulointerstitial nephritis with preference of T-cell infiltrates around the collecting ducts. Compared with the treated right kidney, the histological findings of the untreated left kidney and the remaining organs were unremarkable in sense of no systemic reactions.

Discussion

Our study is discussed in context to previous results of renal IRE. Tracy et al. [19] histologically evaluated eight pigs after laparoscopic IRE of the kidney (18 ablations ≤7 days and 6 ablations after 14 days). Deodhar et al. [2] analyzed histological and CT imaging features in 15 swine after percutaneous renal IRE (23 ablations ≤36 h and six ablations after 21 days). Both groups demonstrated the potential of IRE for renal parenchyma ablation while sparing the urine collecting system. Our presented study is the first differentiated histological evaluation of the renal parenchyma with a longer follow-up of 28 days.

Pathological Analysis

In contrast to Tracy et al. [19] and Deodhar et al. [2], we observed different results on tubules ablation. Tracy et al. [19] did not report persisting tubules and did not differentiated histologically the renal parenchyma. Deodhar et al. [2] observed persisting tubules in the IRE ablation area without differentiation of the tubules entity while a complete necrosis of the glomeruli was seen.

Our histological findings allowed the following conclusions: 28 days after IRE, the picture of the tissue showed ablation areas that were surrounded by normal parenchyma. The ablation zones could be structured in the basic inner ablation zone surrounded by a small (<1 mm) transition zone (Table 1).

In the scar (central ablation zone), the tubuli, the majority of collecting ducts, and glomeruli are almost nonreactively replaced by fibrous tissue. Both in the cortex and medulla, the scar contains only few tubular structures, which most likely can be interpreted as collecting ducts with regenerative epithelium. The same observation was made by Deodar et al. [2], who could not clarify the entity of the tubuli as well as the question of whether such regeneration represented regrowth of cells that escaped ablation or repopulation in the ablation field by migrant stem cells. The phenomenon of remaining collecting ducts is may be based on two facts: (1) the larger lumen and the more surrounding matrix of the collecting ducts compared with the proximal and distal tubules; (2) the regeneration potential of the collecting ducts endothelium is similar to the transitional endothelium of the collecting system due to the same embryological origin. In the area of transition (<1 mm) between scar and normal tissue, IRE did not result in a complete destruction of the tubuli but only a high-grade tubulus atrophy, which may due to the reversible electroporation at the margin. The alterations on the glomeruli (hyaline degeneration and microcystic transformation) in the

Table 2 SI (mean ± SEM) of the renal parenchyma (all renal parts) in close vicinity to the ablation zones of each MR sequence and point of time in comparison between the right/IRE-treated and the left/untreated kidney

Kidney	Time to IRE	SSH	T2SPIR	T2RT	DWI	Dual	Thrive1	Thrive2	Thrive3	Thrive4	Thrive5
Right/IRE-treated	Before	769 ± 94	1,005 ± 115	835 ± 114	1,529 ± 104	781 ± 51	616 ± 64	1,061 ± 118	1,296 ± 88	1,429 ± 78	1,159 ± 68
	Immediately after	918 ± 101	830 ± 120	597 ± 120	1,726 ± 111	1,185 ± 55	963 ± 74	1,203 ± 137	1,337 ± 107	1,256 ± 95	1,476 ± 76
	Short-term after	1,247 ± 94	978 ± 115	995 ± 114	1,865 ± 104	1,114 ± 51	867 ± 64	1,678 ± 118	1,412 ± 88	1,380 ± 78	1,170 ± 68
	Mid-term after	1,161 ± 94	832 ± 115	894 ± 114	1,781 ± 104	1,067 ± 51	1,062 ± 64	2,615 ± 118	2,280 ± 88	2,261 ± 78	1,371 ± 68
Left/untreated	Before	876 ± 108	1,162 ± 128	896 ± 107	1,481 ± 102	883 ± 51	725 ± 68	1,189 ± 126	1,420 ± 96	1,568 ± 81	1,285 ± 79
	Immediate after	845 ± 113	780 ± 134	526 ± 111	1,679 ± 109	1,192 ± 59	972 ± 79	1,203 ± 143	1,301 ± 116	1,254 ± 100	1,364 ± 93
	Short-term after	1,237 ± 108	946 ± 128	976 ± 107	1,881 ± 102	1,110 ± 51	893 ± 68	1,621 ± 126	1,360 ± 96	1,339 ± 81	1,126 ± 79
	Mid-term after	1,167 ± 108	855 ± 128	884 ± 107	1,780 ± 102	1,117 ± 51	1,055 ± 68	2,556 ± 126	2,260 ± 96	2,252 ± 81	1,323 ± 79

Table 3 *P* values ($\alpha = 0.05$) for differences between the SI (ROI) of the renal parenchyma in close vicinity to the ablation zones depending on the renal part of the treated kidney (upper pole = UP vs. middle part = MP vs. lower pole = LP), laterality (right treated vs. left untreated kidney for each renal part) and observation time to IRE (before resp. 30 min/immediate, 7 days/short-term and 28 days/mid-term after IRE)

MRI sequences	Renal part (UP vs. MP vs. LP)	Laterality (right/treated vs. left/untreated kidney)	Time to IRE (before resp. 30 min, 7 days, and 28 days after IRE)	Renal part * time to IRE
SSH	0.799	0.737	0	0.318
T2SPIR	0.71	0.501	0	0.092
T2RT	0.425	0.716	0	0.502
DWI	0.07	0.563	0	0.877
Dual	0.502	0.092	0	0.367
Thrive1	0.455	0.328	0	0.638
Thrive2	0.607	0.901	0	0.653
Thrive3	0.38	0.895	0	0.737
Thrive4	0.432	0.712	0	0.674
Thrive5	0.546	0.58	0	0.162

transition zone are obviously due to primary tubulus atrophy and not to a direct consequence of IRE.

In six of nine ablations scars, we found partly massive calcifications with foreign-body-giant cell granulomatous reactions. These calcifications were obviously caused by IRE, because these usually do not occur for example in infarct necroses of the kidney. Deodhar et al. [2] described such a mineralization in three of six IRE scars in the kidney of swine. Rubinsky et al. [14], investigating the liver of swine, reported on calcifications in necroses induced by IRE. According to experimental studies, an increased calcium accumulation due to an increased intracellular Ca^{2+} influx through the electrically increased permeability of the cell membrane as possible mechanism of IRE-induced apoptosis is suggested [18]. The specific calcifications induced by IRE have no functional significance.

The large number of siderophages at the rim of ablation scars is residue of stronger bleeding in necrosis as of the kidney [2, 19] as well as the liver [14]. Obviously, IRE directly damages the walls of the capillaries with consecutive capillary hemorrhage because of the absent tunica intima and adventitia.

The obliterated and sclerosed vessels in the scars can be explained by reduced blood flow through the scars, although a direct effect of IRE on the vessel walls is possible. Rubinsky et al. [14] found wall necroses of portal vessels in ablation areas in the liver of swine. Tracy et al. [19] described thickening with focal thrombosis of intralobar arteries, whereas Deodhar et al. [2] did not mention any alteration of renal vessels. The small necrotic infarct

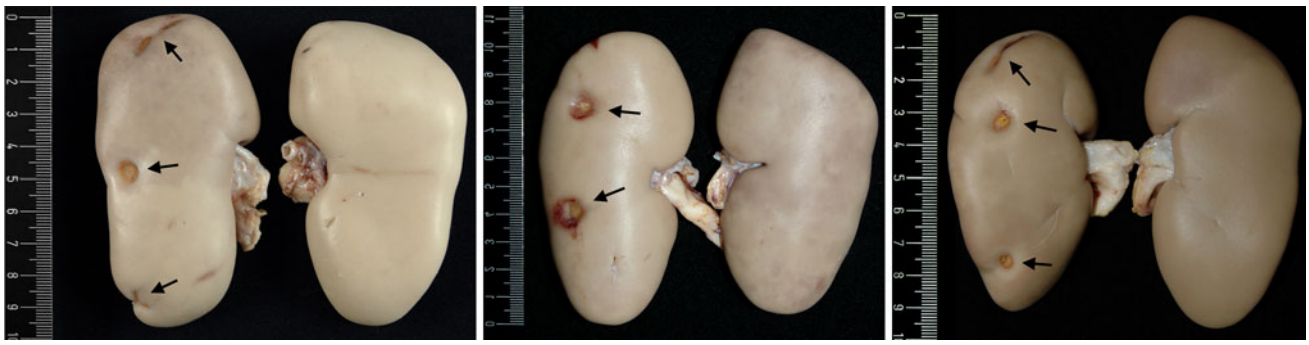

Fig. 2 Renal ablation zones (*arrows*) compared with contralateral, untreated kidney 28 days after IRE. pig 1 (*left* ventral view); pig 2 (*center* dorsal view); pig 3 (*right* ventral view)

within an ablation scar (Fig. 3O) is the consequence of an obliterated artery by IRE-induced arteriosclerotic-like alteration or direct lesion by electrode placement. The sclerosis of an interlobar artery and the calcifications around (Fig. 3P) seem to be the consequence of IRE. It seems to induce arteriosclerosis-like alteration without acute damage. It could be the consequence of the IRE-induced endothelial damage combined with the supposed IRE-related Ca^{2+} release. The residues of bleeding seen in the surrounding of the artery suggest that the applicator needle electrode was placed beside or into the artery.

Obviously, in four lesions, ablation had reached the urothelium of a renal calix, which was completely regenerated in three cases. In only one lesion, the urothelium, which was not completely regenerated, had a small central defect, possibly in the region of a puncture site. Tracy et al. [19] more frequently found an ulceration of the urothelium after direct puncture of the collecting system 14 days after IRE. The connective tissue and the smooth musculature of the collecting system are not altered by IRE, so a regeneration of the urothelium is possible. A time of 6 weeks should be taking into account for whole urothelial regeneration.

MR Imaging

This is the first MRI evaluation of renal IRE with the longest follow-up of 4 weeks after IRE. MRI reveals more differentiated functional information about the renal parenchyma compared with CT follow-up [2]. Our study showed inhomogenous ablation areas in different MRI sequences, whereas Deodhar et al. [2] observed homogenous texture in CT scan of the ablation area immediately and 7 days after IRE. Simultaneous histological analysis is warranted to differentiate the MRI findings immediately and up to 7 days after IRE. It should be noted that there is a vague border and a time-dependent unpredictable course between reversible and irreversible electroporation of the perifocal zone [2, 6, 7, 14, 19, 22]. A radiological differentiation between postinterventional inflammation and electroporation of the margin cannot be made. Guo et al. [6] demonstrated that contrast-enhanced, tissue-nulled, inversion-recovery MRI could be used for quantitative differentiation of reversible "IRE penumbra" in the rodent liver. That could be used for near-term evaluation of the tumor ablation success. In contrast to CT 3 weeks after IRE [2], we observed nonintense scar-like lesions that were well delimitable from the spared renal parenchyma 28 days after IRE. There was a cortical shrinkage without contrast enhancement or perifocal edema. This indicates a completed tissue repair and cicatrization with complete localized parenchyma ablation in the IRE treatment zone after 28 days, which correlated with the histological analysis. Therefore, we propose a first follow-up of IRE ablation by DCI-MRI at least 4 weeks after treatment to evaluate the ablation success.

Study limitations

This preliminary study is limited by its preclinical character and the missing renal tumor model. A different ablation efficacy of IRE in renal tumor tissue should be taken into account. Moreover, it is limited by the small number of cases and the histological analysis after a chronic period of 28 days only. It shall be considered as a contribution to discussions of previous and further renal IRE studies. Noncontrast-enhanced CT for IRE guidance was limited by the low-contrast demarcation of the kidney from the surrounded tissue (especially intestine), mainly because of the absent adipose capsule of the kidney in these animals, making the IRE probe placement difficult. The authors cannot draw a final conclusion about the histological extension of the "real" ablation zone and the relation to the transition zone and scar, due to the missing MRI and histology at the same point of time (short-term after IRE), the unknown tissue shrinkage of the scar, and the missing tumor model as index target volume. Because of the specific IRE effects with local parenchyma decellularization as well as preservation of the matrix and vascularization, a faster tissue repair can be expected in contrast to lesions of a general coagulation necrosis after thermal ablation methods.

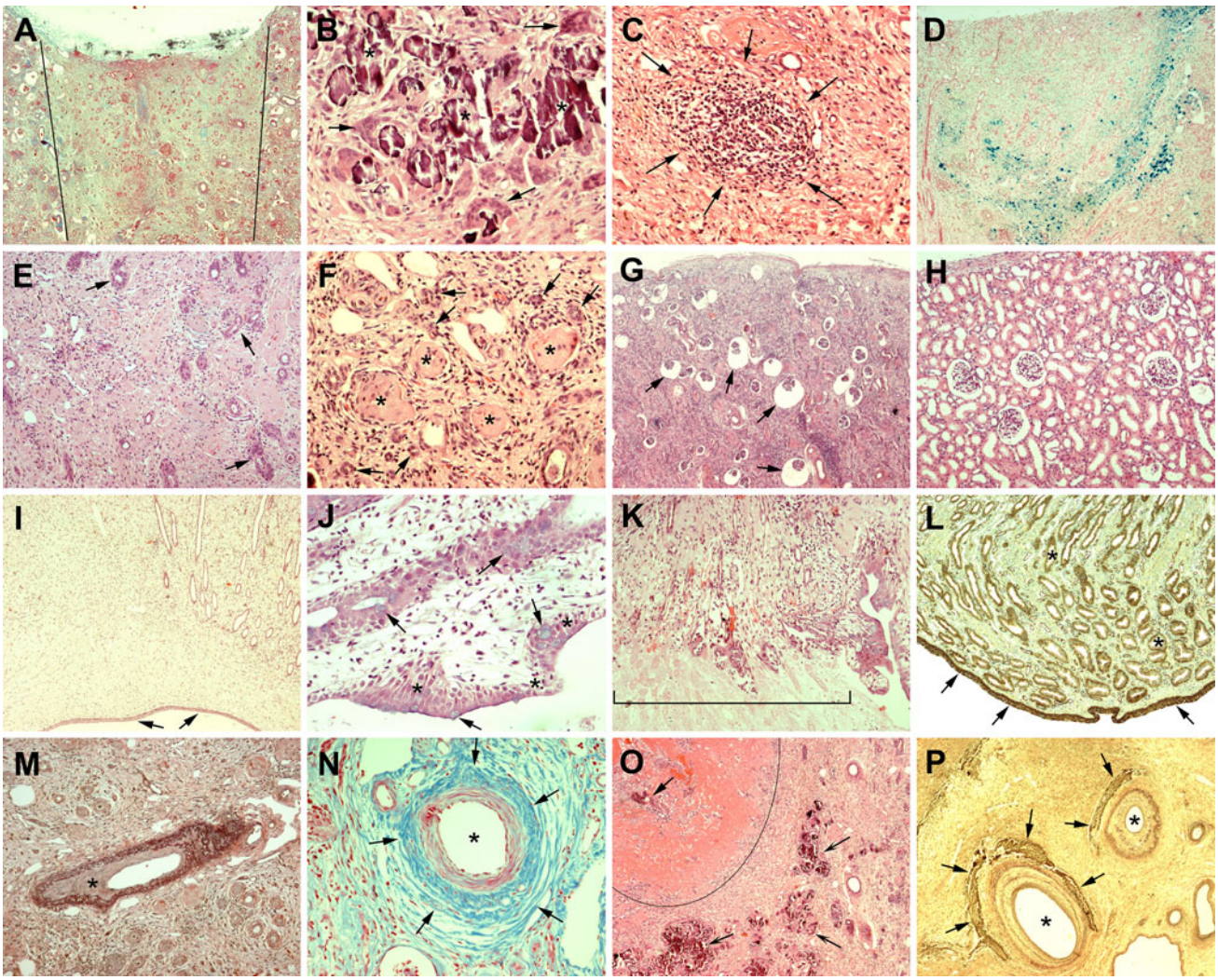

Fig. 3 Histopathology of the kidney 28 days after IRE. **A** Sharp delineated IRE-ablation zone (*between slashes*) with retraction of the surface. **B** Calcium deposits (*asterisks*) with foreign-body giant cells (*arrows*). **C** Lymphocytic infiltration in the cortical scar (*arrows*). **D** Rim of siderophages (*blue*) at the scar margin. **E** Center of cortical scar with loss of glomeruli and reduction of tubuli. The remaining tubular structures (*arrows*) show partly epithelial regeneration. Rim of the cortical scar with hyalinised sclerotic (**F** *asterisks*) and microcystic (**G** *arrows*) glomeruli and atrophic tubuli (**F** *arrows*) between (**F**). **H** Normal cortex parenchyma immediately besides the scar. **I** Medullar scar with complete loss of collecting ducts and Henle's loop (*left*). The marginal zone (*right*) shows preserved collecting ducts and loss of Henle's loop. Obviously regenerated calyx urothelium (*arrows*). **J** Tip of scarred papilla. Flat regenerated urothelium (*asterisks*) with mucinous metaplasia (*arrows*). Mucinous metaplasia also in ductus papillares (*black arrows*). **K** Calyx lesion with still missing urothelial regeneration (*square bracket, left*) resp. ongoing urothelial regeneration (*right*). **L** Normal parenchyma with urothelial coating of the papilla (*arrows*) and collecting ducts (*asterisks*) adjacent to the scar (*arrows*). **M** Interlobular artery in the centre of the cortical scar with intima fibrosis (*asterisk*). **N** Interlobular artery (*asterisk*) in the rim of the scar with surrounding circular fibrosis (*arrows*). **O** Infarct in the center of the scar (*open square*) with foreign-body giant cell (*black closed arrow*). Large calcium deposits in the adjacent scar (*open arrows*). **P** Arteriosclerotic-like altered interlobular arteries (*asterisk*) surrounded by clasp-like calcifications (*arrows*). HE stain: **B**, **C**, **E**, **F**, **G**, **H**, **I**, **J**, **K**, **O**. Azan-stain: **A**, **N**. Berlin-blue reaction: **D**. Cytokeratin-7-immunoreaction: **L**. Van-Gieson-stain: **M**. Elastica-van-Gieson-stain: **P**

Conclusions

Compared with CT imaging, MRI permits a better monitoring of the ablation zones after renal IRE due to the higher soft tissue contrast, especially T2-SPIR-w-MRI. Multifocal IRE led to sharp delineated, complete ablations of the tubuli and glomeruli. The adjacent renal parenchyma, connective tissue, and urinary system were preserved. The destructed urothelium of the IRE ablation zone involved urinary system can regenerate without scarification after IRE because of the obtained basement membrane. Renal IRE as a minimally invasive ablation method

could indicate prevention of renal function to reduce the risk of collateral damage by vascular or parenchymal injury and urinary obstruction with kidney failure, which could be superior to thermal ablation methods. Pathologists will be confronted with new and specific histological phenomenons after IRE. Further human IRE studies of resectable, primary bioptic verified kidney tumors, followed by curative surgical resection approximately 4 weeks after IRE, are warranted to determine the IRE ablation efficacy in renal masses. Parallel, functional MRI and contrast-enhanced, tissue-nulled, inversion-recovery MRI should be performed to evaluate its predictive value.

Conflict of interest The authors declare that they have no conflict of interest. This study was performed independently of the manufacturer of the devices used.

References

1. Bello AK, Nwankwo E, El Nahas AM (2005) Prevention of chronic kidney disease: a global challenge. Kidney Int 98(Suppl): S11–S17
2. Deodhar A, Monette S, Single GW Jr, Hamilton WC Jr, Thornton R, Maybody M, Coleman JA, Solomon SB (2011) Renal tissue ablation with irreversible electroporation: preliminary results in a porcine model. Urology 77(3):754–760
3. Duffey BG, Kyle Anderson J (2010) Current and future technology for minimally invasive ablation of renal cell carcinoma. Indian J Urol 26(3):410–417
4. Goldberg SN, Charboneau JW, Dodd GD 3rd, Dupuy DE, Gervais DA, Gillam AR, Kane RA, Lee FT, Livraghi T, McGahan JP, Rhim H, Silverman SG, Solbiati L, Vogl TJ, Wood BJ (2003) International working group on image-guided tumor ablation image-guided tumor ablation: proposal for standardization of terms and reporting criteria. Radiology 228(2):335–345
5. Granot Y, Ivorra A, Maor E, Rubinsky B (2009) In-vivo imaging of irreversible electroporation by means of electrical impedance tomography. Phys Med Biol 54(16):4927–4943
6. Guo Y, Zhang Y, Nijm GM, Sahakian AV, Yang GY, Omary RA, Larson AC (2011) Irreversible electroporation in the liver: contrast-enhanced inversion-recovery MR imaging approaches to differentiate reversibly electroporated penumbra from irreversibly electroporated ablation zones. Radiology 258(2):461–468
7. Hjouj M, Rubinsky B (2010) Magnetic resonance imaging characteristics of nonthermal irreversible electroporation in vegetable tissue. J Membr Biol 236(1):137–146
8. Kosiek O, Strach K, Ricke J, Pech M (2012) Irreversible electroporation: a new kid on the block? (in German). Radiologe 52(1):38–43
9. Ljungberg B, Cowan N, Hanbury DC, Hora M, Kuczyk MA, Merseburger AS, Mulders PFA, Patard JJ, Sinescu IC (2010) Guidelines on Renal Cell Carcinoma. European Association of Urology (EAU). http://www.uroweb.org/. Accessed 25 May 2011
10. Miller DC, Schonlau M, Litwin MS, Lai J (2008) Urologic diseases in America project. Renal and cardiovascular morbidity after partial or radical nephrectomy. Cancer 112(3):511–520
11. Notohamiprodjo M, Reiser MF, Sourbron SP (2010) Diffusion and perfusion of the kidney (review). Eur J Radiol 76(3):337–347
12. Pech M, Janitzky A, Wendler JJ, Strang C, Blaschke S, Dudeck O, Ricke J, Liehr UB (2011) Irreversible electroporation of renal cell carcinoma: a first-in-man phase I clinical study. Cardiovasc Interv Radiol 34(1):132–138
13. Rosner M, Abdel-Rahman E (2010) ASN advisory group on geriatric nephrology geriatric nephrology: responding to a growing challenge. Clin J Am Soc Nephrol 5(5):936–942
14. Rubinsky B, Onik G, Mikus P (2007) Irreversible electroporation: a new ablation modality-clinical implications. Technol Cancer Res Treat 6(1):37–48
15. Rubinsky B (2009) Irreversible electroporation, 1st edn. Springer, Berlin Heidelberg, p 328. ISBN-10: 3642054196
16. Sutherland SE, Resnick MI, Maclennan GT, Goldman HB (2002) Does the size of the surgical margin in partial nephrectomy for renal cell cancer really matter? J Urol 167(1):61–64
17. Thomson KR, Cheung W, Ellis SJ, Federman D, Kavnoudias H, Loader-Oliver D, Roberts S, Evans P, Ball C, Haydon A (2011) Investigation of the safety of irreversible electroporation in humans. J Vasc Interv Radiol 22(5):611–621
18. Tovar O, Tung L (1992) Electroporation and recovery of cardiac cell membrane with rectangular voltage pulses. Am J Physiol 263(4 Pt 2):H1128–H1136
19. Tracy CR, Kabbani W, Cadeddu JA (2011) Irreversible electroporation (IRE): a novel method for renal tissue ablation. BJU Int 107(12):1982–1987
20. Wendler JJ, Pech M, Porsch M, Janitzky A, Fischbach F, Buhtz P, Vogler K, Hühne S, Borucki K, Strang C, Mahnkopf D, Ricke J, Liehr UB (2011) Urinary tract effects after multifocal nonthermal irreversible electroporation of the kidney: acute and chronic monitoring by magnetic resonance imaging, intravenous urography, and urinary cytology. Cardiovasc Interv Radiol 35:921–926
21. Wendler JJ, Pech M, Blaschke S, Porsch M, Janitzky A, Ulrich M, Dudeck O, Ricke J, Liehr UB (2012) Angiography in the isolated perfused kidney: radiological evaluation of vascular protection in tissue ablation by nonthermal irreversible electroporation. Cardiovasc Interv Radiol 35:383–390
22. Zhang Y, Guo Y, Ragin AB, Lewandowski RJ, Yang GY, Nijm GM, Sahakian AV, Omary RA, Larson AC (2010) MR imaging to assess immediate response to irreversible electroporation for targeted ablation of liver tissues: preclinical feasibility studies in a rodent model. Radiology 256(2):424–432

8.5

Irreversible electroporation of renal cell carcinoma: **a first-in-man phase I clinical study**.

Pech M, Janitzky A, Wendler JJ, Strang C, Blaschke S, Dudeck O, Ricke J, Liehr UB.

Cardiovasc Intervent Radiol. 2011 Feb;34(1):132-8.

PURPOSE: Irreversible electroporation (IRE) is a newly developed nonthermal tissue-ablation technique in which high-voltage electrical pulses of microsecond duration are applied to induce irreversible permeabilisation of the cell membrane, presumably through nanoscale defects in the lipid bilayer, leading to apoptosis. The purpose of this study was to assess the feasibility and safety of ablating renal cell carcinoma (RCC) tissue by IRE.

METHODS: Six patients scheduled for curative resection of RCC were included. IRE was performed during anaesthesia immediately before the resection with electrographic synchronisation. Central haemodynamics were recorded before and 5 min after electroporation. Five-channel electrocardiography (ECG) was used for detailed analysis of ST waveforms. Blood sampling and 12-lead ECG were performed before, during, and at scheduled intervals after the intervention.

RESULTS: Analysis of ST waveforms and axis deviations showed no relevant changes during the entire study period. No changes in central haemodynamics were seen 5 min after IRE. Similarly, haematological, serum biochemical, and ECG variables showed no relevant differences during the investigation period. No changes in cardiac function after IRE therapy were found. One case of supraventricular extrasystole was encountered. Initial histopathologic examination showed no immediate adverse effects of IRE (observation of delayed effects will require a different study design).

CONCLUSION: IRE seems to offer a feasible and safe technique by which to treat patients with kidney tumours and could offer some potential advantages over current thermal ablative techniques.

Cardiovasc Intervent Radiol (2011) 34:132–138
DOI 10.1007/s00270-010-9964-1

CLINICAL INVESTIGATION

Irreversible Electroporation of Renal Cell Carcinoma: A First-in-Man Phase I Clinical Study

Maciej Pech · Andreas Janitzky · Johann Jacob Wendler · Christof Strang · Simon Blaschke · Oliver Dudeck · Jens Ricke · Uwe-Bernd Liehr

Received: 16 February 2010 / Accepted: 28 July 2010 / Published online: 15 August 2010

Abstract
Purpose Irreversible electroporation (IRE) is a newly developed nonthermal tissue-ablation technique in which high-voltage electrical pulses of microsecond duration are applied to induce irreversible permeabilisation of the cell membrane, presumably through nanoscale defects in the lipid bilayer, leading to apoptosis. The purpose of this study was to assess the feasibility and safety of ablating renal cell carcinoma (RCC) tissue by IRE.
Methods Six patients scheduled for curative resection of RCC were included. IRE was performed during anaesthesia immediately before the resection with electrographic synchronisation. Central haemodynamics were recorded before and 5 min after electroporation. Five-channel electrocardiography (ECG) was used for detailed analysis of ST waveforms. Blood sampling and 12-lead ECG were performed before, during, and at scheduled intervals after the intervention.
Results Analysis of ST waveforms and axis deviations showed no relevant changes during the entire study period. No changes in central haemodynamics were seen 5 min after IRE. Similarly, haematological, serum biochemical, and ECG variables showed no relevant differences during the investigation period. No changes in cardiac function after IRE therapy were found. One case of supraventricular extrasystole was encountered. Initial histopathologic examination showed no immediate adverse effects of IRE (observation of delayed effects will require a different study design).
Conclusion IRE seems to offer a feasible and safe technique by which to treat patients with kidney tumours and could offer some potential advantages over current thermal ablative techniques.

Keywords Irreversible electroporation · Ablation · Renal carcinoma · Interventional radiology

M. Pech (✉) · O. Dudeck · J. Ricke
Department of Radiology and Nuclear Medicine, University of Magdeburg, Leipziger Straße 44, 39120 Magdeburg, Germany
e-mail: maciej.pech@med.ovgu.de

A. Janitzky · J. J. Wendler · S. Blaschke · U.-B. Liehr
Department of Urology, University of Magdeburg, Leipziger Straße 44, 39120 Magdeburg, Germany

C. Strang
Department of Anaesthesiology and Intensive Care Medicine, University of Magdeburg, Leipziger Straße 44, 39120 Magdeburg, Germany

Introduction

Like radiofrequency ablation (RFA), irreversible electroporation (IRE) is performed by applying a voltage to needle-like electrodes inserted at the site of the tumour to be ablated. However, the physiologic principles underlying the two techniques are entirely different: whereas RFA depends on thermal destruction of carcinoma tissue, IRE, a novel technique, employs high-voltage electrical pulses on the microsecond timescale to induce irreversible opening of pores in the cell membrane, with consequent cell death [1]. IRE has a clear potential for application in surgical oncology, and special instrumentation has been designed for the clinical use of IRE [1–3].

For this first-in-man study, renal tumours were selected as suitable targets because IRE may offer a clinical advantage over local thermal ablation in this organ. They can be detected at a relatively early stage (<3 cm) and may thus be treated by procedures that conserve the renal

parenchyma, such as partial resection in case of contraindication for surgical treatment. They are also excellently accessible for local ablative procedures. However, they are associated with several problems. Certain options, such as chemotherapy or radiotherapy, are not promising because in general renal tumours respond poorly to these treatments. Furthermore, the location of the tumour within the kidney may influence the success of thermal ablation because regional vascular flow can provide a heat sink, especially in cases in which renal tumours are centrally located [4, 5]. Renal cell carcinoma represents 80 to 90% of all renal tumours and is the most malignant of these, with poor (60% at 5 years) survival prognosis (see [6] for an up-to-date review).

The potential of IRE to overcome the limitations of RFA has been demonstrated in animal models [7–10]. It appears to offer a number of advantages as follows:

1. Because it does not require heating of the tissue to be ablated, it is not sensitive to the cooling effects that result from normal circulation or hypervascularisation.
2. Important structures are conserved [10].
3. Shrinkage of the renal pelvis and calices or necrosis in the access area, a special risk in centrally located tumours, is avoided [4].

Surgical nephrectomy of renal carcinoma leads to 5-year survival rates from 97 to 87% (pT1a/pT1b) to only 20% (pT4) [11], with similar rates for partial resection. For tumours with a largest diameter measuring <4 cm, the 5- and 10-year survival rates are 92 and 80%, respectively [12]. The progression of small renal masses is not well defined: Tumours measuring <3 cm diameter were formerly classified as adenomas [13] and later as "renal carcinomas of low metastatic potential" [14]. The growth rate of such small neoplasms is 0 to 1.3 cm/year [15], and only few cases exhibit multicentricity (<4% [16]). They have an average metastatic rate of approximately 1% after 34 months of follow-up [17]. However, total and nephron-sparing nephrectomy are not ideal for many patients, such as those who cannot tolerate surgery because of serious comorbidities or those in whom the tumour is unfavourably located. Alternative procedures, above all involving thermoablative procedures, for parenchyma-sparing renal tumour excision are topics of much current research. Dependence of the degree of tumour destruction on tumour size, geometry, and vascularisation has been demonstrated [18–21].

This first-in-man pilot study with IRE was therefore designed to investigate the feasibility and safety of IRE treatment. This study addressed in particular the possible risks associated with the need for general anaesthesia (to induce muscular relaxation) and with the need to synchronise IRE pulses with the refractory period of the cardiac rhythm (to avoid rhythm disorders).

Patients and Methods

Approval for this good clinical practice (GCP)-compliant study was granted by the Ethics Committee of the Medical Faculty of the University of Magdeburg. The study design and conduct complied with the precepts of good clinical practice. Patients were only treated by IRE if they had given their written informed consent to do so.

Six patients, already scheduled for surgical resection of renal tumours of size measuring <4 cm and without any signs of metastasis, were treated with IRE during their surgery, and the entire procedure was monitored by ultrasonography. For all patients we used a NanoKnife bipolar probe (length 15 cm) and a NanoKnife IRE electroporator (AngioDynamics, Latham, NY). The electrode was positioned under ultrasound guidance. On the basis of in vitro porcine data with a bipolar probe, this electrode typically ablates a prolate ellipsoid with axes of approximately 30 and 15 mm. IRE was followed by a 15-min rest period; after this, blood was sampled, and the resection was conducted according to the normal procedure.

For the safety assessment, laboratory values, electrocardiography (ECG), and blood gas analyses were performed. Blood was sampled before, during, 6 h after, and 1, 3, and 5 days after the intervention. Twelve-lead ECGs were taken before, 6 h after, 1, 3, and 5 days, and 12 weeks after the intervention. The laboratory values recorded and analysed included erythrocyte count, haemoglobin, haematocrit, mean corpuscular volume, mean corpuscular haemoglobin (amount and concentration), leucocyte count, electrolytes (Na^+, K^+, Cl^-, Ca^{2+}), urea, creatinine, creatine kinase MM (isoenzymic form for skeletal muscle), creatine kinase MB (isoenzymic form for myocardium), troponin T, alanine and aspartate aminotransferases, lactate and lactate dehydrogenase and C-reactive protein, prothrombin time, partial thromboplastin time, thrombocyte count, and D-dimers.

Standard histopathologic analyses of the electroporated and resected tissue were performed with haematoxylin-and-eosin staining. (It should be noted that these can only be of preliminary value when the tissue is removed immediately after IRE; see "Discussion" section.)

In a further analysis, the changes in the variables assessed were compared with those found for six patients selected from the institution's database and matched with the study patients with respect to tumour size, operative technique, age, and renal function.

Cardiac and laboratory variables were subjected to statistical testing at an exploratory level; in view of the very small sample size of this first-in-man study, no formal testing was appropriate. Cardiac, respiratory, and acid–base values (before and 15 min after IRE) were compared by Wilcoxon's test, and coagulation values (before IRE and

5 min, 6 h, and 1, 3, and 5 days after IRE) were compared by the Kruskal–Wallace test. A view of the operative procedure is shown in Fig. 1, and a typical sonographic monitor image is shown in Fig. 2.

Results

The patients' basic demographic and disease characteristics are listed in Table 1. The IRE procedure was conducted in each case according to plan. The lesions were fully covered by the IRE (dimensions listed in Table 1); depending on the shape and size of the tumour growth, and one to three positionings of the needle electrodes were required. All resections were conducted by the same surgeon with approximately 10 years' experience, and the needles were positioned by a nephrological surgeon with approximately 15 years' experience.

The most important (as presumably most sensitive) cardiac values were those measured during the surgery. These are listed in Table 2. None of the individual or mean differences were clinically significant, and all statistical comparisons (Wilcoxon's test) yielded $p > 0.05$.

There was a single case of intraoperative supraventricular extrasystole. In the postoperative monitoring phase ($\leq$5 days) and at follow-up examination (after 12 weeks), no ECG-related changes were detected. No changes in cardiac function were found after IRE.

Acid–base and respiratory values are listed in Table 3. Again, none of the individual or group differences were clinically significant, and all comparisons yielded $p > 0.05$.

Relative changes in the most important clinical laboratory variables, as measured at the various time points, are shown in Figs. 3, 4 and 5. Changes are expressed as percentages of the mean of the respective normal range.

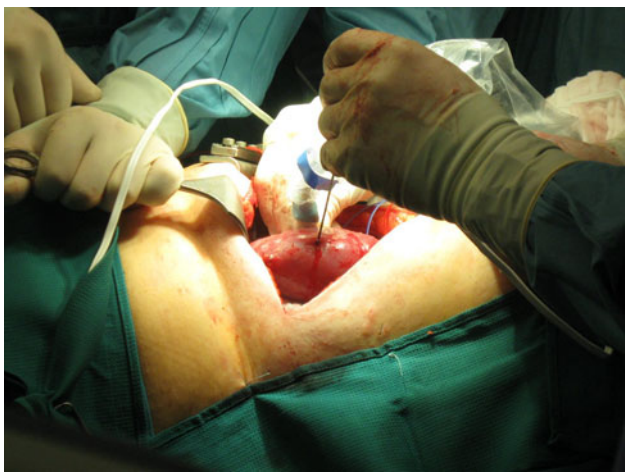

Fig. 1 A view of the IRE procedure being conducted. The needle in the operator's hand is a bipolar electrode

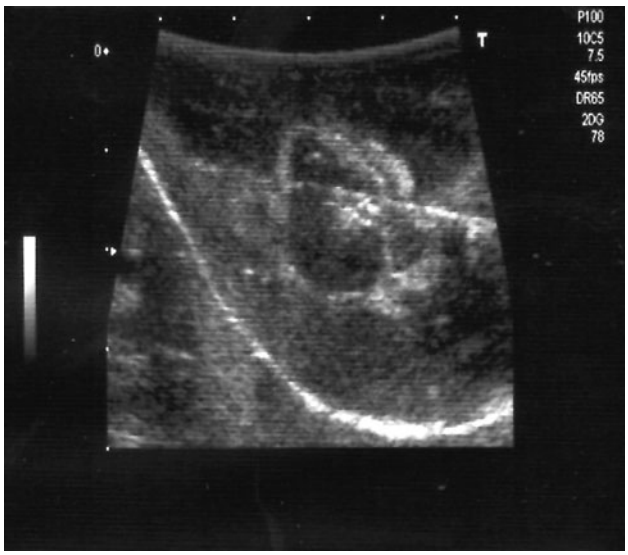

Fig. 2 A typical sonographic image obtained during monitoring of the positioning of the needle electrode (see Fig. 1) for IRE. The "hockey-stick" curve shows the envelope of the kidney; the dark central mass is the tumour; and the slightly off-horizontal line passing through it is the electrode

Coagulation values showed no changes: Specifically, the absence of changes in creatine kinase MB and troponin T indicated no risk of cardiac infarction, although the stability of the lactate and lactate dehydrogenase values indicated, as expected, no ischaemia or cell death (these would only be observed later). Myoglobin and creatine kinase MM increased because of the surgery.

Urea and creatinine are markers of renal function. Increases in creatinine values are to be expected because a part or the whole of a kidney is removed in the surgery, with resulting impairment of the detoxification function (Fig. 3).

The destruction of muscle cells (including heart muscle) results in increased creatine kinase MM levels; in the case of heart muscle, CK-MB and troponin levels are also increased. Therefore, these were monitored to allow differentiation between the effects of the surgical intervention and those of the high-voltage electroporation. Results are shown in Figs. 4 and 5.

The kidneys play an important part in the regulation of arterial blood pressure. The relative changes in systolic and diastolic arterial pressure are shown in Fig. 6. As expected, a decrease was seen for the perioperative period, and values were restored by 24 h after surgery.

Statistically relevant changes were observed in the coagulation variables as follows: partial thromboplastin time ($p = 0.015$), thrombin time ($p = 0.025$), thromboplastin time ($p = 0.010$), and D-dimers ($p < 0.001$). All of these changes are expected in connection with standard surgical intervention, including administration of heparin.

Table 1 Patient characteristics

Patient no.	Sex	Age (year)	Tumour size (mm)	Part of kidney	Nephrectomy	Surgery duration (min)	Artery occlusion (min)
1	M	50.2	25	Central	Partial	168	0[a]
2	F	60.7	24	Central	Partial	226	45
3	F	43.5	35	Upper	Partial	201	30
4	M	73.1	29	Central	Total	205	NA
5	F	53.3	39	Central	Total	156	NA
6	M	69.8	20	Upper	Partial	202	24

NA not applicable for total nephrectomy

[a] This patient had only one kidney; therefore, artery occlusion was not performed, and instead an intraoperative blood transfusion (500 ml) was given. Apart from this, no intraoperative or postoperative transfusions were required

Table 2 Cardiac values

Parameter	Five minutes before IRE			Five minutes after IRE		
	Mean	Median	SD	Mean	Median	SD
Pulse rate (bpm)	49.7	49	7.1	49.5	49.5	5.75
mBP arterial (mmHg)	82.9	82	8.9	81.5	81.5	7.56
CVP (mmHg)	16	16	4.1	15.7	15	3.78
ST II (mV)	0.42	0.45	0.21	0.4	0.4	0.25
ST aVL (mV)	−0.07	0	0.2	−0.1	−0.1	0.25
ST V5 (mV)	0.28	0.3	0.18	0.28	0.25	0.15

mBP mean blood pressure, *CVP* central venous pressure, *ST* segment derivatives II, aVL, and V5

Table 3 Acid–base and respiratory values

Parameter	Five minutes before IRE			Five minutes after IRE		
	Mean	Median	SD	Mean	Median	SD
pH arterial	7.4	7.4	0	7.4	7.4	0
pH venous	7.35	7.35	0.05	7.35	7.35	0.05
CO_2 arterial (mmHg)	38.17	38.5	2.64	37.5	38	2.81
CO_2 venous (mmHg)	46.5	46.5	0.05	46.3	45.5	2.25
O_2 arterial (mmHg)	213.8	192.5	48.52	210.5	195	47.24
O_2 venous (mmHg)	47	47	3.35	46.3	47	3.56
HCO_3 arterial (mM)	24.3	24.0	1.74	24.42	24.5	1.61
HCO_3 venous (mM)	23.9	23.9	2.32	23.7	22.9	2.15
BE arterial (mM)	0.15	0.4	2.06	−0.12	−0.25	1.87
BE venous (mM)	0.53	0.6	2.27	0.75	0.8	2
O_2 sat arterial (%)	99.3	99.5	2.06	99.4	99.5	0.35
O_2 sat venous (%)	79.9	80.2	9.7	79.2	79.1	3.96

BE base excess, *sat* saturation. HCO_3 = standard bicarbonate

None of the six patients showed any signs of an infection, as assessed by C-reactive protein or leucocyte count.

The other laboratory values (as listed in the "Patients and methods" section; results not shown) did not show any conspicuous changes or effects of IRE. No complications associated with loss of blood (e.g., decreased red cell counts) were encountered.

In the matched-pair comparison, no statistically significant differences were found except for duration of surgery, which was longer for the study subjects, as

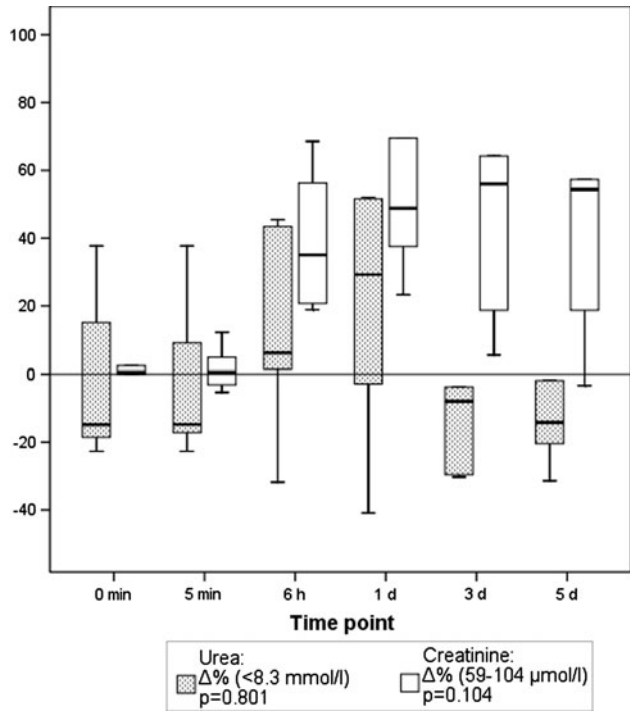

Fig. 3 Urea and creatinine measured before IRE and at the previously stated times after IRE. The conventional *box*-and-*whisker symbols* are used. For easier representation, values are shown as percentage deviations from the preoperative range

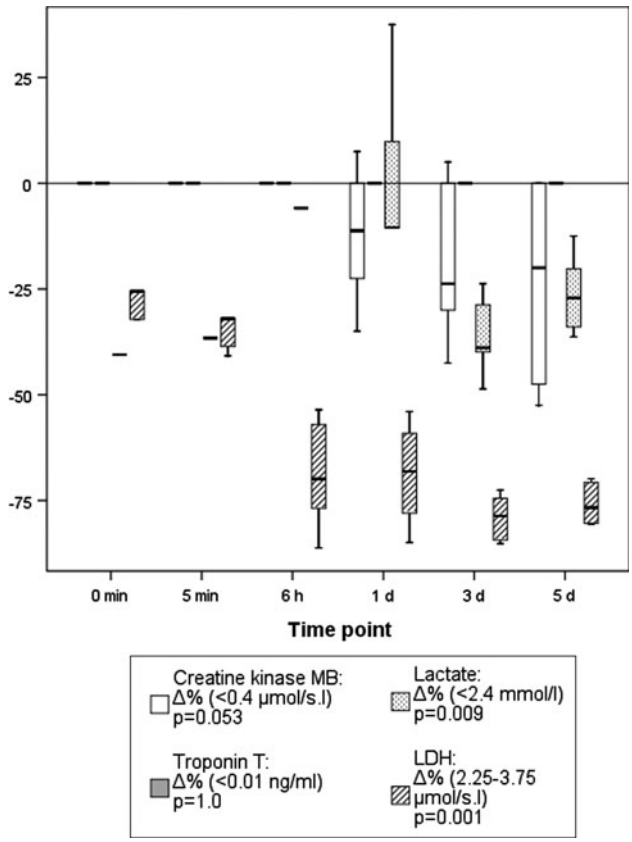

Fig. 4 Creatine kinase MB, troponin T, lactate, and lactate dehydrogenase values. Details as in Figure 3

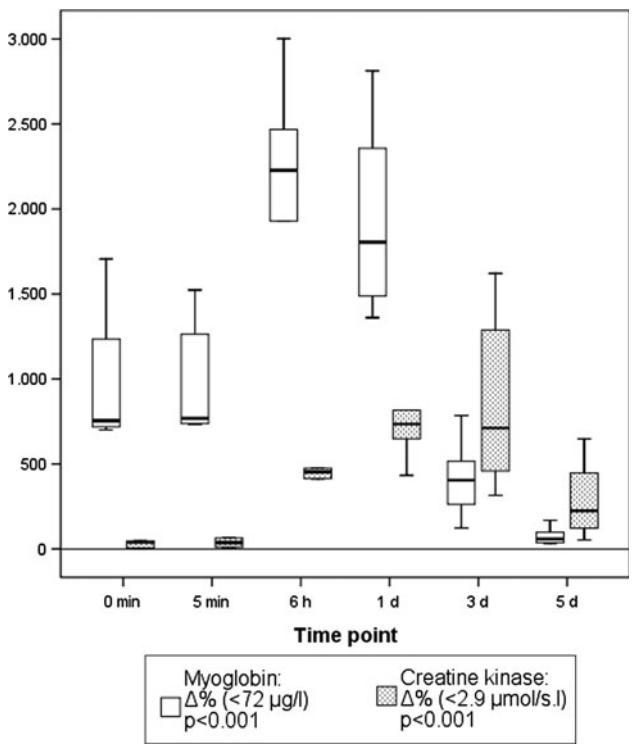

Fig. 5 Myoglobin and creatine kinase MM. Details as in Figure 3

expected in view of the additional procedure that was conducted.

In the histopathologic examination, cells showed a mismatch between plasma and nuclear volume, i.e., the cells had begun to swell but were not dead (no dead cells were found in the specimens).

In summary, the safety assessments gave no suggestion of any deleterious short-term effect of intraoperative IRE. Most importantly, the application of electrical pulses did not interfere with the patients' cardiac parameters as measured by ECG.

Discussion

Because no clinically or statistically significant changes were found in the laboratory analysis (including the respiratory values) or in the ECG assessment, IRE can be regarded as safe enough to allow the design of a further study. The first task of such a study will be to conduct IRE several days before resection to investigate the success of this technique in destroying tumour cells. Because the results presented previously suggest that IRE may be a useful complement to, or may even one day supplant, thermal ablation, we therefore consider in turn the relevant technical aspects and associated safety factors.

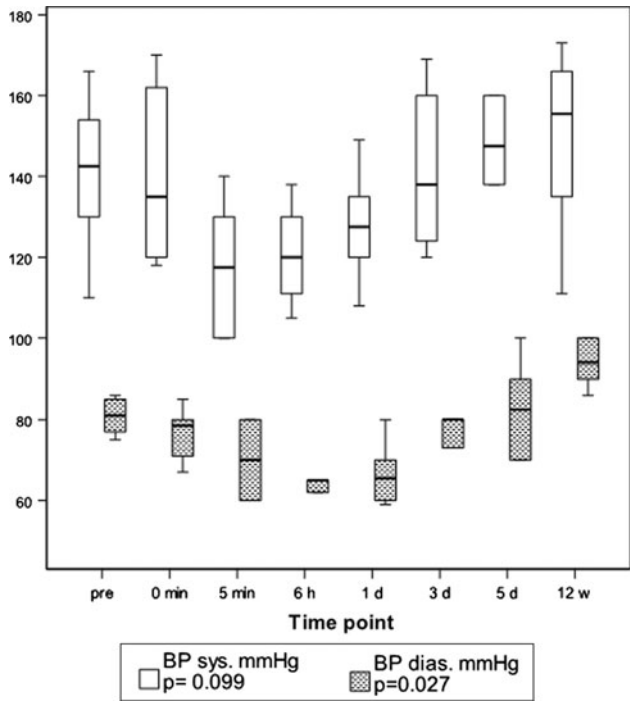

Fig. 6 Blood pressure

In thermal ablation, the cooling effect in hypervascularised lesions and the enlargement of renal tumours has been successfully avoided by selective preinterventional embolisation [22, 23]. However, the nature of the surrounding perirenal fatty tissue also influences the ablation zone: Both normal fatty tissue and fibrotic tissue (the latter resulting from chronic renal disorder) have an insulating effect and can decrease heat dissipation, thus increasing the temperature attained in the tumour and amplifying the thermal effect [20]. It is possible that the rates of local tumour recurrence found in a meta-analysis of 71 studies of RFA in the kidney region were due to the problem of thermal ablation and temperature monitoring. Other serious complications that can occur with RFA include uretral stricture and loss of a renal unit [24]. From a technical perspective, IRE—as a nonthermal procedure—may possess considerable potential in the treatment of inoperable renal tumours, as appears to be confirmed by animal studies in which cell destruction right up to the large "cooling" vessels has been observed [25] as has preservation of the integrity of the ureter, the nerve trunk, and the renal blood vessels [10, 26].

Another issue is the recovery of normal tissue in the treated region. Early work in liver showed rapid resolution of IRE lesions to a minimal scar in approximately 2 weeks [2]; this was attributed to preservation of the microvasculature throughout the IRE lesion. Compared with this, lesions deriving from RFA and cryotherapy must resolve from the edges inward [10]. Therefore, a lower complication rate may be expected with IRE than with thermoablation or cryoablation.

Another major limitation of thermal ablation technologies has been the nonselective nature of the destructive process. IRE destroys the cellular components of a tissue but does not affect the underlying collagen network, thereby allowing the basic tissue structure to be preserved. Consequently, tissue with regenerative capacities (such as the ureter) may replace its mucosal cells with time. Although RFA and cryoablation cause complications to normal structures within the ablation zone, IRE lesions have been observed to leave intact bile ducts within liver lesions, and similar results in the prostatic urethra and the periprostatic nerves have been obtained (reviewed by Onik et al. [10]). Similar considerations should apply to the possible sparing of healthy nephron tissue in renal IRE. Thus, again, IRE appears to offer a treatment with a lower complication rate than thermoablation or cryoablation.

A further anticipated difference between IRE and RFA in clinical application is the overall duration of the electrical treatment. IRE is coupled to the cardiac rate only and typically requires 90 to 100 pulses (corresponding to the same number of heartbeats) for treatment. In contrast, thermal procedures can require up to 30 min.

Finally, studies in vitro suggest that different tumour cells may respond with greater or lesser sensitivity to treatment by IRE and that ablation may be steered by optimising such parameters as the voltage gradient and the duration, number, frequency, and polarity of the pulses applied [27]. Optimising these could provide further possibilities for minimising the side effects of treatment.

Potential limitations of the IRE procedure, and of the selection of appropriate patients, could be the need for the use of muscle relaxant, electrocardiographic synchronisation, and placement of several electrodes in cases of larger tumours. Our results give a first indication that the procedure is generally safe and does not constitute an additional risk for patients when applied in an intraoperative setting.

The present pilot study was intentionally restricted to a small patient population and to an overall procedure that deviated as little as possible from the standard resection. The next step in development of the method will be a further study to establish the long-term safety of the procedure. Furthermore, to assess the efficacy of this technique, it will be necessary to conduct the IRE well in advance of resection to discover the histological effects of IRE, which necessarily require some time to develop. In the present study, the 15 min between IRE and resection was only sufficient to show any immediate histological effects, but the longer-term effects will be decisive for possible application of this method. In addition, it will be necessary to include larger patient cohorts into the design strategy. If the long-term safety of IRE is confirmed, then it

is anticipated that the way will be open for the first clinical studies of the method's efficacy.

Conclusion

This safety-only study indicates that IRE is potentially a feasible and safe technique to treat patients with tumour of the kidney.

Conflict of interest The authors declare that they have no conflict of interest. This study was performed independently of the manufacturer of the devices used.

References

1. Bertacchini C, Margotti PM, Bergamini E, Lodi A, Ronchetti M, Cadossi R (2007) Design of an irreversible electroporation system for clinical use. Technol Cancer Res Treat 6(4):313–320
2. Rubinsky B, Onik G, Mikus P (2007) Irreversible electroporation: a new ablation modality—clinical implications. Technol Cancer Res Treat 6(1):37–48
3. Rubinsky B (2007) Irreversible electroporation in medicine. Technol Cancer Res Treat 6(4):255–260
4. Hines-Peralta A, Goldberg SN (2004) Review of radiofrequency ablation for renal cell carcinoma. Clin Cancer Res 10(18 Pt 2):6328S–6334S
5. Yoon SK, Choi JC, Cho JH, Oh JY, Nam KJ et al (2009) Radiofrequency ablation of renal VX2 tumors with and without renal artery occlusion in a rabbit model: feasibility, therapeutic efficacy, and safety. Cardiovasc Intervent Radiol 32(6):1241–1246
6. Ljungberg B, Hanbury DC, Kuczyk MA, Merseburger AS, Mulders PF, Patard JJ et al (2007) Renal cell carcinoma guideline. Eur Urol 51(6):1502–1510
7. Al Sakere B, André F, Bernat C, Connault E, Opolon P, Davalos RV, et al (2007) Tumor ablation with irreversible electroporation. PLoS One 2(11):e1135
8. Garcia PA, Rossmeisl JH, Robertson J, Ellis TL, Davalos RV (2009) Pilot study of irreversible electroporation for intracranial surgery. Conf Proc IEEE Eng Med Biol Soc 1:6513–6516
9. Granot Y, Ivorra A, Maor E, Rubinsky B (2009) In vivo imaging of irreversible electroporation by means of electrical impedance tomography. Phys Med Biol 54(16):4927–4943
10. Onik G, Mikus P, Rubinsky B (2007) Irreversible electroporation: implications for prostate ablation. Technol Cancer Res Treat 6(4):295–300
11. Frank I, Blute ML, Leibovich BC, Cheville JC, Lohse CM, Zincke H (2005) Independent validation of the 2002 American Joint Committee on cancer primary tumor classification for renal cell carcinoma using a large, single institution cohort. J Urol 173(6):1889–1892
12. Hafez KS, Fergany AF, Novick AC (1999) Nephron-sparing surgery for localized renal cell carcinoma: impact of tumor size on patient survival, tumor recurrence and TNM staging. J Urol 162(6):1930–1933
13. Bell ET (1950) Renal diseases. Lippincott, Philadelphia, PA, pp 428–439
14. Peterson RO (1986) Urologic pathology. Lippincott, Philadelphia, PA, pp 85–110
15. Bosniak MA (1995) Observation of small incidentally detected renal masses. Semin Urol Oncol 13(4):267–272
16. Nissenkorn, Bernhelm J (1995) Multicentricity in renal cell carcinoma. J Urol 153(3 Pt 1):620–622
17. Chawla SN, Crispen PL, Hanlon AL, Greenberg RE, Chen DY, Uzzo RG (2006) The natural history of observed enhancing renal masses: meta-analysis and review of the world literature. J Urol 175(2):425–431
18. Mayo-Smith WW, Dupuy DE, Parikh PM, Pezzullo JA, Cronan JJ (2003) Imaging-guided percutaneous radiofrequency ablation of solid renal masses: techniques and outcomes of 38 treatment sessions in 32 consecutive patients. AJR Am J Roentgenol 180(6):1503–1508
19. Matlaga BR, Zagoria RJ, Woodruff RD, Torti FM, Hall MC (2002) Phase II trial of radio frequency ablation of renal cancer: evaluation of the kill zone. J Urol 168(6):2401–2405
20. Gervais DA, McGovern FJ, Arellano RS (2003) Renal cell carcinoma: clinical experience and technical success with radiofrequency ablation of 42 tumors. Radiology 226(2):417–424
21. Pavlovich C, Walther M, Choyke P, Pautler SE, Chang R, Linehan WM et al (2002) Percutaneous radiofrequency ablation of small renal tumors: initial results. J Urol 167(1):10–15
22. Tacke J, Mahnken A, Bucker A, Rohde D, Günther RW (2001) Nephron-sparing percutaneous ablation of a 5 cm renal cell carcinoma by superselective embolization and percutaneous RF-ablation. Rofo 173(11):980–983
23. Gebauer B, Werk M, Lopez-Hanninen E, Felix R, Althaus P (2007) Radiofrequency ablation in combination with embolization in metachronous recurrent renal cancer in solitary kidney after contralateral tumor nephrectomy. Cardiovasc Intervent Radiol 30(4):644–649
24. Dib RE, Touma NJ, Kapoor A (2009) Review of the efficacy and safety of radiofrequency ablation for the treatment of small renal masses. Can Urol Assoc J 3(2):143–149
25. Lee EW, Loh CT, Kee ST (2007) Imaging-guided percutaneous irreversible electroporation: ultrasound and immunohistological correlation. Technol Cancer Res Treat 6(4):287–294
26. Maor E, Ivorra A, Leor J, Rubinsky B (2007) The effect of irreversible electroporation on blood vessels. Technol Cancer Res Treat 6(4):307–312
27. Miller L, Leor J, Rubinsky B (2005) Cancer cells ablation with irreversible electroporation. Technol Cancer Res Treat 4(6): 699–705

8.6

Letter to the Editor Concerning "Irreversible Electroporation (IRE) Fails to Demonstrate Efficacy in a Prospective Multicenter Phase II Trial on Lung Malignancies: The ALICE Trial" by Ricke et al. 2015 (doi:10.1007/s00270-014-1049-0).

Wendler JJ, Porsch M, Fischbach F, Pech M, Schostak M, Liehr UB.

*Cardiovasc Intervent Radiol. 2015 Aug;38(4):1064-*5.

No abstract available. Comment on:

Irreversible electroporation (IRE) fails to demonstrate efficacy in a prospective multicenter phase II trial on lung malignancies: the ALICE trial.

Ricke J, Jürgens JH, Deschamps F, Tselikas L, Uhde K, Kosiek O, De Baere T.

Cardiovasc Intervent Radiol. 2015 Apr;38(2):401-8.

PURPOSE: To assess safety and efficacy of irreversible electroporation (IRE) of lung malignancies.

MATERIALS AND METHODS: Patients with primary and secondary lung malignancies and preserved lung function were included in this prospective single arm trial. Primary and secondary endpoints were safety and efficacy. Recruitment goal was 36 subjects in 2 centers. Patients underwent IRE under general anesthesia with probe placement performed in Fluoroscopy-CT. The IRE system employed was NanoKnife® (Angiodynamics). System settings for the ablation procedure followed the manufacturer's recommendations. The Mann-Whitney U test was used to evaluate the correlation of nine technical parameters with local tumor control. Median follow up was 12 months.

RESULTS: The expected efficacy was not met at interim analysis and the trial was stopped prematurely after inclusion of 23 patients (13/10 between both centers). The dominant tumor entity was colorectal (n = 13). The median tumor diameter was 16 mm (8-27 mm). Pneumothoraces were observed in 11 of 23 patients with chest tubes required in 8 (35 %). Frequently observed alveolar hemorrhage never led to significant hemoptysis. 14/23 showed progressive disease (61 %). Stable disease was found in 1 (4 %), partial remission in 1 (4 %) and complete remission in 7 (30 %) patients. The relative increase of the current during ablation was significantly higher in the group treated successfully as compared to the group presenting local recurrence ($p < 0.05$). Needle tract seeding was found in three cases (13 %).

CONCLUSIONS: IRE is not effective for the treatment of lung malignancies. We hypothesize that the energy deposition with current IRE probes is highly sensitive to air exposure.

Cardiovasc Intervent Radiol (2015) 38:1064–1065
DOI 10.1007/s00270-015-1096-1

LETTER TO THE EDITOR

Letter to the Editor Concerning "Irreversible Electroporation (IRE) Fails to Demonstrate Efficacy in a Prospective Multicenter Phase II Trial on Lung Malignancies: The ALICE Trial" by Ricke et al. 2015 (doi:10.1007/s00270-014-1049-0)

Johann Jakob Wendler[1] · Markus Porsch[1] · Frank Fischbach[2] · Maciej Pech[2] · Martin Schostak[1] · Uwe-Bernd Liehr[1]

Received: 16 February 2015 / Accepted: 3 March 2015 / Published online: 23 April 2015

Dear Editor,

We would like to compliment the authors for the first controlled prospective human trial to determine the safety and efficacy of irreversible electroporation (IRE) in lung malignancies that was stopped prematurely because of a high rate of treatment failure (69 %) [1]. We would like to supplement the discussion of IRE treatment failure by reflecting the actual discrepancy between the approval of IRE, the theoretical basis of mechanism, the current knowledge in clinical tumor studies, and the potential efficacies of IRE in different tissues. Up to now, there is only one clinical IRE system available on the market (NanoKnife® System; AngioDynamics Inc., Latham, NY). In 2007, the NanoKnife® has received a 510(k) clearance for surgical ablation of soft tissue by the US FDA and is approved for commercialization in the E.U. (CE mark for medical devices 93/42/EWG), although it has not been cleared for the treatment of any specific disease or condition, and the treatment parameters have been mostly developed in ex vivo models, especially in the liver [1, 2]. A priori, that general approval for soft tissue ablation is surprising because IRE could be dependent on the different tissue texture and conductivity [3]. Physiological differences of organ specific conductivities have been described [4]. There is a lack of knowledge in specific conductivity of different tumors because of quite variable texture. Up to now, international databank shows experimental and mathematical IRE data primarily. Yet, IRE in tumor patients has been performed in prospective trial phase I (safety) for kidney, pancreas, prostate, liver, and lung with preliminary results of ablation efficacy only. Altogether, there is still no evidence on IRE in prospective clinical trials about curative treatment of localized primary tumors. For tissue ablation, IRE electrodes need a close contact to a solid tissue with sufficient, relative homogenous conductivity as target tissue. This issue could be not given for small lung masses, bone tumors, and maybe ducts or larger vessels when IRE electrodes have to be placed around or close to the target edge for complete intended ablation. Lung tissue is not dense but more sponge-like with pulmonary alveoli as air chambers while air is a strong isolator, which may explain the failure of IRE ablation in small lung masses [1]. Bile ducts are no homogenous tissue but rather like tubes with isolation of matrix and liquid content. Up to now, all known IRE publications on liver and bile ducts demonstrated not the ablation, but rather the preservation of bile ducts [5] which was one reason to mention IRE as tissue selective with the potential of preserving sensitive and essential structures [2]. Equally, the preservation of larger vessels, the renal calicopelvic

✉ Johann Jakob Wendler
Johann.wendler@med.ovgu.de

Markus Porsch
Markus.porsch@med.ovgu.de

Frank Fischbach
Frank.fischbach@med.ovgu.de

Maciej Pech
Maciej.pech@med.ovgu.de

Martin Schostak
Martin.schostak@med.ovgu.de

Uwe-Bernd Liehr
Uwe-bernd.liehr@med.ovgu.de

[1] Department of Urology and Pediatric Urology, University of Magdeburg, Magdeburg, Germany

[2] Department of Radiology, University of Magdeburg, Magdeburg, Germany

system, and the urethra with endothelial and epithelial regeneration have been described [6–8]. How far a curative IRE in preserving those structures in the treatment of related malignoma such as angiosarcoma, transitional cell carcinoma, or cholangiocarcinoma (especially Klatskin tumor) is possible has to be proofed. According to bone, IRE may ablate soft tissue metastasis in bone or soft tissue bone sarcomas [9]. In that case, IRE electrodes have to be placed closed to the tumor margin, certainly. An adequate conductivity may be disturbed by isolating large calcifications or may be different in osteoclastic and osteoplastic metastases.

Basically, we really believe in the high potential of the IRE technology as a focal tissue, especially tumor ablation method. Whether the biophysical models and postulated IRE characteristics (non-thermal and homogenous ablation with tissue selectivity and sharp demarcation) can be transferred to the clinical routine has to be still investigated. Since the market launch, IRE can be performed outside of studies as an off-label-use procedure financed by interested patients. Currently, IRE treatment in non-controlled, non-standardized, and non-organ-selective settings as well as promising articles in the (lay) press could influence the development of this very promising technique negatively. Therefore, it is important to discuss recommendations and indications for its usage and to set up comparable application standards [10]. Due to all above-mentioned facts, we strongly recommend an implementation of IRE in only clinical studies.

Acknowledgments AngioDynamics Inc. (NY, USA) supports the current IRENE study (www.ClinicalTrials.gov: NCT01967407) by providing the NanoKnife electroporator device and technical maintenance. The company has had no involvement in devising, writing or editing a protocol, and study conduct and will have no contentual input in presenting the results in conferences, congresses, and/or papers.

Conflict of interest The authors Wendler Johann Jakob, Porsch Markus, Fischbach Frank, Pech Maciej, Schostak Martin, and Liehr Uwe-Bernd declare that they have no conflict of interest.

References

1. Ricke J, Jürgens JH, Deschamps F, Tselikas L, Uhde K, Kosiek O, De Baere T. Irreversible electroporation (IRE) fails to demonstrate efficacy in a prospective multicenter phase II trial on lung malignancies: the ALICE trial. Cardiovasc Intervent Radiol. 2015;38(2):401–8.
2. Edd JF, Horowitz L, Davalos RV, Mir LM, Rubinsky B. In vivo results of a new focal tissue ablation technique: irreversible electroporation. IEEE Trans Biomed Eng. 2006;53(7):1409–15.
3. Golberg A, Bruinsma BG, Uygun BE, Yarmush ML. Tissue heterogeneity in structure and conductivity contribute to cell survival during irreversible electroporation ablation by "electric field sinks". Sci Rep. 2015;5:8485. doi:10.1038/srep08485.
4. Rubinsky B. Irreversible electroporation, Series in Biomedical Engineering. Berlin: Springer; 2010. doi:10.1007/978-3-642-05420-4.
5. Choi JW, Lu DS, Osuagwu F, Raman S, Lassman C. Assessment of chronological effects of irreversible electroporation on hilar bile ducts in a porcine model. Cardiovasc Intervent Radiol. 2014;37(1):224–30. doi:10.1007/s00270-013-0731-y.
6. Wendler JJ, Pech M, Blaschke S, Porsch M, Janitzky A, Ulrich M, Dudeck O, Ricke J, Liehr UB. Angiography in the isolated perfused kidney: radiological evaluation of vascular protection in tissue ablation by nonthermal irreversible electroporation. Cardiovasc Intervent Radiol. 2012;35(2):383–90. doi:10.1007/s00270-011-0187-x.
7. Wendler JJ, Pech M, Porsch M, Janitzky A, Fischbach F, Buhtz P, Vogler K, Hühne S, Borucki K, Strang C, Mahnkopf D, Ricke J, Liehr UB. Urinary tract effects after multifocal nonthermal irreversible electroporation of the kidney: acute and chronic monitoring by magnetic resonance imaging, intravenous urography and urinary cytology. Cardiovasc Intervent Radiol. 2012;35(4):921–6. doi:10.1007/s00270-011-0257-0.
8. Onik G, Mikus P, Rubinsky B. Irreversible electroporation: implications for prostate ablation. Technol Cancer Res Treat. 2007;6(4):295–300.
9. Yu Z, Zhang X, Ren P, Zhang M, Qian J. Therapeutic potential of irreversible electroporation in sarcoma. Expert Rev Anticancer Ther. 2012;12(2):177–84. doi:10.1586/era.11.211.
10. Ahmed M, International Working Group on Image-Guided Tumor Ablation, Interventional Oncology Sans Frontières Expert Panel, Technology Assessment Committee of the Society of Interventional Radiology, Standard of Practice Committee of the Cardiovascular and Interventional Radiological Society of Europe, et al. Image-guided tumor ablation: standardization of terminology and reporting criteria—a 10-year update. J Vasc Interv Radiol. 2014;25(11):1691–1705.e4. doi:10.1016/j.jvir.2014.08.027.

8.7

Irreversible electroporation - Current value for focal treatment of prostate cancer.

Wendler JJ, Ganzer R, Hadaschik B, Blana A, Henkel T, Köhrmann KU, Machtens S, Roosen A, Salomon G, Sentker L, Witzsch U, Schlemmer HP, Baumunk D, Köllermann J, Schostak M, Liehr UB; Working Group for Focal and Microtherapy, Academy of the German Society of Urology.

Urologe A. 2015 Jun;54(6):854-62.

BACKGROUND: Irreversible electroporation (IRE), a new tissue ablation procedure available since 2007, could meet the requirements for ideal focal therapy (FT) with its postulated features, especially the absence of a thermal ablative effect. Thus far, there is no adequate tumor-entity-specific proof of its effectiveness, and its clinical application has hitherto been confined to very small patient cohorts. This also holds true for prostate cancer (PCA). Nevertheless, it is now being increasingly applied outside clinical trials-to a certain extent due to active advertising in the lay press.

AIM OF THE STUDY: In this study, current discrepancies between the clinical application and study situation and the approval and market implementation of the procedure are described. The media portrayal of IRE is discussed from different perspectives, particularly with reference to the FT of PCA. This is followed by a final clinical assessment of IRE using the NanoKnife® system.

DISCUSSION: Strict requirements govern new drug approvals. According to the German Drug Act (AMG), evidence of additional benefit over existing therapy must be provided through comparative clinical trials. For medicotechnical treatment procedures, on the other hand, such trial-based proof is not required according to the Medical Devices Act (MPG). The use of IRE even outside clinical trials has been actively promoted since the NanoKnife® system was put on the market. This has led to an increase in the number of uncontrolled IRE treatments of PCA in the last 2 years. The patients have to cover the high treatment costs themselves in these cases. If articles in the lay press advertise the procedure with promising but unverified contents, false hopes are raised in those concerned. This is disastrous if it delays the use of truly effective treatment options.

CONCLUSION: IRE basically still has high potential for the treatment of malignancies; however, whether it can really be used for FT remains unclear due to the lack of data. This also holds true for the treatment of PCA. Only carefully conducted scientific research studies can clarify the unresolved issues regarding IRE of PCA. The urgently needed development of universally valid treatment standards for IRE is unnecessarily hampered by the flow commercially driven patients.

Urologe 2015 · 54:854–862
DOI 10.1007/s00120-015-3864-6
Online publiziert: 31. Mai 2015

J.J. Wendler[1] · R. Ganzer[5] · B. Hadaschik[3] · A. Blana[4] · T. Henkel[6] · K.U. Köhrmann[7] · S. Machtens[8] · A. Roosen[9] · G. Salomon[10] · L. Sentker[11] · U. Witzsch[12] · H.P. Schlemmer[13] · D. Baumunk[1] · J. Köllermann[2] · M. Schostak[1] · U.B. Liehr[1] · Arbeitskreis für fokale und Mikrotherapie der Akademie der Deutschen Gesellschaft für Urologie e.V.

[1] Universitätsklinik für Urologie und Kinderurologie Medizinische Fakultät, Otto-von-Guericke-Universität Magdeburg, Universitätsklinikum Magdeburg, Magdeburg
[2] Institut für Pathologie, Sana Klinikum Offenbach, Offenbach am Main
[3] Urologische Klinik und Poliklinik, Ruprecht-Karls-Universität Heidelber g, Heidelberg
[4] Klinik für Urologie und Kinderurologie, Klinikum Fürth, Fürth
[5] Urologische Klinik und Poliklinik, Universität Leipzig, Leipzig
[6] Urologische Praxis Dr. Henkel & Dr. Kahmann, Berlin
[7] Klinik für Urologie, Theresienkrankenhaus Mannheim, Mannheim
[8] Klinik für Urologie, Marienkrankenhaus Bergisch-Gladbach, Bergisch-Gladbach
[9] Urologische Klinik und Poliklinik, Ludwig-Maximilians-Universität, Klinikum Großhadern, München
[10] Martini-Klinik am UKE GmbH, Hamburg
[11] Urologische Gemeinschaftspraxis, Sinsheim
[12] Klinik für Urologie und Kinderurologie, Krankenhaus Nordwest, Frankfurt/Main
[13] Abteilung für Radiologie, Deutschen Krebsforschungszentrums Heidelberg, Heidelberg

Irreversible Elektroporation

Aktueller Stellenwert in der fokalen Therapie des Prostatakarzinoms

Hintergrund

Das Ziel einer möglichst geringen Umfeldschädigung bei vollständiger Tumorablation (fokale Therapie, FT) nimmt einen zunehmenden Stellenwert in der Onkotherapie ein. Der Entscheidungskonflikt beim Low-risk-Prostatakarzinom (-PCA) zwischen der vermeintlichen Übertherapie durch definitive Standardtherapieverfahren (radikale Prostatektomie, Strahlentherapie) mit teils erheblichen Nebenwirkungen und dem Risiko einer fehlenden Tumorkontrolle bei aktiver Krankheitsüberwachung („Active Surveillance“) führt zur Suche nach Therapiealternativen [1, 2].

Bei der FT des PCA soll nur der tumortragende Teil der Prostata behandelt werden. Je nach Tumorausdehnung und -lokalisation kann damit eine subtotale Behandlung der Prostata bis hin zur ausschließlichen Behandlung des Tumors gemeint sein. Aufgrund ihrer kritischen Beurteilung hat die FT des PCA bislang keine Verbreitung gefunden, da bei dem häufig vorliegenden multifokalen, heterogenen Wachstum das Risiko einer Untertherapie wesentlicher Tumorareale besteht.

In bisherigen Übersichtsarbeiten wurden die für die FT des PCA wichtigen Aspekte sowie die Eigenschaften der Ablationsverfahren hochintensiver fokussierter Ultraschall (HIFU), Kryotherapie (KT), fokale Laserablation (FLA), photodynamische Therapie (PDT) und Brachytherapie (BT) beschrieben [2, 3, 4, 5, 19]. Die irreversible Elektroporation (IRE) stellt ein seit 2007 verfügbares neuartiges Gewebeablationsverfahren dar, das mit seinen postulierten Eigenschaften die Anforderungen einer idealen fokalen Therapie erfüllen könnte.

Methodik

In dieser Arbeit wird die aktuelle Diskrepanz zwischen der bisherigen klinischen Anwendung und Studienlage und der Zulassung bzw. Marktimplementierung des Verfahrens, sowie der Mediendarstellung der IRE, insbesondere im Hinblick auf die FT des PCA, aus unterschiedlichen Blickwinkeln diskutiert. Aus Verständnisgründen erfolgt eine Diskussion in Teilbereichen vor einer abschließenden klinischen Bewertung der IRE mittels NanoKnife®-System (http://www.angiodynamics.com).

Grundlagen zur IRE

Die irreversible Elektroporation (IRE) ist ein 2005 entwickeltes nonthermales Gewebeablationsverfahren [6], das bereits seit den 1960er Jahren kommerziell als in-

dustrielles Lebensmittelsterilisationsverfahren genutzt wird [7]. Durch die lokale Applikation von repetitiven Starkstromimpulsen mit 2000–3000 V und 30–50 A im Mikrosekundenbereich über in das Zielgewebe eingebrachte nadelförmige Elektroden wird ein elektrischer Zusammenbruch der Zellmembran im Zielbereich verursacht [8]. Dabei entstehen Nanoporen (Ø 80–490 nm) in der Zellmembran [9], welche zum unkontrollierten Ioneneinstrom sowie Verlust von Makromolekülen mit konsekutiver Störung der Zellhomöostase und Apoptose innerhalb von 1–7 Tagen führen sollen [9, 10]. Ein Erhalt der extrazellulären Matrix wird diskutiert, ebenso die nonthermale Ablationswirkung der IRE. Bisher konnten Temperaturanstiege für eine Thermoablation nicht nachgewiesen werden [11, 12]. Aufgrund der postulierten nonthermalen Ablationswirkung der IRE (daher auch nonthermale IRE, NTIRE) sollen vaskularisationsbedingte Kühleffekte („heat-sink-effect" wie bei der Radiofrequenzablation, RFA) keine Rolle spielen [13].

Durch die postulierte Alles-oder-Nichts-Reaktion ab einem „kritischen" induzierten Transmembranpotential (ca. 1000 V/cm) innerhalb des Zielvolumens soll das Ablationsareal eine sehr kleine Transitionszone (≤1 mm) und damit scharfe Begrenzung zum unveränderten Umgebungsgewebe aufweisen [8, 14]. Die Größe des gesamten Ablationsareals ist von der verwendeten Elektrodenanzahl und -konfiguration abhängig [8, 13]. Für die IRE wird eine gewisse Gewebeselektivität postuliert, wobei unter Erhalt der extrazellulären Matrix größere Gewebestrukturen und anatomische Grenzstrukturen innerhalb des Zielvolumens oder im Randbereich geschont werden, denen ein matrixbasiertes Grundgerüst zugrundeliegt [8]. So wurde in präklinischen Untersuchungen demonstriert, dass Blutgefäße, intrahepatische Gallengänge, das Nierenbeckenkelchsystem, die Urethra und Nervenbündel trotz umgebender Parenchymablation erhalten bleiben [15, 16, 17, 18, 19, 20, 21, 22]. Aus diesen publizierten Eigenschaften wurde ein scheinbarer klinischer Vorteil der IRE gegenüber anderen Ablationsmethoden (insbesondere gegenüber Thermoablationstechniken) postuliert [6, 8, 9, 13]. Unterschiedliche elektrische Eigenschaften verschiedener Zielgewebe lassen jedoch eine unterschiedliche Wirkung vermuten [23]. Darüber hinaus gibt es bislang keine systematische Evaluation der spezifisch elektrischen Konduktivität in verschiedenen Tumorgeweben.

Die perkutane Platzierung der nadelförmigen IRE-Elektroden muss bildgeführt erfolgen [Sonographie, Computertomographie (CT)]. Eine MRT-gestützte (Magnetresonanztomographie) Elektrodenapplikation ist derzeit nicht möglich, da bislang kein MRT-taugliches System zur Verfügung steht [14]. Zur Vermeidung von impulsinduzierten Herzrhythmusstörungen sollte die IRE zumindest in Herznähe EKG-getriggert erfolgen. Zur Reduktion von elektroinduzierten, starken Muskelkontrationen muss die IRE-Behandlung in tiefer Muskelrelaxation mit konsekutiv notwendiger Beatmung in Vollnarkose durchgeführt werden. Als ausgewiesene Kontraindikation für die IRE gelten nach Herstellerangaben eine unbehandelte Epilepsie, Schwangerschaft, elektronische oder metallische Implantate in direkter Nähe zum Zielvolumen, Herzrhythmusstörungen mit nicht möglicher EKG-Triggerung, ein QT-Intervall >550 ms, Herzschrittmacher oder Defibrillatoren bei v. a. intrathorakaler Applikation sowie die Anwendung im Augenbereich [14].

Allgemeine Studienlage und Zulassung zur IRE

Gegenwärtig ist ein zur klinischen Anwendung zugelassenes IRE-System verfügbar (NanoKnife®-System; AngioDynamics Inc., http://www.angiodynamics.com). Eine kommerzielle Zulassung erfolgte für Kanada, die Europäische Union (CE-Kennzeichnung für Medizinprodukte nach 93/42/EWG) und Australien (http://www.investors.angiodynamics.com). Bereits 2007 erhielt das NanoKnife®-System von der US-amerikanischen „Food and Drug Administration" (FDA) die 510(k)-Anwendungszulassung zur Ablation von Weichgewebe ohne Beschränkung auf spezifische Erkrankungen oder Organe (http://www.angiodynamics.com), wobei die Behandlungsparameter an Ex-vivo-Modellen, insbesondere am Lebermodell entwickelt wurden [6, 8, 10].

Bisher liegen keine ausreichenden tumorentitätsspezifischen Wirksamkeitsnachweise vor. Die klinische Anwendung beschränkt sich bislang auf sehr kleine Patientenkohorten.

Durch das Institut für Medizinische Dokumentation und Information (DIMDI) des Deutschen Bundesministeriums für Gesundheit (BMG) erfolgte 2015 die Bekanntgabe von OPS-Kodes (Operationen- und Prozedurenschlüssel) für die IRE mittels NanoKnife® auf Beantragung durch den Hersteller AngioDynamics Inc. (https://www.dimdi.de/dynamic/de). Elf neue OPS-Kodes für die IRE an Gallengängen (5–513.44), Knochen (5–789.9), Leber (5–501.7), Lunge (5–339.22), Magen (5–433.7), Nebennieren (5–073.42), Nieren (5–552.9), Ösophagus (5–422.7), Prostata (5–601.8), Pankreas (5–521.3) und Rektum (5–482.e) wurden eingeführt (https://www.dimdi.de). Dies erscheint überraschend, erklärt sich aber durch die fehlende Notwendigkeit einer wissenschaftlichen Begründung für OPS-Kodes.

So gibt es laut internationaler Datenbanken bisher keine experimentellen und klinischen Untersuchungen zur IRE von Gallengängen, Magen, Nebennieren und Ösophagus. Weiterhin fehlen wissenschaftliche Erkenntnisse zur Anwendung am menschlichen Rektum, Ösophagus, Magen, Gallengängen und Nebennieren. Die einzigen auswertbaren Daten zur IRE bei Tumorpatienten resultieren aus prospektiven Phase-1- (Safety-)Studien zu Niere, Pankreas, Prostata, Leber und Lunge an sehr kleinen Kohorten bzw. Einzelfällen mit nur vorläufigen Ergebnissen zur Ablationseffektivität (bildgebend und bioptisch). Darüber hinaus gibt es keine Ergebnisse von prospektiven klinischen Studien mit kurativer Behandlung von lokal begrenzten, primären Tumoren [30]. Die technische Durchführbarkeit lässt nicht auf eine Wirksamkeit schließen. Irreführend erscheint deshalb die Vergabe von OPS-Kodes für die IRE an Knochen, Lunge und Gallengängen. Die Gewebeablation mittels IRE benötigt einen ausreichend engen Kontakt der nadelförmigen Elektroden zu solidem Gewebe und eine adäquate Konduktivität des Zielgewebes. Diese Bedingungen erscheinen für kleine Lungen-, Knochen-Gallengang-Karzinome und bei großen Tumorgefäßen zumin-

Zusammenfassung · Abstract

Urologe 2015 · 54:854–862 DOI 10.1007/s00120-015-3864-6

J.J. Wendler · R. Ganzer · B. Hadaschik · A. Blana · T. Henkel · K.U. Köhrmann · S. Machtens · A. Roosen · G. Salomon · L. Sentker · U. Witzsch · H.P. Schlemmer · D. Baumunk · J. Köllermann · M. Schostak · U.B. Liehr · Arbeitskreis für fokale und Mikrotherapie der Akademie der Deutschen Gesellschaft für Urologie e.V.

Irreversible Elektroporation. Aktueller Stellenwert in der fokalen Therapie des Prostatakarzinoms

Zusammenfassung

Hintergrund. Die irreversible Elektroporation (IRE) stellt ein seit 2007 verfügbares, neuartiges Gewebeablationsverfahren dar, das mit seinen postulierten Eigenschaften, allen voran die fehlende, thermoablativ wirkende Hitzewirkung, die Anforderungen einer idealen fokalen Therapie (FT) erfüllen könnte. Bisher liegen keine ausreichenden tumorentitätsspezifischen Wirksamkeitsnachweise vor. Die klinische Anwendung beschränkt sich bislang auf sehr kleine Patientenkohorten. Dies gilt auch für das Prostatakarzinom (PCA). Trotzdem erfolgt aktuell zunehmend eine Anwendung außerhalb von Studien. Nicht zuletzt durch aktive Werbung für das Verfahren in der Laienpresse.

Ziel der Arbeit. In dieser Arbeit wird die aktuelle Diskrepanz zwischen der bisherigen klinischen Anwendung und Studienlage und der Zulassung bzw. Marktimplementierung des Verfahrens aufgezeigt und die Mediendarstellung der IRE, insbesondere im Hinblick auf die FT des PCA, aus unterschiedlichen Blickwinkeln diskutiert. Gefolgt von einer abschließenden klinischen Bewertung der IRE mittels NanoKnife®-System.

Diskussion. Bei der Neuzulassung eines Medikaments gelten strengste Anforderungen. Der Nachweis eines Zusatznutzens zur bestehenden Therapie ist durch Vergleichsstudien nach Arzneimittelgesetz (AMG) zu erbringen. Bei medizinisch-technischen Behandlungsverfahren werden solche Ansprüche durch Studien nach Medizinproduktgesetz (MPG) nicht eingefordert. Seit der Markteinführung des NanoKnife®-Systems wird die IRE-Anwendung auch außerhalb von Studien aktiv beworben. Dies hat in den letzten 2 Jahren zu einer Zunahme der unkontrollierten IRE-Behandlungen des PCA geführt. Die Patienten müssen in diesen Fällen die hohen Behandlungskosten selbst zahlen. Werben zusätzlich Laienpresseartikel mit vielversprechenden, aber ungeprüften Inhalten, werden aktuell unberechtigte Hoffnungen bei den Betroffenen geweckt. Fatal, wenn dies zur Verzögerung tatsächlich wirksamer Therapieoptionen führt.

Schlussfolgerung. Grundsätzlich besitzt die IRE auch weiterhin ein hohes Potential für die Therapie von Malignomen. Ob sie tatsächlich als FT einsetzbar ist, bleibt aufgrund fehlender Daten unklar. Dies gilt auch für die Therapie des PCA. Nur wissenschaftliche Fragestellungen mit adäquater Studiendurchführung können die bislang ungeklärten Fragen zur IRE des PCA auflösen. Die dringend benötigte Entwicklung allgemeingültiger geprüfter Behandlungsstandards für die IRE wird durch wirtschaftlich gelenkte Patientenströme unnötig erschwert.

Schlüsselwörter

Gewebeablationsverfahren · NanoKnife®-System · Medizinproduktgesetz · Malignom · Onkotherapie

Irreversible electroporation. Current value for focal treatment of prostate cancer

Abstract

Background. Irreversible electroporation (IRE), a new tissue ablation procedure available since 2007, could meet the requirements for ideal focal therapy (FT) with its postulated features, especially the absence of a thermal ablative effect. Thus far, there is no adequate tumor-entity-specific proof of its effectiveness, and its clinical application has hitherto been confined to very small patient cohorts. This also holds true for prostate cancer (PCA). Nevertheless, it is now being increasingly applied outside clinical trials—to a certain extent due to active advertising in the lay press.

Aim of the study. In this study, current discrepancies between the clinical application and study situation and the approval and market implementation of the procedure are described. The media portrayal of IRE is discussed from different perspectives, particularly with reference to the FT of PCA. This is followed by a final clinical assessment of IRE using the NanoKnife® system.

Discussion. Strict requirements govern new drug approvals. According to the German Drug Act (AMG), evidence of additional benefit over existing therapy must be provided through comparative clinical trials. For medicotechnical treatment procedures, on the other hand, such trial-based proof is not required according to the Medical Devices Act (MPG). The use of IRE even outside clinical trials has been actively promoted since the NanoKnife® system was put on the market. This has led to an increase in the number of uncontrolled IRE treatments of PCA in the last 2 years. The patients have to cover the high treatment costs themselves in these cases. If articles in the lay press advertise the procedure with promising but unverified contents, false hopes are raised in those concerned. This is disastrous if it delays the use of truly effective treatment options.

Conclusion. IRE basically still has high potential for the treatment of malignancies; however, whether it can really be used for FT remains unclear due to the lack of data. This also holds true for the treatment of PCA. Only carefully conducted scientific research studies can clarify the unresolved issues regarding IRE of PCA. The urgently needed development of universally valid treatment standards for IRE is unnecessarily hampered by the flow commercially driven patients.

Keywords

Ablation techniques · NanoKnife® system · Medical Devices Act · Tumors · Oncotherapy

dest zweifelhaft erfüllt, da die IRE-Elektroden in unmittelbarer Nähe zum Tumorrand für eine komplette Ablation platziert werden müssen.

Lungengewebe ist kein homogenes solides Gewebe, sondern schwammartig aufgebaut, wobei die Lungenalveolen als Luftkammern wie starke Isolatoren wirken, was das Therapieversagen der IRE von Lungentumoren erklären könnte [24, 51]. Gallengänge stellen kein homogenes Parenchym dar, sondern röhrenartige Strukturen mit einer isolierenden Matrix und flüssigkeitsgefülltem Lumen. Bisher wurde in allen Publikationen zur IRE der Leber ein Erhalt der Gallengänge bei gleichzeitiger Leberparenchymablation demonstriert [6, 16], weshalb für

Tab. 1 Studienübersicht zur IRE der Prostata. (Nach [33, 34, 35, 36, 37, 38, 39, 40, 41, 42, 43, 44, 45, 46])

Publikation	Design	Material	IRE	Analyse	Ergebnisse
Valerio M et al. 2014 [33]	Klinische Studie Phase 1–2, multizentrisch, prospektiv, „single intervention", einarmig	34 Patienten mit Low-/Intermediate-/High-risk-PCA nach D'Amico („small volume") der anterioren Prostata nach initialer Templatebiopsie der Prostata mit Sonographie-MRT-Fusion	Fusionsgestützte TRUS-MRT, fokale, transperineale IRE (monopolar) mittels NanoKnife® nur in anteriorer, rektum-, apex- und basisferner Prostata, ohne EKG-Triggerung	mpMRI des Beckens/Prostata, PSA, CTCAE-Klassifikation der UAW, urogenitale Funktion	100% Kontinenzerhalt (24/24 Patienten) und 95% Potenzerhalt (19/20 Patienten); 22-mal Grad 1 und 2, keine Grad ≥3 UAW; 18% residuales PCA im mpMRI (24 Patienten)
Van den Bos W et al. 2014 [34]	Klinische Studie Phase 2a, multizentrisch, prospektiv, RPVE 30 Tage nach IRE der Prostata, „double intervention", einarmig	16 Patienten mit PCA (mit Inidkation zur RPVE, nicht weiter definiert) nach initialer Templatebiopsie der Prostata mit Sonographie-MRT-Fusion	Fusionsgestützte TRUS-MRT, fokale, transperineale IRE mittels NanoKnife®	Initiale Templatebiopsie der Prostata mit Sonographie-MRT-Fusion, mpMRI des Beckens/Prostata, Histologie nach RPVE, PSA, QoL	Keine, Studienprotokoll
Valerio M et al. 2014 [35]	Klinische Studie Phase 2a, monozentrisch, „single intervention", einarmig	20 Patienten mit PCA (PSA ≤15 ng/ml, Gleason-Score 7b T2 cN0cM0) nach initialer Templatebiopsie der Prostata mit Sono-MRT-Fusion	Fusionsgestützte TRUS-MRT, fokale, transperineale IRE mittels NanoKnife®, nur in anteriorer, rektum-, apex- und basisferner Prostata, ohne EKG-Triggerung	mpMRI des Beckens/Prostata, Templaterebiopsie der Prostata mit Sono-mpMRT-Fusion nach 6 Monaten, PSA, QoL, FU 12 Monate	Keine, Studienprotokoll
Neal RE et al. 2014 [36]	Tierexperimentelle Untersuchung und Safety-Fall-Studie	1 Hundeprostata, 2 PCA-Patienten (cT1c und T2a)	In-vivo-IRE (monopolar) mittels NanoKnife®	Resektionshistologie bis 3 h und 3–4 Wochen nach IRE, numerische Simulation	Komplette Nekrose im Ablationsareal, variable Randeffekten, spezifische elektrische Feldstärke für Prostata postuliert
Polascik T 2013 [37]	Klinische Studie Phase 1–2, multizentrisch, prospektiv, „single intervention", einarmig	6 Patienten mit Low-risk-PCA (PSA <10 ng/ml, cT1-T2a, Gleason-Score 6, „low-volume", ≤33% positive Biopsien)	Fusionsgestützte TRUS-MRT, fokale, transperineale IRE (monopolar) mittels NanoKnife®	Sicherheit, mpMRI des Beckens/Prostata, Templaterebiopsie der Prostata mit Sono-mpMRT-Fusion, PSA, QoL, FU 2 Jahre	Keine, Studienprotokoll
Neal RE et al. 2013 [38]	Experimentell, tierexperimentell	Kartoffelknollenbrachytherapie-Seed-Modell, 2 Hundeprostatae mit und ohne Brachytherapie-Seeds, Rechen- und Simulationsmodell	Postulierte IRE-Parameter für Prostatagewebe, In-vivo-IRE	Resektionshistologie bis 5 h nach IRE, numerische Simulation	Keine signifikante Alteration des elektrischen Feldes oder thermischer Effekte durch Brachytherapie-Seeds, komplette Nekrose der Prostata auch in Seed- und Elektrodennähe in Ablationsareal
Van de Bos W et al. 2013 [39]	Klinische Studie Phase 2a, multizentrisch, prospektiv, „single intervention", randomisiert, zweiarmig (Hemiablation vs. komplette Ablation der Prostata)	200 Patienten mit therapienaivem Low- und Intermediate-risk-PCA (cT1-T2, Gleason-Score 6–7a, PSA <20 ng/ml, Ausschluss TURP)	Fusionsgestützte TRUS-MRT, fokale und organumfassende transperineale IRE (monopolar) mittels NanoKnife®	Sicherheit, mpMRI des Beckens/Prostata, Templaterebiopsie der Prostata mit Sono-mpMRT-Fusion, PSA, QoL, FU 3 Jahre	Keine, Studienprotokoll
Korohoda W et al. 2013 [40]	Experimentell	Zellsuspension, PCA-Zell-Line AT-2	IRE in vitro	Zytologie, IRE-Parameteranalyse	Reversible und irreversible Elektroporation
Qin Z et al. 2013 [40]; Jiang C et al. 2012 [41]	Experimentell	Implantationstumor PCA-Zelllinie LNCaP Pro 5 in Mäusen	Perkutane IRE	Intrainterventionelle intratumorale Temperaturmessung, Resektionshistologie nach 2 Wo.	Keine thermoablativ wirksame Temperaturerhöhung, lokale elektrische Heterogenität des Tumors reduziert Effektivität der IRE

Tab. 1 Studienübersicht zur IRE der Prostata. (Nach [33, 34, 35, 36, 37, 38, 39, 40, 41, 42, 43, 44, 45, 46]) (Fortsetzung)

Publikation	Design	Material	IRE	Analyse	Ergebnisse
Onik G u. Rubinsky B [42]	Klinische Phase-1-Fallserie, monozentrisch, „single-inervention"	16 Patienten mit Low- bis Intermediate-risk-PCA (15-mal cT1c; einmal T2a; PSA 2.2–7; Gleason-Score 6–8; 2-mal residual nach Radiatio) nach initialer Template-TRUS-gestützter Biopsie der Prostata	TRUS-gestützte, fokale, transperineale IRE (monopolar) mittels NanoKnife®	Histologie aus Template-TRUS-gestützter Biopsie der Prostata nach 3 Wochen	100% Potenzerhalt, 100% Kontinenzerhalt, 0% residuales PCA im Ablationsareal, Blasenkatheter 0–3 Tage
Golberg A u. Rubinsky B 2010 [43]	Statistisch	Rechen- und Simulationsmodell	Postulierte IRE-Parameter für Prostatagewebe	Kalkulation der kritischen Parameter, 2D-Simulation zur IRE	IRE-Parameter zur akkuraten Behandlungsplanung
Daniels C u. Rubinsky B 2009 [44]	Statistisch	Rechen- und Simulationsmodell	Postulierte IRE-Parameter für Weichgewebe	Kalkulation der kritischen Parameter, 2D-Simulation zur IRE für heterogenes Gewebe	Berechneter Erhalt von Nerven, Blutgefäßen und Duktus im Ablationsgebiet, Übertragung auf Prostata möglich
Rubinsky J et al. 2008 [45]	Experimentell	Zellsuspension PCA-Zelllinie PC3	IRE in vitro	Zytologie in Abhängigkeit der IRE-Parameter	Komplette IRE der PCA-Zellen ohne thermale Effekte, mögliche Anwendung beim PCA
Onik et al. 2007 [46]	Tierexperimentell	6 Hunde	TRUS-gestützte, fokale transperineale IRE (monopolar), Hemiablation der Prostata	Resektionshistologie nach 2 Wochen	Hemiablation der Prostata mit scharfer Demarkierung des Ablationsareals unter Erhalt des neurovaskulären Bündels und der Urethra, kein Einfluss durch Blutfluss, Vorteil gegenüber Thermoablation

CTCAE „Common Terminology Criteria for Adverse Events", *TRUS* transrektaler Ultraschall, *UAW* unerwünschte Arzneimittelwirkungen, *MRT* Magnetresonanztomographie, *PCA* Prostatakarzinom, *EKG* Elektrokardiogramm, *QoL* „quality of life", *FU* Follow-up, *IRE* irreversible Elektroporation, *PSA* prostataspezifisches Antigen.

die IRE eine gewebe- bzw. strukturselektive Eigenschaft mit Schonung sensibler oder essentieller Strukturen vermutet wurde [6, 8, 10, 25, 46]. Ebenso wurde der Erhalt von größeren Blutgefäßen, des Nierenbeckenkelchsystems und der Urethra mit endothelialer bzw. epithelialer Regeneration beschrieben [6, 10, 15, 17, 18, 46]. Inwieweit eine kurative IRE von Tumoren (cholangiozelluläre Karzinome, Angiosarkome, Nierenzell-, Urothel-, Prostatakarzinome) an diesen Organen mit gleichzeitigem Erhalt dieser anatomischen Strukturen möglich ist, bleibt nachzuweisen. Im Knochen ist eine IRE von Weichgewebemetastasen oder primären Knochentumoren denkbar [26]. Für eine vollständige Ablation ist auch hier die Platzierung der IRE-Elektroden nahe am Tumorrand notwendig. Eine für die IRE ausreichende elektrische Konduktivität könnte durch isolierend wirkende Kalzifikationen gestört sein. Ein unterschiedliches Verhalten osteolytischer und osteoplastischer Metastasen ist ebenfalls zu vermuten. Dass dieses Phänomen Gegenstand aktueller wissenschaftlicher Diskussionen ist, zeigt sich auch in Ausschlusskriterien aktuell laufender oder angekündigter Studien zur IRE des PCA. Hier gelten Kalzifikationen ab einer Größe von 5 mm im Zielvolumen als Kontraindikation [34, 36, 39].

Pressespiegel zur IRE der Prostata

Im Wochenmagazin „Focus" (Ausgabe 5/2015) wurde erneut über die IRE als „… neue Waffe gegen Prostatakrebs …" und „… schonende Methode …" berichtet. Potenz und Schließmuskelfunktion würden nicht beeinträchtigt, Harnröhre sowie die Erektionsfähigkeit blieben erhalten [27, 28].

Die Deutsche Gesellschaft für Urologie e. V. (DGU) reagierte daraufhin umgehend: Derartige Werbung sei aktuell ungerechtfertigt, irreführend und deshalb gefährlich. Der Wert dieser Behandlung ist derzeit ungesichert [29]. Niemand könne zum gegenwärtigen Zeitpunkt Aussagen zur therapeutischen Beeinflussbarkeit von PCA mittels IRE machen. Der Stellenwert der IRE im Vergleich zu den Standardtherapien oder zu anderen fokalen Therapieverfahren ist unklar, ein Zusatznutzen nicht bewiesen [29, 31, 32]. Die Behandlung außerhalb von Studien ist zusätzlich für den Patienten mit sehr hohen Kosten verbunden, da diese aufgrund des nicht bewiesenen Nutzens von den Krankenkassen nicht übernommen werden [29, 31, 32].

Das Unternehmen AngioDynamics sieht die aktuelle Entwicklung zum NanoKnife® folgendermaßen:

- „This is the first step in securing reimbursement for new medical technologies in Germany …"
- "… the issuance … is an enormous advancement in the successful implementation of the NanoKnife technology in the German market …",
- "… with OPS in-hand, the Ministry can now document the technology's benefits and determine an appropriate level of reimbursement according to German Diagnosis Related Groups (G-DRGs) for a variety of specific procedures …" (http://www.investors.angiodynamics.com).

Eine behördliche Beurteilung des Therapienutzens durch die IRE ist nach unserem Ermessen nur nach Durchführung systematischer Studien möglich.

Studienlage zur IRE der Prostata

Eine Evidenz zur Anwendung der IRE als Therapiealternative zur Behandlung des PCA wurde bisher nicht erzielt. Derzeit liegen mathematische Simulationen, experimentelle Untersuchungen, vier Studienprotokollpublikationen von geplanten, teilweise nicht-rekrutierenden (n=2), klinischen Phase-1- und -2-Studien, eine erste Fallserie zur fokalen IRE beim PCA sowie eine Phase-1- und -2-Studie mit ersten vorläufigen Ergebnissen zur Behandlungssicherheit und Durchführbarkeit der fokalen IRE beim lokal begrenzten PCA vor (**Tab. 1,** [33, 34, 35, 36, 37, 38, 39, 40, 41, 42, 43, 44, 45, 46]). Dabei ist zu berücksichtigen, dass mehr als die Hälfte der experimentellen Untersuchungen nicht mittels NanoKnife® durchgeführt wurden. Nach Herstellerangaben und laut Laienpresse lägen zahlreiche „positive" Behandlungsfälle vor. Hierzu existieren keine publizierten Belege. Die Erfahrungen zur IRE der Prostata bzw. des PCA sind nach den wissenschaftlichen Literaturdatenbanken aus unserer Sicht für eine unkritische Anwendung unvollständig.

Spezielle Aspekte zur IRE für die Behandlung des PCA

Wie bei den etablierten Therapieverfahren sind in der Betrachtung zur IRE der Prostata die anatomischen Risikostrukturen wie periprostatisches Gefäßnervenbündel, M. sphincter externus urethrae, Rektum, Harnblase bzw. Blasenhals zu berücksichtigen. Publizierte Studiendaten zur IRE der Harnblase, des Schließmuskels und des Gefäßnervenbündels liegen nicht vor. Lediglich eine Studie berichtet vom Erhalt funktioneller Parameter (Kontinenz, Erektion).

Tierexperimentelle Untersuchungen zur IRE am Dünndarm und Rektum sowie an peripheren Nervenfasern und quergestreifter Skelettmuskulatur werden als übertragbare Modelle diskutiert.

Die Wirkung der IRE auf Darmgewebe untersuchten zwei Arbeitsgruppen. Nach IRE am Dünndarm wurde von einer fokalen Nekrose mit erhaltener Organstruktur und beginnender epithelialer Regeneration nach 1 Woche berichtet [47]. Nach perirektaler rektumnaher IRE wurde ohne Verwendung einer fixierenden Rektumspule nur von fokal entzündlichen Reaktionen des Rektums und bei Verwendung einer fixierenden Rektumspule auch von transmuralen Nekrosen des Rektums berichtet. Perforationen traten nicht auf. Daraus wurde geschlussfolgert, dass es ohne Kompression auf das Rektum im Bereich des Applikationsfeldes zu keiner relevanten Rektumschädigung kommt [48]. Endorektal applizierte IRE des Rektums führte in Abhängigkeit der IRE-Parametereinstellungen zur fokalen Schleimhautläsion, aber auch zur Ablation der gesamten Rektumwand [49]. Über entsprechend schwere Komplikationen nach IRE wurde bereits berichtet [50].

Die Wirkung der IRE auf periphere Nerven untersuchten zwei Arbeitsgruppen im In-vivo-Tierversuchsmodell am N. ischiadiucus von Schweinen. Ein akuter Schaden der Nervenfaser mit Fragmentierung und Axondegeneration (Waller-Degeneration) zeigte sich nach 1–2 Wochen. Nach 8–10 Wochen stellte sich teilweise eine beginnende Axonregeneration dar, dies bei erhaltener und regenerierter Myelinscheide aus Neurofilamenten und Schwann-Zellen [20, 21, 22]. Gleichzeitig zeigte sich perineural eine fokale Nekrose der quergestreiften Skelettmuskulatur mit narbigem Bindegewebsersatz [20, 21, 22].

Analog zu den thermischen FT ist bei der IRE des PCA deshalb grundsätzlich ebenfalls davon auszugehen, dass funktionell sensible Strukturen (Gefäßnervenbündel, Sphinkter und Rektum) geschädigt werden können, wenn diese im Ablationsgebiet liegen. Inwiefern eine Schonung dieser Strukturen bei kapsel- oder sphinkternaher IRE gelingt, ist völlig unklar.

Diskussion

Bei einer Neuzulassung eines Medikaments gelten strengste Anforderungen. Der Nachweis eines Zusatznutzens zur bestehenden Therapie ist durch Vergleichsstudien nach Arzneimittelgesetz (AMG) zu erbringen. Bei medizinisch-technischen Behandlungsverfahren werden solche Ansprüche durch Studien nach Medizinproduktgesetz (MPG) nicht eingefordert. Allein die technische Durchführbarkeit und vermeintliche Applikationssicherheit werden für eine Anwendung am Menschen als ausreichend angesehen [31, 32]. Seit der Markteinführung des NanoKnife®-Systems wird die IRE-Anwendung auch außerhalb von Studien aktiv beworben. Dies hat in den letzten 2 Jahren zu einer Zunahme der unkontrollierten IRE-Behandlungen des PCA geführt. Die Patienten müssen in diesen Fällen die hohen Behandlungskosten selbst zahlen. Von Fall zu Fall können so Kosten in Höhe von 20.000–30.000 € für den Patienten entstehen. Für eine Kostenübernahme durch die Krankenkassen fordert der Medizinische Dienst der Krankenkassen (MDK) berechtigterweise den Nachweis eines Therapienutzens, auch wenn der Gesetzgeber dies für die prinzipielle Anwendung nicht verlangt. Werben zusätzlich Laienpresseartikel mit vielversprechenden, aber ungeprüften Inhalten [27, 28], werden aktuell unberechtigte Hoffnungen bei den Betroffenen geweckt. Fatal, wenn dies zur Verzögerung des Einsatzes tatsächlich wirksamer Therapieoptionen führt.

Diesen Konflikt können nur wissenschaftliche Fragestellungen mit adäquater Studiendurchführung auflösen. Bisher ungeklärte Fragen zur IRE des PCA sind adressiert. Unklar ist z. B., in wie weit die histopathologische Heterogenität sowohl des PCA als auch der Prostata (Grading, Lithiasis, Gewebedichte) den Ablationserfolg beeinflusst. Im Fall einer notwendigen Ganzdrüsen- oder kapselnahen Therapie muss die Volumengeometrie der Prostata mit der Ablationsgeometrie des IRE-Feldes kongruieren. Das nur eingeschränkt adaptierbare Zielvolumen scheint hierfür mit gleichzeitiger Schonung funktionell wichtiger Strukturen nur bedingt geeignet. Betrachtet man die international publizierten IRE-Anwendungen bei PCA-Patienten, handelt es sich insgesamt um 42 Behandlungsfälle (**Tab. 1,** [33, 36, 42]):

- Neal et al. [36] führten bei 2 Patienten (einmal „low risk", einmal „intermediate risk" nach D'Amico-Krite-

rien) eine jeweils bifokale, transperineal TRUS-gestützte IRE der Prostata durch [36]. In der histologischen Aufarbeitung der Prostatektomiepräparate 3 und 4 Wochen nach IRE erfolgte lediglich eine deskriptive Beschreibung der Ablationszonen. Eine Stellungnahme hinsichtlich einer Tumorablation fehlt sowohl in der Behandlungsplanung als auch im Resektat. Die Behandlungssicherheit wurde nicht bewertet.

- Valerio et al. [35] behandelten zur Beurteilung der Therapiesicherheit 34 Patienten (9-mal „low risk", 24-mal „intermediate risk", einmal „high risk" nach D'Amico-Kriterien; mittlerer PSA-Wert von 6,1 ng/ml) mittels transperineal templategestützter, mpMRT-TRUS-fusionierter, fokaler IRE in anterioren Bereichen der Prostata [33]. Eine Beurteilung der Wirksamkeit erfolgte bisher nur bei 24 Patienten und ausschließlich nur mittels PSA-Messung und mpMRT der Prostata 1–24 Monate nach IRE. Bei 6 Patienten (17%) zeigte sich ein Therapieversagen mit nachfolgend anderen FT. Dazu ist anzumerken, dass es bisher keine validierten Kriterien zur Beurteilung der MRT-Morphologie nach IRE gibt [17]. Die im Studienprotokoll vorgesehene und geforderte Überprüfung des Therapieerfolgs mittels Prostatastanzbiopsie wurde nicht publiziert [33, 35]. Die Bewertung der Nebenwirkungen bei 24 Patienten ergab in 35% einen Grad 1 und in 29% einen Grad 2 nach CTCAEv4.0 („Common Terminology Criteria for Adverse Events"): Harnverhalte [(n=2), Hämaturien (n=6), Dysurien (n=5), Harnwegsinfekte (n=5)]. Eine Harnableitung war in 9 Fällen suprapubisch und in 16 Fällen transurethral notwendig. Es fanden sich keine urethralen Strikturen oder rektourethralen Fisteln bei 100% Kontinenzerhalt (24/24 Patienten) und 95% Potenzerhalt (19/20 Patienten).
- Onik u. Rubinsky (2010) therapierten 16 Patienten (7-mal „low risk", 5-mal „intermediate risk", 2-mal „high risk" nach D'Amico-Kriterien; 2 nach EBRT („external beam radiation therapy") mit Therapieversagen; mittlerer PSA-Wert von 4,57 ng/ml) mittels perineal templategeführter, TRUS-gestützter IRE [42]. Die Ablationen erfolgten mono-, bi- und trifokal sowie halbseitig. Eine Beurteilung der Wirksamkeit erfolgte 3 Wochen nach IRE mittels transperinealer TRUS-geführter Biopsie der Tumorareale und deren Umgebung ohne Verwendung eines Templates. Negative Biopsiekontrollen und Potenzerhalt fanden sich in jeweils 100%. Diese nur als Buchbeitrag veröffentlichen Ergebnisse wurden nicht weiter publiziert [8, 42].

Die aktuell geführte Diskussion zur IRE des PCA kann lediglich auf diesen 3 Veröffentlichungen zurückgreifen [33, 36, 42]. Diese Datenlage rechtfertigt derzeit keine verantwortungsvolle Anwendung der IRE in der klinischen Therapieroutine des PCA.

Grundsätzlich besitzt die IRE auch weiterhin ein hohes Potential für die Therapie von Malignomen. In wie fern sie tatsächlich als FT einsetzbar ist, bleibt aufgrund fehlender Daten weiterhin unklar. Dies gilt auch für die Therapie des PCA. Darüber sollten auch nicht wirtschaftlich intendierte Marketingstrategien von Industrie und Anwender hinwegtäuschen. Die oft weitaus aufwendigere, aber notwendige Überprüfung des Verfahrens in Studien wird so verzögert. Die dringend benötigte Entwicklung allgemeingültiger, geprüfter Behandlungsstandards für die IRE wird durch wirtschaftlich gelenkte Patientenströme unnötig erschwert. Ein verantwortungsbewusster Journalismus sollte dies berücksichtigen.

Fazit für die Praxis

- **Die IRE besitzt aufgrund ihrer molekularen Wirkweise auch weiterhin ein hohes Potential zur FT. Viele postulierte Eigenschaften sind aktuell nicht ausreichend in klinischen Studien belegt.**
- **Das Vorliegen von OPS-Codes belegt keine Wirksamkeit oder Zulassung einer Therapie. Die bisherige Darstellung in der Laienpresse suggeriert eine Effektivität der NanoKnife®-IRE, für die es keine hinreichenden Belege gibt.**
- **Die IRE stellt aufgrund der bisherigen Datenlage keine Alternative zu etablierten Behandlungsmethoden des PCA dar.**
- **Eine Anwendung der IRE außerhalb von Studien kann aktuell nicht empfohlen werden.**

Korrespondenzadresse

Dr. J.J. Wendler
Universitätsklinik für Urologie und Kinderurologie Medizinische Fakultät, Otto-von-Guericke-Universität Magdeburg, Universitätsklinikum Magdeburg
Leipziger Straße 44, 39108 Magdeburg
johann.wendler@med.ovgu.de

Einhaltung ethischer Richtlinien

Interessenkonflikt. J.J. Wendler, R. Ganzer, B. Hadaschik, A. Blana, T. Henkel, K.U. Köhrmann, S. Machtens, A. Roosen, G. Salomon, L. Sentker, U. Witzsch, H.P. Schlemmer, D. Baumunk, J. Köllermann, M. Schostak und U.B. Liehr geben an, dass kein Interessenkonflikt besteht.

Dieser Beitrag beinhaltet keine Studien an Menschen oder Tieren.

Literatur

1. Cooperberg MR, Carroll PR, Klotz L (2011) Active surveillance for prostate cancer: progress and promise. J Clin Oncol 29(27):3669–3676. doi:JCO.2011.34.9738
2. Schostak M, Köllermann J, Hadaschik B et al (2015) Cancer control in focus insights and future perspectives for the focal treatment of prostate cancer. Aktuelle Urol 46(1):39–44. doi:10.1055/s-0034-1396803 (PubMed PMID: 25658230)
3. Roosen A, Ganzer R, Hadaschik B et al (2014) Focal therapy for prostate cancer in Germany – 2014 status. Urologe A 53(7):1040–1045. doi:10.1007/s00120-014-3532-2. (PubMed PMID: 24941932)
4. Baumunk D, Blana A, Ganzer R et al (2013) Focal prostate cancer therapy: capabilities, limitations and prospects. Urologe A 52(4):549–556. doi:10.1007/s00120-012-3002-7. (PubMed PMID: 23073701)
5. Baumunk D, Schostak M (2015) Treatment of localized prostate cancer with high-intensity focused ultrasound. Urologe A 54(2):183–190. doi:10.1007/s00120-014-3666-2 (PubMed PMID: 25588324)
6. Davalos RV, Mir IL, Rubinsky B (2005) Tissue ablation with irreversible electroporation. Ann Biomed Eng 33(2):223–231
7. Doevenspeck H (1961) Influencing cells and cell walls by electrostatic impulses. Fleischwirtschaft 13:986–987
8. Rubinsky B (2010) Irreversible electroporation. Springer, Berlin Heidelberg New York. DOI 10.1007/978-3-642-05420-4, ISBN: 978-3-642-05419-8 (Print) 978-3-642-05420-4 (Online)

9. Lee EW, Wong D, Prikhodko SV et al (2012) Electron microscopic demonstration and evaluation of irreversible electroporation-induced nanopores on hepatocyte membranes. J Vasc Interv Radiol 23(1):107–113
10. Edd JF, Horowitz L, Davalos RV et al (2006) In vivo results of a new focal tissue ablation technique: irreversible electroporation. IEEE Trans Biomed Eng 53(7):1409–1415
11. Gemert MJ van, Wagstaff PG, Bruin DM de et al (2015) Irreversible electroporation: just another form of thermal therapy? Prostate 75(3):332–335. doi:10.1002/pros.22913 (PubMed PMID: 25327875; PubMed Central PMCID: PMC4305196)
12. Faroja M, Ahmed M, Appelbaum L et al (2013) Irreversible electroporation ablation: is all the damage nonthermal? Radiology 266(2):462–470. doi:10.1148/radiol.12120609 (PubMed PMID: 23169795)
13. Kosiek O, Strach K, Ricke J, Pech M (2012) Irreversible electroporation – a new kid on the block? Radiologe 52(1):38–43. doi:10.1007/s00117-011-2210-2 (PubMed PMID: 22249700)
14. AngioDynamics (2011) Manual NanoKnife® System Procedure & Trouble Shouting Guide. Software version 2.2.0. AngioDynamics®. AngioDynamics Inc., Hamburg, P1-159
15. Wendler JJ, Pech M, Blaschke S et al (2012) Angiography in the isolated perfused kidney: radiological evaluation of vascular protection in tissue ablation by nonthermal irreversible electroporation. Cardiovasc Intervent Radiol 35(2):383–390. doi:10.1007/s00270-011-0187-x (PubMed PMID: 21633883)
16. Choi JW, Lu DS, Osuagwu F et al (2014) Assessment of chronological effects of irreversible electroporation on hilar bile ducts in a porcine model. Cardiovasc Intervent Radiol 37(1):224–230. doi:10.1007/s00270-013-0731-y (PubMed PMID: 24196262)
17. Wendler JJ, Porsch M, Hühne S et al (2013) Short- and mid-term effects of irreversible electroporation on on normal renal tissue: an animal model. Cardiovasc Intervent Radiol 36(2):512–520. doi:10.1007/s00270-012-0452-7 (PubMed PMID: 22893419)
18. Wendler JJ, Pech M, Porsch M et al (2012) Urinary tract effects after multifocal nonthermal irreversible electroporation of the kidney: acute and chronic monitoring by magnetic resonance imaging, intravenous urography and urinary cytology. Cardiovasc Intervent Radiol 35(4):921–926. doi:10.1007/s00270-011-0257-0 (PubMed PMID: 21870207)
19. Kasivisvanathan V, Shah TT, Donaldson I et al (2015) Focal therapy for prostate cancer: German version. Urologe A 54(2):202–209. doi:10.1007/s00120-014-3668-0 (PubMed PMID: 25690574)
20. Schoellnast H, Monette S, Ezell PC et al (2013) The delayed effects of irreversible electroporation ablation on nerves. Eur Radiol 23(2):375–380. doi:10.1007/s00330-012-2610-3 (PubMed PMID: 23011210)
21. Schoellnast H, Monette S, Ezell PC et al (2011) Acute and subacute effects of irreversible electroporation on nerves: experimental study in a pig model. Radiology 260(2):421–427. doi:10.1148/radiol.11103505. (PubMed PMID: 21642418)
22. Li W, Fan Q, Ji Z et al (2011) The effects of irreversible electroporation (IRE) on nerves. PLoS One 6(4):e18831. doi:10.1371/journal.pone.0018831 (PubMed PMID: 21533143; PubMed Central PMCID: PMC3077412)
23. Golberg A, Bruinsma BG, Uygun BE, Yarmush ML (2015) Tissue heterogeneity in structure and conductivity contribute to cell survival during irreversible electroporation ablation by „electric field sinks". Sci Rep 5:8485. doi:10.1038/srep08485 (PubMed PMID: 25684630; PubMed Central PMCID: PMC4329566)
24. Ricke J, Jürgens JH, Deschamps F et al (2015) Irreversible Electroporation (IRE) fails to demonstrate efficacy in a prospective multicenter phase II trial on lung malignancies: the ALICE trial. Cardiovasc Intervent Radiol (PubMed PMID: 25609208)
25. Liehr UB, Wendler JJ, Blaschke S et al (2012) Irreversible electroporation: the new generation of local ablation techniques for renal cell carcinoma. Urologe A 51(12):1728–1734. doi:10.1007/s00120-012-3038-8. (PubMed PMID: 23139026)
26. Yu Z, Zhang X, Ren P et al (2012) Therapeutic potential of irreversible electroporation in sarcoma. Expert Rev Anticancer Ther 12(2):177–184. doi:10.1586/era.11.211 (PubMed PMID: 22316365)
27. Focus Magazin (2015) Die neue Waffe gegen Prostatakrebs. Focus Magazin 05/2015; http://www.focus.de. Zugegriffen 24.01.2015
28. Focus Online (2014) Elektrisches Feld zerstört gezielt Prostatakrebs. Heidelberger Klinik für Prostatatherapie nutzt erstmals die irreversible Elektroporation zur schonenden Behandlung von Prostatakrebs. http://www.focus.de. Zugegriffen: 20. Jan. 2014
29. Ärzteblatt (2015) Nutzen der irreversiblen Elektroporation bei Prostatakrebs nicht belegt. http://www.aerzteblatt.de/nachrichten/61695
30. Wendler JJ, Porsch M, Nitschke S, Köllermann J et al (2015) A prospective Phase 2a pilot study investigating focal percutaneous irreversible electroporation (IRE) ablation by NanoKnife in patients with localised renal cell carcinoma (RCC) with delayed interval tumour resection (IRENE trial). Contemp Clin Trials (Epub ahead of print) pii: S1551-7144(15)00088-9. doi: 10.1016/j.cct.2015.05.002. PubMed PMID: 25962890
31. Gesundheitsstadt Berlin (2015) Urologen warnen vor zu viel Optimismus. Gesundheitsstadt Berlin, http://www.gesundheitsstadt-berlin.de. Zugegriffen 10. Februar 2015
32. DGU (20159 Ungerechtfertigte Werbung für Außenseitertherapie „IRE" bei Prostatakrebs. DGU, Düsseldorf. http://www.krebs-nachrichten.de. Zugegriffen 4.02.2015
33. Valerio M, Stricker PD, Ahmed HU et al (2014) Initial assessment of safety and clinical feasibility of irreversible electroporation in the focal treatment of prostate cancer. Prostate Cancer Prostatic Dis 17(4):343–347. doi:10.1038/pcan.2014.33 (PubMed PMID: 25179590; PubMed Central PMCID: PMC4227889)
34. Bos W van den, Bruin DM de, Muller BG et al (2014) The safety and efficacy of irreversible electroporation for the ablation of prostate cancer: a multicentre prospective human in vivo pilot study protocol. BMJ Open 4(10):e006382. doi:10.1136/bmjopen-2014-006382 (PubMed PMID: 25354827; PubMed Central PMCID: PMC4216863)
35. Valerio M, Dickinson L, Ali A et al (2014) A prospective development study investigating focal irreversible electroporation in men with localised prostate cancer: Nanoknife Electroporation Ablation Trial (NEAT). Contemp Clin Trials 39(1):57–65. doi:10.1016/j.cct.2014.07.006 (PubMed PMID: 25072507; PubMed Central PMCID: PMC4189798)
36. Neal RE II, Millar JL, Kavnoudias H et al (2014) In vivo characterization and numerical simulation of prostate properties for non-thermal irreversible electroporation ablation. Prostate 74(5):458–468. doi:10.1002/pros.22760 (PubMed PMID: 24442790)
37. Polascik T (2014) Clinicaltrials. https://clinicaltrials.gov. North Carolina. U.S.A., study first received Oct 23, 2013; last updated June 30, 2014
38. Neal RE II, Smith RL, Kavnoudias H et al (2013) The effects of metallic implants on electroporation therapies: feasibility of irreversible electroporation for brachytherapy salvage. Cardiovasc Intervent Radiol 36(6):1638–1645. doi:10.1007/s00270-013-0704-1 (PubMed PMID: 23942593)
39. Bos W van den, Muller BG, Rosette JJ de la (2013) A randomized controlled trial on focal therapy for localized prostate carcinoma: hemiablation versus complete ablation with irreversible electroporation. J Endourol 27(3):262–264. doi:10.1089/end.2013.1568 (PubMed PMID: 23469828.; https://clinicaltrials.gov)
40. Korohoda W, Grys M, Madeja Z (2013) Reversible and irreversible electroporation of cell suspensions flowing through a localized DC electric field. Cell Mol Biol Lett 18(1):102–119. doi:10.2478/s11658-012-0042-3 (PubMed PMID: 23271434)
41. Qin Z, Jiang J, Long G et al (2013) Irreversible electroporation: an in vivo study with dorsal skin fold chamber. Ann Biomed Eng 41(3):619–629. doi:10.1007/s10439-012-0686-1 (PubMed PMID: 23180025)
42. Onik A, Rubinsky B (2010) Irreversible electroporation: first patient experience focal therapy of prostate cancer. Irreversible Electroporation (Book). Series in Biomedical Engineering 2010, Springer, Berlin Heidelberg New York, S 235–247. doi: 10.1007/978-3-642-05420-4, ISBN: 978-3-642-05419-8 (Print) 978-3-642-05420-4 (Online)
43. Golberg A, Rubinsky B (2010) A statistical model for multidimensional irreversible electroporation cell death in tissue. Biomed Eng Online 9:13. doi:10.1186/1475-925X-9-13 (PubMed PMID: 20187951; PubMed Central PMCID: PMC2839970)
44. Daniels C, Rubinsky B (2009) Electrical field and temperature model of nonthermal irreversible electroporation in heterogeneous tissues. J Biomech Eng 131(7):071006. doi:10.1115/1.3156808. (PubMed PMID: 19640131)
45. Rubinsky J, Onik G, Mikus P, Rubinsky B (2008) Optimal parameters for the destruction of prostate cancer using irreversible electroporation. J Urol 180(6):2668–2674. doi:10.1016/j.juro.2008.08.003 (PubMed PMID: 18951581)
46. Onik G, Mikus P, Rubinsky B (2007) Irreversible electroporation: implications for prostate ablation. Technol Cancer Res Treat 6(4):295–300 (PubMed PMID: 17668936)
47. Phillips MA, Narayan R, Padath T, Rubinsky B (2012) Irreversible electroporation on the small intestine. Br J Cancer 106(3):490–495. doi:10.1038/bjc.2011.582 (PubMed PMID: 22223084; PubMed Central PMCID: PMC3273351)
48. Schoellnast H, Monette S, Ezell PC et al (2013) Irreversible electroporation adjacent to the rectum: evaluation of pathological effects in a pig model. Cardiovasc Intervent Radiol 36(1):213–220. doi:10.1007/s00270-012-0393-1 (PubMed PMID: 22562481)
49. Srimathveeravalli G, Wimmer T, Monette S et al (2013) Evaluation of an endorectal electrode for performing focused irreversible electroporation ablations in the Swine rectum. J Vasc Interv Radiol 24(8):1249–1256. doi:10.1016/j.jvir.2013.04.025 (PubMed PMID: 23796856)
50. Månsson C, Nilsson A, Karlson BM (2014) Severe complications with irreversible electroporation of the pancreas in the presence of a metallic stent: a warning of a procedure that never should be performed. Acta Radiol Short Rep 3(11):2047981614556409. doi:10.1177/2047981614556409 (PubMed PMID: 25535573; PubMed Central PMCID: PMC4271709)
51. Wendler JJ, Porsch M, Fischbach F et al (2015) Letter to the editor concerning „Irreversible electroporation (IRE) fails to demonstrate efficacy in a prospective multicenter phase II trial on lung malignancies: The ALICE Trial" by Ricke et al. Cardiovasc Intervent Radiol (Epub ahead of print). (doi:10.1007/s00270-014-1049-0). PubMed PMID: 25902855

8.8

Why we should not routinely apply irreversible electroporation as an alternative curative treatment modality for localized prostate cancer at this stage.

Wendler JJ, Ganzer R, Hadaschik B, Blana A, Henkel T, Köhrmann KU, Machtens S, Roosen A, Salomon G, Sentker L, Witzsch U, Schlemmer HP, Baumunk D, Köllermann J, Schostak M, Liehr UB.

World J Urol. 2017 Jan;35(1):11-20.

Irreversible electroporation (IRE), a new tissue ablation procedure available since 2007, could meet the requirements for ideal focal therapy of prostate cancer with its postulated features, especially the absence of a thermal ablation effect. Thus far, there is not enough evidence of its effectiveness or adverse effects to justify its use as a definitive treatment option for localized prostate cancer. Moreover, neither optimal nor individual treatment parameters nor uniform endpoints have been defined thus far. No advantages over established treatment procedures have as yet been demonstrated. Nevertheless, IRE is now being increasingly applied for primary prostate cancer therapy outside clinical trials, not least through active advertising in the lay press. This review reflects the previous relevant literature on IRE of the prostate or prostate cancer and shows why we should not adopt IRE as a routine treatment modality at this stage.

World J Urol (2017) 35:11–20
DOI 10.1007/s00345-016-1838-y

INVITED REVIEW

Why we should not routinely apply irreversible electroporation as an alternative curative treatment modality for localized prostate cancer at this stage

J. J. Wendler[1] · R. Ganzer[5] · B. Hadaschik[3] · A. Blana[4] · T. Henkel[6] · K. U. Köhrmann[7] · S. Machtens[8] · A. Roosen[9] · G. Salomon[10] · L. Sentker[11] · U. Witzsch[12] · H. P. Schlemmer[13] · D. Baumunk[1] · J. Köllermann[2] · M. Schostak[1] · U. B. Liehr[1]

Received: 8 June 2015 / Accepted: 22 April 2016 / Published online: 4 May 2016

Abstract Irreversible electroporation (IRE), a new tissue ablation procedure available since 2007, could meet the requirements for ideal focal therapy of prostate cancer with its postulated features, especially the absence of a thermal ablation effect. Thus far, there is not enough evidence of its effectiveness or adverse effects to justify its use as a definitive treatment option for localized prostate cancer. Moreover, neither optimal nor individual treatment parameters nor uniform endpoints have been defined thus far. No advantages over established treatment procedures have as yet been demonstrated. Nevertheless, IRE is now being increasingly applied for primary prostate cancer therapy outside clinical trials, not least through active advertising in the lay press. This review reflects the previous relevant literature on IRE of the prostate or prostate cancer and shows why we should not adopt IRE as a routine treatment modality at this stage.

Keywords Focal therapy · Ablation · Irreversible electroporation · Prostate · Localized prostate cancer · Definitive treatment

Introduction

The goal of achieving complete tumor ablation with minimal damage to surrounding structures (focal therapy, FT) is becoming increasingly important in oncotherapy. A search for alternative treatment options has been prompted by the decisional conflict in low-risk prostate cancer (PCA) between definitive standard approaches (radical

J. J. Wendler, R. Ganzer, B. Hadaschik, A. Blana, T. Henkel, K. U. Köhrmann, S. Machtens, A. Roosen, G. Salomon, L. Sentker, U. Witzsch, H. P. Schlemmer, D. Baumunk, J. Köllermann, M. Schostak and U. B. Liehr: Working Group for Focal and Microtherapy (AKFM) of the Academy of the German Urological Association (DGU) e. V., Düsseldorf, Germany.

✉ J. J. Wendler
johann.wendler@med.ovgu.de

[1] Department of Urology and Pediatric Urology, Magdeburg University Medical Center, Leipziger Str. 44, 39120 Magdeburg, Germany

[2] Institute of Pathology, Sana Medical Center Offenbach, Offenbach, Germany

[3] Department of Urology, Ruprecht-Karls University, Heidelberg, Germany

[4] Department of Urology and Pediatric Urology, Medical Center Fürth, Nuremberg, Germany

[5] Department of Urology, University of Leipzig, Leipzig, Germany

[6] Urological Practice of Dr. Henkel and Dr. Kahmann, Berlin, Germany

[7] Department of Urology, St. Theresa Hospital, Mannheim, Germany

[8] Department of Urology, St. Maria Hospital, Bergisch-Gladbach, Germany

[9] Department of Urology, Augusta-Krankenanstalt gGmbH Bochum, Bochum, Germany

[10] Martini Clinic, Hamburg-Eppendorf University Medical Center, Hamburg, Germany

[11] Joint Urological Practice, Sinsheim, Germany

[12] Department of Urology and Pediatric Urology, Northwest Hospital & Medical Center, Frankfurt/Main, Germany

[13] Department of Radiology, German Cancer Research Center, Heidelberg, Germany

prostatectomy, radiation therapy) with the risk of overtreatment and serious side effects on the one hand and active surveillance with the risk of inadequate tumor control on the other hand [1, 2]. FT of PCA aims to treat only tumor-bearing prostate tissues. Depending on tumor spread and localization, this can vary from subtotal treatment of the prostate to treatment of only the tumor. Due to its critical assessment, FT of PCA has not found wide acceptance thus far; it harbors the risk of undertreating crucial tumor areas, since growth is frequently multifocal and heterogeneous. Survey studies published thus far have described important aspects of FT for PCA as well as the features of high-intensity focused ultrasound (HI-FU) ablation, cryotherapy (CT), focal laser ablation (FLA), photodynamic therapy (PDT) and brachytherapy (BT) [3]. Irreversible electroporation (IRE), a new tissue ablation procedure available since 2007, could meet the requirements for ideal focal therapy (FT) of localized prostate cancer. The postulated features of this molecular nonthermal ablation technique include precise organ-confined homogeneous prostate cancer tissue ablation achieved via nonthermal damage with potential for minimal toxicity to surrounding structures as well as the urethra and ejaculatory ducts. This may lead to optimal treatment with improved preservation of continence and erectile function as well as micturition and ejaculation. IRE is now being increasingly applied for primary prostate cancer therapy outside clinical trials—not least through active advertising in the lay press—despite the lack of knowledge regarding its effectiveness or its spectrum and rate of adverse events. The aim of this review is to elucidate the current status of IRE for definitive treatment of localized nonmetastatic PCA and to examine whether this new procedure can now be applied as an alternative to the hitherto established treatment modalities.

Methods, structure

This review summarizes the literature published thus far on the development of IRE of the prostate. After an initial introduction to the active principle of IRE and the procedure of IRE of the prostate, the state of research on IRE of the prostate as well as special safety aspects of IRE for the treatment of PCA is discussed with reference to critical adjacent structures. The relevant literature on IRE of the prostate is subsequently described in tabular form for experimental (Table 1) and clinical (Table 2) data in publication order and, then, discussed with regard to safety aspects and effectiveness. In order to assess the relevant literature, a systematic search of the PubMed database and ResearchGate database was conducted (date: up to March 2016). The search focused on "prostate" or "prostate cancer (and synonyms)" and "irreversible electroporation (and synonyms)". The search query to identify questions was "irreversible electroporation". No exclusion criteria were defined. The main points of the original studies mentioned are described and assessed in this review conducted by the Working Group for Focal and Microtherapy (AKFM) of the Academy of the German Urological Association (DGU). The group deals with scientific analyses relating to all aspects of focal therapy. This study aims at elucidating the current scientific status and clinical potential of irreversible electroporation as a new tissue ablation procedure for definitive treatment of localized nonmetastatic prostate cancer.

Fundamental principles of IRE

IRE was developed as a tissue ablation procedure in 2005 [4]. Electrical disruption of the cell membranes in the target area is caused by local application of repetitive heavy current pulses with 2000–3000 V and 30–50 A in the microsecond range via needle electrodes placed in the target tissue [5]. This creates nanopores (Ø 80–490 nm) in the cell membranes, which should lead to an uncontrolled ion influx as well as a loss of macromolecules with a consecutive disturbance of cell homeostasis and apoptosis within 1–7 days [5]. Preservation of the extracellular matrix is discussed as well as the nonthermal ablation effect of IRE [6]. Due to the postulated nonthermal ablation effect of IRE, the cooling effect of blood flow (heat-sink effect as in radiofrequency ablation, RFA) should be of no consequence [5, 6]. Through the postulated all-or-nothing reaction above a "critical" induced transmembrane potential (approx. 1000 V/cm) within the target volume, the ablated area should exhibit a very small transition zone ($\leq$1 mm) and a sharp delineation between treated and unchanged surrounding tissue [5, 7]. A certain tissue selectivity is postulated for IRE: While preserving the extracellular matrix, it spares larger tissue structures and anatomic border structures within the target volume or marginal area that have a matrix-based framework such as blood vessels, intrahepatic bile ducts, the pelvicalyceal system, the urethra, the ureter and nerve bundles [5, 6]. From these published features, IRE was postulated to have an apparent clinical advantage over other ablation methods, particularly over thermoablation techniques [4–6]. However, different electrical properties of various target tissues suggest a varying effect [8]. Moreover, the specific electrical conductivity of various tumor tissues has not yet been systematically evaluated [8]. To avoid pulse-induced cardiac arrhythmias and strong electrically induced muscle contractions, IRE treatment should be carried out under general anesthesia with ECG triggering, deep muscle relaxation and mechanical ventilation [7, 9]. An IRE system has been approved for clinical use and is currently available with commercial approval (NanoKnife® system; AngioDynamics Inc.). As early as

2007, the NanoKnife system was granted FDA 510(k) approval for ablation of soft tissue without restriction to specific diseases or organs, although the treatment parameters were developed in ex vivo models, particularly the liver model [4–6]. Thus far, there is no adequate proof of its effectiveness for specific tumor entities, and its clinical application has hitherto been confined to very small patient cohorts.

Data available on IRE of the prostate: from the in vitro prostate model to the patient's prostate cancer

Valerio et al. [10] and Ting et al. [24] provided a comprehensive step-by-step description of the technique applied for focal transperineal TRUS-mpMRI fusion and template-guided IRE in selected patients with localized prostate cancer in an operating room setting under general anesthesia with continuous electrocardiography [10, 37]. Valerio et al. recommend strict indicational criteria for localized low- to intermediate-risk PCA: tumor volume ≤3 ccm, safety margin of 5 mm, limitation to the transition zone and sufficient distance from the rectal wall. A transrectal biplanar ultrasound probe and a 5-mm prostate brachytherapy grid are compulsory to achieve correct needle placement with parallel alignment and to enable pull-in or pull-back electrode movement (session) for basal or apical treatment extension. The NanoKnife is set to deliver 90 IRE pulses with a pulse length of 70 µs to produce an optimal electric field between 20 and 40 A [10].

No evidence has as yet been obtained on the application of IRE as an alternative curative PCA treatment. The following are available at present: mathematical simulations, experimental investigations (Table 1, [11–17]) and first clinical phase 1–2 results on focal IRE of PCA (Table 2, [18–26]).

It should be noted in this context that more than half the experimental investigations were not carried out using the NanoKnife (AngioDynamics). Most clinical publications on IRE of the prostate are reviews, discussion papers and published study protocols, which are not listed separately here due to the lack of primary data. The clinical application of IRE in men with prostate cancer already ran parallel to basic research experiments on prostate cancer cell lines and animal models. The current application of IRE for primary therapy of localized prostate cancer is based on the clinical data summarized in the following table; results are considered separately under the aspects of side effects and radio- or histomorphological proof of effectiveness.

Analysis of side effects after IRE ablation of the prostate

- Tomihama et al. ([21], congress abstract only) examined 103 patients with PCA T1aN0M0-T4NXM1c (in some cases after TURP, IRE, EBRT, HIFU or RPVE) 3 months after IRE of the prostate. Twenty-three patients underwent whole-gland ablation and 80 partial-gland IRE ablation. The complications were described without specifying a classification: 1 rectourethral fistula, 11 % of patients with temporary and 2 % with chronic erectile dysfunction, 3 % with transient dysuria, 13 % with transient urinary retention, 7 % with transient incontinence, 4 % with transient urgency, 4 % with dysejaculation and 3 % with postprocedural urogenital infection. A statement or histological confirmation regarding tumor or prostate ablation is lacking [21].
- Valerio et al. [10] assessed the side effects in 24 of 34 patients 1–24 months after IRE and found grade 1 in 35 % and grade 2 in 29 % according to CTCAEv4.0: urinary retention in 2 cases, hematuria in 6, dysuria in 5 and urinary tract infections in 5 cases. Nine patients required a suprapubic and 16 a transurethral catheter. There were no urethral strictures or rectourethral fistulas with preservation of continence in 100 % (24/24 patients) and potency in 95 % (19/20 patients) [20].
- Onik et al. [18] described 100 % preservation of potency, 100 % preservation of continence and an indwelling urinary catheter time of 0–3 days in 16 patients (2 with treatment failure after EBRT) 3 weeks after uni-, bi-, trifocal or hemiglandular IRE ablations [5, 18].
- Brausi et al. [35] observed in 11 treated patients 9 % ($n = 1$) acute urinary retention and 27 % ($n = 3$) transient urge incontinence. Continence rate was 100 %; IPSS reduced from 7.72 to 4; and IIEF was between 13.18 and 17.3 over a 19-month period [37].
- Ting et al. [24] assessed unwanted side effects after transperineal IRE of the prostate in 25/32 PCA patients. They found 1 case with grade 3 and 5 cases with grade 1 complications according to Clavien–Dindo. Functional follow-up using the Expanded Prostate Cancer Index Composite (EPIC) questionnaire revealed no significant change in sexual or bowel function up to 6 months after IRE [24].
- Murray et al. ([22], congress abstract only) analyzed 30 PCA patients with a median follow-up of 11.6 months and at least 6 months after IRE. Complications according to Clavien–Dindo were found in 5 patients (18 %): grade 1 in 3 (acute urinary retention) and grade 3 in 2 (1 with epididymitis and 1 with urethral stricture). No cases of rectal injury were reported. Questionnaires of 21 patients 6 months after IRE showed no significant change from baseline in the symptom score for potency, urinary function, bowel function or overall health [22].
- Van den Bos et al. [25] observed in 16 patients no serious adverse events perioperatively with discharge from the hospital 1 day after IRE. No rectal wall damage

Table 1 Overview of studies on statistical and experimental IRE of the prostate or prostate model [11–17]

Publication	Design, material	IRE application	Analysis, results
Onik et al. Aug 2007 [11]	6 Dogs	TRUS-guided focal transperineal IRE (monopolar), hemiablation of the prostate	Resection histology after 2 weeks, hemiablation with sharp demarcation of the ablation area while preserving the neurovascular bundle and urethra, no influence exerted by blood flow, advantage over thermoablation
Rubinsky et al. Dec 2008 [12]	Cell suspension PCA cell line PC3	In vitro	Cytology in relation to IRE parameters, complete IRE of PCA cells without thermal effects, possible application in PCA
Daniels et al. July 2009 [13]	Calculation and simulation model	Use of postulated IRE parameters for soft tissue	Calculation of critical parameters, 2D simulation of IRE for heterogeneous tissue, preservation of nerves, blood vessels and duct in the ablation area, transfer to the human prostate possible
Golberg et al. Feb 2010 [14]	Calculation and simulation model	Use of postulated IRE parameters for prostate tissue	Calculation of critical parameters, 2D simulation of IRE, definition of IRE parameters for accurate treatment planning
Korohoda et al. March 2013 [15]	Cell suspension PCA cell line AT-2	In vitro	Cytology, IRE ablation parameter analysis, is reversible and irreversible electroporation possible
Qin et al. March 2013 [16]	Implantation tumor PCA cell line LNCaP Pro 5 in mice	Percutaneous	Intrainterventional intratumoral temperature measurement, resection histology after 2 weeks. No thermoablative temperature rise, local electrical tumor heterogeneity reduces the effectiveness of IRE
Neal et al. Aug 2013 [17]	Statistical: calculation and simulation model; experimental: potato tuber brachytherapy seed model; animal experimental: 2 canine prostates with and without brachytherapy seeds	Postulated IRE parameters for prostate tissue, in vivo IRE	Resection histology up to 5 h after IRE, numerical simulation, no significant alteration of the electrical field or thermal effects through brachytherapy seeds

Table 2 Clinical study results on IRE of the prostate or prostate cancer (PCA) [18–26, 35, 36]

Publication	Design	N	Material	IRE	Analysis
Onik et al. 2010 [18]	Phase 1 case series, monocenter, single intervention	16	Low- to intermediate-risk PCA (15x cT1c; 1x T2a; PSA 2.2-7; Gleason score 6–8; 2x residual after EBRT) after initial template TRUS-guided prostate biopsy, mean PSA 4.57	TRUS-guided, focal, transperineal IRE, monopolar, NanoKnife, mono-, bi- and trifocal ablations as well as hemiablations	Histology of template TRUS-guided prostate biopsy after 3 weeks
Brausi et al. March 2011 [35]	Phase 1, monocenter, single intervention, single arm	11	Low-risk PCA 10x cT1c; 1x cT2a; PSA 2.7-9.75	TRUS-guided, focal, transperineal IRE, monopolar, electrode 4-10, NanoKnife	Follow-up 2 weeks and 1, 3, 6, 19 months; IIEF, IPSS, PSA; histology of biopsy after 1 month
Neal et al. May 2014 [19]	Safety case study	2	PCA (cT1c and T2a)	TRUS-guided, monopolar, NanoKnife	Resection histology up to 3 h and 3–4 weeks after IRE, numerical simulation
Valerio et al. Dec 2014 [20]	Phase 1–2 trial, multicenter, prospective, single intervention, single arm	34	low-/intermediate-/high-risk PCA according to D'Amico (small volume) of the anterior prostate after initial prostate template biopsy with ultrasound-MRI fusion, mean PSA 6.1	TRUS-MRI fusion-guided focal transperineal IRE (monopolar), NanoKnife, only in the anterior prostate distant from rectum, apex and base, without ECG triggering, pulses à 70 µs	mpMRI of the pelvis/prostate, PSA, CTCAE classification of UAW, urogenital function
Tomihama et al. Feb 2015 [21]	Phase 1–2 trial, multicenter, retrospective, single intervention, single arm, safety	103	PCA T1aN0M0-T4NXM1c, 25 had history of recurrences after other treatments (5 TURPs, 8 IRE, 4 irradiations, 3 HIFUs, 3 prostatectomies alone, 2 prostatectomies EBRT)	139 treatments, whole-gland ablation ($n = 23$), partial-gland ablation ($n = 80$), mean percentage of ablated prostate tissue was 64 %. Ablation field included the urethra, neurovascular bundle, bladder, rectum, urethral sphincter, seminal vesicles and small bowel ($n = 93$, 82, 24, 2, 12, 27, 1, respectively). NanoKnife, monopolar	3-Month follow-up: MRI before and 10–24 h after, 3D-MRI mapping biopsies in 47 %
Murray et al. April 2015 [22]	Phase 1–2, prospective, single arm, single intervention	30	Low- to intermediate-risk PCA (Gleason score 6 = 19, Gleason score 7 = 9), 4 after EBRT, mean PSA 4.48	3–6 Electrodes, monopolar, transperineal TRUS-guided, NanoKnife	Clavien–Dindo, mpMRI 6 weeks after IRE, questionnaires, template TRUS-guided biopsies 6 months after IRE
Niessen et al. Sep 2015 [23]	Phase 1–2, retrospective, single center, single arm, single intervention	13	Low- to intermediate-risk PCA	TRUS-guided percutaneous transperineal IRE, NanoKnife, monopolar	Transabdominal and transrectal contrast-enhanced ultrasound (CEUS) before, immediately after, and 1 day after IRE
Ting et al. Oct 2015 [24]	Phase 1–2, prospective, single center, single arm, single intervention	25	Low- to intermediate-risk PCA	3–6 Electrodes, minimum of 5-mm safety margin around the visible magnetic resonance imaging (MRI) lesion, NanoKnife, monopolar	Baseline, and after 1.5, 3 and 6 months: Clavien, Expanded Prostate Cancer Index Composite (EPIC) questionnaire; after 6 months: mpMRI; after 7 months: biopsy

Table 2 continued

Publication	Design	N	Material	IRE	Analysis
Van den Bos et al. Aug 2015 [25], Oct 2015 [26, 36]	Clinical phase 1–2 trial, multicenter, prospective, double intervention, single arm	16	IRE 30 days before radical prostatectomy (RP). Gleason score 6–8, T1c-T3a, $n = 14$ bilateral PCA, mean PSA 9	TRUS-MRT fusion-guided, focal transperineal IRE using NanoKnife, monopolar, pulses à 90 µs, pull-back 1/16	Prior to and 4 weeks after IRE, imaging by US, CEUS and mpMRI. Following RP assessed on the H&E-stained whole-mount sections. Safety/functional assessment with CTCAE, EPIC, IPSS, VAS, IIEF, uroflowmetry

occurred with electrodes placed at a minimum distance of 5 mm from the rectum [25, 26, 36]. Mainly mild adverse events (grade 1–2 CTCAEv4.0) were reported: grade 1 in 94 % (15/16) with mild hematuria, hematospermia, grade 2 in 50 % (8/16) with urge incontinence (7/16) or acute urinary retention (6/16). EPIC concerning the urinary function decreased significantly ($p = 0.01$). A significant rise was observed between the first and fourth week after treatment concerning sexual function of EPIC. When analyzing the outcomes per treatment protocol (focal vs extended), decreases in the urinary domain of the EPIC with a significant p value were observed in the extended ablation group between baseline and one- and 4-week follow-up ($p = 0.02$ and $p = 0.04$ resp.). In the focal ablation group, no significant differences were noted. IPSS and erectile functions (IIEF-5) outcomes did not differ significantly between baseline and follow-up. Furthermore, uroflowmetry showed a mean maximal flow of 17.2 mL/s at baseline, followed by 14.1 mL/s at 1 week and 14.3 mL/s at 4 weeks [36].

Imaging and histological analysis of the IRE ablation zone of the prostate

- Niessen et al. [23] investigated the microcirculation of 13 PCA patients by transrectal and transabdominal CEUS directly before percutaneous IRE of the prostate and up to 1 day later. The microcirculation was found to be significantly reduced in the ablation area [23].
- Van den Bos et al. [25] examined 16 PCA patients directly before IRE of the prostate and 4 weeks later by TRUS-GSUS, CEUS and mpMRI as well as histologically in radical prostatectomy (RP) specimens. The IRE ablation zone could not be sufficiently visualized by TRUS-GSUS. Whole-mount sections showed sharply delineated ablation zones that closely matched the volumes on T2MRI and CEUS. The area within the IRE electrode configuration was completely ablated and consisted only of hemorrhagic, necrotic and fibrotic tissues with no viable cells in H&E. The ablation zones were ≥2.5 times larger depending on the electrode number and configuration. The ablation effects extended beyond the prostatic capsule in 87 % ($n = 13/15$) and into the neurovascular bundle in 80 % ($n = 12/15$); the urethra was affected in 60 % ($n = 9/15$). No viable cells were found in the IRE ablation zone. There was no rectal wall damage; the electrodes were placed at a minimum distance of 5 mm from the rectum [25, 26].
- Valerio et al. [20] measured PSA levels and performed mpMRI of the prostate in 24 patients 1–24 months after IRE. Treatment failed in 17 % ($n = 6$). Verification of

treatment success by punch biopsy of the prostate was not published.

- Neal et al. [19] conducted bifocal transperineal TRUS-guided IRE in 2 patients followed by radical prostatectomy (RP) 3–4 weeks later. The histological workup of specimens yielded only a descriptive depiction of the ablation zones. A statement regarding tumor ablation is lacking in conjunction with both the treatment planning and the resected tissue. Treatment safety was not assessed [19].
- Brausi et al. [35] mentioned a biopsy-proven persistent PCA in 27 % (3/11 patients) 30 days after IRE. Coagulative necrosis, granulomatosis, fibrosis and hemosiderosis were commonly reported [37].
- Ting et al. [24] examined 24/32 patients by mpMRI 6 months after IRE with a minimum safety margin of 5 mm and by biopsy 7 months later. Findings on examining the treatment zone by mpMRI and biopsy were subdivided into infield, adjacent or outfield. Neither mpMRI ($n = 24$) nor biopsy ($n = 21$) of the IRE ablation zone revealed suspicious infield findings in any of the patients. Cancer was detected adjacent to the treatment zone in 21 % ($n = 5$) by mpMRI and in 19 % ($n = 4$) by biopsy. Outfield cancer findings were obtained in 8 % ($n = 2$) by mpMRI and in 5 % ($n = 1$) by biopsy [24].
- Onik et al. [18] performed uni-, bi-, trifocal or hemiglandular IRE ablations in 16 patients (2 with treatment failure after EBRT). Transperineal TRUS-guided biopsy (no template) of the ablation zones and their surroundings revealed no residual tumor in any of the patients 3 weeks after IRE [5, 18].
- Murray et al. ([22], congress abstract only) analyzed 30 PCA patients by mpMRI 6 weeks after IRE and by template-guided TRUS biopsy 6 months later. There was no significant difference between the prostate volume before the intervention and 6 weeks later. Biopsy results in the treatment zone were positive in 25 % ($n = 7$) after 6 months [22].

Special safety aspects for the treatment of PCA: IRE of nerves and bowel

For IRE of the prostate as well as for the established treatment procedures, it is important to take into account the anatomic risk structures such as periprostatic neurovascular bundles, the external urethral sphincter, the rectum and the bladder neck. No published study data are available on IRE of the bladder, sphincter or neurovascular bundle. Only one study reports on preservation of functional parameters (continence, erection). Animal experimental studies on IRE in the small bowel and rectum as well as in peripheral nerve fibers and striated skeletal muscles are being discussed as transferable models. After IRE in the small bowel, focal necrosis with preserved organ structure and incipient epithelial regeneration was reported after 1 week [27]. After perirectal IRE adjacent to the rectum, only focal inflammatory reactions of the rectum were reported when a fixed rectal coil was not used, while transmural necroses of the rectum were also found when it was. No perforations occurred. This led to the conclusion that no relevant rectal damage is caused without rectal compression in the application field [28]. Depending on the parameter settings, endorectally applied IRE of the rectum led to a focal mucosal lesion but also to ablation of the entire rectal wall [29].

An in vivo experimental animal model was used by two study groups to investigate the effect of IRE on peripheral branches of the sciatic nerve in pigs. Acute damage to the nerve fibers with fragmentation and axon degeneration (Waller degeneration) was seen after 1–2 weeks. After 8–10 weeks, partial incipient axon regeneration was found with preserved and regenerated myelin sheath composed of neurofilaments and Schwann cells [20–22]. At the same time, perineural focal necrosis of striated skeletal muscles with scarred connective tissue replacement became apparent [30–32].

In analogy to thermal FT, it must basically also be assumed in IRE of PCA that functionally sensitive structures (neurovascular bundle, sphincter and rectum) can be damaged if they lie in the ablation area. It is completely unclear to what extent these structures can be spared if IRE is performed adjacent to the capsule or sphincter. Neal et al. [17] postulated no significant differences in the electric field or thermal effects between tissue with and without a grid of expired radiotherapy seeds, suggesting that IRE can be used as a salvage therapy option for brachytherapy. In contrast, Månsson et al. [33] concluded that adjacent metallic implants may cause unwanted extracapsular extension of the IRE ablation field.

Discussion

Stringent requirements govern new drug approvals. Evidence of additional benefit over the existing therapy must be provided through comparative clinical trials. For medicotechnical treatment procedures, such trial-based proof is not required to the same extent. Merely, technical feasibility and putative application safety are regarded as formally sufficient for use in humans. At this stage, scientific validation in suitable studies is a conditio sine qua non. The use of IRE even outside clinical trials has been actively promoted since the NanoKnife system was put on the market. This has led to a worldwide increase in the number of IRE treatments of PCA in the last 3 years. Patients have to cover the high

treatment costs themselves in these cases. If articles in the lay press advertise the procedure with promising but unverified contents, false hopes are raised in those concerned. This is disastrous if it delays the development of truly effective treatment options. Only scientific research with adequate study implementation can resolve this conflict. Hitherto unclarified questions on IRE of PCA are addressed. It is unclear, for example, to what extent the histopathological heterogeneity of both PCA and the prostate (grading, lithiasis, tissue density) influences the success of ablation. If the whole gland or the area adjacent to the capsule has to be treated, the volume geometry of the prostate must be congruent with the ablation geometry of the IRE field. The only partially adaptable target volume appears to be of only limited suitability to achieve this with concomitant sparing of functionally important structures. The internationally published IRE applications in PCA patients (Table 2) involve a total of 239 analyzed treatment cases that primarily illuminate safety aspects in a short- or medium-term follow-up.

Safety of IRE of the prostate

In general, only mild side effects have been reported up to 24 months after IRE with a concomitant high rate of continence and potency preservation. However, the authors sometimes used different assessment tools in an often very heterogeneous patient population (with and without previous therapy, localized low-risk and locally advanced high-risk PCA). Another shortcoming is the lack of objective systematic functional testing by urodynamics, uroflowmetry, PAD tests and morphological imaging as well as, for example, by assessment tools such as the International Index of Erectile Function (*IIEF*-5) score and the *International Prostate Symptom Score (IPSS) to evaluate urinary continence/incontinence, potency/erectile dysfunction and obstructive dysuria.* In particular, it is not possible to basically classify side effects reported in the various studies due to differences in the IRE treatment localization in the prostate, the extension of the IRE ablation zone and the individual IRE treatment parameters and endpoints. Contrary to the initially postulated tissue selectivity or confinement to anatomical borders, the IRE field can inadvertently extend beyond the prostatic capsule into the neurovascular bundle and to the rectal wall [21, 25, 26]. A thus far incalculable variability of the electrical field arises through inter- and intraindividual tissue heterogeneity or through metallic foreign bodies [16, 17, 25, 26, 33]. Ablation-induced nerve degeneration can thus lead to erectile impotence and stress urinary incontinence [15, 30–32]. An ablation-induced rectal lesion can lead to perforation and fistulas [21, 27–29]. Damage to the bladder neck and urethral sphincter also seems possible. Formally, there is thus no fundamental difference between the risk profile of IRE and that of hitherto established procedures for treating localized prostate cancer.

Efficacy of IRE for ablation of localized prostate cancer

The discussion on the efficacy of IRE has thus far focused on the question of whether it is possible to completely ablate a defined prostate tissue zone by IRE. It is crucial for ablative therapies to ensure that the targeted zone is entirely ablated, without leaving any viable cells. Radical prostatectomy (RP) as the gold standard enables complete resection of tumor tissue. Several studies on ablative therapies or radiation followed by RP yielded various results, including cases with incomplete tumor destruction and persistent residual tumor cells in the treatment zone. There is still no imaging modality to reliably visualize and assess the ablation zone after IRE, though CEUS and mpMRI seem most feasible for this purpose [22, 25, 26]. Since it is representative for the entire treatment zone, biopsy punch monitoring after IRE of PCA is less accurate than the examination of prostatectomy specimens [1, 25] and has thus far shown nonuniform results ranging from complete tumor ablation to 25 % positive biopsies in the ablation zone or its margin [5, 18, 22, 24]. Van den Bos et al. [25] conducted the only study on RP after IRE of localized PCA (Gleason score 6–8, PSA 3.6–25 ng/ml), and, on examining whole-gland specimens 4 weeks after IRE ablation, they detected no viable cells (i.e., compete ablation) within the IRE electrode configuration area using an H&E stain (no application of vital markers) [25]. Though focal IRE of the prostate with complete tumor cell ablation (inconstant) seems possible [22, 24, 25], contrary to initially postulated potential features of IRE, the IRE ablation field varies in size and currently cannot be strictly limited to the prostate gland. Thus, van den Bos et al. [25] found $\geq$2.5 times larger ablation zones than those calculated in the IRE treatment planning as well as extracapsular extension of the ablation field when IRE was performed close to the prostate capsule. Moreover, localized PCA cannot yet be detected and ablated safely enough by focal IRE. Thus, residual PCA was detected in biopsy specimens by Ting et al. [24] adjacent to the treatment zone in 19 % and by Murray et al. [22] within the treatment zone in 25 %. Van den Bos et al. [25] were able to detect PCA outside the focal IRE ablation zone in 94 % with RP specimens. According to guidelines for (thermal) ablation methods, the target tumor should be completely covered by the ablation zone, which includes a safety margin of at least 5–10 mm around the expected tumor margin, in order to achieve successful ablation and eliminate micrometastases around the index tumor [34]. The treatment margin around the needles has been estimated to be 5 mm [7, 10]. The optimal or minimum safety margin for IRE ablation has not yet been

defined. According to data reported by Ting et al. [24], a 5-mm safety margin appears to be inadequate, and it seems necessary to leave a safety margin of 10 mm.

Conclusion

IRE has high potential for FT of malignancies due to its molecular mode of action. Many postulated features have not been sufficiently verified in clinical studies. The data available cannot justify the use of IRE in the routine clinical, focal treatment of PCA as an alternative to established treatment methods at this stage. Application of IRE outside clinical trials cannot be currently recommended.

Authors' contributions J. J. Wendler is the corresponding author, wrote the manuscript, collected and analyzed the data, and developed the project. R. Ganzer, B. Hadaschik, A. Blana, T. Henkel, K. U. Köhrmann, S. Machtens, A. Roosen, G. Salomon, L. Sentker, U. Witzsch, H. P. Schlemmer and J. Köllermann edited and critically revised the manuscript and voted for internal consensus. D. Baumunk wrote and edited the manuscript. M. Schostak is the chief of academy, wrote the manuscript and developed the project. U. B. Liehr is a senior author, wrote the manuscript and developed the project.

Compliance with ethical standards

Conflicts of interest The authors declare that they have no conflict of interest.

Ethical standards For this type of study (review) formal consent is not required.

References

1. Cooperberg MR, Carroll PR, Klotz L (2011) Active surveillance for prostate cancer: progress and promise. J Clin Oncol 29(27):3669–3676. doi:10.1200/JCO.2011.34.9738
2. Schostak M, Köllermann J, Hadaschik B, Blana A, Ganzer R, Henkel T, Köhrmann KU, Liehr UB, Machtens S, Roosen A, Salomon G, Sentker L, Witzsch U, Schlemmer HP, Baumunk D (2015) Cancer control in focus insights and future perspectives for the focal treatment of prostate cancer. Aktuelle Urol 46(1):39–44. doi:10.1055/s-0034-1396803 (**Epub 2015 Feb 6**)
3. Kasivisvanathan V, Shah TT, Donaldson I, Kanthabalan A, Moore CM, Emberton M, Ahmed HU (2015) Focal therapy for prostate cancer: German version. Urologe A 54(2):202–209. doi:10.1007/s00120-014-3668-0 (**German**)
4. Davalos RV, Mir IL, Rubinsky B (2005) Tissue ablation with irreversible electroporation. Ann Biomed Eng 33(2):223–231
5. Rubinsky B, Irreversible Electroporation (Book), Series in Biomedical Engineering, Springer, Berlin (2010). doi:10.1007/978-3-642-05420-4. ISBN: 978-3-642-05419-8 (print) (online)
6. Davalos RV, Bhonsle S, Neal RE II (2015) Implications and considerations of thermal effects when applying irreversible electroporation tissue ablation therapy. Prostate 75(10):1114–1118. doi:10.1002/pros.22986 (**Epub 2015 Mar 23**)
7. Manual NanoKnife® System Procedure and Trouble Shooting Guide. Software version 2.2.0. AngioDynamics®, ©2011 AngioDynamics, Inc. P1-159
8. Golberg A, Bruinsma BG, Uygun BE, Yarmush ML (2015) Tissue heterogeneity in structure and conductivity contribute to cell survival during irreversible electroporation ablation by "electric field sinks". Sci Rep 5:8485. doi:10.1038/srep08485
9. Sano MB, Arena CB, Bittleman KR, DeWitt MR, Cho HJ, Szot CS, Saur D, Cissell JM, Robertson J, Lee YW, Davalos RV (2015) Bursts of bipolar microsecond pulses inhibit tumor growth. Sci Rep 13(5):14999. doi:10.1038/srep14999
10. Valerio M, Ahmed HU, Emberton M (2015) Focal therapy of prostate cancer using irreversible electroporation. Tech Vasc Interv Radiol 18(3):147–152. doi:10.1053/j.tvir.2015.06.005 (**Epub 2015 Jun 18**)
11. Onik G, Mikus P, Rubinsky B (2007) Irreversible electroporation: implications for prostate ablation. Technol Cancer Res Treat 6(4):295–300
12. Rubinsky J, Onik G, Mikus P, Rubinsky B (2008) Optimal parameters for the destruction of prostate cancer using irreversible electroporation. J Urol 180(6):2668–2674. doi:10.1016/j.juro.2008.08.003 (**Epub 2008 Oct 31**)
13. Daniels C, Rubinsky B (2009) Electrical field and temperature model of nonthermal irreversible electroporation in heterogeneous tissues. J Biomech Eng 131(7):071006. doi:10.1115/1.3156808
14. Golberg A, Rubinsky B (2010) A statistical model for multidimensional irreversible electroporation cell death in tissue. Biomed Eng Online 9:13. doi:10.1186/1475-925X-9-13
15. Korohoda W, Grys M, Madeja Z (2013) Reversible and irreversible electroporation of cell suspensions flowing through a localized DC electric field. Cell Mol Biol Lett 18(1):102–119. doi:10.2478/s11658-012-0042-3 (**Epub 2012 Dec 27**)
16. Qin Z, Jiang J, Long G, Lindgren B, Bischof JC (2013) Irreversible electroporation: an in vivo study with dorsal skin fold chamber. Ann Biomed Eng 41(3):619–629. doi:10.1007/s10439-012-0686-1 (**Epub 2012 Nov 22**)
17. Neal RE II, Smith RL, Kavnoudias H, Rosenfeldt F, Ou R, McLean CA, Davalos RV, Thomson KR (2013) The effects of metallic implants on electroporation therapies: feasibility of irreversible electroporation for brachytherapy salvage. Cardiovasc Intervent Radiol 36(6):1638–1645. doi:10.1007/s00270-013-0704-1 (**Epub 2013 Aug 14**)
18. Onik A, Rubinsky B (2010) Irreversible electroporation: first patient experience focal therapy of prostate cancer. Irreversible Electroporation (Book). Series in Biomedical Engineering, pp 235–247. Springer, Berlin. doi:10.1007/978-3-642-05420-4. ISBN: 978-3-642-05419-8 (print), (online)
19. Neal RE II, Millar JL, Kavnoudias H, Royce P, Rosenfeldt F, Pham A, Smith R, Davalos RV, Thomson KR (2014) In vivo characterization and numerical simulation of prostate properties for non-thermal irreversible electroporation ablation. Prostate 74(5):458–468. doi:10.1002/pros.22760 (**Epub 2014 Jan 17**)
20. Valerio M, Stricker PD, Ahmed HU, Dickinson L, Ponsky L, Shnier R, Allen C, Emberton M (2014) Initial assessment of safety and clinical feasibility of irreversible electroporation in the focal treatment of prostate cancer. Prostate Cancer Prostatic Dis 17(4):343–347. doi:10.1038/pcan.2014.33 (**Epub 2014 Sep 2**)
21. Tomihama RT, Günther E, Kim D, Stehling M (2015) Irreversible electroporation treatment for prostate adenocarcinomas: a safety outcome study. J Vasc Interv Radiol 26(2):S121–S122. Abstract only. Published in issue: February, 2015
22. Murray K, Musser J, Mashni J, Srimathveeravalli G, Durack J, Solomon S, Coleman J (2015) PD47-08 irreversible electroporation (IRE) as a localized treatment for prostate cancer: a report on safety and outcomes. J Urol 193(4):e964. doi:10.1016/j.juro.2015.02.2752

23. Niessen C, Jung EM, Beyer L, Pregler B, Dollinger M, Haimerl M, Scheer F, Stroszczynski C, Wiggermann P (2015) Percutaneous irreversible electroporation (IRE) of prostate cancer: contrast-enhanced ultrasound (CEUS) findings. Clin Hemorheol Microcirc 61(2):135–141. doi:10.3233/CH-151985
24. Ting F, Tran M, Böhm M, Siriwardana A, Van Leeuwen PJ, Haynes AM, Delprado W, Shnier R, Stricker PD (2015) Focal irreversible electroporation for prostate cancer: functional outcomes and short-term oncological control. Prostate Cancer Prostatic Dis 19(1):46–52. doi:10.1038/pcan.2015.47
25. van den Bos W, de Bruin DM, Jurhill RR, Savci-Heijink CD, Muller BG, Varkarakis IM, Skolarikos A, Zondervan PJ, Laguna-Pes MP, Wijkstra H, de Reijke TM, de la Rosette JJ. The correlation between the electrode configuration and histopathology of irreversible electroporation ablations in prostate cancer patients. World J Urol. 2015 Aug 22. (**Epub ahead of print**)
26. van den Bos W, de Bruin DM, van Randen A, Engelbrecht MR, Postema AW, Muller BG, Varkarakis IM, Skolarikos A, Savci-Heijink CD, Jurhill RR, Zondervan PJ, Laguna Pes MP, Wijkstra H, de Reijke TM, de la Rosette JJ. MRI and contrast-enhanced ultrasound imaging for evaluation of focal irreversible electroporation treatment: results from a phase I-II study in patients undergoing IRE followed by radical prostatectomy. Eur Radiol. 2015 Oct 8. (**Epub ahead of print**)
27. Phillips MA, Narayan R, Padath T, Rubinsky B (2012) Irreversible electroporation on the small intestine. Br J Cancer 106(3):490–495. doi:10.1038/bjc.2011.582 **(Epub 2012 Jan 5)**
28. Schoellnast H, Monette S, Ezell PC, Single G, Maybody M, Weiser MR, Fong Y, Solomon SB (2013) Irreversible electroporation adjacent to the rectum: evaluation of pathological effects in a pig model. Cardiovasc Intervent Radiol 36(1):213–220. doi:10.1007/s00270-012-0393-1 **(Epub 2012 May 5)**
29. Srimathveeravalli G, Wimmer T, Monette S, Gutta NB, Ezell PC, Maybody M, Weiser MR, Solomon SB (2013) Evaluation of an endorectal electrode for performing focused irreversible electroporation ablations in the Swine rectum. J Vasc Interv Radiol 24(8):1249–1256. doi:10.1016/j.jvir.2013.04.025 **(Epub 2013 Jun 21)**
30. Schoellnast H, Monette S, Ezell PC, Maybody M, Erinjeri JP, Stubblefield MD, Single G, Solomon SB (2013) The delayed effects of irreversible electroporation ablation on nerves. Eur Radiol 23(2):375–380. doi:10.1007/s00330-012-2610-3 **(Epub 2012 Aug 16)**
31. Schoellnast H, Monette S, Ezell PC, Deodhar A, Maybody M, Erinjeri JP, Stubblefield MD, Single GW Jr, Hamilton WC Jr, Solomon SB (2011) Acute and subacute effects of irreversible electroporation on nerves: experimental study in a pig model. Radiology 260(2):421–427. doi:10.1148/radiol.11103505 (**Epub 2011 Jun 3**)
32. Li W, Fan Q, Ji Z, Qiu X, Li Z (2011) The effects of irreversible electroporation (IRE) on nerves. PLoS ONE 6(4):e18831. doi:10.1371/journal.pone.0018831
33. Månsson C, Nilsson A, Karlson BM (2014) Severe complications with irreversible electroporation of the pancreas in the presence of a metallic stent: a warning of a procedure that never should be performed. Acta Radiol Short Rep 3(11):2047981614556409. doi:10.1177/2047981614556409. eCollection 2014 Dec
34. Ahmed M, Solbiati L, Brace CL, Breen DJ, Callstrom MR, Charboneau JW, Chen MH, Choi BI, de Baère T, Dodd GD 3rd, Dupuy DE, Gervais DA, Gianfelice D, Gillams AR, Lee FT Jr, Leen E, Lencioni R, Littrup PJ, Livraghi T, Lu DS, McGahan JP, Meloni MF, Nikolic B, Pereira PL, Liang P, Rhim H, Rose SC, Salem R, Sofocleous CT, Solomon SB, Soulen MC, Tanaka M, Vogl TJ, Wood BJ, Goldberg SN; International Working Group on Image-Guided Tumor Ablation; Interventional Oncology Sans Frontières Expert Panel; Technology Assessment Committee of the Society of Interventional Radiology; Standard of Practice Committee of the Cardiovascular and Interventional Radiological Society of Europe (2014) Image-guided tumor ablation: standardization of terminology and reporting criteria–a 10-year update. J Vasc Interv Radiol 25(11):1691–1705.e4. doi:10.1016/j.jvir.2014.08.027. (**Epub 2014 Oct 23**)
35. Brausi MA, Giliberto GL, Simonini GL, Botticelli L, Di Gregorio C (2011) 960 Irreversible electroporation (IRE), a novel technique for focal ablation of prostate cancer (PCA): results of a interim pilot study in low risk patients with PCA. Eur Urol Suppl. doi:10.1016/S1569-9056(11)60942-1
36. Van den Bos W, De Bruin DM, Veelo DP, Postema AW, Muller BG, Varkarakis IM, Skolarikos A, Zondervan PJ, Laguna Pes MP, Savci-Heijink CD, Wijkstra H, De Reijke TM, De La Rosette JJMCH (2015) Quality of life and safety outcomes following irreversible electroporation treatment for prostate cancer: results from a phase I–II study. J Cancer Sci Ther 7(10):312–321. doi:10.4172/1948-5956.1000369
37. Ting F, Van Leeuwen PJ, Stricker PD (2016) Step-by-step technique for irreversible electroporation of focal prostate cancer: an instructional video guide. J Vasc Interv Radiol 27(4):568. doi:10.1016/j.jvir.2016.01.003

8.9

Irreversible Electroporation of Prostate Cancer: Patient-Specific Pretreatment Simulation by Electric Field Measurement in a 3D Bioprinted Textured Prostate Cancer Model to Achieve Optimal Electroporation Parameters for Image-Guided Focal Ablation.

Wendler JJ, Klink F, Seifert S, Fischbach F, Jandrig B, Porsch M, Pech M, Baumunk D, Ricke J, Schostak M, Liehr UB.

Cardiovasc Intervent Radiol. 2016 Nov;39(11):1668-1671.

No abstract available.

Cardiovasc Intervent Radiol (2016) 39:1668–1671
DOI 10.1007/s00270-016-1390-6

LETTER TO THE EDITOR

Irreversible Electroporation of Prostate Cancer: Patient-Specific Pretreatment Simulation by Electric Field Measurement in a 3D Bioprinted Textured Prostate Cancer Model to Achieve Optimal Electroporation Parameters for Image-Guided Focal Ablation

Johann Jakob Wendler[1,5,6] · Fabian Klink[2] · Sven Seifert[3] · Frank Fischbach[4,6] · Burkhard Jandrig[1] · Markus Porsch[1] · Maciej Pech[4,6] · Daniel Baumunk[1,5] · Jens Ricke[1] · Martin Schostak[1,5] · Uwe-Bernd Liehr[1,5,6]

Received: 28 March 2016 / Accepted: 23 May 2016 / Published online: 2 June 2016

Irreversible electroporation (IRE) of localized prostate cancer (PCA) for curatively intended treatment is still considered experimental, though first study results confirm its high developmental potential as an organ- and function-preserving focal therapy. Current limitations thus far include exact calculation of the ablation field, congruence between tumor localization and extension of the ablation field, and organ confinement of the ablation field with sparing of structures/organs at risk. Van den Bos et al. [1], for example, described the ablation field as being two-to-three times larger than expected and extending beyond the prostatic capsule into the neurovascular bundle with the corresponding risks of stress incontinence and erectile dysfunction. Two important factors are discussed. For one thing, electric field configuration strongly depends on tissue heterogeneity and conductivity [2]. The aging prostate with PCA is a very inhomogeneous tissue or organ (PCA, nodular hyperplasia, inflammatory infiltrates, cysts, prostatoliths, urethra, anatomic zones, and capsule). IRE planning with the NanoKnife system, however, developmentally assumes the target tissue to be homogeneous and not organ specific. This limits individual tissue-texture-related prostate-specific IRE ablation planning. For another thing, a spheroidal IRE field coaxially aligned with the needle electrodes in the longitudinal axis is generated in transperineal grid-directed IRE of the prostate. However, the prostate displays pyramidal-to-spheroid asymmetry. Moreover, PCA is often characterized by multifocal, peripheral, asymmetric, nonspheroidal, and capsule-infiltrating or transmural growth (apex, not capsule). This

✉ Johann Jakob Wendler
johann.wendler@med.ovgu.de

Fabian Klink
fabian.klink@ovgu.de

Sven Seifert
seifert.s@fug-elektronik.de

Frank Fischbach
frank.fischbach@med.ovgu.de

Burkhard Jandrig
burkhard.jandrig@med.ovgu.de

Markus Porsch
markus.porsch@med.ovgu.de

Maciej Pech
macej.pech@med.ovgu.de

Daniel Baumunk
daniel.baumunk@med.ovgu.de

Jens Ricke
jens.ricke@med.ovgu.de

Martin Schostak
martin.schostak@med.ovgu.de

Uwe-Bernd Liehr
uwe-bernd.liehr@med.ovgu.de

[1] Department of Urology and Pediatric Urology, University of Magdeburg, Leipziger Str. 44, 39120 Magdeburg, Germany

[2] Department of Mechanical Engineering, Otto von Guericke University, Magdeburg, Germany

[3] FuG Elektronik GmbH, 83135 Schechen, Bavaria, Germany

[4] Department of Radiology, University of Magdeburg, Magdeburg, Germany

[5] Working Group for Focal and Microtherapy of the German Society of Urology (AKFM of DGU e.V.), Magdeburg, Germany

[6] German Academy of Microtherapy (DAfMT e.V.), 39120 Magdeburg, Germany

makes it very difficult to adjust the IRE ablation field to tumor and prostate geometry, especially in the peripheral areas. Previous approaches to mathematical pretreatment simulation and intra-interventional monitoring by electrical impedance tomography could not be clinically implemented to solve the problem [3, 4].

Current advancements in medical technology involving the use of 3D procedures and IRE gave rise to the project idea of performing an individual pretreatment simulation of IRE ablation by electric field measurement in a 3D bioprinted model composed of matrix, cells, and possibly anorganic structures with a resulting heterogeneous tissue structure based on patient-specific multiparametric MRI (mpMRI) imaging of the prostate and periprostatic structures. This could enable pretreatment determination of optimal individual IRE parameters for focal, tumor-congruent, organ-confined IRE ablation of PCA as the solution to the above problem. This is achieved by combining three aspects:

First Modern commercially available plastic 3D printers make it possible to create accurate bodies for a wide variety of applications. In the field of medicine, they can be used to make detailed 3D models of patients' organs for preoperative visualization and surgical planning in order to counterbalance disadvantages of the limited depth perception associated with a 2D screen display [5]. In some cases, we use this procedure to counsel patients and plan their treatment for localized PCA with the aid of an mpMRI-based 3D model for patient-specific visualization of the prostate with PCA foci (Fig. 1) [6].

Second In vitro tissue models are useful platforms that can facilitate systematic laboratory investigations of complex culture systems. Bioprinting makes it possible to create highly complex 3D architectures with living cells. Bioprinting techniques have been developed to precisely and rapidly generate patterns of living cells, biological macromolecules, and biomaterials facilitating physiologically relevant cell–cell and cell–matrix interactions. These technologies hold great potential for applications in cancer research [7, 8]. 3D bioprinted organ/tumor models with individual textures could enable pretreatment in vitro simulation of tissue-structure-dependent ablation procedures. The development of a 3D cell culture model for PCA also seems possible [9].

Third IRE ablation uses a series of brief but intense electric pulses delivered by paired needle-like electrodes into a targeted region of tissue, killing the cells by irreversibly disrupting cellular membrane integrity within a localized electric field with a critical potential at about 1500 V/cm or more. This potential can be measured via working electrodes in relation to the distance of the IRE electrodes (Fig. 2). Inactive IRE electrodes placed in the target tissue can also be used as working electrodes to determine the potential of an adjacent active pair of electrodes in that particular area of the target volume (Fig. 3).

Taken together, more individual IRE planning would be possible for focal treatment of localized PCA, and the following simulation approach should be discussed: First,

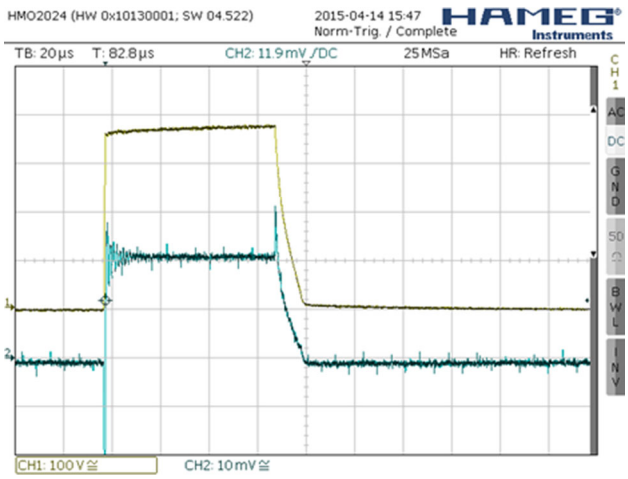

Fig. 2 Graph experimental setup voltage measurement (V) in gel phantom using PF 753, oscilloscope, 2 isolating transformers, and PFO 224 (current clamp): Channel 1 voltage curve IRE electrode (*yellow-black*) and channel 2 voltage curve working electrode (*blue-black*). Distance between IRE and working electrode 20 mm. Different voltage distribution and field strength in the target volume in relation to conductivity (transmission ratio)

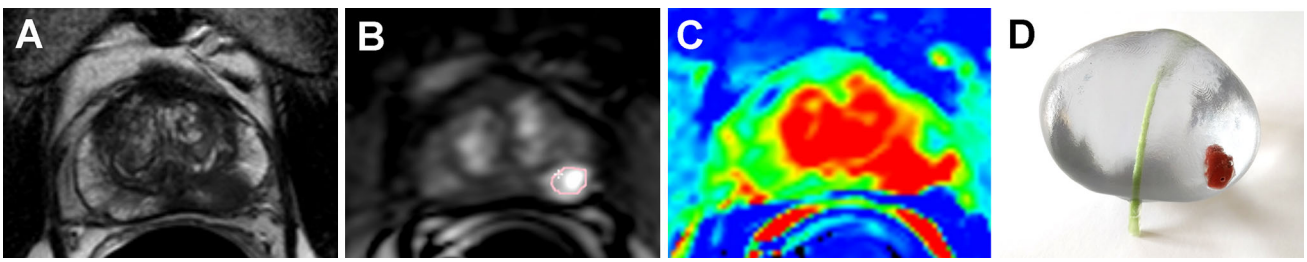

Fig. 1 **A–C** mpMRI prostate transverse view. **D** 3D printed model (rapid prototyping, stereolithography with transparent UV-curable plastic, and colored silicon structures) of a patient-specific prostate based on mpMRI (*left*) with tumor structure (*red*) and urethra (*green*) (Color figure online)

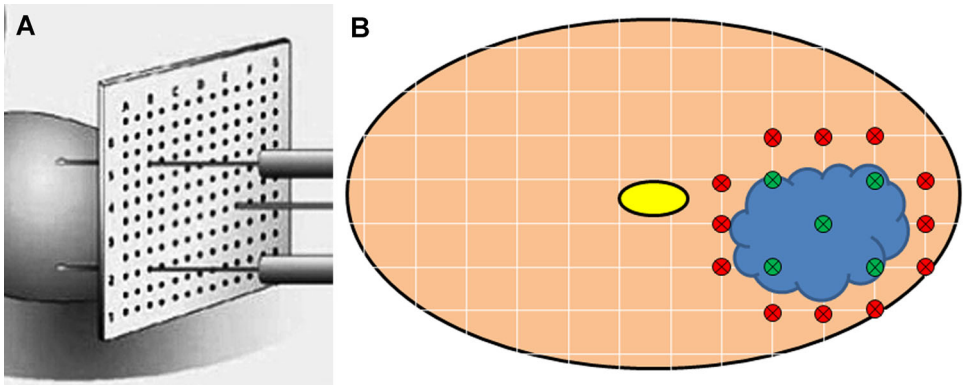

Fig. 3 Diagram IRE prostate/model via template (table of fields or white checkered pattern); prostate in transverse section with urethra (*yellow*) and PCA (*blue cloud*), inactive IRE electrodes (*green*) also utilizable as working electrodes, outer working electrodes (*red*)

creation of an ex vivo 3D biomodel (3D bioprinting) based on individual mpMRI data. This model ideally has the characteristics of the gland to be treated (tissue inhomogeneity, individual tissue conductivity, special structural features, cysts, calcifications, etc.). Template-based ablation simulation is subsequently carried out in this model: after positioning the IRE needles, specific local measurement of the electric potential is performed via the non-conducting needles or working electrodes during pulse emission in the biomodel. Systematic potential measurement via several working electrodes would enable three-dimensional concentric spheroidal determination of the electric field and critical potential. Thus, the optimal IRE ablation parameters (potential and electrode geometry) could be determined prior to treatment. The measurement results are then used to adjust the IRE parameters (potential, electrode geometry for the active pair of electrodes, and ultimately for the definitive ablation). Finally, the experimental approach is translated into the clinical setting.

At present, mpMRI is the imaging technique that provides the most accurate diagnostic and morphologic image data for the prostate and PCA. Current limitations consist in the sensitivity and specificity for PCA detection as well as translation from the morphologic image features of the prostate (texture) into tissue-specific features of the prostate tissue (density, cell–matrix ratio, nucleus–plasma ratio, and conductivity). Further limitations arise from subjective mistakes made by the examiner (interpreting MRI findings, determining outer prostate borders and tumor volumes, and performing a biopsy and histopathological examination) as well as from objective technology-related errors (mpMRI algorithms, image fusion algorithms, and biopsy technique). Corresponding discrepancies between the imaging/evaluation and the true status influence the effectiveness of focal therapies. First comparative analyses have been carried out using 3D printing methods [10]. Automatic segmentation of the prostate and PCA in 3D magnetic resonance images is a challenging task due to the varying shapes, sizes, and textures involved [11]. The introduction and implementation of the above-mentioned principles based on patient-specific data could enable a more precise and reliable IRE application for PCA in the future.

Acknowledgments AngioDynamics Inc. (NY, USA) supports the current IRENE study [ClinicalTrials.gov: NCT01967407] by providing the NanoKnife electroporator device and technical maintenance. The authors declare that they have no conflict of interest.

Compliance with Ethical Standards

Conflict of Interest The authors declare that they have no conflict of interest.

Ethical Approval All procedures performed in studies involving human participants were in accordance with the ethical standards of the institutional and/or national research committee and with the 1964 Helsinki Declaration and its later amendments or comparable ethical standards.

Informed Consent Informed consent was obtained from all individual participants included in the study.

References

1. Van den Bos W, de Bruin DM, Jurhill RR et al. The correlation between the electrode configuration and histopathology of irreversible electroporation ablations in prostate cancer patients. World J Urol. 2016;34(5):657–64. doi:10.1007/s00345-015-1661-x.
2. Golberg A, Bruinsma BG, Uygun BE, et al. Tissue heterogeneity in structure and conductivity contribute to cell survival during irreversible electroporation ablation by "electric field sinks". Sci Rep. 2015;16(5):8485.
3. Neal RE 2nd, Millar JL, Kavnoudias H, et al. In vivo characterization and numerical simulation of prostate properties for non-thermal irreversible electroporation ablation. Prostate. 2014;74(5):458–68.
4. Kranjc M, Markelc B, Bajd F, et al. In situ monitoring of electric field distribution in mouse tumor during electroporation. Radiology. 2015;274(1):115–23.
5. Takagi K, Nanashima A, Abo T, et al. Three-dimensional printing model of liver for operative simulation in perihilar cholangiocarcinoma. Hepatogastroenterology. 2014;61(136):2315–6.
6. Priester A, Natarajan S, Le JD, et al. A system for evaluating magnetic resonance imaging of prostate cancer using patient-

specific 3D printed molds. Am J Clin Exp Urol. 2014;2(2):127–35.
7. Pati F, Gantelius J, Svahn HA. 3D bioprinting of tissue/organ models. Angew Chem Int Ed Engl. 2016;55(15):4650–65.
8. Knowlton S, Onal S, Yu CH, et al. Bioprinting for cancer research. Trends Biotechnol. 2015;33(9):504–13.
9. Jung V, Saar M, Grobholz R, et al. Development of a three-dimensional primary prostate cancer cell culture model. Urologe A. 2008;47(9):1199–204.
10. Priester A, Natarajan S, Le JD, et al. A system for evaluating magnetic resonance imaging of prostate cancer using patient-specific 3D printed molds. Am J Clin Exp Urol. 2014;2(2):127–35.
11. Korsager AS, Fortunati V, van der Lijn F, et al. The use of atlas registration and graph cuts for prostate segmentation in magnetic resonance images. Med Phys. 2015;42(4):1614–24.

8.10

Irreversible Electroporation (IRE): Standardization of Terminology and Reporting Criteria for Analysis and Comparison.

Wendler JJ, Fischbach K, Ricke J, Jürgens J, Fischbach F, Köllermann J, Porsch M, Baumunk D, Schostak M, Liehr UB, Pech M.

Pol J Radiol. 2016 Feb 17;81:54-64.

BACKGROUND: Irreversible electroporation (IRE) as newer ablation modality has been introduced and its clinical niche is under investigation. At present just one IRE system has been approved for clinical use and is currently commercially available (NanoKnife® system). In 2014, the International Working Group on Image-Guided Tumor Ablation updated the recommendation about standardization of terms and reporting criteria for image-guided tumor ablation. The IRE method is not covered in detail. But the non-thermal IRE method and the NanoKnife System differ fundamentally from established ablations techniques, especially thermal approaches, e.g. radio frequency ablation (RFA).

MATERIAL/METHODS: As numerous publications on IRE with varying terminology exist so far - with numbers continuously increasing - standardized terms and reporting criteria of IRE are needed urgently. The use of standardized terminology may then allow for a better inter-study comparison of the methodology applied as well as results achieved.

RESULTS: Thus, the main objective of this document is to supplement the updated recommendation for image-guided tumor ablation by outlining a standardized set of terminology for the IRE procedure with the NanoKnife Sytem as well as address essential clinical and technical informations that should be provided when reporting on IRE tumor ablation.

CONCLUSIONS: We emphasize that the usage of all above recommended reporting criteria and terms can make IRE ablation reports comparable and provide treatment transparency to assess the current value of IRE and provide further development.

Signature: © Pol J Radiol, 2016; 81: 54-64
DOI: 10.12659/PJR.896034

Polish Journal of Radiology
www.PolRadiol.com
ORIGINAL ARTICLE

Received: 2015.09.20
Accepted: 2015.09.22
Published: 2016.02.17

Irreversible Electroporation (IRE): Standardization of Terminology and Reporting Criteria for Analysis and Comparison

Authors' Contribution:
A Study Design
B Data Collection
C Statistical Analysis
D Data Interpretation
E Manuscript Preparation
F Literature Search
G Funds Collection

Johann J. Wendler[1ABCDEF], Katharina Fischbach[2E], Jens Ricke[2B], Julian Jürgens[2B], Frank Fischbach[2BC], Jens Köllermann[3BC], Markus Porsch[1D], Daniel Baumunk[1DF], Martin Schostak[2A], Uwe-Bernd Liehr*[1AE], Maciej Pech*[2AE]

* These authors contributed equally
[1] Department of Urology, University of Magdeburg, Magdeburg, Germany
[2] Department of Radiology, University of Magdeburg, Magdeburg, Germany
[3] Department of Pathology, Sana Klinikum Offenbach a. M., Offenbach Am Main, Germany

Author's address: Johann J. Wendler, Department of Urology, University of Magdeburg, Magdeburg, Germany, e-mail: johann.wendler@med.ovgu.de

Summary

Background: Irreversible electroporation (IRE) as newer ablation modality has been introduced and its clinical niche is under investigation. At present just one IRE system has been approved for clinical use and is currently commercially available (NanoKnife® system). In 2014, the International Working Group on Image-Guided Tumor Ablation updated the recommendation about standardization of terms and reporting criteria for image-guided tumor ablation. The IRE method is not covered in detail. But the non-thermal IRE method and the NanoKnife System differ fundamentally from established ablations techniques, especially thermal approaches, e.g. radio frequency ablation (RFA).

Material/Methods: As numerous publications on IRE with varying terminology exist so far – with numbers continuously increasing – standardized terms and reporting criteria of IRE are needed urgently. The use of standardized terminology may then allow for a better inter-study comparison of the methodology applied as well as results achieved.

Results: Thus, the main objective of this document is to supplement the updated recommendation for image-guided tumor ablation by outlining a standardized set of terminology for the IRE procedure with the NanoKnife Sytem as well as address essential clinical and technical informations that should be provided when reporting on IRE tumor ablation.

Conclusions: We emphasize that the usage of all above recommended reporting criteria and terms can make IRE ablation reports comparable and provide treatment transparency to assess the current value of IRE and provide further development.

MeSH Keywords: Ablation Techniques • Current Procedural Terminology • Electroporation • Irreversible Electroporation • Reference Standards • Research Design • Therapy, Soft Tissue

PDF file: http://www.polradiol.com/abstract/index/idArt/896034

Background

Focal ablation therapy is playing an increasingly important role in oncology and may reduce risks and toxicity of current surgical and radiation treatments while achieving complete tumor destruction with an adequate oncologic outcome. Newer ablation modalities, such as irreversible electroporation (IRE), have been introduced and their respective clinical niches are under investigation [1–6]. IRE causes cell death through the repeated application of short-duration high-voltage electrical pulses that create irreversible damage to cell membranes by electrical breakdown of the cell membrane [7]. While there may be some hyperthermic ablative changes with

high-power applications, the mechanism of cell death with IRE is thought to be predominantly non-thermal [7,8]. Nonthermal ablative irreversible electroporation has been proposed to be "tissue-selective" by leading to apoptosis without affecting the extracellular matrix with potential advantages compared with current thermal-ablation technologies or radiotherapy. Therefore matrix-based tissue borders and surrounded structures can be preserved [7,8]. At present only one IRE system has been approved for clinical use and is currently commercially available (NanoKnife® system; AngioDynamics Inc.). In 2007, NanoKnife® received a 510(k) medical product clearance for surgical ablation of soft tissue by the U.S. FDA. However, it has not been cleared for the treatment of any specific disease or condition and the treatment parameters have been mostly developed in *ex vivo* models, particularly the liver model [9]. Thus far there are no adequate tumor entity-specific proofs of its effectiveness, and its clinical application has hitherto been confined to very small patient cohorts.

In 2014, the International Working Group on Image-Guided Tumor Ablation updated the recommendation about standardization of terms and reporting criteria for image-guided tumor ablation [10]. The main objective of this document is to improve precision in communication in the field of image-guided tumor ablation, leading to a more accurate comparison of technologies, results, and ultimately to improved patient outcomes. Herein, they outlined a standardized set of general terminology to be used and essential clinical and technical information that should be provided when reporting on tumor ablation. The IRE method is not covered in detail. As numerous publications on IRE with varying terminology exist so far – with numbers continuously increasing – standardized terms and reporting criteria of IRE are needed urgently. The use of standardized terminology may then allow for a better inter-study comparison of the methodology applied as well as results achieved. Hence, parameters for successful ablation may be identified and undesired side effects such as reversible electroporation or thermal ablation may be detected when performing a meta-analysis and looking at larger patient collectives.

Material and Methods

Whereas the NanoKnife-System manual explains general conditions for use, the efficacy of several service parameters has not been studied extensively in prospective clinical studies [11]. Additionally, the specific terminology used does not comply entirely with the updated recommendations of the International Working Group on Image-Guided Tumor Ablation and dedicated reporting criteria are completely missing. Last but not least, the IRE method and the NanoKnife System differ fundamentally from established ablation techniques, especially thermal approaches (e.g. RFA) [12,13]. Otherwise, IRE efficacy will be compared with thermal ablation techniques, mainly RFA, as the most prevalent technique [12,13].

Thus, the main objective of this document is to supplement the updated recommendation for image-guided tumor ablation [10] by outlining a standardized set of terminology for the IRE procedure with the NanoKnife Sytem as well as address essential clinical and technical information that should be provided when reporting on IRE tumor ablation.

Results

General terminology for IRE ablation

According to the proposal for standardization of terms and reporting criteria for image-guided tumor ablation by the International Working Group on Image-Guided Tumor Ablation [10], classifying terminology for IRE is defined:

IRE as '**energy-based ablation method**' is used as '**focal therapy**' (FT) for localized soft '**tissue ablation**' (TA), usually under image guidance. IRE or '**IRE ablation**' is based on a '**nonthermal ablation mechanism**'. Decisive of that is the '**electrical conductivity**' of the target tissue that mainly depends on the tissue entity, tissue homogeneity and anatomical structures. In case of tumor ablation '**malignant tissue**' and '**non-malignant tissue**' can be treated. IRE ablation of malignant tumor mainly focused on debulking should be classified as treatment with '**debulking intent**' compared to treatment with '**curative intent**' or '**palliative (symptomatic) intent**'. IRE,with debulking intent (tumor downsizing) could be used as '**neoadjuvant pre-surgical treatment**' to achieve negative resection margins (R0 resection, curative intent), especially close to vital structures that have to be preserved [5,14,15].

The specific tumor which is supposed to be treated with IRE is called '**target tumor**'. The term '**targeting**' is used to describe the step during an IRE ablation procedure that involves placement of the electrodes into the tumor. The applicators for IRE are electrodes and should be addressed as such; the term 'probes' of the NanoKnife system manual [11] should not be used. The term '**needle-like electrodes**' needs to be further specified with respect to diameter (in '**Gauge' [G]**) and length (in centimeters [cm]). IRE can be performed with one '**bipolar (single) electrode**' applicator or with two to six '**monopolar (single) electrode**' applicators, whereby two electrodes constitute one '**monopolar electrode pair**'. The length of the '**exposure**' of the monopolar IRE NanoKnife system electrodes can be manually changed and should be described as the '**active tip length**' (Figure 1).

The monopolar electrodes are usually placed in '**multipolar applicator insertions**'. One 'IRE procedure' as a single event (operation) is counted as one '**IRE session**' (number of procedures = number of IRE sessions). If more than one 'IRE ablation' is performed during one IRE session, this series of IRE ablation is called '**IRE course of treatment**'. Monitoring of IRE ablation by imaging, the process by which the IRE therapy effects with its definitive extent and effectiveness are viewed during the procedure, is not yet available. The term '**intraprocedural modification**' is used to describe the intraprocedural tools and techniques that are used to perform intraprocedural modification of the ablation treatment. Up to now there is only one approved NanoKnife system-based tool to monitor the IRE treatment by reviewing the IRE current graphs to determine the overall current draw after each completed IRE course (see also Reporting Criteria and Figure 2). An

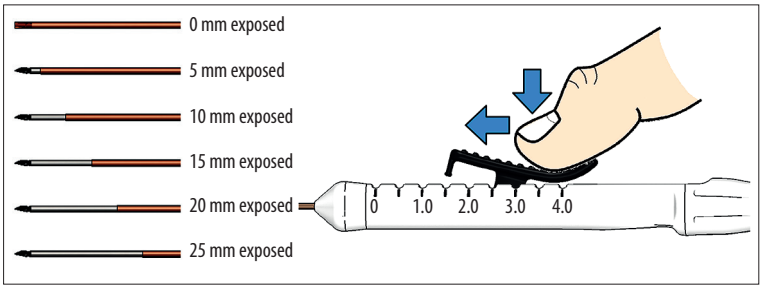

Figure 1. The active tip length of the monopolar IRE electrodes of the NanoKnife system can be manually changed in exposure.

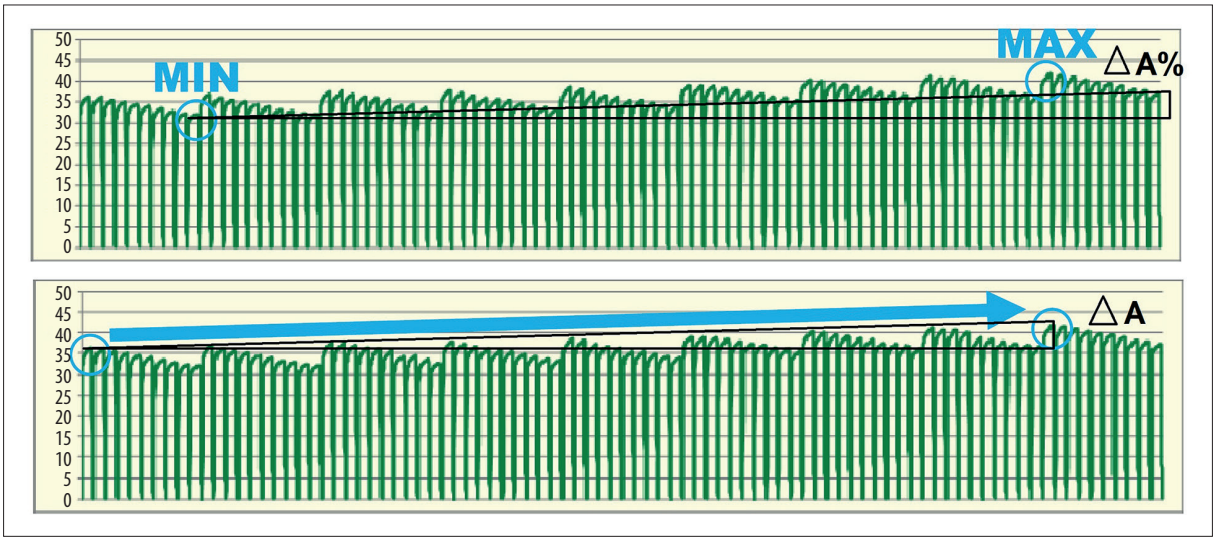

Figure 2. Output of current graphs with 9 clusters of 10 pulses each of 1 electrode pair for 1 IRE round. Marking the bottom and the peak of one cluster of 10 pulses. One can deduce a successful IRE ablation by reviewing the current graphs for an overall upward trend for each probe pair and for a slightly angled upwards cluster plateau (blue arrow in Figure 2). 1 Cluster of 10 pulses – small bracket. 1 session of 1 electrode pair with 9 clusters resp. 90 pulses – 1 burst – large bracket.

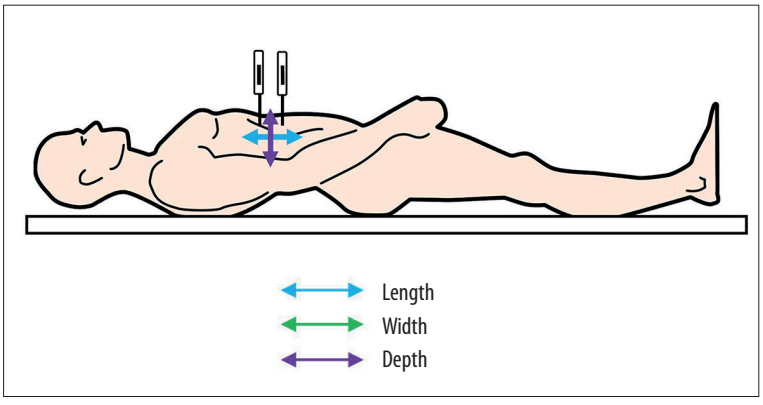

Figure 3. Specification of the tumor size in three anatomical dimensions of the patient´s body (sagittal – depth, transversal – width and longitudinal – length) in order to make follow-up measurements systematically comparable.

automated system that automatically terminates the ablation at a critical point in the IRE procedure is still not available.

The preferred term for the initially identified tumor prior to IRE ablation is '**index tumor**'. The term 'lesion' should not be used. CT and MRI are the best currently available and reproducible methods to measure target lesions (tumor) selected for response assessment [16]. When the primary endpoint of the study is objective response evaluation, ultrasound (US) should not be used to measure tumor lesions. In diagnostics and follow-up of oncologic patients, CT or MRI are the commonly used methods that enable 3D measurements of the targets, even if IRE is not performed under CT guidance but sonography guidance. The WHO (1979) and RECIST (2000) criteria were introduced to unify and standardize therapy response or course of disease in the studies [16]. The WHO criteria use 2D and RECIST 1D measurements. However, widespread use of multidetector CT, MR imaging, and post-imaging processing procedures enables to view targets from any arbitrary plane and even to measure the volume three-dimensionally (3D measurement) [16]. To evaluate studies of the new and very complex Nanoknife IRE ablation technique, a 3D measurement should be adopted. The IRE ablation zone diameters depend on the intraindividual IRE electrode and ablation settings (number and

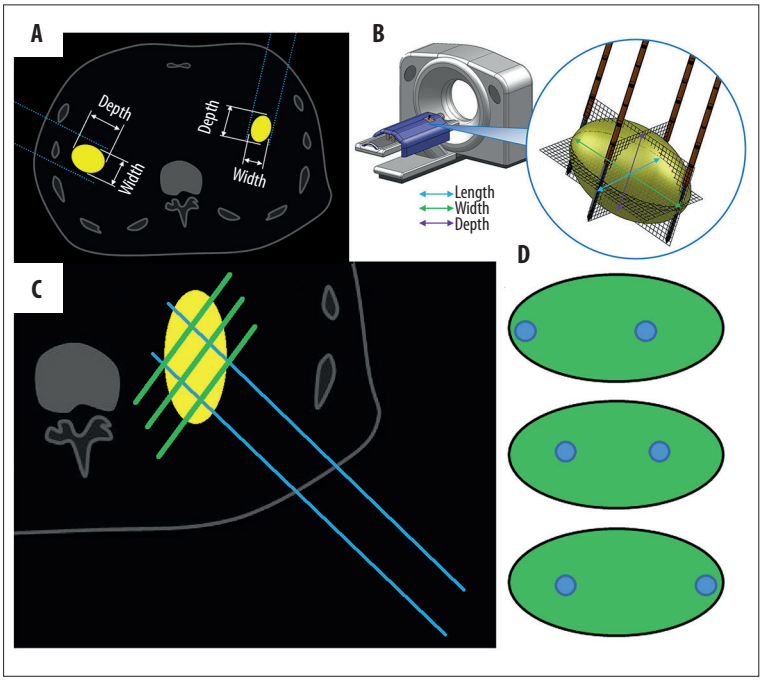

Figure 4. (**A, B**): The sketch of description of the IRE electrode-based tumor dimensions. Idealized coaxial IRE electrode placement in elliptic tumors. Green line in Figure 4A – IRE treatment planning sectional plane (2D) according to Figure 3. (**C, D**): Required oblique-angled IRE electrode placement in an elliptic tumor. Green lines in Figure 4C – different IRE treatment planning sectional planes (2D) in Figure 4D according to Figure 3 depending on the sectional plane level.

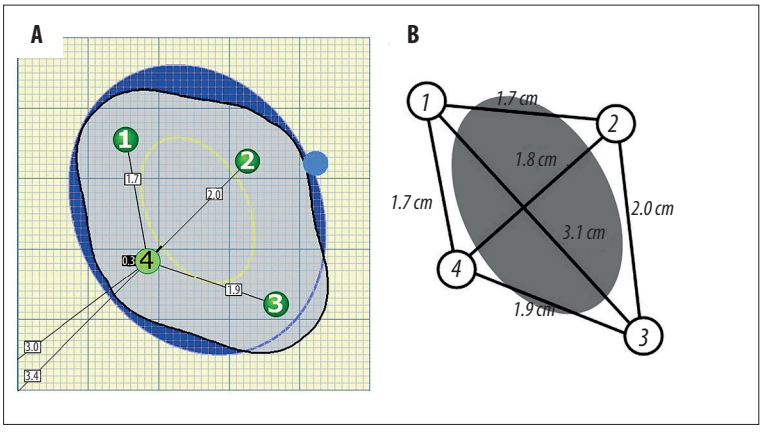

Figure 5. The sketch of monopolar IRE ablation with all interelectrode spacings and spacings between the electrodes (numbered green dots) and the shortest distance to the tumor margin (targeted edge, yellow circle).

position of electrodes, active tip/ exposure, voltage setting, overlapping ablation) in all three dimensions. Therefore, in IRE trials and publications, the actual tumor sizes should be specified in three anatomical dimensions of the patient´s body (sagittal, transversal and longitudinal) as well as in their maximum diameter in order to make follow-up measurements systematically comparable (Figure 3).

Moreover, the IRE ablation index tumor size should be reported in one dimension coaxial to the IRE electrode direction and in the other two vertical dimensions in order to make the extent of the index tumor compared to the 2D visualization of the estimated '**ablation zone**' comprehensible (see also Reporting Criteria and Figures 4, 5). The NanoKnife manual and software terminology uses the term '**estimated ablation zone**' (Figure 6) to describe the treatment zone that is visualized in 2D only. The term '**ablation zone**' should be used after ablation of the target index tumor. Therefore, the term 'estimated ablation zone' should be replaced by '**planned treatment zone**' **(PTV)**. The IRE index tumor should be classified according to the Standardization of Terms and Reporting Criteria for Image-Guided Tumor Ablation by the International Working Group on Image-Guided Tumor Ablation in the following scale: tumors <3 cm as 'small', tumors of 3–5 cm as 'intermediate', and tumors >5 cm as 'large'.

The '**planned treatment volume (PTV)**' consists of the '**target volume**' (= tumor) and the **circumferential** '**ablative margin**' that should be described separately. The term '**ablative IRE margin**' ('margin'), analogous to the surgical margin, is used to describe the region around the target that should ideally be ablated. At present, the ideal peritumoral IRE margin size is still under investigation and thus no definite recommendation can be made. Guidelines for (thermal) ablation methods recommend that the target tumor should be completely covered by the ablation zone that includes at least a 5–10-mm margin all around the expected tumor margin, in order to be considered successful ablation. The presence of micrometastases around the index tumor has to be taken into account [17]. As long as no specific data for IRE exist, this recommendation should be adopted at the minimum likewise. The thickness of that **margin** around the tumor can be adjusted per NanoKnife system

Table 1. Recommended IRE electrode settings for different tumor sizes based on calculations of IRE treatment planning using the PC-based NanoKnife® planning software demo tool (ProcedureManager-2_2_0_23 for Windows, AngioDynamics) for spherical masses and an approx. 5-mm safety ablation margin orthogonal to the electrodes. The ablation margin longitudinal to the electrodes (depth) is 5 mm as specified by the manufacturer [11].

Index tumor size [mm]	8	10	13	15	18	20	23	25	28	30	33	35	38	40
Margin circumferential (example) [mm]	5	5	5	5	5	5	5	5	5	5	5	5	5	5
Width of target zone, orthogonal to probes [mm]	18	20	23	25	28	30	33	35	38	40	43	45	48	50
Probe configuration	2	3	3	3	3	3	4	4	4 or 5 (DIE FACE-5)	6 (pentagonal with center)	6 (pentagonal with center) alternative: 5 + OL (mirrored trapezoid)	5 + OL (mirrored trapezoid) alternative: 6 (pentagonal with center)	5 + OL (mirrored trapezoid)	5 + OL (mirrored trapezoid)
Active tip, electrode exposure [mm], Pull-back (PB)	10, no PB	10–15, no PB	15, no PB	15–20, no PB	20, no PB	20–25, no PB	25, no PB	15, 1×PB	15, 1x PB	20, 1×PB	20, 1x PB	20, 1×PB	20-25, 1×PB	20-25, 1×PB
Depth of target zone, longitudinal to probes [mm]	20	20–25	25	25–30	30	30–35	35	Variable due to PB	Variable due to PB	Variable due to PB	Variable due to PB	Variable due to PB	Variable due to PB	Variable due to PB

Ablation zones reach a more or less spherical shape depending on the electrode count, probe configuration, tissue conductivity and technical conditions. PB – pull-back of the probes. OL – overlapping ablation.

software (Figure 6). This setting just serves the visualization of NanoKnife IRE treatment planning (target zone, margin zone) and orientation for IRE electrode configuration only. It differs from the estimated ablation zone depending on the electrode setting (Figure 6). The aim of IRE ablation is a complete coverage of the tumor zone (yellow) and as far as possible of the margin zone (blue) by the estimated ablation zone (grey). The coaxial dimension to the IRE electrode direction is named '**depth**' of the target zone and is not visualized in the NanoKnife system planning software.

The ideal electrode configuration depends on the tumor size and aimed ablation margin. Fixed IRE electrode configuration settings for tumor categories in 5–10-mm increments are not practicable. Due to the complex and parallel image-guided IRE electrode placement, the aim is to receive complete tumor ablation with the smallest possible ablation margin and as few as possible electrodes. The following table (Table 1) provides recommended IRE electrode settings according to the NanoKnife System Manual and the NanoKnife System Treatment planning software.

IRE ablation method reporting criteria

As treatment criteria the '**operating room time (OR)**', the '**operating time (OT)**' between first electrode insertion and last electrode removal, the IRE '**electrode placement time (EPT)**', the '**application time (AT)**' of the IRE pulse application, the general anaesthesia or intubation time between the beginning and ending should be reported separately. In the complex setting of IRE ablation the anaesthesia, the electrode placement time (EPT) and the duration of intraprocedural modification or treatment planning take up most of the time of the operation room time (ORT) and operating time (OT) compared to the IRE pulse application time.

The IRE pulse application speed (pulse per minute = ppm) has to be mentioned according to the eligible options 90 ppm, 240 ppm or ECG-triggered, whereas the heart rate for ECG triggering has to be reported. A pulse frequency of 240 ppm is not recommended anymore (unpublished data) due to possible thermal ablation effects (unpublished data, no official distributor statement).

The IRE ablation index tumor size (yellow ellipsoid) should be reported in one dimension coaxial **(depth)** to the IRE electrode direction (blue dotted lines) and in the other two vertical dimensions (width and length) in order to make the extent of the index tumor compared to the ablation zone comprehensible according to Figure 6 (Figure 4A, 4B). Figure 4A and 4B show idealized situations whereby the longest diameter of an elliptic tumor is parallel/coaxial to the IRE electrodes. It is getting more difficult if placement of an oblique-angled IRE electrode is required (Figure 4C, 4D). Different diameter and distances have to be taken into account.

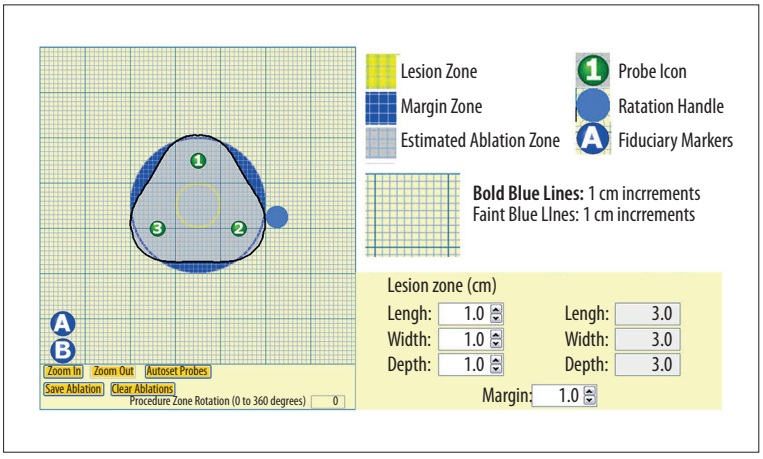

Figure 6. The planning margin (blue area) around the tumor ('lesion zone', yellow circle) can be adjusted initially per NanoKnife software (right down) for visualization of NanoKnife IRE treatment planning (grey triangular area) and orientation for IRE electrode configuration (numbered green spots). The named term 'lesion' should not be used; the term 'tumor' should be used instead. The discrepancy between the term `lesion' of the NanoKnife system manual and the recommended term 'tumor' by the International Working Group on Image-Guided Tumor Ablation may result from the received clearance for surgical ablation of soft tissues in general but not for tumor exclusively.

The electrode positions and the treatment planning (target) zone have to be reported reproducibly in relation to the tumor location to analyze possible incomplete tumor ablations (positive margin or skip lesions). That complex situation is getting obvious for IRE application per monopolar IRE electrodes: For the use of monopolar IRE electrodes, all electrodes have to be numbered, whereas the IRE activator electrode should be labeled as IRE electrode 1. For monopolar IRE ablation all inter-electrode spacings have to be mentioned (Figure 5). Moreover, all spacings between the electrodes and the shortest distance to the tumor margin (targeted edge) have to be documented (Figure 5). All these parameters should be reported in a figure (Figure 5).

A basic problem of the visualization of the IRE treatment planning (Figures 5, 6) is the depiction of the transverse plain (just 2D) to the IRE electrodes by the NanoKnife System Software only. The depth of the target and the active tips of the electrodes are not depicted.

The term '**IRE ablation zone**' can be used to describe the radiologic region or zone of induced treatment effect. Reporting of the ablation zone should be made in the transversal plain of the electrode axis with relation to the target tumor and planned treatment zone, if possible. According to the ablation zone, ablation should be classified as complete or partial, whereas the report on the degree (percentage) of partial ablation should be avoided. Intermediate or large targets can be treated with overlapping IRE ablations. The term '**overlapping IRE ablation**' is used for the creation of a complex overlapping ablation zone in the transversal plane of the electrode axis (Figure 7A). The term '**pull-back IRE ablation**' is used for the creation of a complex overlapping ablation zone in the coaxial axis of the electrodes by using ablation zones behind one another with pulling the electrodes back stepwisely and applicating IRE ablation again (Figure 7B). Pull-back IRE ablation seems to be very intricate and not very practicable even with electrode length markings, especially in cases of small margins and small overlapping ablation zones.

Needle tract seeding has thus far been described by Ricke et al. [4] after IRE of lung tumors and by Fredericks et al. [18] after IRE of colorectal carcinomas. A higher rate of needle tract seeding after IRE than after RFA is under discussion. The risk of seeding is reduced in RFA by thermal ablation of the needle tract, a technique that IRE cannot utilize [18]. In IRE with the NanoKnife system, the cover is pulled back at the electrode (as an active tip) in the tumor before insertion. The tip should be covered again on withdrawal. However, it is unclear whether this would reduce the risk of seeding [4]. A higher needle tract tumor seeding for pull-back IRE ablation should be discussed. If a complex IRE ablation with coaxial overlapping in the electrode axis is necessary, we propose a '**push-forward IRE ablation**' instead of the pull-back ablation to reduce the hypothetical risk of needle tract tumor seeding (Figure 7C).

Micrometastases close to the primary index tumors or macrometastases have been observed in different entities that had been seeded from the primary index tumor or originated from the macrometastatic lesions as satellite lesions [17].

For different IRE sessions in one IRE course of treatment different electrode pairs can be selected as an intraprocedural modification (Figure 8). Here, for example, only 3 IRE electrode pairs can be selected for IRE ablation in spite of 4 inserted IRE electrodes and 6 possible IRE electrode pairs. IRE electrode pairs should be recorded as a cathode (P–) and anode (P+) analogous to the pulse parameter table (Figure 8). Before starting IRE ablation the user can set the number of pulses in the pulse parameter table. The NanoKnife system tests automatically each electrode pair with one '**test pulse**' application with reduced voltage. We recommend applying each 10 test pulses (1 '**test run**') with the aimed planning voltage set in the pulse parameter table in order to check for a high current risk within that planning voltage setting (Figure 8). The number of IRE pulses can be adjusted in a group of ten pulses (decadic), where 10 pulses count as 1 '**IRE pulse cluster**' (10 pulses = 1 cluster). The number of clusters can be set up to nine for one session per pair (9 clusters = 90 pulses) (Figure 2). The terms 'burst' and 'train' are not common for IRE description. But the term 'IRE cluster' is similar to 'RFA train'. All clusters of one IRE session for one electrode pair can be described as one '**IRE burst**', analogous to 'RFA burst'.

Up to now, there has been only one approved NanoKnife-based tool to monitor the IRE treatment for

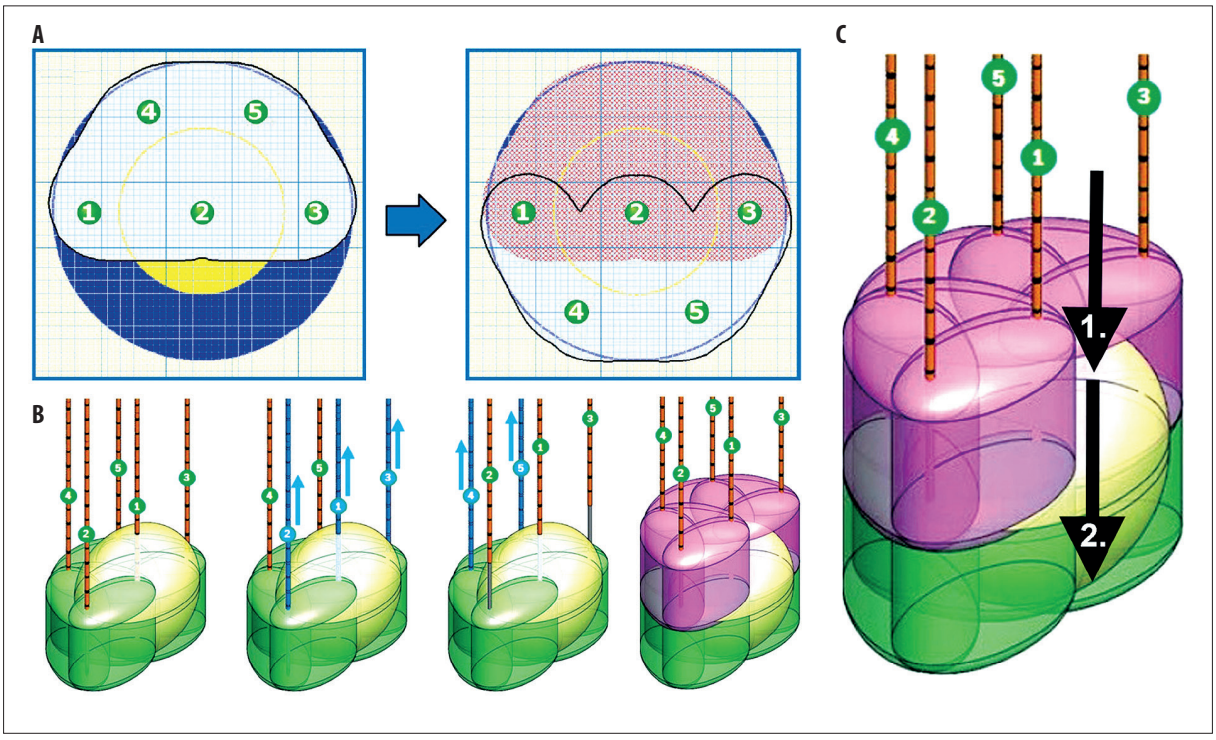

Figure 7. Overlapping IRE ablation (**A**). Pull-back IRE ablation (**B**). Push-forward IRE ablation (**C**).

	P+	P–	Voltage	Pulse length	Num Pulses	V/cm	Distance
	1	2	2550	90	70	1500	1.7
▶	1	3	3000	90	70	1500	3.1
	2	3	3000	90	70	1500	2.0
	3	4	2850	90	70	1500	1.9
	4	1	2550	90	70	1500	1.7
	2	4	3000	90	70	1500	2.0

Adjust Dist Apply

Figure 8. IRE NanoKnife pulse parameter table. Cathode (P–) and anode (P+). The current direction between the IRE electrodes can be adjusted for each electrode pair during IE treatment planning (table column anode [P+] and cathode [P–]). The relevance between the current direction and the grade of IRE ablation has not been still examined systematically – especially for overlapping ablations and centrifugal plus peripheral-concentric ablation for 5–6 electrodes with one central electrode.

intraprocedural modification by reviewing the '**IRE current graphs**' to determine the overall current draw after each completed IRE course (Figure 2). Reviewing the '**IRE result graphs**' is recommended upon the completion of each IRE ablation before removing or repositioning the IRE electrodes. The result graphs should be assessed for abnormalities which may require an additional ablation session. An automated system that automatically terminates the ablation at a critical point in the IRE procedure is still not available. The graphs display the voltage output and the current output of each pulse delivered between all probe pairs (Figure 2). For a successful IRE ablation an output of uniform voltage graphs within each probe pair's results should be reported. By reviewing the current graphs for an overall upward trend for each probe pair and for a slightly angled upwards cluster plateau (blue arrow in Figure 2), one can deduce a successful IRE ablation. This indicates a decrease in soft-tissue resistance throughout the pulse delivery. A flat trend does not indicate an unsuccessful pulse delivery (only the area may have been previously ablated within this course of treatment). Current draws exceeding 45 Amps may lead to high current conditions during a subsequent ablation with undesirable thermal ablation.

The range of minimum and maximum current of each IRE electrode pair for each session ('**session pair current range**') should be reported as IRE ablation method

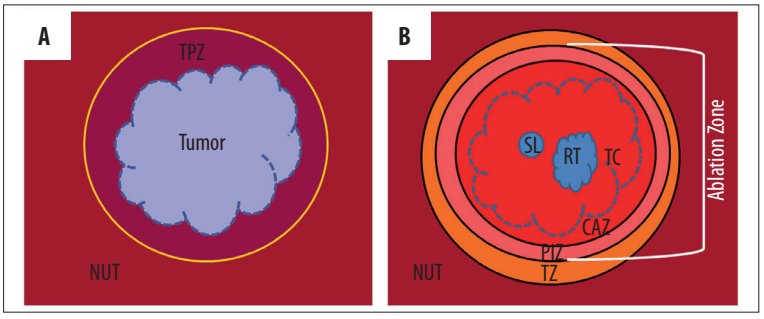

Figure 9. Pre-IRE description (**A**): NUT – natural untreated tissue, TPZ – treatment planning zone. Post-IRE description (**B**): NUT – natural untreated tissue, TZ – transition zone, PIZ – peripheral inflammation zone, CAZ – central ablation zone, TC – tumor contour, RT – residual tumor, SL – skip lesion, CAZ + PIZ – ablation zone.

Table 2. IRE method reporting criteria with reporting data example (fictive) of 1 IRE ablation in 1 IRE session/course of treatment for 1 target with intraprocedural modification.

Patient	Tumor/target	Ablation	Round	No. of electrode	Intraprocedural modification	Active tip [mm]	Sketch electrode configuration	Electrode configuration	Electrode – tumor-margin distance [mm]	Electrode end/tip – tumor margin distance [mm]	Electrode pairs	Current flow direction [– > +]	Inter-elec-trode space [mm]	Voltage setting [V/cm]	Voltage Setting Total [V]	Pulse length [µs]	No of pul-ses	Application -speed [bpm]	E [kJ]	ΔA burst [A]	ΔA% burst [A]
1	1	1	0	1	Test	20		Trape-	1–R: +3	1T–R:	1–2	1+>2–	20	1500	3000	90	10	HR	X	–	–
				2		20		zoid/	2–R: +2	+1	2–3	2+>3–	17	1700	2890	90	10	HR	X	–	–
				3		20		square	3–R: 0	2T–R:	3–4	3+>4–	15	1800	2700	90	10	HR	X	–	–
				4		20			4–R: 0	+2	1–3	1+>3–	21	1450	3000	90	10	HR	X	–	–
										3T–R: 0	1–4	1+>4–	20	1500	3000	90	10	HR	X	–	–
										4T–R:	2–4	2+>4–	22	1300	2860	90	10	HR	X	–	–
										+1											
			1	1	Pulse	20		Trape-	1–R: +3	1T–R:	1–2	1+>2–	20	1500	3000	90	70	HR	X	X	X
				2	Count	20		zoid/	2–R: +2	+1	2–3	2+>3–	17	1700	2890	90	70	HR	X	X	X
				3		20		square	3–R: 0	2T–R:	3–4	3+>4–	15	1800	2700	90	70	HR	X	X	X
				4		20			4–R: 0	+2	1–3	1+>3–	21	1450	3000	90	70	HR	X	X	X
										3T–R: 0	1–4	1+>4–	20	1500	3000	90	70	HR	X	X	X
										4T–R:	2–4	2+>4–	22	1300	2860	90	70	HR	X	X	X
										+1											
			2	1	Pull-	20		Trape-	1–R: +5	1T–R:	1–2	1+>2–	20	1500	3000	90	70	HR	X	X	X
				2	back	20		zoid/	2–R: +3	–14	2–3	2+>3–	17	1700	2890	90	70	HR	X	X	X
				3	–15	20		square	3–R: +2	2T–R:	3–4	3+>4–	15	1800	2700	90	70	HR	X	X	X
				4	Mm	20			4–R: +2	–13	1–3	1+>3–	21	1450	3000	90	70	HR	X	X	X
										3T–R:	1–4	1+>4–	20	1500	3000	90	70	HR	X	X	X
										–15	2–4	2+>4–	22	1300	2860	90	70	HR	X	X	X
										4T–R:											
										–14											
1	1	1	Total (3 rounds):	4	Pull-	20	–	Trape-	Min:	+Max:	6	–	Min:	Min:	Min:	90	900	HR	X	X	X
					Back			zoid/	0Max:	+2			15	1300	2700						
								square	+5	–Max:			Max:	Max:	Max:						
										–15			22	1800	3000						
													Med:	Med:	Med:						
													19	1540	2900						

reporting criteria. Moreover, the difference between the maximum current of the first cluster and the maximum current of the last cluster of each IRE electrode pair of each session (blue arrow in Figure 2) should be reported ('**session pair current delta**'). Due to the claimed increase, this difference of each burst should be reported in case of a positive increase (+) or a negative decrease (–), as well as reported as delta Ampere **[ΔA burst]** and delta of percentage **[ΔA% burst]** of the current graph plateaus (Figure 2). The value of this delta may allow for drawing conclusions on IRE ablation success [4,11].

For IRE ablation method reporting, the following table with the mentioned variables should be reported in each publication (Table 2).

The NanoKnife system includes no automatically prepared report of the applied energy (Joule [J]) for each ablation. This makes the comparison with the applied energy of other ablation modalities impossible. A detailed, clinically oriented calculation of the electric energy of the electric field seems to be not practicable, but it is approximately possible. In a simplified case of a constant voltage per

electrode pair and constant current (level of current result graphs), the electric energy [E] can be calculated by the multiplication of the applied voltage [U], the applied current [I] and the total pulse length of all applied pulses [t]:

Example for 6 used IRE electrode pairs of one IRE session:
$Etotal = E1–2 + E2–3 + E3–4 + E1–4 + E2–4 + E1–3$
$= [(U_{1–2}) \times (I_{1–2}) \times number\ of\ pulses_{1–2} \times pulse\ length_{1–2}] +$
$[(U_{2–3}) \times (I_{2–3}) \times number\ of\ pulses_{2–3} \times pulse\ length_{2–3}] +$
$[(U_{3–4}) \times (I_{3–4}) \times number\ of\ pulses_{3–4} \times pulse\ length_{3–4}] +$
$[(U_{1–4}) \times (I_{1–4}) \times number\ of\ pulses_{1–4} \times pulse\ length_{1–4}] +$
$[(U_{2–4}) \times (I_{2–4}) \times number\ of\ pulses_{2–4} \times pulse\ length_{2–4}] +$
$[(U_{1–3}) \times (I_{1–3}) \times number\ of\ pulses_{1–3} \times pulse\ length_{1–3}].$

IRE pre-treatment and outcome reporting criteria

The difference between pathological findings and imaging findings of IRE ablation must be stressed by an appropriate selection of terminology. For ablation therapy, given that many tumors undergo central necrosis without ablation therapy, the term 'coagulation' is preferred over the use of 'necrosis', as it denotes that the ablation intervention actively leads to tumor destruction. The term '**coagulation**' should also be used to describe pathological findings caused by newer ablation technologies, such as microwave ablation and IRE, as well. The more generalized term 'coagulation' is preferred over the term '**coagulative necrosis**', as the latter has a well-defined meaning within the pathology literature including the absence of visible nuclei within the dead cells. When histopathological evaluation of the ablation zone is performed, tumor cells identified in morphologic stains (hematoxylin-eosin) should undergo additional evaluation with specialized immunohistochemical stains to determine the viability or irreversible cell death. The optimal method for specialized immunohistochemical stains for IRE coagulation has not been evaluated conclusively.

For histopathological description of the IRE ablation zone the terminology '**central ablation zone**' and '**peripheral inflammation zone**' should be used (Figure 9). This should be differentiated from the thickness of the IRE ablation '**transition zone**', which describes how much spatial zone resides between coagulative necrosis or dead tissue and normal/unaffected tissue (Figure 9). The true correlation and imaging of these zones have not been evaluated for imaging methods after IRE ablation conclusively. Residual tumor zones and skip lesions should be reported separately. The dimensions and locations of these zones or lesions are of special interest (Figure 9).

IRE ablation zones may show shrinkage of the ablation volume after IRE. The term '**involution**' should be used to describe this process over weeks to months. It is important to note that the lack of or minimal involution after IRE does not imply treatment failure. This is a finding that has been described for multiple thermal ablation modalities and IRE as well. Finally, a successful IRE ablation zone will be significantly larger than the target tumor and therefore traditional Response Evaluation Criteria in Solid Tumors, or RECIST, do not address successful ablation. Cicatrization may accompany involution, where nearby normal tissue is retracted toward the IRE treatment zone. The amount of contraction varies with ablation time.

Finally, zones of IRE coagulation often demonstrate spherical shapes, but can show variations in the cross-sectional axis which can introduce variability in ablation size measurements. A three-dimensional, or whenever possible, volumetric evaluation, should be performed to measure the IRE ablation zone according to both above mentioned measuring methods (Figures 3, 4).

The optimal follow-up imaging method after IRE ablation seems to be multiparametric MRI whenever possible. Previous IRE reports used different follow-up terms for outcome inhomogenously, especially for short-term imaging or histopathological data.

According to the proposal for standardization of the International Working Group on Image-Guided Tumor Ablation (a) technical success and early safety data should have a 6-month follow-up, (b) clinical outcome results up to 1 year of follow-up should be named as preliminary or short-term, (c) 1–5-year follow-up as intermediate-term, (d) and at least 5-year (and ideally longer) follow-up as long-term.

The '**primary IRE efficacy rate**' is defined as the percentage of target tumors successfully eradicated following the initial or IRE treatment (adequate ablation, '**local control**'). The '**secondary or assisted IRE efficacy rate**' is defined as including tumors that have undergone successful repeat IRE ablation following identification of '**local tumor progression**' ('**retreatment**').

The term '**IRE (technical) success**' should be used to report whether the tumor was treated according to the protocol. A tumor that is treated according to the protocol and covered completely (i.e. ablation zone completely overlaps or encompasses the target tumor with the ablative margin), as determined at the time of the procedure, is 'technically successful'.

The term '**IRE (technique) efficacy**' should be used to report whether the tumor was ablated effectively (local control). IRE efficacy can only be demonstrated with appropriate clinical follow-up, and should therefore refer to a prospectively-defined time point at which point 'complete ablation' of macroscopic tumor, as evidenced by imaging follow-up or histopathological analysis of a resection specimen or biopsies.

For IRE ablation outcome reporting, the following table with the mentioned variables of pre-treatment variables and outcome variables should be reported in each publication (Table 3).

Complication reporting

Complications should be stratified on the basis of the outcome by using the most recent version of the unified standardized SIR grading system of the Society of Interventional Radiology (SIR) [10,19]. The SIR grading system is the most commonly used complication-reporting system for interventional radiological procedures according to the severity of the complications. Alternative classifications exist, and can be used if a compelling reason is provided [10]. The

Table 3. Tabular IRE pre-treatment and outcome reporting criteria.

	Patient X
Pre-IRE data	
No. targets	
Tumor location/anatomy	
Pre-IRE tumor size, index tumor size [mm × mm × mm]	Length × width × depth
Pre-IRE tumor volume, index tumor volume [ccm]	Ellipsoid formula
Index tumor shape and class	
Biopsy histopathology	
Index tumor texture	Homogeneity?, solid?, cystic?, calcifications?
TNM	
Planned treatment zone size [mm × mm × mm]	Length × width × depth
Planned treatment zone volume [ccm]	Ellipsoid formula
Post-IRE data (histological)	
Ablation zone size [mm x mm x mm]	Length × width × depth
Ablation zone volume [ccm]	Ellipsoid formula
Post-IRE tumor contour/ structure size [mm × mm × mm]	Length × width × depth
Post-IRE tumor contour/ structure volume [ccm]	Ellipsoid formula
Tumor ablation degree	'Complete ablation' or 'partial ablation' (incomplete)
Regression grade (if available)	
Residual tumor zones	Number? location?
Post-IRE volume of histologically residual tumour [ccm]	Ellipsoid formula
Assessment method of viability of tumor tissue	
Skip lesions in the ablation zone	Number? location?
Difference of pre-post-IRE tumour volume [ccm]: Post – Pre	Negative value demonstrates involution with size reduction
Difference of pre-post-IRE tumour volume [%]: Post – Pre	Negative value demonstrates involution with size reduction
Difference of treatment planning zone volume and ablation zone volume [ccm]	

Common Terminology Criteria for Adverse Events (CTCAE) v4.0 of the National Cancer Institute [20] and the Clavien-Dindo Classification system [21] are commonly used systems in oncological and surgical practice. The CTCAE is the most detailed system for each symptom and organ system.

IRE, as a new treatment modality, will not be compared with different interventional procedures only, but with surgical therapies as well. Therefore, we propose using simultaneously the SIR grading system, the Clavien-Dindo Classification system and the CTCAE system [19–21].

Discussion

The original intent of this standardization of IRE terminology was to provide an appropriate vehicle for reporting the various aspects of image-guided IRE ablation therapy. Our intent continues to be to provide such a framework which would facilitate the clearest communication between investigators, and enable the greatest flexibility in comparisons in IRE ablation technology. We encourage all of our colleagues to adopt the terminology and reporting strategies outlined in this updated proposal to facilitate worldwide communication on scientific advances in IRE.

Conclusions

We would like to emphasize that using all the above recommended reporting criteria and terms can make IRE ablation reports comparable and provide treatment transparency to assess the current value of IRE and provoke further development.

Acknowledgements

All authors declare that they have no conflict of interest.

References:

1. Wendler JJ, Porsch M, Nitschke S et al: A prospective Phase 2a pilot study investigating focal percutaneous irreversible electroporation (IRE) ablation by NanoKnife in patients with localised renal cell carcinoma (RCC) with delayed interval tumour resection (IRENE trial). Contemp Clin Trials, 2015; 43: 10–19
2. van den Bos W, de Bruin DM, Muller BG et al: The safety and efficacy of irreversible electroporation for the ablation of prostate cancer: a multicentre prospective human *in vivo* pilot study protocol. BMJ Open, 2014; 4(10): e006382
3. Valerio M, Dickinson L, Ali A et al: A prospective development study investigating focal irreversible electroporation in men with localised prostate cancer: Nanoknife Electroporation Ablation Trial (NEAT). Contemp Clin Trials, 2014; 39(1): 57–65
4. Ricke J, Jürgens JH, Deschamps F et al: Irreversible electroporation (IRE) fails to demonstrate efficacy in a prospective multicenter phase II trial on lung malignancies: the ALICE trial. Cardiovasc Intervent Radiol, 2015; 38(2): 401–8
5. Paiella S, Butturini G, Frigerio I et al: Safety and feasibility of Irreversible Electroporation (IRE) in patients with locally advanced pancreatic cancer: results of a prospective study. Dig Surg, 2015; 32(2): 90–97
6. Martin RC, Schwartz E, Adams J et al: Intra – operative anesthesia management in patients undergoing surgical irreversible electroporation of the pancreas, liver, kidney, and retroperitoneal tumors. Anesth Pain Med, 2015; 5(3): e22786
7. Rubinsky B: Irreversible electroporation. 1st ed. Berlin: Springer, 2009; 328
8. Davalos RV, Bhonsle S, Neal RE II: Implications and considerations of thermal effects when applying irreversible electroporation tissue ablation therapy. Prostate, 2015; 75(10): 1114–18
9. Wendler JJ, Porsch M, Fischbach F et al: Letter to the Editor Concerning "Irreversible Electroporation (IRE) Fails to Demonstrate Efficacy in a Prospective Multicenter Phase II Trial on Lung Malignancies: The ALICE Trial" by Ricke et al. 2015. Cardiovasc Intervent Radiol, 2015; 38(4): 1064–65
10. Ahmed M, Solbiati L, Brace CL et al., International Working Group on Image-Guided Tumor Ablation; Interventional Oncology Sans Frontières Expert Panel; Technology Assessment Committee of the Society of Interventional Radiology; Standard of Practice Committee of the Cardiovascular and Interventional Radiological Society of Europe: Image-guided tumor ablation: standardization of terminology and reporting criteria – a 10-year update. J Vasc Interv Radiol, 2014; 25(11): 1691–705.e4
11. Manual NanoKnife® System Procedure & Trouble Shouting Guide. Software version 2.2.0. AngioDynamics®, © AngioDynamics, Inc., 2011; 1–159
12. Kang TW, Rhim H, Lee MW et al: Terminology and reporting criteria for radiofrequency ablation of tumors in the scientific literature: systematic review of compliance with reporting standards. Korean J Radiol, 2014; 15(1): 95–107
13. Crocetti L, de Baere T, Lencioni R: Quality improvement guidelines for radiofrequency ablation of liver tumours. Cardiovasc Intervent Radiol, 2010; 33(1): 11–17
14. Martin RC, Philips P, Ellis S et al: Irreversible electroporation of unresectable soft tissue tumors with vascular invasion: effective palliation. BMC Cancer, 2014;14: 540
15. Narayanan G, Bhatia S, Echenique A et al: Vessel patency post irreversible electroporation. Cardiovasc Intervent Radiol, 2014; 37(6): 1523–29
16. Suzuki C, Jacobsson H, Hatschek T et al: Radiologic measurements of tumor response to treatment: practical approaches and limitations. Radiographics, 2008; 28(2): 329–44
17. Nanko M, Shimada H, Yamaoka H et al: Micrometastatic colorectal cancer lesions in the liver. Surg Today, 1998; 28(7): 707–13
18. Fredericks C, Arslan B, Mullane M et al: Needle tract seeding following irreversible electroporation (IRE) of metastatic colorectal carcinoma to the liver. Cardiovasc Intervent Radiol, 2015; 38(5): 1349–51
19. Sacks D, McClenny TE, Cardella JF, Lewis CA: Society of Interventional Radiology clinical practice guidelines. J Vasc Interv Radiol, 2003; 14(9 Pt 2): S199–202
20. Common Terminology Criteria for Adverse Events (CTCAE) v4.0. National Cancer Institute. *http://evs.nci.nih.gov/ftp1/CTCAE/CTCAE_4.03_2010-06-14_QuickReference_5x7.pdf*
21. Clavien PA, Barkun J, de Oliveira ML et al: The Clavien-Dindo classification of surgical complications: five-year experience. Ann Surg, 2009; 250(2): 187–96

8.11

A prospective Phase 2a pilot study investigating focal percutaneous irreversible electroporation (IRE) ablation by NanoKnife in patients with localised renal cell carcinoma (RCC) with delayed interval tumour resection (IRENE trial).

Wendler JJ, Porsch M, Nitschke S, Köllermann J, Siedentopf S, Pech M, Fischbach F, Ricke J, Schostak M, Liehr UB.

Contemp Clin Trials. 2015 Jul;43:10-9.

INTRODUCTION: Focal ablation therapy is playing an increasing role in oncology and may reduce the toxicity of current surgical treatments while achieving adequate oncological benefit. Irreversible electroporation (IRE) has been proposed to be tissue-selective with potential advantages compared with current thermal-ablation technologies or radiotherapy. The aim of this pilot trial is to determine the effectiveness and feasibility of focal percutaneous IRE in patients with localised renal cell cancer as a uro-oncological tumour model.

METHODS: Prospective, monocentric Phase 2a pilot study following current recommendations, including those of the International Working Group on Image-Guided Tumor Ablation. Twenty patients with kidney tumour (T1aN0M0) will be recruited. This sample permits an appropriate evaluation of the feasibility and effectiveness of image-guided percutaneous IRE ablation of locally confined kidney tumours as well as functional outcomes. Percutaneous biopsy for histopathology will be performed before IRE, with magnetic-resonance imaging one day before and 2, 7, 27 and 112 days after IRE; at 28 days after IRE the tumour region will be completely resected and analysed by ultra-thin-layer histology.

DISCUSSION: The IRENE study will investigate over a short-term observation period (by magnetic-resonance imaging, post-resection histology and assessment of technical feasibility) whether focal IRE, as a new ablation procedure for soft tissue, is feasible as a percutaneous, tissue-sparing method for complete ablation and cure of localised kidney tumours. Results from the kidney-tumour model can provide guidance for designing an effectiveness and feasibility trial to assess this new ablative technology, particularly in uro-oncology.

Contemporary Clinical Trials 43 (2015) 10–19

Contents lists available at ScienceDirect

Contemporary Clinical Trials

journal homepage: www.elsevier.com/locate/conclintrial

A prospective Phase 2a pilot study investigating focal percutaneous irreversible electroporation (IRE) ablation by NanoKnife in patients with localised renal cell carcinoma (RCC) with delayed interval tumour resection (IRENE trial)

J.J. Wendler [a,*,1], M. Porsch [a], S. Nitschke [a], J. Köllermann [b,2], S. Siedentopf [c], M. Pech [d,1], F. Fischbach [d,1], J. Ricke [d,1], M. Schostak [a,2], U.B. Liehr [a,1,2]

[a] Department of Urology, University Hospital, Otto von Guericke University of Magdeburg, Germany
[b] Institute of Pathology, Sana Klinikum Offenbach, Offenbach am Main, Germany
[c] Institute of Pathology, University Hospital, Otto von Guericke University of Magdeburg, Germany
[d] Department of Radiology, University Hospital, Otto von Guericke University of Magdeburg, Germany

ARTICLE INFO

Article history:
Received 25 February 2015
Received in revised form 30 April 2015
Accepted 4 May 2015
Available online 9 May 2015

Keywords:
Focal therapy
Health technology assessment
Irreversible electroporation
Renal cell carcinoma
Renal mass
Ablation
Kidney

ABSTRACT

Introduction: Focal ablation therapy is playing an increasing role in oncology and may reduce the toxicity of current surgical treatments while achieving adequate oncological benefit. Irreversible electroporation (IRE) has been proposed to be tissue-selective with potential advantages compared with current thermal-ablation technologies or radiotherapy. The aim of this pilot trial is to determine the effectiveness and feasibility of focal percutaneous IRE in patients with localised renal cell cancer as a uro-oncological tumour model.

Methods: Prospective, monocentric Phase 2a pilot study following current recommendations, including those of the International Working Group on Image-Guided Tumor Ablation. Twenty patients with kidney tumour (T1aN0M0) will be recruited. This sample permits an appropriate evaluation of the feasibility and effectiveness of image-guided percutaneous IRE ablation of locally confined kidney tumours as well as functional outcomes. Percutaneous biopsy for histopathology will be performed before IRE, with magnetic-resonance imaging one day before and 2, 7, 27 and 112 days after IRE; at 28 days after IRE the tumour region will be completely resected and analysed by ultra-thin-layer histology.

Discussion: The IRENE study will investigate over a short-term observation period (by magnetic-resonance imaging, post-resection histology and assessment of technical feasibility) whether focal IRE, as a new ablation procedure for soft tissue, is feasible as a percutaneous, tissue-sparing method for complete ablation and cure of localised kidney tumours. Results from the kidney-tumour model can provide guidance for designing an effectiveness and feasibility trial to assess this new ablative technology, particularly in uro-oncology.

Abbreviations: BfArM, German Federal Institute for Drugs and Medical Devices; CE, Community of Europe; CRF, case report form; CT, computer tomography; DIMDI, German Institute of Medical Documentation and Information; DRKS, German Clinical Trials Registry; EAU, European Association of Urology; ECG, electrocardiogram; ECOG, Eastern Co-operative Oncology Group; EORTC, European Organisation for Research and Treatment of Cancer; EUDAMED, European Databank on Medical Devices; FACT, Functional Assessment for Cancer Therapy; FKSI, FACT Kidney Symptoms Index; GCP, Good Clinical Practice; ICTRP, International Clinical Trials Registry Platform; IIT, investigator-initiated trial; IRE, irreversible electroporation; IRENE, IRreversible Electroporation of kidney tumours before partial NephrEctomy; KKS, German network of co-ordination centres for clinical studies; MPG, German Medical Devices Act; MRI, magnetic-resonance Imaging; NIH, U.S. National Institute of Health; OVGU, Otto von Guericke University of Magdeburg Germany; QLQ, Quality-of-Life Questionnaire; RCC, renal cell carcinoma; SAE, severe adverse event; TSC, Trial Steering Committee; US, ultrasound; UTN, Universal Trial Number; WHO, World Health Organisation.

* Corresponding author at: Department of Urology, University Hospital, Otto von Guericke University of Magdeburg, Leipziger Str. 44, 39120 Magdeburg, Germany.
E-mail address: johann.wendler@med.ovgu.de (J.J. Wendler).
[1] German Academy for Microtherapy (DAfMT), Magdeburg, Germany.
[2] Working Group for Focal and Microtherapy of the Academy for German Urologists, Magdeburg, Germany.

http://dx.doi.org/10.1016/j.cct.2015.05.002
1551-7144/

1. Introduction

Focal ablation therapy is playing an increasingly important role in oncology and may reduce the toxicity of current surgical treatments while achieving complete tumour destruction with a satisfactory oncological outcome. Newer ablation modalities, such as irreversible electroporation (IRE), have been introduced and their respective clinical niches are being defined [1]. IRE causes cell death through the repeated application of short-duration high-voltage electrical pulses that create irreversible damage to cell membranes [1,2]. While there may be some hyperthermic ablative changes with high-power applications, the mechanism of cell death with IRE is thought to be predominantly non-thermal [2,3,18,42].

In urology, the trend in surgery as the standard treatment is moving toward minimally invasive procedures [4]. In localised renal cell carcinoma, partial nephrectomy should be performed whenever technically feasible, so as to avoid chronic renal failure [4]. For this reason, cryoablation and radiofrequency ablation (RFA) have been put forward as alternatives by the EAU for small renal masses (<4 cm) in selected patients [4]. IRE has been proposed to be tissue-selective and possibly to convey advantages compared with currently used thermal ablative technologies or radiotherapy [5]. Therefore, IRE represents an interesting option for nephron-sparing treatment of renal tumours, even for those with unfavourable anatomic location (e.g., centrally located and close to the renal pelvis and/or the large hilar vessels).

Conclusive reports on the use of IRE in kidney malignancies, especially renal cell carcinoma, are not yet available. Previous investigations on renal IRE were exclusively experimental or safety-oriented [6–21]. A complete histological analysis is still required to assess the completeness of tumour ablation and the nephron-sparing potential of IRE in RCC. Studies published so far – mainly case reports or series reports of patients undergoing palliative treatment – do not permit systematic analysis. However, one of the criticisms of published ablation studies in general is the sparse tissue outcome data, because most studies are based only on radiographic or post-biopsy assessments [1]. With this study (the "IRENE study") we present the first detailed histopathological data on the short-term effect of IRE-treated renal tumours in humans after secondary surgical tumour resection. To the best of our knowledge this is the first study determining the safety and effectiveness of IRE of localised renal cell carcinomas with curative treatment intention.

2. IRENE study protocol

2.1. Study title for registration

"Prospective, monocentric clinical Phase 2a study of the effectiveness of the percutaneous irreversible electroporation (IRE) as primary ablation therapy of locally confined kidney tumours (renal cell carcinomas)." Acronym and short title "IRENE — IRreversible Electroporation of kidney tumours before partial NephrEctomy" [22–24].

2.2. Study registration

The trial has been registered as follows:

- ClinicalTrials.gov of the U.S. National Institutes of Health: NCT01967407 [22].
- International Clinical Trials Registry Platform (ICTRP) of the World Health Organisation (WHO): DRKS00004266 [23].
- German Clinical Trials Registry (DRKS): DRKS00004266 [24].
- Universal Trial Number (UTN) of the World Health Organisation (WHO): U1111-1140-0415 [23].
- German Federal Institute for Drugs and Medical Devices (BfArM) and German Institute of Medical Documentation and Information (DIMDI) with the European Databank on Medical Devices (EUDAMED) number: CIV-12-04-006021.
- Study protocol number for the ethics committee responsible: MD-URO-001.

2.3. Study approval

The study was registered at the German Institute of Medical Documentation and Information (DIMDI). Approval for this study was granted by the BfArM and the Ethics Committee of the Medical Faculty of the Otto von Guericke University of Magdeburg (OVGU) [no. 73/12].

The NanoKnife System has been CE-certified for the ablation of soft tissue (all parenchymatous organs and tumours of the soft tissues) under the number CE 0086 (formerly CE 0050 Generator and CE 0051 electrodes) [25]. The system is classified as a Class II device according to the Risk Classification for Medicinal Products of the FDA and as belonging to Class IIb according to the European regulation 93/42/EWG.

2.4. Study management

IRENE is an interventional, investigator-initiated trial (IIT), compliant with Good Clinical Practice (GCP) and the German Medical Devices Act (MPG) guidelines as well with those of the International Working Group on Image-Guided Tumor Ablation [1]. Investigators from the University Hospital designed the protocol under due consideration of feedback from the Ethics Committee of the OVGU and the Clinical Study Centre of the Medical Faculty of the OVGU. The study is sponsored by the Medical Faculty of the OVGU, and will be conducted at the University Hospital in Magdeburg. The Trial Steering Committee (TSC) is composed of an independent chairperson, the principal investigator, the study co-ordinator, a patient representative, a leading study nurse, the leading co-investigators of the both clinical departments involved, all other co-investigators and the study statistician. The independent data-monitoring committee includes independent urologists, radiologists and pathologists in the field of tumour therapy and focal therapy (all of whom are independent of the study and are reviewers of the German academies of focal therapy and microtherapy).

2.5. Trial design

This is a prospective, monocentric, non-randomised, uncontrolled, non-blinded, single-arm Phase 2a interventional pilot study to assess the clinical effectiveness of a novel 2007 CE-certified procedure and medicinal product (NanoKnife Electroporation Ablation System, AngioDynamics Inc., Latham, NY 12110, USA). In spite of the strict selection criteria and anticipated slow recruitment, the duration of the study has at present been set to two years. The follow-up period is 4 months after IRE.

2.6. Study rationale

Animal experiments, clinical case reports and safety application studies all indicate that the use of IRE to treat kidney tumours is safe and without relevant side effects. Furthermore, experiments have shown that IRE efficiently ablates target tissue. Thorough histological investigations following complete tumour resection by IRE in localised kidney tumours are not described in the literature. Therefore, post-procedural imaging findings provide only a rough guide to the success of ablation therapy, because microscopic foci of residual disease cannot be expected to be identified by standard imaging [1,26]. The gold standard for treatment of localised RCC is surgical resection, increasingly as nephron-sparing surgery. Therefore, in this study the tumour ablation region will be removed surgically four weeks after IRE. Imaging, in conformity with the relevant guidelines (EAU [4]), will be conducted by repeated MRI and results will be compared with histological findings.

The study is intended to reveal the current value of percutaneous IRE, guided by CT and/or sonography with MRI-fusion.

2.7. Aim of the study

The objective of the study is to evaluate percutaneous IRE as a novel ablation procedure performed with the only electroporation system at present available for this the NanoKnife Electroporation Ablation System (AngioDynamics Inc., Latham, NY 12110, USA) in the treatment of localised kidney tumours with subsequent operative tumour resection (partial kidney resection) after four weeks. The success of IRE will be assessed by MRI and histological testing (short-term and medium-term effects). The hypothesis that kidney tumours of ≤4 cm can be completely ablated will be tested. The sample size will be 20 (see Section 2.17).

2.7.1. Primary objective

- To assess the "probable oncotherapeutic effectiveness", measured by the proportion of residual viable tumour in the kidney, as revealed by histopathology and imaging 28 days after IRE.

2.7.2. Secondary objective

- To assess the technical feasibility of percutaneous IRE performed with the NanoKnife (see above) and guided by CT and/or sonography with MRI fusion, under clinical conditions, on human kidney tumours.
- To assess, 28 days after IRE, by imaging and histology, peritumoural tissue damage during nephron-sparing focal tumour ablation.
- To acquire information on the procedural tolerability of IRE and the subsequent tumour resection and intervention-independent quality of life up to 4 months after IRE.

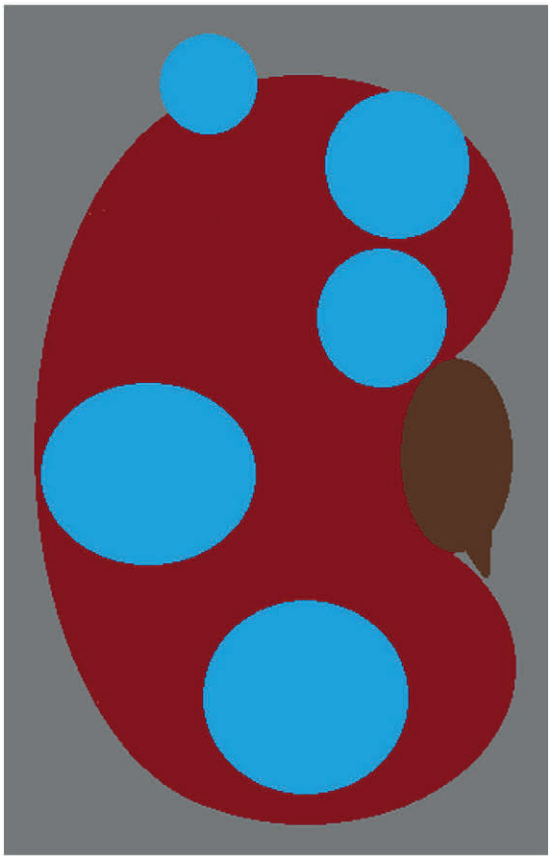

Fig. 1. Schematic example of localised T1a kidney tumour/kidney cell carcinoma (blue circles) suitable for IRE. Kidney parenchyma (reddish brown) and renal pelvis (brown).

2.8. Study population eligibility

Men and women with imaging-based evidence of a localised, solid renal mass with suspicion of RCC ≤4 cm without any sign of metastasis (and, if applicable, kidney carcinoma confirmed by biopsy; TNM classification T1a cN0 cM0, Stage I, EAU criteria; for an example see Fig. 1) will be considered for inclusion in the study. Imaging will be performed by contrast-enhanced CT or MRI. All histological kidney carcinoma subtypes and Fuhrman grades will be included. Selection of patients in pre-screening and screening will be performed according to the complete list of criteria in Table 1. Sample size is 20 (see Section 2.17).

2.9. Trial entry

All patients with a new diagnosis of suspected localised kidney tumour or RCC will be counselled about the standard treatment option with curative intention (partial kidney resection/tumour nephrectomy). Those meeting all the inclusion and none of the exclusion criteria (see Table 1) will be offered a Patient's Information Sheet and invited to attend a screening and consent visit if they are interested in study

Table 1
Inclusion and exclusion criteria.

Inclusion criteria:

- One or more localised, resectable kidney tumours (≤4 cm) with suspicion of malignancy *OR* histologically confirmed renal cell cancer,
- Patient's desire for non-surgical and surgical therapy,
- Karnofsky Index > 70% and ECOG ≤ 1,
- Age ≥ 18 years,
- Life expectancy ≥ 12 months,
- Compliance of the patient taking part in a study,
- Informed consent.

Exclusion criteria:

- Cardiac pacemaker or other electrical implant(s),
- QT interval > 550 ms or cardiac arrhythmias or any condition after myocardial infarction that makes an ECG-synchronisation unfeasible,
- Known cardiac ejection fraction < 30% or NYHA 3–4,
- Known epilepsy,
- Second malignancy (except basal-cell carcinoma and cervical carcinoma in situ),
- Immunosuppression or HIV-positivity,
- Active infection or severe health impairment that makes taking part in a study unfeasible,
- Pregnancy or lactation,
- Metastatic disease,
- Palliative status,
- Current or completed therapy for RCC,
- Taking part in another clinical study in RCC,
- Rejection of interventional or surgical therapy by the patient,
- Circulatory instability,
- Inoperable or general contra-indications for anaesthesia, endotracheal anaesthesia and/or muscle relaxation,
- Psychiatric disorders that make taking part in a study or giving informed consent unfeasible,
- Haemorrhage, impossibility of taking a blood-thinner, untreatable thrombophilia, thromboplastin time ≤ 50%, thrombocytes ≤ 50 Gpt/l; partial thromboplastin time > 50 s,
- MRI incompatibility,
- Metal implants <1 cm close to the kidney/kidney tumour,
- Contraindication for biopsy and puncture of the renal tumour under CT guidance,
- Suspicion of renal pelvic tumour/urothelial carcinoma of the kidney,
- Untreated urinary retention of the kidney/hydronephrosis.

participation (see Fig. 2, Table 2). Central to the patient's information therapy decision will be the tissue-sparing, kidney-preserving removal of the tumour. The study rationale, the basics of IRE and the current state of scientific knowledge will be discussed with the patient, and possible advantages and disadvantages of participating in the study will be explained.

2.10. Trial flow

See Fig. 2.

2.11. Single visit schedule

See Table 2.

2.12. Interventions

2.12.1. Pre-treatment biopsy

Percutaneous biopsy is obligatory before ablation of renal masses [4], in order to obtain an initial histological tumour classification in cases of complete ablation. If not performed previously, the IRE intervention starts with a percutaneous full-core biopsy (two-cylinder) guided by CT and/or MRI–sonography under general anaesthesia. Immediately thereafter the IRE electrodes are placed and IRE is performed. Biopsy specimens will be analysed histologically according to current guidelines [27].

2.12.2. Focal irreversible electroporation (Intervention 1)

IRE procedure is to be performed under general anaesthesia and deep muscle paralysis (the latter only during IRE pulse application) to avoid severe muscle contractions and patient movement. Maximum muscle relaxation cannot completely prevent IRE-triggered muscle contractions. The optimum level of muscle relaxation is described as 0–1 twitches per 10 IRE pulses [28]. The complex IRE electrode placement, IRE treatment planning and intermediate graph analysis require prolonged anaesthesia. Muscle relaxation, prone position, prolonged intervention, and possible IRE-triggered muscle contraction make endotracheal anaesthesia necessary. IRE requires separate ECG synchronisation (R-wave triggering, using an external synchronisation device: AccuSync® 72, AccuSync Medical Research Corporation, Milford, CT,

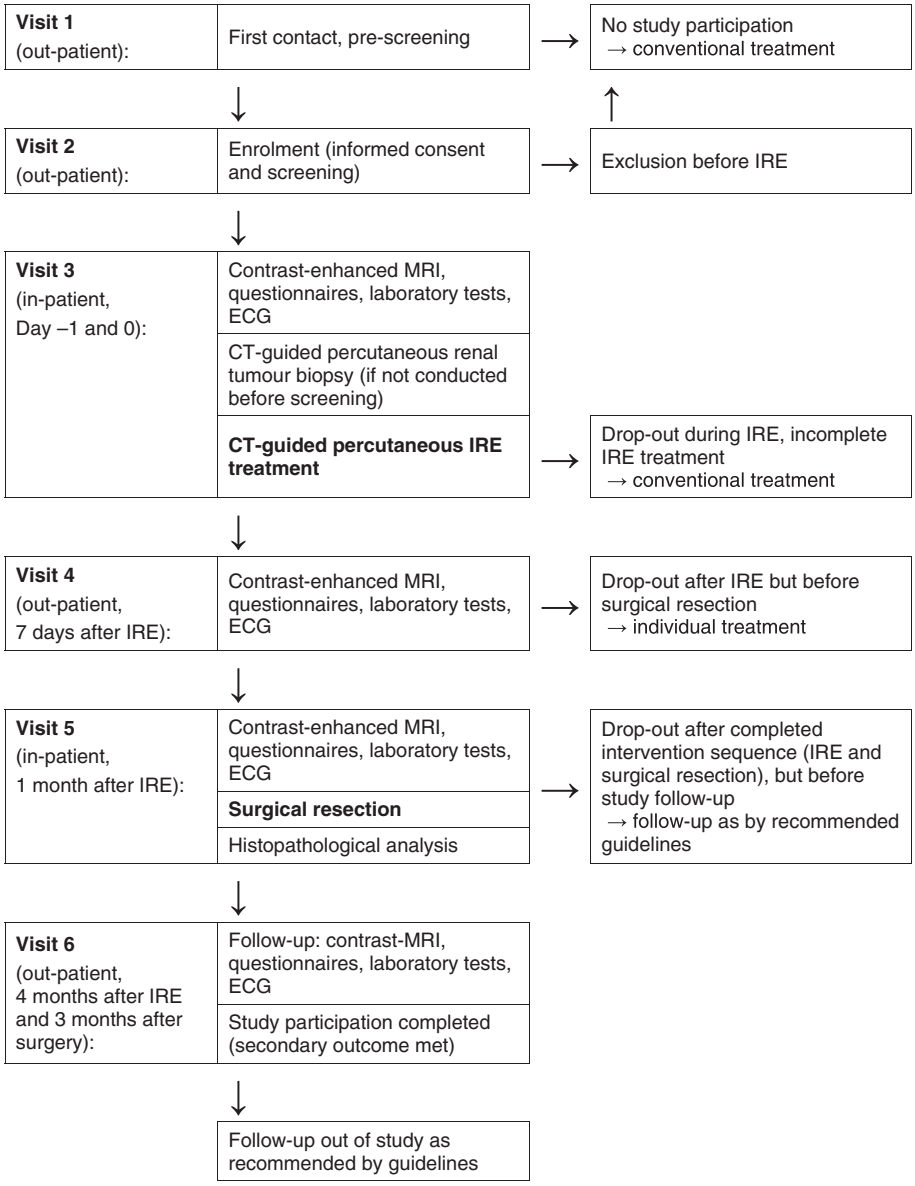

Fig. 2. Trial flow chart.

Table 2
Schedule of visits and procedures.

Time of event	Visit 2	Visit 3		Visit 4		Visit 5		Visit 6	
	Days −29 to −2	Day −1	Day 0	Days 1 to 2	Day 7	Day 27[a]	Day 28[a]	Days 29[a] to 38[a]	Day 112[b]
Milestones	Enrolment, screening	Preparation	Intervention 1 (IRE)	Surveillance	Surveillance	Surveillance and preparation	Intervention 2 (surgery)	Surveillance	Follow-up, completion of study participation
Informed consent	X								
Anamnesis	X	X			X	X			X
QOL questionnaires	X	X	X	X	X	X	X	X	X
Physical examination	X	X	X	X	X	X	X	X	X
Evaluation anaesthesia	X	X				X			
Blood and urine tests	X	X	X	X	X	X	X	X	X
Chest CT	X[c]								
Abdomen contrast CT	X[c]								
ECG	X	X	X	X	X	X	X		X
Kidney/abdomen contrast-enhanced MRI	X[d]	X[c]		X	X	X			X
CT-guided kidney tumour biopsy			X						
Percutaneous IRE of the kidney tumour			X						
Open kidney tumour resection (partial kidney resection)							X		
Endotracheal general anaesthesia			X				X		
Histopathological analysis			X				X		

[a] Time point: +1 to +7 days, if the patient's general condition or other circumstances make treatment at the scheduled time point temporarily impossible.
[b] Time point: ±7 days, if the patient's general condition or other circumstances make treatment at the scheduled time point temporarily impossible.
[c] If not already done in pre-screening.
[d] If medically indicated according to the current guideline of the EAU.

USA). The optimum IRE electrode configuration and the optimum probe-pair voltage setting (V/cm) for the target zone (tumour zone plus a safety margin of 5–10 mm) [1,4,28] is planned by using the PC-based NanoKnife® planning software demonstration tool (ProcedureManager-2_2_0_23 for Windows, AngioDynamics® [29]). The 15 cm 19G single IRE electrodes are placed under CT guidance or MRI–sonography in accordance with the pre-interventional treatment planning. A CT scan or MRI–sonography is then performed to check the current position of the IRE electrodes relative to each other and to the adjoining tumour edge. This allows precise placing of the needle-like electrodes. On the basis of these data, IRE treatment is planned by using the NanoKnife® generator-based planning software tool (AngioDynamics®). The optimum electrode-pair voltage setting is chosen for the lesion zone. IRE electrode placement has to be adjusted, if necessary, and the above-mentioned interventional planning process is repeated. IRE pulses can be applied after the optimum electrode position has been checked by 10 test pulses per electrode pair. IRE pulses are applied consecutively for each predetermined IRE probe pair. Abnormal graphs, abnormal current warnings or pulse delivery failures necessitate modification of the interventional treatment planning and probe placement, and the IRE pulse application has then to be repeated. The number of electrodes used depends on the size and the shape of the target (Fig. 3). The device is set to deliver 70–90 pulses with a pulse length of 70–90 μs in order to achieve an electrical field of 20–50 A. This current has been shown to cause complete ablation in the target area without also causing an ablative heating effect, which is possible when the current is higher [2]. If the electric field is in the optimum range, then 80–90 pulses per pair are delivered; otherwise, the voltage is modified and treatment is repeated if necessary.

2.12.3. Tumour resection (Intervention 2)

Partial renal resection or radical nephrectomy (if necessary) with complete resection [4] of the tumour area/IRE area is conducted

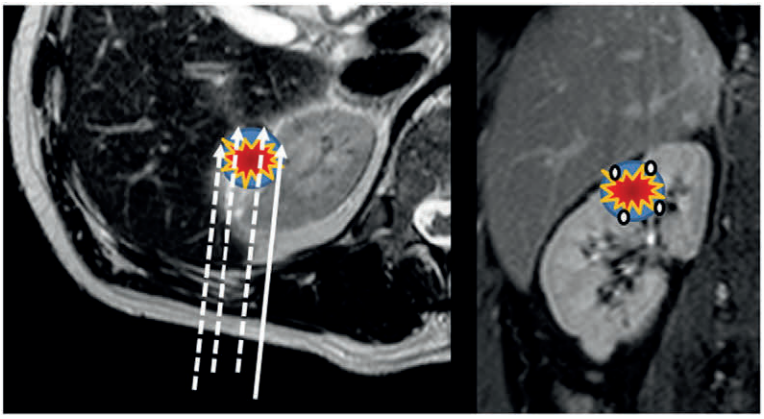

Fig. 3. This a representative sketch of the treatment (planning) for IRE of the kidney tumour (blue circle). The left image is a transversal view of a renal MRI with a lateral view of the dorsolumbar inserted IRE probes (white arrows). The right image is a coronal view of a renal MRI with coaxial view of the dorsolumbar inserted IRE electrodes (white spots). The highlighted red and yellow spots typify the IRE energy input in whole target (tumour plus safety margin).

28 days after the IRE. The intervention is performed by open surgery (to allow better assessment of the organ and its surroundings; lumbar or transperitoneal access) under general anaesthesia. Depending upon the results of the first, interim analysis, the procedures may be adapted to a laparoscopic resection. This analysis will be performed when the first three patients have been fully assessed. To obtain first insights into the IRE ablation environment in situ in the kidney, the intervention is initially planned as an open surgery to allow better assessment of the organ and its surroundings as well as lumbar or transperitoneal access. Depending on the first interim analysis, laparoscopic nephrectomy (total or partial) may be performed. To identify the spatial position of the resectate or tumour for the resection, the resectate will be marked intraoperatively with threads, as is usual.

2.13. Investigations

2.13.1. Contrast MRI of the kidney/abdomen

The image-morphological assessment of the kidneys is performed by contrast-enhanced MRI (1.5 T scanner, gadobutrol: 0.1 ml/kg Gadovist 1.0 mmol/ml; Bayer, Leverkusen, Germany) on planned study days 1, 1–2, 7, 27 and 112, whereby the contrast medium sequences 'arterial', 'portal-venous', 'venous' and 'urographic' are carried out. The sequences to be used are shown in Table 3. The above MRI parameters were defined as ideal settings in clinical routine for kidney MRI, and in earlier animal studies we found them to be optimum parameters for MRI diagnosis before and after IRE of kidney tissue [6]. DW-MRI will be analysed by two specialised urological radiologist focusing on: ablation zone, ablation zone shape/symmetry, ablation volume, residual tumour at the ablation zone border, skip lesions within ablation zone, transition zone between ablated and normal renal or perirenal tissue, and damage to vital structures. MRI images will be stacked to render a 2D–3D reconstruction of the kidney and the IRE ablation zone within it.

2.13.2. Laboratory tests — blood and urine

The following laboratory values are to be determined in the screening and/or in the course of the study (for time points see Table 2):

- Haematological and clinico-chemical values: aspartate transaminase, alanine transaminase, lactate dehydrogenase, alkaline phosphatase, albumin, C-reactive protein, sodium, potassium, chloride, calcium, creatinine, urea, uric acid, thyroid-stimulating hormone, free thyroid hormone T4, human β-choriogonadotrophin (for women of child-bearing age), Quick's test, partial thromboplastin time, thrombin time, coagulation time; serology for human immunodeficiency virus and hepatitis; standard haematological values, and blood group.
- Urine tests: sediment, bacteria (culture), and urine cytology [30].

2.13.3. Scores and questionnaires on morbidity and quality of life

The patients' morbidity and quality of life will be recorded systematically by means of standardised scores and questionnaires [1]. Inter alia, the effects of the therapeutic interventions – IRE and surgery – on quality of life will be investigated. The following scores and questionnaires will be used:

- Life expectancy of the patient by age and sex as given in the mortality statistics issued by the German *Statistisches Bundesamt*, Wiesbaden, 2013 [31].
- Charlson Comorbidity Index/Score [32].
- Degree of pain on a numerical rating scale (NRS) from 1 to 10 according to the *Ärztliches Zentrum für Qualität in der Medizin* [33] in the context of a pain diary.
- Quality of life according to EORTC QLQ-C30, Version 3.0, German [34].
- Disease-specific morbidity and quality of life (kidney carcinoma) according to FKSI-15 (Functional Assessment of Cancer Therapy (FACT) Kidney Symptom Index-15), Version 4.0, German [35].
- Study-specific quality of life as assessed by using a study-specific questionnaire (questions 1–9) according to Wendler, adapted from EORTC QLQ-C30, Version 3.0, German (aEORTC-QLQ-C30-Wendler).
- ECOG Score and Karnofsky Index.
- Grading of adverse events following the Common Terminology Criteria for Adverse Events (CTCAE), Version 4.0, of the U.S. NIH and following the Clavien–Dindo classification [36].
- Grading of adverse events following the SIR (Society of Interventional Radiology) classification system for complications by outcome [1,26,37].

2.13.4. Histopathological analysis

After resection, preparation sections are fixed in buffered 4% formaldehyde solution for at least 24 h and then examined by microscopy. This includes the complete sectioning of the ablation area including a border of macroscopically inconspicuous kidney tissue in 0.5 cm thick slices [27]. The slices are numbered and photographed for documentation. The ablation area is measured. In cases of nephrectomy, coarse sectioning of the remaining preparation to exclude other pathologies is done. Thereafter the ablation area, including the border, is completely embedded in paraffin wax in standard tissue cassettes after topographic assignment based on macrophotography. Each tissue block is used to prepare 3 μm thick sections and these are stained with haematoxylin–eosin (the number of sections depends on the thickness of the tissue) for morphological assessment in 500 μm steps with one unstained section each

Table 3
MRI imaging sequences (kidney programme).

Sequence	Method	Section plane	TR (ms)	TE (ms)	Flip (°)	LT (mm)	Matrix (pixel)
T_1w-2D-GRE (Scout)	T_1-weighted 2D gradient echo sequence in three planes for general orientation and planning of treatment						
T_2w-SShTSE	Coronary T_2-weighted SSH–TSE sequence in 4 mm LT in breathing pause	Coronary	476	80	90	5	236 × 116
T_2w-FS-TSE	Transversal T_2-weighted TSE sequence with fat saturation in 4 mm LT, T2-SPIR = T2 with fat saturation; triggered	Transversal	1600	100	90	4	288 × 130
T_2w-RT-TSE	Transversal T_2-weighted TSE sequence without fat saturation in 4 mm LT; triggered	Transversal	1600	100	90	4	324 × 230
DWI (b = 0/500)	Transversal diffusion-weighted sequence in 8 mm LT; triggered	Transversal	3899	68	90	8	136 × 117
T_1w-GRE	Transversal T_1-weighted 2D gradient-echo sequence in 4 mm LT; in breathing pause	Transversal	222	2.3/4.6	80	4	176 × 98
T_1w-FS-3DGRE (transversal)	Transversal T_1-weighted 3D gradient echo sequence with contrast enhancement in native, arterial, portal-venous and venous perfusion phase as dynamic measurement in 4 mm LT, beginning with bolus track (aorta), in breathing pause	Transversal	4	1.96	10	2	164 × 138
T_1w-FS-3DGRE (coronal)	Coronary T_1-weighted 3D gradient-echo sequence in 2 mm LT after 3 min and 4 mm LT after 15 min (late venous phase); in breathing pause	Coronary	4.3	2.1	10	2	188 × 147

LT, layer thickness; TSE, turbo spin-echo; SSH, single-shot; RT, respiratory triggers.

for transmission microscopy. Additional immunohistological staining (e.g., Mib-1) is performed to determine viability or irreversible cell death [1]. Further detailed analysis includes the measurement, mapping and photo-documentation of the histological preparation by transmission microscopy.

The histological work-up will be conducted in the marked plane with corresponding mapping as 2D fusion sketches and possibly 3D reconstruction. In each specimen, the complete ablation area, the tumour area and non-affected renal tissue on each slide will be precisely outlined in multicoloured ink. On the basis of this marking, sequential outline maps will be traced for each level of section. The maps from each subject will be computer-scanned and inspected serially. The area of tumour at each level of section will be determined by using a digitising pad (Bamboo One™) and image-manipulation software (GIMP 2.8.14®). This reconstruction will be used to assess the exact lesion volume (volumetry) and shape.

2.14. Observation and follow-up

The total period of observation and follow-up is 16 weeks (approximately 4 months), i.e., 16 weeks after IRE and 12 weeks after surgical resection. After this, the patient's participation in the study will be complete. At the final study follow-up examination (16 weeks after IRE) the following measurements and assessments will be performed: general clinical examination, body weight and height, vital signs (blood pressure, pulse, temperature), general health status, recording of quality of life and morbidity (by ECOG status, Karnofsky Index, FACT-FKSI-15-Kidney-V4D, EORTC-QLQ-C30-V3D and aEORTC-QLQ-C30-Wendler-T + 112 questionnaires and NRS pain scale), 12-lead ECG, laboratory values (aspartate transaminase, alanine transaminase, lactate dehydrogenase, C-reactive protein, sodium, potassium, chloride, calcium, creatinine, thyroid-stimulating hormone, free thyroid hormones T3 and T4, standard haematological values), urine tests (sediment, bacterial culture, cytology), sonography of the kidney and urinary bladder, and three-phase contrast-enhanced MRI (high-field MRI, 1.5 T) of the kidneys.

Thereafter, continued care, on an individual basis and within the responsibility of the patient's own urologist, is recommended. This should follow the EAU guidelines [4] and may involve referral back to the study centre; it should include CT of the thorax and abdomen as practised after focal treatment, after 6, 12, 24, 36, 48 and 60 months and then every two years.

2.15. Management of serious adverse events

For all patients in this clinical trial, all adverse events after the giving of informed consent will be recorded in a GCP-compliant manner and followed up as necessary. Lack of effectiveness of the study treatment will not be regarded as an adverse event.

Serious adverse events (SAEs) are those that fulfil at least one of the following criteria (note that the list is based upon those set out in GCP, but goes beyond them in the inclusion of certain procedure-related events). SAEs are listed in Table 4 Appendix.

Every SAE will be assessed by the principal investigator, in order to allow the continual evaluation of the risk–benefit ratio of the study treatment and to ensure the patient's safety during the subsequent course of the trial.

The trial's Steering Committee, the principal investigator and the sponsor (the Clinical Study Centre of the Medical Faculty of the OVGU) are legally obliged to report all SAEs and all adverse events leading to discontinuation of a patient's participation in the study to the BfArM (as responsible regulatory authority) and to the Ethics Committee of the Medical Faculty of the OVGU.

2.16. Stopping rules

The following events are to be regarded as sufficient grounds for withdrawing individual patients from the study:

- Personal wish of the patient;
- Decision of the principal investigator, if in his considered view the patient is likely to profit from a change in treatment according to the EAU guidelines [4];
- Decision of the sponsor, for major regulatory or ethical reasons;
- If in the view of the investigation team the risks for the patient outweigh the benefits;
- If the recruitment of patients is clearly delayed for objective reasons.

The reasons for premature withdrawal of a patient from the trial are to be documented in the source data (patient's records) by the investigator and, within the framework of SAE management, to be reported to the Clinical Study Centre of the Medical Faculty of the OVGU. After every SAE report the trial's Steering Committee and sponsor (the latter usually represented by the Clinical Study Centre of the Medical Faculty of the OVGU) will assess whether it is safe to proceed with the trial. After every SAE report the BfArM will assess whether it is safe to continue the study and other studies or to allow the conduct of other studies – and treatment outside clinical studies – with the NanoKnife Electroporation Ablation System. After every SAE report Ethics Committee of the Medical Faculty of the OVGU will issue a recommendation as to whether it is ethically justified to continue the study.

2.17. Statistical analysis and sample-size calculation

On the basis of the aims and goals and the primary and secondary objectives of this Phase 2a pilot study the sample size was set at $N = 20$ [39,41,43]. This cohort size was chosen by the sponsor on the basis of experience with similar studies and was not based upon a formal calculation. It was agreed to by the BfArM and the Ethics Committee of the Medical Faculty of the OVGU. This cohort size will allow meaningful assessment of technical feasibility and of the success or failure of the ablation, by histological and imaging criteria. Precedence is here given to obtaining a detailed descriptive evaluation, without significance testing, for which the study would in any case presumably be underpowered. Statistical analysis will be performed by a study statistician of the medical faculty of the OVGU with IBM SPSS Statistics (SPSS; version 22). This pilot study is intended to provide the basis for a confirmatory, multicentric trial.

2.17.1. Primary outcomes

Primary outcomes will be measured by conventional histopathological analysis and special proliferation markers for formalin-fixed paraffin-embedded specimens to determine the success of the tumour ablation and to detect any persisting viable tumour tissue.

2.17.2. Secondary outcomes

Secondary outcomes will be measured by conventional histopathological analysis and by kidney imaging by diffusion-weighted contrast-enhanced MRI for the determination of damage to healthy peritumoural kidney tissue (collateral damage) in the context of the intended nephron-sparing effect. Furthermore, the tolerability of the procedure and the intervention-dependent quality of life following IRE and the subsequent tumour resection will be assessed on the basis of quality-of-life questionnaires (EORTC QLQ-C30, V3.0D, FKSI-15 V4.0D, adapted EORTC QLQ-C30 V3.0D (aEORTC-QLQ-C30-Wendler), ECOG status, Karnofsky Index) and the NRS, and by classification of adverse events according to CTCAE version 4.0, the Clavien–Dindo and the SIR classifications.

In the context of the complete documentation of the procedure and adverse events, the trial is aimed at assessing the technical feasibility of the percutaneous IRE, supported by CT and/or by MRI–sonography, of localised kidney tumours using the commercially available NanoKnife Electroporation Ablation System under study conditions close to those of clinical practice.

2.18. Monitoring and audit

Regular monitoring will be performed by the external and independent Co-ordinating Centre for Clinical Trials of the Medical Faculty of the Martin Luther University of Halle-Wittenberg (KKS Halle), which is a member of the German network of co-ordination centres for clinical studies (KKS network). Audits will be regularly performed by independent staff of the Clinical Study Centre of the Medical Faculty of the OVGU. The purpose of the monitoring and the audits is to contribute to ensuring patient safety and adherence to GCP.

2.19. Legal and ethical principles

The study will be conducted in conformity with the most recent version of the Declaration of Helsinki (October 2013). It will adhere to GCP (German version, "Good Clinical Practice" — Verordnung; GCP-V, most recent version, of 19.10.2012); *Grundsätze für die ordnungsgemäße Durchführung der klinischen Prüfung von Medizinprodukten* ("Principles of good practice in the conduct of clinical trials of medicinal products", Bundesanzeiger, DIMDI), the German law governing medicinal products (MPG; most recent version, 21.07.2014), the European norm for the application of risk management for medicinal products (Norm EN ISO 14971:2012 according to the European guideline 93/42/EWG) and international operating procedures for medicinal products (ISO 14155:2011).

3. Discussion

Following on from pre-clinical studies testing IRE in phantoms (immediate evaluation), ex vivo porcine kidney (immediate evaluation), in vivo porcine kidney (short- and medium-term evaluation) and human kidney tumours in situ (immediate evaluation; Phase 1 safety study), the prospective Phase 2a trial IRENE represents the natural next step in the assessment of this new technology for treating localised renal cell cancer [38]. The IRE procedure and the NanoKnife offer a number of user-dependent variables, so that the parameters of IRE treatment can be specified exactly and used to compare various study results in evaluating the effectiveness and safety of the treatment and the results obtained from imaging and histology [1]. Authors should also set out to describe the tissue homogeneity of the target tumours and to stratify/quantify any inhomogeneity in tumour-specific tissue and in organ structures [1]. Post-procedural imaging findings are only a rough guide to the success of ablation therapy, because microscopic foci of residual disease cannot be expected to be identified by standard imaging techniques [1,26]. Absence of – or a minimal involution of – the ablation zone does not imply treatment failure [1,26]. Any residual tumour tissue or tumour cells should result in the result being classified as incomplete ablation [1], independently of how small the amount of residual tumour may be in relation to the untreated tumour. IRE may be reversible or irreversible, depending on the voltage applied and the peripheral decrease in field strength (edge area), whereby however only the irreversible region leads to visible tissue ablation [5]. One of the shortcomings of IRE today is the absence of dedicated, clinically validated protocols to be used in different tissue environments and for different tumour biologies [39,40]. In addition, no technical endpoint has yet been described that reliably predicts successful ablation of a tumour during the course of the intervention procedure [1,39]. So far, there is a lack of adequate experience of how long it takes for complete tumour involution to occur after correctly performed ablation by IRE, or of how long after IRE one may expect to observe residual tumour cells if the ablation was incomplete. Preliminary studies in renal IRE suggested the 4-week interval to be used in the present study, without however, having been conducted on a tumour model. It is possible that tumour tissue behaves differently from healthy kidney parenchyma. It is also unclear whether residual nests of tumour cells in coagulation necrosis of the ablation zone can influence the oncological outcome. For that reason a secondary objective of the IRENE study is also defined as "'probable oncotherapeutic effectiveness' measured by the proportion of residual viable tumour in the kidney, as revealed by histopathology and imaging 28 days after IRE" (see Aim of the study). It is to be expected that post-interventional, reversible effects of IRE in the period after 28 days will no longer be detectable, either by imaging or by histology. The monitoring by MRI and post-interventional biopsy probably does not provide adequate proof of the success of therapy. For this reason the study includes a complete resection of the tumour – or ablation area – with a complete histological work-up. The oncotherapeutic security of the patient is guaranteed by the inclusion of standard, guideline-compliant tumour resection. IRE is a procedure with potentially attractive characteristics and may be ideal for delivering focal therapy in the kidney, especially as it has been shown to have tissue-selectivity in animal studies that have demonstrated a homogeneous ablation of renal tissue with preservation of larger vessels and the urine-collecting system [6,11,12,14,15].

To our knowledge, there is no description of needle-tract tumour seeding after coaxial biopsy and thermal RCC ablation by RFA or cryotherapy [4]. Needle-tract tumour seeding was first described for IRE in the context of IRE ablation of lung tumours [39]. However, in the context of IRE of kidney tumours this has not been observed [13,17]. Although the design includes repeated MR imaging before and after IRE, MRI seems to be the ideal but not validated imaging tool for local monitoring after IRE [6]. As a consequence of these considerations, the only reliable measure of ablation in this study remains the histological analysis of the completely resected tissue in the treatment area.

3.0.1. Study limitations

The study is a single-centre trial in a tertiary university hospital that has especial expertise in focal therapy, image-guided therapy and minimally invasive percutaneous kidney procedures; therefore, the results of this study are unlikely to allow wide generalisation. Furthermore, the small cohort size (20 patients) will clearly leave a need for future multi-centre studies. This single-centre expert setting is the preferred context to allow the development of new technologies and treatment procedures such as percutaneous image-guided renal IRE. At present, a technical limitation of IRE by the NanoKnife Electroporation Ablation System is the absence of any real-time monitoring of the energy applied or of therapeutic success; to date no clinically applicable solution to meet this need was been found. The position of the kidney tumour does not constitute a criterion for participation in the IRENE trial. Therefore, systematic measurement errors due to the technically imposed limits on slice thinness have to be taken into account. In the assessment of quality of life, some of the questionnaires to be used record only approximately, on a "best possible" basis, in the absence of validated alternatives, the patient's actual life quality in the context of his/her localised kidney tumour or carcinoma and its ablation. Differences in tumour biology and response rate of different histological entities (RCC vs. transitional cell cancer or renal metastasis) must be taken into account in any consideration of the generalisability of the study's results. The possible disadvantages of participation in the study vis-à-vis standard tumour-resection therapy are puncture and IRE as additional invasive procedures under general anaesthesia. In CT/fluoroscopy-supported IRE electrode placement there is also additional exposure to X-rays. Furthermore, with 4 weeks an especially short interval was chosen, so as to avoid any prognostically relevant delay of the definitive therapy (R0 resection, gold standard). On account of the postulated massive tumour damage by IRE, the risk of a secondary carry-over of tumour cells

by the resection may be regarded as very slight. A simpler partial renal resection with kidney preservation after IRE might be possible. All in all, the additional risk of progression, on account of the 4 week interval, is to be regarded as very slight.

4. Conclusion

The IRENE trial will allow an appropriate evaluation in a clinical setting of the feasibility and effectiveness of CT-guided and/or MRI–sonography-guided percutaneous IRE ablation of localised renal cell cancer as well as functional outcomes, using pre- and post-treatment MRI and ultra-thin-section histology after complete surgical resection in the short-term interval. The outcomes of the IRENE trial may be used to plan a larger multi-centre confirmation study. Our pilot study protocol of renal IRE as a potential universal tumour model can provide guidance for designing an effectiveness and feasibility trial to asses a new ablative technology in the challenging landscape of surgical and focal treatment particularly for RCC. A different tumour biology and ablation response of the different tumour entities respectively RCC subtypes have to be taken into account and discussed.

Conflict of interest

M. Schostak has received funding for conference attendance from AngioDynamics Inc. (New York, USA). J.J. Wendler has received trial funding support from AngioDynamics Inc. for previous experimental studies. Neither of these sources provided any input whatsoever into this article or this study.

Acknowledgements

AngioDynamics Inc. (CIV-12-04-00621) (New York, USA) supports the study by providing the NanoKnife electroporator device and technical maintenance cost-free for the duration of the study. The company will meet the publication costs. The company has had, and will have, no involvement in devising, writing or editing the protocol or in the study conduct and will have no contentual influence on presenting the results at conferences and congresses and/or in papers. The academies and the authors have no collaboration with AngioDynamics Inc. AngioDynamics Inc. will not receive any of the results of this study or parts of the study until its publication.

Appendix A

Table 4

SAE definition
— Death during the study or up to 28 calendar days after the ending of study-specific procedures. (Death because of confirmed tumour progression will not be recorded as an SAE and will be recorded in the CRF with the clinical cause of death documented as an adverse event, severity "5 = death". An SAE report for this is not requirEd.)
— The adverse event is immediately life-threatening.
— The adverse event leads to unplanned hospitalisation.
— A stationary hospital stay is extended by ≥2 days (after IRE > 3 days; after resection of the kidney tumour, >12 days) beyond the usual duration of confinement to bed.
— Persistent and/or interventions-requiring cardiac rhythm disorder leading to abortion of the IRE or occurring after the IRE,
— Circulatory dysregulation leading to abortion of the IRE,
— Epileptic attack after IRE,
— Movement of the IRE electrodes, caused by muscle contraction, with injury of non-target organs or non-target tissue during or after IRE,
— Retroperitoneal, perirenal abscess,
— Post-puncture, symptomatic, retroperitoneal haematoma requiring intervention and/or a symptomatic haemoglobin decrease after puncture, requiring intervention (definitions of indication for transfusion according to transfusion guidelines),
— Injury to neighbouring organs caused by puncture,
— Renal, ureteral or gastro-intestinal fistula formation,
— Post-puncture urinoma requiring intervention,
— Repeated operation after kidney tumour resection,
— Acute or sub-acute renal failure requiring dialysis,
— Renal infarction of the IRE-treated kidney after IRE (before or after resection),
— Complete loss of function of the IRE-treated kidney after IRE (before or after resection),
— Wound-healing disorder after IRE,
— Re-appearance of urinary blockage,
— Technically caused abortion of IRE,
— Permanent or significant handicap or impairment,
— Any other side effect that the investigator regard as serious (an important medical event), that may endanger the patient's health and/or requires measures to prevent one of the above events.

References

[1] Ahmed M, Solbiati L, Brace CL, Breen DJ, Callstrom MR, Charboneau JW, et al. International Working Group on Image-Guided Tumor Ablation; Interventional Oncology Sans Frontières Expert Panel; Technology Assessment Committee of the Society of Interventional Radiology; Standard of Practice Committee of the Cardiovascular and Interventional Radiological Society of Europe. Image-guided tumor ablation: standardization of terminology and reporting criteria — a 10-year update. J Vasc Interv Radiol Nov. 2014;25(11):1691–705. http://dx.doi.org/10.1016/j.jvir.2014.08.027 [e4; Epub 2014 Oct 23. PubMed PMID: 25442132].

[2] Golberg A, Yarmush ML. Nonthermal irreversible electroporation: fundamentals, applications, and challenges. IEEE Trans Biomed Eng Mar. 2013;60(3):707–14. http://dx.doi.org/10.1109/TBME.2013.2238672 [Epub 2013 Jan 9. Review. PubMed PMID: 23314769].

[3] Faroja M, Ahmed M, Appelbaum L, Ben-David E, Moussa M, Sosna J, et al. Irreversible electroporation ablation: is all the damage nonthermal? Radiology Feb. 2013;266(2):462–70. http://dx.doi.org/10.1148/radiol.12120609 [Epub 2012 Nov 20. PubMed PMID: 23169795].

[4] B. Ljungberg (chair), K. Bensalah, A. Bex (vice-chair), S. Canfield, S. Dabestani, F. Hofmann, M. Hora, M.A. Kuczyk, T. Lam, L. Marconi, A.S. Merseburger, P.F.A. Mulders, T. Powles, M. Staehler, A. Volp EAU Guidelines on Renal Cell Carcinoma;http://www.uroweb.org/gls/pdf/10%20Renal%20Cell%20Carcinoma_LR.pdf; 02.02.2015.

[5] Rubinsky B. Irreversible Electroporation. 1st ed. Berlin Heidelberg: Springer; 2009 328[10: 3642054196].

[6] Wendler JJ, Porsch M, Hühne S, Baumunk D, Buhtz P, Fischbach F, et al. Short- and mid-term effects of irreversible electroporation on normal renal tissue: an animal model. Cardiovasc Intervent Radiol Apr. 2013;36(2):512–20. http://dx.doi.org/10.1007/s00270-012-0452-7 [Epub 2012 Aug. 15. PubMed PMID: 22893419].

[7] Sommer CM, Fritz S, Wachter MF, Vollherbst D, Stampfl U, Bellemann N, et al. Irreversible electroporation of the pig kidney with involvement of the renal pelvis: technical aspects, clinical outcome, and three-dimensional CT rendering for assessment of the treatment zone. J Vasc Interv Radiol Dec. 2013;24(12):1888–97.

[8] Ben-David E, Ahmed M, Faroja M, Moussa M, Wandel A, Sosna J, et al. Irreversible electroporation: treatment effect is susceptible to local environment and tissue properties. Radiology Dec. 2013;269(3):738–47.

[9] Olweny EO, Kapur P, Tan YK, Park SK, Adibi M, Cadeddu JA. Irreversible electroporation: evaluation of nonthermal and thermal ablative capabilities in the porcine kidney. Urology Mar. 2013;81(3):679–84.

[10] Neal 2nd RE, Garcia PA, Robertson JL, Davalos RV. Experimental characterization and numerical modeling of tissue electrical conductivity during pulsed electric fields for irreversible electroporation treatment planning. IEEE Trans Biomed Eng Apr. 2012;59(4):1076–85.

[11] Wendler JJ, Pech M, Porsch M, Janitzky A, Fischbach F, Buhtz P, et al. Urinary tract effects after multifocal nonthermal irreversible electroporation of the kidney: acute and chronic monitoring by magnetic resonance imaging, intravenous urography and urinary cytology. Cardiovasc Intervent Radiol Aug. 2012;35(4):921–6.

[12] Wendler JJ, Pech M, Blaschke S, Porsch M, Janitzky A, Ulrich M, et al. Angiography in the isolated perfused kidney: radiological evaluation of vascular protection in tissue ablation by nonthermal irreversible electroporation. Cardiovasc Intervent Radiol Apr. 2012;35(2):383–90.

[13] Thomson KR, Cheung W, Ellis SJ, Federman D, Kavnoudias H, Loader-Oliver D, et al. Investigation of the safety of irreversible electroporation in humans. J Vasc Interv Radiol May 2011;22(5):611–21.

[14] Deodhar A, Monette S, Single Jr GW, Hamilton Jr WC, Thornton R, Maybody M, et al. Renal tissue ablation with irreversible electroporation: preliminary results in a porcine model. Urology Mar. 2011;77(3):754–60.

[15] Tracy CR, Kabbani W, Cadeddu JA. Irreversible electroporation (IRE): a novel method for renal tissue ablation. BJU Int Jun. 2011;107(12):1982–7.

[16] Pech M, Janitzky A, Wendler JJ, Strang C, Blaschke S, Dudeck O, et al. Irreversible electroporation of renal cell carcinoma: a first-in-man phase I clinical study. Cardiovasc Intervent Radiol Feb. 2011;34(1):132–8.

[17] Ball C, Thomson KR, Kavnoudias H. Irreversible electroporation: a new challenge in "out of operating theater" anesthesia. Anesth Analg May 1, 2010;110(5):1305–9.

[18] Wagstaff PG, de Bruin DM, van den Bos W, Ingels A, van Gemert MJ, Zondervan PJ, et al. Irreversible electroporation of the porcine kidney: temperature development and distribution. Urol Oncol Dec. 31, 2014. http://dx.doi.org/10.1016/j.urolonc.2014.11.019 [S1078-1439(14)00440-2; [Epub ahead of print] PubMed PMID: 25557146].
[19] Neal RE, Garcia PA, Kavnoudias H, Rosenfeldt F, Mclean CA, Earl V, et al. In vivo irreversible electroporation kidney ablation: experimentally correlated numerical models. IEEE Trans Biomed Eng Feb. 2015;62(2):561–9. http://dx.doi.org/10.1109/TBME.2014.2360374 [Epub 2014 Sep. 25. PubMed PMID: 25265626].
[20] Wimmer T, Srimathveeravalli G, Gutta N, Ezell PC, Monette S, Maybody M, et al. Planning irreversible electroporation in the porcine kidney: are numerical simulations reliable for predicting empiric ablation outcomes? Cardiovasc Intervent Radiol Feb. 2015;38(1):182–90. http://dx.doi.org/10.1007/s00270-014-0905-2 [Epub 2014 May 17. PubMed PMID: 24831827].
[21] Dunki-Jacobs EM, Philips P, Martin 2nd RC. Evaluation of thermal injury to liver, pancreas and kidney during irreversible electroporation in an in vivo experimental model. Br J Surg Aug. 2014;101(9):1113–21. http://dx.doi.org/10.1002/bjs.9536 [Epub 2014 Jun. 24. PubMed PMID: 24961953].
[22] https://clinicaltrials.gov/ct2/show/NCT01967407?term=IRENE&rank=1.
[23] http://apps.who.int/trialsearch/Trial2.aspx?TrialID=DRKS00004266.
[24] https://drks-neu.uniklinik-freiburg.de/drks_web/navigate.do?navigationId=trial.HTML&TRIAL_ID=DRKS00004266.
[25] http://www.angiodynamics.com/products/nanoknife.
[26] Ahmed M, Technology Assessment Committee of the Society of Interventional Radiology. Image-guided tumor ablation: standardization of terminology and reporting criteria — a 10-year update: supplement to the consensus document. J Vasc Interv Radiol Nov. 2014;25(11):1706–8. http://dx.doi.org/10.1016/j.jvir.2014.09.005 [Epub 2014 Oct 23. PubMed PMID: 25442133].
[27] http://www.pathologie.de/fachinfos/nachschlagewerke-handbuchreihe/handbuch-leitlinien-pathologie/leitfaeden-detailansicht/?tx_ttnews%5Btt_news%5D=268&cHash=73875b5f47d3e8ac0b970cf6987ab03b.
[28] Manual NanoKnife® System Procedure & Trouble Shouting Guide. Software Version 2.2.0. AngioDynamics®, © 2011 AngioDynamics, Inc. P1–159.
[29] ProcedureManager-2_2_0_23 for Windows, AngioDynamics®, © 2011 AngioDynamics, Inc.
[30] Böhm M, Schostak M, Hakenberg OW. Urinary immunocytology—promise or nonseller? A review with an opinion. Urol Oncol May 2014;32(4):383–90. http://dx.doi.org/10.1016/j.urolonc.2013.11.002 [Epub 2014 Mar 5. PubMed PMID: 24618288].
[31] https://www.destatis.de/EN/Homepage.html;jsessionid=1F6FAE698FB976BB1F6DA1391FA58335.cae4.
[32] Charlson M, Peterson J, Szatrowski TP, MacKenzie R, Gold J. Long-term prognosis after peri-operative cardiac complications. J Clin Epidemiol Dec. 1994;47(12):1389–400 [PubMed PMID: 7730848].
[33] http://www.dgss.org/versorgung/leitlinien-zur-schmerzbehandlung/von-der-deutschen-schmerzgesellschaft-ev-initiierte-leitlinien/.
[34] Poulakis V, Witzsch U, de Vries R, Moeckel M, Becht E. Quality of life after surgery for localized renal cell carcinoma: comparison between radical nephrectomy and nephron-sparing surgery. Urology Nov. 2003;62(5):814–20 [PubMed PMID: 14624900].
[35] Cella D, Yount S, Du H, Dhanda R, Gondek K, Langefeld K, et al. Development and validation of the Functional Assessment of Cancer Therapy — Kidney Symptom Index (FKSI). J Support Oncol Apr. 2006;4(4):191–9 [PubMed PMID: 16669463].
[36] http://evs.nci.nih.gov/ftp1/CTCAE/CTCAE_4.03_2010-06-14_QuickReference_5x7.pdf.
[37] Sacks D, McClenny TE, Cardella JF, Lewis CA. Society of Interventional Radiology clinical practice guidelines. J Vasc Interv Radiol Sep. 2003;14(9 Pt 2):S199–202.
[38] Liehr UB, Wendler JJ, Blaschke S, Porsch M, Janitzky A, Baumunk D, et al. Irreversible electroporation: the new generation of local ablation techniques for renal cell carcinoma. Urol Androl 2012 Dec;51(12):1728–34. http://dx.doi.org/10.1007/s00120-012-3038-8 [German. PubMed PMID: 23139026].
[39] Ricke J, Jürgens JH, Deschamps F, Tselikas L, Uhde K, Kosiek O, et al. Irreversible electroporation (IRE) fails to demonstrate efficacy in a prospective multicenter phase II trial on lung malignancies: the ALICE trial. Cardiovasc Intervent Radiol Apr 2015;38(2):401–8. http://dx.doi.org/10.1007/s00270-014-1049-0 [Epub 2015 Jan 22. PubMed PMID: 25609208].
[40] Ben-David E, Ahmed M, Faroja M, Moussa M, Wandel A, Sosna J, et al. Irreversible electroporation: treatment effect is susceptible to local environment and tissue properties. Radiology Dec 2013;269(3):738–47. http://dx.doi.org/10.1148/radiol.13122590 [Epub 2013 Oct. 28. PubMed PMID: 23847254; PubMed Central PMCID: PMC4228712].
[41] Valerio M, Dickinson L, Ali A, Ramachandran N, Donaldson I, Freeman A, et al. A prospective development study investigating focal irreversible electroporation in men with localised prostate cancer: NanoKnife Electroporation Ablation Trial (NEAT). Contemp Clin Trials Sep. 2014;39(1):57–65. http://dx.doi.org/10.1016/j.cct.2014.07.006 [Epub 2014 Jul 26. PubMed PMID: 25072507; PubMed Central PMCID: PMC4189798].
[42] Davalos RV, Bhonsle S, Neal 2nd RE. Implications and considerations of thermal effects when applying irreversible electroporation tissue ablation therapy. Prostate Mar. 23, 2015. http://dx.doi.org/10.1002/pros.22986 [[Epub ahead of print] PubMedPMID: 25809014].
[43] Wagstaff PG, de Bruin DM, Zondervan PJ, Savci Heijink CD, Engelbrecht MR, van Delden OM, et al. The efficacy and safety of irreversible electroporation for the ablation of renal masses: a prospective, human, in-vivo study protocol. BMC Cancer Mar. 22, 2015;15:165. http://dx.doi.org/10.1186/s12885-015-1189-x [PubMed PMID: 25886058; PubMed Central PMCID: PMC4376341].

8.12

First Delayed Resection Findings After Irreversible Electroporation (IRE) of Human Localised Renal Cell Carcinoma (RCC) in the IRENE Pilot Phase 2a Trial.

Wendler JJ, Ricke J, Pech M, Fischbach F, Jürgens J, Siedentopf S, Roessner A, Porsch M, Baumunk D, Schostak M, Köllermann J, Liehr UB.

Cardiovasc Intervent Radiol. 2016 Feb;39(2):239-50.

INTRODUCTION: It is postulated that focal IRE affords complete ablation of soft-tissue tumours while protecting the healthy peritumoral tissue. Therefore, IRE may be an interesting option for minimally invasive, kidney-tissue-sparing, non-thermal ablation of renal tumours.

AIM: With this current pilot study ("IRENE trial"), we present the first detailed histopathological data of IRE of human RCC followed by delayed tumour resection. The aim of this interim analysis of the first three patients was to investigate the ablation efficiency of percutaneous image-guided focal IRE in RCC, to assess whether a complete ablation of T1a RCC and tissue preservation with the NanoKnife system is possible and to decide whether the ablation parameters need to be altered.

METHODS: Following resection 4 weeks after percutaneous IRE, the success of ablation and detailed histopathological description were used to check the ablation parameters.

RESULTS: The IRE led to a high degree of damage to the renal tumours (1 central, 2 peripheral; size range 15-17 mm). The postulated homogeneous, isomorphic damage was only partly confirmed. We found a zonal structuring of the ablation zone, negative margins and, enclosed within the ablation zone, very small tumour residues of unclear malignancy.

CONCLUSION: According to these initial, preliminary study results of the first three renal cases, a new zonal distribution of IRE damage was described and the curative intended, renal saving focal ablation of localised RCC below <3 cm by percutaneous IRE by the NanoKnife system appears to be possible, but needs further, systematic evaluation for this treatment method and treatment protocol.

Cardiovasc Intervent Radiol (2016) 39:239–250
DOI 10.1007/s00270-015-1200-6

First Delayed Resection Findings After Irreversible Electroporation (IRE) of Human Localised Renal Cell Carcinoma (RCC) in the IRENE Pilot Phase 2a Trial

Johann Jakob Wendler[1] · Jens Ricke[3] · Maciej Pech[3] · Frank Fischbach[3] · Julian Jürgens[3] · Sandra Siedentopf[4] · Albert Roessner[4] · Markus Porsch[1] · Daniel Baumunk[1] · Martin Schostak[1] · Jens Köllermann[2] · Uwe-Bernd Liehr[1]

Received: 6 May 2015 / Accepted: 7 August 2015 / Published online: 4 September 2015

Abstract

Introduction It is postulated that focal IRE affords complete ablation of soft-tissue tumours while protecting the healthy peritumoral tissue. Therefore, IRE may be an interesting option for minimally invasive, kidney-tissue-sparing, non-thermal ablation of renal tumours.

Aim With this current pilot study ("IRENE trial"), we present the first detailed histopathological data of IRE of human RCC followed by delayed tumour resection. The aim of this interim analysis of the first three patients was to investigate the ablation efficiency of percutaneous image-guided focal IRE in RCC, to assess whether a complete ablation of T1a RCC and tissue preservation with the NanoKnife system is possible and to decide whether the ablation parameters need to be altered.

Methods Following resection 4 weeks after percutaneous IRE, the success of ablation and detailed histopathological description were used to check the ablation parameters.

Results The IRE led to a high degree of damage to the renal tumours (1 central, 2 peripheral; size range 15–17 mm). The postulated homogeneous, isomorphic damage was only partly confirmed. We found a zonal structuring of the ablation zone, negative margins and, enclosed within the ablation zone, very small tumour residues of unclear malignancy.

Jens Köllermann and Uwe-Bernd Liehr have contributed equally.

Johann Jakob Wendler, Jens Ricke, Maciej Pech, Frank Fischbach and Uwe-Bernd Liehr are with the German Academy for Microtherapy (DAfMT).
Daniel Baumunk, Martin Schostak, Jens Köllermann and Uwe-Bernd Liehr are with the Working Group for Focal and Microtherapy of the Academy for German Urologists.

✉ Johann Jakob Wendler
johann.wendler@med.ovgu.de

Jens Ricke
jens.Ricke@med.ovgu.de

Maciej Pech
macej.pech@med.ovgu.de

Frank Fischbach
frank.fischbach@med.ovgu.de

Julian Jürgens
julian.juergens@med.ovgu.de

Sandra Siedentopf
sandra.siedentopf@med.ovgu.de

Albert Roessner
albert.roessner@med.ovgu.de

Markus Porsch
markus.porsch@med.ovgu.de

Daniel Baumunk
daniel.baumunk@med.ovgu.de

Martin Schostak
martin.schostak@med.ovgu.de

Jens Köllermann
jens.koellermann@sana.de

Uwe-Bernd Liehr
uwe-bernd.liehr@med.ovgu.de

[1] Department of Urology, University Hospital, Otto von Guericke University of Magdeburg, Leipziger Str. 44, 39120 Magdeburg, Germany

[2] Institute of Pathology, Sana Klinikum Offenbach Am Main, Offenbach Am Main, Germany

[3] Department of Radiology, University of Magdeburg, Magdeburg, Germany

[4] Institute of Pathology, University of Magdeburg, Magdeburg, Germany

Conclusion According to these initial, preliminary study results of the first three renal cases, a new zonal distribution of IRE damage was described and the curative intended, renal saving focal ablation of localised RCC below <3 cm by percutaneous IRE by the NanoKnife system appears to be possible, but needs further, systematic evaluation for this treatment method and treatment protocol.

Keywords Irreversible electroporation (IRE) · Renal cell carcinoma (RCC) · Small renal mass (SRM) · Kidney · Focal therapy (FT) · Ablation

Introduction

In the treatment of RCC, focal therapy (FT) with the goal of minimising damage to the surroundings while still achieving total destruction of the tumour tissue is receiving increasing attention [1–4]. For focal IRE, it has been postulated that complete ablation of soft-tissue tumours with protection of the healthy peritumoral tissue is possible [2, 5–12]. Therefore, IRE represents an interesting potential option for nephron-sparing treatment of renal tumours. However, there is still a lack of clinical data for its application in RCC [13–16], and most studies have been based on radiological or post-biopsy assessment only. With this pilot study [17], we present the first detailed histopathological data of IRE treated RCC followed by delayed resection. The aims of the present interim analysis of the first three patients were to evaluate the ablation efficacy and accuracy of percutaneous focal IRE in RCC and to obtain a preliminary assessment of whether a histologically complete ablation of localised RCC with preservation of kidney tissue, using the NanoKnife™ system, is possible and to decide whether the ablation parameters need to be altered.

Methods

Study Approval

The detailed study protocol was published separately [17]. Approval for this GCP-compliant study [ClinicalTrials.gov: NCT01967407 (10/2013), ICTRP/WHO: DRKS00004266] was granted by German Federal Institute for Drugs and Medical Devices (BfArM) and Ethics Committee of University Magdeburg [73/2012].

Procedures

Metastatic disease was excluded by contrast-enhanced, thoracic CT and abdominopelvic CT or MRI. Renal MRI was performed one day before IRE for current tumour measurement and pretreatment planning (see Pretreatment planning) [17]. Due to the protocol, required tumour biopsy prior to ablation could precede IRE as initial diagnosis for histological proof of RCC in uncertain imaging or in the same session using the general anaesthesia required for IRE in obvious malignant imaging [1, 17].

Before IRE treatment, CT-guided coaxial core biopsies were taken from all tumours for initial histological assessment (case 1-3 with delay between). For IRE treatment, we used the NanoKnife™ IRE electroporator (AngioDynamics Inc.,® USA; firmware V3.29, software V2.2.0.23) and NanoKnife™ monopolar probes (15 cm, 19G). The electrodes were positioned under CT guidance (Aquillion prime CT scanner, Toshiba Inc.,® USA) and on the basis of individual treatment-planning data (ProcedureManager-2_2_0_23 for Windows, AngioDynamics®). IRE was performed with ECG triggering, under general anaesthesia and deep muscle paralysis. After 28 days, open partial kidney resection or radical nephrectomy with complete resection of the ablation region was performed [1]. To identify the spatial position of the resectate or tumour for the resection, the resectate will be anatomically land-marked intraoperatively with threads, as is usual. Renal MRI was performed one day before IRE.

The patient and treatment parameters are shown in Table 1. Intraprocedural modification was performed after immediately evaluation of post-IRE ablation graphs by interelectrode voltage modulation and separate electrode pair ablation. A complete ablation was defined as end-point with following characteristics: at least a complete ablation per electrode pair; simulated complete coverage of the tumour (target zone) by the treatment-planning zone; ideal (typically configurated) IRE ablation pulse graphs according to the manual [18]. The evaluation of the graphs was performed immediately after each pulse train application by at least two IRE experienced urologists and two IRE experienced interventional radiologists on the NanoKnife generator display.

Histopathological Analysis

Pre-IRE tumour biopsy specimens were fixed in 4 % buffered formalin, paraffin embedded, cut at 3 µm and stained with haematoxylin and eosin (HE). The resection specimens were fixed in buffered 4 % formaldehyde solution for at least 24 h followed by complete sectioning of the ablation area including a border of macroscopically inconspicuous kidney tissue in 0.4-cm-thick slices [19]. The ablation area was measured two dimensionally. In the case of nephrectomy, coarse sectioning of the remaining preparation was performed to exclude other pathologies. Thereafter, the ablation area, including the border, was completely embedded in paraffin in standard tissue cassettes after topographic assignment based on

Table 1 Patient and treatment parameters according to the Standardization of Terminology and Reporting Criteria for Image-Guided Tumor Ablation [21, 31]

	Patient 1 (44 years)	Patient 2 (78 years)	Patient 3 (74 years)
Tumour data			
No. targets	1	1	1
Tumour location	Upper pole, right, cortical, exophytic, ventrolateral	Upper to mid-pole region, right, cortical, exophytic, dorsomedial	Upper to mid-pole region, right, cortical, exophytic, dorsomedial, close to hilus
Tumour size (cm)	1.7 × 1.7 × 1.6	1.5 × 1.5 × 1.4	1.6 × 1.5 × 1.5
Tumour volume (ccm)	2.4	1.6	1.9
Tumour shape and class	Spherical, small	Spherical, small	Spherical, small
Biopsy	Pap RCC Typ 1, Fuhrman G2	Eosinophils cc RCC, Fuhrman G1	cc RCC, Fuhrman G1
Tumour texture	Inhomogeneous, solid, no cysts/calcification	Inhomogeneous, solid, no cysts/calcification	Inhomogeneous, solid, no cysts/calcification
TNM	pT1a G2 (C3)	pT1a G1 (C3)	pT1a G1 (C3)
	cN0 cM0 (C2) stage I	cN0 cM0 (C2) stage I	cN0 cM0 (C2) stage I
IRE parameter			
Procedures/sessions	1	1	1
Electrode type	Monopolar	Monopolar	Monopolar
No. of electrodes	4	3	4
No. of ablation pairs	6	3	6
Tip exposure[a] (cm)	2.5	1.5	2.0
Electrode configuration	Square	Triangular	Square
Interelectrode spaces (cm)	edge: 0.9–1.1, diagonal: 1.3–1.5	edge: 1.0–1.3; diagonal: n.a.	edge: 1.4–2.3, diagonal: 1.4–1.7
Ablation margin (cm)	0.2–0.6	0.3–0.5	0.5–1.4
Treatment zone (cm)	2.4 × 2.9 × 3.5[a]	2.5 × 2.5 × 2.5[a]	3.5 × 4.0 × 3.0[a]
Treatment zone (ccm)	12.7	8.2	22.0
No. of ablations	4 (plus 1 test run)	2 (plus 1 test run)	3 (plus 1 test run)
Pulse length	90 µs	90 µs	90 µs
Total no. of pulses	1300	450	1320
Current (max.)	49 A	42 A	49 A
Voltage (min./max.)	1800/2800 V	2200/2640 V	1960/3000 V
Surgery			
Resection type	Partial kidney resection	Partial kidney resection	Radical nephrectomy
ypTNM	ypT1a V0 L0 Pn0 R0 (C4)	ypT0 V0 L0 Pn0 R0 (C4)	ypT0 V0 L0 Pn0 R0 (C4)

Tumour and ablation volume ($V = \frac{1}{6}\pi d^3$, respectively, $\frac{4}{3}\pi abc$)

[a] Active tip (exposure) plus postulated ablation field in depth 2 × 0.5 cm [18]

macrophotography. Each tissue block was used to prepare 3-µm-thick sections, and these were stained with HE for morphological assessment in 500 µm steps with one unstained section each for transmission microscopy. Additional immunohistological staining of the tumour region with proliferation marker Mib1 (Dako; dilution 1:100) at least still rudimentary basic structure was performed to determine viability or irreversible cell death.

In each specimen, the complete ablation area, the tumour area and non-affected renal tissue on each slide was precisely outlined in multicoloured ink. The maps from each subject were computer scanned, inspected serially and determined by a digitising pad (Bamboo One™) and image-manipulation software (GIMP 2.8.14®). Volume was calculated as the sum of tumour areas multiplied by the section thickness (0.4 cm) and by a formalin-induced tissue-shrinkage factor of 1.5.

The extent of histologically demonstrable damage was determined by examining the histostructural changes (disorganisation of the original tumour structure) and also the cellular changes (ballooning, vacuolisation and nuclear pyknosis), and a regression grade (RG) was assigned according to the scale shown in Table 2 [19, 20].

Table 2 Histological-cellular grading of the regressive alterations of the RCC after IRE, adapted from Ref. [20]

RG	Histological and cellular morphology
0	No regression: Neither necrosis nor cellular or structural alterations
1	Slight regression: necrosis or disappearance of the tumour and/or cellular or structural alterations in less than 1/3 of the tumour
2	Moderate regression: necrosis or disappearance of the tumour and/or cellular or structural alterations in more than 1/3, but not more than 2/3, of the tumour
3	Strong regression: necrosis or disappearance of the tumour and/or cellular of structural alterations in more than 2/3 of the tumour, but still histomorphologically intact or only slightly altered tumour cells distinguishable
4	Complete regression: tumour completely necrotic and/or replaced by fibrosis. No histomorphologically intact tumour cells distinguishable

DR degree of regression

Results

Case 1 (Fig. 1)

Initial biopsy Initial biopsy revealed papillary RCC of type 1 (Fig. 1D). *Treatment* partial kidney resection. *Macroscopic analysis* Sharply demarcated, approximately ellipsoidal, haemorrhagically altered ablation zone. In the centre of the ablation zone, a round to oval tumour focus was clearly delineated. The greatest width of the peritumoural damage zone was 8 mm, spreading to peritumoural renal tissue and to perirenal fatty tissue (Fig. 1E, F–K). *Microscopic analysis* The tumour focus within the ablation zone showed strong treatment effects (RG III) with almost complete tumour destruction by extended, homogeneously eosinophilic coagulation necrosis (Fig. 1L). Within the necrotic tumour only, a small focus of preserved residual papillary tumour, comprising 18.7 % of the posttreatment tumour zone (12 % of the pretreatment tumour zone), was detected. The residue showed only minor regressive changes without demonstrable proliferative activity (Fig. 1L, O; Tables 2, 3; regression grade 3).

Case 2 (Fig. 2)

Initial biopsy Equivocal oncocytic renal tumour. On account of its staining profile (CD 10+, Vimentin−, cytokeratin 20−, Hale–) classified as clear-cell RCC of the eosinophilic subtype (Fig. 2D). *Treatment* partial kidney resection. *Macroscopic analysis* sharply demarcated, semi-ellipsoidal ablation zone with a broad base at the kidney surface and ellipsoidal intrarenal extension. At the ellipsoidal end clearly demarcated tumour focus. Extensive signs of local haemorrhage. Peritumourally a narrow (1 mm) margin of haemorrhagic surrounding tissue. A 9 mm margin to the kidney surface was present (Fig. 2E, F–I). *Microscopic analysis* The tumour focus within the ablation zone showed extensive coagulation necrosis with intratumoural haemorrhage, partly fresh and partly older as well as focal granulation tissue formation. Within the necrotic tumour, a small tumour focus comprising 2.8 % of the pre- and posttreatment tumour zone with rudimentary preserved histoarchitecture was seen (Fig. 2F–I). This focus showed severe cytological damage (homogeneous cytoplasm eosinophilia, cell hydropsy, cell-wall destruction with only schematically distinguishable cell nuclei and loss of nucleoli) without signs of proliferative activity in Mib-1 staining. The regressive changes were graded as RG 4 (Fig. 2J–L; Tables 2, 3).

Case 3 (Fig. 3)

Initial biopsy Clear-cell RCC (Fig. 3C). *Treatment* radical nephrectomy due to intraoperative findings (severe inflammatoric and fibrotic perifocal reaction with involvement of the hilus) (Fig. 4). *Macroscopic analysis* Extended geographic ablation zone with a central capsule-like, delimited tumour focus (Fig. 3E–L). Far-reaching peritumoural extension of the ablation region (width up to 11 mm) to the renal cortex and medulla, associated vessel structures, renal pelvis and perirenal fat (Fig. 5). *Microscopic analysis* The tumour focus within the ablation zone showed strong treatment effects (RG 4) with formation of extended homogeneous, acellular, eosinophilic coagulation necrosis and inclusion of an area with rudimentary preserved histoarchitecture (62.4 % of the preatreatment tumour zone resp. 91.2 % of the posttreatment tumour zone) which showed massive cytological damage (RG 4) without sign of a residual proliferative activity (Fig. 3M–O; Tables 2, 3).

Volumetry, Histological Planimetry and Volumetry

See Table 3 and Fig. 4

Zonal Histological Structuring of the Ablation Zone

Alongside the case-specific tumour-related histological changes described above, all cases showed a zonal structuring of the ablation region. In the centre, an amorphous necrosis zone of the coagulation-necrosis type (zone Z1 in Fig. 5A, B) was seen [21]. Next to this, there was a

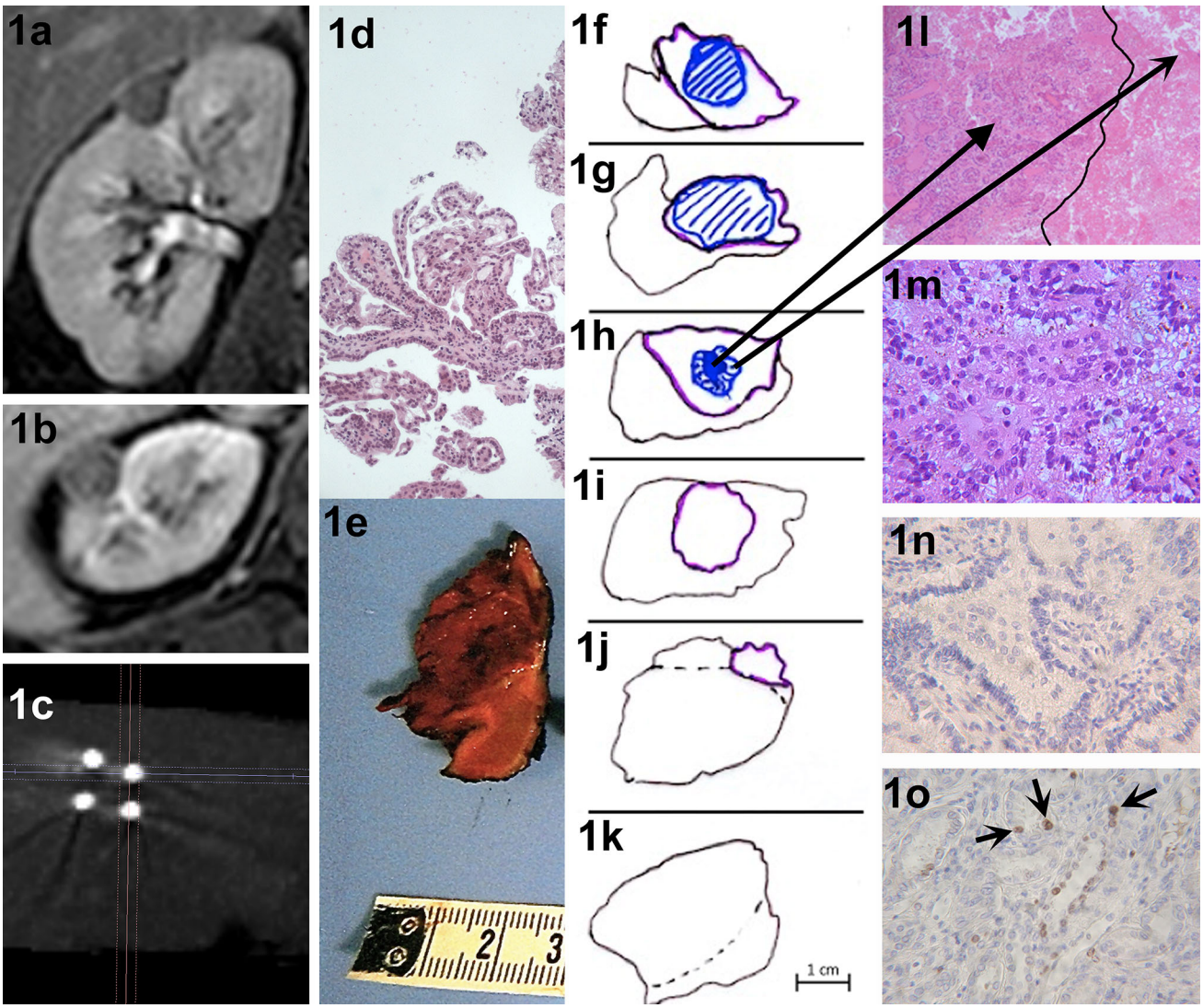

Fig. 1 Case 1: **A**, **B** Pre-interventional MRI coronal/transverse. **C** Check of IRE electrode placing in CT. **D** Histology of initial biopsy showing type 1 papillary RCC. **E** Macroscopic view of renal specimen with sharply demarcated ablation zone. **F–K** Macro- and microscopic fusion sketch of the serially sectioned renal specimen (**F** sketch corresponding to **E**): *violet line* ablation zone (including zone 2 and 3 as shown in Fig. 5), *blue-hatched area* tumour zone, *solid blue area* part of tumour zone with preserved histo- and cytoarchitecture; *black dashed line* border to perirenal fat. **L** Papillary NCC after IRE: ablated tumour area with complete necrosis of coagulation type on the *right of the black line* (corresponding to the *blue-hatched area* in the fusion sketches). Sharply adjacent tumour area with partially preserved histo- and cytomorphology on the *left of the black line* (corresponding to the *solid blue area* in the fusion sketch, haematoxylin–eosin (HE) staining) **M** Histologic detail view of the preserved tumour region from **L** showing papillary architecture and minor signs of cytologic damage (cell hydrops, cytoplasmic vacuolization, isolated pycnotic nuclei) (HE). **N** Same tumour area as in 1 m with negative staining for the proliferation marker Mib-1. **O** Low proliferative activity (individual nuclear-stained cells, *arrows*) of normal renal cortex tissue distant from the lesion (Mib-1 immunohistochemistry)

necrosis zone of variable width, also of the coagulation-necrosis type, in which ghost structures of the tissue affected could still be discerned (e.g., tubuli, glomeruli, fat; zone Z2 in Fig. 5A, C). Some dystrophic areas of calcification and resorptive chronic-inflammatory changes could also be seen, sometimes with the formation of foreign-body giant cells. In sections where the ablation zone included the renal pelvis and papillae, both structures showed necrosis with urothelial sloughing. Adjacent to this zone, there was a gradual transition to a zone of granulation tissue (zone Z3) with a width between 1 to 5 mm (mean 2.45 mm, data not shown). Zone 3 was associated with frequent, in part luminal occlusive intimal hyperplasia of small- and medium-sized arterial renal vessels. Adjacent to this, unaffected renal parenchyma (urp) was found (unaffected renal parenchyma = URP, Fig. 5A, D–F).

Table 3 Volumetry, histological planimetry, degree of regression, residual vitality

	Case 1	Case 2	Case 3
Pretreatment (planning, MRI)			
Tumour size (target size) (cm)	1.7 × 1.7 × 1.6	1.5 × 1.5 × 1.4	1.6 × 1.5 × 1.5
Volume tumour (ccm)	2.4	1.6	1.9
Treatment zone (cm)	2.4 × 2.9 × 3.5[#]	2.5 × 2.5 × 2.5[#]	3.5 × 4.0 × 3.0[#]
Volume treatment (planning) zone (ccm)	12.7	8.2	22.0
Posttreatment (histological)			
Tumour size (cm)	1.6 × 1.5 × 1.2	1.6 × 1.7 × 1.1	1.5 × 1.4 × 1.2
Volume treated tumour (contour) (ccm)	1.5	1.6	1.3
Volume residual tumour (ccm)	0.28	0.045	1.185
Ablation zone[a] size (cm)	2.5 × 2.0 × 1.3	3.0 × 2.5 × 2.0	4.2 × 3.0 × 2.6
Ablation zone[a] volume (ccm)	3.4	7.9	17.2
Tumour characteristics			
RCC type	Papillary	Clear cell	Clear cell
Regression grade (Table 2)	3	4	4
Residual tumour of pretreatment tumour size (%)	12	2.8	62.4
Residual tumour of posttreatment tumour size (%)	18.7	2.8	91.2
Mib-1 labelling index (%)[b]	0	0	0
Assessment of viability	Uncertain	Non-viable	Non-viable
Post–Pre-IRE proportions			
Δ Tumour volume (involution/shrinkage) (ccm)	−0.9	0	−0.6
Δ Tumour volume (involution/shrinkage) (%)	−37.5	0	−31.6
Δ Volume Ablation zone[a]—treatment (plan.) zone (ccm)	−9.3	−0.3	−4.8
Q Volume ablation zone[a]/treatment (plan.) zone (%)	+26.8	+96.3	+79.2

Treated tumour is residual visible tumour shape (volume) with histological signs of posttreatment alteration of the complete tumour area. Residual tumour is histologically residual tumour structure without signs of complete destruction

Volume ($V = \frac{1}{6}\pi d^3$, respectively, $\frac{4}{3}\pi abc$)

[a] Ablation zone includes zone Z2 and Z3 as defined in Fig. 5

[b] Percentage of Mib-1-nuclear-labelled tumour cells

Discussion

This pilot study is intended to assess the results obtained from resection after curative IRE of localised RCC in humans. This allows a first-ever clinical check of the hitherto mostly pre-clinical considerations of the general mechanism, the non-thermal ablation characteristics and the organ-independent effectiveness of IRE. In this preliminary interim analysis, the following hypotheses were considered: Early experiments had shown a shrunk scarring 2–4 weeks after apoptosis induction by IRE, assuming macrophagocytic degeneration of the ablation zone. A concentric-zonal character of the ablation zone has been described [7]. In contrast to this, monitoring of IRE-induced ablation exclusively by imaging and biopsy (for various types of tumour) revealed persistent tumour structures [15]. Assuming that the effect of IRE is non-thermal, this leads to the hypothesis that one must reckon with the continued presence of regressively altered tumour cells, dependent upon the time that has elapsed since IRE. The assessment of viability of these cells is particularly important. The required regression grading of RCC after non-operative treatment does not yet exist and would have to be established for progress-monitoring by biopsy (see e.g. Table 2) [1, 19]. The best time for this assessment must also be established. On the basis of the resection results (ablation and tumour geometry), the study parameters would also require adjustment.

Zonal Structuring of the Ablation Zone

The histological analysis of the tumour specimens confirmed a zonal structuring of the ablation zone as already described in previous animal studies [7, 10, 11]. A conspicuous feature was the detection of a central necrotic region in all of our cases. This largely unreactive

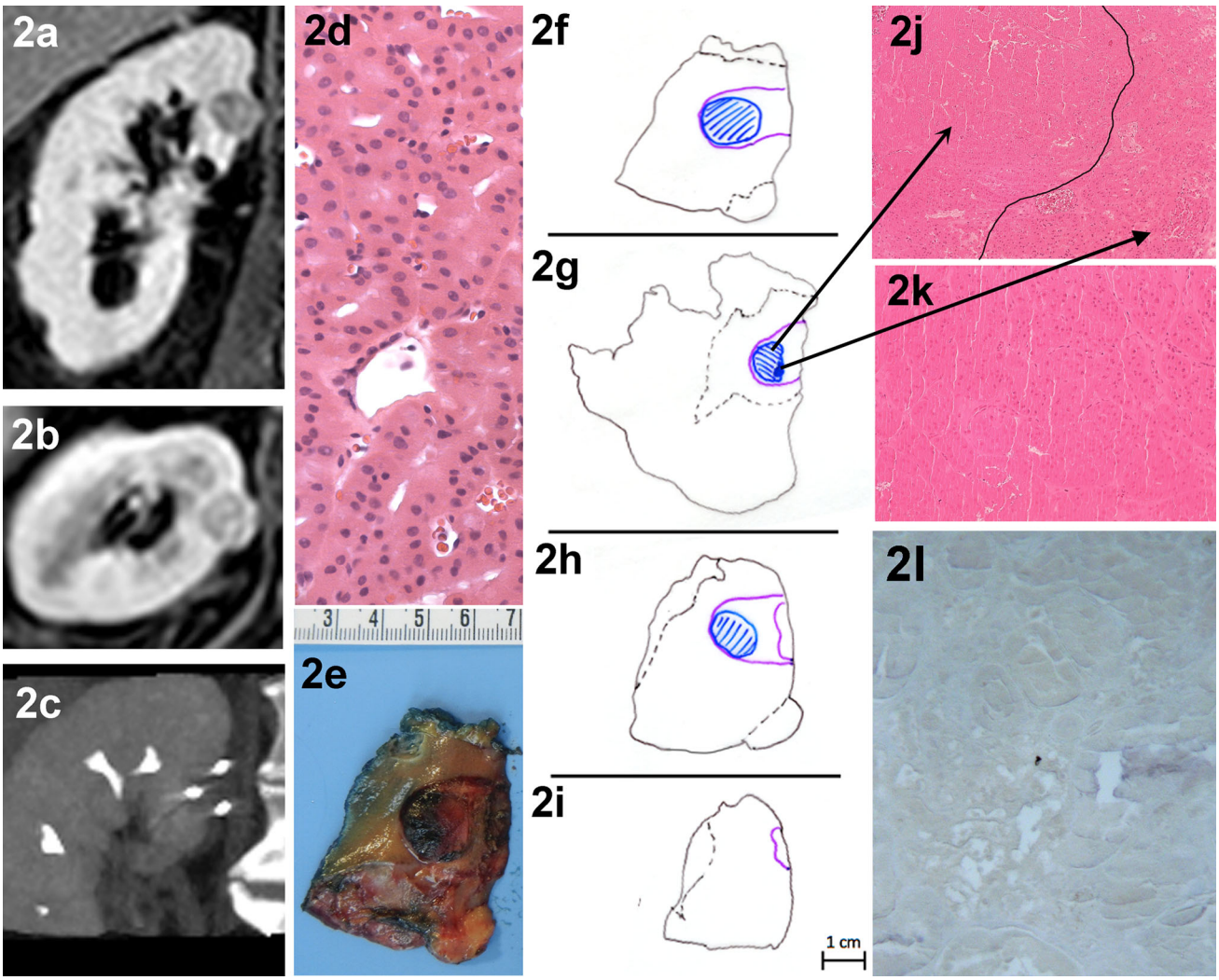

Fig. 2 Case 2: **A**, **B** Pre-interventional MRI coronal/transverse. **C** Check of IRE electrode placing in CT after administration of contrast enhancer. **D** Histology of initial biopsy showing ccRCC of eosinophilic subtype. **E** Macroscopic view of renal specimen with ablation zone. **F**–**I** Macro- and microscopic fusion sketch of the sectioned tumour resectate (sketch **F** corresponding to Fig. 2E): *violet line* ablation zone (including zone 2 and 3 as shown in Fig. 5), *blue-hatched area* tumour zone, *solid blue area* part of tumour zone with rudimentary preserved histo- and cytoarchitecture, *black dashed line* border to perirenal fat. **J** ccRCC after IRE: ablated tumour area with complete necrosis of coagulation type on the *left of the black line* (corresponding to the *blue-hatched area* in the fusion sketches). Sharply adjacent tumour area with hardly recognizable residual histoarchitecture on the *right of the black line* (corresponding to the *solid blue area* in the fusion sketch, haematoxylin-eosin (HE) staining*). **K** Detail view of tumour necrosis with rudimantory tumour architecture and severe signs of cytological damage (destroyed cell walls, cell hydrops, shadow nuclei, (HE)). **L** Same tumour area as shown in **K** with negative staining for the proliferation marker Mib-1

coagulation/infarction necrosis made up the greatest part of the damage zone (zone 1). To date, only one previous study [7] reported on a damage pattern of this kind of limited extend 28 days after IRE, which corresponds to the age of zone 1 in the current study (Figs. 1, 2, 3, 5).

Considering further its size, homogeneity, damage pattern as well as its sharp delineation suggests that zone 1 corresponds to the initial damage zone of IRE (Fig. 5A). In contrast to the finding of initial pre-clinical studies [7], this zone 1 did not pass directly over into normal surrounding tissue. Rather, it was surrounded by two further zones of damage (zones 2 and 3, Fig. 5). The histological picture of zone 2 suggests more recent damage, about 7 days old. One must therefore proceed on the assumption of a two-phase process. In subsequent studies with a defined interval between IRE and resection, it will be necessary to take into account whether, and if so when, this secondary tissue damage increases the initial ablation volume.

Zones 2 and 3 might have their origin in one or both of the following mechanisms:

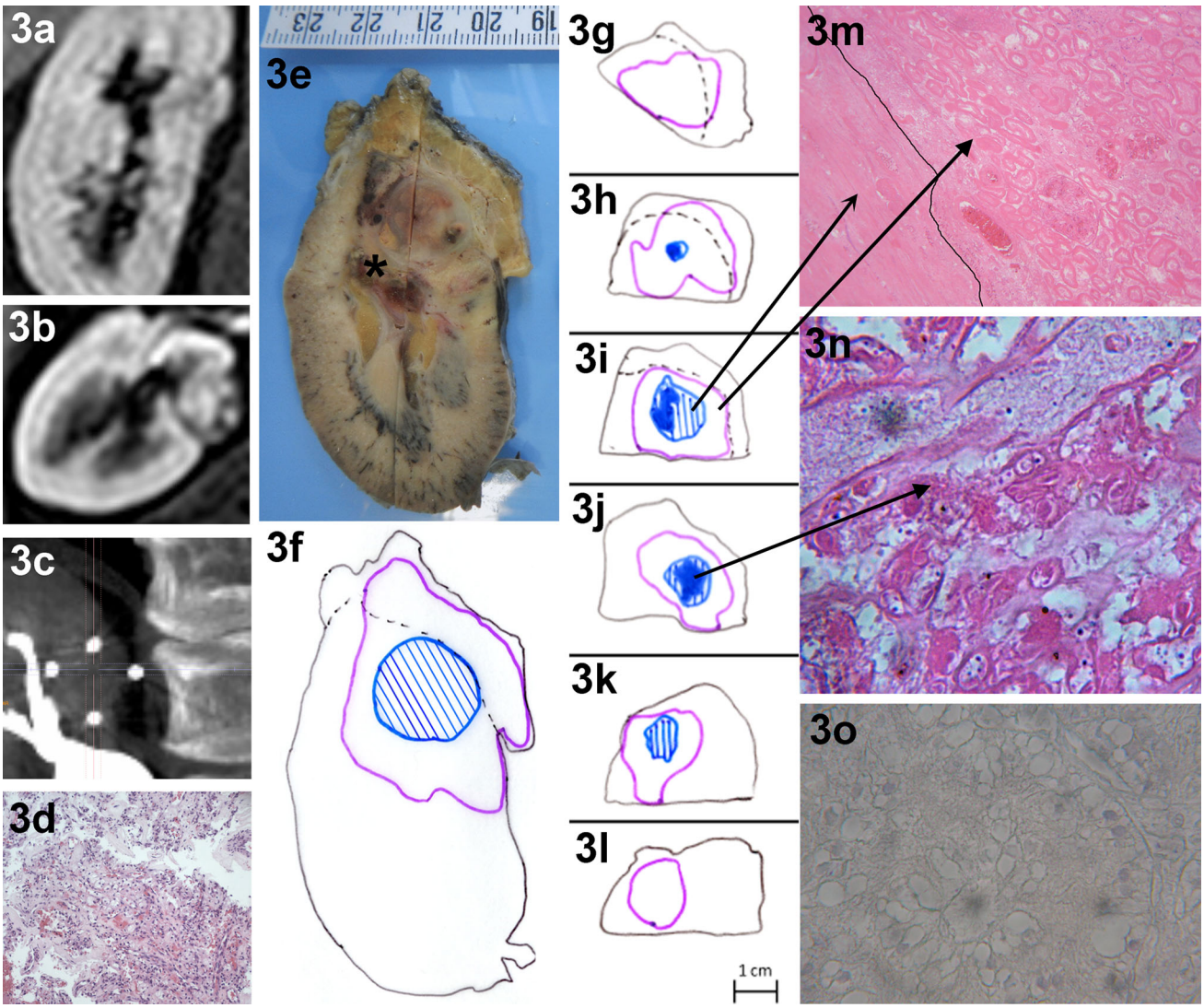

Fig. 3 Case 3: **A**, **B** Pre-interventional MRI coronal/transverse. **C** Check of IRE electrode placing in CT. **D** Histology of initial biopsy showing ccRCC. **E** Macroscopic section of the nephrectomy preparation with ablation region, which covers ca. 2/3 of the cranial kidney region; renal pelvis (*). **F** Macro- and microscopic fusion sketch of the nephrectomy specimen (corresponding to **E**), **G**–**L**: sketches of serially sectioned tumour bearing ablation zone. For all sketches: *violet line* ablation zone (including zone 2 and 3 as shown in Fig. 5), *blue-hatched area* tumour zone, *solid blue area* part of tumour zone with still distinguishable histo- and cytoarchitecture; *black dashed line* border to perirenal fat. **M** Ablated tumour area with complete coagulation necrosis on the *left of the black line* and a sharp transition to the bordering non-tumour parenchyma with less homogeneous coagulation necrosis showing contours of necrotic tubuli on the *right of the dashed line* (HE). **N** Necrotic tumour portion with still recognisable basis structure and signs of severe cytological damage (destroyed cell walls, cytoplasm vacuolisation and nuclear destruction; HE). **O** The absence of detection of proliferative activity (nuclear negativity) of the tumour section from 3n (Mib-1 immunohistochemistry)

– The energy of the electric field decays "centrifugally". A lower voltage gradient—below the postulated lower efficacy limit for IRE—explains the sharp primary demarcation of the ablation region. Histological transformation processes in the ablation region (cell clusters, interstitial processes, capillaries) could lead to secondary, nutritive damage (diffusional changes) by perturbation of cellular homeostasis in the immediately adjacent tissue.

– Zones 2 and 3 show conspicuous vascular alterations. The intralobar arteries show prominent mural thickening, in part with complete luminal obliteration (Fig. 5E, F). This phenomenon is of interest as it was seen clearly, in all cases, in the region of zones 2 and 3. This kind of vessel damage has been described in animal experiments [7]. Hypoxic effects caused by the initial tissue damage is known to induce vascular intima hyperplasia—up to complete obliteration of

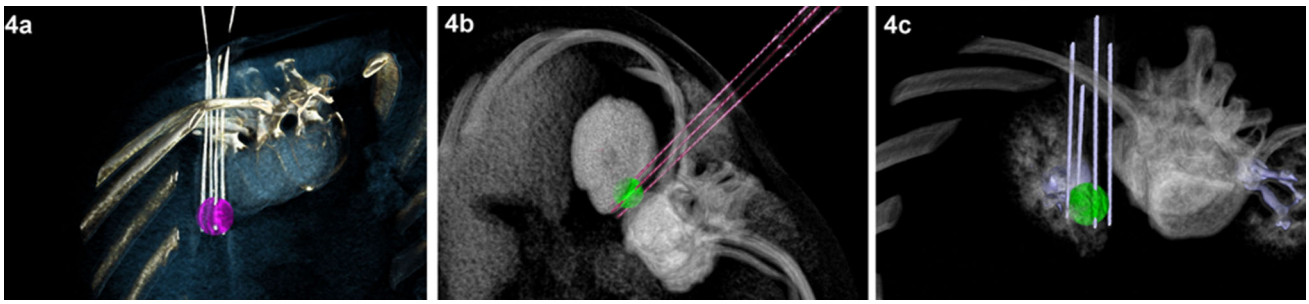

Fig. 4 3D-CT-reconstruction of the IRE electrode placing (case 1, **A**; case 2, **B**; case 3, **C**)

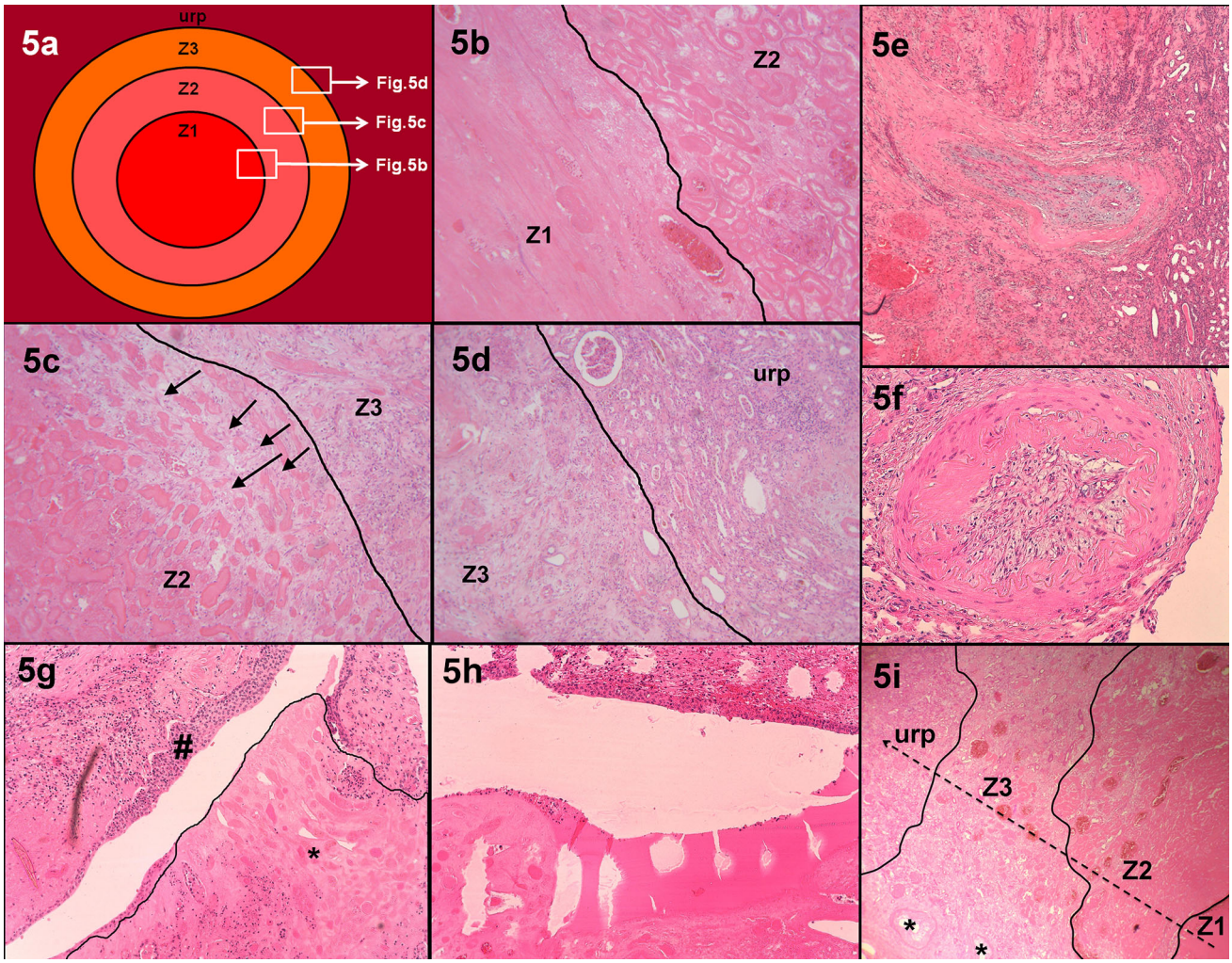

Fig. 5 **A** Macroscopic/microscopic structural sketch of the ablation region with trizonal structuring of tissue damage. **B** Damage zone Z1 of the type amorphous-coagulation necrosis, passing over into damage zone Z2, also of the type amorphous-coagulation necrosis but with discernable basic tissue structure. **C** Zone Z2, at the periphery, with sprouting by connective tissue (*arrows*) and, adjacent to this, transition to damage zone Z3, which consists of a fibrosis seam with formation of granulations tissue. **D** Transition from zone Z3 to unaffected renal parenchyma (urp). **E** Zone 3 arterial vessel with vaso-occlusive intima hyperplasia. **F** Detail of a zone 3 small arterial vessel with vaso-occlusive intima hyperplasia. (**B**–**F**: HE staining). **G** Treatment effect on renal pyelon showing necrotic renal papilla* covered by partially necrotic urothelium with urothelial sloughing. # non-affected intact urothelium. Yet no signs of stricture formation or luminal obliteration. **H** Histologic details from **G**. **I** low power microphotograph showing the zonal distribution of the ablation zone (Z1–Z3) as described above. * zone 3 vessels with prominent intima proliferation

surrounding vessels which could lead to ischaemia-based secondary necrosis. The origin of this might lie in the vascular-lock phenomenon described above [3, 9, 22, 23].

Volumetry

The ablation volumes found by histology corresponded to the planned ablation volumes in that in each case the actual ablation volume (zone 1–3) completely included the tumour volume. In the histological volumetry the reduction in tumour volume (delta post-minus pretreatment tumour volume) was −37.5 %, 0 % and −31.6 % for cases 1, 2 and 3, respectively. The proportion of in ablation versus treatment (planning) zone/volume (quotient) was 26.8, 96.3 and 79.2 % for cases 1, 2 and 3, respectively. The differences (pre–post) in both ablation and tumour volumes are best explained by a combination of shrinkage induced by IRE (tissue remodelling), by resection (lack of perfusion) and by formalin fixation.

On the basis of the very small number of patients investigated so far, no meaningful statistical assessment is possible. However, it already appears that a parallel shrinkage of both volumes takes place. The secondary necrosis could also possibly have a quantitative influence on this tissue shrinkage (Fig. 5). To what extent the region of secondary necrosis in zones 2 and 3 (Fig. 5) exceeds the area of the primary ablation field cannot at present be decided, on account of the shrinkage of the ablation region and the difficulty in calculating it. However, this is probably not relevant in clinical application, because of the inherent inaccuracy of 1–2 mm in the CT-guided placing of the IRE electrodes, even with layer thicknesses of 1 mm (Fig. 4). Because of the tissue remodelling after 28 days (involution), and shrinkage due to formalin fixation, an exact correlation of the observed ablation volumes to the planned treatment volumes is not possible. However, the goal of completely coveraging the tumour area by the ablation zone was achieved while at the same time the kidney was preserved.

Summary of Tumour Histopathology

In this study, histologically altered tumour structures were observed after an interval of 4 weeks between IRE and resection; these showed various degrees of change. To assess these findings systematically, we used an adapted regression grading (Table 2). These histologies represented "snapshots" 4 weeks after IRE, with specific findings. Although the choice of a different interval between IRE and histological analysis could of course influence this result, the optimum interval between IRE and histological assessment is at present still unclear.

In each of the three cases investigated, IRE-induced massive damage to the tumour tissue. In no case did a tumour residue appear at the edge of the ablation zones. The minimum safety margin was ca. 1 mm (medullary), and the greatest margin was 8–11 mm (cortical), on account of the tumour's position.

The tumour damage comprised complete tumour necrosis in cases 2 and 3, while in case 1 almost complete tumour necrosis was observed, with a residual tumour that measured 8 mm and made up 12 % of the original tumour volume; according to Mib-1 staining, it had no proliferative activity (Case 1). However, Mib-1 immunohistochemistry is only of limited in assessing the viability of slowly proliferating tumours such as RCC, especially of small residues comprising only few cells. Therefore, a residual viability cannot be excluded with certainty on a histological basis, in spite of the negative immunohistochemical reaction to the proliferation marker Mib-1. The assessment of apoptosis or programmed cell death by the terminal transferase-mediated nick end labelling technique represents an additional technique of tissue viability testing. Due to well-known technical pitfalls [24], we initially decided to abstain from TUNEL staining. However, due to the remaining uncertainty concerning residual tumour viability, we will apply TUNEL staining in future investigations.

It is also unclear whether, the massive perifocal structure and vessel damage would here also have led to complete necrosis of this tumour region. It remains uncertain as to whether the basic histological structure of this tumour residue (papillary RCC) and/or a non-optimised IRE field was the cause of this [25, 26].

At least the meta-analyses of patients with positive surgical margin after nephron-sparing surgery of RCC suggests a lack of prognostic relevance of small tumour residues. Therefore, a surveillance strategy seems preferable to surgical reintervention [27, 28]. Small, dubious tumour residues remaining in the non-viable ablation region 4 weeks after IRE must be assessed in the light of this. Similarly, residual tumour areas are seen following RFA that possess a residual viability immediately and one week after ablation [29, 30]. Following IRE of liver tumours, for comparison, 29 % showed recurrent tumour after 6 months [25].

Conclusion

IRE (with used recommended clinical parameters in this treatment protocol) could be an effective treatment and led to near-total or total destruction of various histological RCC subtypes. 4 weeks after IRE, novel histological findings were made. The postulated homogeneous, isomorphic tissue damage by IRE could not be confirmed.

Instead of this, a new zonal distribution of IRE damage was described. The assessment of the viability and clinical relevance of very small amounts of residual tumour is difficult. Viable tumour cells may be possible within an IRE ablation zone. Up to that preliminary point an alteration of the ablation parameters cannot be recommended. Because of the tissue remodelling after 28 days (involution), and shrinkage due to formalin fixation, an exact correlation of the observed ablation volumes to the planned treatment volumes is not possible. However, at least, the goal of complete coverage of the tumour by ablation zone while focal ablation with preserving of the kidney was achieved. On the basis of various observables (depth of target, breathing movement, puncture window, manual CT-guided electrode placement), an ablation volume reduced to that of the renal tumour appears feasible (Fig. 4). According to these initial, preliminary study results of the first three renal cases, the curative intended, renal saving focal ablation of localised RCC below <3 cm by percutaneous IRE by the NanoKnife system appears to be possible but needs further, systematic evaluation for optimation of this treatment method and treatment protocol.

Compliance with Ethical Standards

Conflict of Interest Author 10 (Martin Schostak) has received funding for conference attendance from AngioDynamics Inc. (New York, USA). Neither of these sources provided any input whatsoever into this article or this study. The other authors declare that they have no conflict of interest.

Ethical Approval All procedures performed in studies involving human participants were in accordance with the ethical standards of the institutional and/or national research committee and with the 1964 Helsinki declaration and its later amendments or comparable ethical standards.

Informed Consent Informed consent was obtained from all individual participants included in this study. Additional informed consent for identifying information does not apply.

References

1. Ljungberg B, Bensalah K, Bex A, Canfield S, Dabestani S, Hofmann F, Hora M, Kuczyk MA, Lam T, Marconi L, Merseburger AS, Mulders PFA, Powles T, Staehler M, Volpe A. EAU guidelines on renal cell carcinoma. http://uroweb.org/guideline/renal-cell-carcinoma/#. Accessed 26 April 2015.
2. Castro A Jr, Jenkins LC, Salas N, Lorber G, Leveillee RJ. Ablative therapies for small renal tumours. Nat Rev Urol. 2013;10(5):284–91. doi:10.1038/nrurol.2013.68.
3. Rubinsky B. Irreversible electroporation. 1st ed. Berlin: Springer; 2009. p. 328. ISBN 3642054196.
4. Silk M, Tahour D, Srimathveeravalli G, Solomon SB, Thornton RH. The state of irreversible electroporation in interventional oncology. Semin Intervent Radiol. 2014;31(2):111–7. doi:10.1055/s-0034-1373785.
5. Sommer CM, Fritz S, Wachter MF, Vollherbst D, Stampfl U, Bellemann N, Gockner T, Mokry T, Gnutzmann D, Schmitz A, Knapp J, Longerich T, Kuhn-Neureuther C, Pereira PL, Kauczor HU, Werner J, Radeleff BA. Irreversible electroporation of the pig kidney with involvement of the renal pelvis: technical aspects, clinical outcome, and three-dimensional CT rendering for assessment of the treatment zone. J Vasc Interv Radiol. 2013;24(12):1888–97. doi:10.1016/j.jvir.2013.08.014.
6. Olweny EO, Kapur P, Tan YK, Park SK, Adibi M, Cadeddu JA. Irreversible electroporation: evaluation of nonthermal and thermal ablative capabilities in the porcine kidney. Urology. 2013;81(3):679–84. doi:10.1016/j.urology.2012.11.026.
7. Wendler JJ, Porsch M, Hühne S, Baumunk D, Buhtz P, Fischbach F, Pech M, Mahnkopf D, Kropf S, Roessner A, Ricke J, Schostak M, Liehr UB. Short- and mid-term effects of irreversible electroporation on normal renal tissue: an animal model. Cardiovasc Intervent Radiol. 2013;36(2):512–20. doi:10.1007/s00270-012-0452-7.
8. Wendler JJ, Pech M, Porsch M, Janitzky A, Fischbach F, Buhtz P, Vogler K, Hühne S, Borucki K, Strang C, Mahnkopf D, Ricke J, Liehr UB. Urinary tract effects after multifocal nonthermal irreversible electroporation of the kidney: acute and chronic monitoring by magnetic resonance imaging, intravenous urography and urinary cytology. Cardiovasc Intervent Radiol. 2012;35(4):921–6. doi:10.1007/s00270-011-0257-0.
9. Wendler JJ, Pech M, Blaschke S, Porsch M, Janitzky A, Ulrich M, Dudeck O, Ricke J, Liehr UB. Angiography in the isolated perfused kidney: radiological evaluation of vascular protection in tissue ablation by nonthermal irreversible electroporation. Cardiovasc Intervent Radiol. 2012;35(2):383–90. doi:10.1007/s00270-011-0187-x.
10. Deodhar A, Monette S, Single GW Jr, Hamilton WC Jr, Thornton R, Maybody M, Coleman JA, Solomon SB. Renal tissue ablation with irreversible electroporation: preliminary results in a porcine model. Urology. 2011;77(3):754–60. doi:10.1016/j.urology.2010.08.036.
11. Tracy CR, Kabbani W, Cadeddu JA. Irreversible electroporation (IRE): a novel method for renal tissue ablation. BJU Int. 2011;107(12):1982–7. doi:10.1111/j.1464-410X.2010.09797.x.
12. Liehr UB, Wendler JJ, Blaschke S, Porsch M, Janitzky A, Baumunk D, Pech M, Fischbach F, Schindele D, Grube C, Ricke J, Schostak M. Irreversible electroporation: the new generation of local ablation techniques for renal cell carcinoma. Urologe A. 2012;51(12):1728–34. doi:10.1007/s00120-012-3038-8.
13. Ball C, Thomson KR, Kavnoudias H. Irreversible electroporation: a new challenge in "out of operating theater" anesthesia. Anesth Analg. 2010;110(5):1305–9. doi:10.1213/ANE.0b013e3181d27b30.
14. Pech M, Janitzky A, Wendler JJ, Strang C, Blaschke S, Dudeck O, Ricke J, Liehr UB. Irreversible electroporation of renal cell carcinoma: a first-in-man phase I clinical study. Cardiovasc Intervent Radiol. 2011;34(1):132–8. doi:10.1007/s00270-010-9964-1.
15. Thomson KR, Cheung W, Ellis SJ, Federman D, Kavnoudias H, Loader-Oliver D, Roberts S, Evans P, Ball C, Haydon A. Investigation of the safety of irreversible electroporation in humans. J Vasc Interv Radiol. 2011;22(5):611–21. doi:10.1016/j.jvir.2010.12.014 **Epub 2011 Mar 25**.
16. Nielsen K, Scheffer HJ, Vieveen JM, van Tilborg AA, Meijer S, van Kuijk C, van den Tol MP, Meijerink MR, Bouwman RA. Anaesthetic management during open and percutaneous irreversible electroporation. Br J Anaesth. 2014;113(6):985–92. doi:10.1093/bja/aeu256.
17. Wendler JJ, Porsch M, Nitschke S, Köllermann J, Siedentopf S, Pech M, Fischbach F, Ricke J, Schostak M, Liehr UB. A prospective Phase 2a pilot study investigating focal percutaneous irreversible electroporation (IRE) ablation by NanoKnife in patients with localised renal cell carcinoma (RCC) with delayed interval tumour resection (IRENE trial). Contemp Clin Trials. 2015;43:10–9. doi:10.1016/j.cct.2015.05.002.

18. Manual NanoKnife® System Procedure & Trouble Shouting Guide. Software version 2.2.0. AngioDynamics®, © 2011 AngioDynamics, Inc. p. 1–159.
19. http://www.pathologie.de/fachinfos/nachschlagewerke-handbuchreihe/handbuch-leitlinien-pathologie/leitfaeden-detailansicht/?tx_ttnews%5Btt_news%5D=268&cHash=73875b5f47d3e8ac0b970cf6987ab03b.
20. Ninomiya Y, Yanagisawa A, Kato Y, Kitagawa T, Ishihara S, Nakajima T. Histological indications of a favorable prognosis with far-advanced gastric carcinomas after preoperative chemotherapy. J Cancer Res Clin Oncol. 1999;125(12):699–706.
21. DE Dupuy, Gervais DA, Gianfelice D, Gillams AR, Lee FT Jr, Leen E, Lencioni R, Littrup PJ, Livraghi T, Lu DS, McGahan JP, Meloni MF, Nikolic B, Pereira PL, Liang P, Rhim H, Rose SC, Salem R, Sofocleous CT, Sofocleous CT, Solomon SB, Soulen MC, Tanaka M, Vogl TJ, Wood BJ, Goldberg SN, International Working Group on Image-Guided Tumor Ablation, Standard of Practice Committee of the Cardiovascular and Interventional Radiological Society of Europe. Image-guided tumor ablation: standardization of terminology and reporting criteria–a 10-year update. J Vasc Interv Radiol. 2014;25(11):1691–705. doi:10.1016/j.jvir.2014.08.027.
22. Calmels L, Al-Sakere B, Ruaud JP, Leroy-Willig A, Mir LM. In vivo MRI follow-up of murine tumors treated by electrochemotherapy and other electroporation-based treatments. Technol Cancer Res Treat. 2012;11(6):561–70 **Epub 2012 Jun 15**.
23. Ierardi AM, Lucchina N, Duka E, Bacuzzi A, Dionigi G, Carrafiello G. "Vascular lock" causing splenic perfusion defects during irreversible electroporation of a locally advanced pancreatic tumor. JOP. 2014;15(6):604–8. doi:10.6092/1590-8577/2850.
24. Garrity MM, Burgart LJ, Riehle DL, Hill EU, Sebo TJ, Witzig T. Identifying and quantifying apoptosis: navigating technical pitfalls. Mod Pathol. 2003;16(4):389–94.
25. Niessen C, Igl J, Pregler B, Beyer L, Noeva E, Dollinger M, Schreyer AG, Jung EM, Stroszczynski C, Wiggermann P. Factors associated with short-term local recurrence of liver cancer after percutaneous ablation using irreversible electroporation: a prospective single-center study. J Vasc Interv Radiol. 2015. doi:10.1016/j.jvir.2015.02.001.
26. Wendler JJ, Porsch M, Fischbach F, Pech M, Schostak M, Liehr UB. Letter to the Editor Concerning "Irreversible Electroporation (IRE) Fails to Demonstrate Efficacy in a Prospective Multicenter Phase II Trial on Lung Malignancies: The ALICE Trial" by Ricke et al. 2015. Cardiovasc Intervent Radiol. 2015. doi:10.1007/s00270-014-1049-0.
27. Steinestel J, Steffens S, Steinestel K, Schrader AJ. Positive surgical margins in nephron-sparing surgery: risk factors and therapeutic consequences. World J Surg Oncol. 2014;12:252. doi:10.1186/1477-7819-12-252.
28. Marszalek M, Carini M, Chlosta P, Jeschke K, Kirkali Z, Knüchel R, Madersbacher S, Patard JJ, Van Poppel H. Positive surgical margins after nephron-sparing surgery. Eur Urol. 2012;61(4):757–63. doi:10.1016/j.eururo.2011.11.028.
29. Rendon RA, Kachura JR, Sweet JM, Gertner MR, Sherar MD, Robinette M, Tsihlias J, Trachtenberg J, Sampson H, Jewett MA. The uncertainty of radio frequency treatment of renal cell carcinoma: findings at immediate and delayed nephrectomy. J Urol. 2002;167(4):1587–92.
30. Klingler HC, Marberger M, Mauermann J, Remzi M, Susani M. 'Skipping' is still a problem with radiofrequency ablation of small renal tumours. BJU Int. 2007;99(5):998–1001.
31. Ahmed M, Technology Assessment Committee of the Society of Interventional Radiology. Image-guided tumor ablation: standardization of terminology and reporting criteria–a 10-year update: supplement to the consensus document. J Vasc Interv Radiol. 2014;25(11):1706–8. doi:10.1016/j.jvir.2014.09.005.

8.13

Focal therapy for small renal masses: Observation, ablation or surgery.

Wendler JJ, Friebe B, Baumunk D, Blana A, Franiel T, Ganzer R, Hadaschik B, Henkel T, Köhrmann KU, Köllermann J, Kuru T, Machtens S, Roosen A, Salomon G, Schlemmer HP, Sentker L, Witzsch U, Liehr UB, Ricke J, Schostak M.

Urologe A. 2016 May;55(5):594-606.

BACKGROUND: The rising incidence of renal cell carcinoma, its more frequent early detection (stage T1a) and the increasing prevalence of chronic renal failure with higher morbidity and shorter life expectancy underscore the need for multimodal focal nephron-sparing therapy.

DISCUSSION: During the past decade, the gold standard shifted from radical to partial nephrectomy. Depending on the surgeon's experience, the patient's constitution and the tumor's location, the intervention can be performed laparoscopically with the corresponding advantages of lower invasiveness. A treatment alternative can be advantageous for selected patients with high morbidity and/or an increased risk of complications associated with anesthesia or surgery. Corresponding risk stratification necessitates previous confirmation of the small renal mass (cT1a) by histological examination of biopsy samples. Active surveillance represents a controlled delay in the initiation of treatment.

RESULTS: Percutaneous radiofrequency ablation (RFA) and laparoscopic cryoablation are currently the most common treatment alternatives, although there are limitations particularly for renal tumors located centrally near the hilum. More recent ablation procedures such as high intensity focused ultrasound (HIFU), irreversible electroporation, microwave ablation, percutaneous stereotactic ablative radiotherapy and high-dose brachytherapy have high potential in some cases but are currently regarded as experimental for the treatment of renal cell carcinoma.

Urologe 2016 · 55:594–606
DOI 10.1007/s00120-016-0075-8
Online publiziert: 27. April 2016

J. J. Wendler[1,2] · B. Friebe[3] · D. Baumunk[1,2] · A. Blana[1,6] · T. Franiel[1,7] · R. Ganzer[1,4] · B. Hadaschik[1,5] · T. Henkel[1,8] · K. U. Köhrmann[1,9] · J. Köllermann[1,17] · T. Kuru[1,10] · S. Machtens[1,11] · A. Roosen[1,12] · G. Salomon[1,13] · H. P. Schlemmer[1,16] · L. Sentker[1,14] · U. Witzsch[1,15] · U. B. Liehr[1,2] · J. Ricke[3] · M. Schostak[1,2]

[1] Arbeitskreis für fokale und Mikrotherapie der Akademie (AKFM), Deutsche Gesellschaft für Urologie (DGU) e. V., Düsseldorf, Deutschland
[2] Universitätsklinik für Urologie und Kinderurologie, Otto-von-Guericke-Universität Magdeburg, Magdeburg, Deutschland
[3] Universitätsklinik für Radiologie und Nuklearmedizin, Otto-von-Guericke-Universität Magdeburg, Magdeburg, Deutschland
[4] Urologische Klinik und Poliklinik, Universität Leipzig, Leipzig, Deutschland
[5] Urologische Klinik und Poliklinik, Ruprecht-Karls-Universität Heidelberg, Heidelberg, Deutschland
[6] Klinik für Urologie und Kinderurologie, Klinikum Fürth, Fürth, Deutschland
[7] Institut für Diagnostische und Interventionelle Radiologie, Universitätsklinikum Jena, Jena, Deutschland
[8] Urologische Praxis Dr. Henkel & Dr. Kahmann, Berlin, Deutschland
[9] Klinik für Urologie, Theresien-Krankenhaus Mannheim, Mannheim, Deutschland
[10] Universitätsklinik für Urologie, Universitätsklinikum Köln, Köln, Deutschland
[11] Klinik für Urologie, Marien-Krankenhaus gGmbH, Bergisch-Gladbach, Deutschland
[12] Klinik für Urologie, Augusta-Krankenanstalt gGmbH Bochum, Bochum, Deutschland
[13] Martini-Klinik, UKE GmbH, Hamburg, Deutschland
[14] Urologische Gemeinschaftspraxis, Sinsheim, Deutschland
[15] Klinik für Urologie und Kinderurologie, Krankenhaus Nordwest, Frankfurt/Main, Deutschland
[16] Abteilung für Radiologie, Deutsches Krebsforschungszentrum Heidelberg, Heidelberg, Deutschland
[17] Institut für Pathologie, Sana Klinikum Offenbach, Offenbach am Main, Deutschland

Fokale Therapie von kleinen Nierentumoren

Beobachtung, Ablation oder Operation

Für die Inzidenz des Nierenzellkarzinoms (NZK) in Deutschland wird von der Gesellschaft der Epidemiologischen Krebsregister in Deutschland (GEKID) und dem Robert-Koch-Institut (RKI) weiterhin ein kontinuierlicher Anstieg prognostiziert [1].

Neben der mit zunehmendem Alter ansteigenden Krebserkrankungsrate kommt es auch zu einem Anstieg der Komorbidität bis Multimorbidität anderer Organ- oder Systemerkrankungen, die sowohl direkten oder indirekten Einfluss auf die Therapie und den Verlauf der malignen Erkrankungen als auch die Nierenfunktion haben [2]. Insbesondere die chronische Niereninsuffizienz geht mit einer schlechteren Lebenserwartung und -qualität einher [3]. Aufgrund des Fortschritts in der schnittbildgebenden Diagnostik und zunehmenden prätherapeutisch histologischen Sicherung per Biopsie erfolgt zunehmend die Erkennung des NZK im Frühstadium mit dem Vorteil einer fokalen nierenerhaltenden Behandlung [4].

» Die Erkennung des NZK erfolgt zunehmend im Frühstadium

Die radikale Tumornephrektomie galt historisch als das Mittel der Wahl auch bei kleinen lokal begrenzten NZK. Inzwischen ist die nierenerhaltende, nierenfunktionssparende Tumorresektion (wenn möglich) der Goldstandard, da diese eine gleichermaßen hohe Tumorkontrolle bei möglichst viel Nierenfunktionserhalt mit prognostisch besserem Überleben bietet [5]. Bei ausgewählten Patienten kommen laut Leitlinien der Deutschen Krebsgesellschaft (DKG) bzw. der Deutschen Gesellschaft für Urologie (DGU) und der Europäischen Gesellschaft für Urologie (EAU) zum T1a-NZK (≤ 4 cm) bzw. bei kleinen Nierentumoren („small renal masses“, SRM) auch die primär aktive Überwachung (Active Surveillance) mit möglicher sekundärer Therapie und die fokale Tumorablation mittels Radiofrequenz- oder Kryoablation als Behandlungsalternative in Frage [6, 7]. Zahlreiche andere, derzeit noch als experimentell geltende Ablationstechniken werden auf einen möglichen Behandlungsvorteil geprüft.

Diagnosesicherung – von SRM zum NZK

Die Biopsie zur histologischen Diagnosesicherung einer bildgebend unklaren Nierenraumforderung cT1a sollte nur erfolgen, wenn dies die Therapiewahl beeinflussen könnte bzw. vor einer geplanten ablativen Therapie [7]. Zwar gilt ein bildmorphologisch malignomsuspekter Befund eines Nierentumors ohne bioptische Sicherung als ausreichend für eine operative Therapie bei fehlenden Kontraindikationen, jedoch ist der Nutzen einer präoperativen Biopsie mit einer negativen Histologie und möglichen Vermeidung einer Operation zu diskutieren [8]. Bei soliden Tumoren wird eine 2fache koaxiale Zylinderbiopsie (18 gg) außerhalb der möglichen zentralen Tumornekrose mit histologischer Analyse empfohlen [6].

Eine Besonderheit stellen zystische Tumoren dar, welche nach der CT-morphologischen Bosniak-Klassifikation [9, 10] bereits ab der Kategorie IIF maligne (3–10 %), häufiger papilläre NZK sein können und mindestens einer bildgebenden Kontrolle bedürfen [11]. Die Biopsie von zystischen Tumoren kann das erhöhte Risiko einer falsch-negativen Biopsie und die potenzielle Gefahr einer punktionsbedingten Verschleppung von Tumorzellen mit dem Austritt von Zystenflüssigkeit bergen [7]. Im Falle einer angestrebten Diagnosesicherung wird hier eine Kombination aus koaxialer Zylinderbiopsie mit histologischer und Feinnadelpunktion mit zytologischer Analyse empfohlen [6].

Bei einem differentialdiagnostischen Verdacht auf ein Urothelkarzinom des Nierenbeckenkelchsystems, insbesondere bei zentraler Lage und/oder Hohlsystemeinbruch (mit und ohne Hämaturie), gilt die perkutane Biopsie wegen der erhöhten Gefahr einer Punktionskanalmetastasierung als kontraindiziert [12, 13]. Trotz der relativ hohen Sensitivität (94–98 %) und Spezifität (100 %) der diagnostischen Genauigkeit zum bioptischen Nachweis eines NZK existiert eine hohe Rate (bis zu jeder 5. Biopsie) an falsch-negativen oder nicht aussagekräftigen Proben sowie eine Gradingungenauigkeit von 31 % [8, 14, 15]. Eine negative Biopsie (normales Parenchym) sollte eine Rebiopsie aufgrund einer hohen Erfolgsrate um 90 % nach sich ziehen [6, 7, 15]. Eine Limitation der bioptischen Diagnostik mit Festlegung der Entität stellt zudem die intratumorale biologische Heterogenität das NZK dar [16]. Ebenso wird beim als benigne klassifizierten Onkozytom die Differenzierung zum onkozytären NZK und Entartungspotenz diskutiert [17]. Insgesamt korreliert die zunehmende Biopsierate von SRM mit einer Therapieeinleitung [18].

Active Surveillance und Watchful Waiting

Active Surveillance

Aktive Überwachung bis zur Therapieeinleitung

Das Konzept der aktiven Überwachung (Active Surveillance, AS) sieht im Falle kleiner, lokal begrenzter asymptomatischer Nierentumoren (SRM, cT1a, ≤ 4 cm) mit geringer Größenprogredienz und Metastasierungstendenz ein Kontrollieren mittels regelmäßiger Bildgebung vor. Definiert wird dieses Risiko durch die Tumorgröße und den pathologischen Subtyp nach histologischer Sicherung des Tumors mittels Stanzbiopsie. Erst im Falle einer Größenprogredienz des Tumors oder auf Patientenwunsch soll die kurativ intendierte Behandlung eingeleitet werden. Somit ist die AS-Strategie direkt abhängig von der „natürlichen" Tumorbiologie und der diagnostischen „Sicherheit".

Es gibt weder objektive Kriterien zur Selektion adäquater Patienten noch eine einheitliche Definition zur AS (EG0, LE3, [7]). Für die „richtige Indikationsstellung oder Praktizierung" der AS bedarf es demnach der Berücksichtigung bestimmter Fakten im interdisziplinären Setting aus Urologen, Radiologen und Pathologen. Zahlreiche Studien zum Progress kleiner cT1a-Nierentumoren (≤ 4 cm, SRM) zeigten eine relativ langsame Wachstumsrate mit 0,2–0,4 cm pro Jahr und eine sehr geringe Metastasierungsrate 1–2 % in den ersten 2–4 Jahren Follow-up, wobei diese Daten eine nicht unerhebliche Anzahl histologisch ungesicherter oder benigner Tumoren und verschiedene NZK-Subtypen enthalten [7, 19].

Chawla et al. [20] errechneten aus einer Metaanalyse für die Subgruppe bioptisch gesicherter pT1a-NZK (n = 120) mit einer medianen Tumorgröße von 2,48 (1,7–4,0) cm eine mediane Wachstumsrate von 0,35 cm pro Jahr (0,42–1,6 cm pro Jahr) bei einem mittleren Nachbeobachtungszeitraum von 30 (25–39) Monaten, wobei die initiale Tumorgröße nicht mit der Wachstumsrate signifikant korrelierte [1]. Thompson et al. [21] beschrieben eine Metastasierungsquote von 0,13 % bei NZK < 3 cm (1/178), wobei das Metastasierungsrisiko um 24 %/cm zusätzlichem Wachstum stieg.

Prognostisch ungünstige Faktoren und somit Gründe gegen eine AS stellen zudem eine bildgebende Gefäß-, Nierenkapsel-, Nebennieren- und Nierenbeckenkelchsysteminvasion, sowie ein biopsiehistologischer Fuhrman-Kerngrad 3–4 bzw. „high grade" des klarzelligen NZK und nicht-klarzelligen NZK dar [6]. Auch anatomische Klassifikationssysteme wie PADUA-Score („preoperative aspects and dimensions used for an anatomical classification"), RENAL-Score („radius, exophytic/endophytic, nearness to collecting system or sinus, anterior/posterior and location relative to polar lines") oder C-Index können frühzeitig richtungsweisend für die Option oder Art der verzögerten Therapie und damit bereits eine Entscheidungshilfe für oder gegen eine AS sein [6, 22].

» Als AS wird die bildgebende Kontrolluntersuchung definiert

Ein Tumormarker zur Verlaufskontrolle des Nierentumors existiert nicht; das Konzept der Rebiopsie zur Verlaufskontrolle des Nierentumors unter AS ist nicht etabliert [7]. Somit wird als AS lediglich die bildgebende Kontrolluntersuchung definiert. Ein empfohlenes Schema zu Bildgebungsart und Intervall im Rahmen der AS existiert bislang nicht [6, 7].

Tendenziell zeigt sich im Staging für den Thorax ein Vorteil zugunsten der

Zusammenfassung · Abstract

Urologe 2016 · 55:594–606 DOI 10.1007/s00120-016-0075-8

J. J. Wendler · B. Friebe · D. Baumunk · A. Blana · T. Franiel · R. Ganzer · B. Hadaschik · T. Henkel · K. U. Köhrmann · J. Köllermann · T. Kuru · S. Machtens · A. Roosen · G. Salomon · H. P. Schlemmer · L. Sentker · U. Witzsch · U. B. Liehr · J. Ricke · M. Schostak

Fokale Therapie von kleinen Nierentumoren. Beobachtung, Ablation oder Operation

Zusammenfassung

Hintergrund. Die gleichzeitig steigende Inzidenz des Nierenzellkarzinoms mit zunehmend häufigerer Diagnose im Frühstadium T1a und die zunehmende Prävalenz der chronischen Niereninsuffizienz mit konsekutiv erhöhter Morbidität sowie kürzerer Lebenserwartung bedingen die Notwendigkeit einer multimodalen fokalen Therapie mit Nierenerhalt.

Diskussion. In der letzten Dekade verschob sich der Goldstandard von der radikalen Nephrektomie hin zur Nierenteilresektion. Je nach Erfahrung des Operateurs, Patientenkonstitution und Lage des Tumors kann der Eingriff laparoskopisch mit entsprechenden Vorteilen der geringeren Invasivität erfolgen. Für ausgewählte Patienten mit hoher Morbidität, hohem Narkose- oder Operationsrisiko kann eine Behandlungsalternative von Vorteil sein. Eine entsprechende Risikostratifizierung macht die vorherige biotisch-histologische Sicherung des kleinen Nierentumors („small renal mass", cT1a) notwendig. Die aktive Überwachung (Active Surveillance) stellt einen kontrolliert verzögerten Behandlungsbeginn dar.

Ergebnisse. Die perkutane Radiofrequenzablation und die laparoskopische Kryoablation stellen die derzeit gängigsten Therapiealternativen dar, wobei sich v. a. Limitationen für zentral gelegene hilusnahe Nierentumoren ergeben. Jüngere Ablationsverfahren, wie der hochintensive fokussierte Ultraschall, die irreversible Elektroporation, Mikrowellenablation, perkutane stereotaktische ablative Radiotherapie und die Hochdosisbrachytherapie, weisen teilweise ein hohes Potenzial auf, gelten derzeit jedoch für die Therapie des Nierenzellkarzinoms als experimentell.

Schlüsselwörter

Nierenzellkarzinom · Fokale Therapie · Nierenteilresektion · Active Surveillance · Ablation

Focal therapy for small renal masses. Observation, ablation or surgery

Abstract

Background. The rising incidence of renal cell carcinoma, its more frequent early detection (stage T1a) and the increasing prevalence of chronic renal failure with higher morbidity and shorter life expectancy underscore the need for multimodal focal nephron-sparing therapy.

Discussion. During the past decade, the gold standard shifted from radical to partial nephrectomy. Depending on the surgeon's experience, the patient's constitution and the tumor's location, the intervention can be performed laparoscopically with the corresponding advantages of lower invasiveness. A treatment alternative can be advantageous for selected patients with high morbidity and/or an increased risk of complications associated with anesthesia or surgery. Corresponding risk stratification necessitates previous confirmation of the small renal mass (cT1a) by histological examination of biopsy samples. Active surveillance represents a controlled delay in the initiation of treatment.

Results. Percutaneous radiofrequency ablation (RFA) and laparoscopic cryoablation are currently the most common treatment alternatives, although there are limitations particularly for renal tumors located centrally near the hilum. More recent ablation procedures such as high intensity focused ultrasound (HIFU), irreversible electroporation, microwave ablation, percutaneous stereotactic ablative radiotherapy and high-dose brachytherapy have high potential in some cases but are currently regarded as experimental for the treatment of renal cell carcinoma.

Keywords

Renal cell carcinoma · Focal therapy · Partial kidney resection · Active surveillance · Ablation

Computertomographie (CT) und für das Abdomen bzw. des Nierentumors insbesondere bezüglich weiterer Differenzierung zu Malignität und Grading zugunsten der Magnetresonanztomographie (MRT, [23–25]). Die bildgebende Kontrolle im Rahmen der AS sollte mindestens einmal pro Jahr erfolgen. Zur AS von SRM und pT1a-NZK liegen neben retrospektiven Studien und Metaanalysen keine prospektiv randomisierten Studiendaten vor [7]. Weiterhin fehlen großen Serien oder Metaanalysen zu bioptisch gesicherten pT1a-NZK mit AS.

Jewett et al. [26] analysierten bei 101 bioptisch gesicherten pT1a-NZK eine Progressionsrate von 0,13 cm/Jahr und einer Metastasierungsrate von 1,1 % über eine mediane Nachbeobachtungszeit von 28 Monaten. Lane et al. [27] fanden bei 537 SRM-Patienten mit einem Alter ≥ 75 Jahren keinen signifikanten Überlebensunterschied zwischen AS, Nierenteilresektion und Tumornephrektomie, wobei von 148 Todesfällen in einer medianen Nachbeobachtungszeit von 3,9 Jahren lediglich 4 % auf einen klinischen Progress eines NZK zurückzuführen waren. Dazu beschrieben Pierorazio et al. [28] keinen Unterschied in der Lebensqualität (QoL) zwischen einer sofortigen Intervention und AS ab einem Jahr Follow-up. Insgesamt wird die AS nicht für Nierentumoren mit einer Größe > 3cm, unscharfer Begrenzung, deutlicher Inhomogenität sowie bei bioptisch aggressivem NZK und nichtmorbiden Patienten mit nicht wesentlich eingeschränkter Lebenserwartung mit bildmorphologischem Verdacht auf Malignität empfohlen [19]. Mit den Möglichkeiten einer bildgestützten lokalen Ablation neben der nierenerhaltenden Chirurgie tritt die aktive Überwachung aufgrund ihrer Limitationen zunehmend in den Hintergrund.

Watchful Waiting/Wait-and-see

Abwarten ohne gezielte Diagnostik oder Therapie

Von der Active Surveillance definitionsgemäß abzugrenzen ist die Watchful-Waiting- oder besser Wait-and-see-Strategie, bei der nach einer bildgebenden Diagnosestellung des asymptomatischen, nicht-metastasierten Nierentumors zunächst von einer weiteren, gezielten Diagnostik oder Therapie Abstand genommen wird. Hierfür werden Patienten mit einer geringen statistischen Lebenserwartung aufgrund eines sehr hohen Alters mit einer sehr hohen Komorbidität und damit reduzierten biologischen Lebenserwartung sowie hohen Behandlungsrisiken oder wegen einer prognostisch stark eingeschränkten Lebenserwartung aufgrund einer anderen aggressiven fortgeschrittenen, klinisch führenden Tumorerkrankung triagiert. Die Patienten werden somit einer palliativen, symptomkontrollierten Therapie zugeführt („best supportive care"). Daten hierfür liegen nicht vor; häufig werden hier Publikationen zur Active-Surveillance-Strategie angegeben.

Ablation

Leitlinienbasierte Ablationsverfahren

Die Radiofrequenzablation (RFA) und Kryoablation (KA) werden in den Leitlinien der deutschen, europäischen und US-amerikanischen Gesellschaften für Urologie und Radiologie als alternative kurative Therapieoption kleiner Nierentumoren gewertet. Zwar existieren hierzu aufgrund ihrer längeren Anwendung die meisten Daten, jedoch liegen keine prospektiv randomisierten Studiendaten vor [29]. Neben der Effektivität zur Tumorkontrolle spielt die Bewertung der Komplikationsraten und Lebensqualität eine entscheidende Rolle. Im direkten Vergleich von RFA und KA konnte keine Überlegenheit eines der beiden Verfahren bezogen aufs krankheitsspezifische, rezidivfreie und Gesamtüberleben nachgewiesen werden [6]. Entscheidend für die Erfolgs- und Komplikationsrate ist die Lage und Größe des Nierentumors.

Camacho et al. [22] demonstrierten, dass eine RENAL-Score > 8 eine höhere Lokalrezidiv- und Komplikationsrate für RFA und KA vorhersagen kann. Eine endgültige Bewertung der RFA oder KA als Therapiealternative kann bei der aktuellen Datenlage nicht getroffen werden, so dass dieses Verfahren aktuell als Therapieoption bei nicht zentral gelegenen T1a- Nierentumoren für ältere Patienten mit höherer Morbidität und erhöhten operativen bzw. anästhesiologischen Risiken oder Kontraindikationen empfohlen wird [6, 7].

Radiofrequenzablation

Die RFA stellt ein hyperthermes Ablationsverfahren dar, bei dem es durch die Applikation von hochfrequentem Wechselstrom (375–480 kHz) über aktive Elektroden zum alternierenden Ionenstrom mit resultierender Reibungswärme (Joule-Effekt) über 100 °C und Koagulationsnekrose im Zielgewebe kommt. Diese Friktionswärme wird radiär zur Elektrode durch das Gewebe fortgeleitet (Konduktionsprinzip). Insgesamt werden somit Temperaturen von 50–105 °C mit multipelvariabler Wirkung erreicht. Im niedrigeren Temperaturbereich kommt es zur Proteindenaturierung, chromosomalen Alteration, Membranschädigung der Zellen und Zellorganellen sowie zur Schädigung des Gefäßsystems. Im höheren Temperaturbereich um ca. 100 °C kommt es zur Verkochung, Vaporisation (Verdampfung) und Karbonisation (Verkohlung) des Gewebes [30]. Als Elektroden werden monopolare oder bipolare Elektroden, kompakte Einzel-, Cluster- oder vorrangig expandierbare Schirmelektroden unterschiedlicher Größen verwendet.

Zur Behandlung von Nierentumoren wurde die RFA erstmals 1997 eingesetzt [31]. Die Sondenart, Applikationszeit (ca. 10–12 min) und Temperaturhöhe beeinflusst dabei die Größe und Homogenität der Ablationszone (2–7 cm). Ein Sicherheitssaum von 5–10 mm wird empfohlen. Die RFA ist bei zentral gelegenen NZK wegen der Nähe zum Nierenhilus und Nierenbeckenkelchsystems (NBKS) neben den möglichen Perforationsrisiken wegen des Hitzeabtransports durch Blut- und Harnfluss (konvektionsbedingter „heat sink effect") eingeschränkt anwendbar. Zur Reduzierung des Heatsink-Effekts durch arterielle Nierengefäße kann die vorherige transarterielle Embolisation des Ziel- und Grenzgewebes eingesetzt werden.

Bisherige Anwendungsversuche an der Niere schlossen offen-chirurgische, perkutane und laparoskopische Verfahren ein. Die perkutane RFA ist die am häufigsten angewendete energieablative Methode zur alternativen Behandlung des NZK, da sie technisch sehr einfach und mit relativ geringem zeitlichen (10–20 min Ablationsdauer) und apparativen Aufwand durchgeführt werden kann. Aufgrund der sehr guten Platzierungsmöglichkeit der RFA-Applikatoren unter Fluoroskopie (CT oder MRT) und Effektivität wurde und wird die RFA vorrangig perkutan in Analgosedierung angewandt. Für die hypertherme, möglichst vollständige Gewebezerstörung sind etwa Temperaturen von ca. 80 °C über 8–10 min notwendig.

Die starke Inhomogenität und Vaskularisation von Nierentumoren führt durch den oben genannten Heat-sink-Effekt und durch entsprechende Impedanzsprünge häufig zur inkompletten Ablation (Skipping-Läsionen, [32, 33]). Die primäre Erfolgsrate der RFA bei SRM liegt zwischen 90–100 % in Abhängigkeit von der Tumorgröße und -lage, wobei die Rate technisch bedingt bei SRM < 3 cm und kortikalperipherer Lokalisation höher ist [34–38].

Diverse Studien beschrieben eine Lokalrezidivrate für pT1a-NZK zwischen 2 und 12 % in den ersten 5 Jahren nach RFA [36, 39–43]. Darüber hinaus ermöglicht die RFA eine Wiederholung, wobei deren Sekundärerfolgsrate auf nahezu 100 % steigt [44].

» Komplikationen nach renaler RFA treten meist leichtgradig auf

Die Metastasierungsraten nach RFA sind vergleichbar mit Active-Surveillance-Daten (metastasenfreie und erkrankungsspezifische Überlebensraten von 95–99 %, [26, 37, 38, 44, 45]). Komplikationen nach renaler RFA treten meist leichtgradig zwischen 0–19 % auf [7, 34,

37, 38, 40, 46]. Insbesondere von einer renalen RFA im Kontakt zum NBKS oder Harnleiter wird wegen der Perforations-, Fistel- und Strikturgefahr abgeraten [6, 7, 40]. Insgesamt zeigen sich bei der RFA vergleichbare Ergebnisse zur Nierenteilresektion unter Vorbehalt fehlender randomisierter Studien [6, 7, 41, 47]. Mit ausstehenden Langzeitdaten ist eine Indikationsausweitung und breitere Anwendung der RFA zur Therapie von T1a-NZK zu erwarten.

Kryoablation

Die KA stellt das einzige hypotherme Ablationsverfahren dar und wurde als älteste thermale Ablationstechnik erstmal 1995 zur Behandlung von Nierentumoren eingesetzt [48]. Über eine eingeführte Kältesonde kommt es durch 2–3 zyklische aktive Einfrier- (–60 ° bis –70 °C) und passive Auftauphasen (>°C) mit konsekutiver Zelldehydrierung, mechanischer Zerreißung durch Eiskristallbildung und minderperfusionsbedingter Ischämie schließlich zur Koagulationsnekrose im Zielgewebe [49]. Die KA bietet im Gegensatz zu hyperthermalen Ablationstechniken keinen ausreichend hämostyptischen Effekt mit entsprechend erhöhtem Blutungsrisiko [50].

Die KA ist bei zentral gelegenen NZK wegen der Nähe zum Nierenhilus und NBKS neben den möglichen Perforations- und Thrombembolierisiken wegen der Erwärmung durch den Blut- und Harnfluss (konvektionsbedingter „cold sink effect“) eingeschränkt anwendbar.

Die Thermoregulation erfolgt über gasdurchströmte Kryosonden mit thermoisoliertem Schaft und nichtisolierter Spitze per Joule-Thomson-Effekt (dichte- und druckabhängige Temperaturveränderung), wobei Argongas (–180 °C) zur Kühlung und Heliumgas zur Erwärmung genutzt wird [50]. Je nach Tumorgröße werden 3–5 Kryonadeln und 2 Thermonadeln bildgeführt platziert. Ein Sicherheitssaum von 5–10 mm wird empfohlen. Die starke Inhomogenität und Vaskularisation von Nierentumoren führt durch den oben genannten Cold-sink-Effekt und durch entsprechende Impedanzsprünge häufig zur inkompletten Ablation (Skipping-Läsionen, [22, 50]). Zur Reduzierung des Cold-sink-Effekts kann die vorherige, transarterielle Embolisation des Ziel- und Grenzgewebes eingesetzt werden [30].

Bisherige Anwendungsversuche der renalen KA schlossen offen-chirurgisch, perkutane, laparoskopische, transluminale und endoskopische Verfahren ein. Zwar erreicht die perkutane Anwendung bei günstiger Tumorlage akzeptable Ergebnisse, jedoch stellt die laparoskopische Anwendung in Allgemeinnarkose die gängigste und sicherste Technik aufgrund der endoskopischen und endosonographischen Kontrollmöglichkeit der KA-Applikation (Eisball) und größeren Blutungskontrolle dar [6]. Hierfür muss zuvor die Niere wie bei einer standardisierten laparoskopischen Nierenteilresektion vom anlagernden Fett operativ befreit werden. Nach der KA wird der Eisball für 5–10 min mechanisch komprimiert und für weitere 5–10 min unter einem reduzierten intraabdominellen Gasdruck kontrolliert. Die Hämostase kann durch Applikation von Hämostyptika oder Klebstoffen und bei persistierende Blutungen auch mittels Umstechung versorgt werden [49, 51].

Die primäre Erfolgsrate der KA bei SRM liegt zwischen 90–100 % in Abhängigkeit von der Tumorgröße und -lage, wobei die Rate technisch bedingt bei SRM < 3 cm und kortikalperipherer Lokalisation höher ist [52, 53]. Diverse Studien beschrieben in den ersten 5 Jahren nach KA eine Lokalrezidivrate für pT1a-NZK zwischen 3 und 17 % [54–59]. Die Metastasierungsraten nach KA entsprechen Active-Surveillance-Daten (metastasenfreie und erkrankungsspezifische Überlebensraten von 93–98 %, [6, 7, 56, 60]). Das perioperative Outcome der laparoskopischen KA ist vergleichbar zur laparoksopischen Nierenteilresketion [6, 51, 58, 60, 61]. Komplikationen nach renaler KA treten meist leichtgradig zwischen 2–19 % auf [7, 58, 60]. Von einer renalen KA im Kontakt zum NBKS oder Harnleiter wird wegen der Perforations-, Fistel- und Strikturgefahr abgeraten [6, 7, 56]. Aufgrund des hohen apparativen und kostenintensiveren Aufwands wird diese Technik eher wenigen Zentren vorbehalten bleiben.

Potenziell alternative Ablationstechniken

Hochintensiver fokussierter Ultraschall

Die hochintensive fokussierte Ultraschalltherapie (HIFU) stellt ein hyperthermales Ablationsverfahren (>80 °C) durch auf das Zielgewebe gebündelte Ultraschallwellen eines Piezokristalls (1–4 MHz, Pulsdauer 4–6 s, Spitzenenergie von 2000 kJ/cm^2) mit folglicher Koagulationsnekrose dar. Bei der perkutanen HIFU-Therapie wird mittels sog. Split-beam-Technologie (externe HIFU-Sonde mit integrierter Ultraschallkopplung) eine Ablation in einer Eindringtiefe von 3,5–8,0 cm in Vollnarkose erzeugt.

Zusammenfassend ist aufgrund der respiratorischen Nierenbewegung, des skelettbedingten eingeschränkten Schallfensters und der dynamisch-manuellen Ultraschallsteuerung eine gezielte und sichere komplette Ablation von SRM mittels perkutaner HIFU technisch schwer umsetzbar [62, 63]. Eine Umgehung dieses Problems sollte die laparoskopische HIFU-Therapie darstellen, bei der zuvor die Niere wie bei einer standardisierten laparoskopischen Nierenteilresektion vom anlagernden Fett operativ befreit werden muss [64, 65]. Durch eine 18 mm lange laparoskopische HIFU-Sonde („side firing dual focal length“, Fa. Misonix, USA) wird der Tumor mit >90 °C über 10–40 min unter Real-time-Ultraschallmonitoring unter möglicher Ultraschallkontrolle (intraoperativen Powerdopplerendoultraschalls mit einer 10-Hz-Sonde) ablatiert.

» Die laparoskopische HIFU ist technisch aufwendig

Klingler et al. [64] resezierten das Tumorablationsareal einer cT1a-SRM (Median 2,2 cm; 1,1–4,0 cm) nach laparoskopischer HIFU bei 7 Patienten und konnten bei 4 eine komplette und bei 3 Tumoren eine inkomplette Ablation bei fehlenden HIFU-abhängigen Komplikationen demonstrieren. Ritchie et al. [65] analysierten 12 SRM (Median 3,8 cm, 2,0–4,7 cm, 2 endophytisch, 10 kortikal-exophytisch, 4 Onkozytome, 8 NZK) nach komplikati-

onsloser laparoskopischer HIFU gefolgt von einer laparoskopischen Nierenteilresektion, wobei 8 SRM eine inkomplette Ablation mit vorrangig subkapsulären Residuen (Skipping-Läsionen, $n = 2$: 90–95 %, $n = 6$: 0 %) aufwiesen. Insgesamt stehen für die HIFU von SRM nur begrenzte Daten mit einer hohen Rate an inkompletter Ablation zur Verfügung, wobei die laparoskopische HIFU zwar effektiver scheint, jedoch technisch wesentlich aufwendiger ist.

Irreversible Elektroporation

Die irreversible Elektroporation (IRE) ist ein neues minimal-invasives, nonthermal wirkendes Gewebeablationsverfahren, bei dem es durch eine lokale, kritische, elektrisch induzierte Störung des dipolelektrischen Zellmembranpotenzials mit konsekutiver irreversibler Bildung von Membranporen zu einer permanenten Erhöhung der Zellmembranpermeabilität und Verlust der Zellhomöostase mit folglicher Zytolyse in 1–7 Tagen kommt. Über 2–6 Nadelelektroden werden lokal je Elektrodenpaar 90–100 hochenergetische, ultrakurze rektanguläre Starkstrompulse (mindestens 90 pro Elektrodenpaar, 1500–3000 V, Stromstärke 30–50 A, Pulsdauer 70–100 µs) unter vollständiger Muskelrelaxation in Intubationsnarkose und EKG-Triggerung appliziert. Durch die postulierte Alles-oder-Nichts-Reaktion ab einem „kritischen" induzierten Transmembranpotenzial sowie der zellulären Wirkung (Erhalt der Matrix) soll das Ablationsareal eine sehr kleine Transitionszone und scharfe Begrenzung zum Umgebungsgewebe aufweisen [66].

Seit 2007 ist ein IRE-System (NanoKnife® System; AngioDynamics Inc, 2–6 Nadelelektroden) zur klinischen Anwendung zugelassen (allgemeine Zulassung für Weichgewebe). Bisherige experimentelle und Phase-1-Publikation konnten eine sichere Applikation bei Erhalt des NBKS und renaler Gefäße demonstrieren [67]. Thomson et al. [68] beschrieben nach CT-gestützter IRE bei 7 Patienten mit einem pT1a-NZK (1,6–3,1 cm) per CT-Kontrolle nach 3 Monaten in 5 Fällen eine komplette Ablation und in 2 Fällen einen Tumorprogress (29 %). Trimmer et al. [69] beobachteten nach CT-gestützter IRE bei 20 peripheren T1a-Nierentumoren (1,5–2,9 cm; davon stanzbioptisch gesichert 13 NZK) CT- oder MRT-morphologisch ein Tumorresiduum nach 6 Wochen in 2 von 20 Fällen (10 %) und eine Rezidiv in 1 von 6 Fällen (17 %) nach 1 Jahr.

> » Die IRE ist bei zentralen Tumoren für den Nierenerhalt günstig

Erste resektionshistologische Ergebnisse 4 Wochen nach IRE von soliden, stanzbioptisch gesicherten pT1a-NZK lieferte eine Phase-IIa-Studie von Wender et al. [70, 71]. Die Tumorresektate nach IRE wiesen fokal zonale Umbauprozesse mit einem massiven Schaden am Tumorgewebe ohne Tumorresiduen bei gleichzeitigem Erhalt größerer Nierengefäße und des NBKS auf. Entsprechend diesen ersten vorläufigen Studienergebnissen scheint die perkutane Ablation von soliden NZK mittels IRE möglich und bei zentralen Tumoren für einen Nierenerhalt günstig.

Mikrowellenablation

Bei der Mikrowellenablation (MWA) erfolgt die Hitzeinduktion durch die Entstehung von Reibungswärme der Wassermoleküle im Zielgewebe. Diese werden durch ihr Dipolmoment mittels dielektrischer Hysteresis (rotierende Dipole) mit einer Frequenz von 915–2450 MHz über Mikrowellengeneratoren (45–200 W) und entsprechende Antennen zu rotierenden Bewegungen angeregt. Damit werden Temperaturen von 100 ° bis über 150 °C lokal über ca. 10–15 min erzeugt, aus denen eine hyperthermale Koagulationsnekrose mit einem variablen von der Antennengeometrie abhängigen Wirkradius resultiert [72, 73].

In der Literatur sind neben zahlreichen experimentellen Tierversuchen am In-vivo-Nierengewebe nur eine kleine Anzahl klinischer Studien zur Mikrowellentherapie von SRM mit vorläufigen Ergebnissen beschrieben. Yu et al. [74] beobachten nach perkutaner sonographiegestützter MWA bei 98 Patienten mit pT1a-NZK (0,6–4 cm) eine Erfolgsrate von 97 % im Median von 26 Monaten und in einen Fall einen Progress nach 32 Monaten bei einer Majorkomplikationsrate von 1,7 % in CEUS („contrast-enhanced ultrasound"), CT oder MRT.

Moreland et al. [75] behandelten 53 Patienten mit einen bioptisch gesicherten NZK-pT1a (0,8–4,0 cm) mittels perkutaner sonographiegestützter MWA. In der Kontroll-CT oder -MRT zeigte sich kein Lokalrezidiv oder -persistiv bei 38 Patienten nach medianen 8 Monaten. Klinisch zeigte sich keine signifikante Änderung der Nierenfunktion bei insgesamt 6 Minorkomplikationen (11,3 %) mit u. a. Harnstauung ($n = 1$) und transfusionspflichtiger Hämorrhagie ($n = 1$).

Aufgrund der spezifischen Wirkungsweise auf Wassermoleküle könnte die MWA eine spezifische Ablationsmethode für zystische Nierentumoren bzw. komplizierte/maligne Nierenzysten darstellen. Carrafiello et al. [76] zeigten bei 7 Bosniak-Zysten Klasse III oder IV (1,4,–2,7 cm) eine Ablationsrate von 100 % und Rezidivfreiheit über 24 h mittels perkutaner, CT- oder sonographiegestützter MWA. Durch ihren hohen technischen Aufwand und die relative große Antennengröße konnte sich die MWA bisher gegenüber anderen perkutanen, hyperthermen Ablationsverfahren insbesondere zur Nierentumortherapie nicht durchsetzen.

Perkutane Strahlentherapie

Die primäre, perkutane, konventionelle, fokale Strahlentherapie des lokal begrenzten NZK gilt historisch als unwirksam und unbrauchbar. Grundlage dafür ist die relativ hohe „Strahlenunempfindlichkeit" des NZK und die durch mangelnde technische Aussparungsmöglichkeit bedingte, hohe Nebenwirkungsrate der strahlensensiblen, perirenalen Risikoorgane (radiogene Enteritis und Harnleiterstriktur). Neuere radiotherapeutische Techniken ermöglichen als stereotaktische ablative Radiotherapie („sterotactic ablative body radiotherapy", SABR) eine präzise, fokale, hypofraktionierte Bestrahlung („Radiochirurgie") über eine oder wenige Fraktionen (24–40 Gy über 1–5 Fraktionen à 4–25 Gy Einzeldosen). Dies ermöglicht

eine Bandbreite an Techniken (robotergestützte Linearbeschleuniger, moderne Immobilisationsmaßnahmen, neue softwarebasierte Bestrahlungsgeometrie und -algorithmen, 3D/4D-CT-Simulation, Atmungstriggerung, Bestrahlungsmarker, Cone-Beam, intensitätsmodulierte Radiotherapie [IMRT] etc.).

Im Kontrast zur konventionellen Strahlentherapie, die über eine DNA-Schädigung zur Apoptose führt, wirkt die SABR auf verschiedene strukturelle und signaltransduktorische Bereiche der Zelle mit konsekutiv letaler, nonthermaler Zellschädigung. Campbell et al. [77] fassten die Ergebnisse der SABR von lokal begrenzten Nierenzellkarzinomen von 138 Patienten respektive 166 T1a- bis T1b-Tumoren aus 14 Studien von 2003–2015 zusammen. Für eine einheitliche Beurteilung ist hierbei die Heterogenität der Behandlungsschemata, Tumordaten und Bewertungskriterien zur Lokalkontrolle limitierend. Die Autoren schließen auf eine mögliche künftige Therapieoption des lokalen NZK mittels primärer SABR.

Brachytherapie

Bei der Brachytherapie (BT) werden im Zielgewebe sehr hohe Strahlendosen über temporär eingebrachte Strahlenquellen erreicht. Durch den typischen steilen Dosisabfall kann eine hohe unerwünschte Strahlenexposition des Umgebungsgewebes bzw. der benachbarten Risikoorgane vermieden werden. Beim bildgeführten Afterloading werden sekundär zu beladende, d. h. zunächst inaktive Applikatoren im Tumor (interstitielle Brachytherapie) unter CT- oder MR-Fluoroskopie platziert und dann sekundär durch das Nachladegerät mit der divergenten Strahlenquelle beladen. Ein exakter Bestrahlungsplan (Dosisverteilung) wird durch die räumlich individuelle Lage und Verweildauer der Applikatoren kalkuliert.

Die High-dose-rate-Brachytherapie (HDR-BT) zeichnet sich durch eine kontinuierliche Hochdosisleistung (HDR > 12 Gy/h) aus, wobei aktuell vorzugsweise 192-Iridium als β-strahlendes Isotop verwendet wird. Dies führt über die Wirkung auf verschiedene strukturelle und signaltransduktorische Bereiche der Zelle zu einer letalen, nonthermalen Zellschädigung. Nach Positionierung der Brachytherapiekatheter in Seldinger-Technik und in intravenöser Analgosedierung eingebrachte fixierte Schleusen (z. B. Angiographieschleusen) wird eine kontrastmittelgestützte Planungs-CT oder -MRT (Atemanhaltetechnik, Schichtdicke ≤ 5 mm) zur Determinierung der exakten Lage in Beziehung zur Tumorausdehnung (Koordinaten x, y, z) akquiriert. Die Bestrahlungszeit von etwa 20–90 min ist von der Größe des zu therapierenden Tumorvolumens (GTV) abhängig, wobei idealerweise 100 % (D100) des Zielvolumens (GTV + Sicherheitssaum von wenigen Millimetern) von der avisierten Dosis erfasst werden sollten. Gegebenenfalls werden in einer zweiten Sitzung unterexponierte Tumoranteile erneut behandelt.

Mit dieser Technik können irregulär geformte Tumoren ohne Größenlimitation und unabhängig von der respiratorischen Bewegung behandelt werden. Klinische Daten zur Behandlung des lokal begrenzten NZK mittels perkutaner HDR-BT wurden bisher nicht publiziert. In einer prospektiven Phase-I- bis -II-Studie wird derzeit die Bestrahlung von NZK und die Toleranzdosis des nichttumorösen Nierenparenchyms untersucht (Ricke et al. [78], Universität Magdeburg, Deutschland). Die noch unveröffentlichten Zwischenergebnisse zeigen eine gute Steuerbarkeit und ein gutes Ansprechen von Nierenkarzinomen.

Operation

Nierenteilresektion und Nierentumorenukleation

Die operative Nierentumorentfernung gilt als Therapie der Wahl, aber es sollte – wann immer möglich – eine Nierenteilresektion (NTR) mit Erhalt der Restniere (Organerhalt) durchgeführt werden. In erfahrenen Zentren besteht im Gesamt- und tumorspezifischen Überleben der Betroffenen kein Unterschied zwischen offenen und laparoskopischen Eingriffen, allerdings ist der intraoperative Blutverlust geringer und der stationäre Aufenthalt bei der Laparoskopie kürzer als bei einer offenen Operation [6, 7, 79–82].

Die Indikationsstellung bezüglich des Zugangswegs hängt stark von der Patientenkonstitution, der Tumorlage (RENAL-Score) und v. a. der Laparoskopieerfahrung des jeweiligen Operateurs ab. Die konsekutive Nierenleistung ist nicht abhängig vom Zugang. Trotz kürzerer Operations- und Ischämiezeiten bei der offenen NTR mit geringerem postoperativen GFR-Abfall und andererseits geringerer Morbidität bei der laparoskopischen NTR fand sich nach 3,6 Jahren Nachbeobachtungszeit kein Unterschied im Niereninsuffizienzgrad [69, 81–83].

Den wichtigsten Outcomeparameter stellt die Ischämiezeit des zu erhaltenden gesunden Nierenparechyms dar, welche zum maximalen Nierenfunktionserhalt so kurz wie möglich sein muss. Bei einer zu erwartenden Ischämiezeit > 25 min wird eine Kühlung (kalte Ischämie) empfohlen. Bei einer günstigen, insbesondere peripheren Tumorlage und einer zu erwartenden geringen Blutung kann auch ohne Nierengefäßausklemmung (Zeroischämie) nierenteilreseziert werden [84]. Weiterhin sollte maximal viel gesundes Parenchym im Sinne einer möglichen Tumorenukleation belassen werden („nephron-sparing surgery"). Hierbei fanden sich gleiche Raten zum progressionsfreien und krebsspezifischen Überleben im Vergleich zur Nierenteilresektion und Tumornephrektomie [85, 86].

Metaanalysen nach Tumorenukleation von NZK zeigen eine Rate von 0–7 % für positive Resektionsränder (R1), deren Mehrheit keinen Einfluss auf die Rezidiv- sowie krebsspezifische und gesamte Überlebensrate zu haben scheint, so dass in diesem Fall eine Kontrolle gegenüber einer Reoperation präferiert werden kann [87, 88]. Vergleichsstudien zur Wertigkeit der laparoskopisch Single-port-NTR („laparoskopic endoscopic single site", LESS) und der roboterassistierten NTR stehen noch aus [89–92].

Fazit für die Praxis

- **Die fokale Therapie von kleinen Nierentumoren bzw. lokal begrenzten**

Nierenzellkarzinomen ermöglicht den Nierenorganerhalt mit möglichem Erhalt der Nierenfunktion.

- **Bei kleinen Nierentumoren ist eine Nierenteilresektion Goldstandard.**
- **Vor ablativen Therapiemaßnahmen sowie AS soll und vor operativer Therapieerwägung kann eine perkutane Biopsie zur histologischen Sicherung bzw. Risikostratifizierung durchgeführt werden.**
- **Die AS stellt nur für ausgewählte Patienten mit einem Low-risk-NZK < 3 cm eine empfohlene Option mit engmaschiger Befundkontrolle und kurativ-intendierter Therapieeinleitung ab einem Lokalprogress dar. Watchful Waiting zeichnet sich durch eine aufgeschobene Behandlung und Kontrolle bis zur notwendigen palliativen, symptomkontrollierten Therapie aus.**
- **Als Ablationsverfahren sind bisher nur die RFA und die Kryotherapie zur Therapie der SRM/NZK laut Leitlinien zugelassen.**
- **Die genannten potenziell alternativen Ablationstechniken gelten weiterhin für die renale Anwendung als experimentell.**

Korrespondenzadresse

Dr. med. J. J. Wendler
Universitätsklinik für Urologie und Kinderurologie, Otto-von-Guericke-Universität Magdeburg
Leipziger Straße 44, 39120 Magdeburg, Deutschland
Johann.wendler@med.ovgu.de

Einhaltung ethischer Richtlinien

Interessenkonflikt. J.J. Wendler, B. Friebe, D. Baumunk, A. Blana, T. Franiel, R. Ganzer, B. Hadaschik, T. Henkel, K.U. Köhrmann, J. Köllermann, T. Kuru, S. Machtens, A. Roosen, G. Salomon, H.P. Schlemmer, L. Sentker, U. Witzsch, U.B. Liehr, J. Ricke und M. Schostak geben an, dass kein Interessenkonflikt besteht.

Dieser Beitrag beinhaltet keine von den Autoren durchgeführten Studien an Menschen oder Tieren.

Literatur

1. Robert Koch-Institut, Gesellschaft der epidemiologischen Krebsregister in Deutschland e. V. (2013) Krebs in Deutschland 2009/2010, 9. Aufl. ruksaldruck, Berlin
2. Kirchberger I, Meisinger C, Heier M, Zimmermann AK, Thorand B, Autenrieth CS, Peters A, Ladwig KH, Döring A (2012) Patterns of multimorbidity in the aged population. Results from the KORA-Age study. PloS One 7(1):e30556 doi:10.1371/journal.pone.0030556
3. http://www.kdigo.org/clinical_practice_guidelines/pdf/CKD/KDIGO_2012_CKD_GL.pdf. Zugegriffen: 19. Jan. 2016
4. Tsili AC, Argyropoulou MI (2015) Advances of multidetector computed tomography in the characterization and staging of renal cell carcinoma. World J Radiol 7(6):110–127. doi:10.4329/wjr.v7.i6.110
5. Olbert PJ, Maier M, Heers H, Hegele A, Hofmann R (2015) Indications for nephron-sparing surgery. Analysis over a 13-year period in the context of changing guidelines. Urologe A 54(6):804–810. doi:10.1007/s00120-014-3710-2
6. Ljungberg B, Bensalah K, Bex A, Canfield S, Dabestani S, Giles RH, Hofmann F, Hora M, Kuczyk MA, Lam T, Marconi L, Merseburger AS, Powles T, Staehler M, Volpe A (2015) Guidelines on Renal Cell Carcinoma. European Association of Urology (EAU) 2015, Update March 2015, S 8–23. http://uroweb.org/wp-content/uploads/10-Renal-Cell-Carcinoma_LR1.pdf. Zugegriffen: 19. Jan. 2016
7. Leitlinienprogramm Onkologie (Deutsche Krebsgesellschaft, Deutsche Krebshilfe, AWMF) (2015) Diagnostik, Therapie und Nachsorge des Nierenzellkarzinoms, S3-Leitlinie, Langversion 1.0, 2015, AWMF Registernummer: 043/017OL. http://leitlinienprogramm-onkologie.de/Leitlinien.7.0.html. Zugegriffen: 19. Jan. 2016
8. Volpe A, Finelli A, Gill IS, Jewett MA, Martignoni G, Polascik TJ, Remzi M, Uzzo RG (2012) Rationale for percutaneous biopsy and histologic characterisation of renal tumours. Eur Urol 62(3):491–504. doi:10.1016/j.eururo.2012.05.009
9. Warren KS, McFarlane J (2005) The Bosniak classification of renal cystic masses. BJU Int 95(7):939–942
10. Graumann O, Osther SS, Karstoft J, Hørlyck A, Osther PJ (2015) Bosniak classification system: a prospective comparison of CT, contrast-enhanced US, and MR for categorizing complex renal cystic masses. Acta Radiol 27:pii: 0284185115588124
11. Visapää H, Glücker E, Haukka J, Taari K, Nisen H (2013) Papillary renal cell cancer is strongly associated with simple renal cysts. Urol Int 91(3):269–272. doi:10.1159/000351751
12. Robertson EG, Baxter G (2011) Tumour seeding following percutaneous needle biopsy: the real story! Clin Radiol 66(11):1007–1014. doi:10.1016/j.crad.2011.05.012
13. Horstmann M, Franiel T, Grimm MO (2014) Differential diagnosis of hematuria. Urologe A 53(8):1215–1226. doi:10.1007/s00120-014-3506-4
14. Remzi M, Marberger M (2009) Renal tumor biopsies for evaluation of small renal tumors: why, in whom, and how? Eur Urol 55(2):359–367. doi:10.1016/j.eururo.2008.09.053
15. Menogue SR, O'Brien BA, Brown AL, Cohen RJ (2013) Percutaneous core biopsy of small renal mass lesions: a diagnostic tool to better stratify patients for surgical intervention. BJU Int 111(4 Pt B):E146–E151. doi:10.1111/j.1464-410X.2012.11384.x
16. Höfflin R, Roth W, Sültmann H, Grüllich C, Hatiboglu G, Nyarangi-Dix J, Schönberg G, Teber D, Hadaschik B, Pahernik S, Hohenfellner M, Duensing S (2015) Intratumoral heterogeneity in renal cell carcinoma. Molecular basis and translational implications. Urologe A 54(6):800–803. doi:10.1007/s00120-015-3800-9
17. Trpkov K, Yilmaz A, Uzer D, Dishongh KM, Quick CM, Bismar TA, Gokden N (2010) Renal oncocytoma revisited: a clinicopathological study of 109 cases with emphasis on problematic diagnostic features. Histopathology 57(6):893–906. doi:10.1111/j.1365-2559.2010.03726.x
18. Maurice MJ, Zhu H, Kiechle JE, Kim SP, Abouassaly R (2015) Increasing Biopsy Utilization for Renal Cell Carcinoma Is Closely Associated With Treatment. Urology 86(5):906–913. doi:10.1016/j.urology.2015.08.020
19. Wein A, Kavoussi L, Partin A, Peters C (2016) Campbell-Walsh Urology, 11. Aufl. Elsevier, Philadelphia.
20. Chawla SN, Crispen PL, Hanlon AL, Greenberg RE, Chen DY, Uzzo RG (2006) The natural history of observed enhancing renal masses: meta-analysis and review of the world literature. J Urol 175(2):425–431
21. Thompson RH, Hill JR, Babayev Y, Cronin A, Kaag M, Kundu S, Bernstein M, Coleman J, Dalbagni G, Touijer K, Russo P (2009) Metastatic renal cell carcinoma risk according to tumor size. J Urol 182(1):41–45. doi:10.1016/j.juro.2009.02.128
22. Camacho JC, Kokabi N, Xing M, Master VA, Pattaras JG, Mittal PK, Kim HS, R. E. N. A. L. (2015) Radius, exophytic/endophytic, nearness to collecting system or sinus, anterior/posterior, and location relative to polar lines) nephrometry score predicts early tumor recurrence and complications after percutaneous ablative therapies for renal cell carcinoma: a 5-year experience. J Vasc Interv Radiol 26(5):686–693. doi:10.1016/j.jvir.2015.01.008
23. Vargas HA, Delaney HG, Delappe EM, Wang Y, Zheng J, Moskowitz CS, Tan Y, Zhao B, Schwartz LH, Hricak H, Russo P, Akin O (2013) Multiphasic contrast-enhanced MRI: single-slice versus volumetric quantification of tumor enhancement for the assessment of renal clear-cell carcinoma fuhrman grade. J Magn Reson Imaging 37(5):1160–1167. doi:10.1002/jmri.23899
24. Platzek I, Zastrow S, Deppe PE, Grimm MO, Wirth M, Laniado M, Stroszczynski C (2010) Whole-body MRI in follow-up of patients with renal cell carcinoma. Acta Radiol 51(5):581–589. doi:10.3109/02841851003724846
25. Hallscheidt PJ et al (2004) Diagnostic accuracy of staging renal cell carcinomas using multidetector-row computed tomography and magnetic resonance imaging: a prospective study with histopathologic correlation. J Comput Assist Tomogr 28(3):333–339
26. Jewett MA, Mattar K, Basiuk J, Morash CG, Pautler SE, Siemens DR, Tanguay S, Rendon RA, Gleave ME, Drachenberg DE, Chow R, Chung H, Chin JL, Fleshner NE, Evans AJ, Gallie BL, Haider MA, Kachura JR, Kurban G, Fernandes K, Finelli A (2011) Active surveillance of small renal masses: progression patterns of early stage kidney cancer. Eur Urol 60(1):39–44. doi:10.1016/j.eururo.2011.03.03
27. Lane BR, Abouassaly R, Gao T, Weight CJ, Hernandez AV, Larson BT, Kaouk JH, Gill IS, Campbell SC (2010) Active treatment of localized renal tumors may not impact overall survival in patients aged 75 years or older. Cancer 116(13):3119–3126. doi:10.1002/cncr.25184
28. Pierorazio P, McKiernan J, Allaf M (2013) Quality of life on active surveillance for small renal masses versus immediate intervention: interim analysis of the DISSRM (delayed intervention and surveillance for small renal masses) registry. J Urol 189(3S):e259

29. Whitson JM, Harris CR, Meng MV (2012) Population-based comparative effectiveness of nephron-sparing surgery vs ablation for small renal masses. BJU Int 110(10):1438–1443
30. Duffey BG, Kyle AJ (2010) Current and future technology for minimally invasive ablation of renal cell carcinoma. Indian J Urol 26(3):410–417
31. Zlotta AR, Wildschutz T, Wood BJ et al (1997) Radiofrequency interstitial tumor ablation (RITA) is a possible new modality for treatment of renal cancer: ex vivo and in vivo experience. J Endourol 11:251–258
32. Rendon RA, Kachura JR, Sweet JM, Gertner MR, Sherar MD, Robinette M, Tsihlias J, Trachtenberg J, Sampson H, Jewett MA (2002) The uncertainty of radio frequency treatment of renal cell carcinoma: findings at immediate and delayed nephrectomy. J Urol 167(4):1587–1592
33. Klingler HC, Marberger M, Mauermann J, Remzi M, Susani M (2007) „Skipping" is still a problem with radiofrequency ablation of small renal tumours. BJU Int 99(5):998–1001
34. Varkarakis IM, Allaf ME, Inagaki T et al (2005) Percutaneous radio frequency ablation of renal masses: results at a 2-year mean followup. JURO 174(460):456–460
35. Clark TWI, Malkowicz B, Stavropoulos SW et al (2006) Radiofrequency ablation of small renal cell carcinomas using multitined expandable electrodes: preliminary experience. J Vasc Interv Radiol 17:513–519
36. Breen DJ, Rutherford EE, Stedman B et al (2007) Management of renal tumors by image-guided radiofrequency ablation: Experience in 105 tumors. Cardiovasc Intervent Radiol 30:936–942
37. Ferakis N, Bouropoulos C, Granitsas T, Mylona S, Poulias I (2010) Longterm results after computed-tomography-guided percutaneous radiofrequency ablation for small renal tumors. J Endourol 24:1909–1913
38. Zagoria RJ, Pettus JA, Rogers M, Werle DM, Childs D, Leyendecker JR (2011) Long-term outcomes after percutaneous radiofrequency ablation for renal cell carcinoma. URL 77:1393–1397
39. Kunkle DA, Uzzo RG (2008) Cryoablation or radiofrequency ablation of the small renal mass : a meta-analysis. Cancer 113(10):2671–2680. doi:10.1002/cncr.23896
40. Wah T, Irving H, Gregory W, Cartledge J, Joyce A, Selby P (2014) Radiofrequency ablation (RFA) of renal cell carcinoma (RCC): experience in 200 tumours. BJU Int 113(3):416–428. doi:10.1111/bju.12349
41. Olweny EO, Park SK, Tan YK, Best SL, Trimmer C, Cadeddu JA (2012) Radiofrequency ablation versus partial nephrectomy in patients with solitary clinical T1a renal cell carcinoma: comparable oncologic outcomes at a minimum of 5 years of follow-up. Eur Urol 61:1156–1161
42. Psutka SP, Feldman AS, McDougal WS, McGovern FJ, Mueller P, Gervais DA (2013) Long-term oncologic outcomes after radiofrequency ablation for T1 renal cell carcinoma. Eur Urol 63:486–492
43. Kroeger N, Choueiri TK, Lee JL, Bjarnason GA, Knox JJ, Mackenzie MJ, Wood L, Srinivas S, Vaishamayan UN, Rha SY, Pal SK, Yuasa T, Donskov F, Agarwal N, Tan MH, Bamias A, Kollmannsberger CK, North SA, Rini BI, Heng DY (2013) Survival outcome and treatment response of patients with late relapse from renal cell carcinoma in the era of targeted therapy. Eur Urol 65:1086–1092. doi:10.1016/j.eururo.2013.07.031
44. Tracy CR, Raman JD, Donnally C, Trimmer CK, Cadeddu JA (2010) Durable oncologic outcomes after radiofrequency ablation: experience from treating 243 small renal masses over 7.5 years. Cancer 116:3135–3142
45. Georgiades C, Rodriguez R (2013) Renal tumor ablation. Tech Vasc Interv Radiol 16:230–238
46. Gervais DA, McGovern FJ, Arellano RS, McDougal WS, Mueller PR (2005) Radiofrequency ablation of renal cell carcinoma: part 1, indications, results, and role in patient management over a 6-year period and ablation of 100 tumors. AJR 185:64–71
47. Takaki H, Yamakado K, Soga N et al (2010) Midterm results of radiofrequency ablation versus nephrectomy for T1a renal cell carcinoma. Jpn J Radiol 28(6):460–468 (Jul)
48. Uchida M, Imaide Y, Sugimoto K, Uehara H, Watanabe H (1995) Percutaneous cryosurgery for renal tumours. Br J Urol 75(2):132–137 (Feb)
49. Bischoff JT, Chen RB, Lee BR et al (1999) Laparoscopic renal cryoablation: acute and long-term clinical radiographic, and pathologic effects in an animal model and application in a clinical trial. J Endourol 13:233–239
50. Berger A, Kamoi K, Gill IS, Aron M (2009) Cryoablation for renal tumors: current status. Curr Opin Urol 19(2):138–142
51. Gill IS, Matin SF, Desai MM, Kaouk JH, Steinberg A, Mascha E et al (2003) Comparative analysis of laparoscopic versus open partial nephrectomy for renal tumors in 200 patients. J Urol 170:64–68
52. Atwell TD, Farrell MA, Leibovich BC et al (2008) Percutaneous renal cryoablation: experience treating 115 tumors. J Urol 179:2136–2140 (discussion 2140–2141)
53. Georgiades CS, Hong K, Bizzell C, Geschwind JF, Rodriguez R (2008) Safety and efficacy of CT-guided percutaneous cryoablation for renal cell carcinoma. J Vasc Interv Radiol 19:1302–1310
54. Pirasteh A, Snyder L, Boncher N, Passalacqua M, Rosenblum D, Prologo JD (2011) Cryoablation vs. radiofrequency ablation for small renal masses. Acad Radiol 18:97–100
55. Atwell TD, Schmit GD, Boorjian SA et al (2013) Percutaneous ablation of renal masses measuring 3.0 cm and smaller: comparative local control and complications after radiofrequency ablation and cryoablation. AJR 200:461–466
56. Gill IS, Remer EM, Hasan WA, Strzempkowski B, Spaliviero M, Steinberg AP et al (2005) Renal cryoablation: outcome at 3 years. J Urol 173:1903–1907
57. Finley DS, Beck S, Box G, Chu W, Deane L, Vajgrt DJ et al (2008) Percutaneous and laparoscopic cryoablation of small renal masses. J Urol 180:492–498
58. KlatteT, Mauermann J, Heinz-Peer G, Waldert M, Weibl P, Klingler HC, Remzi M (2011) Perioperative, oncological and functional outcomes of laparoscopic renal cryoablation and open partial nephrectomy: a matched pair analysis. J Endourol 25(6):991–997
59. Strom KH, Derweesh I, Stroup SP, Malcolm JB, L'Esperance J, Wake RW et al (2011) Second prize: recurrence rates after percutaneous and laparoscopic renal cryoablation of small renal masses: does the approach make a difference? J Endour 25:371–375
60. Haber GP, Lee MC, Crouzet S et al (2012) Tumour in solitary kidney: laparoscopic partial nephrectomy vs laparoscopic cryoablation. BJU Int 109(1):118–124
61. Desai MM, Aron M, Gill IS (2005) Laparoscopic partial nephrectomy versuslaparoscopic cryoablation for the small renal tumor. Urology 66(5 Suppl):23–28
62. Wu F, Wang ZB, Chen WZ, Bai J, Zhu H, Qiao TY (2003) Preliminary experience using high intensity focused ultrasound for the treatment of patients with advanced stage renal malignancy. J Urol 170(6 Pt 1):2237–2240
63. Ritchie RW, Leslie T, Phillips R, Wu F, Illing R, ter Haar G, Protheroe A, Cranston D (2010) Extracorporeal high intensity focused ultrasound for renal tumours: a 3-year follow-up. BJU Int 106(7):1004–1009. doi:10.1111/j.1464-410X.2010.09289.x
64. Klingler HC, Susani M, Seip R, Mauermann J, Sanghvi N, Marberger MJ (2008) A novel approach to energy ablative therapy of small renal tumours: laparoscopic high-intensity focused ultrasound. Eur Urol 53(4):810–816 (discussion 817–818)
65. Ritchie RW, Leslie TA, Turner GD, Roberts IS, D'Urso L, Collura D, Demarchi A, Muto G, Sullivan ME (2011) Laparoscopic high-intensity focused ultrasound for renal tumours: a proof of concept study. BJU Int 107(8):1290–1296. doi:10.1111/j.1464-410X.2010.09620.x
66. Rubinsky B (2010) Irreversible Electroporation. Series in Biomedical Engineering. Springer, Berlin Heidelberg
67. Narayanan G, Doshi MH (2016) Irreversible Electroporation (IRE) in Renal Tumors. Curr Urol Rep 17(2):15 doi:10.1007/s11934-015-0571-1
68. Thomson KR, Cheung W, Ellis SJ, Federman D, Kavnoudias H, Loader-Oliver D, Roberts S, Evans P, Ball C, Haydon A (2011) Investigation of the safety of irreversible electroporation in humans. J Vasc Interv Radiol 22(5):611–621. doi:10.1016/j.jvir.2010.12.014
69. Trimmer CK, Khosla A, Morgan M, Stephenson SL, Ozayar A, Cadeddu JA (2015) Minimally Invasive Percutaneous Treatment of Small Renal Tumors with Irreversible Electroporation: A Single-Center Experience. J Vasc Interv Radiol 26(10):1465–1471. doi:10.1016/j.jvir.2015.06.028
70. Wendler JJ, Ricke J, Pech M, Fischbach F, Jürgens J, Siedentopf S, Roessner A, Porsch M, Baumunk D, Schostak M, Köllermann J, Liehr UB (2015) First Delayed Resection Findings After Irreversible Electroporation (IRE) of Human Localised Renal Cell Carcinoma (RCC) in the IRENE Pilot Phase 2a Trial. Cardiovasc Intervent Radiol 39:239–250
71. Wendler JJ, Porsch M, Nitschke S, Köllermann J, Siedentopf S, Pech M, Fischbach F, Ricke J, Schostak M, Liehr UB (2015) A prospective Phase 2a pilot study investigating focal percutaneous irreversible electroporation (IRE) ablation by NanoKnife in patients with localised renal cell carcinoma (RCC) with delayed interval tumour resection (IRENE trial). Contemp Clin Trials 43:10–19. doi:10.1016/j.cct.2015.05.002
72. Brace CL (2009) Microwave ablation technology: what every user should know. Curr Probl Diagn Radiol 38(2):61–67
73. Floridi C, De Bernardi I, Fontana F, Muollo A, Ierardi AM, Agostini A, Fonio P, Squillaci E, Brunese L, Fugazzola C, Carrafiello G (2014) Microwave ablation of renal tumors: state of the art and development trends. Radiol Med 119(7):533–540. doi:10.1007/s11547-014-0426-8
74. Yu J, Zhang G, Liang P, Yu XL, Cheng ZG, Han ZY, Zhang X, Dong J, Li QY, Mu MJ, Li X (2015) Midterm results of percutaneous microwave ablation under ultrasound guidance versus retroperitoneal laparoscopic radial nephrectomy for small renal cell carcinoma. Abdom Imaging 40(8):3248–3256. doi:10.1007/s00261-015-0500-2
75. Moreland AJ, Ziemlewicz TJ, Best SL, Hinshaw JL, Lubner MG, Alexander ML, Brace CL, Kitchin

DR, Hedican SP, Nakada SY, Lee FT Jr, Abel EJ (2014) High-powered microwave ablation of t1a renal cell carcinoma: safety and initial clinical evaluation. J Endourol 28(9):1046–1052. doi:10.1089/end.2014.0190
76. Carrafiello G, Dionigi G, Ierardi AM, Petrillo M, Fontana F, Floridi C, Boni L, Rovera F, Rausei S, Mangano A, Spampatti S, Marconi A, Carcano G, Dionigi R (2013) Efficacy, safety and effectiveness of image-guided percutaneous microwave ablation in cystic renal lesions Bosniak III or IV after 24 months follow up. Int J Surg 11(Suppl 1):S30–S35. doi:10.1016/S1743-9191(13)60010-2
77. Campbell SP, Song DY, Pierorazio PM, Allaf ME, Gorin MA (2015) Stereotactic Ablative Radiotherapy for the Treatment of Clinically Localized Renal Cell Carcinoma. J Oncol 2015:1–6. doi:10.1155/2015/547143
78. Bretschneider T, Peters N, Hass P, Ricke J (2012) Update on interstitial brachytherapy. Radiologe 52(1):70–73. doi:10.1007/s00117-011-2213-z
79. Gill IS, Kavoussi LR, Lane BR et al (2007) Comparison of 1,800 laparoscopic and open partial nephrectomies for single renal tumors. J Urol 178(1):41–46
80. Lane BR, Gill IS (2010) 7-year oncological outcomes after laparoscopic and open partial nephrectomy. J Urol 183(2):473–479
81. Gong EM, Orvieto MA, Zorn KC et al (2008) Comparison of laparoscopic and open partial nephrectomy in clinical T1a renal tumors. J Endourol 22(5):953–957
82. Marszalek M, Meixl H, Polajnar M et al (2009) Laparoscopic and open partial nephrectomy: a matchedpair comparison of 200 Patients. Eur Urol 55(5):1171–1178
83. Muramaki M, Miyake H, Sakai I et al (2012) Prognostic factors influencing postoperative development of chronic kidney disease in patients with small renal tumors who underwent partial nephrectomy. Curr Urol 6:129–135
84. Gill IS et al (2011) „Zero ischemia" partial nephrectomy: novel laparoscopic and robotic technique. Eur Urol 59(1):128–134
85. Minervini A, Serni S, Tuccio A et al (2012) Simple enucleation versus radical nephrectomy in the treatment of pT1a and pT1b renal cell carcinoma. Ann Surg Oncol 19(2):694–700
86. Minervini A, Ficarra V, Rocco F et al (2011) SATURN Project-LUNA Foundation. Simple enucleation is equivalent to traditional partial nephrectomy for renal cell carcinoma: results of a nonrandomized, retrospective, comparative study. J Urol 185(5):1604–1610
87. Steinestel J, Steffens S, Steinestel K, Schrader AJ (2014) Positive surgical margins in nephron-sparing surgery: risk factors and therapeutic consequences. World J Surg Oncol 8(12):252 doi:10.1186/1477-7819-12-252
88. Marszalek M, Carini M, Chlosta P, Jeschke K, Kirkali Z, Knüchel R, Madersbacher S, Patard JJ, Van Poppel H (2012) Positive surgical margins after nephron-sparing surgery. Eur Urol 61(4):757–763. doi:10.1016/j.eururo.2011.11.028
89. Bazzi WM, Stroup SP, Kopp RP et al (2012) Comparison of laparoendoscopic single-site and multiport laparoscopic radical and partial nephrectomy: a prospective, nonrandomized study. Urology 80(5):1039–1045
90. Masson-Lecomte A, Bensalah K, Seringe E et al (2013) A prospective comparison of surgical and pathological outcomes obtained after robot-assisted or pure laparoscopic partial nephrectomy in moderate to complex renal tumours: results from a French multicentre collaborative study. BJU Int 111(2):256–263
91. Aboumarzouk OM, Stein RJ, Eyraud R et al (2012) Robotic versus laparoscopic partial nephrectomy: a systematic review and meta-analysis. Eur Urol 62(6):1023–1033
92. Froghi S et al (2013) Evaluation of robotic and laparoscopic partial nephrectomy for small renal tumours (T1a). BJU Int 112(4):E322–E333

8.14

Follow-up after focal therapy in renal masses: an international multidisciplinary Delphi consensus project.

Zondervan PJ, Wagstaff PG, Desai MM, de Bruin DM, Fraga AF, Hadaschik BA, Köllermann J, Liehr UB, Pahernik SA, Schlemmer HP, Wendler JJ, Algaba F, de la Rosette JJ, Laguna Pes MP.

World J Urol. 2016 Dec;34(12):1657-1665.

PURPOSE: To establish consensus on follow-up (FU) after focal therapy (FT) in renal masses. To formulate recommendations to aid in clinical practice and research.

METHODS: Key topics and questions for consensus were identified from a systematic literature research. A Web-based questionnaire was distributed among participants selected based on their contribution to the literature and/or known expertise. Three rounds according to the Delphi method were performed online. Final discussion was conducted during the "8th International Symposium on Focal Therapy and Imaging in Prostate and Kidney Cancer" among an international multidisciplinary expert panel.

RESULTS: Sixty-two participants completed all three rounds of the online questionnaire. The panel recommended a minimum follow-up of 5 years, preferably extended to 10 years. The first FU was recommended at 3 months, with at least two imaging studies in the first year. Imaging was recommended biannually during the second year and annually thereafter. The panel recommended FU by means of CT scan with slice thickness ≤3 mm (at least three phases with excretory phase if suspicion of collecting system involvement) or mpMRI. Annual checkup for pulmonary metastasis by CT thorax was advised. Outside study protocols, biopsy during follow-up should only be performed in case of suspicion of residual/persistent disease or radiological recurrence.

CONCLUSIONS: The consensus led to clear FU recommendations after FT of renal masses supported by a multidisciplinary expert panel. In spite of the low level of evidence, these recommendations can guide clinicians and create uniformity in the follow-up practice and for clinical research purposes.

World J Urol (2016) 34:1657–1665
DOI 10.1007/s00345-016-1828-0

ORIGINAL ARTICLE

Follow-up after focal therapy in renal masses: an international multidisciplinary Delphi consensus project

P. J. Zondervan[1] · P. G. K. Wagstaff[1] · M. M. Desai[2] · D. M. de Bruin[1,3] · A. F. Fraga[4] · B. A. Hadaschik[5] · J. Köllermann[6] · U. B. Liehr[7] · S. A. Pahernik[5] · H. P. Schlemmer[7] · J. J. Wendler[8] · F. Algaba[9] · J. J. M. C. H. de la Rosette[1] · M. P. Laguna Pes[1]

Received: 26 February 2016 / Accepted: 4 April 2016 / Published online: 22 April 2016

Abstract
Purpose To establish consensus on follow-up (FU) after focal therapy (FT) in renal masses. To formulate recommendations to aid in clinical practice and research.
Methods Key topics and questions for consensus were identified from a systematic literature research. A Web-based questionnaire was distributed among participants selected based on their contribution to the literature and/or known expertise. Three rounds according to the Delphi method were performed online. Final discussion was conducted during the "8th International Symposium on Focal Therapy and Imaging in Prostate and Kidney Cancer" among an international multidisciplinary expert panel.
Results Sixty-two participants completed all three rounds of the online questionnaire. The panel recommended a minimum follow-up of 5 years, preferably extended to 10 years. The first FU was recommended at 3 months, with at least two imaging studies in the first year. Imaging was recommended biannually during the second year and annually thereafter. The panel recommended FU by means of CT scan with slice thickness $\leq$3 mm (at least three phases with excretory phase if suspicion of collecting system involvement) or mpMRI. Annual checkup for pulmonary metastasis by CT thorax was advised. Outside study protocols, biopsy during follow-up should only be performed in case of suspicion of residual/persistent disease or radiological recurrence.
Conclusions The consensus led to clear FU recommendations after FT of renal masses supported by a multidisciplinary expert panel. In spite of the low level of evidence, these recommendations can guide clinicians and create uniformity in the follow-up practice and for clinical research purposes.

Keywords Focal therapy · Follow-up · Renal masses · Consensus · Delphi method

Abbreviations

CA	Cryoablation
CEUS	Contrast-enhanced ultrasound

P. J. Zondervan and P. G. K. Wagstaff have contributed equally to this work.

Electronic supplementary material The online version of this article (doi:10.1007/s00345-016-1828-0) contains supplementary material, which is available to authorized users.

✉ P. J. Zondervan
p.j.zondervan@amc.uva.nl

[1] Department of Urology, AMC University Hospital, PO box 22660, 1100DD Amsterdam, The Netherlands

[2] Department of Urology, Keck School of Medicine USC, Los Angeles, CA, USA

[3] Department of Biomedical Engineering and Physics, AMC University Hospital, Amsterdam, The Netherlands

[4] Department of Urology, Centro Hospitalar do Porto, Porto, Portugal

[5] Department of Urology, University Hospital Heidelberg, Heidelberg, Germany

[6] Department of Pathology, Sana Klinikum Offenbach, Offenbach, Germany

[7] Department of Urology, Otto-von-Guericke University Magdeburg, Magdeburg, Germany

[8] Department of Radiology, German Cancer Research Center, Heidelberg, Germany

[9] Department of Pathology, Fundació Puigvert, Barcelona, Spain

CKD	Chronic kidney disease
FT	Focal therapy
HIFU	High-intensity focused ultrasound
IRE	Irreversible electroporation
KT	Key topic
MWA	Microwave
mpMRI	Multiparametric magnetic resonance imaging
PN	Partial nephrectomy
RCC	Renal cell cancer
RFA	Radio-frequency ablation
RM	Renal mass
RN	Radical nephrectomy

Introduction

Treatment of RMs has shifted from RN to nephron-sparing interventions. Conversely, increasing life expectancy has resulted in increased number of elderly patients with multiple severe comorbidities and concomitant RM. In poor surgical candidates or patients suffering from a genetic predisposition for developing multiple tumors, FT competes strongly with minimally invasive surgery [1, 2]. Interest in kidney FT has been fueled by promising reports on mid- to long-term oncological outcome combined with preservation or marginal loss of renal function [3–10].

The literature is abundant on safety and efficacy reports on CA and RFA. However, follow-up protocols are ill-defined, and the major urological associations guidelines (EAU/AUA) provide sparse guidance on the subject [2, 11, 12]. Efforts on standardization of terminology and reporting criteria by the "International Working Group on Image-Guided Tumor Ablation" have resulted in recommendations that, although non-consensually structured, are valid so far [13, 14]. However, practical guidance in terms of follow-up schedules or specific tests is not provided. With the aim of filling this gap in follow-up recommendations after FT of RMs and to provide straightforward protocols, a multidisciplinary international consensus was organized on the subject of follow-up after FT in RMs.

Materials and methods

A consensus project based on the four Delphi method stages [15] was organized prior to and during the "8th International Symposium on Focal Therapy and Imaging in Prostate and Kidney Cancer" on June 21, 2015, in Noordwijk, The Netherlands. The four stages included:

1. Systematic literature search

   In order to assess the relevant literature, a systematic search of the PubMed database was conducted (date: January 2005–February 2015). The search focused on "renal masses" (and synonyms), "focal therapy" (and synonyms), and "follow-up" (and synonyms). The full search query and inclusion criteria to identify manuscripts are listed below (Table 1).
2. Defining consensus topics, formulating questions and selecting experts

   From the systematic literature review, key topics were identified, questions formulated, and online questionnaire created.

   Participants were selected based on their contribution to the literature, academic involvement or recognized expertise in the field. The multidisciplinary panel of experts in FT included urologists, radiologists, pathologists, radiation oncologists, and biomedical engineers. Biomedical engineers were asked for their involvement in new ablation technologies and diagnostics in the future.
3. Online questionnaires

   Three consecutive rounds of online questionnaires (www.surveymonkey.com) were sent to the selected experts in the period from March 29, 2015, till June 16, 2015. In the first and second rounds, the participants were encouraged to provide suggestions and feedback. Results of the previous round were incorporated in successive rounds (2nd and 3rd). Questions on which consensus was not reached were reformulated, new questions incorporated following suggestions of the participants and similar questions collated.
4. Consensus meeting

   A 6-h consensus meeting to discuss the results of the questionnaire was conducted during the 8th International Symposium on "Focal Therapy and Imaging in Prostate and Kidney Cancer" in Noordwijk, The Netherlands (www.Focaltherapy.org) from June 21, 2015, to June 23, 2015. During this last phase of the process, the results of the Web-based questionnaires were presented and discussed.

Results

Systematic literature search and key topics

Overall, 300 potentially eligible articles were identified by the systematic literature search. After review of titles and abstracts, 68 full-text articles were assessed for eligibility.

Table 1 Complete search query, filters used for the systematic literature search and inclusion criteria of the articles previous to identification of the key topics

Search query
(“Kidney neoplasms”[Mesh] OR kidney neoplasm*[tiab] OR kidney cancer*[tiab] OR kidney tumo*[tiab] OR kidney neoplasm*[tiab] OR kidney malignan*[tiab] OR kidney carcinoma*[tiab] OR kidney adenoma*[tiab] OR nephroma*[tiab] OR renal mass*[tiab] OR renal tumor*[tiab] OR renal tumor*[tiab] OR renal neoplasm*[tiab] OR renal cancer*[tiab] OR renal malignan*[tiab] OR renal carcinoma*[tiab] OR renal adenoma*[tiab]) AND (“Ablation Techniques”[Mesh] OR “Cryosurgery”[Mesh] OR cryotherap*[tiab] OR ablat*[tiab] OR cryoablat*[tiab] OR cryosurger*[tiab] OR RFA [tiab] OR radiofrequency ablat*[tiab] OR radio frequency ablat*[tiab] OR focal therap*[tiab]) AND (“follow-up studies”[Mesh] OR “minimally invasive surgical procedures”[Mesh] OR follow-up[tiab] OR follow-up[tiab] OR follow-up [tiab] OR CT [tiab] OR “tomography, X-ray computed”[Mesh] OR “ultrasonography”[Mesh] OR “magnetic resonance imaging”[Mesh] OR “biopsy”[Mesh] OR computed tomography[tiab] OR imaging[tiab] OR ultraso*[tiab] OR MRI[tiab] OR magnetic resonance imaging[tiab] OR biops*[tiab] OR “neoplasm recurrence, local”[Mesh] OR neoplasm persist*[tiab]) NOT (“animals”[Mesh] NOT “humans”[Mesh]) NOT (“letter” [Publication Type] OR “comment”[pt] OR “editorial”[pt])
Filters
Published last 10 years
English
Humans
Inclusion criteria
≥50 Patients included
≥24 Months follow-up

Table 2 Key topics identified in the literature search and pertinent questions for follow-up

Key topic	Questions
1. Definitions	What is the proper definition of persistent/residual disease? What is the proper definition of recurrent disease?
2. Follow-up intervals	What is the first time point for imaging during follow-up? What is the ideal follow-up interval? What is the ideal length of follow-up?
3. Imaging modality	Which one is the imaging modality of choice? Which alternative imaging modality in case of CKD? What are the proper CT/MRI protocols to be used? Is radiation exposure an issue during the follow-up?
4. Follow-up for metastasis	Which imaging test is recommended in the follow-up for metastasis? Which is the recommended follow-up schedule for metastasis?
5. Role of biopsy in follow-up	What is the role of biopsy in case of suspicion of residual/persistence or recurrence?
6. Risk stratification-adapted follow-up	Should follow-up be adapted to risk stratification? Which risk factors should be used?

Finally, 31 publications were selected after quality assessment (Addendum 1 in ESM). Most of these were case–control and cohort studies describing a single type of FT, comparing FT to PN outcomes or laparoscopic versus percutaneous approach. When assessing the follow-up topic, a lack of proper description of protocols was observed. Furthermore, overlap between the definitions of residual/persistent and recurrent disease frequently made it difficult to assess the results of these different outcomes separately.

Based on the lack of clarity from the literature search, we formulated five key topics. An additional query related to risk-adapted stratification follow-up showed up persistently during the online survey and was incorporated among the key topics (Table 2).

Participants

From 130 experts invited, 76 (58 %) accepted to participate in the project. The group consisted of 57 (75 %) urologists, 11 (14.5 %) radiologists, 5 (6.5 %) pathologists, 2 (2.6 %) engineers and 1 (1.4 %) radiation oncologist. The experience of the participants with FT of renal masses was: CA for 82 %, RFA for 67 %, HIFU for 13 %, MWA for 10 % and IRE for 17 % of the participants.

First, second and third round questionnaires were completed by 72 (95 %), 67 (88 %) and 63 (83 %) of the experts, respectively. A total of 62 (82 %) participants completed all three rounds of the online questionnaire. A panel of 12 experts, consisting of 9 urologists, 1 pathologist, 1

radiologist and 1 engineer/physicist, attended the consensus meeting in Noordwijk. Addendum 2 in ESM lists participants and their affiliations.

Consensus

In the online questionnaires, 98 % of the participants set the cutoff for consensus at ≥80 % agreement for a specific question. A total of 51 questions were considered for consensus. Online agreement and near-agreement were reached for 19 and 6 of the questions, respectively. Online agreement was not reached in 13 questions, and 13 were exploratory with multiple possible responses. Percentage of agreement and at which round it was reached are displayed in Addendum 3 in ESM.

There was online agreement on the lack of clear recommendation on follow-up after FT, on a unique protocol after CA and RFA and on the multidisciplinary character of the follow-up protocol. During the present meeting, the composition of the follow-up team was defined as including at least one urologist, one radiologist and one pathologist with experience in FT.

KT 1. Definition of residual/persistent and recurrent disease

Residual or persistent disease was strictly defined as the *"presence of any radiological enhancement at the first radiologic follow-up*". After consensus was reached on the timing of the first radiological FU (KT 2), *the* term "at 3 months" was added (Table 3).

Online questionnaires showed agreement on that "any new enhancement inside the ablated zone or in the margin of the ablated zone after a period of non-enhancement, preferably with positive biopsy" was considered as locally recurrent disease. Of the participants, 57 % considered a growing mass without enhancement as recurrence, and 1/3 of the participants would indicate a biopsy in this circumstance. Conversely, half of the participants did not consider biopsy mandatory for diagnosis of recurrence (Fig. 1a). The panel reviewed the definitions, results and suggestions and constructed a definition of radiological recurrence, as follows: "a *new (after a period of non-enhancement) enhancing or growing lesion, inside or in the margin of the ablated zone"* (Table 3).

Results of the online questionnaire and the panel meeting emphasized the differentiation between locally recurrent or "de novo" ipsilateral tumor (outside the treated area).

KT 2. Follow-up intervals

The majority of the participants (74 %) recognized that contrast enhancement might persist several months after FT.

Table 3 Summary of definitions and follow-up recommendations

1. Definitions
Residual/persistent disease: "presence of any radiological enhancement at 3 months radiological follow-up"
Radiological recurrence: "a new (after a period of non-enhancement) enhancing or growing lesion, inside or in the margin of the ablated zone"
2. Multidisciplinary composition of follow-up team
At least 1 urologist, 1 pathologist and 1 radiologist (experienced in post-ablation imaging)
3. Follow-up schedules
Follow-up interval:
Minimum FU period of 5 years, preferably extended to 10 years
First FU imaging at 3 months post-treatment
A minimum of two imaging studies in the first year
Biannual imaging in the second year
Annual imaging from the third year onwards
Strongly advised not to skip on the minimum recommended number of imaging studies
Imaging modalities
First option 3-phase CT scan (non-enhanced, arterial and nephrographic/cortico-medular), slice thickness ≤3 mm, IVP phase (delayed phase) advised if suspicion of urinary tract involvement or hydronephrosis
Second option MRI with multiparametric protocol including at least: T1, T2, DWI, DCE
In case of CKD 4/5 non-contrast-enhanced MRI or CEUS
Follow-up of metastasis
Annual examination for pulmonary metastasis, using CT thorax
Besides chest and abdomen, no other routine imaging for distant metastasis
4. Biopsy
Only in case of suspicion of residual disease/persistence or recurrence
5. Risk-adapted follow-up
Stage and grade are main determinants

During the consensus meeting, it was confirmed that a certain degree of tiny peripheral enhancement might be noted up to 6–9 months after FT that disappears subsequently. The opinion of the participants was divided at 40 % on the first timing for determination of residual disease (3 or 6 months after FT). The panel reached consensus on recommending first imaging after FT 3 months post-treatment.

No agreement was reached for number of radiological FUs in the first year. Majority (69 %) favored biannual imaging in the first year post-treatment although, when asked in consecutive round to choose between three and two imaging studies during the first year, 56 % of the participants supported imaging at 3, 6 and 12 months against 36.5 % at 6 and 12 months. Based on this apparent discordance, the panel recommended "at least" two imaging studies in the first year.

Concerning imaging FU during the second year after FT, opinions were divided between biannually and annually (55 vs 43 %, respectively). After discussion on the risk of local radiological recurrence, the panel recommended biannual imaging in the second year. From 3 years onward, annual imaging was recommended by participants' agreement (92.5 %) and supported by the panel.

The panel stressed the lack of reliable data in the literature, the need for more frequent imaging and prolonged FU in case of aggressive pathology (high grade and cT1b) (Fig. 1b), the lack of pathological staging in FT, and that eGFR should not dictate FU intervals.

Regarding the length of the follow-up after FT, the majority of participants favored 10 years (66 %). The panel recommended a minimum follow-up term of 5 years, with the advice to prolong to 10 years because of the absence of long-term data.

KT 3. Imaging modality

Considering participants' response, the panel recommended three-phase CT scan (non-enhanced, arterial, and nephrographic/cortico-medular) with $\leq$3 mm slice thickness protocol as the imaging of choice for the follow-up after FT. Delayed or IVP phase was advised if suspicion of urinary tract involvement (leak or hydronephrosis). The second preferred imaging modality was mpMRI (T1, T2, DWI and DCE sequences, 94 % consensus) (Fig. 1d).

In case of CKD IV–V, the panel advised non-contrast-enhanced MRI as the first choice instead of non-contrast-enhanced CT. Contrast-enhanced ultrasound (CEUS) was also considered as suitable option when available and if applied by experienced hands (Fig. 1c). Of participants, 80 % considered changing imaging policy on the basis of radiation exposure. The panel emphasized that concerns on radiation exposure must not lead to skip the minimum recommended amount of imaging studies, but rather to consider a different imaging modality (e.g., MRI for young age at FT or conditions at risk of radiation accumulation).

Follow-up intervals and type of imaging did not differ between CA and RFA.

KT 4. Follow-up for metastasis

The majority of participants (77 %) recommended regular checkup for pulmonary metastasis, at yearly intervals (89 % agreement). Based on "near-consensus" online (79 %), the panel recommended the use of CT thorax instead of X-ray thorax because of its higher sensitivity. Besides imaging of chest and abdomen, no other routine follow-up for metastasis is advised (consensus 83 %).

KT 5. The role of biopsy during follow-up

Online agreement (85 %) was reached that post-FT biopsy should not be acquired routinely during follow-up. The participants agree (85 %) that the literature was not clear on the reliability of the biopsy to confirm residual disease. Biopsy was used by 72 % of participants to make the diagnosis or residual/recurrent disease and 2/3 recommended it for this indication. After discussion on the literature, the panel recommended biopsy during follow-up only if suspicion of residual/recurrent disease. Regarding the need to confirm radiological recurrence by biopsy, 51 % of online participants and the panel agreed that biopsies are not mandatory to confirm recurrent disease. However, the panel strongly emphasized that biopsy might be of benefit to individual patient counseling and treatment strategy.

Regarding initial biopsy results, the panel recommended to stop follow-up only in case of angiomyolipoma (Fig. 1e). In follow-up setting, opinions were divided on labeling biopsy as "non-diagnostic" in case of fibrosis, necrosis or inflammation on pathology. The panel could not find evidence in the literature to solve this question.

KT 6. Risk stratification-adapted follow-up

There was online consensus (88 %) on "risk stratification" to guide follow-up after FT in renal masses instead of depending on procedural quality control. There was an agreement that patient and tumor factors dictate additional testing. When ranking four possible stratification factors, 1/3 of the participants found both stage and grade the most important, followed by RCC subtype. Clinical history of RCC was the least important. The panel agreed that patient and tumor factors should guide follow-up after FT, but concern was expressed on the value of adapting the currently known risk factors to the more restrictive RM population treated by FT.

Discussion

Based on the Delphi methodology, an International multidisciplinary panel of experts discussed and formulated consensus definitions of residual/persistent and locally recurrent disease after FT of RMs. Recommendations were formulated for relevant key topics on FT follow-up including the choice of imaging modality, follow-up intervals, checkup for metastasis and the role of biopsy. Furthermore the consensus unveiled that after FT, stage and grade are the main drivers of additional testing during follow-up. The

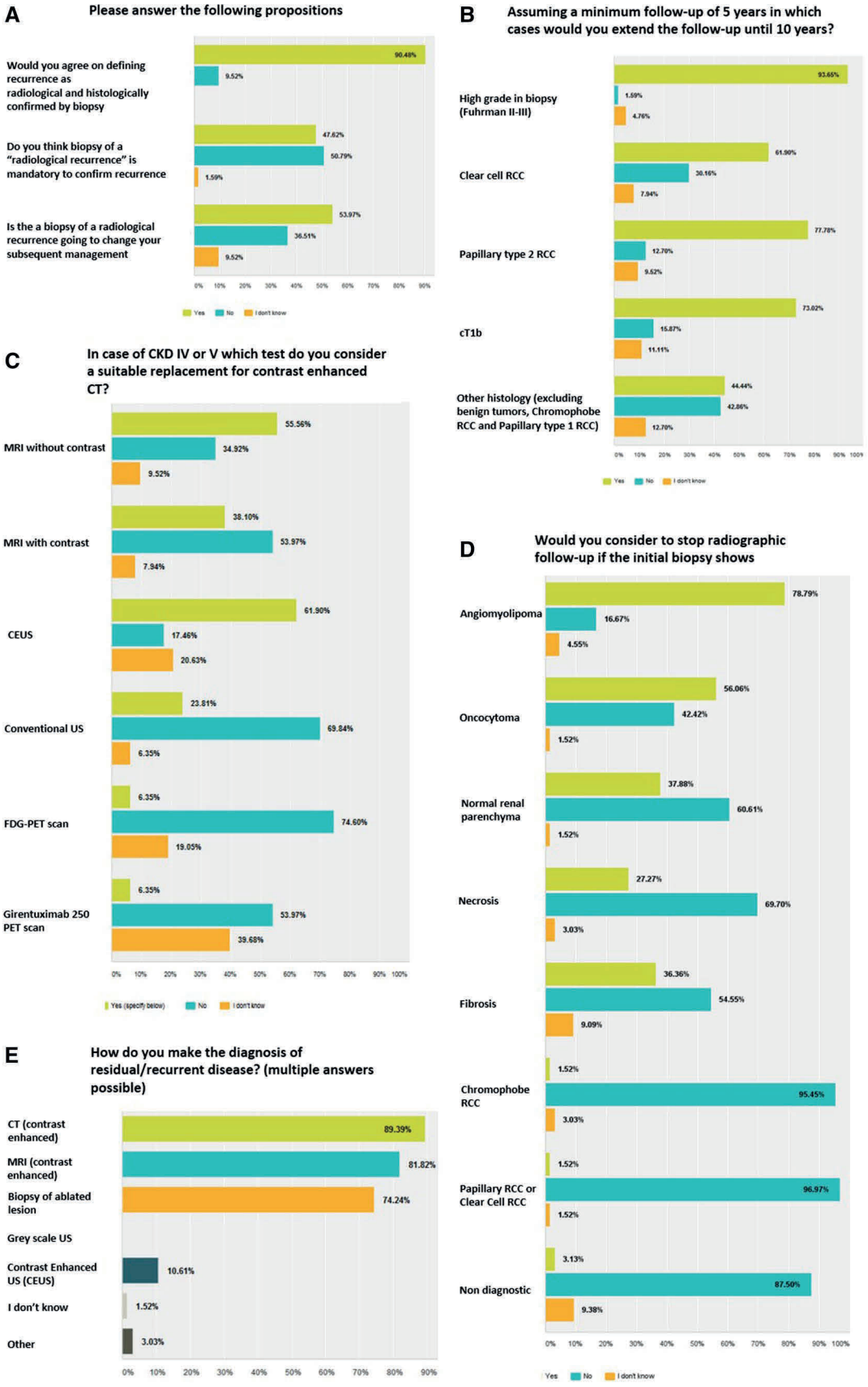

Fig. 1 Composite figure of questions from the Delphi survey

presented recommendations avoid overlap between residual and recurrent disease definitions and represent a comprehensive quality of care document.

So far, no formal recommendation process has been undertaken for follow-up of RMs after FT although the International Working Group on Image-Guided Tumor Ablation previously presented a consensus document for standardization in terminology and reporting criteria for FT in general [13, 14, 16]. EAU and AUA guidelines on RCC advise risk-adapted follow-up considering ablated tumors as intermediate- and low-risk category [2, 11, 12]. The aim of the present consensus was neither to interfere with previous documents nor to define imaging patterns of persistence or recurrence or specific recommendations on how to interpret a given test. For this purpose, a whole body of descriptive literature on post-FT imaging patterns for CT scan and MRI exists [17]. Conversely, the consensus aimed to establish clear and concise definitions of persistent and recurrent disease and to produce recommendations on which and when to apply alternative tests during FU.

Because of the absence of a well-designed comparative diagnostic study in follow-up after kidney FT and the difficulty in applying a reliable standard for comparison, we choose the Delphi method as an adequate tool to draw recommendations based on expert opinion in the medical field [15, 18]. By reformulating the questions, providing the answers of the previous rounds and narrowing the possibility for feedback, the process of achieving consensus was stimulated. Two facts strengthened the present consensus recommendations, the interdisciplinary character of the consensus Panel meeting and the high response rate reached during the three online rounds. Rather unusual in medical questionnaires, this high response rate likely reflects the strong interest and commitment of the participants [19, 20]. Furthermore, the participant's comments forced the inclusion and discussion of a new topic: the risk-adapted follow-up. Although agreement is not necessary to reach a consensus, participants massively set a cutoff at $\geq$80 % as an agreement facilitating the discussion and the recommendation process.

After FT, tumor activity relies mostly on radiological evolution of the treated lesion after contrast administration. The need for repeated imaging during FT follow-up was early recognized and fully accepted. The panel agreed unanimously that a clear distinction between persistent/residual disease and local recurrence was necessary. These definitions coincide with the ones previously stated by other panels composed mainly by radiologists [13].

Follow-up schedules after FT have been erratically described and not standardized. It distillates from the literature that early contrast evaluation within the first month after treatment may not be representative of the secondary vascular necrosis and apoptotic phenomenon that ultimately condition the evolution of the ablated lesion [21, 22]. Three months was unanimously chosen as the moment for the first evaluation outside trial protocols irrespective of the ablation technology used, recognizing that the size of the lesion may be larger at this point. Rather than establishing a rigid imaging interval, the panel emitted minimal recommendations for both the period (minimum of 5 years) and interval (minimum of 2 imaging studies in the first year). Recent data suggesting that 5-year follow-up may miss up to 30 % of the recurrences in T1 tumors [23] support this recommendation especially in young or healthy patients treated by FT.

A significant percentage of patients with ablated renal masses are already known with CDK $\geq$ 3 at the moment of diagnosis, or will develop CKD $\geq$ 3 during the follow-up. The toxicity of iodine contrast agents adds to the radiation burden especially when long survival is expected [24]. Both concerns are solved by using mpMRI with or without contrast, although availability and costs may constrain the use. CEUS is the alternative test recommended by the consensus. However, this test is not available in all countries worldwide for renal tumor diagnostics or follow-up and expert interpretation is needed [25].

Data gathered by the consensus also clarifies the role of the biopsy during follow-up. Not mandatory to pronounce the diagnosis of "radiological recurrence", the panel considered that the majority of participants used biopsy as a tool to definitive diagnosis of residual/recurrent disease and when growing mass without evidence of enhancement. In view of the scarce publications on the subject, the panel recognized that there may be a poor correlation between radiographic imaging and histopathology of the biopsy post-RFA, but probably not for Cryoablation [3, 26]. The panel recommended unanimously biopsy during FU in case of radiological suspicion of recurrence. With the limitations of expert opinion level of evidence, this seems to be the general policy in those centers practicing FT. Lastly, participants and the panel recommended stopping follow-up only in those cases with initial biopsy showing angiomyolipoma. The panel, considering the online results, recommended follow-up in case of any other biopsy results at treatment. However, in view that 56 % of respondents would stop follow-up when initial diagnostic of oncocytoma, the panel acknowledged that future studies should address this specific point. In spite of some data reporting the high reliability of oncocytoma diagnosis, the current pathology guidelines advise the use of the term "oncocytic features" specifying the preference for oncocytoma or chromophobe RCC [27].

The key topic of "risk stratification" as a guide for follow-up schedules after FT in RMs was strongly supported (88 %) in the first round of the consensus. The concept was extended in successive rounds according to participants'

feedback. It was the unanimous opinion that both patient and tumor factors should guide the risk stratification. Specifically, tumor characteristics overpowered the reliability of the procedural ablation, and tumor stage and grade were the main drivers of a "risk stratification" adapted follow-up. These two factors are universally recognized in the follow-up of any RCC, and size and stage are the most important risk factors for recurrence after kidney FT [4, 5, 28, 29]. In FT, information on grade is depending exclusively on biopsy with the consequent limitations in terms of accuracy and diagnostic yield [30]. The panel emphasized the importance of the subject and the need to strive to define "risk profiles" in the FT subpopulation of clinical renal tumors, mainly cT1a in which the classical "risk stratification" factors may require refinements.

Limitations

In spite of its strength, the Delphi methodology is not exempt of limitations. A consensus has low level of evidence but reflects clinical practice in a topic where no RCT or well-conducted studies exist. In our specific topic, there is no literature comparing the efficacy of different follow-up schedules after FT. One should question whether such a study makes sense and will ever show a sound clinical or statistical result for an event (persistence or local recurrence) that presents scarcely in the follow-up [31].

Arguments may arise on the composition of the panel. Major difference from our expert panel when compared with previous ones on kidney FT is the high prevalence of urologists. Although there seems to be a trend from laparoscopic to percutaneous FT, it is still the responsibility and privilege of the urologist to follow up patients with localized kidney cancers after curative treatment. Thus, the panel composition and the strong recommendation on multimodal composition of the team performing the follow-up rather represent a strong than a weak point.

Lastly, the key topic "risk stratification" was explored based on participants' feedback. While recognizing the importance of patient factors as follow-up tailoring to our surprise, previous history of RCC was ranked as the least important by almost 2/3 of the participants. Age and comorbidity were not truly explored due to complexity of the subject and the length of the survey. The panel recognized the importance of patients' factors as determinants of a less stringent follow-up in clinical practice, but stressed the lack of a proper classification of such factors.

Conclusions

The present consensus document defines the concepts of residual (persistent) and recurrent disease after FT of a renal mass. It recommends minimum time intervals and type of imaging to be performed during the first 5 years of follow-up. Biopsy is recommended to confirm radiological recurrence, and an extended follow-up to 10 years is advisable due to the lack of long-term data. Imaging options in case of CKD $\geq$3 or because of radiation exposure concerns were discussed. "risk stratification" according to patient and tumor characteristics was strongly supported by participants and the panel with so far only tumor factors (stage and grade) defined as stratifying forces.

Acknowledgments P. G. K. Wagstaff received an unrestricted research Grant from the Cure for Cancer Foundation.

Authors' contribution P. J. Zondervan contributed to protocol/project development, data collection or management, and manuscript writing/editing. P. G. K. Wagstaff contributed to protocol/project development, data collection or management, and manuscript writing/editing. M. M. Desai contributed to data collection or management, and manuscript writing/editing. D. M. de Bruin contributed to data collection or management, and manuscript writing/editing. A. F. Fraga contributed to data collection or management, and manuscript writing/editing. B. A. Hadaschik contributed to data collection or management, and manuscript writing/editing. J. Köllermann contributed to data collection or management, and manuscript writing/editing. U. B. Liehr contributed to data collection or management, and manuscript writing/editing. S. A. Pahernik contributed to data collection or management, and manuscript writing/editing. H. P. Schlemmer contributed to data collection or management, and manuscript writing/editing. J. J. Wendler contributed to data collection or management, and manuscript writing/editing. F. Algaba contributed to data collection or management, and manuscript writing/editing. J. J. M. C. H. de la Rosette contributed to data collection or management, and manuscript writing/editing. M. P. Laguna Pes contributed to protocol/project development, data collection or management, and manuscript writing/editing.

Compliance with ethical standards

Conflict of interest All authors of this manuscript declare no conflict of interest.

Ethical standards All human studies have been approved by the appropriate ethics committee and have therefore been performed in accordance with the ethical standards laid down in the 1964 Declaration of Helsinki and its later amendments.

References

1. Van Poppel H, Becker F, Cadeddu JA, Gill IS, Janetschek G, Jewett MA, Laguna MP, Marberger M, Montorsi F, Polascik TJ, Ukimura O, Zhu G (2011) Treatment of localised renal cell carcinoma. Eur Urol 60:662–672

2. Ljungberg B, Bensalah K, Canfield S, Dabestani S, Hofmann F, Hora M, Kuczyk MA, Lam T, Marconi L, Merseburger AS, Mulders P, Powles T, Staehler M, Volpe A, Bex A (2015) EAU guidelines on renal cell carcinoma: 2014 update. Eur Urol 67:913–924
3. Aron M, Kamoi K, Remer E, Berger A, Desai M, Gill I (2010) Laparoscopic renal cryoablation: 8-year, single surgeon outcomes. J Urol 183:889–895
4. Best SL, Park SK, Yaacoub RF, Olweny EO, Tan YK, Trimmer C, Cadeddu JA (2012) Long-term outcomes of renal tumor radio frequency ablation stratified by tumor diameter: size matters. J Urol 187:1183–1189
5. Psutka SP, Feldman AS, McDougal WS, McGovern FJ, Mueller P, Gervais DA (2013) Long-term oncologic outcomes after radiofrequency ablation for T1 renal cell carcinoma. Eur Urol 63:486–492
6. Johnson S, Pham KN, See W, Begun FP, Langenstroer P (2014) Laparoscopic cryoablation for clinical stage T1 renal masses: long-term oncologic outcomes at the Medical College of Wisconsin. Urology 84:613–618
7. Tracy CR, Raman JD, Donnally C, Trimmer CK, Cadeddu JA (2010) Durable oncologic outcomes after radiofrequency ablation: experience from treating 243 small renal masses over 7.5 years. Cancer 116:3135–3142
8. Ramirez D, Ma YB, Bedir S, Antonelli JA, Cadeddu JA, Gahan JC (2014) Laparoscopic radiofrequency ablation of small renal tumors: long-term oncologic outcomes. J Endourol 28:330–334
9. Caputo PA, Ramirez D, Zargar H, Akca O, Andrade HS, O'Malley C, Remer EM, Kaouk JH (2015) Laparoscopic cryoablation for renal cell carcinoma: 100-month oncologic outcomes. J Urol 194:892–896
10. Thompson RH, Atwell T, Schmit G, Lohse CM, Kurup AN, Weisbrod A, Psutka SP, Stewart SB, Callstrom MR, Cheville JC, Boorjian SA, Leibovich BC (2015) Comparison of partial nephrectomy and percutaneous ablation for cT1 renal masses. Eur Urol 67:252–259
11. Novick AC, Campbell SC, Belldegrun A, Blute ML, Chow GK, Derweesh IH (2010) Guideline for management of the clinical stage 1 renal mass. Am Urol Assoc. https://www.auanet.org/education/guidelines/renal-mass.cfm. Accessed 17 Apr 2016

Ref Type: Online Source

12. Donat SM, Diaz M, Bishoff JT, Coleman JA, Dahm P, Derweesh IH, Herrell SD III, Hilton S, Jonasch E, Lin DW, Reuter VE, Chang SS (2013) Follow-up for clinically localized renal neoplasms: AUA guideline. J Urol 190:407–416
13. Ahmed M, Solbiati L, Brace CL, Breen DJ, Callstrom MR, Charboneau JW, Chen MH, Choi BI, de Baere T, Dodd GD, Dupuy DE, Gervais DA, Gianfelice D, Gillams AR, Lee FT, Leen E, Lencioni R, Littrup PJ, Livraghi T, Lu DS, McGahan JP, Meloni MF, Nikolic B, Pereira PL, Liang P, Rhim H, Rose SC, Salem R, Sofocleous CT, Solomon SB, Soulen MC, Tanaka M, Vogl TJ, Wood BJ, Goldberg SN (2014) Image-guided tumor ablation: standardization of terminology and reporting criteria-A 10-year update. Radiology 273:241–260
14. Goldberg SN, Grassi CJ, Cardella JF, Charboneau JW, Dodd GD, Dupuy DE, Gervais D, Gillams AR, Kane RA, Lee FT, Livraghi T, McGahan J, Phillips DA, Rhim H, Silverman SG (2005) Image-guided tumor ablation: standardization of terminology and reporting criteria. Radiology 235:728–739
15. Linstone HA, Turoff M (1975) The Delphi method: techniques and applications. Addison-Wesley, London
16. Goldberg SN, Charboneau JW, Dodd GD, Dupuy DE, Gervais DA, Gillams AR, Kane RA, Lee FT, Livraghi T, McGahan JP, Rhim H, Silverman SG, Solbiati L, Vogl TJ, Wood BJ (2003) Image-guided tumor ablation: proposal for standardization of terms and reporting criteria. Radiology 228:335–345
17. Iannuccilli JD, Grand DJ, Dupuy DE, Mayo-Smith WW (2014) Percutaneous ablation for small renal masses-imaging follow-up. Semin Interv Radiol 31:50–63
18. Williams PL, Webb C (1994) The Delphi technique—a methodological discussion. J Adv Nurs 19:180–186
19. Archer TM (2007) Characteristics associated with increasing the response rates of web-based surveys. Pract Assess Res Eval 12(12). Available online: http://pareonline.net/getvn.asp?v=12&n=12. Accessed 17 Apr 2016
20. Grava-Gubins I, Scott S (2008) Effects of various methodologic strategies survey response rates among Canadian physicians and physicians-in-training. Can Fam Phys 54:1424–1430
21. Beemster P, Phoa S, Wijkstra H, de la Rosette J, Laguna P (2008) Follow-up of renal masses after cryosurgery using computed tomography; enhancement patterns and cryolesion size. BJU Int 101:1237–1242
22. Lagerveld BW, van Horssen P, Laguna MP, van den Wijngaard JPHM, Siebes M, Wijkstra H, de la Rosette JJMC, Spaan JAE (2011) Gradient changes in porcine renal arterial vascular anatomy and blood flow after cryoablation. J Urol 186:681–686
23. Kiechle JE, Abouassaly R, Smaldone MC, Shah ND, Dong S, Cherullo EE, Nakamoto D, Zhu H, Cooney MM, Kim SP (2015) National trends of local ablative therapy among young patients with small renal masses in the United States. Urology 86:962–967
24. Eisenberg JD, Gervais DA, Singh S, Kalra MK, Sabir SH, Paul AB, Pandharipande PV (2015) Radiation exposure from CT-guided ablation of renal masses: effects on life expectancy. AJR Am J Roentgenol 204:335–342
25. Barwari K, Wijkstra H, van Delden OM, de la Rosette JJ, Laguna MP (2013) Contrast-enhanced ultrasound for the evaluation of the cryolesion after laparoscopic renal cryoablation: an initial report. J Endourol 27:402–407
26. Weight CJ, Kaouk JH, Hegarty NJ, Remer EM, O'Malley CM, Lane BR, Gill IS, Novick AC (2008) Correlation of radiographic imaging and histopathology following cryoablation and radiofrequency ablation for renal masses. J Urol 179:1277–1283
27. Brimo F, Epstein JI (2012) Selected common diagnostic problems in urologic pathology: perspectives from a large consult service in genitourinary pathology. Arch Pathol Lab Med 136:360–371
28. Wah TM, Irving HC, Gregory W, Cartledge J, Joyce AD, Selby PJ (2014) Radiofrequency ablation (RFA) of renal cell carcinoma (RCC): experience in 200 tumours. BJU Int 113:416–428
29. Kim EH, Tanagho YS, Bhayani SB, Saad NE, Benway BM, Figenshau RS (2013) Percutaneous cryoablation of renal masses: Washington University experience of treating 129 tumours. BJU Int 111:872–879
30. Richard PO, Jewett MA, Bhatt JR, Kachura JR, Evans AJ, Zlotta AR, Hermanns T, Juvet T, Finelli A (2015) Renal tumor biopsy for small renal masses: a single-center 13-year experience. Eur Urol 68:1007–1013
31. Zargar H, Atwell TD, Cadeddu JA, de la Rosette JJ, Janetschek G, Kaouk JH, Matin SF, Polascik TJ, Zargar-Shoshtari K, Thompson RH (2016) Cryoablation for small renal masses: selection criteria, complications, and functional and oncologic results. Eur Urol 69:116–128

8.15

Initial assessment of clinical feasibility, safety and efficacy of NanoKnife irreversible electroporation (IRE) in the focal treatment of localized renal cell carcinoma (RCC) with delayed interval tumor resection (IRENE trial).

Wendler JJ, Ricke J, Pech M, Fischbach F, Jürgens J, Porsch M, Janitzky A, Baumunk D, Siedentopf S, Köllermann J, Schostak M, Liehr UB.

Eur Urol Suppl 2017; 16(3);e102.

INTRODUCTION & OBJECTIVES: To evaluate the feasibility, adverse event profile, functional outcome and efficacy of focal irreversible electroporation (IRE) for pT1a renal cell carcinoma (RCC) in consecutive patients of the first prospective, monocentric Phase 2a pilot ablate-and-resect study (IRENE trial). For this new technology a complete ablation of soft-tissue tumors with protection of healthy peritumoral tissue and anatomical structures has been postulated.

MATERIAL & METHODS: Approval for this GCP-compliant study [NCT01967407 (10/2013)] was granted by the German Federal Institute for Drugs and Medical Devices BfArM (CIV-12-4 006021) and authorized ethics [73/2012]. 7 patients (mean age 68 y; ECOG 0-2; Charlson Score 0-2) with biopsy proven RCC pT1a cN0cM0 (5/7 clear-cell, 2/7 papillary; located cortically 5/7 and centrally 2/7) with a mean tumor size of 22 mm (range 15-39) underwent percutaneous CT-guided (Aquillion prime CT scanner, Toshiba, USA) IRE (NanoKnife system, AngioDynamics, USA). IRE was performed ECGtriggered in general anaesthesia and deep muscle paralysis with 3-6 monopolar electrodes positioned within the renal tumor (90 µs pulse length; 2-4 ablations per tumor in 1 session). At 28 days after IRE the tumor region was completely resected surgically. A contrast-enhanced, diffusion-weighted MRI was carried out 1 day before as well as 2, 7, 27 and 112 days after IRE. Clinical parameter, quality of life, pain feeling and complications were recorded 1 day before as well as 1, 2, 7, 27, 29, 30, 35 and 112 days after IRE. Restaging CT was ensued 6 and 12 month after IRE, then annually.

RESULTS: Technical feasibility was achieved in all patients, but electrode placement and ablation was complex with mean overall procedure time of 129 min and anaesthesia time of 165 min. There were no major or residual procedure-related complications. Minor complications occurred including slight selflimiting macrohematuria (7/7), perirenal hematomas (2/7) and drug-treated temporary post-puncture pain (7/7). In all cases MR imaging demonstrated a complete coverage of the tumor areal by the ablation zone, nearly size persistent tumor areas with contrast enhancement but degenerative change of hypoperfusion and diffusion restriction. Intrasurgically examinations showed severe local perirenal adhesions. Renal function after IRE was retained in all cases with no urinary leakage or retention, no renal infarction and no significant change of creatinine. Partial kidney resection was performed in 5 of 7 patients and radical nephrectomy in 2 of 7 due to central tumor ablation areas. Resection exhibited in 4/7 cases ypT0V0N0Pn0R0; and 3/7 cases with ypT1aV0N0Pn0R1 due to small residual tumor areas with viable tumor cells in 2 cases and uncertain viable tumor cells in 1 case. Mean follow-up of 25 month had no evidence of local recurrence or metastasis.

CONCLUSIONS: Renal percutaneous NanoKnife IRE appears to be a safe treatment for small renal tumors but needs a high procedural effort. According to these initial study results the curative intended, renal saving focal ablation of T1a RCC appears to be possible, but needs further technical improvement and evaluation for a certain complete ablation by this still experimental method.

62

Initial assessment of clinical feasibility, safety and efficacy of NanoKnife irreversible electroporation (IRE) in the focal treatment of localized renal cell carcinoma (RCC) with delayed interval tumor resection (IRENE trial)

Eur Urol Suppl 2017; 16(3);e102

Wendler J.J.[1], Ricke J.[2], Pech M.[2], Fischbach F.[2], Jürgens J.[2], Porsch M.[1], Janitzky A.[3], Baumunk D.[3], Siedentopf S.[4], Köllermann J.[5], Schostak M.[3], Liehr U-B.[3]

[1]University Magdeburg, Dept. of Urology, Magdeburg, Germany, [2]University Magdeburg, Dept. of Radiology, Magdeburg, Germany, [3]University Magdeburg, Dept. of Urolgy, Magdeburg, Germany, [4] University Magdeburg, Dept. of Pathology, Magdeburg, Germany, [5]Sana Medical Center, Dept. of Pathology, Offenbach, Germany

INTRODUCTION & OBJECTIVES: To evaluate the feasibility, adverse event profile, functional outcome and efficacy of focal irreversible electroporation (IRE) for pT1a renal cell carcinoma (RCC) in consecutive patients of the first prospective, monocentric Phase 2a pilot ablate-and-resect study (IRENE trial). For this new technology a complete ablation of soft-tissue tumors with protection of healthy peritumoral tissue and anatomical structures has been postulated.

MATERIAL & METHODS: Approval for this GCP-compliant study [NCT01967407 (10/2013)] was granted by the German Federal Institute for Drugs and Medical Devices BfArM (CIV-12-4-006021) and authorized ethics [73/2012]. 7 patients (mean age 68 y; ECOG 0-2; Charlson Score 0-2) with biopsy proven RCC pT1a cN0cM0 (5/7 clear-cell, 2/7 papillary; located cortically 5/7 and centrally 2/7) with a mean tumor size of 22 mm (range 15-39) underwent percutaneous CT-guided (Aquillion prime CT scanner, Toshiba, USA) IRE (NanoKnife system, AngioDynamics, USA). IRE was performed ECG-triggered in general anaesthesia and deep muscle paralysis with 3-6 monopolar electrodes positioned within the renal tumor (90 µs pulse length; 2-4 ablations per tumor in 1 session). At 28 days after IRE the tumor region was completely resected surgically. A contrast-enhanced, diffusion-weighted MRI was carried out 1 day before as well as 2, 7, 27 and 112 days after IRE. Clinical parameter, quality of life, pain feeling and complications were recorded 1 day before as well as 1, 2, 7, 27, 29, 30, 35 and 112 days after IRE. Restaging CT was ensued 6 and 12 month after IRE, then annually.

RESULTS: Technical feasibility was achieved in all patients, but electrode placement and ablation was complex with mean overall procedure time of 129 min and anaesthesia time of 165 min. There were no major or residual procedure-related complications. Minor complications occurred including slight self-limiting macrohematuria (7/7), perirenal hematomas (2/7) and drug-treated temporary post-puncture pain (7/7). In all cases MR imaging demonstrated a complete coverage of the tumor areal by the ablation zone, nearly size persistent tumor areas with contrast enhancement but degenerative change of hypoperfusion and diffusion restriction. Intrasurgically examinations showed severe local perirenal adhesions. Renal function after IRE was retained in all cases with no urinary leakage or retention, no renal infarction and no significant change of creatinine. Partial kidney resection was performed in 5 of 7 patients and radical nephrectomy in 2 of 7 due to central tumor ablation areas. Resection exhibited in 4/7 cases ypT0V0N0Pn0R0; and 3/7 cases with ypT1aV0N0Pn0R1 due to small residual tumor areas

62

Initial assessment of clinical feasibility, safety and efficacy of NanoKnife irreversible electroporation (IRE) in the focal treatment of localized renal cell carcinoma (RCC) with delayed interval tumor resection (IRENE trial)

Eur Urol Suppl 2017; 16(3);e103

with viable tumor cells in 2 cases and uncertain viable tumor cells in 1 case. Mean follow-up of 25 month had no evidence of local recurrence or metastasis.

CONCLUSIONS: Renal percutaneous NanoKnife IRE appears to be a safe treatment for small renal tumors but needs a high procedural effort. According to these initial study results the curative intended, renal saving focal ablation of T1a RCC appears to be possible, but needs further technical improvement and evaluation for a certain complete ablation by this still experimental method.

Patient Data	P1	P2	P3	P4	P5	P6	P7
Age / Sex	44 / M	78 / M	74 / M	73 / M	74 / M	71 / F	61 / M
ECOG / Karnofsky / Charlson Score	0 / 100 / 0	0 / 90 / 2	0 / 100 / 0	0 / 100 / 1	1 / 80 / 1	0 / 100 / 0	0 / 100 / 0
Tumor Data							
No. Targets, index tumor	1	1	1	1	2	1	1
Tumor location	UP, right, cortical, exophytic, ventrolateral	UP/MP, right, cortical, exophytic, dorsomedial	UP/MP, right, cortical, exophytic, dorsomedial, hilum	UP, right, cortical, exophytic, lateral	LP/MP, right, cortical, exophytic, lateral, medio-central satellite	UP/MP, right, cortical, exophytic, ventrolateral	LP, left, cortical, exophytic, dorsomedial
MR imaging pre-IRE (1 day before, selected sequences)	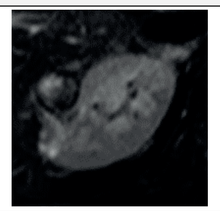	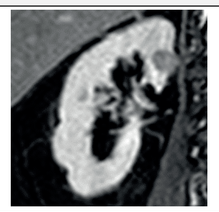	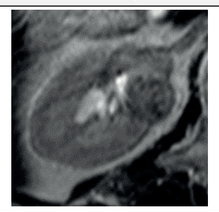	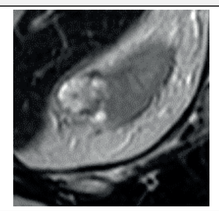	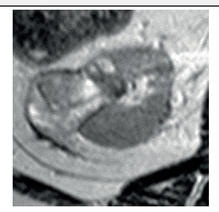	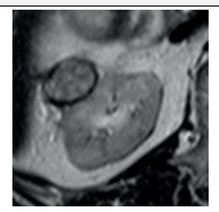	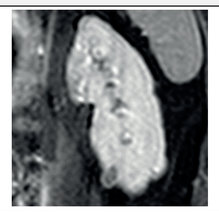
PADUA-Score	6	8	11	6	8	6	7
Tumor/ target size (cm)	1.7 x 1.7 x 1.6	1.5 x 1.5 x 1.4	1.6 x 1.5 x 1.5	2.2 x 2.1 x 1.9	3.9 x 3.8 x 3.1 and 1.8 x 1.5 x 1.7	2.4 x 2.4 x 2.0	1.4 x 1.1 x 1.8
Tumor volume (ccm)	2.4	1.6	1.9	4.6	24.1 + 2.8 = 26.9	6.0	1.5
Tumor shape and class	spherical, small	spherical, small	Spherical, small	spherical, small	elliptical-spherical, small	spherical, small	spherical, small
Biopsy	Pap RCC Typ 1, G2	Eosinophils cc RCC, G1	cc RCC, G1	cc RCC, G1	cc RCC, G1	cc RCC, G2	pap RCC, G2
Tumor texture	Inhomog., solid	Inhomog., solid	Inhomog., solid	Inhomog., cystic-solid	Inhomog., solid	Inhomog., solid	Inhomog., solid
TNM	pT1a G2 (C3) cN0 cM0 (C2) stage I	pT1a G1 (C3) cN0 cM0 (C2) stage I	pT1a G1 (C3) cN0 cM0 (C2) stage I	pT1a G1 (C3), cN0 cM0 (C2) stage I	pT1a G1 (C3), cN0 cM0 (C2) stage I	pT1a G2 (C3), cN0 cM0 (C2) stage I	pT1a G2 (C3), cN0 cM0 (C2) stage I
IRE Data							
Procedures/sessions; total ablations	1; 1	1; 1	1; 1	1; 1	1; 2	1; 1	1; 1
Rounds total	4 (plus 1 test run)	2 (plus 1 test run)	3 (plus 1 test run)	3 (plus 2 test runs)	2 + 2 (plus 1 test run each)	2 (plus 1 test run)	2 (plus 1 test run)
No. of electrodes / electrode pairs / configuration	4 / 6 / square	3 / 3 / triangular	4 / 6 / square	4 / 6 / square	3 / 3 / triangular and 6 / 10 / pentagonal with center	3 / 3 / triangular	3 / 3 / triangular
IRE electrode placement (3D CT simulation)	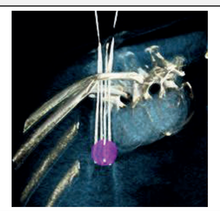	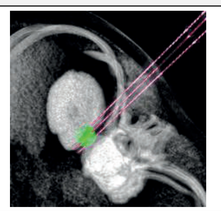	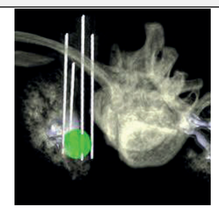	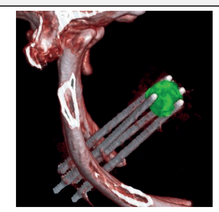	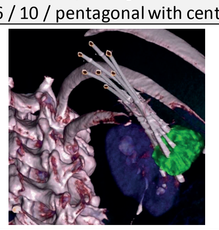	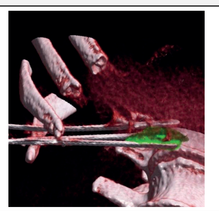	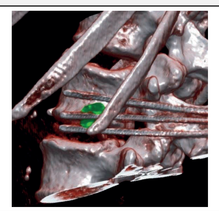
Electrode tip exposure (cm)	2.5	1.5	2.0	2.0	2.0 and 2.5 (pull-back)	2.5	2.0
Planned Treatment zone (cm) / (ccm)	2.4 x 2.9 x 3.5 / 12.7	2.5 x 2.5 x 2.5 / 8.2	3.5 x 4.0 x 3.0 / 22.0	3.0 x 3.0 x 2.9 / 13.7	2.7 x 2.7 x 2.7 / 10.3 and 4.4 x 4.4 x 4.5 / 45.6	3.0 x 3.3 x 3.0 / 15.6	2.4 x 2.9 x 2.8 / 10.2
Urine collecting system involvement	yes	yes	yes	yes	yes	yes	yes
Pulse length (µs)	90	90	90	90	70, 80 and 90	90	70 and 90
No. of pulses total	1300	450	1320	840	570 + 880	450	510
Current min./ max. (A)	30 / 49	30 / 42	30 / 49	25 / 49	22 / 50	28 / 50	20/ 35
Voltage min./max. (V)	1800 / 2800	2200 / 2640	1960 / 3000	2160 / 3000	1800 / 2800	1850 / 2600	1820 / 2660
Intervention time (min) / Anesthesia time (min)	131 / 193	126 / 162	163 / 208	123 / 194	203 / 317	53 / 91	104 / 181
MR imaging pre-surgical (27 days after IRE, selected sequences)	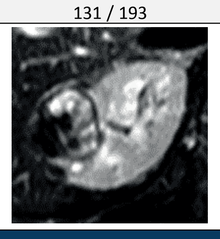	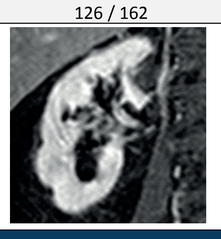	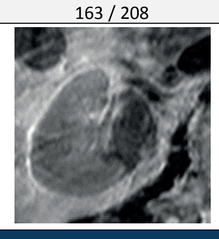	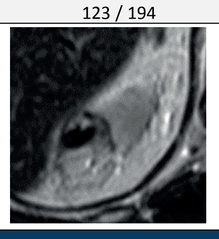	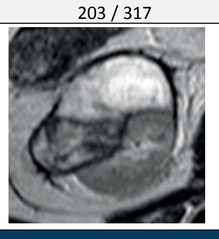	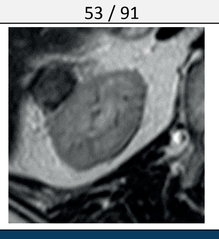	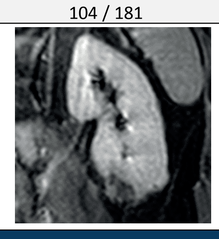
Surgery Data							
Pres-surgical kidney preservation	Yes	yes	yes	yes	yes	yes	yes
Initial / pre-surgical serum creatinine	73 / 96	69/ 88	92 / 73	96 / 63	84 / 72	101 / 47	95 / 80
Resection type; access	Partial resection; open lumbar	Partial resection; open lumbar	Radical nephrectomy; open lumbar	Partial resection; open abdominal	Radical nephrectomy; open lumbar	Partial resection; open abdominal	Partial resection; open lumbar
Specimen macroscopy (28 days after IRE; selected slices)	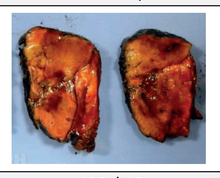	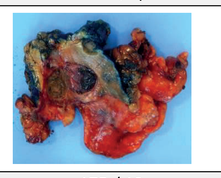	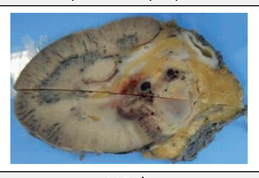	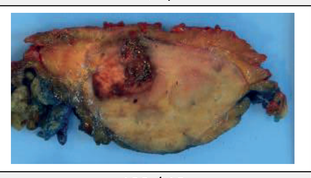	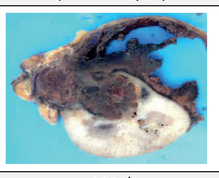	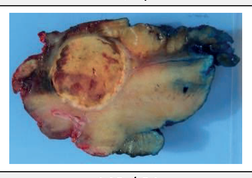	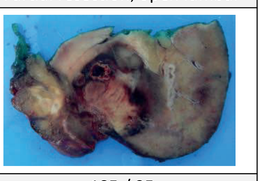
Operating time (min) / ischemia time (min)	185 / 16	175 / 19	115 / -	190 / 18	130 / -	140 / 21	185 / 35
Resection Pathology Data							
Specimen mapping (selected slices) black line = resection border beige area = kidney purple line = ablation zone blue hatched area = destructed tumor blue filled area = residual tumor	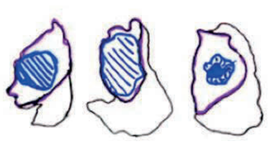	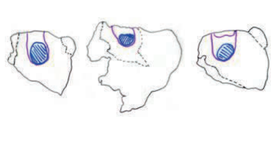	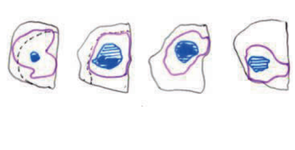	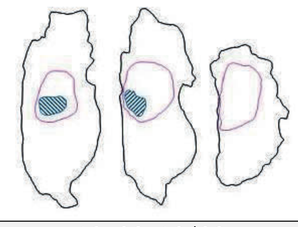	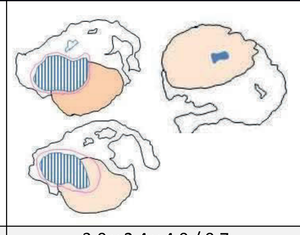	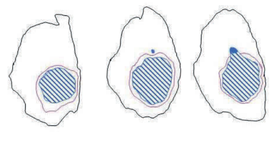	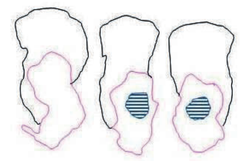
Tumor size (cm) / (ccm)	1.6 x 1.5 x 1.2 / 1.6	1.6 x 1.7 x 1.1 / 1.6	1.5 x 1.4 x 1.2 / 1.3	1.2 x 0.8 x 1.0 / 0.2	3.0 x 2.4 x 4.0 / 9.7	3.0 x 2.2 x 2.0 / 2.0	1.3 x 1.2 x 1.0 / 0.2
Ablation zone size (cm) / (ccm)	2.5 x 2.0 x 1.3 / 3.4	3.0 x 2.5 x 2.0 / 7.9	4.2 x 1.4 x 1.2 / 17.2	2.8 x 2.2 x 2.0 / 3.5	4.2 x 2.8 x 3.5 / 19.2	2.9 x 2.5 x 3.5 / 4.5	4.6 x 2.2 x 3.0 / 8.4
Residual tumor zones / skip lesions	1 / 1	1 / 1	1 / 1	0 / 0	1 / 0	1 / 0	0 / 0
Residual tumor infield or margin / outfield (ccm)	0.28 / 0	0.045 / 0	1.185 / 0	0 / 0	0 / 0.009	0.03 / 0.009	0 / 0
Residual tumor of pretreatment tumor size (%)	12	2.8	62.4	0	0.03	0.15	0
Residual tumor of posttreatment tumor size (%)	18.7	2.8	91.2	0	0.1	0.45	0
Mib-1 labelling index (%)[d]	0	0	0	-	1	1	-
Assessment of viability	uncertain	non-viable	non-viable	non-viable	viable	viable	non-viable
Specimen histology (selected sections)	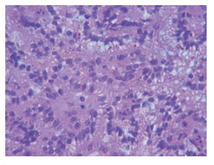 Preserved tumor region showing papillary RCC architecture and minor signs of cytologic damage (HE).	 Tumor necrosis with rudimantory tumor architecture and severe signs of cytological damage (HE).	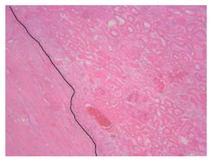 Ablated tumor area with complete coagulation necrosis on (left) and sharp border to parenchyma (HE).	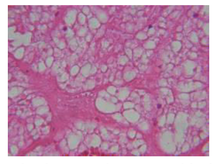 Completely necrotic tumor with shadowy cell contours (HE).	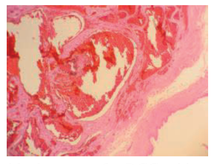 Residual tumor of ccRCC with cystic degeneration and fresh bleeding adjacent to urinary collecting system (HE).	Viable residual tumor of ccRCC with proliferating colored nuclei (Mib-1).	Completely necrotic tumor with shadowy cell contours (HE).
Q volume ablation zone tumor / total (%)	+26.8	+96.3	+79.2	+94.6	+50.5	+55.4	+93.2
Tumor ablation degree (incomplete / complete)	uncertain	complete	complete	complete	incomplete	incomplete	complete
ypTNM	ypT0-1a V0 L0 Pn0 R1 (C4)	ypT0 V0 L0 Pn0 R0 (C4)	ypT0 V0 L0 Pn0 R0 (C4)	ypT0 V0 L0 Pn0 R0 (C4)	ypT1a V0 L0 Pn0 R1 (C4)	ypT1a V0 L0 Pn0 R1 (C4)	ypT0 V0 L0 Pn0 R0 (C4)

8.16

Upper-Urinary-Tract Effects After Irreversible Electroporation (IRE) of Human Localised Renal-Cell Carcinoma (RCC) in the IRENE Pilot Phase 2a Ablate-and-Resect Study.

Wendler JJ, Pech M, Köllermann J, Friebe B, Siedentopf S, Blaschke S, Schindele D, Porsch M, Baumunk D, Jürgens J, Fischbach F, Ricke J, Schostak M, Böhm M, Liehr UB.

Cardiovasc Intervent Radiol. 2018 Mar;41(3):466-476.

PURPOSE: Irreversible electroporation (IRE) is a new potential ablation modality for small renal masses. Animal experiments have shown preservation of the urine-collecting system (UCS). The purpose of this clinical study was to perform the first evaluation and comparison of IRE's effects on the renal UCS by using urinary cytology, magnetic-resonance imaging, and resection histology in men after IRE of pT1a renal-cell carcinoma (RCC).

METHODS: Seven patients with biopsy-proven RCC pT1a cN0cM0 underwent IRE in a phase 2a pilot ablate-and-resect study (IRENE trial). A contrast-enhanced, diffusion-weighted MRI and urinary cytology was performed 1 day before and 2, 7, and 27 days after IRE. Twenty-eight days after IRE the tumour region was completely resected surgically.

RESULTS: Technical feasibility was demonstrated in all patients. In all cases, MRI revealed complete coverage of the tumour area by the ablation zone with degenerative change. The urographic late venous MRI phase (urogram scans) demonstrated normal morphological appearances. Urine cytology showed a temporary vacuolisation of the cyto- and caryoplasmas after IRE. Whereas the urothelium showed signs of regeneration 28 days after IRE-ablation, the tumour and parenchyma below it showed necrosis and permanent tissue destruction.

CONCLUSIONS: Renal percutaneous IRE appears to be a safe treatment for pT1a RCC. The preservation of the UCS with unaltered normal morphology as well as urothelial regeneration and a phenomenon (new in urinary cytology) of temporary degeneration with vacuolisation of detached transitional epithelium cells were demonstrated in this clinical pilot study.

Cardiovasc Intervent Radiol (2018) 41:466–476
DOI 10.1007/s00270-017-1795-x

Upper-Urinary-Tract Effects After Irreversible Electroporation (IRE) of Human Localised Renal-Cell Carcinoma (RCC) in the IRENE Pilot Phase 2a Ablate-and-Resect Study

J. J. Wendler[1] M. Pech[2] J. Köllermann[4] B. Friebe[2] S. Siedentopf[3] S. Blaschke[1] D. Schindele[1] M. Porsch[5] D. Baumunk[6] J. Jürgens[2] F. Fischbach[2] J. Ricke[7] M. Schostak[1] M. Böhm[8] U. B. Liehr[1]

Received: 11 July 2017 / Accepted: 5 September 2017 / Published online: 19 September 2017

Abstract

Purpose Irreversible electroporation (IRE) is a new potential ablation modality for small renal masses. Animal experiments have shown preservation of the urine-collecting system (UCS). The purpose of this clinical study was to perform the first evaluation and comparison of IRE's effects on the renal UCS by using urinary cytology, magnetic-resonance imaging, and resection histology in men after IRE of pT1a renal-cell carcinoma (RCC).

Methods Seven patients with biopsy-proven RCC pT1a cN0cM0 underwent IRE in a phase 2a pilot ablate-and-resect study (IRENE trial). A contrast-enhanced, diffusion-weighted MRI and urinary cytology was performed 1 day before and 2, 7, and 27 days after IRE. Twenty-eight days after IRE the tumour region was completely resected surgically.

Results Technical feasibility was demonstrated in all patients. In all cases, MRI revealed complete coverage of the tumour area by the ablation zone with degenerative change. The urographic late venous MRI phase (urogram scans) demonstrated normal morphological appearances. Urine cytology showed a temporary vacuolisation of the cyto- and caryoplasmas after IRE. Whereas the urothelium showed signs of regeneration 28 days after IRE-ablation, the tumour and parenchyma below it showed necrosis and permanent tissue destruction.

Conclusions Renal percutaneous IRE appears to be a safe treatment for pT1a RCC. The preservation of the UCS with unaltered normal morphology as well as urothelial regeneration and a phenomenon (new in urinary cytology) of temporary degeneration with vacuolisation of detached transitional epithelium cells were demonstrated in this clinical pilot study.

Keywords Irreversible electroporation · Renal-cell carcinoma · Small renal masses · Kidney tumour · Focal therapy · Ablation · Urinary cytology · Upper urinary tract · IRENE study

M. Böhm and U. B. Liehr have contributed equally to this work.

M. Böhm: Working group urine cytology and urine-based markers of the German Society of Urology (DGU).

Study group IRENE trial featured by AKFM-DGU (J. J. Wendler, J. Köllermann, D. Schindele, D. Baumunk, M. Schostak, U. B. Liehr) and DAfMT (J. J. Wendler, M. Pech, B. Friebe, J. Jürgens, F. Fischbach, J. Ricke, U. B. Liehr), Germany.

✉ J. J. Wendler
johann.wendler@med.ovgu.de

1 Department of Urology, Otto von Guericke University of Magdeburg, Leipziger Str. 44, 39120 Magdeburg, Germany

2 Department of Radiology, Otto von Guericke University of Magdeburg, Magdeburg, Germany

3 Department of Pathology, Otto von Guericke University of Magdeburg, Magdeburg, Germany

4 Department of Pathology, Sana Medical Center Offenbach, Offenbach, Germany

5 Urological Practice, Magdeburg, Germany

6 Urological Practice, Stuttgart, Germany

7 Department of Radiology, Ludwig Maximilians University of Munich, Munich, Germany

8 Urological Practice, Dill-Clinics, Dillenburg, Germany

Introduction

For the treatment of renal cell carcinoma (RCC), focal therapy (FT), with the goal of minimising damage to the surroundings while still achieving total destruction of the

tumour tissue, is receiving increasing attention [1, 2, 16, 21]. For irreversible electroporation (IRE), it has been postulated that complete ablation of soft-tissue tumours with protection of the healthy peritumoral tissue is possible [3–6, 20, 21]. Therefore, IRE represents an interesting potential option for nephron- and urinary-tract-sparing treatment of renal (centrally located) tumours [7–11]. Animal studies in healthy swine have shown preservation of the urine-collecting system (UCS) with unaltered normal morphology as well as urothelial regeneration and a phenomenon, new in urinary cytology, of temporary degeneration with vacuolisation of detached transitional epithelial cells [5, 6, 20, 21].

First transureteral endoluminal catheter-directed IRE showed full-thickness IRE ablation of the normal ureteral wall with no leakage and full recovery of the urethelium but caused ureter stricture with consecutive proximal urinary retention in all cases [24, 25]. However, there is still a lack of clinical data regarding the application of IRE in RCC [7–11], and most studies have been based on computed tomography (CT) or magnetic resonance (MR) or postbiopsy assessment only [10, 11]. The purpose of this clinical study was to perform first evaluation and comparison of IRE's effects on the renal urine collecting system (UCS) and upper urinary tract (UUT) by using urinary cytology, magnetic-resonance imaging, and resection histology in men after IRE of pT1a renal-cell carcinoma (RCC). The detailed histological and MRI morphological analysis of the tumour region and renal parenchyma will be published separately.

Materials and Methods

Study Design, Approval and Recruitment

This pilot study was planned to achieve histological, cytological, and imaging data of percutaneous CT-guided IRE treated localized RCC followed by delayed ablation zone resection 4 weeks after IRE. The patients received no neoadjuvant, concomitant, or adjuvant targeted therapy. The protocol of this GCP-compliant, prospective, monocentric, nonrandomised, uncontrolled, nonblinded, single-arm, Phase 2a, single-centre, interventional pilot study ("IRENE"—IRreversible Electroporation of kidney tumours before partial NephrEctomy; ClinicalTrials.gov NCT01967407 (10/2013), WHO ICTRP DRKS00004266) has been published separately [12]. Approval according to German medical product law (MPG) was granted by the German Federal Institute for Drugs and Medical Devices (BfArM) [CIV-12-4-006021] and the Ethics Committee of Magdeburg University [73/2012].

Patients

Seven patients (P1–P7) with biopsy-proven localized, nonmetastatic, untreated RCC pT1a cN0cM0 were recruited (5 clear-cell RCC, 2 papillary RCC) [22, 23]. One patient (P5) had two adjacent tumours. Overall, eight tumours with a mean tumour size of 22 mm (range 15–39 mm) and PADUA score 6–11 were treated. Two patients had a centrally located RCC adjacent to the hilum or renal pelvis (P3 and P5). Five patients had a cortically located RCC with adjacency to a renal calyx and therefore to the renal pelvis-calyceal (urine collecting) system as well (Table 1).

IRE Treatment

For IRE Treatment, we used the NanoKnife™ IRE electroporator (AngioDynamics Inc., Latham, NY; firmware V3.29, software V2.2.0.23) and NanoKnife™ monopolar probes (15 cm, 19G). The electrodes were positioned under CT guidance (Aquillion™ prime CT scanner, Toshiba Inc., Tustin, CA, USA) and on the basis of individual treatment-planning data (ProcedureManager-2_2_0_23 for Windows™, AngioDynamics) [19]. The IRE electrodes should be placed CT guided at the tumour rim approximately. The simulated tumour contour should be covered completely by the IRE ablation zone, mostly calculated with a safety margin of 5 mm in all dimensions. The IRE electrode positions and tip exposure as well as the planned IRE treatment zone and IRE ablation parameters are shown in Table 1. This was performed with ECG triggering under general anaesthesia and deep muscle paralysis with 3–6 monopolar electrodes positioned within the renal tumour. Intraprocedural modification was performed after immediate evaluation of post-IRE ablation graphs by interelectrode voltage modulation, separate electrode-pair ablation, and IRE electrode placement [13, 19]. For complete ablation, we performed more than one round per ablation for each electrode pair.

Imaging

Metastatic disease was excluded by contrast-enhanced, thoracic CT, and abdominopelvic CT or MRI. The image-morphological assessment of the kidneys was performed by contrast-enhanced, diffusion-weighted MRI (1.5T scanner, gadobutrol: 0.1 ml/kg Gadovist 1.0 mmol/ml; Bayer, Leverkusen, Germany) on planned study days, one day before IRE and 1–2, 7, and 27 days after IRE. Contrast-enhanced sequences arterial, portal-venous, venous, and urographic (late venous phase) were performed (T1w-2D-GRE (Scout), T2w-SShTSE, T2w-FS-TSE, T2w-RT-TSE,

Table 1 Tumour data, treatment parameters and histological results

	Patient P1	Patient P2	Patient P3	Patient P4	Patient P5	Patient P6	Patient P7
Tumour data							
No. targets, index tumour	1	1	1	1	2	1	1
Tumour location	UP, right, cortical, exophytic, ventrolateral	UP/MP, right, cortical, exophytic, dorsomedial	UP/MP, right, cortical, exophytic, dorsomedial, hilum	UP, right, cortical, exophytic, lateral	LP/MP, right, cortical, exophytic, lateral, medio-central satellite	UP/MP, right, cortical, exophytic, ventrolateral	LP, left, cortical, exophytic, dorsomedial
PADUA score	6	8	11	6	8	6	7
Tumour/target size (cm)	1.7 × 1.7 × 1.6	1.5 × 1.5 × 1.4	1.6 × 1.5 × 1.5	2.2 × 2.1 × 1.9	3.9 × 3.8 × 3.1 and 1.8 × 1.5 × 1.7	2.4 × 2.4 × 2.0	1.4 × 1.1 × 1.8
Tumour volume (cm^3)	2.4	1.6	1.9	4.6	24.1 2.8 = 26.9	6.0	1.5
Biopsy	Pap RCC Typ 1, G2	Eosinophils cc RCC, G1	cc RCC, G1	cc RCC, G1	cc RCC, G1	cc RCC, G2	pap RCC, G2
TNM [22, 23]	pT1a G2 (C3), cN0 cM0 (C2) Stage I	pT1a G1 (C3), cN0 cM0 (C2) Stage I	pT1a G1 (C3), cN0 cM0 (C2) Stage I	pT1a G1 (C3), cN0 cM0 (C2) Stage I	pT1a G1 (C3), cN0 cM0 (C2) Stage I	pT1a G2 (C3), cN0 cM0 (C2) Stage I	pT1a G2 (C3), cN0 cM0 (C2) Stage I
IRE data							
Procedures/sessions; total ablations	1; 1	1; 1	1; 1	1; 1	1; 2	1; 1	1; 1
Rounds total	4 (plus 1 test run)	2 (plus 1 test run)	3 (plus 1 test run)	3 (plus 2 test runs)	2 2 (plus 1 test run each)	2 (plus 1 test run)	2 (plus 1 test run)
No. of electrodes/electrode pairs/configuration	4/6/square	3/3/triangular	4/6/square	4/6/square	3/3/triangular and 6/10/ pentagonal with centre	3/3/triangular	3/3/triangular
Electrode tip exposure (cm)	2.5	1.5	2.0	2.0	2.0 and 2.5 (pull–back)	2.5	2.0
Planned treatment zone (cm)/(cm^3)	2.4 × 2.9 × 3.5/ 12.7	2.5 × 2.5 × 2.5/8.2	3.5 × 4.0 × 3.0/22.0	3.0 × 3.0 × 2.9/ 13.7	2.7 × 2.7 × 2.7/10.3 and 4.4 × 4.4 × 4.5/45.6	3.0 × 3.3 × 3.0/15.6	2.4 × 2.9 × 2.8/ 10.2
Pulse length (μs)	90	90	90	90	70, 80 and 90	90	70 and 90
No. of pulses total	1300	450	1320	840	570 880	450	510
Current min./max. (A)	30/49	30/42	30/49	25/49	22/50	28/50	20/35
Voltage min./max. (V)	1800/2800	2200/2640	1960/3000	2160/3000	1800/2800	1850/2600	1820/2660

Table 1 continued

	Patient P1	Patient P2	Patient P3	Patient P4	Patient P5	Patient P6	Patient P7
Surgery data							
Initial/pre-surgical serum creatinine (umol/l)	73/75	69/66	92/89	96/101	84/90	101/102	87/89
Initial/pre-surgical eGFR (ml/min)	107/106	86/88	70/73	67/63	78/72	48/47	82/80
Resection type; access	Partial resection; open lumbar	Partial resection; open lumbar	Radical nephrectomy; open lumbar	Partial resection; open abdominal	Radical nephrectomy; open lumbar	Partial resection; open abdominal	Partial resection; open lumbar
Pathology data							
Ablation zone (cm)/(cm^3)	2.5 × 2.0 × 1.3/3.4	3.0 × 2.5 × 2.0/7.9	4.2 × 1.4 × 1.2/17.2	2.8 × 2.2 × 2.0/3.5	4.2 × 2.8 × 3.5/19.2	2.9 × 2.5 × 3.5/4.5	4.6 × 2.2 × 3.0/8.4
Tumour shape (cm)/(cm^3)	1.6 × 1.5 × 1.2/1.6	1.6 × 1.7 × 1.1/1.6	1.5 × 1.4 × 1.2/1.3	1.2 × 0.8 × 1.0/0.2	3.0 × 2.4 × 4.0/9.7	3.0 × 2.2 × 2.0/2.0	1.3 × 1.2 × 1.0/0.2
Coverage of tumour shape by ablation zone	Complete	Complete	Complete	Complete	Incomplete	Incomplete	Complete
Residual tumour (cm^3); location	0.28; in-field	0.045; in-field	1.185; in-field	None	0.009; out-field/margin	0.03; out-field/margin	None
ypTNM classification (IRE, tumour) [22, 23]	ypT0-1a V0 L0 Pn0 R0-1 (C4)	ypT0 V0 L0 Pn0 R0 (C4)	ypT0 V0 L0 Pn0 R0 (C4)	ypT0 V0 L0 Pn0 R0 (C4)	ypT1a V0 L0 Pn0 R1 (C4)	ypT1a V0 L0 Pn0 R1 (C4)	ypT0 V0 L0 Pn0 R0 (C4)
R status (resection)	R0	R0	R0	R0	R0	R0	R0
Renal pelvis or calyx	Involved	Involved	Involved	Involved	Involved	Involved	Involved
Urothelium	Regeneration	Regeneration	Regeneration	Regeneration	Regeneration	Regeneration	Regeneration
Urine cytology	Temporary degeneration and vacuolisation	Temporary degeneration and vacuolisation	Temporary degeneration and vacuolisation	Temporary degeneration and vacuolisation	Temporary degeneration and vacuolisation	Temporary degeneration and vacuolisation	Temporary degeneration and vacuolisation

Active tip (exposure) plus postulated ablation field in depth 2 × 0.5 cm. Volume for ellipsoidal tumour, $V = 4/3\ \pi\ a \times b \times c$

UP upper pole, *MP* mid-pole, *LP* lower pole, *cc* clear-cell

DWI (b = 0/500), T1w-GRE, T1w-FS-3DGRE transversal, T1w-FS-3DGRE coronal). MRI scans were evaluated using Infinitt PACS software (INFINITT PACS, INFINITT Europe GmbH, Germany).

Histopathological Analysis

Before IRE treatment, CT-guided coaxial core biopsies were taken from all tumours for initial histological assessment. Partial renal resection or (if necessary) radical nephrectomy, with complete resection of the tumour area/ablation area, was performed by open surgery 28 days after IRE. The resection specimens were fixed in buffered 4% formaldehyde solution followed by complete sectioning of the ablation area including a border of macroscopically inconspicuous kidney tissue in 0.4-cm-thick slices. Thereafter, the ablation area, including the border, was completely embedded in paraffin. Each tissue block was used to prepare 3-µm-thick sections, and these were stained with HE for morphological assessment in 500-µm steps with one unstained section each for transmission microscopy. In each specimen, the complete ablation area, the tumour area, and nonaffected renal tissue on each slide were outlined manually.

Urinary Cytology

Urinary cytology was investigated on planned study days, 1 day before IRE and 1, 2, 7, and 27 days after IRE. Urine-cytological preparations were pipetted onto two microscope slides with 500 µl of the urine into prepared cytochambers and centrifuged for 5 min in a Rotofix 32 at 1000 rpm and room temperature. After withdrawal of the supernatant from the cytochamber with a filter pump, the preparations on the slides were allowed to dry in the air at ambient temperature. Urinary cytology centrifugates were stained with May–Grünwald–Giemsa stain (by Pappenheim's method) and then fixed with Canada balm for transmitted-light microscopy with and without oil immersion. The examination was performed with a Leica DM2500 microscope (Leica Microsystems GmbH, Wetzlar, Germany) using transmitted light, partly with differential interference contrast (DIC) at a magnification of 200× with an HC PLAN APO 20×/0.70 Ph2, ∞/0.17/C objective and 630× with an N PLAN 63×/0.80, ∞/0.17/C objective. Examination was performed according to the rules of the Working Group for Urine Cytology and urine-bound markers of the *Deutsche Gesellschaft für Urologie* (German Society for Urology), taking account of The Paris System for reporting urinary cytology (TPS). Typical findings were documented by photography with a Leica DFC290 camera.

Results

IRE Treatment

Seven patients, who had biopsy-proven RCC pT1a cN0cM0 with a mean tumour size of 22 mm (range 15–39 mm), underwent lumbar percutaneous CT-guided IRE with the NanoKnife™ system (Table 1). IRE (70–90 µs, 450–1300 pulses per target, 1.8–3 kV, 28–50 A). IRE was performed for one session for one ablation in six patients and for two ablations in one patient (total, 8 ablations; Table 1). The mean planned IRE treatment zone was 17.3 cm^3 (8 ablations; range 8.2–45.6 cm^3). Technical feasibility was attained in all patients, but IRE electrode placement was time-consuming due to CT-guided IRE electrode placement control and due to IRE electrode reposition if required according to the treatment planning measurements. The mean overall procedure time was 129 min (range 53–203 min). The anaesthesia time was 165 min (range 91–317 min).

Side Effects

In all of the seven renal tumour IRE ablations, the renal pelvis-calyceal system was involved in the IRE ablation zone, either with adjacent renal calyxes (7/7) or the renal pelvis (2/7). There were no major or residual procedure-related complications. All patients had slight transient macrohaematuria due to the IRE electrode placement and puncture of the renal pelvis-calyceal system. Minor complications included slight self-limiting macrohaematuria (in 7/7 patients), perirenal haematomas (2/7), and temporary post-puncture pain, treated by drugs (7/7). Renal function after IRE was retained in all cases, with no urinary leakage or retention, no renal infarction, and consistent creatinine or eGFR level (Table 1).

MR Imaging

The detailed analysis of the MRI of the tumour texture and renal parenchyma has to be published separately. In all cases, MRI demonstrated macroscopically complete coverage of the tumour area by the ablation zone (size of ablation zone ≥ tumour size in three dimensions) with nearly size-persistent tumour areas four weeks after IRE. MRI images demonstrated a preserved renal hilum vessels 27 days after IRE (Fig. 1M). All tumours showed 4 weeks after IRE ablation a slight shrinkage, a clear restriction of diffusion in MRI with correspondingly low ADC values and a sign of greater cellularity and no more trace of image-morphological perfusion. The urographic MRI phase (T1-Thrive5-3D-GE urogram scans) demonstrated normal morphological appearances and normal timing of

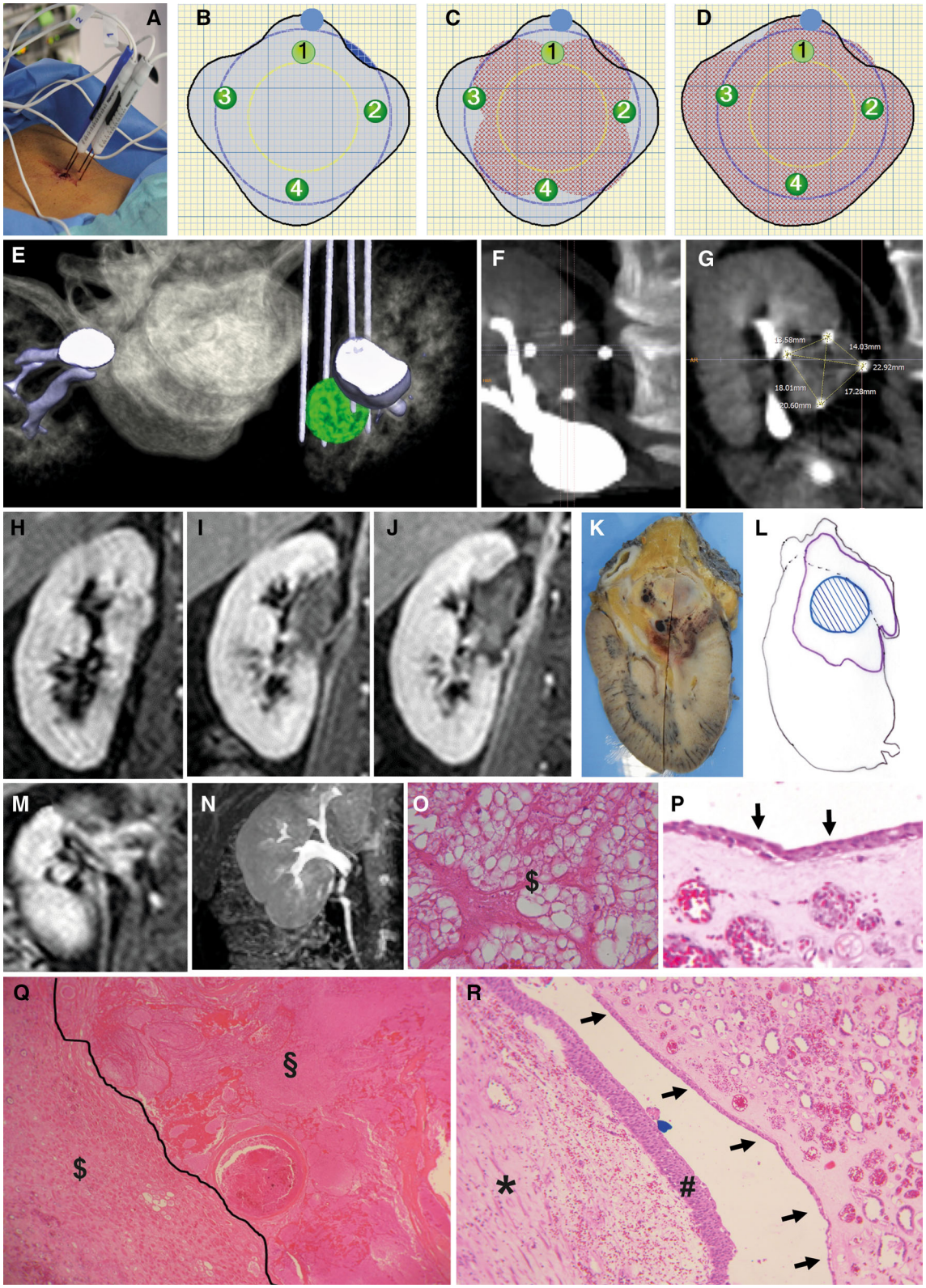
A
B
C
D
1
2
3
4
E
F
G
12.58mm
14.03mm
22.92mm
18.01mm
17.28mm
20.60mm
H
I
J
K
L
M
N
O
$
P
Q
§
$
R
*
#

Fig. 1 Percutaneous renal IRE treatment planning and effects (patient P3 [Table 1]). **A** Percutaneous IRE of RCC with 4 NanoKnife electrodes. **B–D** NanoKnife IRE planning and representation of the calculated ablation zone (grey) und calculated ablation (red-brown) in relation to the tumour (yellow circle) by using 4 electrodes (green dots 1–4). **E** Computer-tomographic representation of the 4 IRE electrodes in the kidney tumour (green) in relation to the directly adjacent renal pelvis-calyceal system (RPCS; blue–white) by 3D reconstruction. **F–G** 2D computer-tomographic transversal representation of the 4 IRE electrodes (white dots) in the kidney tumour in relation to the directly adjacent RPCS system (white) and measurement of the interelectrode distances. **H** Initial representation of the tumour: cortical RCC 1.6 cm from dorsomedial to the right kidney close to the hilum, imaged by MRI before IRE. **I–J** Representation of the ablation zone in the tumour region by MRI 7 days after IRE (**I**) and 27 days after IRE (**J**; tumour no longer demarcatable). **K–L** Longitudinally sectioned nephrectomy preparation (black line) and corresponding sketch showing the zones of ablation (violet line) and of the degenerative renal tumour (blue-hatched area) without microscopic tumour residue 28 days after IRE. **M–N** MRI images of the preserved renal hilus vessels (**M**) and the RPCS without extravasation or urinary tension (**N**) 7 and 27 days after IRE. **O** Completely necrotic RCC ($) with only faintly recognisable cell contours and preserved extracellular matrix. **P** Medulla with stroma fibrosis and regenerating, still flat, urothelium (arrows) after irreversible electroporation. **R** Sharp demarcation of the completely necrotic RCC ($) from the adjacent, likewise necrotic tumour-free renal parenchyma (§). **S** RPCS with signs of regeneration after mild perifocal damage. Renal papilla with stroma fibrosis of the renal medulla (right-hand side) with covering by flat regenerated urothelium (arrows). Unaltered part of the calyx ($) with regular, normal-width urothelium (#)

contrast-agent excretion with no urine leakage or urinary obstruction (Fig. 1).

Resection and Histological Analysis

The detailed histological analysis of the tumour region and renal parenchyma will be published separately. The current analysis is focused on the IRE's effects on the renal urine collecting system (UCS) and upper urinary tract (UUT). Four weeks after IRE, residual tumour shape was persistent in all cases and was similar to the initial size. Partial kidney resection was performed in five of the seven patients and radical nephrectomy in the other two because of the central location of the tumour ablation areas. Despite the relatively small tumour sizes, these two nephrectomies had to be performed to obtain a complete resection of the tumour and ablation zone analogous to the study protocol, whereas the unfavourable location and central expansion near the hilum made a partial resection not feasible in surgeon´s indication (e.g., Fig. 1H–L). Complete macroscopic coverage of the tumour by the IRE ablation field was achieved in 100% of cases. The histological ablation IRE zone was larger than expected in the treatment planning zone in three of seven cases (Table 1). Macroscopic analysis showed sharply demarcated, approximately ellipsoidal, haemorrhagically altered IRE ablation zones. The peritumoral damage zones had spread to peritumoral renal tissue and perirenal fatty tissue. In sections where the ablation zone included the renal pelvis and papillae, both structures showed necrosis with urothelial sloughing and incipient regeneration of the urothelium (Fig. 1O–S). Whereas the urothelium showed signs of regeneration 28 days after IRE, the parenchyma below it showed necrosis and chronic tissue destruction (Fig. 1P, S). Resection revealed complete tumour ablation (ypT0V0N0Pn0R0) in four cases; in the other three, due to microscopic residual tumour areas with viable tumour cells (in 2 patients), ypT1aV0N0Pn0R1, and to tumour cells of uncertain viability (in the third), ypT0-1aV0N0Pn0R0-1, was found according to the current TNM classification [22, 23] (Table 1). Alongside the tumour-related histological changes, all cases showed zonal structuring of the ablation region, as described earlier in detail [9]. In the centre, an amorphous necrosis zone of the coagulation-necrosis type without differentiation of stromal and cellular structures was seen. Next to this, there was a necrosis zone of variable width, also of the coagulation-necrosis type, in which ghost structures with preserved extracellular matrix and medulla fibrosis of the tissue affected could still be discerned (e.g., tubules, glomerules, fat). Lymphocytic infiltrations and resorptive chronic-inflammatory changes also could be seen.

Urinary Cytology

Urinary cytology had fundamentally changed by days 1 and 2 after IRE application (Fig. 2D–F). There were an increased number of isolated and partly aggregated transitional urothelium cells with massive degeneration: pale and partly cloudy cytoplasm with ongoing dissolution of the cell membrane as well as swollen cell nuclei with anisokaryosis, hypochromasia, and a dissolute structure revealed by differently sized pale vacuoles of cytoplasm and karyoplasm (Fig. 2D–F). A typical feature, seen for all patients, was cytoplasmic vacuolisation: partly with small vacuoles and partly with displacement and crescent-shaped deformation of the nucleus. Additionally, for some patients, alterations in the nucleus and even fragmentation (meaning cell death) were seen. From day 7 on, these findings diminished. By day 27, these alterations were no longer detectable, with normal urinary cytology of isolated transitional epithelial cells (regular relation between homogenous cytoplasm and cell nucleus), comparable to the finding at the start, 1 day before IRE (Fig. 2G–L).

Discussion

Despite first clinical publications on IRE of the kidney or in RCC, there is still a lack of clinical and histological data on the application of IRE in RCC, and most studies

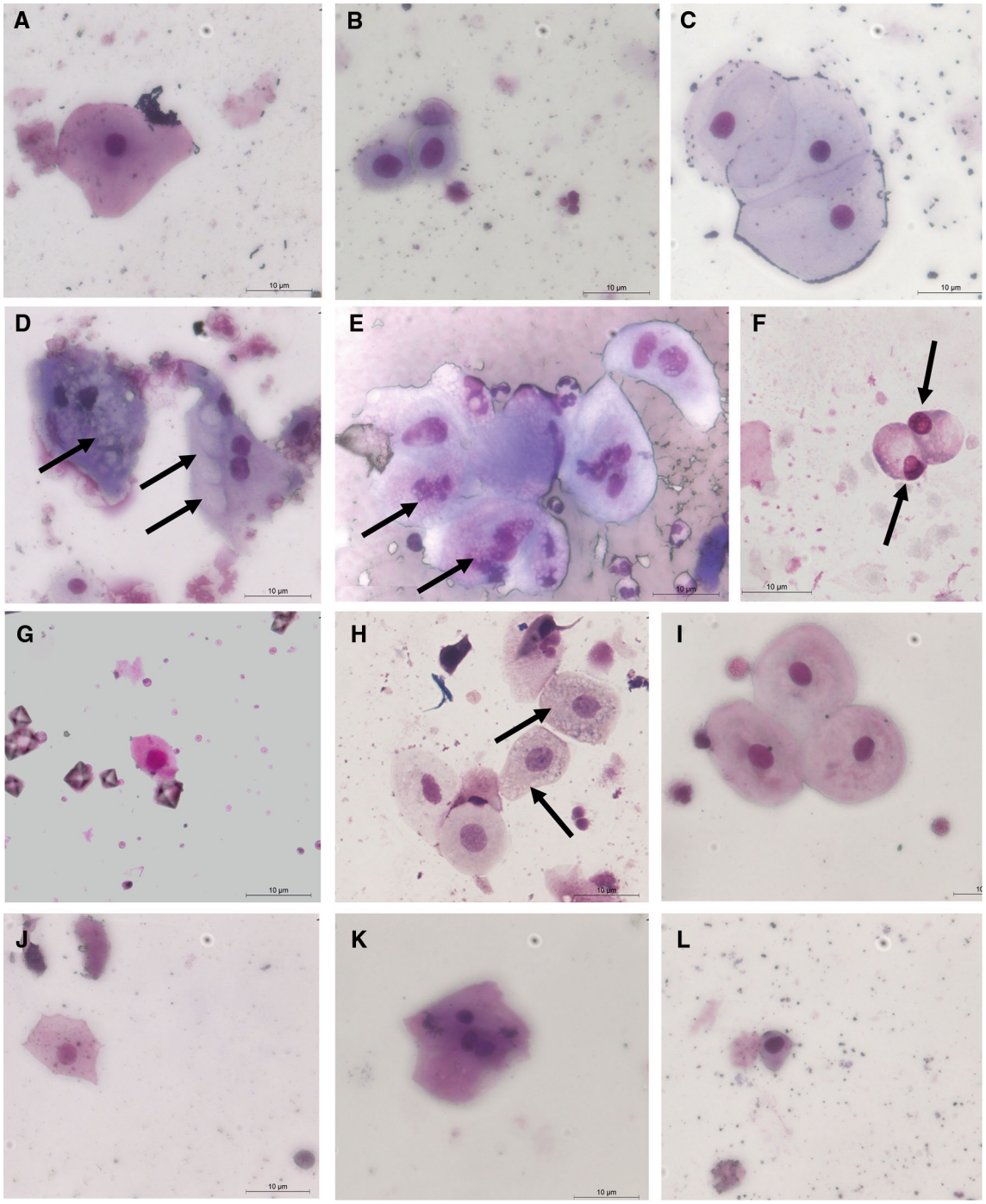

Fig. 2 Urine cytological examination of the urothelial changes by IRE. **A–C** Urocytology before IRE. Inconspicuous urothelial cells with regular nucleus–cytoplasm ratio, no vacuolisation, and some debris. **D–F** Urocytology 1 day after IRE with vacuoles (arrows) of varying size in the cytoplasm (**D–E**) and caryoplasm (**E**), with partial nuclear disintegration (**E**) and displacement (**F**). Some erythrocytes and leucocytes are visible. **G–I** Urocytology 7 days after IRE. Overall, fewer cytoplasmic and karyoplasmic, smaller vacuoles in the cytoplasm (arrows), relatively few karyoplasmic vacuoles. Partly normal urothelial cells. Oxalate crystals are seen (**G**) and hyperchromatic leucocytes (**H**, **I**). **J–L** Urocytology 27 days after IRE and 1 day before resection. Inconspicuous urothelial cells, no vacuoles or, at worst, minimal cytoplasmic vacuolisation (**K**); some debris, few leucocytes and erythrocytes

have been based on radiological or post-biopsy assessment only [7–11]. Diehl et al. [10] treated seven small renal masses (SRMs) with percutaneous IRE in five patients with a single kidney and a mean tumour diameter 24 mm (range 15–38 mm), but that study was limited to an unknown SRM entity. Canvasser et al. [11] reported

suboptimum oncological efficacy and imaging features after IRE of 42 SRMs (of which 20 were RCC) with a mean tumour size of 20 mm (range 10–36 mm). So far, only preclinical studies have demonstrated histologically the potential of sparing the urine-collecting system by IRE of renal parenchyma in a normal porcine kidney [5, 6, 20, 21].

With this current clinical pilot study of IRE of human pT1a RCC followed by delayed tumour resection, the IRENE trial [9, 12, 18], we present the first examination of the effect of IRE on the renal urine-collecting system using resection histology, MRI with urogram scan, and urinary cytology. The detailed histological and MRI morphological analysis of the tumour region and renal parenchyma will be published separately. The histological and MRI morphological findings represented "snapshots" taken 4 weeks after IRE according to the study protocol, with procedure-specific findings. Although the choice of a different interval between IRE and histological analysis could of course influence this result, the optimum interval between IRE and histological assessment is at present still unclear. In each of the seven cases investigated, IRE induced massive damage to the tumour tissue. Intrasurgical examination at resection showed severe local perirenal/peritumoral adhesions due to a local, unspecific inflammatory reaction resulting from puncture and/or IRE. Complete macroscopic coverage of the tumour by the IRE ablation field was achieved in 100% of cases. The histological ablation IRE zone was larger than expected in the treatment planning zone in three of seven cases.

In sections where the ablation zone included the renal pelvis and papillae, both structures showed necrosis with urothelial sloughing and incipient regeneration of the urothelium (Fig. 1O–S). Whereas the urothelium showed signs of regeneration 28 days after IRE-ablation, the parenchyma below it showed necrosis and chronic tissue destruction (Fig. 1P, S). The initial macrohaematuria resulted most likely from the puncture of the tumour adjacent renal pelvis-calyceal system (calyx) by the IRE electrode placement. The histological changes of the urothelial and submucosal tissue constitute unspecific and specific reactions to the ablation 4 weeks earlier. The postulated preservation of the noncellular tissue matrix, such as submucosa matrix and the basement membrane of the urine-collecting system, as well as the regeneration capability of the urothelium, may stimulate healing of the renal calyxes and pelvis after IRE [3]. Tracy et al. [21], Deodhar et al. [20], and Wendler et al. [5] showed histologically the regeneration of ablated urothelium after renal IRE in healthy swine.

Srimathveeravalli et al. [24, 25] evaluated the effect of transureteral endoluminal catheter-directed irreversible electroporation (IRE) on the integrity, patency, and function of the normal porcine ureter. They observed a full-thickness IRE ablation of the ureteral wall with the preservation of the ureteral wall integrity with no leakage and full recovery of the urethelium at 28 days after IRE. The IRE affected ureteral tunica muscularis showed progressive granulation tissue with extensive scarring as a lumen patency reductive ureter stricture and consecutive proximal urinary retention in all cases [24, 25]. Despite the pelvico-ureteral junction the renal pelvis-calyceal system has no tunica muscularis; therefore, a wall thickening of the renal pelvis-calyceal system by granulation seems to be unlikely, but calyx stricture could be possible, which we have not observed. Compared with the ureteral wall thickening [25], Wendler et al. [9] demonstrated luminal occlusive intimal hyperplasia of the tunica muscularis of small- and medium-sized arterial renal vessels, which might be an IRE-specific side effect.

MRI of the ablation zones on day 28 after IRE correlated well with histological analysis on the same day. The increased diffusion restriction 4 weeks after IRE could be explained by the lymphocytic infiltrations and resorptive chronic-inflammatory changes as a reaction and decomposition process of the IRE induced necrosis. There could be a dynamic process with a change of the histological and MRI morphological sight over time more than 4 weeks after IRE ablation. The urographic MRI phase (T1-Thrive5-3D-GE urogram scans) demonstrated normal morphological appearances and normal timing of contrast-agent excretion with no urine leakage or urinary obstruction (Fig. 1). Wendler et al. [5] demonstrated normal MRI urogram scans after renal IRE in healthy swine. These observations are in direct contrast to the acute effects and early complications in the urine-collecting system seen when RFA and CRA are used [14, 15, 17, 19].

The urinary cytology findings changed fundamentally during days 1–7 after IRE, with massive degeneration through cytoplasmic and karyoplasmic vacuolisation (Fig. 2D–H). By day 27, these alterations were no longer detectable, with normal urinary cytology of the isolated transitional epithelium cells (regular relation between homogenous cytoplasm and cell nucleus) comparable to the finding at the start, 1 day before IRE (Fig. 2A–C; J–L). This suggests a temporary alteration in the cytoplasmic metabolism, similar to the temporary vacuolisation of transitional cells in urine cytology observed after renal IRE in swine [5]. The current literature provides no similar observations of urothelial cell alteration. We interpret this vacuolisation of the detached urothelial cells as an IRE-caused degeneration that seems to be specific in the sense of ongoing apoptosis and necrosis of cells after IRE. This study observation of urinary cytology after IRE represents a qualitative result of a new urinary cytological

phenomenon, which has already been established in animal experiments with no tumour model and which we confirmed clinically [5]. However, urinary cytology after IRE is unable to monitor the success of IRE ablation; yet it still reflects IRE's individual effect on transitional cells of the urinary tract. Therefore, this new phenomenon must be taken into account when evaluating urinary cytology during the first days after IRE.

Limitations

Our study is limited statistically by the small number of patients, although this fact was ameliorated by the consistency of the results obtained with the small initial patient cohort. The study was planned at a time when not all technical variables of the NanoKnife™ system and renal IRE ablation conditions were completely understood. On the basis of this initial analysis, we conclude that complete ablation of T1a RCC in different locations, and renal preservation, is possible with IRE. The results do not lead to a recommendation of specific changes in IRE ablation parameters. The procedures in this study place a substantial burden on the patients because of the two-stage intervention principle with general anaesthesia for IRE ablation and again for delayed resection; moreover, the specimens had to be obtained by open surgery. If they had not taken part in the study these patients would have undergone a single intervention (ablation, possibly without general anaesthesia or by laparoscopy), a factor that also made it difficult to recruit a larger patient collective. The result of this interim analysis indicates that laparoscopic nephrectomy (total or partial) may be performed according to the protocol. However, it does not seem likely that further recruitment to reach the originally planned total of 20 patients would lead to different results, so that termination of the study is under consideration.

Conclusions

This first human study of kidney IRE of pT1a RCC with urographic, urine-cytological, and resection-histological analysis shows complete tumour destruction with protection or regeneration of the urine-collecting system and vacuolisation of urothelial cells in der urine cytology. Renal percutaneous IRE using the NanoKnife appears to be a safe tissue ablation treatment. New cytological and histological phenomena should be considered by pathologists when evaluating histology and cytology after IRE. Irreversible electroporation might be useful for ablation of centrally located renal tumours.

Compliance with Ethical Standards

Conflict of interest The authors declare that they have no conflict of interest.

Ethical Approval All procedures performed and the conduct of the study as a whole was in accordance with the 1964 Helsinki declaration and its later amendments and comparable ethical standards. Approval was obtained for the study by the national research committee (BfArM) and the institutional ethics committee.

Informed Consent Informed consent was obtained from all subjects in this study. Additional informed consent for identifying information was not required.

References

1. Ljungberg B, Albiges L, Bensalah K, Bex A, Giles RH, Hora M, Kuczyk MA, Lam T, Marconi L, Merseburger AS, Powles T, Staehler M, Volpe A, Dabestani S, Fernandez-Pello Montes S, Hofmann F, Tahbaz R. EAU Guidelines on renal cell carcinoma. European Association of Urology 2017. Update March 2017. http://uroweb.org/wp-content/uploads/10-Renal-Cell-Carcinoma_2017_web.pdf. Accessed 4 July 2017.
2. D'Andrea D, Shariat SF, Klatte T. Update on ablative therapies of renal tumors. Curr Opin Urol. 2016;26(5):410–6. doi:10.1097/MOU.0000000000000306.
3. Rubinsky B (2009) Irreversible electroporation. 1st ed. Berlin: Springer; p. 328. ISBN 3642054196.
4. Wendler JJ, Pech M, Blaschke S, Porsch M, Janitzky A, Ulrich M, Dudeck O, Ricke J, Liehr UB. Angiography in the isolated perfused kidney: radiological evaluation of vascular protection in tissue ablation by nonthermal irreversible electroporation. Cardiovasc Interv Radiol. 2012;35(2):383–90. doi:10.1007/s00270-011-0187-x.
5. Wendler JJ, Pech M, Porsch M, Janitzky A, Fischbach F, Buhtz P, Vogler K, Hühne S, Borucki K, Strang C, Mahnkopf D, Ricke J, Liehr UB. Urinary tract effects after multifocal nonthermal irreversible electroporation of the kidney: acute and chronic monitoring by magnetic resonance imaging, intravenous urography and urinary cytology. Cardiovasc Interv Radiol. 2012;35(4):921–6. doi:10.1007/s00270-011-0257-0.
6. Wendler JJ, Porsch M, Hühne S, Baumunk D, Buhtz P, Fischbach F, Pech M, Mahnkopf D, Kropf S, Roessner A, Ricke J, Schostak M, Liehr UB. Short- and mid-term effects of irreversible electroporation on normal renal tissue: an animal model. Cardiovasc Interv Radiol. 2013;36(2):512–20. doi:10.1007/s00270-012-0452-7.
7. Pech M, Janitzky A, Wendler JJ, Strang C, Blaschke S, Dudeck O, Ricke J, Liehr UB. Irreversible electroporation of renal cell carcinoma: a first-in-man phase I clinical study. Cardiovasc Interv Radiol. 2011;34(1):132–8. doi:10.1007/s00270-010-9964-1.
8. Thomson KR, Cheung W, Ellis SJ, Federman D, Kavnoudias H, Loader-Oliver D, Roberts S, Evans P, Ball C, Haydon A. Investigation of the safety of irreversible electroporation in humans. J Vasc Interv Radiol. 2011;22(5):611–21. doi:10.1016/j.jvir.2010.12.014.
9. Wendler JJ, Ricke J, Pech M, Fischbach F, Jürgens J, Siedentopf S, Roessner A, Porsch M, Baumunk D, Schostak M, Köllermann J, Liehr UB. First delayed resection findings after irreversible electroporation (IRE) of human localised renal cell carcinoma (RCC) in the IRENE pilot Phase 2a trial. Cardiovasc Interv Radiol. 2016;39(2):239–50. doi:10.1007/s00270-015-1200-6.

10. Diehl SJ, Rathmann N, Kostrzewa M, Ritter M, Smakic A, Schoenberg SO, Kriegmair MC. Irreversible electroporation for surgical renal masses in solitary kidneys: short-term interventional and functional outcome. J Vasc Interv Radiol. 2016;27(9):1407–13. doi:10.1016/j.jvir.2016.03.044.
11. Canvasser NE, Sorokin I, Lay AH, Morgan MS, Ozayar A, Trimmer C, Cadeddu JA. Irreversible electroporation of small renal masses: suboptimal oncologic efficacy in an early series. World J Urol. 2017. doi:10.1007/s00345-017-2025-5.
12. Wendler JJ, Porsch M, Nitschke S, Köllermann J, Siedentopf S, Pech M, Fischbach F, Ricke J, Schostak M, Liehr UB. A prospective Phase 2a pilot study investigating focal percutaneous irreversible electroporation (IRE) ablation by NanoKnife in patients with localised renal cell carcinoma (RCC) with delayed interval tumour resection (IRENE trial). Contemp Clin Trials. 2015;43:10–9. doi:10.1016/j.cct.2015.05.002.
13. Manual NanoKnife_ System Procedure & Trouble Shouting Guide. Software version 2.2.0. AngioDynamics_, _ 2011 AngioDynamics, Inc. p. 1–159.
14. Dupuy DE, Gervais DA, Gianfelice D, Gillams AR, Lee FT Jr, Leen E, Lencioni R, Littrup PJ, Livraghi T, Lu DS, McGahan JP, Meloni MF, Nikolic B, Pereira PL, Liang P, Rhim H, Rose SC, Salem R, Sofocleous CT, Sofocleous CT, Solomon SB, Soulen MC, Tanaka M, Vogl TJ, Wood BJ, Goldberg SN. International Working Group on Image-Guided Tumor Ablation, Standard of Practice Committee of the Cardiovascular and Interventional Radiological Society of Europe. Image-guided tumor ablation: standardization of terminology and reporting criteria—a 10-year update. J Vasc Interv Radiol. 2014;25(11):1691–705. doi:10.1016/j.jvir.2014.08.027.
15. Ahmed M. Technology Assessment Committee of the Society of Interventional Radiology. Image-guided tumor ablation: standardization of terminology and reporting criteria—a 10-year update: supplement to the consensus document. J Vasc Interv Radiol. 2014;25(11):1706–8. doi:10.1016/j.jvir.2014.09.005.
16. Wendler JJ, Friebe B, Baumunk D, Blana A, Franiel T, Ganzer R, Hadaschik B, Henkel T, Köhrmann KU, Köllermann J, Kuru T, Machtens S, Roosen A, Salomon G, Schlemmer HP, Sentker L, Witzsch U, Liehr UB, Ricke J, Schostak M. Focal therapy for small renal masses: observation, ablation or surgery [in German]. Urologe A. 2016;55(5):594–606. doi:10.1007/s00120-016-0075-8.
17. Zondervan PJ, Wagstaff PG, Desai MM, de Bruin DM, Fraga AF, Hadaschik BA, Köllermann J, Liehr UB, Pahernik SA, Schlemmer HP, Wendler JJ, Algaba F, de la Rosette JJ, Laguna Pes MP. Follow-up after focal therapy in renal masses: an international multidisciplinary Delphi consensus project. World J Urol. 2016;34(12):1657–65.
18. Wendler JJ, Ricke J, Pech M, Fischbach F, Jürgens J, Porsch M, Janitzky A, Baumunk D, Siedentopf S, Köllermann J, Schostak M, Liehr U-B. Initial assessment of clinical feasibility, safety and efficacy of NanoKnife irreversible electroporation (IRE) in the focal treatment of localized renal cell carcinoma (RCC) with delayed interval tumor resection (IRENE trial). Eur Urol Suppl. 2017;16(3):e102–3. doi:10.1016/S1569-9056(17)30129-X.
19. Wendler JJ, Fischbach K, Ricke J, Jürgens J, Fischbach F, Köllermann J, Porsch M, Baumunk D, Schostak M, Liehr UB, Pech M. Irreversible electroporation (IRE): standardization of terminology and reporting criteria for analysis and comparison. Pol J Radiol. 2016;81:54–64. doi:10.12659/PJR.896034.
20. Deodhar A, Monette S, Single GW Jr, Hamilton WC Jr, Thornton R, Maybody M, Coleman JA, Solomon SB. Renal tissue ablation with irreversible electroporation: preliminary results in a porcine model. Urology. 2011;77(3):754–60. doi:10.1016/j.urology.2010.08.036.
21. Tracy CR, Kabbani W, Cadeddu JA. Irreversible electroporation (IRE): a novel method for renal tissue ablation. BJU Int. 2011;107(12):1982–7. doi:10.1111/j.1464-410X.2010.09797.x.
22. Brierley JD, Gospodarowicz MK, Wittekind C. TNM classification of malignant tumours. 8th ed. New York: Wiley; 2017.
23. Wittekind C, Compton CC, Brierley J, Sobin LH. TNM supplement. A commentary on uniform use. 4th ed. New York: Wiley; 2012.
24. Srimathveeravalli G, Silk M, Wimmer T, Monette S, Kimm S, Maybody M, Solomon SB, Coleman J, Durack JC. Feasibility of catheter-directed intraluminal irreversible electroporation of porcine ureter and acute outcomes in response to increasing energy delivery. J Vasc Interv Radiol. 2015;26(7):1059–66. doi:10.1016/j.jvir.2015.01.020.
25. Srimathveeravalli G, Cornelis F, Wimmer T, Monette S, Kimm SY, Maybody M, Solomon SB, Coleman JA, Durack JC. Normal porcine ureter retains lumen wall integrity but not patency following catheter-directed irreversible electroporation: imaging and histologic assessment over 28 days. J Vasc Interv Radiol. 2017;28(6):913–919.e1. doi:10.1016/j.jvir.2017.02.032.

8.17

Initial Assessment of the Efficacy of Irreversible Electroporation in the Focal Treatment of Localized Renal Cell Carcinoma With Delayed-interval Kidney Tumor Resection (Irreversible Electroporation of Kidney Tumors Before Partial Nephrectomy [IRENE] Trial - An Ablate-and-Resect Pilot Study).

Wendler JJ, Pech M, Fischbach F, Jürgens J, Friebe B, Baumunk D, Porsch M, Blaschke S, Schindele D, Siedentopf S, Ricke J, Schostak M, Köllermann J, Liehr UB.

Urology. 2018 Apr;114:224-232.

OBJECTIVES: To assess the efficacy of irreversible electroporation (IRE) ablation of pT1a renal-cell carcinoma (RCC) in the first prospective, monocentric Phase 2a pilot ablate-and-resect study (IRENE trial). It has been postulated that focal IRE can bring about complete ablation of soft-tissue tumours with protection of healthy peritumoral tissue and anatomical structures.

METHODS: The first seven study patients, with biopsy-proven pT1a RCC (15-39mm) underwent IRE. Percutaneous computed-tomography-guided IRE was performed with electrocardiographic triggering under general anaesthesia and deep muscle paralysis with 3-6 monopolar electrodes positioned within the renal tumour. 28 days later the tumour region was completely resected to confirm tumour destruction pathologically. Individual results for these patients are displayed, described and discussed.

RESULTS: Technical feasibility was attained in all patients, but electrode placement and ablation were complex, with a mean overall procedure time of 129min. There were no major complications. Partial kidney resection was performed in five patients and, in two, radical nephrectomy because of central tumour location and ablation areas. Resections revealed by TNM classification no residual tumour as complete ablation in four cases (ypT0V0N0Pn0R0), and microscopic residual tumour cells as incomplete ablation in the other three (ypT1aV0N0Pn0R1).

CONCLUSIONS: Renal percutaneous IRE appears to be a safe treatment for pT1a RCC but requires substantial procedural effort. Resection specimens of the ablation zone revealed a high rate of microscopic incomplete ablation four weeks after IRE. According to these initial study results curative, kidney-sparing ablation of T1a RCC appears possible, but needs technical improvement to ensure complete ablation.

Initial Assessment of the Efficacy of Irreversible Electroporation in the Focal Treatment of Localized Renal Cell Carcinoma With Delayed-interval Kidney Tumor Resection (Irreversible Electroporation of Kidney Tumors Before Partial Nephrectomy [IRENE] Trial—An Ablate-and-Resect Pilot Study)

Johann J. Wendler,[2,3] Maciej Pech,[3] Frank Fischbach,[3] Julian Jürgens,[3] Björn Friebe,[3] Daniel Baumunk,[2] Markus Porsch, Simon Blaschke, Daniel Schindele, Sandra Siedentopf, Jens Ricke,[3] Martin Schostak,[2] Jens Köllermann,[1,2] and Uwe B. Liehr[1,2,3]

OBJECTIVE To assess the efficacy of irreversible electroporation (IRE) ablation of pT1a renal cell carcinoma (RCC) in the first prospective, monocentric phase 2a pilot ablate-and-resect study (Irreversible Electroporation of Kidney Tumors Before Partial Nephrectomy [IRENE] trial). It has been postulated that focal IRE can bring about complete ablation of soft-tissue tumors with protection of healthy peritumoral tissue and anatomic structures.

PATIENTS AND METHODS The first 7 study patients with biopsy-proven pT1a RCC (15-39 mm) underwent IRE. Percutaneous computed tomography-guided IRE was performed with electrocardiographic triggering under general anesthesia and deep muscle paralysis with 3-6 monopolar electrodes positioned within the renal tumor. Twenty-eight days later, the tumor region was completely resected to confirm tumor destruction pathologically. Individual results for these patients are displayed, described, and discussed.

RESULTS Technical feasibility was attained in all patients, but electrode placement and ablation were complex, with a mean overall procedure time of 129 minutes. There were no major complications. Partial kidney resection was performed in 5 patients, and radical nephrectomy was performed in 2 patients because of central tumor location and ablation areas. Resections revealed by tumor, node, and metastasis classification of the International Union for Cancer Control 2017 no residual tumor as complete ablation in 4 cases (ypT0V0N0Pn0R0) and microscopic residual tumor cells as incomplete ablation in the other 3 cases (ypT1aV0N0Pn0R1).

CONCLUSION Renal percutaneous IRE appears to be a safe treatment for pT1a RCC but requires substantial procedural effort. Resection specimens of the ablation zone revealed a high rate of microscopic incomplete ablation 4 weeks after IRE. According to these initial study results, curative, kidney-sparing ablation of T1a RCC appears possible but needs technical improvement to ensure complete ablation. UROLOGY 114: 224–232, 2018. © 2017 Elsevier Inc.

[1] *These authors contributed equally to this work.*
[2] *Study group IRENE trial featured by AKFM-DGU, Germany.*
[3] *Study group IRENE trial featured by DAfMT, Germany.*

Financial Disclosure: *The authors declare that they have no relevant financial interests.*

Compliance with Ethical Standards: *All procedures performed and the conduct of the study as a whole were in accordance with the 1964 Helsinki Declaration and its later amendments and comparable ethical standards.*

From the Department of Urology, Otto von Guericke University of Magdeburg, Germany; the Department of Radiology, Otto von Guericke University of Magdeburg, Germany; the Department of Pathology, Otto von Guericke University of Magdeburg, Germany; the Department of Pathology, Sana Medical Center Offenbach, Germany; Urological practice, Magdeburg, Germany; Urological practice, Stuttgart, Germany; and the Department of Radiology, Ludwig Maximilians University of Munich, Germany

Address correspondence to: Johann J. Wendler, M.D., Department of Urology, University of Magdeburg, Leipziger Str. 44, Magdeburg 39120, Germany. E-mail: johann.wendler@med.ovgu.de

Submitted: July 7, 2017, accepted (with revisions): December 9, 2017

https://doi.org/10.1016/j.urology.2017.12.016
0090-4295

Focal therapy of small renal cell carcinoma (RCC) has the goal of achieving total destruction of the tumor tissue while minimizing damage to the surroundings.[1-5] For irreversible electroporation (IRE), it has been postulated that complete ablation of soft-tissue tumors with protection of the healthy peritumoral tissue is possible.[6-9] IRE is mostly investigated for percutaneous ablation of prostate and pancreatic cancer, cholangiocarcinoma, hepatic and pulmonal malignancies, and small renal masses (SRMs). However, there is still a lack of clinical data for its application in RCC.[10-14] Most IRE studies have been based on computed tomography (CT) or magnetic resonance radiological or inconsistent postbiopsy assessment only.[13,14] With this pilot ablate-and-resect study,[12,15,16] we present detailed histopathologic resection data of IRE-treated RCC to evaluate the ablation efficacy and accuracy of percutaneous focal IRE, in RCC, using the NanoKnife system (Figs. 1, 2).

PATIENTS AND METHODS

Study Design and Approval

This pilot study was planned to achieve histologic data (primary objective) of percutaneous CT-guided IRE-treated localized RCC followed by delayed ablation zone resection 4 weeks after IRE (primary end point), according to previous animal swine studies of RCC in normal kidneys. The resection was performed to assess histologic changes of the IRE ablation area within the tumor and the surrounding tissue (primary objective). The protocol of this good clinical practice-compliant, prospective, monocentric, nonrandomized, uncontrolled, nonblinded, single-arm phase 2a interventional pilot study (Irreversible Electroporation of Kidney Tumors Before Partial Nephrectomy [IRENE]; ClinicalTrials.gov NCT01967407 (10/2013), World Health Organization International Clinical Trials Registry Platform DRKS00004266) has been published separately.[15] Approval according to German medical product law was granted by German Federal Institute for Drugs and Medical Devices (CIV-12-4-006021) and the Ethics Committee of Magdeburg University (73/2012). Informed consent was obtained from all subjects in the present study. The study was planned to include up to 20 patients with an interim analysis after the first 10 recruited patients. According to plan, 10 patients were recruited into the study. For 2 of the 10 patients, the study biopsy showed that their disease was not RCC, so they were not IRE treated and were withdrawn from the study. A third patient could not be treated for technical reasons (persistent boot failure of the NanoKnife generator) and was also withdrawn before IRE.

Procedures

Before IRE treatment, CT-guided coaxial core biopsies were taken from all tumors for initial histologic assessment and selection of patients. For IRE treatment, we used the NanoKnife IRE electroporator (firmware V3.29, software V2.2.0.23; AngioDynamics Inc., Latham, NY) and NanoKnife monopolar probes (15 cm, 19G). The electrodes were positioned under CT guidance (Aquillion Prime CT scanner; Toshiba Inc., Tustin, CA) and on the basis of individual treatment-planning data (ProcedureManager-2_2_0_23 for Windows, AngioDynamics Inc.). Before each ablation, a test run (10 pulses per electrode pair) was performed to determine conductivity. IRE (70-90 μs, 450-1300 pulses per target, 1.8-3.0 kV, 28-50 A, at least 2 rounds per electrode pair) was performed with electrocardiogram triggering under general anesthesia and deep muscle paralysis with 3-6 monopolar electrodes positioned within the renal tumor (see Table 1). Intraprocedural IRE modification was performed after immediate evaluation of post-IRE ablation graphs by interelectrode voltage modulation, separate electrode-pair ablation, and IRE electrode placement.[17,18] After 28 days, open lumbar or transperitoneal resection of the complete ablation region (partial renal resection or nephrectomy if necessary) was performed to allow better assessment of the organ and its surroundings.

Imaging

Contrast-enhanced, diffusion-weighted magnetic resonance imaging (MRI) (1.5-T scanner, gadobutrol: 0.1 mL/kg Gadovist 1.0 mmol/mL; Bayer, Leverkusen, Germany) of the kidneys was carried out 1 day before and 2, 7, and 27 days after IRE. Contrast-enhanced sequences, "arterial," "portal-venous," "venous," and "urographic" (late venous phase), were carried out (T1w-2D-GRE [Scout], T2w-SShTSE, T2w-FS-TSE, T2w-RT-TSE, diffusion-weighted imaging [b = 0/500], T1w-GRE, T1w-FS-3DGRE transversal, and T1w-FS-3DGRE coronal). INFINITT PACS software (INFINITT Europe GmbH, Germany) was used for evaluation.

Histopathologic Analysis

The resection specimens were fixed in buffered 4% formaldehyde solution for at least 24 hours followed by complete sectioning of the ablation area, including a border of macroscopically inconspicuous kidney tissue in 0.4-cm-thick slices. The ablation area was measured 2-dimensionally. Thereafter, the specimens were completely embedded in paraffin in standard tissue cassettes after topographic assignment based on macrophotography. Each tissue block was used to prepare 3-μm-thick sections, and these were stained with hematoxylin and eosin for morphologic assessment in 500-μm steps with 1 unstained section each for transmission microscopy. The extent of histologically demonstrable damage was determined by a regression grade.[12] Additional immunohistologic staining of the tumor region with proliferation marker Mib1 (dilution 1:100; Dako, Santa Clara, CA), if at least there was still a rudimentary basic structure seen, was performed to determine viability or irreversible cell death. In each specimen, the complete ablation area, the tumor area, and the nonaffected renal tissue on each slide were outlined manually. The maps from each subject were scanned with a digitizing pad (Bamboo One, Wacom, Japan) using

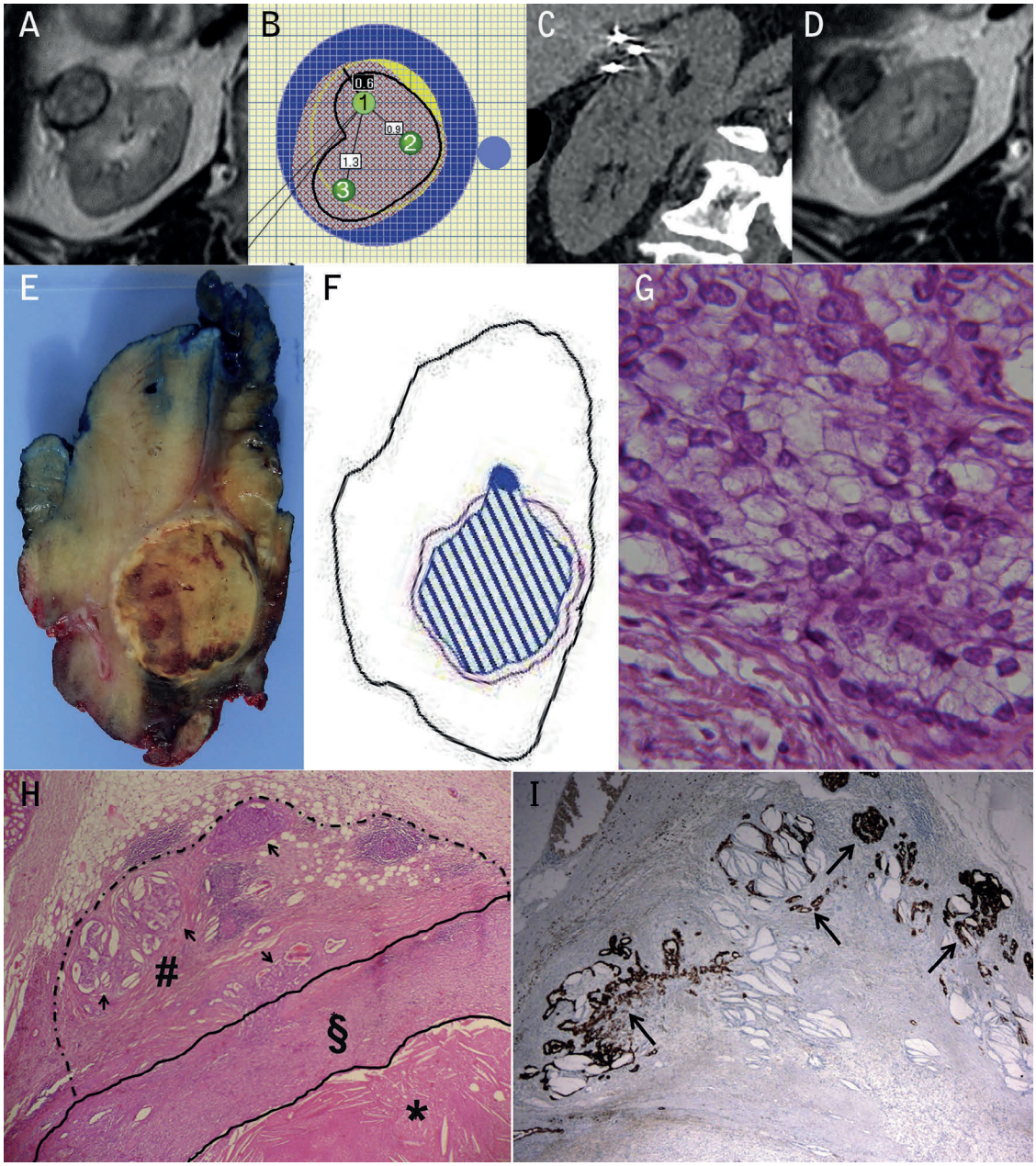

Figure 1. Patient 6—example of incomplete ablation. **(A)** Initial MRI representation of the tumor before IRE: cortical renal cell carcinoma 2.4 cm from the ventrolateral lower pole to the midlevel of the right kidney, imaged by MRI before IRE. **(B)** NanoKnife IRE planning and representation of the calculated ablation zone (red-brown) in relation to the tumor (yellow). The labels 1, 2, and 3 represent the IRE electrode positions (transversal view of treatment planning). **(C)** Computed tomographic 2D transversal representation of the IRE electrodes in the kidney tumor. **(D)** MRI representation of the tumor 27 days after IRE. **(E)** Partial kidney resection with macroscopic tumor contour 28 days after IRE, fixed and cut open. **(F)** A microscopic tumor residue at the edge of the tumor (solid blue area) resulting from incomplete coverage of the tumor in ablation (blue hatched area) and the ablation zone (violet line). (**G**) Viable carcinoma focus without signs of regression seen by HE staining. **(H)** Viable microscopic tumor residue (like cell nests, dashed line with # and arrows) in the edge zone of the ablation area (outfield) with a fibrotic peritumoral border (area § between the solid lines) and bordering, completely necrotic tumor (asterisk). **(I)** Viable tumor residue marked by pancytokeratin antibodies AE1 and AE3 (arrows). IRE, irreversible electroporation; MRI, magnetic resonance imaging. (Color version available online.)

image-manipulation software (GNU Image Manipulation Program [GIMP 2.8.14]) and inspected serially in the computer, and the volume was determined; the volume was calculated as the sum of tumor areas multiplied by the section thickness (0.4 cm) and by a factor of 1.5 to take account of formalin-induced tissue shrinkage.

RESULTS

IRE Treatment

Seven patients who had biopsy-proven RCC pT1a cN0cM0 with a mean tumor size of 22 mm (range 15-39 mm) underwent lumbar percutaneous CT-guided IRE with the

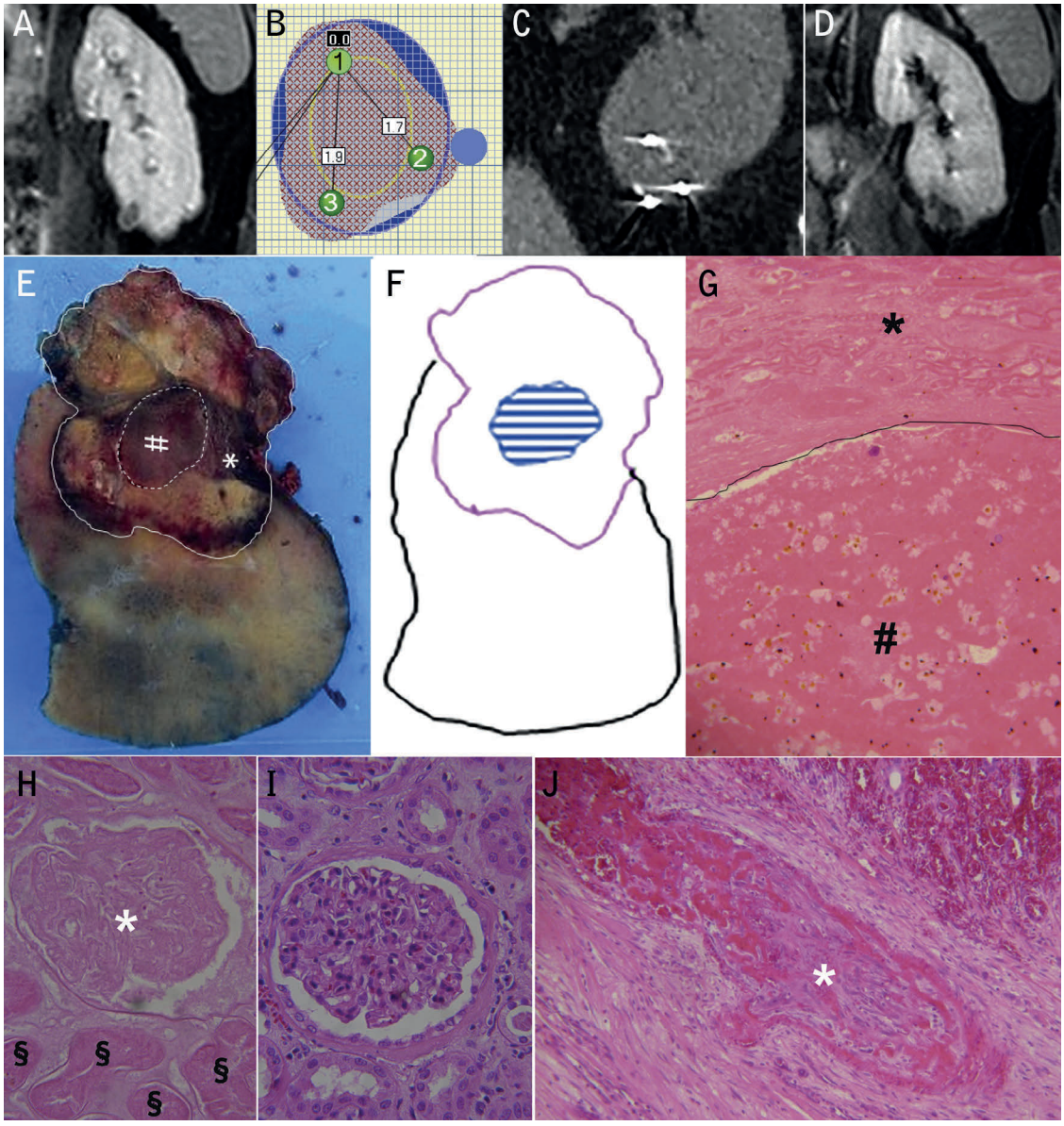

Figure 2. Patient 7—example of complete ablation. **(A)** Initial magnetic resonance imaging representation of the tumor: cortical renal cell carcinoma 1.8 cm from the lower pole dorsomedial to the left kidney, before IRE. **(B)** NanoKnife IRE planning and representation of the calculated ablation zone (red-brown) in relation to the tumor (yellow). The labels 1, 2, and 3 represent the IRE electrode positions (transversal view of treatment planning). **(C)** Computer-tomographic 2D transversal representation of the IRE electrodes in the kidney tumor. **(D)** Magnetic resonance imaging representation of the tumor 27 days after IRE. **(E)** Partial kidney resection with tumor contour 28 days after IRE, fixed and cut open, with tumor contour (#), peritumoral ablation zone (asterisk), and healthy parenchyma outside the ablation zone. **(F)** Complete ablation without microscopic tumor residue (blue hatched area) in the ablation zone (violet line). **(G)** The border (black line) between the completely necrotic tumor (#) and the necrotic tumor-free parenchyma (asterisk), seen by hematoxylin and eosin staining. **(H)** Magnified detail of completely necrotic tubules (§) and a nonviable glomerule (asterisk) from the ablation zone. **(I)** For comparison, unchanged viable parenchyma (glomerule and tubules) in the adjacent tissue. **(J)** Vessel with fresh, partly organized thrombus (asterisk) from the edge zone of the necrosis. IRE, irreversible electroporation. (Color version available online.)

NanoKnife system (Table 1). In 6 patients, 1 IRE ablation in 1 session was performed, and in 1 patient, 2 IRE ablations in 1 session were performed (total of 8 ablations, Table 1). The mean planned IRE treatment zone was 17.3 cm^3 (8 ablations, range 8.2-45.6 cm^3). Because of the proximity between the kidney (and renal tumor) and the adjoining colon, an expandable balloon was placed in between to move the colon out of the IRE ablation field, thus avoiding a possible perforation. Technical feasibility was attained in all patients, but electrode placement and ablation were complex, with a mean overall procedure time of 129 minutes (range 53-203 minutes) and an anesthesia time of 165 minutes (range 91-317 minutes).

Table 1. Patient, treatment, and resection parameters

Patient	P1	P2	P3	P4	P5	P6	P7
Age, sex	44, M	78, M	74, M	73, M	74, M	71, F	61, M
ECOG score, Charlson score	0, 0	0, 2	0, 0	0, 1	1, 1	0, 0	0, 0

Tumor	P1	P2	P3	P4	P5	P6	P7
Targets	1	1	1	1	2	1	1
Location	UP, ventrolateral	UP-MP, dorsomedial	UP-MP, dorsomedial, hilum	UP, lateral	LP-MP, lateral, mediocentral satellite	UP-MP, ventrolateral	LP, left, dorsomedial
PADUA	6	8	11	6	8	6	7
Size (cm)	1.7 × 1.7 × 1.6	1.5 × 1.5 × 1.4	1.6 × 1.5 × 1.5	2.2 × 2.1 × 1.9	3.9 × 3.8 × 3.1, 1.8 × 1.5 × 1.7	2.4 × 2.4 × 2.0	1.4 × 1.1 × 1.8
Volume (cm^3)	2.4	1.6	1.9	4.6	24.1 + 2.8 = 26.9	6.0	1.5
Shape	Spherical	Spherical	Spherical	Spherical	Elliptic-spherical	Spherical	Spherical
Biopsy	papRCC, G2	Eosin-ccRCC, G1	ccRCC, G1	ccRCC, G1	ccRCC, G1	ccRCC, G2	papRCC, G2
Texture	Solid	Solid	Solid	Cystic-solid	Solid	Solid	Solid
TNM	pT1a G2	pT1a G1	pT1a G1	pT1a G1	pT1a G1	pT1a G2	pT1a G2

IRE	P1	P2	P3	P4	P5	P6	P7
Sessions, ablations	1, 1	1, 1	1, 1	1, 1	1, 2	1, 1	1, 1
Rounds	4	2	3	4	2 + 2	2	2
No. of electrodes, electrode pairs, configuration	4, 6, square	3, 3, triangular	4, 6, square	4, 6, square	3, 3, triangular; 6, 10, pentagonal with center	3, 3, triangular	3, 3, triangular
Tip exposure (cm)	2.5	1.5	2.0	2.0	2.0 and 2.5 (pullback)	2.5	2.0
Planned treatment zone (cm)/(cm^3)	2.4 × 2.9 × 3.5/ 12.7	2.5 × 2.5 × 2.5/8.2	3.5 × 4.0 × 3.0/ 22.0	3.0 × 3.0 × 2.9/ 13.7	2.7 × 2.7 × 2.7/ 10.3 and 4.4 × 4.4 × 4.5/ 45.6	3.0 × 3.3 × 3.0/ 15.6	2.4 × 2.9 × 2.8/ 10.2
Pulse length (μs)	90	90	90	90	70, 80, and 90	90	70 and 90
Pulses	1300	450	1320	840	570 + 880	450	510
Current min and max (A)	30 and 49	30 and 42	30 and 49	25 and 49	22 and 50	28 and 50	20 and 35
Voltage min and max (V)	1800 and 2800	2200 and 2640	1960 and 3000	2160 and 3000	1800 and 2800	1850 and 2600	1820 and 2660
Intervention and anesthesia (min)	131 and 193	126 and 162	163 and 208	123 and 194	203 and 317	53 and 91	104 and 181

Surgery	P1	P2	P3	P4	P5	P6	P7
Initial and presurgical eGFR (mL/min)	107 and 106	86 and 88	70 and 73	67 and 63	78 and 72	48 and 47	82 and 80
Resection type, access	Partial resection, open lumbar	Partial resection, open lumbar	Nephrectomy, open lumbar	Partial resection, open abdominal	Nephrectomy, open lumbar	Partial resection, open abdominal	Partial resection, open lumbar
Surgery and ischemia (min)	185 and 16	175 and 19	115 and 0	190 and 18	130 and 0	140 and 21	185 and 35

Continued

Table 1. Continued

Pathology	P1	P2	P3	P4	P5	P6	P7
Ablation zone (cm)/(cm^3)	2.5 × 2.0 × 1.3/3.4	3.0 × 2.5 × 2.0/7.9	4.2 × 1.4 × 1.2/ 17.2	2.8 × 2.2 × 2.0/3.5	4.2 × 2.8 × 3.5/ 19.2	2.9 × 2.5 × 3.5/4.5	4.6 × 2.2 × 3.0/8.4
Tumor shape (cm)/(cm^3)	1.6 × 1.5 × 1.2/1.6	1.6 × 1.7 × 1.1/1.6	1.5 × 1.4 × 1.2/1.3	1.2 × 0.8 × 1.0/0.2	3.0 × 2.4 × 4.0/9.7	3.0 × 2.2 × 2.0/2.0	1.3 × 1.2 × 1.0/0.2
Coverage of tumor shape by ablation zone	Complete	Complete	Complete	Complete	Incomplete	Incomplete	Complete
Residual ablated tumor texture	0.28 cm^3; infield	0.045 cm^3; infield	1.185 cm^3; infield	None	0.009 cm^3; outfield, margin	0.03 cm^3; outfield, margin	None
Regression	3°	4°	4°	4°	3°	3°	4°
Mib-1 index (%)	0	0	0	0	1	1	0
Viability	Uncertain	Nonviable	Nonviable	Nonviable	Viable	Viable	Nonviable
TNM (IRE)	Uncertain ypT0-1a V0 L0 Pn0 R0-1	Complete ypT0 V0 L0 Pn0 R0	Complete ypT0 V0 L0 Pn0 R0	Complete ypT0 V0 L0 Pn0 R0	Incomplete, ypT1a V0 L0 Pn0 R1	Incomplete, ypT1a V0 L0 Pn0 R1	Complete, ypT0 V0 L0 Pn0 R0
TNM (OP)	R0	R0	R0	R0	R0	R0	R0

cc, clear-clear cell; ccRCC, clear cell renal cell carcinoma; ECOG, performance status of Eastern Cooperative of Oncology Group; eGFR, estimated glomerular filtration rate; F, female; IRE, irreversible electroporation; LP, lower pole; M, male; MP, mid-pole; OP, operation or surgery; PADUA, Preoperative Aspects and Dimensions Used for an Anatomical score; papRCC, papillary renal cell carcinoma; TNM, tumor, node, and metastasis classification of the International Union for Cancer Control 2017; UP, upper pole.
Active tip (exposure) plus postulated ablation field in depth 2 × 0.5 cm. Volumes are calculated for ellipsoidal tumor: $V = 4/3\ \pi\ a \times b \times c$.

Magnetic Resonance Imaging

The analysis of the MRI of the tumor texture and the renal parenchyma and its correlation with the histologic results have yet to be published separately.

Side Effects

There were no major or residual procedure-related complications. Minor complications included slight self-limiting gross hematuria (in 7/7 patients), perirenal hematomas (2/7), and temporary postpuncture pain, treated by drugs (7/7) with Clavien-Dindo grades I and II.[19] Renal function after IRE was retained in all cases, with no urinary leakage or retention, no renal infarction, and no significant change in the creatinine level. After a mean follow-up time of 25 months (range 15-36), no evidence of local recurrence or metastasis was seen.

Resection and Histologic Analysis

Four weeks after IRE, a residual tumor contour within the ablation area was macroscopically by MRI persistent in all cases and was similar to the initial tumor size. Partial kidney resection was performed in 5 of the 7 patients. Two patients had a centrally located RCC adjacent to the hilum or the renal pelvis (P3 and P5). Despite the relatively small tumor sizes, these 2 nephrectomies had to be performed to obtain a complete resection of the tumor ablation zone analogous to the study protocol, whereas the unfavorable location and the central expansion near the hilum made a partial resection not feasible in the surgeon's indication. Intrasurgical examination at resection showed severe local perirenal and peritumoral adhesions due to a local inflammatory unspecific reaction resulting from puncture or IRE. Complete macroscopic coverage of the tumor by the IRE ablation field was achieved in 100% of the cases. In each of the 7 cases investigated, IRE induced massive damage to the tumor tissue. Macroscopic analysis showed sharply demarcated, approximately ellipsoidal, hemorrhagically altered IRE ablation zones. The peritumoral damage zones had spread to peritumoral renal tissue and, in some cases, to perirenal fatty tissue. The ablation IRE zone was larger than expected in 3 of the 7 cases.

Microscopic analysis showed the tumor focus within the ablation zone with strong treatment effects (regression grades III and IV, strongest effect = IV[12]) with almost complete tumor destruction by extended, homogeneously eosinophilic coagulation necrosis. Alongside the tumor-related histologic changes, all cases showed zonal structuring of the ablation region, as described earlier in detail.[12] In the center, an amorphous necrosis zone of the coagulation-necrosis type was seen. Next to this, there was a necrosis zone of variable width, also of the coagulation-necrosis type, in which ghost structures of the tissue affected could still be discerned (eg, tubules, glomerules, and fat). Some dystrophic areas of calcification and resorptive chronic-inflammatory changes could also be seen, sometimes with the formation of foreign-body giant cells. In sections where the ablation zone included the renal pelvis and papillae, both structures showed necrosis with urothelial slough-

ing and incipient regeneration. Adjacent to this zone, there was a gradual transition to a zone of granulation tissue associated with frequent, in part luminal, occlusive intimal hyperplasia of small- and medium-sized arterial renal vessels. Adjacent to this, an unaffected renal parenchyma was found.

Within or close to the necrotic tumor only, a small focus of preserved residual tumor texture was detected in 5 of the 7 patients. (Table 1). In 3 of these 5 cases, the microscopic tumor texture residues showed only minor regressive changes (grade 3 or 4) with a mean volume of 0.11 cm^3 (range 0.009-0.280). (Table 1). According to Mib-1 staining, the tumor ablation zone had proliferative activity in 2 of these 3 cases (ypT1a R1 according to tumor, node, and metastasis classification of the International Union for Cancer Control 2017 [TNM classification]) and intermediate or uncertain viability in the third (ypT0–1a R0-1 according to TNM classification) (Table 1).[20,21] One of these 3 cases showed intratumoral microscopic skip lesions (infield residual tumor), and in 2 of the 3 cases, a microscopic tumor residue appeared at the edge of the ablation zone (outfield or field-margin residual tumor). According to the TNM classification, resection revealed ypT0V0N0Pn0R0 in 4 cases as complete ablation. In the other three tumor patients, ablations were classified as incomplete ablation due to residual microscopic tumor cells (Table 1).[20,21]

DISCUSSION

Diehl et al[13] treated 7 SRMs (range 15-18 mm) with percutaneous IRE in 5 patients with a solitary kidney. A progressive, significant decrease in contrast-enhanced magnetic resonance signal intensity of the ablated area was seen at follow-up, suggesting a treatment response rate of 100% at a mean follow-up of 6.4 months (range 3-11). The study was limited to an unknown SRM entity and did not include histologic evaluation after ablation.[13]

Canvasser et al[14] reported "suboptimal oncological efficacy" and imaging features after IRE of 42 SRMs (10-36 mm), observed by CT or MRI immediately, 6 weeks, 6 months, and 12 months after percutaneous IRE ablation. CT or MRI after IRE ablation demonstrated an area of nonenhancement in the treatment zone that became involuted over about 6 months. Three cases showed incomplete ablation with a margin of residual enhancing tumor consistent with viable malignancy; the patients proceeded to salvage therapy. One patient showed local recurrence after 1 year. Canvasser et al's study was limited to a mixed entity of malignant (20 RCCs) and benign or unknown SRMs; no histologic evaluation after ablation was performed.[14]

In contrast to these studies, we present the first results of resection following IRE of human biopsy-proven pT1a RCC.[22] These histologies represented "snapshots" taken 4 weeks after IRE, with procedure-specific findings. The histologic remodeling process of necrosis, vessels and inflammation of the ablated area seemed to be not completed at the point of time. Previous animal studies of renal IRE in healthy swine suggested a favorable follow-up of 4 weeks, knowing to have no tumor, only ablation of renal parenchyma.[8,9] On that concept, this subsequent clinical pilot study in human RCC was based. Although the choice of a different interval between IRE and histologic analysis could of course influence this result, the optimum interval between IRE and histologic assessment is at present still unclear.

In the context of the initial results, it was discussed whether the basic histologic structures of papillary and cystic RCCs cause incomplete ablation due to reduced tissue connectivity and homogeneity.[12] Nevertheless, the results presented here demonstrate complete ablation of 1 of 2 papillary RCCs and 1 of 1 cystic clear cell RCC, so that no conclusion of different IRE ablation responses for specific RCC subtypes can be drawn.

Complete coverage of the tumor by the IRE ablation field was possible, but microscopic residual tumor areas could be found in 3 of the 7 cases. The ablation quality and success with a homogenous, complete IRE ablation with no infield or outfield residual tumor areas could not be predicted certainly. On the basis of this initial analysis, we conclude that complete ablation of T1a RCC in different locations, and renal preservation also in case of centrally located tumors, is possible with IRE. The nephrectomy was performed in 2 cases because of central tumor location and ablation areas. As opposed to this, these 2 patients revealed a functional kidney after central IRE ablation that would not have required nephrectomy out of the study protocol. Our study demonstrated that IRE might be useful for ablation of centrally located renal tumors showing severe tumor destruction with protection or regeneration of the urine-collecting system.[16] This fact may point out the advantage of IRE application over surgical resection and thermal ablation techniques in centrally located kidney tumors.

The rate of residual tumor or incomplete ablation is also dependent on the follow-up tool. Resection histology may evaluate microscopic cancer cell areas more effectively and therefore in a higher rate than imaging, especially in specimens with remodeling process after ablation. The issue of residual tumor cells is common to all ablation and radiation methods and is not specific for IRE.[5,23-25] It should be considered that IRE studies with imaging and biopsy control only may fail to detect microscopic tumor residues or recurrences.[23-25] That fact may explain the higher rate of microscopic incomplete ablation of 43% in our study. However, the ablation success is also dependent on the ablation technique and its feasibility. Despite this finding, each of the known ablation modalities has a unique working principle and biophysics underlying the ablative effect, which largely determines the clinical indication for its application and the specific histologic presentation.[26] Similarly, after radiofrequency ablation (RFA), residual tumor areas are seen that possess a residual viability immediately and 1 week after ablation.[27,28] The primary ablation success of RFA and cryoablation of SRM is about 90%-100%, depending on the tumor size and location. Several studies reported a local recurrence rate of pT1a RCC between 2%

and 12% for RFA and between 3% and 17% for cryoablation within the first 5 years.[3,29] Small case studies of laparoscopic high intensity focused ultrasound (hyperthermal ablation method) of SRMs showed incomplete ablation between 42% and 75% in resection specimens.[3,29] Following IRE of liver tumors, for comparison, 29% showed recurrent tumors after 6 months.[30]

Meta-analyses of patients with positive surgical margins after nephron-sparing surgery of RCC have suggested that small tumor residues lack prognostic relevance.[31,32] Therefore, a surveillance strategy seems preferable to surgical or ablative reintervention. That fact is also based on the known low progression rate of 0.13 cm/y and the low dissemination rate of 1.1% for pT1a RCC.[33] Finally, the detection of residual tumor or local recurrence after ablation offers the possibility of a repetition of the ablation. Microscopic, dubious tumor residues remaining in the nonviable ablation region 4 weeks after IRE must be assessed in light of this.

According to these study experiences, the intended curative IRE ablation of located RCCs sized below 4 cm is feasible but makes a high procedural demand (especially the aimed CT-guided IRE electrode placement and the intrainterventional 2-dimensional treatment-planning control) and is not reliable or reproducible. Maybe, the application of MRI usable IRE electrodes, a combination of 3-dimensional-navigated IRE electrode placement and treatment planning of IRE, as well as the development of clinical applicable high-frequency IRE for muscle relaxation-free and anesthesia-free IRE ablation, could adopt a broad utilization.

Limitations

The strength of our pilot study, according to the German medical product law, was to obtain first histologic resection analyses of the IRE tumor-ablated area of biopsy-proven RCC in all patients. But the procedures in the present study place a substantial burden on the patients because of the 2-stage intervention principle, with general anesthesia for IRE ablation and again for delayed resection. Moreover, the specimens had to be obtained by open surgery, a factor that also made it difficult to recruit a larger patient collective. Hence, our study is limited statistically by the small number of patients. The results do not lead to a recommendation of specific changes in IRE ablation parameters. Finally, it does not seem likely that further recruitment, to reach the originally planned total of 20 patients, would lead to different results, so that termination of the study is under consideration.

CONCLUSION

According to these limited and initial study results, renal percutaneous IRE using the NanoKnife appears to be a safe treatment for SRMs, including centrally located tumors with kidney preservation. The intended curative IRE ablation of located RCCs sized below 4 cm may be feasible but makes a high procedural demand and was inconstant and not reliable or reproducible. We observed by histologic resection analysis a high rate 43% of microscopic residual cancer cells within the IRE ablation zone in a short follow-up setting of 4 weeks. Percutaneous NanoKnife IRE still needs further technical improvement and evaluation in trials to ensure complete ablation by this still experimental and not reliable method. This method needs to be improved before being recommended to patients as an option for cure. Larger studies of renal IRE of biopsy-proven RCC pT1a with MRI and biopsy follow-up according to current recommendations are needed to draw consistent conclusions.[25]

References

1. Ljungberg B, Albiges L, Bensalah K, et al. EAU guidelines on renal cell carcinoma. European Association of Urology 2017. Update March 2017. Available at: http://uroweb.org/wp-content/uploads/10-Renal-Cell-Carcinoma_2017_web.pdf. Accessed November 11, 2017.
2. D'Andrea D, Shariat SF, Klatte T. Update on ablative therapies of renal tumors. *Curr Opin Urol*. 2016;26:410-416.
3. Wendler JJ, Friebe B, Baumunk D, et al. [Focal therapy for small renal masses: observation, ablation or surgery]. *Urologe A*. 2016;55:594-606.
4. Hayes MC, Breen DJ. Excision versus ablation in renal cancer: optimising outcome and minimising risk. *Eur Urol*. 2016;69:683-684.
5. Thompson RH, Atwell T, Schmit G, et al. Comparison of partial nephrectomy and percutaneous ablation for cT1 renal masses. *Eur Urol*. 2015;67:252-259.
6. Rubinsky B. *Irreversible Electroporation*. 1st ed. Berlin: Springer; 2009:328. ISBN 3642054196.
7. Wendler JJ, Pech M, Blaschke S, et al. Angiography in the isolated perfused kidney: radiological evaluation of vascular protection in tissue ablation by nonthermal irreversible electroporation. *Cardiovasc Intervent Radiol*. 2012;35:383-390.
8. Wendler JJ, Pech M, Porsch M, et al. Urinary tract effects after multifocal nonthermal irreversible electroporation of the kidney: acute and chronic monitoring by magnetic resonance imaging, intravenous urography and urinary cytology. *Cardiovasc Intervent Radiol*. 2012;35:921-926.
9. Wendler JJ, Porsch M, Hühne S, et al. Short- and mid-term effects of irreversible electroporation on normal renal tissue: an animal model. *Cardiovasc Intervent Radiol*. 2013;36:512-520.
10. Pech M, Janitzky A, Wendler JJ, et al. Irreversible electroporation of renal cell carcinoma: a first-in-man phase I clinical study. *Cardiovasc Intervent Radiol*. 2011;34:132-138.
11. Thomson KR, Cheung W, Ellis SJ, et al. Investigation of the safety of irreversible electroporation in humans. *J Vasc Interv Radiol*. 2011;22:611-621.
12. Wendler JJ, Ricke J, Pech M, et al. First delayed resection findings after irreversible electroporation (IRE) of human localised renal cell carcinoma (RCC) in the IRENE Pilot Phase 2a Trial. *Cardiovasc Intervent Radiol*. 2016;39:239-250.
13. Diehl SJ, Rathmann N, Kostrzewa M, et al. Irreversible electroporation for surgical renal masses in solitary kidneys: short-term interventional and functional outcome. *J Vasc Interv Radiol*. 2016;27:1407-1413.
14. Canvasser NE, Sorokin I, Lay AH, et al. Irreversible electroporation of small renal masses: suboptimal oncologic efficacy in an early series. *World J Urol*. 2017;35:1549-1555.
15. Wendler JJ, Porsch M, Nitschke S, et al. A prospective Phase 2a pilot study investigating focal percutaneous irreversible electroporation (IRE) ablation by NanoKnife in patients with localised renal cell carcinoma (RCC) with delayed interval tumour resection (IRENE trial). *Contemp Clin Trials*. 2015;43:10-19.
16. Wendler JJ, Pech M, Köllermann J, et al. Upper-urinary-tract effects after irreversible electroporation (IRE) of human localised renal-

cell carcinoma (RCC) in the IRENE pilot phase 2a ablate-and-resect study. *Cardiovasc Intervent Radiol.* 2017;doi:10.1007/s00270-017-1795-x.
17. *Manual NanoKnife_ System Procedure & Trouble Shouting Guide. Software Version 2.2.0. AngioDynamics*. AngioDynamics, Inc.; 2011:1-159.
18. Wendler JJ, Fischbach K, Ricke J, et al. Irreversible electroporation (IRE): standardization of terminology and reporting criteria for analysis and comparison. *Pol J Radiol.* 2016;81:54-64.
19. Dindo D, Demartines N, Clavien PA. Classification of surgical complications: a new proposal with evaluation in a cohort of 6336 patients and results of a survey. *Ann Surg.* 2004;240:205-213.
20. Brierley JD, Gospodarowicz MK, Wittekind C. *TNM Classification of Malignant Tumours*. 8th ed. Wiley-Blackwell; 2017. ISBN-10: 1119263573, ISBN-13: 978-1119263579.
21. Wittekind C, Compton CC, Brierley J, Sobin LH. *TNM Supplement. A Commentary on Uniform Use*. 4th ed. 2012. ISBN-10: 1444332430, ISBN-13: 978-1444332438.
22. Wendler JJ, Ricke J, Pech M, et al. Initial assessment of clinical feasibility, safety and efficacy of NanoKnife irreversible electroporation (IRE) in the focal treatment of localized renal cell carcinoma (RCC) with delayed interval tumor resection (IRENE trial). *Eur Urol Suppl.* 2017;16:e102-e103. doi:10.1016/S1569-9056(17)30129-X.
23. Dupuy DE, Gervais DA, Gianfelice D, et al. Image-guided tumor ablation: standardization of terminology and reporting criteria—a 10-year update. *J Vasc Interv Radiol.* 2014;25:1691-1705.
24. Ahmed M, Technology Assessment Committee of the Society of Interventional Radiology. Image-guided tumor ablation: standardization of terminology and reporting criteria–a 10-year update: supplement to the consensus document. *J Vasc Interv Radiol.* 2014;25:1706-1708.
25. Zondervan PJ, Wagstaff PG, Desai MM, et al. Follow-up after focal therapy in renal masses: an international multidisciplinary Delphi consensus project. *World J Urol.* 2016;34:1657-1665.
26. Vroomen LGPH, Petre EN, Cornelis FH, Solomon SB, Srimathveeravalli G. Irreversible electroporation and thermal ablation of tumors in the liver, lung, kidney and bone: what are the differences? *Diagn Interv Imaging.* 2017;98:609-617.
27. Rendon RA, Kachura JR, Sweet JM, et al. The uncertainty of radio frequency treatment of renal cell carcinoma: findings at immediate and delayed nephrectomy. *J Urol.* 2002;167:1587-1592.
28. Klingler HC, Marberger M, Mauermann J, Remzi M, Susani M. "Skipping" is still a problem with radiofrequency ablation of small renal tumours. *BJU Int.* 2007;99:998-1001.
29. Wah TM. Image-guided ablation of renal cell carcinoma. *Clin Radiol.* 2017;72:636-644.
30. Niessen C, Igl J, Pregler B, et al. Factors associated with short-term local recurrence of liver cancer after percutaneous ablation using irreversible electroporation: a prospective single-center study. *J Vasc Interv Radiol.* 2015;26:694-702.
31. Steinestel J, Steffens S, Steinestel K, Schrader AJ. Positive surgical margins in nephron-sparing surgery: risk factors and therapeutic consequences. *World J Surg Oncol.* 2014;12:252.
32. Marszalek M, Carini M, Chlosta P, et al. Positive surgical margins after nephron-sparing surgery. *Eur Urol.* 2012;61:757-763.
33. Jewett MA, Mattar K, Basiuk J, et al. Active surveillance of small renal masses: progression patterns of early stage kidney cancer. *Eur Urol.* 2011;60:39-44.

9. Danksagung

Mein Hauptinteresse in der Urologie gilt neuen Diagnostik- und Therapieverfahren. Seit 2009 konnte ich die Entwicklungen des Fachgebietes an der Universitätsklinik für Urologie Magdeburg hautnah miterleben. Gerade die fachliche und räumliche Nähe zur Universitätsklinik für Radiologie Magdeburg mit ihrem großen Spektrum an interventionellen Techniken machte für uns eine interdisziplinäre Zusammenarbeit sowohl in der klinischen Routine als auch wissenschaftlich interessant. So ergab sich die Chance der systematischen Evaluation der Irreversiblen Elektroporation als neuartiges, nonthermales Gewebeablationsverfahren. Dieser langjährige, aufwendige Prozess wurde als gemeinsames Projekt durch ein Team beteiligter Wissenschaftler anderer Fachgebiete und der Urologie mit hoher Unterstützung und starkem Rückhalt ermöglicht.

Mein ganz besonderer Dank gilt deshalb meinem Chef, Herrn Prof. Dr. med. Martin Schostak, der mit seinem sehr erfahrenem, wissenschaftlichem Blick stets auf mein Vorankommen achtete und mich uneingeschränkt mit jeder erdenklichen Hilfe förderte.

Von ganzem Herzen danke ich Herrn PD Dr. med. Uwe-Bernd Liehr, Herr Prof. Dr. med. Jens Ricke und Herr Prof. Dr. med. Maciej Pech für ihren stetigen Enthusiasmus für die wissenschaftlichen und organisatorischen Fragestellungen dieser Arbeit, auch über das Kernthema hinaus. Ihre Überzeugungsarbeit und ihr fachlicher Weitblick waren von unschätzbarem Wert und trugen wesentlich zum Gelingen dieser Arbeit bei.

Weiterhin bedanke ich mich außerordentlich bei alle beteiligten Personen, Fachrichtungen und Institutionen, ohne deren fachliche Kompetenz und Hilfe dieser Weg nicht möglich gewesen wäre: Herr Dr. med. Simon Blaschke, Herrn PD Dr. med. Markus Porsch, Frau Dr. med. Sarah Hühne, Herr Prof. Dr. med. Malte Böhm und Frau Simone Nitschke (Urologie); Frau Antje Mittag, Herr Dirk Mahnkopf und das Team (IMTR Rottmersleben); Herr Prof. Dr. med. Frank Fischbach, Frau PD Dr. med. Katharina Fischbach, Herr Dr. Julian Jürgens, Herr Dr. med. Björn Friebe und das gesamte MTRA-Team (Radiologie); Herr Dr. med. Peter Buhtz, Herr PD Dr. med. Jens Köllermann, Frau Dr. med. Sandra Siedentopf, Herr Dr. med. Klaus Vogler und dem MTA-Team (Pathologie), Herr Prof. Dr. med. Siegfried Kropf (Biometrie und Medizinische Informatik), Herr PD Dr. med. Christof Strang und den Anästhesie-Teams (Anästhesiologie), Herr Prof. Dr. med. Frank Grothues (Kardiologie), Frau Prof. Dr. med. Katrin Borucki und dem MTLA-Team (Klinische Chemie), der Deutschen Akademie für Mikrotherapie (DAfMT) und dem Arbeitskreis für Fokale und Mikrotherapie der Akademie der Deutschen Gesellschaft für Urologie (AKFM/ DGU), Frau Dr. med. Patricia J. Zondervan, Herrn Prof. Dr. med. Jean J.M.C.H. de la Rosette und Frau Prof. Dr. med. Maria Pilar Laguna Pes (Urologie), Frau Dr. rer. nat. Antje Wiede und dem KKS-Team (Koordinierungszentrum für Klinische Studien, KKS UMMD).

Meiner Frau Sarina Wendler und meinen Kindern Jakob und Julius Wendler danke ich für ihr Verständnis für meine zum Teil aufwendige wissenschaftliche Arbeit. Ohne ihre volle Unterstützung und Wertschätzung wäre das nicht möglich gewesen.

Allen hier nicht namentlich genannten Kollegen, Mitarbeitern und Freunden sei an dieser Stelle für ihre Unterstützung ebenfalls gedankt.

10. Eidesstattliche Erklärung

Ich erkläre, dass ich die der Medizinischen Fakultät zur Habilitation eingereichte Habilitationsschrift mit dem Titel:

„Irreversible Elektroporation in der Uroonkologie – die systematische Evaluation eines neuartigen, non-thermalen Gewebe-ablationsverfahrens am Nierentumormodell zur minimal-invasiven, perkutanen, kurativ-intendierten Therapie des lokal begrenzten Nierenzellkarzinoms und Prostatakarzinoms“

in der Universitätsklinik für Urologie und Kinderurologie der Medizinischen Fakultät der Otto-von-Guericke-Universität Magdeburg selbständig und ohne sonstige fremde Hilfe durchgeführt und bei der Abfassung keine anderen als die dort aufgeführten Hilfsmittel benutzt habe. Bei der Abfassung der Habilitationsschrift sind Rechte Dritter nicht verletzt worden.

Ich habe die Habilitationsschrift bisher an keiner in- oder ausländischen Hochschule/ Universität zur Habilitation eingereicht oder mich anderweitig um Zulassung zur Habilitation beworben.

Ich übertrage der Medizinischen Fakultät der Otto-von-Guericke-Universität das Recht, weitere Kopien meiner Habilitationsschrift herzustellen und zu vertreiben.

Magdeburg, den 30.04.2019

Unterschrift